Université de Montréal

Faculté des études supérieures

Réseaux étendus construits par autoassemblage de ligands flexibles dithiolatés et de centres métalliques du groupe 11, argent(I) et or(I).

Par
Mohamed Osman Awaleh

Département de Chimie
Faculté des Arts et des Sciences

Thèse présentée à la Faculté des études supérieures
en vue de l'obtention du grade de Philosophiæ Doctor (Ph.D.) en chimie

Décembre 2006

Université de Montréal

Faculté des études supérieures

Cette thèse intitulée :

Réseaux étendus construits par autoassemblage de ligands flexibles dithiolatés et de centres métalliques du groupe 11, argent(I) et or(I).

présentée par
Mohamed Osman AWALEH

a été évaluée par un jury composé des personnes suivantes :

Dr. Julian X. Zhu.....Président rapporteur
Dr. François Brisse.....Directeur de recherche
Dr. Antonella Badia.....Codirectrice de recherche
Dr. Frank Schaper.....Membre du jury
Dr. Fernande D. Rochon.....Examinatrice externe
Dr. Julian X. Zhu ..... Représentant du doyen de la FES

Sommaire

Des composés de coordination d'argent(I) et d'or(I) comportant des ligands ditopiques L^{n-R} (L^{n-R} = $RS(CH_2)_nSR$, n = 1-10, R = Ph ou Me) ont été synthétisés. Les topologies de ces composés supramoléculaires ont été déterminées par diffraction des rayons X sur des monocristaux.

Afin de sonder l'effet de la coordinabilité des anions sur les complexes d'argent(I), nous avons utilisé une vaste gamme de sels d'argent(I), AgX où X = BF_4^-, PF_6^-, SbF_6^-, ClO_4^-, NO_3^-, $CF_3SO_3^-$, $CH_3SO_3^-$, *p*-TsO^-, $C_{10}H_7SO_3^-$, $C_6H_5COO^-$, CF_3COO^-, $CF_3CF_2COO^-$, $CF_3CF_2CF_2COO^-$ et $^-OOCCF_2CF_2COO^-$.

La majorité des composés étudiés forment soit des polymères de coordination soit des réseaux à deux dimensions. Les complexes contenant des carboxylates ont des architectures métallosupramoléculaires neutres où des distances Ag-Ag courtes ont été observées. Ces distances, inférieures à la somme des rayons de van der Waals de l'argent, pourraient indiquer la présence de faibles interactions argentophiliques.

Les anions faiblement ou non coordonnants favorisent la formation de réseaux cationiques. Par exemple, la combinaison du bis(méthylthio)méthane avec les sels d'argent AgX (X = PF_6^-, SbF_6^-, BF_4^- et $CF_3SO_3^-$) conduit à des réseaux cationiques à une, deux et trois dimensions. Les propriétés d'échange anionique de plusieurs matériaux ont été suivies par spectroscopie infrarouge, analyse élémentaire et diffraction de rayons X sur poudre. Les anions PF_6^-, SbF_6^- et $CF_3SO_3^-$ peuvent être remplacés par des anions plus petits: ClO_4^-, BF_4^- et NO_3^-.

Les ligands dithiolatés jouent un rôle prédominant dans la majorité des complexes. Ils constituent avec les centres métalliques le réseau de base alors que les anions ne font que compenser les charges ou complètent la sphère de coordination de l'argent. Pour d'autres complexes, les anions participent avec les ligands et les atomes d'argent à l'édification des réseaux. Dans ces cas-ci, il y a coexistence de deux sous-réseaux, $(Ag\text{-ligand})_\infty$ et $(Ag\text{-anion})_\infty$, qui imbriqués l'un dans l'autre partagent leurs atomes d'argent. Une analyse thermogravimétrique a montré que les structures où coexistent les réseaux $(Ag\text{-ligand})_\infty$ et $(Ag\text{-anion})_\infty$ ont la même stabilité thermique que les réseaux métallosupramoléculaires contenant seulement le réseau $(Ag\text{-ligand})_\infty$ et où les anions sont simplement coordonnés au métal.

La combinaison du bis(méthylthio)méthane et le trifluoroacétate ou le pentafluoropropionate d'argent a conduit à la formation d'agrégats $Ag_{12}S_6$ cuboctaèdriques qui, liés les uns aux autres par des ligands, forment des polymères de coordination.

Des complexes d'or(I) ont été synthétisés par autoassemblage des ligands $L^{n\text{-}R}$ et de l'acide tétrachloroaurique(III) trihydraté. Les ligands dithiolatés permettent la réduction de l'or(III) en or(I). Certains complexes sont des composés moléculaires alors que d'autres sont constitués de polymères de coordination par le biais d'interactions aurophiliques. Pour certains de ces polymères, des dimères $(Au\text{-ligand})_2$ sont reliés entre eux grâce à des interactions aurophiliques. Alors que pour d'autres polymères, les interactions aurophiliques coopératives sont responsables de l'existence de chaînes $(Au\text{-}Au\text{-})_\infty$. La luminescence à l'état solide des polymères contenant des chaînes $(Au\text{-}Au\text{-})_\infty$, montrent des progressions vibroniques.

MOTS CLÉS: Chimie supramoléculaire, autoassemblage, polymères de coordination, argent(I), or(I), échange anionique, spectroscopie infrarouge, analyse thermogravimétrique, diffraction des rayons X, interaction argentophilique, interaction aurophilique, luminescence, agrégats.

Summary

Silver(I) and gold(I) coordination polymers with $L^{n\text{-}R}$ ($L^{n\text{-}R}$ = $RS(CH_2)_nSR$ and R = Ph or Me) ditopic ligands were synthesized. The topologies of these supramolecular complexes were determined by single-crystal X-ray diffraction.

To probe the effect of the anion coordination ability upon the silver (I) complexes, we used a large variety of silver (I) salts, AgX, where X = BF_4^-, PF_6^-, SbF_6^-, ClO_4^-, NO_3^-; $CF_3SO_3^-$, $CH_3SO_3^-$, *p*-TsO^-, $C_{10}H_7SO_3^-$, $C_6H_5COO^-$, CF_3COO^-; $CF_3CF_2COO^-$; $CF_3CF_2CF_2COO^-$ and $^-OOCCF_2CF_2COO^-$.

Most of the compounds studied form either 1D-coordination polymers or 2D-networks. Carboxylate-bearing anions form neutral metal supramolecular architectures, in which short Ag – Ag contacts were observed. The distances, shorter than the sum of van der Waals radii of the silver atoms, may indicate the presence of weak argentophilic interactions. Weakly coordinating or noncoordinating anions favored the formation of cationic networks. For instance, the combination of the bis(methylthio)methane with AgX silver salts (where X = PF_6^-, SbF_6^-, BF_4^- and $CF_3SO_3^-$) resulted in the formation of one, two and three dimensional cationic networks. The anion exchange behavior of some of these was monitored by infrared spectroscopy, elemental analysis and X-Ray powder diffraction. The PF_6^-, SbF_6^- and $CF_3SO_3^-$ anions may be replaced by small ones such as ClO_4^-, BF_4^- and NO_3^-.

The dithioether ligands play a dominant role in most complexes. The ligands and the metal centers constitute the basic structure, while the anions only balance the charges or complete the coordination spheres of the silver centers. In other complexes, the anions together with the silver atoms and the ligands are involved in the formation of the network. These complexes may be seen as the juxtaposition of two sub-networks, $(Ag\text{-anion})_\infty$ and $(Ag\text{-ligand})_\infty$ that share their silver atoms.

A thermogravimetric investigation was undertaken to determine if the coexistence of the two sub-networks would increase the thermal stability relative to that of a structure formed exclusively of a $(Ag\text{-ligand})_\infty$ network in which the anions only complete the coordination sphere of the metal center.

The reaction of bis(methylthio)methane and silver (I) trifluoroacetate or penfluoropropionate leads to the formation of $Ag_{12}S_6$ cuboctahedral clusters which, connected by ligand molecules, constitute a coordination polymer.

Gold(I) complexes were synthesized by the self-assembly of $L^{n\text{-}R}$ ligands and gold(III) chloride trihydrate. The dithiolate ligands reduce the Au(III) to Au(I). Depending on the ligand used, molecular compounds or coordination polymers were obtained. In some case, $(Au\text{-ligand})_2$ dimers were linked into 1D-coordination polymers through aurophilic interactions. In other cases, cooperative interactions led to $(Au\text{-}Au\text{-})_\infty$ chains. The solid-state luminescence of the coordination polymers, which contain $(Au\text{-}Au\text{-})_\infty$ chains, show vibronic progressions.

KEYWORDS: Supramolecular chemistry, self-assembly, coordination polymers, silver(I), gold(I), networks, anion exchange, infrared, thermogravimetric analysis, X-ray diffraction, argentophilic interaction, aurophilic interaction, luminescence, cluster.

Table de matières

Liste des Tableaux

Liste des Figures

Liste des abréviations

δ	déplacement chimique
ε	coefficient d'absorption
λ	longueur d'onde
Δ	ν_{asym} (CO_2) - ν_{sym} (CO_2)
asym	*asymmetric*
ATG	analyse thermogravimétrique
Benz	benzyle
br	*broad*
Calcd	calculated
cif	*crystallographic information file*
Cp	cyclopentadiényle
CVD	chemical vapor deposition
d	doublet
dcpm	bis(dicyclohexylphosphine)méthane
deg	degrés
DMSO	dimethylsulfoxyde
2,5-DMP	2,5-dimethylpyrazine
2,6-DMP	2,6-dimethylpyrazine
Et	éthyle
Et_2O	diéthyléther
f	faible
F	fort
F_c	facteur de structure calculé
F_o	facteur de structure observé
FTIR	fourrier transform infrared
g	*gauche*
GCMS	*gaz chromatography mass spectrometry*
HOMO	*highest occupied molecular orbital*
IR	infrarouge
$L^{1\text{-}Ph}$	bis(phénylthio)méthane

$L^{2\text{-Ph}}$	1,2-bis(phénylthio)éthane
$L^{3\text{-Ph}}$	1,3-bis(phénylthio)propane
$L^{4\text{-Ph}}$	1,4-bis(phénylthio)butane
$L^{5\text{Ph}}$	1,5-bis(phénylthio)pentane
$L^{6\text{-Ph}}$	1,6-bis(phénylthio)hexane
$L^{8\text{-Ph}}$	1,8-bis(phénylthio)octane
$L^{10\text{-Ph}}$	1,10-bis(phénylthio)décane
$L^{n\text{-Ph}}$	1,n-bis(phénylthio)alcane
$L^{1\text{-Et}}$	bis(éthylthio)méthane
$L^{1\text{-Benz}}$	bis(benzylthio)méthane
$L^{1\text{-Me}}$	bis(méthylthio)méthane
$L^{1\text{-}t\text{Bu}}$	bis(*tert*-butylthio)méthane
$L^{2\text{-Et}}$	1,2-bis(éthylthio)méthane
$L^{2\text{-tBu}}$	1,2-bis(*tert*-butylthio)éthane
$L^{3\text{-Me}}$	1,3-bis(méthylthio)propane
$L^{3\text{-Et}}$	1,3-bis(éthylthio)propane
$L^{4\text{-}t\text{Bu}}$	1,4-bis(*tert*-butylthio)butane
$L^{6\text{-}t\text{Bu}}$	1,4-bis(*tert*-butylthio)hexane
$L^{4\text{-Benz}}$	1,4-bis(benzylthio)butane
$L^{4\text{-Et}}$	1,4-bis(éthylthio)butane
$L^{n\text{-R}}$	1,n-bis(R-thiol)alcane
LUMO	*lowest unoccupied molecular orbital*
m	*multiplet*
m	medium
Me	méthyle
NMR	*nuclear magnetic resonance*
OETQ	S, S'-bis(8-quinolyl)-4-oxa-1,7-dithiaheptane
PCy_3	tricyclohexylphosphine
Pcp	[2.2]paracyclophane
Ph	phényle
ppm	parties par million
py	pyridine

pz	pyrazine
qt	quintuplet
R	groupement alkyle
RMN	résonance magnétique nucléaire
s	*singulet*
s	strong
sym	*symmetric*
t	*trans*
t	triplet
*t*Bu	*tert*-butyle
THF	tétrahydrofurane
TGA	thermogravimetric analysis
vs	very strong
vw	very weak
XRPD	X-ray powder diffraction
w	weak

Remerciements

Je voudrais exprimer ma profonde reconnaissance à mes co-directeurs de recherche, les professeurs François Brisse et Antonella Badia, pour m'avoir accueilli dans leurs groupes de recherches. J'aimerais vous remercier de votre patience, votre support intellectuel et financier, vos conseils judicieux et de votre disponibilité tout au long de ce projet. Merci à vous deux pour m'avoir permis de participer à des congrès scientifiques tant nationaux qu'internationaux. Je voudrais exprimer toute ma gratitude au professeur François Brisse pour m'avoir accordé beaucoup de temps bien qu'il soit en retraite.

J'aimerais adresser mes sincères remerciements aux professeurs Julian X. Zhu, Frank Schaper et Fernande D. Rochon pour avoir acceptés de juger ce travail en tant que président rapporteur, membre du jury et examinatrice externe, respectivement.

Je voudrais associer à ces remerciements le Professeur Davit Zargarian pour m'avoir prêté une hôte, initialement prévu pour six mois mais qui s'est prolongé en 42 mois ! J'aimerais adresser tous mes remerciements aux étudiants de son groupe, Christine Suis-Seng, Annie Castonguay, Daniel Gareau et Sylvain Boucher pour la complicité et la bonne ambiance au laboratoire.

Je ne saurais comment remercier Dr. Michel Simard, Dr. Francine Belanger et Dr. Thierry Maris pour leurs disponibilités, leurs très grandes compétences. Sans votre patience et enthousiasme, je ne crois pas que je serais arrivé au bout de la résolution de mes structures avec des désordres. Je m'estime très chanceux d'avoir eu le privilège de vous avoir côtoyé. Michel et Francine m'ont profondément marqué de par leur qualité humaine et leur compétence. Ces journées de travail au laboratoire de rayons X de l'Université de Montréal n'auraient jamais été aussi agréables sans votre présence.

Un merci spécial aussi à Huguette Dinel et à certains membres du groupe de recherche de Badia. Premièrement, Patricia Morelle pour tous ses judicieux conseils.
En Lana Norman, j'ai trouvé une personne avec une très grande qualité humaine. Enfin, Jackie Sanchez pour tout son aide. Merci à toi et à Patricia pour m'avoir initié à la microscopie à force atomique et pour tous vos conseils.

Je voudrais témoigner toute ma reconnaissance et ma sympathie à l'ensemble des membres de l'Aile A-6 ainsi qu'aux anciens comme aux nouveaux membres du groupe d'Antonella Badia pour la bonne humeur et la camaraderie. J'ai eu le plaisir d'avoir travaillé dans une atmosphère agréable durant ces quatre années. Ça m'a permis entre autres d'endurer les rudes hivers du Québec.

J'aimerais profiter de cette occasion pour remercier Hoche Yonis Hoche et Abdoul Yonis Hoche pour tous les merveilleux moments passés ensemble. Il m'a fait drôle de découvrir les très grandes qualités humaines de mes cousins au Canada plutôt que chez moi à Djibouti. Nous avons vraiment eu le temps de s'apprécier. Mon cher Hoche, tu possèdes toutes les qualités pour devenir un scientifique accompli. Je n'oublierai jamais nos interminables débats autour d'un bon plat dans les restaurants de Montréal.

J'aimerais remercier aussi des amis très proches. Wais, le sage, l'homme de toutes les situations, je ne saurai oublier ton altruisme et ta propension à trouver des solutions à des situations passablement compliquées et Youssouf Djibril Soubagleh, un merveilleux scientifique aux qualités humaines incroyables. Enfin, Wahib Omar un ancien du Quartier 7, avenue 41, 'Walwalague', et sa merveilleuse famille, des bons plats du pays partagés dans la bonne humeur.

J'aimerais associer à ces remerciements mon père qui a toujours été une source d'inspiration pour moi et ma mère qui m'a beaucoup manqué. De même, j'aimerais témoigner toute mon admiration pour mon oncle maternel Yonis Hoche Dembile pour son amour des études et surtout pour sa droiture. Tu resteras pour moi un modèle. À mon frère Diine, pour m'avoir aidé à monter mon dossier de candidature pour cette bourse. Sans toi, je n'aurais pas pu boucler la boucle!

En terminant, j'aimerais remercier très sincèrement l'Organisation Internationale de la Francophonie (OIF), Le Programme Canadien des Bourses de la Francophonie (PCBF) ainsi que les professeurs François Brisse et Antonella Badia de l'appuie financier pour mener à bien ce projet.

À mes parents

À mon oncle Yonis Hoche Dembile

À mon frère Abdoulkader Osman Awaleh, dit Diine

À mes autres frères et sœurs: Mahdi, Idriss, Hawa, Habone, Farah et Djama

À mes cousins Hoche Yonis Hoche et Abdoul Yonis Hoche

À ma grande famille paternelle et maternelle

À tous ceux qui me sont chères

Chapitre 1. Introduction

1.1 La chimie supramoléculaire

La chimie supramoléculaire est basée sur la reconnaissance moléculaire: des molécules de petites tailles s'autoassemblent spontanément pour former des architectures supramoléculaires.[1-4] Généralement, les interactions utilisées pour induire le processus d'autoassemblage sont les liaisons de coordination métal-ligand, les liaisons hydrogènes, les interactions électrostatiques ou des interactions plus faibles comme les interactions π–π ou de van der Waals entre autres.

L'interaction la plus utilisée en chimie supramoléculaire est la liaison hydrogène. Cette liaison met en jeu principalement un groupement donneur portant l'atome d'hydrogène, **D**-H, et un groupement accepteur, **A** (**D** — H ····· **A**). Généralement, **A** et **D** sont des atomes fortement électronégatifs comme l'oxygène, l'azote ou le fluor. Cette liaison est une interaction électrostatique qui se crée entre le doublet d'électrons libres du groupe **A** et l'atome d'hydrogène qui porte une charge positive partielle due à la polarisation de la liaison **D**-H par le groupe **D,** un atome plus électronégatif que l'hydrogène. Ainsi, la liaison hydrogène peut être générée par exemple à partir de groupes fonctionnels organiques tels que les acides carboxyliques, les amines, les amides, les cétones ou les hydroxyles.

La directionnalité de cette interaction peut être mise à profit afin de synthétiser des molécules sur lesquelles des groupements donneur et accepteur sont liés selon une géométrie bien déterminée, dans le but de générer une supramolécule à structure préprogrammée.[1,2a,5] De ce fait, la synthèse de molécules préprogrammées pour s'autoassembler en une architecture périodique prédéfinie est l'essence même de la chimie supramoléculaire.[1]

Cette stratégie d'autoorganisation préprogrammée s'illustre bien avec le cas très simple de l'acide trimésique (Figure 1.1).[6-8] En effet, chaque molécule d'acide trimésique avec ses trois groupements carboxyliques peut être entourée par trois autres acides, via des liaisons hydrogène entre leurs groupes carboxyliques respectifs. Ainsi, l'acide trimésique forme une architecture bidimensionnelle hexagonale comparable à celle du graphite (Figure 1.1). Cet acide cristallise avec un motif périodique de forme 'nid d'abeille' (Figure 1.1).

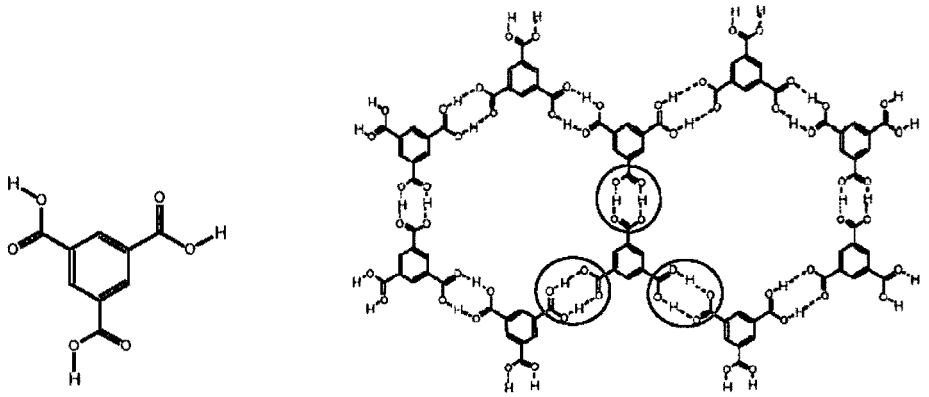

(a) (b)

Figure 1.1. (a) molécule d'acide trimésique; (b) réseau bidimensionnel résultant de l'association par ponts hydrogènes des molécules d'acide trimésique.

Desiraju a conceptualisé l'utilisation des liaisons hydrogènes pour la formation des entités supramoléculaires cristallines.[5] Pour le design de matériaux supramoléculaires à l'aide des liaisons hydrogène, Desiraju préconise de tenir compte de deux notions:
(i) le ''tecton''[9] qui constitue l'entité de base qui se répète.
(ii) le ''synthon supramoléculaire'' est défini par Desiraju comme une unité structurale, existant au sein du composé supramoléculaire, qui assure la propagation du tecton pour générer la supramolécule. Cette unité structurale est formée par le biais d'interactions faibles.[2a,5,9]

Par exemple, dans le cas de l'acide trimésique, le tecton est l'acide lui même (Figure 1.1a). Tandis que le ''synthon supramoléculaire'', entouré en rouge dans la figure 1.1b, est l'unité structurale obtenue par la dimérisation des groupes carboxyliques appartenant à deux acides trimésiques adjacents. Cette unité structurale, le synthon supramoléculaire, permet la propagation du tecton en un réseau bidimensionnel (Figure 1.1b).

Il est possible de concevoir des matériaux supramoléculaires avec une configuration structurale désirée en sélectionnant le bon tecton, l'unité de répétition, et l'emplacement des unités de reconnaissance sur le tecton afin de générer un synthon supramoléculaire approprié pour mener au réseau ciblé.[1,2,5] L'exploitation des concepts de la chimie supramoléculaire dans le but de générer des matériaux avec des architectures contrôlées ouvre la voie à la synthèse de matériaux nouveaux possédant des propriétés qui pourraient être intéressantes.[1,2,5]

Toutefois, il est difficile de contrôler la topologie des matériaux supramoléculaires. Une des raisons de cette difficulté est probablement inhérente aux faibles interactions mises en jeu pour l'élaboration de ces matériaux. Une autre raison pourrait être dans bien des cas l'absence de rigidité du tecton. En effet, comme la reconnaissance moléculaire est principalement basée sur la complémentarité des entités chimiques mises en jeu du point de vue géométrique et énergétique, plus les interactions intermoléculaires seront faibles moins la reconnaissance sera précise, donc la prédictabilité de la topologie de ces composés sera plus difficile à réaliser.

Une alternative à cette problématique pourrait être l'utilisation d'interactions plus fortes pour la formation des unités supramoléculaires. Une très bonne candidate serait la liaison de coordination qui possède une énergie d'environ 200-400 $kJ.mol^{-1}$.[10] Cette interaction est la plus forte de toutes les interactions chimiques exceptée la liaison covalente (tableau 1.1).

Tableau 1.1. Les énergies des principales liaisons chimiques utilisées en chimie supramoléculaire.[10]

Interactions	Énergie ($kJ.mol^{-1}$)
van der Waals	< 5
π···π	0-50
Liaison hydrogène	4-120
Électrostatique	100-350
Coordination	200-400
Covalente	> 400

La liaison de coordination de type σ met en jeu un ligand et un centre métallique. Le ligand est un ion ou une molécule possédant un ou plusieurs doublets d'électrons libres. Un site de coordination ou de complexation pour un ligand donné est une paire d'électron libre portée par un atome de ce ligand. Ainsi, un ligand ditopique est pourvue de deux sites de coordination. Tandis que le centre métallique possède des orbitales vides disposées dans des orientations spécifiques. La liaison de coordination résulte de l'apport d'un doublet d'électron du ligand dans une des orbitales vacantes de l'ion métallique faisant en sorte que ces deux électrons soient partagés par le ligand et le centre métallique.

L'avantage de l'utilisation des liaisons de coordination, par rapport aux interactions intermoléculaires, pour la génération des matériaux supramoléculaires est double :
(i) la liaison de coordination est une interaction forte. Ceci confère aux réseaux supramoléculaires une plus grande stabilité, c'est à dire une plus grande robustesse.
(ii) comme cette liaison est plus forte que les interactions intermoléculaires utilisées le plus souvent en chimie supramoléculaire, on peut espérer une meilleure prévision de la topologie des réseaux métallosupramoléculaires.

Par ailleurs, comme la liaison de coordination est très directionnelle, le nombre de réseaux possibles est réduit. Ceci favorise la prédictabilité de la topologie des réseaux résultants.

D'autre part, les supramolécules possèdent souvent un ordre à longue distance et constituent ainsi des matériaux cristallins. De ce fait, la technique de caractérisation la plus précise des composés supramoléculaires, dans le cas où ils sont cristallins, est la diffraction des rayons X. Un composé est cristallin si l'unité de base qui le caractérise se répète périodiquement dans les trois directions de l'espace. Par contre, un composé est dit amorphe s'il possède seulement un ordre local à très courte distance et aucun ordre à longue distance. La diffraction des rayons X ne permet de déterminer que l'organisation moléculaire des composés cristallins.

Les polymères organiques naturels et synthétiques sont souvent amorphes. Toutefois, les microdomaines cristallins peuvent être orientés à la suite de traitements mécaniques et/ou thermiques. Il est alors possible d'établir la structure du polymère dans ces domaines.[11]

1.2 Polymères de coordination

Les polymères de coordinations sont des composés qui résultent de l'autoassemblage de métaux de transition et de ligands très souvent organiques. La facilité de cet assemblage dépend en grande partie de l'affinité entre les centres métalliques, accepteurs d'électrons, et les sites porteurs de doublets des ligands organiques «constructeurs».

Dans ces matériaux, le métal peut être perçu comme un nœud du réseau alors que le ligand organique est le lien qui interconnecte les nœuds les uns aux autres. Par exemple, le métal peut adopter un ou plusieurs types de coordination (linéaire, triangulaire, tétraédrique ou octaédrique entre autres). D'autre part, les constructeurs organiques doivent posséder au

moins deux sites de coordination de sorte que quand un site est engagé dans une liaison de coordination, l'autre site est en mesure de se connecter à un autre centre métallique et ainsi assurer l'expansion du réseau.

Par conséquent, dépendamment de la coordination du centre métallique, son association avec un ligand ditopique peut générer les réseaux à une, deux ou trois dimensions illustrés schématiquement à la figure 1.2.

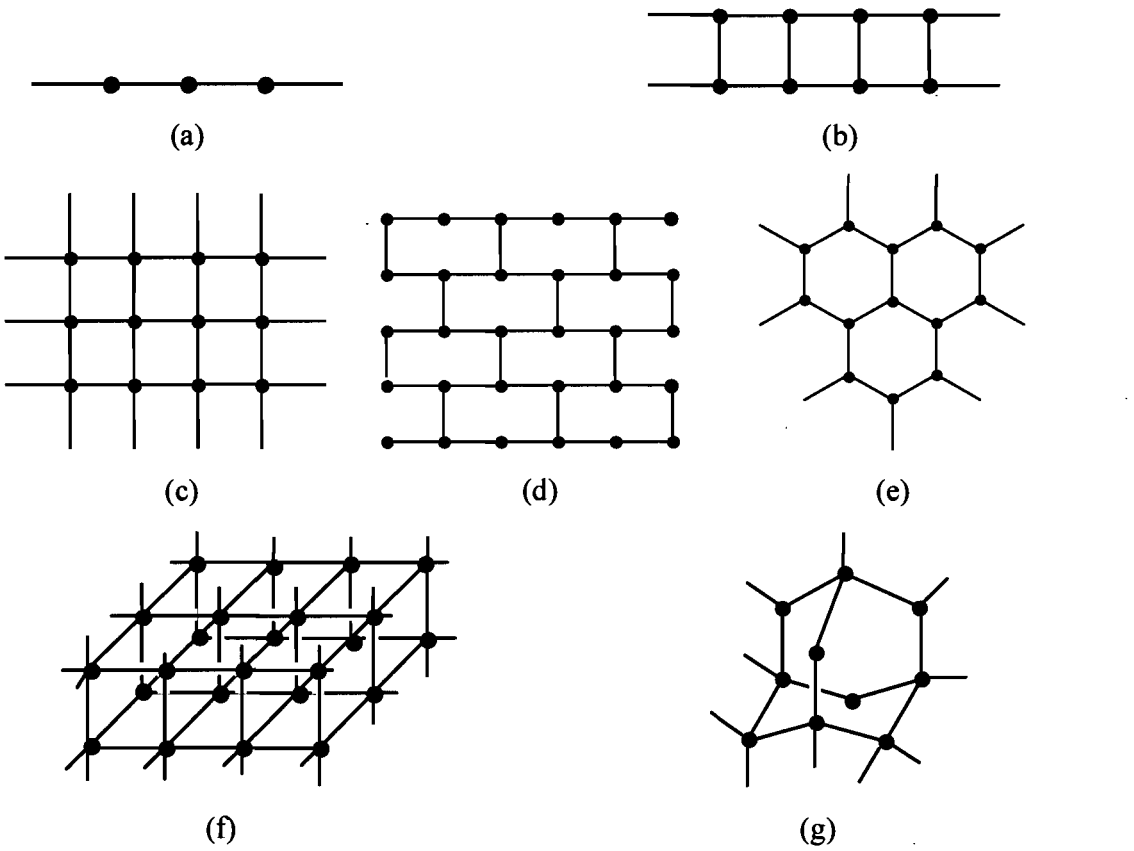

Figure 1.2. Le point noir représente un atome métallique et le bâtonnet reliant deux points voisins est le ligand ditopique. Les réseaux susceptibles de se former par la combinaison d'un métal et d'un ligand ditopique: (a) réseau 1D linéaire, (b) réseau 1D type échelle, (c) réseau 2D carré, (d) réseau 2D brique, (e) réseau 2D hexagonal, (f) réseau 3D octaédrique, (g) réseau 3D diamant. (Adapté de Wells: Structural Inorganic Chemistry).[12]

Contrairement à l'ingénierie cristalline organique,[5,13] nous avons à notre disposition un large éventail de métaux de transition et un choix illimité de ligands pour l'élaboration des polymères de coordination.

Pour notre étude, nous nous sommes intéressés aux réseaux métallosupramoléculaires générés par l'autoassemblage des éléments du groupe 11 du tableau périodique, spécifiquement l'argent(I) et l'or(I), et des ligands flexibles dithiolatés.

1.2.1 Les éléments du groupe 11: Cu, Ag, Au

Ces éléments de transition appartiennent au groupe 11 du tableau périodique et possèdent respectivement les configurations électroniques $[Ar]3d^{10}4s^1$, $[Kr]4d^{10}5s^1$ et $[Xe]4f^{14}5d^{10}6s^1$. Ils constituent un ensemble de métaux précieux, bons conducteurs de la chaleur et de l'électricité, ductile et malléables. Les degrés d'oxydation les plus courants[14] sont donnés ci-dessous:

Cu(I)	Cu(II)	
Ag(I)		
Au(I)		Au(III)

Le cuivre(I) et l'argent(I) possèdent diverses geométries de coordination, allant de la coordination 2 à 6.[14] Les ions cuivre(I) et argent(I) qui ont une configuration d^{10} peuvent adopter une coordination linéaire, triangulaire, tétraédrique, prisme à base triangulaire, pyramide à base carrée ou octaédrique. Alors que l'or(I) adopte généralement la coordination 2 avec une géométrie linéaire.

La richesse de coordination des ions Cu(I) et Ag(I) est mise à profit afin de générer des polymères de coordination en les autoassemblant avec des ligands organiques appropriés. Dans une moindre mesure, les ions Au(I) sont aussi utilisés pour la formation de matériaux hybrides.

La topologie des polymères de coordination est influencée par des paramètres comme la géométrie des ligands, les contre-ions, la stœchiométrie ou le solvant de recristallisation entre autres.[15]

Pour ce qui suit, nous allons nous limiter aux polymères de coordination élaborés avec les éléments du groupe 11 et des ligands ditopiques.

1.2.2 Les polymères de coordination unidimensionnels

Ces polymères peuvent être formés d'une seule chaîne où alternent le métal et le ligand connecteur. Dans ce cas, les chaînes peuvent avoir une géométrie linéaire, en zig-

zag, ondulée ou en hélice.[16-19] D'un autre côté, les polymères peuvent être composés de plusieurs fils[10] et ainsi présenter des géométries dites "échelle"[20] ou "tube".[21]

Quelques chaînes qui se rencontrent dans les polymères de coordination 1D à base d'argent sont illustrés schématiquement à la figure 1.3.

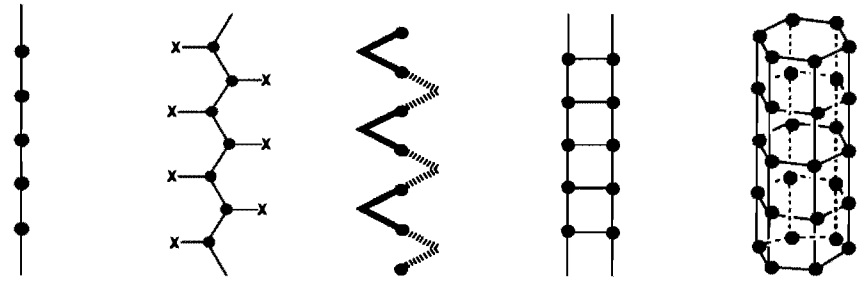

Figure 1.3. Exemples de polymères de coordinations 1D: (a) chaîne linéaire, (b) chaîne en zigzag, (c) chaîne hélicoïdale, (d) chaîne double de forme échelle, (e) tube.

Chaîne linéaire

La chaîne linéaire se rencontre souvent quand des ligands ditopiques rigides joignent les atomes d'argent.[22, 23] En effet, des telles chaînes sont obtenues pour les contre-ions non coordonnants quand la stœchiométrie est 1:1. Dans ces chaînes, le métal adopte la coordination 2 avec une géométrie linéaire. De plus, il faudrait utiliser des solvants de recristallisation non coordonnants afin de permettre à l'argent(I) de garder sa coordination linéaire. Par exemple, l'autoassemblage du 4,4'-bipyridine et du tétrafluoroborate d'argent(I) donne une chaîne linéaire cationique faite de l'alternance du ligand et de l'ion métallique, $[Ag\text{-}(4,4'\text{-bipyridine})]_\infty^+$ (Figure 1.4).[24a]

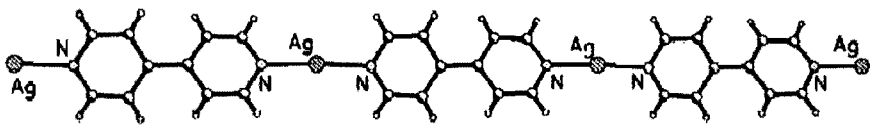

Figure 1.4. La chaîne linéaire dans $\{[Ag(4,4'\text{-bipyridine})]BF_4\}_\infty$. Les anions BF_4^- qui se trouvent à proximité de l'ion argent sans y être coordonnés ont été omis pour plus de clarté.[24a]

Chaîne en zigzag

La chaîne en zigzag se forme en combinant un ligand rigide ditopique avec un ion argent(I) ou cuivre(I) qui est aussi coordonné par une molécule de solvant X. La présence du solvant sur la sphère de coordination de cet ion métallique favorise la formation de la chaîne en zigzag. Ce système est observé en autoassociant le 4,4'-bipyridyl avec $[Cu(MeCN)_4BF_4]$ (Figure 1.5).[24b] Ici, le solvant est coordonné au cuivre (Figure 1.5).[24b]

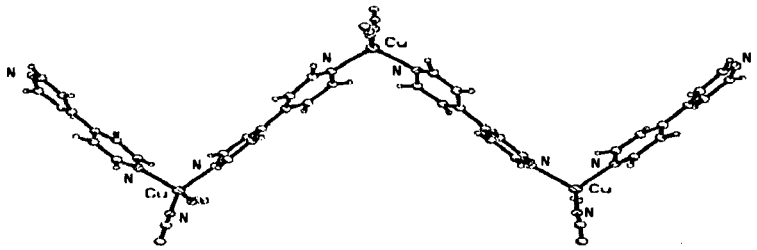

Figure 1.5. La chaîne en zigzag dans $\{[Cu(MeCN)_2(4,4'\text{-bipy})]BF_4\}_\infty$.[24b]

La génération des telles chaînes serait favorisée par l'utilisation de ligands ditopiques rigides, un rapport métal-ligand 1:1, et un anion ou un solvant coordonnant. C'est la présence d'anions ou de molécules de solvant qui se coordonnent au métal, qui force la géométrie zigzag. En d'autres termes, le métal aura une coordination supérieure à deux, par voie de conséquence une géométrie non linéaire. Ainsi, la chaîne résultante ne serait pas linéaire mais aurait plus de chance d'être en zigzag.

Chaîne hélicoïdale

Les polymères de coordination unidimensionnels de forme hélicoïdale sont obtenus en utilisant des ligands ditopiques angulaires avec des sels d'argent d'anions faiblement coordonnants. Par exemple, une hélice a été générée par la réaction du 3,3'-thiobispyridine avec l'hexafluorophosphate d'argent(I) (Figure 1.6).[25] Dans ce polymère de coordination, la charge de l'anion compense celle de l'ion métallique. Une chaîne de même structure est obtenue en combinant la 3,3'-thiobispyridine et le perchlorate d'argent(I). Dans ces chaînes hélicoïdales, l'argent adopte la coordination 2 et l'anion perchlorate se trouve à proximité de l'ion argent sans y être coordonné.

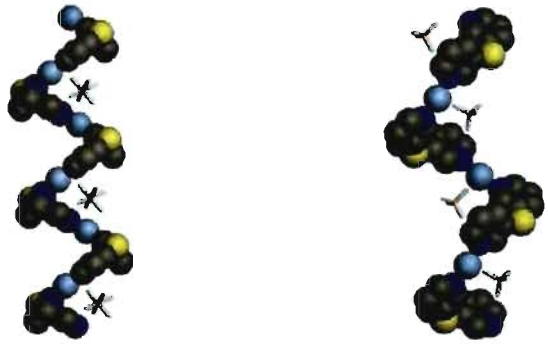

(a) (b)

Figure 1.6. (a) L'hélice $\{[Ag(3,3'\text{-thiobispyridine})]PF_6\}_\infty$. (b) L'hélice $\{[Ag(3,3'\text{-thiobispyridine})]ClO_4\}_\infty$.[25] Les atomes d'hydrogène ont été omis pour plus de clarté. (C: couleur gris; S: jaune; Ag: bleu clair; N: bleu foncé).

Chaîne double ''échelle''

Une chaîne double de type échelle peut être obtenue grâce aux liaisons de coordination des anions qui assurent un pontage métallique entre deux chaînes polymériques contiguës. Bu *et al.* ont rapporté un tel polymère de coordination dans lequel le nitrate relie les ions argent de deux chaînes adjacentes. Ces dernières sont formées par l'alternance de l'ion métallique et le 2,5-bis(4-pyridyl)-1,3,4-thiadiazole (Figure 1.7).[26] Dans ce polymère, l'ion métallique adopte la coordination 3 avec une géométrie triangulaire deformée ou plutôt en forme de T.

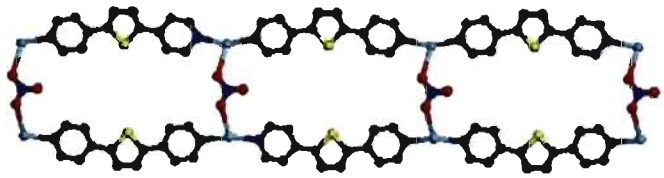

Figure 1.7. Les deux chaînes polymériques sont retenues par des ligands nitrato conduisant à une structure ''échelle''. Les atomes d'hydrogène ont été omis pour plus de clarté.[26] (C: couleur gris; S: jaune; Ag: bleu clair; N: bleu foncé).

Un autre exemple de structure ''échelle'' où deux chaînes sont associées par le biais d'interactions faibles telle que l'interaction intermétallique Ag(I) – Ag(I) est montré à la figure 1.8.[24a] La combinaison du 3,6-bis(pyridin-3-yl)-1,2,4,5-tetrazine avec le triflate d'argent mène à la formation d'une chaîne linéaire cationique composé de l'alternance de

l'ion métallique et du ligand organique. De plus, deux chaînes attenantes sont retenues par de faibles interactions intermétalliques Ag(I) – Ag(I).

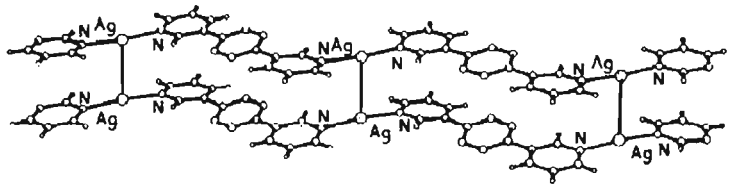

Figure 1.8. La double chaîne de type échelle dans {[Ag(3,6-bis(pyridin-3-yl)-1,2,4,5-tetrazine)]CF_3SO_3}$_\infty$, (Ag···Ag = 3.220 (1) Å).[24a] Les anions triflates qui se trouvent à proximité des ions argent sans y être coordonnés ont été omis pour plus de clarté.

Chaîne double ''tube''

Un autre type de structure rencontré dans les polymères de coordination est l'architecture tubulaire. Ce type de matériau qui est rare dans les polymères de coordination d'argent présente souvent la particularité d'être poreux.[21, 22,27-29] Des polymères d'argent tubulaires topologiquement équivalents sont formés par la combinaison du cis,cis-1,3,5-triaminocyclohexane ou du cis,trans-1,3,5-triaminocyclohexane et le trifluorométhanesulfonate d'argent (Figure 1.9).[21]

(a) (b)

Figure 1.9. (a) Une chaîne de forme tubulaire. (b) Projection le long de l'axe du tube. Les anions, localisés à l'extérieur du tube, et les atomes d'hydrogènes ont été omis pour plus de clarté.[21] (C: couleur gris; Ag: bleu clair; N: bleu foncé).

Nous avons décrit ci-dessus les structures les plus courantes observées pour les polymères de coordination d'argent incorporants des ligands ditopiques. Cependant, cette liste n'est pas exhaustive.[22,30]

1.2.3 Les réseaux de coordination bidimensionnels

Nous avons montré dans la figure 1.2 que les ligands ditopiques peuvent mener à la formation de réseaux bidimensionnels de type carré ou hexagonal entre autres.

Réseau 2D carré

Une structure carrée peut être obtenue en combinant un ligand ditopique et des ions argent en coordination tétraédrique, dans un rapport métal:ligand de 1:2.[22] Par exemple, la réaction du 1,5-pentanedinitrile avec une série de sels d'argent dont les anions sont faiblement ou non coordonnants (ClO_4^-, BF_4^-, PF_6^-, AsF_6^- ou SbF_6^-), conduit à la génération de structures cationiques bidimensionnelles isomorphes de type carré (Figure 1.10).[31] Carlucci *et al.* ont montré que la taille des cavités peut être modulée en faisant varier la longueur du ligand.[31]

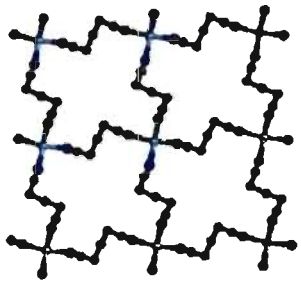

Figure 1.10. Structure bidimensionnelle de type carré, $\{[Ag(1,5\text{-pentanedinitrile})_2](PF_6)\}_\infty$. Les anions localisés entre les feuillets et les atomes d'hydrogène ont été omis pour plus de clarté.[31] (C: couleur gris; Ag: bleu clair; N: bleu foncé).

Réseau 2D hexagonal

L'autoassemblage de ligands ditopiques et des ions argent, adoptant la coordination triangulaire, dans un rapport métal:ligand de 2:3, peut conduire à une structure bidimensionnelle hexagonale du genre nid d'abeille.[22] Cette géométrie est aussi rencontrée lorsque les ions d'argent, qui adoptent la coordination tétraédrique, voient leur quatrième site de coordination bloqué par des anions coordonnants ou des molécules de solvants.[22]

Par exemple Jiang *et al.* ont utilisé cette stratégie pour former une structure hexagonale en faisant réagir du 4,4'-bipyridine avec l'hexafluoroantimonate d'argent(I) (Figure 1.11).[32] Les ions métalliques adoptent la coordination tétraédrique. Une molécule d'acétonitrile et trois molécules de 4,4'-bipyridine entourent chaque atome d'argent (Figure 1.11).[32]

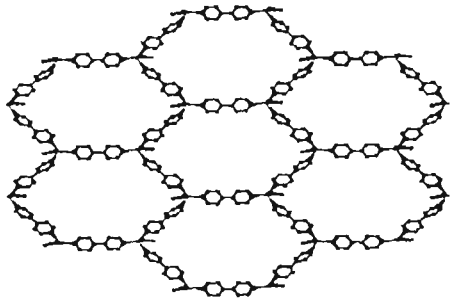

Figure 1.11. Structure bidimensionnelle hexagonale du {[Ag_2(4,4'-bipyridine)$_3$(CH_3CN)$_2$](SbF_6)$_2$}$_\infty$. Les anions, localisés dans les cavités, et les atomes d'hydrogènes ont été omis pour plus de clarté.[32] (C: couleur gris; Ag: bleu clair; N: bleu foncé).

Autres sortes de réseaux 2D

Il faudrait noter que l'autoorganisation spontanée des ions argent(I) et des ligands exhibant deux sites de complexation peut mener à des géométries autres que carrée ou hexagonale. Ces structures pourraient être non seulement de forme oblique, rectangulaire ou losange, mais plus compliquées encore, comme celle qui est reproduite à la figure 1.12.[33]

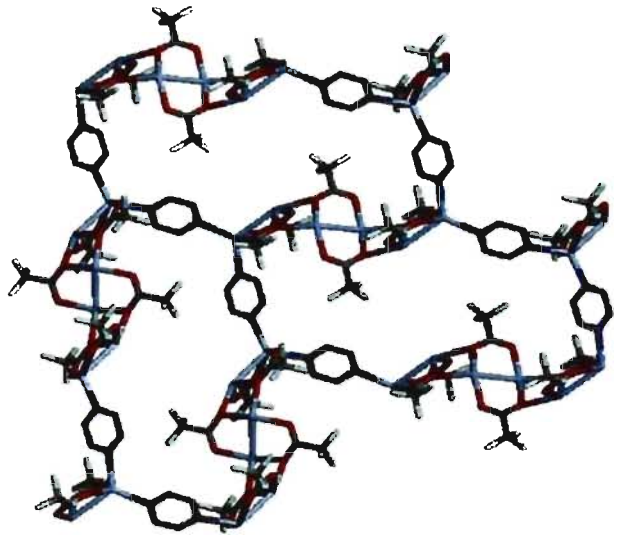

Figure 1.12. Structure bidimensionnelle formée par l'autoassemblage du trifluoroacétate d'argent et le 2-(2',6'-diméthylphenyl)-6-(3'',5''-diméthylphenyl)pyrazine. (C: couleur gris; Ag: bleu clair; N: bleu foncé, pour les groupes de trifluoroacétate l'atome d'oxygène est de couleur rouge).[33]

1.2.4 Les réseaux de coordination tridimensionnels

Réseau 3D diamant

La structure tridimensionnelle de type diamant est la plus courante pour les polymères de coordination de l'argent. Cette organisation est obtenue quand le métal adopte la coordination tétraédrique. Les ligands, avec deux sites de complexation, peuvent joindre les métaux les uns aux autres pour produire un réseau de type diamant (Figure 1.2g).

La réaction du malonitrile et du tétrafluoroborate d'argent(I) génère un réseau type diamant doublement interpénétré (Figure 1.13).[34]

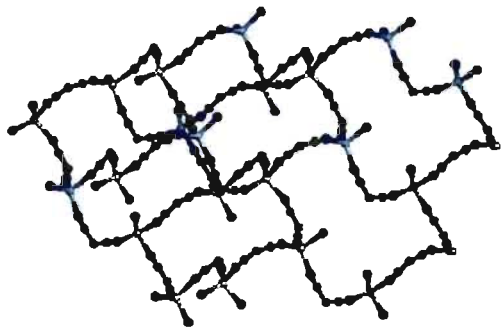

Figure 1.13. Structure de type diamant obtenue par la combinaison du malonitrile et du tétrafluoroborate d'argent(I). Les atomes d'hydrogène et les anions BF_4^- localisés dans les cavités ont été omis pour plus de clarté.[34] (C: gris; N: bleu foncé; Ag: bleu claire).

De telles structures pourraient aussi être obtenues avec des ligands ayant quatre sites de coordination formant entre eux une géométrie tétraédrique et des ions argent en coordination linéaire. Toutefois, ici nous nous sommes limités aux cas des ligands ditopiques.

Réseau 3D octaédrique

Les polymères de coordination d'argent adoptent rarement la structure octaédrique tridimensionnelle.[22] Carlucci *et al.* ont obtenu cette structure en combinant la pyrazine, ligand ditopique très rigide, avec le tétrafluoroborate d'argent(I). Les anions BF_4^-, qui occupent les canaux de section approximativement carrée, sont très désordonnés (Figure 1.14).[35]

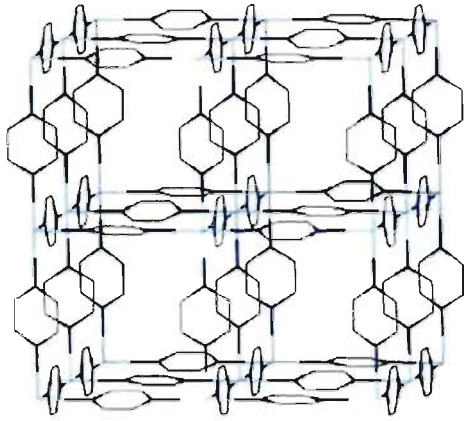

Figure 1.14. Structure tridimensionnelle octaédrique $\{[Ag(pyrazine)_3]BF_4^-\}_\infty$. Les anions tétrafluoroborate et les atomes d'hydrogènes ont été omis pour plus de clarté.[35]

La très grande majorité des polymères de coordination d'argent est construite avec des ligands portants des sites de complexation azotés.[24] Néanmoins, il existe dans une moindre mesure des matériaux hybrides à base d'argent édifiés grâce aux interactions argent-soufre ou avec des ligands dont les sites de coordination sont les atomes d'oxygène, de sélénium, de phosphore, etc.[36]

1.3 Réseaux de coordination basée sur l'interaction argent-soufre

Les ions d'argent, des acides moux, réagissent très facilement avec les composés sulfurés qui sont des bases molles.[37] Pour ce qui suit, nous allons nous limiter aux ligands sulfurés ditopiques. Ces ligands peuvent être classés en deux catégories: (i) les ligands disulfurés rigides et (ii) les ligands disulfurés flexibles.

Ligands rigides

Des exemples de ligands disulfurés rigides sont montrés au schéma 1.1.[38-40] Ces ligands ditopiques rigides génèrent avec les ions argent(I) des réseaux unidimensionnels (1D), bidimensionnels (2D) ou tridimensionnels (3D).

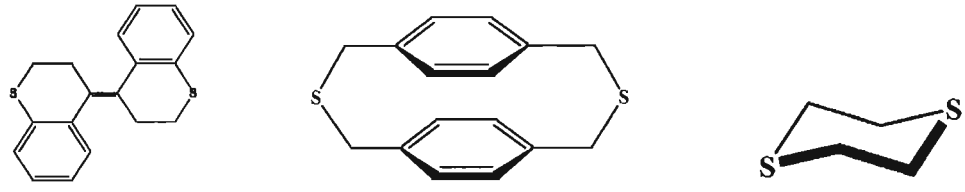

1 **2** **3**

Schéma 1.1. Quelques ligands disulfurés rigides incorporés dans des polymères de coordination d'argent.

Le ligand **1**, 2,2'-3,3'-tétrahydro-4,4'-dithia-1,1'-binaphylidène combiné au perchlorate d'argent ou au triflate d'argent conduit à un réseau unidimensionnel.[38]
D'un autre côté le ligand **2**, 2,11-dithia[3.3]paracyclophane, en forme boîte, a permis l'élaboration de réseaux 1D, 2D voire 3D, quand celui-ci s'autoassocie avec CuBr, CuI, et $AgNO_3$ respectivement.[39]

Des réseaux bidimensionnels hexagonaux sont obtenus avec le 1,4-dithiacyclohexane, **3**, associé au tétrafluoroborate, au triflate ou au nitrate d'argent. Par contre une structure tridimensionnelle de type diamant est obtenue quand le contre-ion est du nitrite d'argent.[40]

Ligands non-rigides

Pour la première fois en 1995, le groupe de Reid a utilisé des ligands dithioéthers constitué d'une chaîne aliphatique flexible entre deux atomes de soufre (schéma 1.2) pour générer des réseaux métallosupramoléculaires.[36a,36b,41] Ainsi, à l'encontre des ligands rigides précédents, ces dithioéthers peuvent adopter différentes conformations. La combinaison du 1,3-bis(phénylthio)propane (schéma 1.2c) avec le tétrafluoroborate d'argent mène à une structure bidimensionnelle. Les anions BF_4^- sont localisés entre les feuillets cationiques contenant les ions d'argent et les ligands.[41] L'autoassemblage de l'homologue à base de sélénium, le 1,3-bis(phénylséléno)propane, avec $AgBF_4$ donne un réseau cationique identique.[36a,41]

Par ailleurs, il a été rapporté que l'autoassemblage du bis(méthylthio)méthane avec $[Cu(MeCN)_4]PF_6$ génère une structure cationique tridimensionnelle où les anions PF_6^- y occupent les canaux.[36b] Par contre, l'homologue sélénié de ce petit ligand, le bis(méthylséléno)méthane, forme une chaîne cationique unidimensionnelle avec le tétrafluoroborate d'argent.[36b]

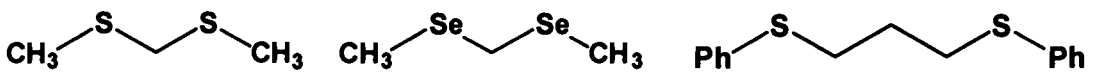

(a) (b) (c)

Schéma 1.2. (a) Bis(méthylthio)méthane; (b) bis(méthylséléno)méthane;
(c) 1,3-bis(phénylthio)propane.

En 2000, Brisse et Bu ont entrepris une étude des paramètres expérimentaux qui peuvent influencer les structures obtenues par l'autoassemblage de ces ligands flexibles et

des ions d'argent(I) ou du cuivre(I).[42] Mon projet de recherche s'inscrit dans cette perspective d'étudier de façon systématique les paramètres pouvant influencer la formation des architectures métallosupramoléculaires à base d'argent(I) et d'or(I). Nous y reviendrons plus en détail dans la section 1.6, où sont décrits les objectifs de cette recherche.

Le terme 'interaction aurophilique' a été employé pour la prémière fois par Schmidbaur.[43a] Cet auteur l'avait utilisé pour décrire l'interaction homophilique entre deux atomes d'or séparés par une distance inférieure à la somme des rayons de van der Waals de l'or (3.32 Å).[43b] Par extension, le terme argentophilique est utilisé dans la littérature pour décrire l'interaction entre deux atomes d'argent séparés par une distance inférieure à la somme des rayons de van der Waals de l'argent (3.44 Å).[43b] Dans cette thèse, les termes argentophilique et aurophilique sont utilisés dans le même sens.

1.4 Polymères de coordination de l'or

Comme l'or appartient au même groupe que l'argent, et qu'ils ont le degré d'oxydation I en commun, il a semblé intéressant d'étudier les structures des complexes d'Au(I) afin de voir s'il y avait un parallèle avec celles des composés d'Ag(I).

En général, l'or adopte le degré d'oxydation I ou III avec les coordinations linéaire et plan carré respectivement.[14] Pour ce qui suit, nous allons nous limiter aux complexes thiolatés d'or(I). Le centre métallique Au(I) est un acide mou et ainsi peut se coordonner très facilement avec les thiols qui sont des bases molles.[37]

Une propriété des ions d'or(I) est leur propension à former des interactions aurophiliques.[43c] Il s'agit d'interactions faibles qui s'établissent entre deux centres Au(I) voisins à une distance approximativement inférieure ou égale à la somme de leurs rayons de van der Waals (3.32 Å).[43b] L'énergie de cette interaction pour deux ions or(I) situés l'un de l'autre d'une distance d'environ 3.05 Å est estimée approximativement à 21-42 kJ. mol^{-1}.[44] C'est pourquoi cette interaction est jugée énergétiquement comparable à la liaison hydrogène.[44]

Le caractère aurophilique des centres métalliques Au(I) est souvent responsable de la formation de polymères de coordination.[45] Individuellement, ces interactions sont faibles. Néanmoins, elles s'additionnent dans les polymères de coordination. C'est cet effet coopératif qui est considéré responsable de la difficulté de dissoudre ces matériaux dans les solvants organiques.[46] Une conséquence directe de ce phénomène est la difficulté de déterminer avec précision la structure de ces complexes à l'état solide ou en solution.

Les polymères de coordination basés sur l'or sont beaucoup moins développés que leurs homologues d'argent ou de cuivre. L'or(I) participe souvent à des structures unidimensionnelles. Les réseaux de coordination d'or(I) possédant une structure bidimensionnelle sont rare.

Chaînes linéaires

Mansour *et al.* ont synthétisé le complexe $[Au(S_2CN(C_5H_{11})_2]_2$ qui a été obtenu sous forme de microcristaux oranges (Figure 1.15). Ce complexe est formé de dimères qui sont retenus par des interactions aurophiliques intermoléculaires pour générer un polymère de coordination unidimensionnel.[47]

Les microcristaux oranges du complexe $[Au(S_2CN(C_5H_{11})_2]_2$ exhibent une très forte luminescence sous irradiation UV. Quand ce composé est exposé plusieurs jours à l'air, il devient incolore et non-émissif. Toutefois, la luminescence se remanifeste quand il est exposé aux vapeurs de solvants aprotiques comme l'acétone, l'acétonitrile, le dichlorométhane ou le chloroforme.[47] Ainsi, ce complexe pourrait être utilisé comme un matériel sensoriel pour la détection des composés organiques volatiles dans l'atmosphère, comme les solvants aprotiques.[47]

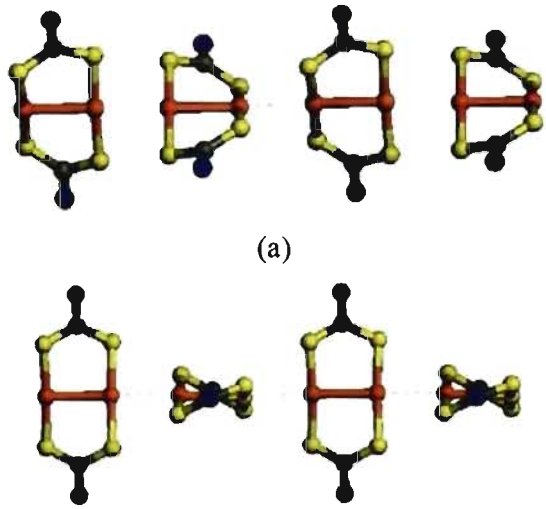

(a)

(b)

Figure 1.15. (a) Chaîne polymérique formée de dimères $[Au(S_2CN(C_5H_{11})_2]_2$ reliés entre eux par des interactions Au – Au. Les distances intermoléculaire et intramoléculaire sont respectivement 3.0241(2) et 2.7653(3) Å. (b) Cette vue montre la perpendicularité des dimères adjacents. Les groupes C_5H_{11} ont été omis afin de ne pas charger la figure. (C: couleur gris; Au: orange; S: jaune; N: bleu).[47]

Généralement, les interactions aurophiliques assurent la formation de structures unidimensionnelles des composés d'or(I). Dans une moindre mesure, il existe des polymères de coordination 1D de l'or(I), où les ligands organiques propagent la sphère de coordination du métal. Ces chaînes sont principalement cationiques et les contre-ions équilibrent uniquement la charge de l'or(I). Par exemple, Puddephatt et ses collaborateurs ont rapporté un polymère de coordination cationique d'or(I) en combinant le trifluoroacétate d'or(I), le trans-1,4-bis(pyridyl)éthylène et le 1,3-diphénylphosphinepropane (Figure 1.16).[30a] Ce matériau hybride, $[\{Ph_2P\text{-}(CH_2)_3PPh_2\text{-}Au\text{-}NC_5H_4CH{=}CHC_5H_4N\text{-}Au\text{-}\}_n]^{2n+}$, forme une chaîne cationique de forme sinusoïdale.

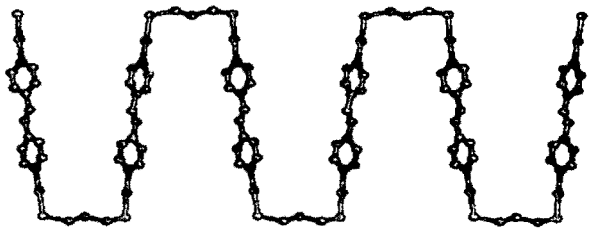

Figure 1.16. $[\{Ph_2P\text{-}(CH_2)_3PPh_2\text{-}Au\text{-}NC_5H_4CH{=}CHC_5H_4N\text{-}Au\text{-}\}_n(CF_3CO_2)_{2n}]$ est constitué d'une chaîne cationique "sinusoïdale". Les phosphines et les atomes d'hydrogène ont été omis afin de ne pas charger la figure. (C: couleur gris; Au: orange; P: violet; N: bleu).[30a]

Réseau à deux dimensions

Puddephatt et Schmidbaur ont beaucoup contribué au développement de la chimie métallosupramoléculaire de l'or.[44,48] Par exemple, Puddephatt *et al.* ont synthétisé un matériau où les phosphines et l'or(I) constituent un squelette bidimensionnel cationique de forme nid d'abeille, $[\{Au_2(\mu\text{-}\ Ph_2P(CH_2)_4PPh_2)_3\}_n][Au(CN)_2]_{2n}.4n(MeOH)$ (Figure 1.17).[49] Les anions $[Au(CN)_2]^-$ et les molécules de méthanol sont localisés dans les cavités de ce réseau (Figure 1.17).[49]

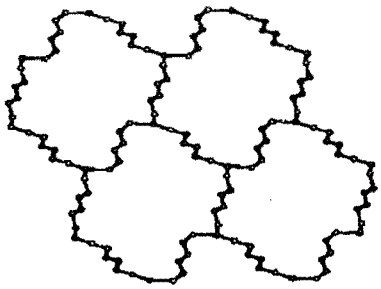

Figure 1.17. Le réseau $[\{Au_2(\mu\text{-}Ph_2P(CH_2)_4PPh_2)_3\}_n][Au(CN)_2]_{2n}.4n(MeOH)$. Les molécules de solvants, les anions $[Au(CN)_2]^-$ ainsi que les atomes d'hydrogène sont omis pour plus de clarté.[49] (C: couleur gris; Au: orange; P: violet).

Les composés thiolatés d'or(I) comme leurs homologues à base de phosphine, présentent des propriétés intéressantes de photoluminescence.[50]

D'un autre côté, les complexes d'or(I) comportant des ligands thiols ont une grande potentialité thérapeutique. Certains de ces complexes comme le myochrysine, le solganol, l'allochrysine ou le ridaura sont utilisés pour traiter l'arthrite rhumatoïde.[46,51] À cause de l'insolubilité de ces matériaux, les structures des médicaments comme le solganol (thioglucose d'or(I)) ou la myochrysine (thiomalate d'or(I) et de sodium) ne sont pas encore connues.[46]

Selon Corbierre et Lennox, il y a encore un débat pour savoir si ces composés forment des macrocycles ou des polymères de coordination,[46] d'où la nécessité de synthétiser des complexes d'or(I) thiolatés qui sont solubles afin d'en faire croître des cristaux possédant une taille convenable pour une analyse cristallographique.

1.5 Applications potentielles des polymères de coordination

Ces matériaux suscitent un certain intérêt de par les propriétés physiques qu'ils possèdent. Ainsi, la force motrice de la recherche sur les polymères de coordination réside principalement dans la compréhension des paramètres qui peuvent influencer leurs formations afin de mieux les exploiter pour générer des matériaux métallosupramoléculaires possédant des architectures désirées, par voie de conséquence des propriétés "voulues".

Échange d'ions

Le groupe de recherche de Rogers a synthétisé un polymère de coordination cationique en associant des ions argent et de la pyrimidine.[52] Le résultat de cette réaction

est une structure en canaux où sont logés les anions nitrates qui compensent les charges du polymère. Ce matériau est utilisé pour échanger les nitrates, NO_3^-, avec des anions radioactifs, comme le pertechnate, TcO_4^-.[52] Ce type de matériaux ouvre des perspectives technologiques importantes pour disposer de certains déchets radioactifs.[53-54]

Stockage de gaz

Dans le contexte du réchauffement planétaire et de la diminution des combustibles fossiles, l'utilisation de source d'énergie propre telle que l'hydrogène est plus que d'actualité. Néanmoins, afin de pouvoir utiliser cette source d'énergie de façon sécuritaire il faudrait parvenir à trouver des matériaux adéquats pour le stockage de l'hydrogène.

L'utilisation des composés métallosupramoléculaires pour le stockage des gaz comme le méthane, le gaz carbonique, l'azote et surtout l'hydrogène se sont révélés prometteurs.[55-57] En effet, Yaghi et ses collaborateurs ont introduit l'utilisation des agrégats métalliques comme nœuds structuraux afin de synthétiser des matériaux hybrides très adaptés au stockage des gaz. En d'autres termes, des agrégats de métaux sont connectés les uns aux autres à l'aide de ligands organiques rigides dans le but de générer des polymères de coordination très robustes avec une très bonne tenue thermique.[56] Certains de ces matériaux ont montré une capacité de stockage du méthane supérieure à celle des zéolites.[2a,57]

Luminescence

L'interaction métal-métal pour l'or(I), et dans une moindre mesure l'argent(I), peut affecter les propriétés de luminescence des complexes de coordination exhibant ces faibles interactions. Flacker a montré l'influence de l'interaction aurophilique sur les propriétés luminescentes des complexes d'or(I) thiolatés à l'état solide.[58] Bien que l'interaction aurophilique soit communément acceptée pour une distance Au(I) – Au(I) inférieure à la somme des rayons de van de Waals de l'or, ce n'est qu'en 2000 qu'a été rapportée la première étude spectroscopique montrant de façon claire la présence de l'interaction argentophilique dans des complexes binucleaires d'argent(I), où les distances Ag(I)-Ag(I) sont 2.936(1) et 2.960(1) Å.[59]

De plus, il a été montré récemment que la présence de l'interaction argentophilique affectait les propriétés de luminescence observées pour des complexes d'argent(I) possédant des distances Ag(I)-Ag(I) courtes (3.110(3) Å).[60]

La finalité de l'ingénierie cristalline demeure le contrôle des architectures supramoléculaires afin de concevoir des matériaux possédant des propriétés spécifiques prédéterminées. En d'autres termes, nous ne pourrons fabriquer de tels matériaux que si nous sommes en mesure d'avoir un vrai contrôle des phénomènes d'autoassociation de ces composés. Par conséquent, il est nécessaire d'étudier les paramètres qui en influencent la formation.

1.6 Objectifs de recherche

Le but de ce projet est d'étudier de façon systématique certains paramètres qui influencent la formation des polymères de coordination obtenus par l'autoassociation d'argent(I) ou d'or(I) et des ligands flexibles dithiolatés. La compréhension de l'influence de ces paramètres sur la topologie des polymères de coordination nous permettrait de mieux les exploiter, afin de générer des matériaux métallosupramoléculaires qui pourraient exhiber des propriétés intéressantes. Les paramètres étudiés pour les polymères de coordination d'argent sont :

(i) l'effet de la longueur, de la flexibilité et de l'encombrement des ligands

(ii) le rôle des anions.

(iii) l'influence des solvants de recristallisation.

(iv) l'effet du rapport métal/ligand

Les ligands choisis pour cette étude sont les dithioéthers $\mathbf{L^{n\text{-}R}}$ (1,n-bis(R-thiol)alcanes). Ces ligands ditopiques linéaires symétriques possèdent une séquence aliphatique de longueur variable intercalée entre les atomes de soufre (Schéma 1.3).

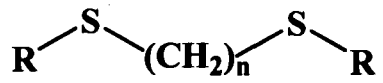

Schéma 1.3. Les ligands connecteurs choisis $\mathbf{L^{n\text{-}R}}$ où **n** est le nombre de groupes méthylène et **R** = Ph, CH_3, sont des substituants plus ou moins encombrants.

Les dithioéthers ont été retenus pour les raisons suivantes :

(i) le thiol, site de complexation de nos ligands, est une basse molle et ainsi présente une très bonne habilité de coordination avec les centres métalliques comme l'argent ou l'or qui sont des acides mous.[37]

(ii) ces ligands dithiolatés ont deux sites de coordination, le nombre minimum requis pour assurer l'expansion des centres métalliques en réseau 1D, 2D ou 3D.

(iii) la variation de la longueur du segment aliphatique (le nombre **n** de groupes méthylènes) entre les atomes de soufre permet d'étudier l'effet de la longueur et de la flexibilité des ligands ditopiques sur la topologie de ces polymères de coordination.
(iv) la taille du groupe **R** lié aux atomes de soufre permet de sonder l'influence de l'encombrement sur les réseaux obtenus.

Bien que la diversité de coordination de l'argent diminue la prédictibilité des topologies des réseaux résultants, ce métal offre l'avantage de donner accès à une large gamme de sels solubles dans les solvants organiques, permettant ainsi l'étude de l'effet des anions sur la formation de ces réseaux.

L'influence des anions sur les architectures supramoléculaires des matériaux hybrides est indéniable.[61] Cependant, il est assez difficile de les classer de façon assez claire. Une classification basée sur la géométrie des anions peut être la suivante:
(i) Anions de forme approximativement sphériques: ClO_4^-, BF_4^-, PF_6^-, SbF_6^-.
(ii) Anions dont le groupe coordonnant est plan: NO_3^-, $C_6H_5COO^-$, CF_3COO^-, $CF_3CF_2COO^-$, $CF_3CF_2CF_2COO^-$ ou $^-OOCCF_2CF_2COO^-$.
(iii) Anions dont le groupe coordonnant est tétraédrique: $CF_3SO_3^-$, $CH_3SO_3^-$, $C_{10}H_7SO_3^-$ ou *p*-TsO^-.

Une autre classification peut être basée sur la possibilité de coordination de ces anions. En générale, tous les anions peuvent exhiber une monocoordination. D'un autre côté, les anions BF_4^-, PF_6^- ou SbF_6^-, réputés non coordonnants, montrent rarement une coordination supérieure à 1. Toutefois, les autres anions peuvent présenter diverses possibilités de coordination (ClO_4^-, NO_3^-, $CF_3SO_3^-$, $CH_3SO_3^-$, $C_{10}H_7SO_3^-$, *p*-TsO^-, $C_6H_5COO^-$, CF_3COO^-, $CF_3CF_2COO^-$, $CF_3CF_2CF_2COO^-$ et $^-OOCCF_2CF_2COO^-$).

Jung et al.[25] ont proposé la classification suivante, basée sur la force de coordination des contre-ions pour des polymères de coordination d'argent:

$$NO_3^- > CF_3CO_2^- > CF_3SO_3^- > PF_6^- > ClO_4^- > BF_4^-$$

Cette difficulté de classification des anions, nous a amené à étudier de façon systématique l'effet de ces derniers sur les structures des matériaux hybrides à base d'argent(I) en faisant varier les anions pour un ligand dithiolaté donné. Les anions choisis pour cette étude sont les suivants: ClO_4^-, BF_4^-, PF_6^-, SbF_6^-, NO_3^-, $CF_3SO_3^-$, $CH_3SO_3^-$, $C_{10}H_7SO_3^-$, *p*-TsO^-, $C_6H_5COO^-$, CF_3COO^-, $CF_3CF_2COO^-$, $CF_3CF_2CF_2COO^-$ et $^-OOCCF_2CF_2COO^-$.

Nous avons aussi utilisé ces mêmes ligands pour les autoassembler avec l'or(I) afin de synthétiser des matériaux hybrides étendus à l'état solide qui sont susceptibles de présenter des propriétés de photoluminescence.

La principale technique de caractérisation utilisée au cours de ce travail est la diffraction des rayons X sur monocristal. Les composés synthétisés sont aussi caractérisés par analyse élémentaire, par spectroscopie RMN en solution et par spectroscopie IR à l'état solide. L'analyse thermogravimétrique (ATG) est mise à profit pour sonder la stabilité thermique de certains composés. La diffraction des rayons X sur poudre est utilisée afin d'identifier les résidus des analyses thermogravimétriques, et dans certains cas, pour suivre la stabilité des réseaux cristallins lors des échanges anioniques. Les spectroscopies UV-visible et de luminescence sont utilisées pour les complexes d'or.

1.7 Description des travaux

Le chapitre 1 de cette thèse consiste en une introduction bibliographique sur les réseaux de coordination d'argent(I) et d'or(I) élaborés avec des ligands ditopiques, tout en soulignant certaines propriétés intéressantes rapportées pour ces types de matériaux hybrides. Ce chapitre est plus particulièrement consacré aux topologies des polymères de coordination d'argent ainsi qu'aux réseaux métallosupramoléculaires basés sur l'interaction Ag-S et Au-S avec des ligands dithiolatés et donne une description des objectifs de cette recherche.

Nous avons présenté la suite des chapitres **2-5** sous forme schématique afin de ressortir les liens entre ces chapitres (schéma 1.4).

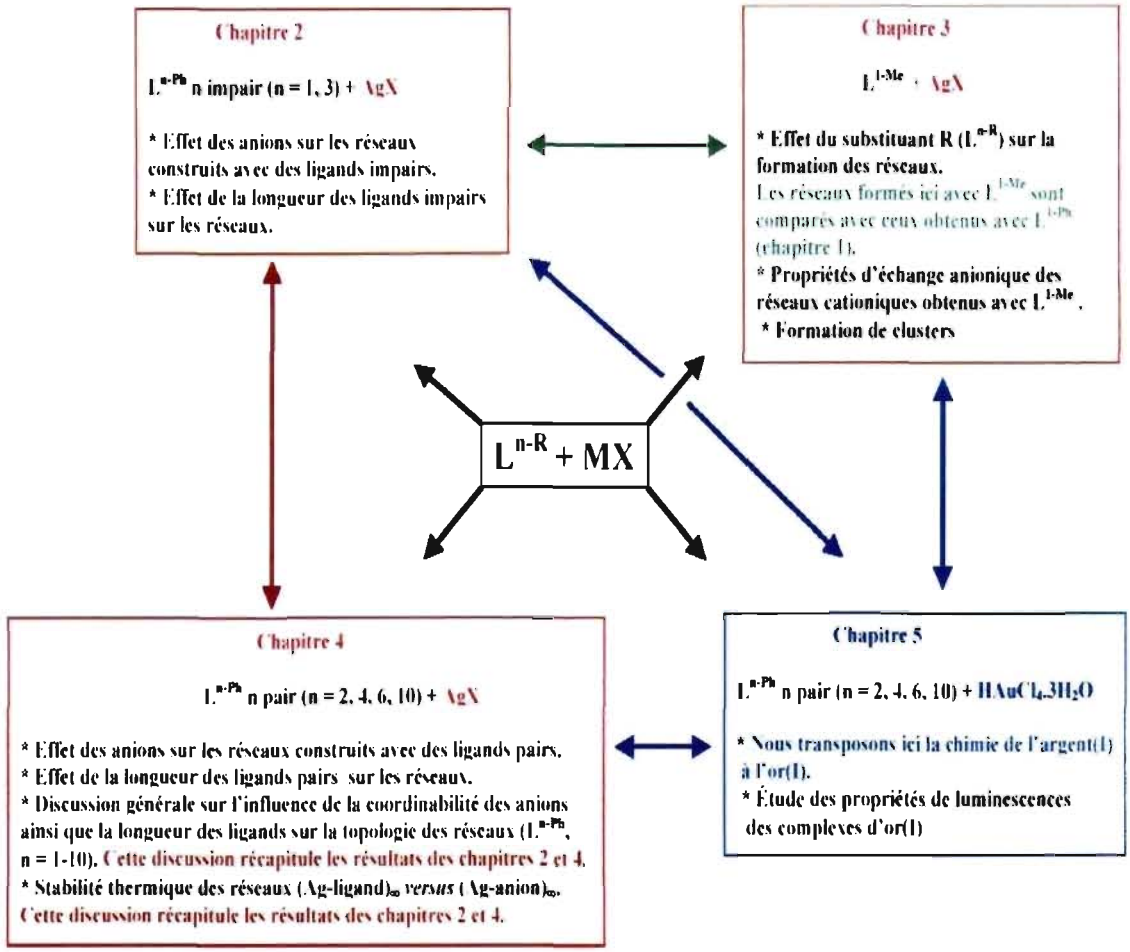

M = Argent(I) ou Or(I)
X = ClO_4^-, BF_4^-, PF_6^-, SbF_6^-, NO_3^-, $CF_3SO_3^-$, $CH_3SO_3^-$, $C_{10}H_7SO_3^-$, *p*-TsO^-, $C_6H_5COO^-$, CF_3COO^-, $CF_3CF_2COO^-$, $CF_3CF_2CF_2COO^-$ et $^-OOCCF_2CF_2COO^-$.

Schéma 1.4. Lien entre les chapitres **2**, **3**, **4** et **5**. **M** représente le métal d^{10} (Ag(I) ou Au(I)). **X** représente les anions des sels d'argent (ClO_4^-, BF_4^-, PF_6^-, SbF_6^-, NO_3^-, $CF_3SO_3^-$, $CH_3SO_3^-$, $C_{10}H_7SO_3^-$, *p*-TsO^-, $C_6H_5COO^-$, CF_3COO^-, $CF_3CF_2COO^-$, $CF_3CF_2CF_2COO^-$ et $^-OOCCF_2CF_2COO^-$). (Les ligands L^{n-R} sont représentés dans le schéma 1.3).

Dans le **chapitre 2**, nous rapportons les réseaux formés par l'autoassemblage du **bis(phénylthio)méthane** et du **1,3-bis(phénylthio)propane** avec des sels d'argent(I). Les contre-ions utilisés sont ClO_4^-; BF_4^-, PF_6^-, SbF_6^-, $CF_3SO_3^-$, *p*-TsO^-, $CF_3CO_2^-$, $CF_3CF_2COO^-$, $CF_3CF_2CF_2COO^-$ et $^-OOCCF_2CF_2COO^-$. Dans le cas du petit ligand, **bis(phénylthio)méthane**, des chaînes polymériques de type $[Ag\text{-ligand-}]_\infty$ sont formées dont les anions ClO_4^-, BF_4^-, $CF_3SO_3^-$ et $CF_3CO_2^-$ complètent la sphère de coordination du métal. De plus, des chaînes voisines sont retenues par des faibles interactions de van der Waals pour former des réseaux bidimensionnels. Les contre-ions $CF_3CF_2CF_2COO^-$ et

$^{-}OOCCF_2CF_2COO^{-}$ ont permis de générer des réseaux unidimensionnels de forme ''échelle''. Dans ces deux structures, des distances Ag-Ag courtes ont été observées.

Avec le **1,3-bis(phénylthio)propane**, les anions faiblement coordonnants ou non coordonnants, comme ClO_4^-, PF_6^- ou SbF_6^-, favorisent la formation des architectures lamellaires cationiques entre lesquels ces anions, souvent accompagnés de solvants, sont localisés. Les anions très coordonnants portant un groupe carboxylique (CF_3COO^-, $CF_3CF_2COO^-$ et $CF_3CF_2CF_2COO^-$) engendrent des réseaux unidimensionnels ou bidimensionnels dont ils font parties. De plus, ces réseaux montrent des faibles interactions métal-métal. Une analyse thermogravimétrique a été entreprise afin de sonder la stabilité des architectures supramoléculaires. L'isomérie supramoléculaire a été mise en évidence pour les complexes du **bis(phénylthio)méthane** et du **1,3-bis(phénylthio)propane.**

Le chapitre 3 de cette thèse traite de la synthèse et de la caractérisation de polymères de coordination obtenus par l'autoorganisation du **bis(méthylthio)méthane** et des sels d'argent. Ce petit ligand, peu flexible et moins encombré, est un candidat idéal pour faire une étude systématique de l'influence des anions sur la formation des réseaux métallosupramoléculaires. Les anions utilisés sont: BF_4^-, PF_6^-, SbF_6^-, ClO_4^-; NO_3^-; $CF_3SO_3^-$, *p*-TsO^-, CF_3COO^-, $C_6H_5COO^-$, $CF_3CF_2CF_2COO^-$ et $HOOCCF_2CF_2COO^-$.
En plus de la méthode de synthèse standard d'autoassemblage direct, nous avons utilisé une procédure de synthèse basée sur l'échange anionique. L'étude des propriétés d'échange anionique de certains de ces matériaux hybrides est rapportée. D'autre part , le trifluoroacétate ou le pentafluoropropionate d'argent ont conduit à la formation d'agrégats $Ag_{12}S_6$ cuboctaédriques qui, liés les uns aux autres par les bis(méthylthio)méthanes, forment des polymères de coordination.

Dans le **chapitre 4**, nous rapportons d'une part l'effet des anions sur la formation des réseaux basés sur l'autoassemblage des ions d'argent et des ligands constructeurs de séquence aliphatique paire, **$PhS(CH_2)_nSPh$** (**n** = 2, 4, 6, 10). Les anions utilisés pour ces ligands sont ClO_4^-, NO_3^-, $CF_3SO_3^-$, CF_3COO^-, $CF_3CF_2COO^-$ et $CF_3CF_2CF_2COO^-$.
Nous comparons ici les réseaux où ces ligands dithiolatés jouent un rôle prédominant dans lesquels les anions compensent seulement la charge des ions métalliques ou complètent la sphère de coordination de l'argent relativement à ceux dont les anions participent avec les ligands à l'édification des réseaux. D'autre part, nous avons utilisé un mélange de solvants de recristallisation (avec une variation du rapport de solvant polaire/solvant apolaire) dans le but de sonder l'effet des solvants sur l'isomérie supramoléculaire observée pour des

matériaux hybrides précédents. Un nouvel isomère supramoléculaire a été isolé. Il est caractérisé par la coexistence de deux réseaux bidimensionnels, imbriqués l'un dans l'autre, $(Ag\text{-ligand})_\infty$ et $(Ag\text{-anion})_\infty$ respectivement. Une analyse thermogravimétrique a été réalisée afin de comparer la stabilité thermique des structures où coexistent les réseaux $(Ag\text{-ligand})_\infty$ et $(Ag\text{-anion})_\infty$ aux réseaux métallosupramoléculaires analogues définis par la présence du seul réseau $(Ag\text{-ligand})_\infty$ et où les anions sont simplement coordonnés au métal.

Le chapitre 5 traite de la synthèse et de la caractérisation des complexes d'or(I) obtenus par l'autoassociation de ligands dithiolatés avec $HAuCl_4.3H_2O$. Les ligands utilisés sont $\mathbf{RS(CH_2)_nSR}$ où **R** = Ph, CH_3 et **n** = 1-4. Ces ligands dithiolatés permettent la réduction de l'or(III) en or(I). Certains complexes forment des composés moléculaires alors que d'autres sont obtenus sous forme de polymères de coordination. Ces derniers sont générés par le biais d'interactions aurophiliques. Pour certains de ces polymères, des dimères $[Au\text{-ligand}]_2$ sont reliés entre eux grâce aux interactions aurophiliques. Alors que pour d'autres polymères, les interactions aurophiliques sont coopératives dans le sens que des chaînes $[Au\text{-}Au]_\infty$ sont présentes. La luminescence à l'état solide des polymères de coordination, caractérisés par la présence des chaînes $[Au\text{-}Au]_\infty$, est rapportée.

Dans le **chapitre 6**, nous discutons de l'influence de certains paramètres sur la topologie des architectures supramoléculaires obtenus avec les ligands $\mathbf{L^{n\text{-}R}}$, $RS(CH_2)_nSR$, et les sels d'argent. Ces paramètres sont l'encombrement du substituant **R**, la longueur du ligand, la nature de l'anion et les rapports métal-ligand des produits de départs. Les interactions métal-métal, ainsi que la spectroscopie infrarouge des complexes formés avec des anions incorporant des groupes carboxylates sont aussi discutées. Enfin, nous parlerons des propriétés d'anions echange et de luminescence exhibées par ces polymères de coordination.

Le chapitre 7 est une conclusion récapitulant l'ensemble des travaux ainsi que quelques perspectives.

Le lecteur qui aimerait avoir une aperçu plus génèrale du contenu des articles pourrait commencer par la lecture du **chapitre 6** où les contenus de ces articles sont discutés d'un point de vue plus génèrale.

1.9 Références

(1) (a) Lehn, J. M. *La chimie supramoléculaire-concepts et perspectives,* De Boeck Université, 1997. (b) Lehn, J.-M. *Supramolecular Chemistry: Concepts and Perspectives;* V. C. H.: Weinheim, 1995.

(2) (a) Brammer, L. *Chem. Soc. Rev.* **2004**, *33*, 476. et références citées. (b) Moulton, B, ; Zaworotko, M. J. *Chem. Rev.* **2001**, *101*, 1629.

(3) http://www.fas.umontreal.ca/CHIMIE/diapos/BIOORG/sld017.htm.

(4) Behr, J. P. *Perspectives in Supramolecular Chemistry, Vol 1. The Lock-and-Key Principle. The State of the Art 1000 Years on.* **1994**, Wiley, Chichester.

(5) Desiraju, G. R. *Crystal Engineering: The Design of Organic Solids,* Elsevier, Amsterdam, 1989.

(6) Duchamp, D. J.; Marsh, R. E. *Acta Crystallogr.* **1969**, *B25*, 5.

(7) Herbstein, F. H.; Kapon, M.; Reisner, G. M. *J. Inclusion Phenom.* **1987**, *5*, 211.

(8) Herbstein, F. H. *Top. Curr. Chem.* **1987**, *140*, 107.

(9) Simard, M.; Su, D.; Wuest, J. D. *J. Am. Chem. Soc.* **1991**, *113*, 4696.

(10) (a) Steed, W. J. ; Atwood, J. L. *Supramolecular Chemistry,* John Wiley and Sons; Chichester, West Sussex, 2000, p19. (b) Pocic, D. *Thèse de doctorat*, **2005**, Université de Strasbourg.

(11) (a) Atfani, M ; Brisse, F. *Macromolecules.* **1999**, *32*, 7741. (b) Wang, S. ; Brisse, F. *Macromolecules.* **1998**, *31*, 2265. (c) Jourdan, N. ; Deguire, S. ; Brisse, F. *Macromolecules.* **1995**, *28*, 8086. (d) Li, X. ; Brisse, F. *Macromolecules.* **1994**, *27*, 2276. (e) Li, X. ; Brisse, F. *Macromolecules.* **1994**, *27*, 7718. (f) Chenite, A ; Brisse, F. *Macromolecules.* **1993**, *26*, 3055. (g) Chenite, A ; Brisse, F. *Macromolecules.* **1992**, *25*, 776.

(12) Wells, A. F. *Structural Inorganic Chemistry,* 3rd ed.; Oxford, 1962.

(13) (a) Schmidt, G. M. J. *Pure Appl. Chem.* **1971**, *27*, 647. (b) Bragga, D. *J. Chem. Soc., Chem. Comm.* **2003**, 2751.

(14) Cotton, F. A.; Wilkinson, G. *Advanced Inorganic Chemistry.* 5rd ed.; John Wiley and Sons, 1988.

(15) (a) Withersby, M. A.; Blake, A. J.; Champness, N. R.; Cooke, P. A.; Hubberstey, P.; Li, W. S.; Schröder, M. *Inorg. Chem.* **1999**, *38*, 2259. (b) Blake, A. J.; Champness, N. R.; Cooke, P. A.; Nicolson, J. E. B.; Wilson, C. *J. Chem. Soc., Dalton Trans.* **2000**, 3811. (c) Noro, S.; Kitaura, R.; Kondo, M.; Kitagawa, S.; Ishii, T.; Matsuzaka, H.; Yamashita, M. *J. Am. Chem. Soc.* **2002**, *124*, 2568. (e) Chatterton, N. P.; Goodgame, D. M. L.; Grachvogel, D. A.; Hussain, I.; White, A. J. P.; Williams, D. J. *Inorg. Chem.* **2001**, *40*, 312.

(16) Lu, J.; Yu, C.; Niu, T.; Paliwala, T.; Crisci, G.; Somosa, F. Jacobson, A. J. *Inorg. Chem.* **1998**, *37*, 4637.

(17) Batsanov, A. S.; Begley, M. J.; Hubberstey, P.; Stroud, J. *J. Chem. Soc., Dalton Trans.* **1996**, 1947.

(18) Beswick, M. A.; Lopez-Casideo, C.; Paver, M. A.; Raithby, P. R.; Russell, C. A.; Steiner, A.; Wright, D. S. *J. Chem. Soc., Chem. Comm.* **1997**, 109.

(19) Mamula, O.; Zelewsky, A. V.; Bark, T.; Bernardinelli, G. *Angew. Chem. Int. Ed.* **1999**, *38*, 2945.

(20) Munakata, M.; Wu, L. P.; Ning, G. L.; Kuroda-Sowa, T.; Maekawa, M.; Suenaga, Y.; Maeno, N. *J. Am. Chem. Soc.* **1999**, *121*, 4968.

(21) Pickering, A. L.; Seeber, G.; Long, D. L.; Cronin, L. *J. Chem. Soc., Chem. Comm.* **2004**, 136.

(22) Chen, C. L.; Kang, B. S.; Su, C. Y. *Aust. J. Chem.* **2006**, *59*, 3.

(23) Patra, G. K.; Goldberg, I. *Cryst. Growth Des.* **2003**, *3*, 321.

(24) (a) Blake, A. J.; Champness, N. R.; Hubberstey, P.; Li, W. S.; Withersby, M. A.; Schröder, M. *Coord. Chem. Rev.* **1999**, *183*, 117. (b) Batsanov, A. S.; Begley, M. J.; Hubberstey, P.; Stroud, J. *J. Chem. Soc., Dalton Trans.* **1996**, 1947.

(25) Jung, O. K.; Kin, Y. J.; Lee, Y. A.; Chae, H. K.; Jang, H. G.; Hong, J. *Inorg. Chem.* **2001**, *40*, 2105.

(26) Huang, Z.; Du, M.; Song, H. B.; Bu, X. H. *Cryst. Growth Des.* **2004**, *4*, 71.

(27) Pickering, A. L.; Cooper, G. J. T.; Long, D. L.; Cronin, L. *Polyhedron* **2004**, 136.

(28) Dong, Y. B.; Zhao, X.; Tang, B.; Wang, H. Y.; Huang, R. Q.; Smith, M. D.; Zur Loye, H. C. *J. Chem. Soc., Chem. Comm.* **2004**, 220.

(29) Fan, J.; Zhu, H. F.; Okamura, T. A.; Sun, W. Y.; Tang, W. X.; Ueyama, N. *Inorg. Chem.* **2003**, *42*, 158.

(30) (a) Irwin, M. J.; Vittal, J. J.; Yap, G. P. A.; Puddephatt, R. J. *J. Am. Chem. Soc.* **1996**, *118*, 13101. (b) Xie, Y. B.; Zhang, C.; Li, J. R.; Bu, X. H. *J. Chem. Soc., Dalton Trans.* **2004**, 562. (c) Pickering, A. L.; Long, D. L.; Cronin, L. *Inorg. Chem.* **2004**, *43*, 4953.

(31) Carlucci, C.; Ciani, G.; Proserpio, D. M.; Rizzato, S. *CrystEngComm.* **2002**, *4*, 413.

(32) Jiang, J. J.; Li, X. P.; Zhang, X. L.; Kang, B. S.; Su, C. Y. *CrystEngComm.* **2005**, *7*, 603.

(33) Schultheiss, N.; Powell, D. R.; Bosh, E. *Inorg. Chem.* **2003**, *42*, 5304.

(34) Westcoot, A.; Whitford, N.; Hardie, M. J. *Inorg. Chem.* **2004**, *43*, 3663.

(35) Carlucci, L.; Ciani, G.; Proserpio, D. M. ; Sironi, A. *Angew. Chem. Int. Ed.* **1995**, *34*, 1895.

(36) (a) Black, J. R.; Champness, N. R.; Levason, W.; Reid, G. *J. Chem. Soc., Dalton Trans.* **1995**, 3439. (b) Black, J. R.; Champness, N. R.; Levason, W.; Reid, G. *Inorg. Chem.* **1996**, *35*, 4432. (c) Brandys, M. C.; Puddephatt, R. J. *J. Am. Chem. Soc.* **2002**, *124*, 3946.

(37) (a) Pearson, R. G. *J. Am. Chem. Soc.* **1963**, *85*, 3533. (b) Pearson, R. G. *J. Chem. Educ.* **1968**, *45*, 581. (c) Pearson, R. G. *J. Chem. Educ.* **1968**, *45*, 643.

(38) Wen, M.; Munakata, M.; Suenaga, Y.; Kuroda-Sowa, T.; Maekawa, M.; Yan, S. G. *Inorg. Chim. Acta* **2001**, *322*, 133.

(39) Munakata, M.; Wu, L. P.; Kuroda-Sowa, T.; Maekawa, M.; Suenaga, Y.; Nakagawa, S. *J. Chem. Soc., Dalton Trans.* **1996**, 1525.

(40) Brooks, N. R.; Blake, A. J.; Champness, N. R.; Cunningham, J. W.; Hubberstey, P.; Teat, S. J.; Wilson, C.; Schröder, M. *J. Chem. Soc., Dalton Trans.* **2001**, 2530.

(41) Black, J. R.; Champness, N. R.; Levason, W.; Reid, G. *J. Chem. Soc., Chem. Comm.* **1995**, 1277.

(42) (a) Bu, X. H.; Chen, W.; Hou, W. F.; Du, M.; Zhang, R. H.; Brisse, F. *Inorg. Chem.* **2002**, *41*, 3477. (b) Bu, X. H.; Chen, W.; Lu, S. L.; Zhang, R. H.; Liao, D. Z.; Bu, W. M.; Shionoya, M.; Brisse, F.; Ribas, J. *Angew. Chem. Int. Ed.* **2001**, *40*, 3201.

(43) (a) Scherbaum, F.; Grohmann, A.; Huber, B.; Krüger, C.; Schmidbaur, H. *Angew. Chem.* **1988**, *100*, 1602; *Angew. Chem. Int. Ed.* **1988**, *27*, 1544. (b) Porterfield, W. W. *Inorganic Chemistry: A Unified Approach*, Addison-Wesley; Reading, MA, 1994, pp.168, 180. (c) Pyykkö, P. *Chem. Rev.* **1997**, *97*, 597. Et références citées.

(44) Schmidbaur, H. *Chem. Soc. Rev.* **1995**, *24*, 391.

(45) (a) Hunks, W. J.; Jennings, M. C.; Puddephatt, R. J. *J. Chem. Soc., Chem. Comm.* **2002**, 1834. (b) Simeling, U.; Rother, D.; Bruhn, C.; Fink, H.; Weidner, T.; Träger, F.; Rothenberger, A.; Fenske, D.; Priebe, A.; Maurer, J.; Winter, R. *J. Am. Chem. Soc.* **2005**, *127*, 1102. (c) Sladek, A.; Schmidbaur, H. *Inorg. Chem.* **1996**, *35*, 3268. (d) Ehlich, H.; Shier, A.; Schmidbaur, H. *Inorg. Chem.* **2002**, *41*, 3721.

(46) Corbierre, M. K.; Lennox, R. B. *Chem. Mater.* **2005**, *17*, 5691 et références citées.

(47) Mansour, M. A.; Connick, W. B.; Lachicotte, R. J.; Gysling, H. J.; Eisenberg, R. *J. Am. Chem. Soc.* **1998**, *120*, 1329.

(48) (a) Tzeng, B. C.; Schier, A.; Schmidbaur, H. *Inorg. Chem.* **1999**, *38*, 3978. (b) Hollatz, C.; Schier, A.; Schimidbaur, H. *J. Am. Chem. Soc.* **1997**, *119*, 8115. (c) Puddephatt, R. J. *Coord. Chem. Rev.* **2001**, *216-217*, 313 et références citées.

(49) Brandys, M. C. ; Puddephatt, R. J. *J. Am. Chem. Soc.* **2001**, *123*, 4839.

(50) (a) Mohamed, A. A.; Kani, I.; Ramirez, A. O.; Flacker, J. P., Jr. *Inorg. Chem.* **2004**, *43*, 3833. (b) Coker, N. L.; Bauer, J. A. K.; Elder, R. C. *J. Am. Chem. Soc.* **2004**, *126*, 12. (c) Lee, Y. A.; Eisenberg, R. *J. Am. Chem. Soc.* **2003**. *125*, 7778. (d) Tzeng, B. C.; Liu, W. H.; Liao, J. H.; Lee, G. H.; Peng, S. M. *Cryst. Growth Des.* **2004**, *4*, 573. (e) Tzeng, B. C.; Huang, Y. C.; Wu, W. M.; Lee, S. Y.; Lee, G. H.; Peng, S. M. *Cryst. Growth Des.* **2004**, *4*, 63.

(51) (a) Brow, D. H.; Smith, W. E. *Chem. Soc. Rev.* **1979**, *9*, 217. (b) Elder, R. C.; Eidness, M. K. *Chem. Rev.* **1987**, *87*, 1027.

(52) Sharma, C. V. K.; Griffin. S. T.; Rogers, R. D. *J. Chem. Soc., Chem. Comm.* **1998**, 215.

(53) Rogers, R. D.; Zhang, J.; Griffin, S. T. *Sep. Sci. Technol.* **1997**, *32*, 699.

(54) Rogers, R. D. ; Bond, A. H.; Zhang, J.; Bauer, C. B. *Appl. Radiat. Isot.* **1996**, *47*, 497.

(55) (a) Rosi, N. L.; Eckert, J. ; Eddaoudi, M.; Vodak, D. T.; Kim, J.; O'Keeffe, M.; Yaghi, O. M. *Science* **2003**, *300*, 1127. (b) Wong-Foy, A. G.; Matzger, A. J.; Yaghi, O. M. *J. Am. Chem. Soc.* **2006**, *128*, 3494. (c) Millward, A. R.; Yaghi, O. M. *J. Am. Chem. Soc.* **2005**, *127*, 17998. (d) Rowsell, J. L. C.; Eckert, J.; Yaghi, O. M. *J. Am. Chem. Soc.* **2005**, *127*, 14904. (e) Rowsell, J. L. C.; Spencer, E. C.; Eckert, J.; Howard, J. A. K.; Yaghi, O. M. *Science* **2005**, *309*, 1350. (f) Rowsell, J. L. C.; Yaghi, O. M. *Ang. Chem. Int. Ed.* **2005**, *44*, 4670.

(56) (a) Chae, H. K.; Siberio-Pérez, D. Y. ; Kim, J. ; Go, Y. B.; Eddaoudi, M.; Matzger, A.

J.; O'Keeffe, M.; Yaghi, O. M. *Nature* **2004**, *427*, 523. (b) Eddaoudi, M.; Moler, D. B.; Li, H.; Chen, B. ; Reineke, T. M. ; O'Keeffe, M, Yaghi, O. M. *Acc. Chem. Res.* **2001**, *34*, 319. (c) Rosi, N. L. ; Eddaoudi, M. ; Kim, J. ; O'Keeffe, M.; Yaghi, O. M. *CrystEngComm*, **2002**, *4*, 401.

(57) Eddaoudi, M.; Kim, J.; Rosi, N.; Vodak, D.; Wachter, J. ; O'Keeffe, M.; Yaghi, O. M. *Science* **2002**, *295*, 469.

(58) (a) Zyl, W. E. V.; López,-de-Luzuriaga, J. M.; Mohamed, A.; Staples, R. J.; Facker, J. P. Jr. *Inorg. Chem.* **2002**, *41*, 4579. (b) King, C.; Wang, J. C.; Khan, M. N. I.; Fackler, J. P., Jr. *Inorg. Chem.* **1989**, *28*, 2145.

(59) Che, C. M. ; Tse, M. C. ; Chan, M. C. W. ; Cheung, K. K. ; Phillips, D. L.; Leung, K. K. *J. Am. Chem. Soc.* **2000**, *122*, 2464.

(60) Omary, M. A. and Patterson, H. H. *Inorg. Chem.* **1998**, *37*, 1060.

(61) (a) Withersby, M. A.; Blake, A. J.; Champness, N. R.; Hubberstey, P.; Li, W. S.; Schröder, M. *Angew. Chem. Int. Ed.* **1997**, *36*, 2327. (b) Chatterton, N. P.; Goodgame, D. M. L.; Grachvogel, D. A.; Hussain, I.; White, A. J. P.; Williams, D. J. *Inorg. Chem.* **2001**, *40*, 312.

Chapitre 2. Architectures métallosupramoléculaires élaborées avec deux ligands ayant un nombre impair de groupe méthylènes.

2.1 Silver coordination polymers with flexible ligands. Syntheses, crystal structures, and effect of the counteranion and the solvent on the structure of complexes $[AgL^{1\text{-}Ph}X]_\infty$ of the bis(phenylthio)methane ligand $L^{1\text{-}Ph}$ with silver(I) salts, X = ClO_4^-, BF_4^-, CF_3COO^-, $CF_3SO_3^-$, $CF_3CF_2CF_2COO^-$ and $^-OOCCF_2CF_2COO^-$.[†]

2.1.1 Abstract

Number of complexes were synthesized to rationalize the structures of Ag(I) complexes with a small flexible bidentate ligand, bis(phenylthio)methane, when the anion is varied. We compared two similar "spherical" anions, ClO_4^- (**1**) and BF_4^- (**2**), as well as two slightly "elongated" ones, CF_3COO^- (**3**) and $CF_3SO_3^-$ (**4, 5**). Complexes with a longer anion, $CF_3CF_2CF_2COO^-$ (**6**), and a diacid, $^-OOCCF_2CF_2COO^-$ (**7**), were also investigated. All the compounds studied form a 1D-coordination polymer. The coordination polymers of **1-4** are of the type [Ag–ligand–]$_\infty$ and adopt two distinct conformations: *gauche-trans-gauche* for **1**, **2** and **4**, and *gauche-gauche-gauche* for **3**. The anions in **1-4** are coordinated to the silver atoms through a single O or F atom. All these 1D-chains are associated through weak van der Waals interactions into 2D-layer structures. Solvent-induced supramolecular isomerism was observed with the $CF_3SO_3^-$ anion. With diethyl ether, the 1D-coordination polymer of **4** was observed, as indicated above, while a two-stranded chain comprising a 16-membered macrocyclic structure, $Ag_4(L^{1\text{-}Ph})_4$, was noted when petroleum ether was used, **5**. The macrocycles are connected through a small cyclic $(CF_3SO_3\cdots Ag\cdots)_2$ dimeric unit. Another type of double-stranded ladder-like structure was noted for **6**. Each of the two heptafluorobutyrate anions is coordinated through its oxygen atoms to two distinct silver atoms to form a dimeric unit. This, in turn, is connected to another unit through two Ag-S coordination bonds. The repeat unit of this coordination polymer is based on a 10-membered $Ag_4(L^{1\text{-}Ph})_2$ macrocycle. In compound **7**, with the tetrafluorosuccinate anion, one observes another type of 1D-polymer best described as a [Ag_2–tetrafuorosuccinate–]$_\infty$ chain reinforced by Ag–ligand–Ag bonds. Most complexes

[†] Awaleh, M. O.; Badia, A.; Brisse, F. *Cryst. Growth Des.* **2005**, *5*, 1897.

containing fluorine atoms have C(H)···F or C(H_2)···F short contacts (2.998 – 3.203 Å) that correlate with an FTIR absorption band around 521 cm^{-1}. Relatively short Ag···Ag interactions are found in both **6** and **7**.

2.1.2 Introduction

One of the interesting aspects of metal-organic polymer coordination is the design of predictable networks with useful catalytic and electronic properties[1]. However, in metal-organic crystal engineering, when flexible ligands are involved in supramolecular networks, the prediction of the topology of the polymer coordination is more difficult, since there are several factors affecting the framework formation, such as the kind of solvent, the counter-anion, and the metal-to-ligand ratio[2]. Nevertheless, to predict a given type of network structure it is necessary to obtain a more representative sampling, especially when dealing with flexible ligands. To this end, the bis(phenylthio)methane spacer is a simple bidentate organic building block that has the advantage of being flexible and at the same time not overly long. In this context, bis(phenylthio)methane is an interesting candidate to attempt to rationalize the topology of a network of metal-organic polymer coordination with flexible ligands. Furthermore, the shortness of the aliphatic chain separating the two thiophenyl groups may be helpful, since the conformational degrees of freedom of this ligand are limited. In addition, the ability of the sulfur atom to bind to the silver atom is well-exploited in this study. In fact, the sulfur atom, being a soft base, is able to coordinate well with the silver atom, which is a soft acid. Therefore, the two dithiol sites can coordinate to metal centers to build up a linear coordination polymer. Bu *et al.* have reported two unusual frameworks for this simple ligand: a 3D-network with the perchlorate anion and a 1D-chain with the nitrate anion.[3] We are extending our previous work[4] by exploring the role of the shape and the length of the spacer upon the topology of the networks. Furthermore, we consider the supramolecular isomerism observed for silver complexes formed with this kind of bifunctional ligand since such behavior was observed in the case of the 1,3-bis(phenylthio)propane ligand.[4c] Recent studies have shown that several factors influence the isomerism of supramolecular structures, such as the presence of a guest molecule[5] or a variation in the metal-to-ligand ratio,[6] among others. In our work,[4c] however, the supramolecular isomerism is associated with the type of solvent used during recrystallization. In an attempt to rationalize the effect of the counteranion upon the topology of the network, we report here the synthesis and the characterization of a number

of silver(I) coordination polymers obtained with the same bis(phenylthio)methane spacer, $\mathbf{L}^{\mathbf{1\text{-}Ph}}$ (Figure 2.1.1), but with different counteranions. Complexes of the following anions were investigated: ClO_4^- (**1**), BF_4^- (**2**), CF_3COO^- (**3**) $CF_3SO_3^-$ (**4**, **5**), $CF_3CF_2CF_2COO^-$ (**6**), and $^-OOCCF_2CF_2COO^-$ (**7**).

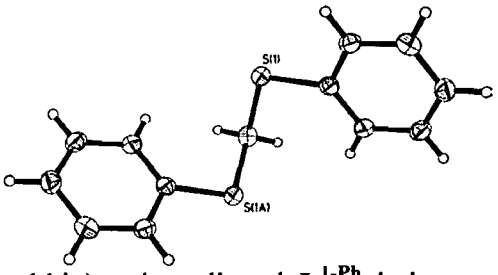

Figure 2.1.1. The bis(phenylthio)methane ligand, $\mathbf{L}^{\mathbf{1\text{-}Ph}}$, in its extended conformation.

2.1.3 Experimental section.

Materials and General Methods. Except for the ligand, the reagents required for the syntheses were commercially available and employed without further purification. The elemental analyses were performed by the Laboratoire d'analyse élémentaire (Université de Montréal), and the IR spectra were recorded on a Perkin-Elmer 1750 FTIR (4000-450 cm^{-1}) with samples prepared as KBr pellets. The ^1H (400 MHz), $^{13}C\{^1H\}$(100.56 MHz) and ^{19}F (376.31 MHz) solution NMR spectra were recorded at 25 °C on Bruker ARX400, AMX300, and AV300 spectrometers. ^1H and ^{13}C chemical shifts are reported in parts per million and are referenced to residual solvent signals of deuterated acetone (δ_{1H} = 2.05; δ_{13C} = 29.8). The ^{19}F spectra were referenced to $C_6H_5CF_3$ (-63.9ppm).

Caution! Although we encountered no problems in handling perchlorate salts, these should be handled with great care due to their potentially explosive nature.

Syntheses. The bis(phenylthio)methane ligand, $\mathbf{L}^{\mathbf{1\text{-}Ph}}$, was synthesized following a published report.[13] Yield 85%. Anal. Found: C, 67.03; H, 5.07. Calcd for $C_{13}H_{12}S_2$: C, 67.20; H, 5.21. The ligand was recrystallized by diffusion of diethyl ether into the solution and gave needlelike crystals suitable for X-ray analysis after one week.

^1H NMR (acetone-d_6, 400 MHz): δ 4.55 (*s*, 2H, -S-(CH_2)-S-), 7.23-7.46 (*m*, 10H, C_6H_5-).

$^{13}C\{^1H\}$ NMR (acetone-d_6, 100.56 MHz): δ 37.4 (S-**C**-S), 124.6-133.1 (C_6H_5).

IR (KBr, cm^{-1}): 3084w, 3072w, 3056w, 2968w, 1934w, 1844w, 1785w, 1713w, 1623w, 1581s, 1478s, 1435s, 1390m, 1327w, 1300w, 1271w, 1190m, 1150w, 1133w, 1085m, 1071m, 1023m, 997w, 883m, 836w, 814m, 732s, 686s, 596w, 472s.

$[AgL^{1\text{-}Ph}(ClO_4)]_\infty$ (1). A solution of $AgClO_4.H_2O$ (237 mg, 1.06 mmol) in acetone (5 mL) was slowly added to a solution of $L^{1\text{-}Ph}$ (241 mg, 1 mmol) in chloroform (5 mL). The mixture was kept under reflux at 50 °C for 30 min, and the filtrate was slowly layered on diethyl ether in the dark to obtain large needle-shaped pale yellow single crystals suitable for X-ray analysis. Yield: 30% based on $AgClO_4.H_2O$. Anal. Found: C, 35.32; H, 3.06. Calcd for $C_{13}H_{12}S_2AgClO_4$: C, 35.51; H, 2.75. ^{1}H NMR (acetone-d_6, 400 MHz): δ 4.74 (*s*, 2H, -S-(CH_2)-S-), 7.36-7.51 (*m*, 10H, C_6H_5-). IR (KBr, cm^{-1}): 3548m, 3056w, 2816w, 2364w, 1796w, 1737w, 1638m, 1582m, 1508w, 1479m, 1438m, 1389m, 1328w, 1301w, 1194w, 1178w, 1143vs, 1114vs, 1088vs, 1024m, 1000w, 940w, 884w, 828w, 815w, 735s, 687s, 636s, 627s, 473m.

$[AgL^{1\text{-}Ph}(BF_4)]_\infty$ (2). $AgBF_4$ (406 mg, 2.08 mmol) in acetone (5 mL) was mixed with a solution of $L^{1\text{-}Ph}$ (239 mg, 1.03 mmol) in chloroform (5 mL). The mixture was refluxed at 70 °C for 40 min. The filtrate was recrystallized in the dark by diffusion of petroleum ether into the solution. A few days later, single crystals suitable for X-ray analysis were deposited. Yield: 40% based on $AgBF_4$. Anal. Found: C, 37.44; H, 2.79. Calcd for $C_{13}H_{12}S_2AgBF_4$: C, 37.51; H, 2.91. ^{1}H NMR (acetone-d_6, 400 MHz): δ 4.65 (*s*, 2H, -S-(CH_2)-S-), 7.21-7.41 (*m*, 10H, C_6H_5-). ^{19}F NMR (acetone-d_6, 376.31 MHz): δ -148.7. IR (KBr, cm^{-1}): 3217m, 3054w, 2963w, 2262w, 1935w, 1845w, 1786w, 1713w, 1641w, 1581m, 1571w, 1478s, 1435s, 1390m, 1327w, 1301w, 1262w, 1193s, 1133m, 1086s, 1070b, 1024s, 884m, 836w, 815m, 732s, 685s, 612w, 546w, 521m, 473s.

$[AgL^{1\text{-}Ph}(CF_3CO_2)]_\infty$ (3). A mixture of $AgCF_3CO_2$ (304 mg, 1.38 mmol) in acetone (5 mL) was stirred in the dark with a solution of $L^{1\text{-}Ph}$ (341 mg, 1.47 mmol) in chloroform (5 mL) at 50 °C for. The mixture was kept under reflux at 50 °C for 160 min. When the filtrate was layered on hexane, single crystals suitable for X-ray analysis were obtained after one week. Yield: 40% based on $AgCF_3SO_3$. Anal. Found: C, 39.77; H, 2.67. Calcd for $C_{15}H_{12}S_2AgF_3O_2$: C, 39.75; H, 2.67. ^{1}H NMR (acetone-d_6, 400 MHz): δ 4.68 (*s*, 2H, -S-(CH_2)-S-), 7.34-7.56 (*m*, 10H, C_6H_5-). ^{19}F NMR (acetone-d_6, 376.31 MHz): δ -74.3.
IR (KBr, cm^{-1}): 3432m, 3055w, 1934w, 1845w, 1690vs, 1581m, 1478s, 1436s, 1390m, 1327w, 1300w, 1222vs, 1193vs, 1134vs, 1086w, 1071w, 1024m, 998w, 884w, 840s, 806s, 727vs, 686vs, 598w, 516w, 473m.

$[AgL^{1\text{-}Ph}(CF_3SO_3)]_\infty$ (4). To a solution of $AgCF_3SO_3$ (472 mg, 1.837 mmol) in acetone (5 mL) was added a mixture of $L^{1\text{-}Ph}$ (374 mg, 1.61 mmol) in chloroform (5 mL). The mixture

was stirred at 50 °C for 90 min in the dark. The resulting solution was layered on diethyl ether and, after 1 week, crystals suitable for X-ray analysis could be harvested. Yield: 50% based on $AgCF_3SO_3$. Anal. Found: C, 34.14; H, 2.17. Calcd for $C_{14}H_{12}S_3AgF_3O_3$: C, 34.37; H, 2.47. ^{1}H NMR (acetone-d_6, 400 MHz): δ 4.65 (*s*, 2H, -S-(CH_2)-S-), 7.22-7.40 (*m*, 10H, C_6H_5-). ^{19}F NMR (acetone-d_6, 376.31 MHz): δ -79.4.

IR (KBr, cm^{-1}): 3480w, 3057m, 1934w, 1845w, 1716w, 1581s, 1572m, 1479s, 1436s, 1390s, 1258(br), 1179vs, 1086m, 1072w, 1032vs, 884m, 836w, 815m, 769m, 732vs, 685vs, 641vs, 581m, 518m, 473m.

$[Ag_2(L^{1\text{-}Ph})_2(CF_3SO_3)_2]_\infty$ (5). This complex was obtained from the same solution as complex **4**, the only difference being the solvent: petroleum ether was used instead of diethyl ether. Yield: 40% based on $AgCF_3SO_3$. Anal. Found: C, 34.14; H, 2.17. Calcd for $C_{28}H_{24}S_6Ag_2F_6O_6$: C, 34.37; H, 2.47. ^{1}H NMR (acetone-d_6, 400 MHz): δ 4.57 (*s*, 2H, -S-(CH_2)-S-), 7.24-7.47 (*m*, 10H, C_6H_5-). ^{19}F NMR (acetone-d_6, 376.31 MHz): δ -79.4.

IR (KBr, cm^{-1}): 3421m, 3055m, 2925w, 1934w, 1713w, 1581s, 1572m, 1479s, 1437s, 1390s, 1254(br), 1180vs, 1086m, 1071w, 1027vs, 884m, 815m, 769m, 734vs, 687vs, 643vs, 580m, 518m, 473m.

$[AgL^{1\text{-}Ph}(CF_3CF_2CF_2CO_2)]_\infty$ (6). A solution of $L^{1\text{-}Ph}$ (254 mg, 1.09 mmol) in diethyl ether (5 mL) was added to a solution of $AgCF_3CF_2CF_2CO_2$ (177 mg, 0.32 mmol) in acetone (5 mL). The mixture was refluxed at 60 °C for 135 min. After evaporation of the solvent (in the dark, at room temperature), single crystals suitable for X-ray analysis were obtained. Yield: 25% based on $AgCF_3CF_2CF_2CO_2$. Anal. Found: C, 37.1; H, 2.07. Calcd for $C_{17}H_{12}S_2AgF_7O_2$: C, 36.90; H, 2.19. ^{1}H NMR (acetone-d_6, 400 MHz): δ 4.70 (*s*, 2H, -S-(CH_2)-S-), 7.34-7.59 (*m*, 10H, C_6H_5-). ^{19}F NMR (acetone-d_6, 376.31 MHz): δ -81.9 (CF_3-), -118.8 ($CF_3CF_2CF_2$-), -127.6 ($CF_3CF_2CF_2$-). IR (KBr, cm^{-1}): 3469m, 3055w, 1934w, 1682vs, 1581s, 1571m, 1478s, 1435m, 1403w,1390s, 1340s, 1274w , 1220vs, 1192w, 1157w, 1117w, 1084s, 1024s, 937s, 935m, 884w, 815s, 733s, 686s, 650w, 586w, 527w, 474m.

$[Ag_2(L^{1\text{-}Ph})_2(CO_2CF_2CF_2CO_2)]_\infty$ (7). Tetrafluorosuccinic acid (245 mg, 1.3 mmol) was added to 156 mg (0.56 mmol) of silver carbonate in 5 mL of acetone. A solution of $L^{1\text{-}Ph}$ (270 mg, 1.16 mmol) in chloroform (5 mL) was added to the vigorously stirred mixture. Then the mixture was kept under reflux at 70 °C for 120 min. The resulting solution was filtered and left to stand. Single crystals suitable for X-ray analysis were found after 1 hour.

Yield: 75% based on $HOOC(CF_2)_2COOH$. Anal. Found: C, 41.49; H, 2.79. Calcd for $C_{30}H_{24}Ag_2F_4O_4S_4$: C, 41.40; H, 2.71. ^1H NMR (acetone-d_6, 400 MHz): δ 4.70 (*s*, 2H, -S-(CH_2)-S-), 7.31-7.55 (*m*, 10H, C_6H_5-). ^{19}F NMR (acetone-d_6, 376.31 MHz): δ -117.7 (CF_2). IR (KBr, cm^{-1}): 3437m, 3057w, 1935w, 1683vs, 1583s, 1480m, 1438m, 1407w, 1391w, 1261w, 1195w, 1164w, 1150w, 1105w, 1087w, 1025m, 985w, 1024s, 822w, 735s, 687s, 632w, 556w, 532vw, 474w.

Crystal Structure Determinations. X-ray diffracted intensities were recorded on a Brucker AXS Platform diffractometer equipped with a SMART 2K CCD area detector using monochromatic Cu Kα (λ = 1.54178 Å). Crystal data for compounds **4** and **5** were collected on a Nonius CAD-4 diffractometer[7] by the ω scan method using the Cu Kα graphite-monochromatized radiation. The program SAINT[8] was used for the data reduction process. An empirical absorption correction, based on the multiple measurements of equivalent reflections, was applied using the program SADABS.[9] The space group was confirmed by the XPREP[10] routine within the SHELXTL program.[11] The structures were solved by direct methods and refined by full-matrix least-squares and difference Fourier techniques with SHELXL-97.[12] All non-hydrogen atoms were refined anisotropically, while the isotropic hydrogen atoms were introduced at calculated positions using a riding model. The structure refinements proceeded smoothly, except for **3**, where the trifluoro group was found to take three different orientations in the ratio 57/23/20. The C-F distances in the trifluoroacetate anion were constrained to be equal (SADI[11]), while the thermal parameters were constrained such that they kept the same values in each orientation (EADP[11]). In complex **5**, the trifluoro groups were found to be disordered over two orientations in a 56/44 proportion. Crystal data and data collection parameters are listed in Table 2.1.1.

Table 2.1.1. Crystal data for the ligand $L^{1\text{-Ph}}$ and its complexes with silver(I) salts AgX (X = BF_4^- (**1**), ClO_4^- (**2**), CF_3COO^- (**3**), $CF_3SO_3^-$ (**4**, **5**), $CF_3CF_2CF_2COO^-$ (**6**) and $^-OOCCF_2CF_2COO^-$ (**7**)).

	$L^{1\text{-Ph}}$	**1**	**2**	**3**
formula	$C_{13}H_{12}S_2$	$C_{13}H_{12}AgClO_4S_2$	$C_{13}H_{12}AgBF_4S_2$	$C_{15}H_{12}AgF_3O_2S_2$
mol wt	232.35	439.67	427.03	453.24
crystal size (mm)	0.28×0.07×0.06	0.64×0.14×0.08	0.27×0.14×0.07	0.38×0.22×0.05
crystal system	orthorhombic	monoclinic	monoclinic	monoclinic
space group	$P2_12_12_1$	$P2_1/n$	$P2_1/n$	$P2_1/c$
a (Å)	10.0741(2)	9.3242(1)	9.2281(1)	4.9373(1)
b (Å)	12.2003(2)	11.1757(2)	11.2482 (1)	19.9552(5)
c (Å)	4.6300(1)	14.5623(2)	14.3353 (1)	16.2439(4)
α (deg)	90	90	90	90
β (deg)	90	96.671(1)	95.738(1)	90.88(1)
γ (deg)	90	90	90	90
volume (Å^3)	569.06(2)	1507.18(4)	1480.54(2)	1600.2(1)
Z	2	4	4	4
D(calcd) (g cm^{-3})	1.356	1.938	1.916	1.881
temp (K)	220(2)	220(2)	220(2)	220(2)
μ (mm^{-1})	3.907	15.067	13.873	12.898
θ_{max}(deg)	72.24	72.84	72.84	73.10
$R1^a$ [$I > 2\sigma(I)$]	0.0314	0.0323	0.0319	0.0534
R_w^b [$I > 2\sigma(I)$]	0.0852	0.0847	0.0766	0.1256
R [*all data*]	0.0328	0.0347	0.0376	0.0852
R_w [*all data*]	0.0864	0.0862	0.0787	0.1375
S^c	1.051	1.006	0.975	0.917

	4	**5**	**6**	**7**
formula	$C_{14}H_{12}AgF_3O_3S_3$	$C_{28}H_{24}Ag_2F_6O_6S_6$	$C_{17}H_{12}AgF_7O_2S_2$	$C_{30}H_{24}Ag_2F_4O_4S_4$
mol wt	489.29	978.57	553.26	868.47
crystal size (mm)	0.57×0.13×0.05	0.56×0.34×0.19	0.55×0.11×0.04	0.23×0.12×0.05
crystal system	monoclinic	triclinic	triclinic	triclinic
space group	$P2_1/n$	P-1	P-1	P-1
a (Å)	8.953(2)	12.526(2)	6.9224(1)	10.9903(2)
b (Å)	19.407(2)	12.905(2)	11.1849(2)	11.3039(2)
c (Å)	10.506(2)	13.186(2)	12.8590(2)	13.0694(2)
α (deg)	90	109.48(2)	87.83(1)	99.34(1)
β (deg)	110.00(2)	109.36(2)	84.06(1)	90.38(1)
γ (deg)	90	100.79(2)	76.03(1)	99.49(1)
volume (Å^3)	1715.3 (5)	1786.5(5)	960.89(3)	1579.27(5)
Z	4	2	2	2
D(calcd) (g cm^{-3})	1.895	1.819	1.912	1.826
temp (K)	220(2)	220(2)	100(2)	100(2)
μ (mm^{-1})	13.241	12.714	11.192	12.934
θ_{max} (deg)	70.02	69.97	72.82	72.78
$R1^a$ [$I > 2\sigma(I)$]	0.0504	0.0480	0.0311	0.0317
R_w^b [$I > 2\sigma(I)$]	0.1232	0.1312	0.0853	0.0792
R [all data]	0.0770	0.0561	0.0317	0.0369
R_w [all data]	0.1302	0.1364	0.0859	0.0839
S^c	0.877	1.017	1.056	0.947

$^aR = \Sigma \| F_o | - | F_c \| / \Sigma | F_o |$. $^bR_w = [\Sigma w(F_o^2 - F_c^2)^2 / \Sigma w(F_o^2)^2]^{1/2}$. $^cS = [\Sigma w(F_o^2 - F_c^2)^2 / (m-n)]^{1/2}$ (m is the number of reflections and n the number of parameters).

2.1.4 Results and Discussion

Ligand. The crystal structure of the bis(phenylthio)methane molecule is shown in Figure 2.1.1. The bis(phenylthio)methane building block is not chiral although the ligand crystallizes in the chiral space group, $P2_12_12_1$. The average C–S distance, 1.796(2) Å, compares well to the values reported in the literature.[4a,14] The ligand molecule adopts a fully extended conformation, that is, the central segment of the molecule is planar within experimental error. The S···S distance is 3.0558(8) Å.

Complexes $[AgL^{1\text{-}Ph}X]_\infty$ (1-4). The discussion in this section deals with compounds **1-4**. Complex **5**, the crystallization of which is influenced by the solvent used, as well as **6** and **7**, which contain a relatively long anion and a dicarboxylate respectively, will be dealt with separately.

The $[AgL^{1\text{-}Ph}X]_\infty$ Complexes **1-4** all form a one-dimensional type of coordination polymer (Figure 2.2 and Scheme 1a), where the basic repeat unit comprises a ligand, an anion, and a silver(I) cation. The polymer may be described as a zigzag chain of alternating silver(I) cations and bridging ligands bonded through the sulfur atoms, while the anions are coordinated to Ag(I). The bond distances and angles involving Ag(I) are compared in Table S1 (Annexe I).

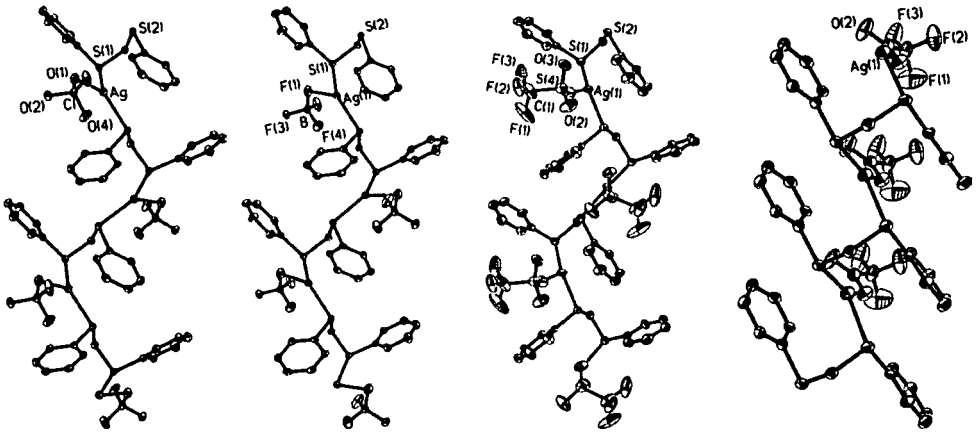

(a) (b) (c) (d)

Figure 2.1.2. Side view of the 1D-coordination polymer structure of (a) **1**, (b) **2**, (c) **4** and (d) **3**. The polymer chain axis is vertical. Note the relative orientations of the phenyl groups. They are always exactly parallel to one another in **3**, but nearly perpendicular in the other complexes. Complexes **1**, **2** and **4** have the gauche-trans-gauche conformation while **3** is gauche-gauche-gauche. The hydrogen atoms have been omitted for clarity.

In $[AgL^{1\text{-}Ph}(ClO_4)]_\infty$, (**1**), each silver is linked to two sulfur atoms from distinct ligands and to one oxygen atom of the perchlorate in a triangular fashion. The sum value of 358.9°of the angles S-Ag-S (121.4(1)°) and O-Ag-S (111.0(1) and 126.5(1)°) confirms a very nearly planar environment around the Ag atom. $[AgL^{1\text{-}Ph}(BF_4)]_\infty$, (**2**), is isostructural to (**1**); the bond angles around Ag(I) are as follows: F-Ag-S: 125.6(1)° and 109.2(1)°; S-Ag-S: 123.5(1)°. The sum of the angles, 358.3°, confirms the planar environment around Ag(I).

The silver coordination in $[AgL^{1\text{-}Ph}(CF_3CO_2)]_\infty$ (**3**) is that of a very distorted trigonal arrangement since the bond angles are in the range: 95.5(1) – 151.4(1)°. The complex $[AgL^{1\text{-}Ph}(CF_3SO_3)]_\infty$ (**4**) is only "approximately isostructural" relative to complexes **1** and **2**. In the trigonally coordinated silver, the bond angles around Ag(I) are in the range 86.7(2)° – 145.9(1)°, making it a clearly distorted environment.

The extreme values of the Ag-S distances are in the range 2.5174(8) – 2.5368(7) Å for **1** and **2**, while their range is 2.468(5) – 2.651(4) Å for **3** and 2.434(2) – 2.477(2) Å for **4**. The Ag-O distance is the shortest, 2.186(12) Å, in **3** compared to 2.412(2) Å in **1** and 2.378(5) Å in **4**. The distance between two consecutive silver atoms in the complexes with tetrahedral counteranions is fairly close, 6.2532(2) and 6.2002(2) Å for ClO_4^- and BF_4^-, respectively. For the trifluoromethanesulfonate counteranion, the Ag···Ag distance is 5.964(2) Å, whereas it is the lowest, 4.9373(2) Å, in the trifluoroacetate **3**. The S···S separation within the ligands is observed to be in the range 3.043(1) – 3.111(2) Å for the complexes and compares well with that in the free ligand, which is 3.056(1) Å. However, the arrangement of the phenyl groups in the complexes is influenced by the nature of the counteranions, as well as the packing of the various structural units.

The dihedral angle between the planes of the phenyl groups of the same ligand, given in Table 2.1.2, falls within the same angular range (23.5(2)°, 22.1(2)°, 17.3(5)°, and 13.6(4)° for complexes **1- 4**, respectively). This differs significantly from that observed for the free ligand, ϕ = 85.22(5)°. In other words, the phenyl groups are approximately orthogonal to one another in the free ligand. However, the conformation of the ligand is considerably different in complexes **1- 4** due to coordination of the Ag(I) to the sulfur atoms. This dihedral angle difference (between the free ligand and the complexes) is ascribed to packing interactions between phenyl groups of adjacent chains. On the other hand, the relative orientations of the aromatic rings vary depending on the counteranions

present (see Figure 2.1.2). The dihedral angles between two phenyl groups of adjacent ligands are 77.4(1)°, 87.1(1)°, and 59.7(3)° respectively for complex **1**, **2** and **4**, while for complex **3**, the dihedral angle is 0°. A ϕ value of 0° was reported by Bu *et* al. in the case of the NO_3^- anion.[3]

Table 2.1.2. Comparison of the dihedral angles (deg) between the phenyl groups of the same ligand, Φ_1, and between adjacent ligands, Φ_2, in complexes **1** – **8**.

		Dihedral angles		
Complex	Anion	Same ligand, Φ_1	Adjacent ligands, Φ_2	group
1	ClO_4^-	23.5(2)	77.4(1)	1
2	BF_4^-	22.1(2)	87.1(1)	1
3	CF_3COO^-	17.3(5)	0	2
4	$CF_3SO_3^-$	13.6(4)	59.7(3)	1
8[a]	NO_3^-	24.5(4)	0	2
5	$CF_3SO_3^-$	20.4(4) 48.4(2)		
6	$CF_3CF_2CF_2COO^-$	11.2(1)	0	
7	$^-OOCCF_2CF_2COO^-$	19.6(1)	9.9(1)	

[a]Reference 3.

On the basis of the above observation, one might infer that for tetrahedral counteranions such as ClO_4^- and BF_4^-, the phenyl groups are approximately orthogonal, ϕ = 77.4(1) and 87.1(1)° respectively, whereas for the planar or "nearly planar" counteranions, such as NO_3^- and $CF_3CO_2^-$, the phenyl groups of two ligands joined through a silver atom in the 1D-coordination polymer are nearly parallel. In the case of $CF_3SO_3^-$, which is a more bulky non planar counteranion, the corresponding phenyl dihedral angle is 59.7(3)°, so the phenyl groups are closer to being orthogonal to one another rather than parallel. Hence, one should consider two types of anions: tetrahedral anions (group 1) and planar or nearly planar anions (group 2). A 1D-coordination polymer is observed even though the counteranions have obviously different coordination strengths.

The torsion angles describing the conformation of the polymer chains are listed in Table 2.1.3. As noted for the dihedral angles, the chains may be classified in the same two groups depending on their torsion angles. Complexes belonging to group 1 have a *gauche-trans-gauche* conformation, with some large deviations noted for **4**. The conformation for

complexes in group 2 is *gauche-gauche-gauche*. Interestingly, these differences may be related to the geometry of the anions involved. In group 1, the coordinating atom is part of a tetrahedral system, which restricts the orientation of the anion. However, in group 2, the planar trigonal coordinating group may adopt a less interfering orientation.

Table 2.1.3. Comparison of the torsion angles (deg) describing the polymer chains in complexes **1-4** and **8**.[a]

	Complex				
Torsion angles	**1**	**2**	**3**	**4**	**8**[b]
Ag(1)-S(1)-C(7)-S(2)	-53.8(2)	55.4(2)	51.4(1)	-46.9(4)	58.5(4)
S(1)-C(7)-S(2)-Ag(1)	-176.4(2)	175.8(1)	53.1(1)	-172.1(3)	65.0(2)
C(7)-S(2)-Ag(1)-S(1)	-80.1(1)	82.9(1)	67.3(6)	-101.0(3)	55.7(4)

[a]**1**, **2** and **4** with the *gauche-gauche-gauche* conformation belong to group 1, while **3** and **8** are in group 2 (*gauche-trans-gauche* conformation). [b]Reference 3.

Scheme 1[a]

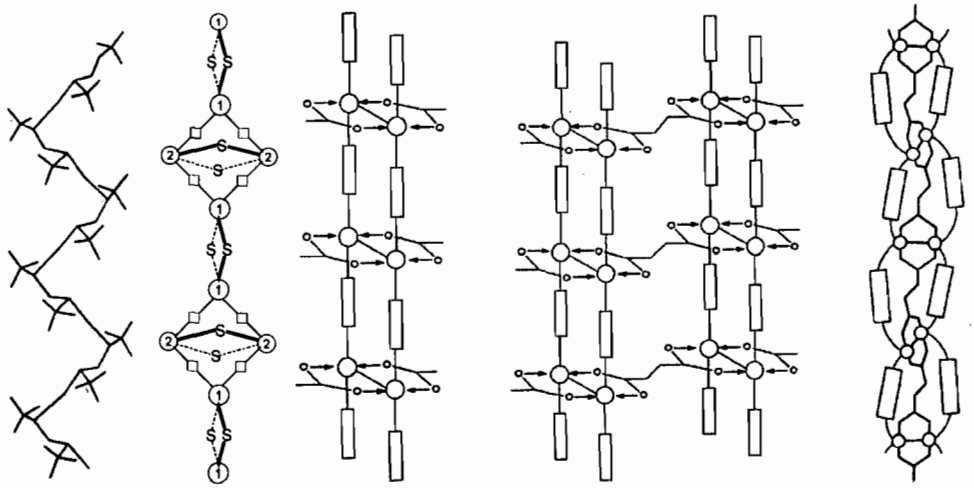

(a) (b) (c) (d) (e)

[a] (a) Single chain [Ag-ligand-]$_\infty$ for **1-4**. (b) Double-stranded chain of **5**. Circles marked 1 and 2 are the silver ions, while the small square represents the ligand. (c) Schematic representation of the double-stranded chain of **6**. (e) Expected extension of **7** into a 2D-network through the replacement of the heptafluorobutyrate anion by the tetrafluoro succinate. (e) Actual structure observed for complex **7** double-stranded chain with the tetrafluorosuccinate anion.

$[Ag_2(L^{1\text{-}Ph})_2(CF_3SO_3)_2]_\infty$ **(5)**. It is worth noting that the complexes obtained with the trifluoromethanesulfonate counteranion display supramolecular isomerism. Complex **5** was synthesized following the same conditions as **4**, except for the solvent used during recrystallization. A new crystalline form, that of **5**, was obtained when petroleum ether was used instead of the diethyl ether that yielded **4**. There are two crystallographically distinct silver atoms in **5**, Ag(1) and Ag(2). They both have the same coordination, although the bond distances and angles differ significantly. Two Ag(1) or two Ag(2) atoms and two different trifluoromethanesulfonate groups form an eight-membered ring through four O-Ag coordinating bonds (Figure 2.1.3a). Each silver atom is also coordinated to two S atoms from distinct ligands. These, in turn, are linked to the second kind of silver atom, Ag(2) to form a centrosymmetric 16-membered metallomacrocycle, $Ag_4(L^{1\text{-}Ph})_4$ (Figure 2.1.5a).

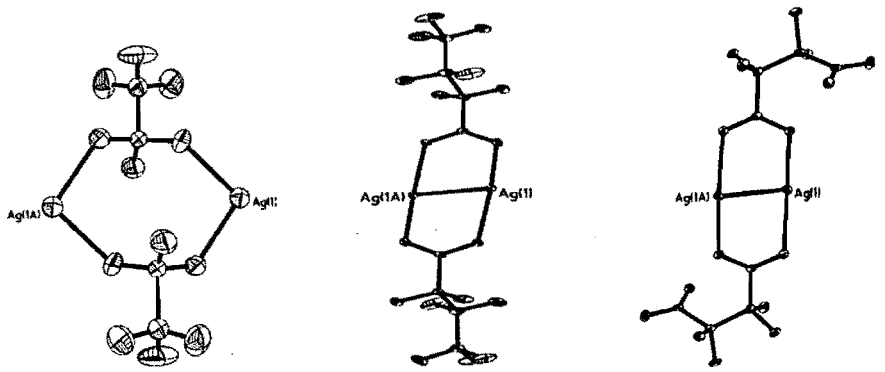

(a) (b) (c)

Figure 2.1.3. (a) An eight-membered ring involving Ag(1) and the trifluoromethanesulfonate anions in **5**, (b) heptafluorocarboxylate anions bridging two silver atoms in **6**, and (c) two tetrafluorosuccinate anions bridging two silver atoms in **7**. The *gauche* conformation of the anion is clearly visible.

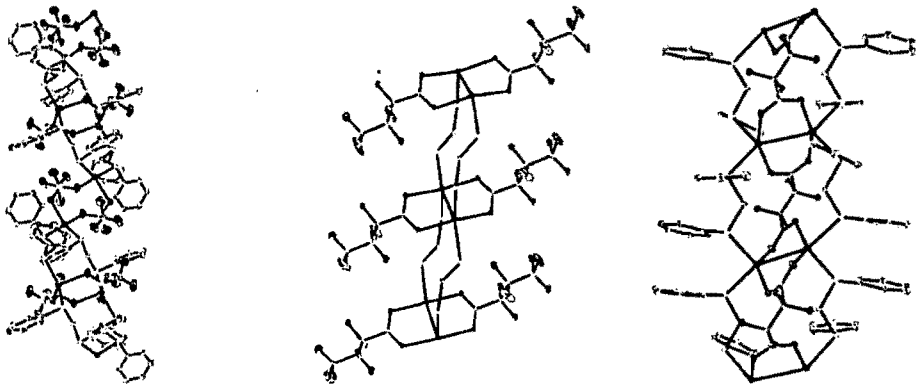

(a) (b) (c)

Figure 2.1.4. (a) The double 1D-chain of **5** extending along the [222]-direction. (b) The double chain of **6** constituted of dimers linked through a 10-membered ring (the double string or ladder-like structure extends in the *a*-axis direction; the H-atoms and the phenyl groups have been omitted for clarity) and (c) the double chain of 7 showing the $Ag_4(L^{1\text{-}Ph})_2$ 10-membered ring and the silver atoms bridged by the tetrafuorosuccinate anions. The H atoms have been omitted for clarity.

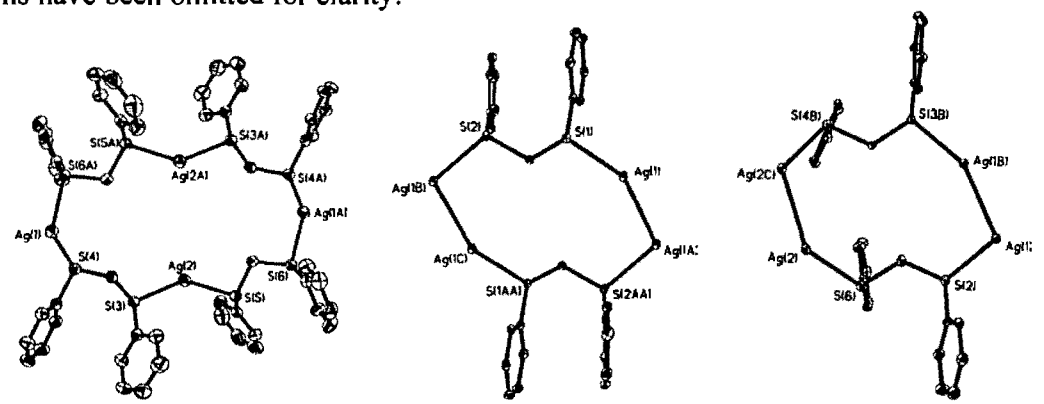

(a) (b) (c)

Figure 2.1.5. The 16-membered ring macrocycle $Ag_4(L^{1\text{-}Ph})_4$ in **5** (a) compared to the $Ag_4(L^{1\text{-}Ph})_2$ 10-membered ring in **6** (b) and in 7 (c). The anions and the H atoms are omitted for clarity.

Two Ag(2) atoms, from adjacent $Ag_4(L^{1\text{-}Ph})_4$ macrometallocycles are also associated with two oxygen atoms from two other trifluoromethanesulfonate anions in a bridging mode and to two sulfur atoms so as to build a double chain coordination polymer extending along the [222]-direction (Figure 2.1.4a, Scheme 1b). The main difference between Ag(1) and Ag(2) is in the relative orientations of the trifluoromethanesulfonate groups. The two kinds of silver atom, Ag(1) and Ag(2), adopt a distorted tetrahedral coordination, that is for Ag(1) O-Ag-O is 99.4(2)° and S-Ag-S is 126.4(1)° and for Ag(2) O-Ag-O is 100.4(2)° and S-Ag-S is 139.6(1)°. The silver···silver separation in the

$Ag_4(L^{1\text{-}Ph})_4$ macrometallocycles are 4.711(1) and 5.524(1) Å for Ag(1)···Ag(1) and Ag(2)···Ag(2), respectively. The S···S separations in this complex are of the same order of magnitude as in the other complexes, 3.0204(2) and 3.005(2) Å.

$[AgL^{1\text{-}Ph}(CF_3CF_2CF_2CO_2)]_\infty$ (6). To study the influence of the length of the counteranion upon the conformation of the ligand and the type of network adopted, the syntheses of complexes with longer anions, such as pentafluoropropionate and heptafluorobutyrate were attempted. Complex **6**, containing the heptafluorobutyrate anion, was successfully crystallized. Since the heptafluorobutyrate anion is elongated, it is expected to have a significant influence on the resulting structure. It is observed that in **6**, two adjacent silver atoms are bonded together in a binuclear bridging mode with two heptafluorobutyrate groups to form the $Ag_2(OOCCF_2CF_2CF_3)_2$ dimer (Figure 2.1.3b). Moreover, adjacent dimers are connected by the ligand molecules, thus building a double chain (ladder-like) structure parallel to the *a*-direction (Figure 2.1.4b, Scheme ac). The two carboxylate groups and the two silver atoms form a nearly coplanar subunit, while the remainder of the anions extend beyond it. All such subunits are parallel to one another and constitute the "steps" of the ladder.

This structure may also be described as that of a corrugated ribbon of adjacent 10-membered rings sharing Ag···Ag edges, while the two heptafluorobutyrate groups coordinated to the silver atoms are in a direction nearly perpendicular to the ribbon axis. In this structure, each Ag(I) is linked to two oxygen atoms (Ag-O = 2.311(2) and 2.321(2) Å) from different anions and to two sulfur atoms from distinct ligands (Ag-S = 2.5826(6) and 2.6154(6) Å). This yields a very distorted trigonal bipyramid coordination since the bond angles (see Table S1, Annexe I) are as follows: S-Ag-Ag: 152.6(1)°, S-Ag-O: 100.0(1), 115.4(1)° and O-Ag-O: 136.6(1)°.

The distance between neighbouring silvers, Ag···Ag, is 3.1593(3) Å, indicating a weak metal-metal interaction.[15] In this organization, a centrosymmetric ten-membered ring $Ag_4(L^{1\text{-}Ph})_2$ is formed (Figure 2.1.5b). Even though the perchlorate (Ag-O = 2.412(1) Å) and the tetrafluoroborate (Ag-F = 2.536(3) Å) are less strongly coordinating anions than the trifluoromethanesulfonate (Ag-O = 2.379(5) Å) or the trifluoroacetate[16] (Ag-O = 2.190(5) Å), they all coordinate to the silver atom. Furthermore, it has been reported that when the aliphatic chain of the ligand increases, the perchlorate and the tetrafluoroborate are not at all or only weakly coordinated to the silver atom.[4a,c,14] When the 1,3-

bis(phenylthio)propane ligand is involved, the weakly coordinating anions ClO_4^- and BF_4^- are sandwiched between the cationic sheets.[4c]

$[Ag_2(L^{1\text{-}Ph})_2(CO_2CF_2CF_2CO_2)]_\infty$ (7). An inspection of the structure of **6** gave us the idea that we could form a 2D-network by linking the chains to one another using a diacid as the counterion (Scheme 1c,d) instead the heptafluorobutyrate. Thus, we chose to synthesize another complex using silver(I) tetrafluorosuccinate. This idea of creating a 2D-network was unsuccessful. Compound **7** only forms a 1D-polymer with a double chain similar to that observed in **6** and also contains an $Ag_4(L^{1\text{-}Ph})_2$ 10-membered ring, shown in Figure 2.1.5c. The 10-membered ring consists of two ligands each bound to two silver atoms. In turn, these are bridged through two anions thus forming a 1D-coordination polymer that extends in the *c*-direction (Figure 2.1.4c, Scheme 1e). As in **6**, the two silver atoms and the two bridging carboxylate groups are almost coplanar. However, two such consecutive units are no longer parallel to one another but form a dihedral angle of 63(1)°, giving rise to a twisted polymeric chain. This chain can also be described as a succession of a pair of silver atoms bridged at one end of the tetrafluorosuccinate anion. Another pair of silver atoms is bridged at the other end and so on. Thus a $[Ag_2\text{-}OOCCF_2CF_2COO\text{-}]_\infty$ ribbon is generated (Figure S1a, Annexe I). This is further reinforced by ligand molecules that bind two consecutive silvers (Figure S1b, Annexe I).

The coordination around Ag(1) and Ag(2) is that of a strongly distorted trigonal bipyramid. The S-Ag1-Ag1 = 154.5(1)°, S-Ag1-O = 106.9(1)° and 109.1(1)° and O-Ag1-O = 139.1(1)°. The angles around Ag(2) are as follows: O-Ag2-O: 158.1(1)°, S-Ag2-Ag2 114.2(1) and 138.7(1)°, and S-Ag2-S 107.1(1)°. The Ag-O distances vary between 2.280(2) and 2.314(2) Å, while the Ag-S distances range from 2.583(1) and 2.654(1) Å. The shorter the Ag-O is, the longer the Ag-S bond is.

Packing of the structures. On the one hand, the ligands and the Ag(I) atoms form 1D-chains in complexes **1-4**. The counteranion is coordinated to the silver(I) atom through an oxygen atom (**1**, **3**, **4**) or a fluorine atom (**2**). In turn, these chains could be seen as being associated through weak van der Waals interactions into 2D-networks. These weak interactions are the short contact interactions of the $C(CH_2)\cdots O$ (or F)-type with values of 3.193(2), and 2.998(4) Å in **1** and **2** respectively. However, in **3** and **4**, the shortest contacts are of the C(CH)···F type. They have values of 3.102(18) and 3.202(11) Å, respectively. The crystal packing adopted by the complexes depends on the chain conformation.

Complexes **1** and **2**, consisting of tetrahedral anions, and **4**, consisting of the trifluoromethanesulfonate anion, belong to the group 1 defined earlier and exhibit an identical packing mode (Figure 2.1.6a).

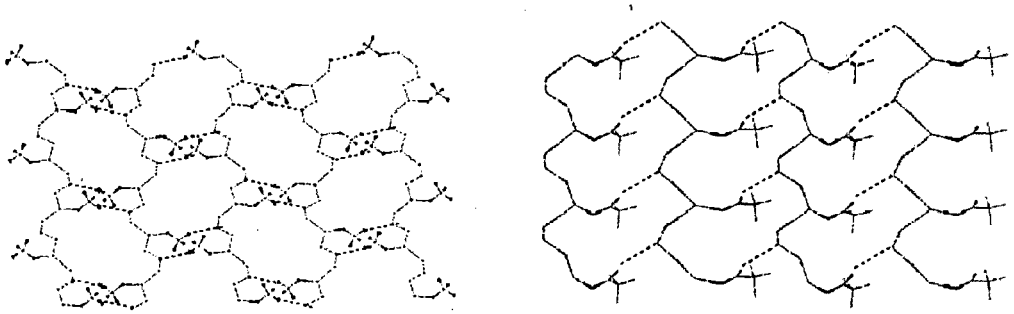

(a) (b)

Figure 2.1.6. Association by van der Waals interactions of the 1D-chains into a "2D-network", view parallel to the (010) plane: (a) anions of group 1 – BF_4^-, ClO_4^- and $CF_3SO_3^-$; (b) anions of group 2 – $CF_3CO_2^-$ and $NO3^-$.

The packing of **3**, with the trifluoroacetate anion, shown in Figure 2.1.6b, differs clearly from that of **1**, **2** and **4**. It is worth noting that a comparable type of packing was reported for **8**, the nitrate complex.[3] The noted packing preference of these two complexes, which belong to group 2, may be attributed to the presence of rather flat anions in complexes **3** and **8**. The packing differences between group 1 and group 2 may be clearly appreciated by the projections along the 1D-polymer chain axis shown in Figure 2.1.7 a, b.

The packing of **5**, shown as a projection along the chain axis, is illustrated in Figure 2.1.7c. The shortest contact is of the C(CH)···F type and is 3.04(3) Å long. As described earlier, complex **6**, with the heptafluorobutyrate anion, forms ribbons extending in the *a*-axis (Figure 2.1.4b). When seen end-on, the ribbons are assembled in a hexagonal compact packing of approximately cylindrical rods (Figure 2.1.7d). The shortest C(H)···F contact is 3.203(4) Å long. The expected 2D-structure for **7** is not observed. As can be observed in Figure 2.1.7e, compound **7** forms a 1D-coordination polymer with deformed hexagonal packing similar to that of **6**. The similarity ends there, since the aromatic rings of **7** are nearly all disposed around the chain axis, while in **6**, they occupy only two diametrically opposed regions. There is a relatively short C(CH)···F contact that is 3.193(4) Å long.

That the 2D-structure is not adopted may be attributed to the fact that the ligand is too short and that the anion is fairly flexible. Indeed, one notes a torsion of 63(1)° about the C(2)-C(3) bond, that is, the fluorine atoms of the succinate are staggered. This is a new

feature for this anion since, in all the structures that contain it, the succinate is always in the trans-conformation and the fluorine atoms are eclipsed.[17-20]

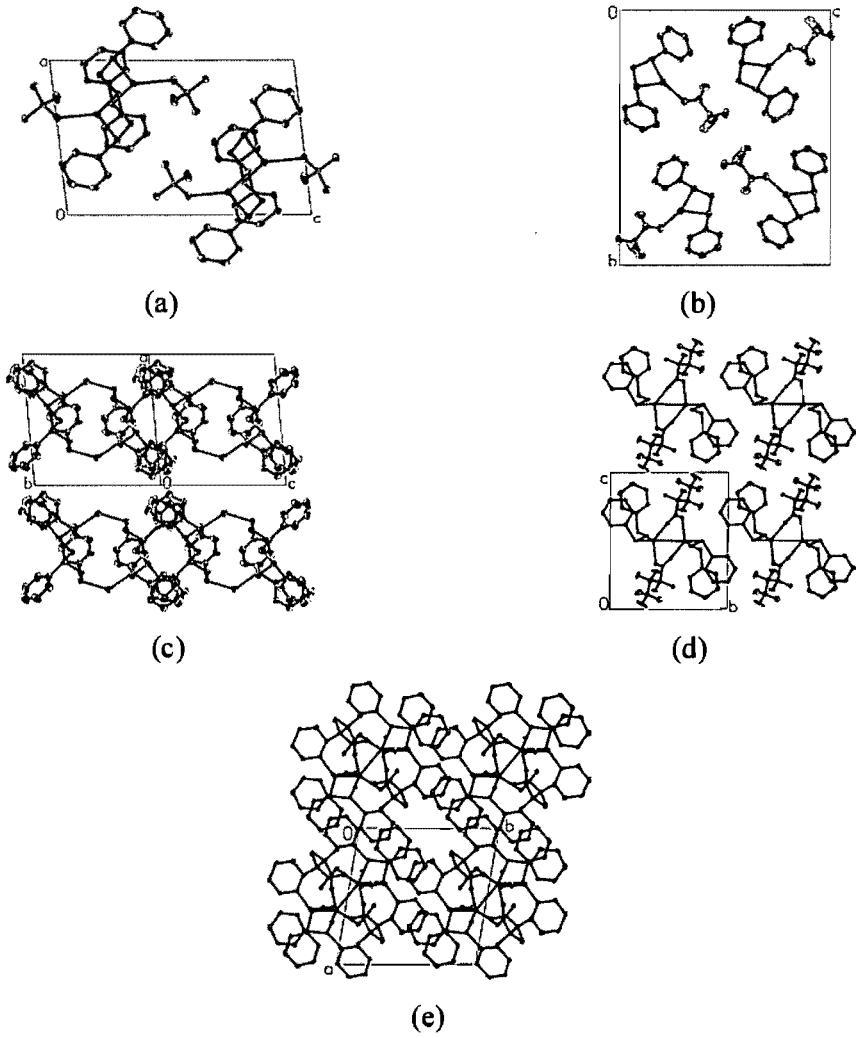

Figure 2.1.7. (a) Unit cell content showing the 1-D chains projected on the *ac*–plane (this arrangement applies to anions of group 1– BF_4^-, ClO_4^- and $CF_3SO_3^-$), (b) projection on the *bc*-plane of the unit cell content of the anions of group 2– CF_3COO^- and NO_3^- anion,[3] (c) projection along the chain axis showing the packing of the double chain in **5**, (d) Projection down the *a*-axis showing the packing of the double-stranded 1D-chains in **6**, and (e) projection onto the *ab*-plane of the chains of **7**.

Supramolecular Isomerism. Solvent induced supramolecular isomerism was observed for complex **4** and **5**. These two trifluoromethanesulfonate complexes have the same molecular composition, $[AgL^{1\text{-}Ph}(CF_3SO_3)]_\infty$, and do not include any solvent molecules. In complex **4**, recrystallized in diethyl ether, the $CF_3SO_3^-$ anion is coordinated to Ag(I) through one of its

oxygen atoms. In complex **5**, obtained from petroleum ether or other nonpolars solvents, two silver atoms are bridged by two trifluoromethanesulfonate anions. To support this observation, other complexes were synthesized using 1,3-bis(phenylthio)propane, ligand $\mathbf{L}^{3\text{-Ph}}$, while the silver salt was either the trifluoromethanesulfonate, $[Ag_2\mathbf{L}^{3\text{-Ph}}(CF_3SO_3)_2]_\infty$, or the *para*-toluenesulfonate, *p*-TsO^-, $[Ag\mathbf{L}^{3\text{-Ph}}(p\text{-TsO})]_\infty$. Supramolecular isomerism was observed[4c] with both anions containing the sulfonate group. Furthermore, all the complexes recrystallized from petroleum ether or other nonpolar solvents, such as pentane or hexane, contain a double-bridged subunit. Obviously one cannot generalize, but clearly, the polarity of the solvent plays a significant role in the way the anion is coordinated to Ag(I). A more systematic study would be required to establish, for example, whether the solvent coordinates first to the silver and is then released, or replaced later when crystallization takes place. This temporary bond could prevent the formation of the double-bridge subunit.

Silver-silver distances. There are some short Ag···Ag distances in both **6** and **7** where the acid ends of two anions form a dinuclear unit with two silver atoms (see Figures 2.1.3b,c). The Ag···Ag distance is 3.1593(3) Å long in **6**. In **7**, the two Ag···Ag distances are even shorter, with values of 2.9836(5) and 3.0168(5) Å. All these distances are slightly longer than the Ag-Ag distance in silver metal, but clearly shorter than the sum of the van der Waals radii[21] (3.44 Å) of the silver atoms, indicating the presence of ligand-supported Ag···Ag interactions. Such short Ag···Ag distances are not unusual in Ag(I) dinuclear complexes, where the anions maintain the Ag atoms close to each other. For example, a Ag-Ag bond of 2.9710(4) Å was reported for trifluoroacetate groups bridging two silver cations in a 2:1 complex of bis(dimethylphenyl)pyrazine and silver(I) trifluoroacetate crystallized in acetonitrile, while a Ag···Ag distance of 3.1014(3) Å was obtained in for the 2:2 complex crystallized in dichloromethane.[22] A distance of 3.116(1) Å is reported for Ag···Ag in a bis(2-pyridylthio)methanedinitrotrisilver(I) nitrate and 3.128(4) Å in bis(2-pyridylthio)propane dinitro disilver(I)[23].

Short Ag···Ag distances, 2.9246(5) and 2.9731(4) Å, have been reported, in a complex of silver trifluoroacetate and 2,4,6-trimesityl-1,3,5-triazine,[24] 3.1300(3) Å in the tetrameric silver thiolate phosphine complex,[25] and 3.032(2) and 3.053(2) Å in a bipyridyl-based silver iodide.[26] It is only in the tetrafluorosuccinate silver acetylenediide that the Ag-Ag distances are close to that in silver metal: in the crown-like [C2@Ag7] cage they range from 2.8848(8) to 2.9526(8) Å.[20] Following the discussion of Wheatley and coworkers,[25]

we can infer that there is a significant metal-metal bonding contribution in the above compounds especially at these short distances.

Infrared spectroscopy. The infrared absorptions band frequencies recorded for our fluorine containing complexes and the shortest C(H)···F contacts are listed in Table 2.1.4. Our results are in agreement with the very well documented work of Reger *et al.*,[27] which reports a good correlation between the existence of a short C(H)···F contact and the presence of an absorption band at around 521 cm^{-1}. Except for **6** and **7**, all our complexes exhibit an absorption band in the 516-521 cm^{-1} range and short C(H)···F contacts. Thus, in accordance with Reger *et* al., we conclude that weak hydrogen bonds exist in these complexes.[27, 28] In the perchlorate –containing complex **1**, the peaks at 1143 ($\nu_4(E)$), 1080 ($\nu_1(A_1)$) and 940 cm^{-1} ($\nu_2(A_1)$) indicate the presence of a monodentate ClO_4^- anion,[29] while the peaks at 1070 and 1024 cm^{-1} in complex **2** confirm the presence of the BF_4^- ligand.[30]

Tableau 2.1.4. Short contacts C(H)···F or $C(H_2)$···F (Å), and infrared absorption frequencies (cm^{-1}).

Complex	Anion	Contact	Frequency	Type
2	BF_4^-	2.998(4)	521m	$C(H_2)$ F
3	CF_3COO^-	3.102(18)	516w	C(H) F
4	$CF_3SO_3^-$	3.202(11)	518w	C(H) F
5	$CF_3SO_3^-$	3.04(3)	518m	C(H) F
6	$CF_3CF_2CF_2COO^-$	3.203(4)	527w	C(H) F[a]
7	$^-OOCCF_2CF_2COO^-$	3.193(4)	532vw	C(H) F[a]

[a]Although complexes **6** and **7** also have relatively short contacts, the infrared absorption frequencies are very weak and broad.

The peaks observed at 1690 and 1390 cm^{-1} in the IR spectrum of complex **3** are assigned to the characteristic antisymmetric and symmetric stretching bands of the carboxylate group respectively. In addition, the value of $\Delta = [\nu_{asym}(CO_2) - \nu_{sym}(CO_2)]$, 300 cm^{-1}, obviously points to the occurrence of the monoatomic binding mode[31] shown by the X-ray analysis of **3**. The IR spectrum of complex **6** shows two peaks at 1682 and 1403 cm^{-1}, which correspond to the carboxylate the antisymmetric and symmetric stretching bands. The Δ value of 279 cm^{-1} points to the presence of a dimer in a bridging mode,[32] corroborating the structure shown in Figure 2.1.3b. The IR spectrum of complex **7** presents

two absorptions at 1683 and 1407 cm^{-1}, which are assigned as above. The Δ value of 276 cm^{-1} confirms the presence of the bridging mode, in agreement with the crystal structure.

In structures **4** and **5** containing the trifluoromethanesulfonate anion, $CF_3SO_3^-$, the unambiguous assignment of the vibration modes of the anion is difficult because of the mixing of the CF_3 and SO_3 vibrations in the stretching region between 1000 and 1300 cm^{-1}.[33, 34] However, according to Lawrance,[34] the silver atom in silver trifluoromethanesulfonate is coordinated to the anion, which has absorption bands at 1270 and 1043 cm^{-1}. These bands have been assigned to the $\nu[SO_3(E)]$ and $\nu[SO_3(A_1)]$ vibrations. The bands observed at 1258 and 1033 cm^{-1} for complex **4** are consistent with the triflate coordinated to a silver atom (published frequencies 1257 and 1035 cm^{-1}).[35] Since the IR spectra of complexes **4** and **5** are strikingly similar, the different coordinations of the silver atom, that is monoatomic coordination *vs* diatomic bridging mode in **4** and **5**, respectively, cannot be distinguished by means of their IR spectra.

2.1.5 Conclusions

We have synthesized and structurally characterized seven different coordination polymers consisting of Ag(I) salts of bis(phenylthio)methane ligand. The complexes all form 1D-polymer-like structures. These polymers are either single- or double-stranded. The single-stranded chains are of the type $[Ag–ligand–]_\infty$, and the anions are coordinated to the silver ions. These polymeric chains have two distinct conformations: when the anions are tetrahedral (**1**, **2**, and **4**), the conformation is *gauche-trans-gauche*, while it is *gauche-gauche-gauche* for planar anions (**3**, **8**). Furthermore, the single-stranded chains are, in turn, associated through weak van der Waals interactions into 2D-layer structures, the packings of which are of two distinct types depending on the conformation of the chains. Complex **5** and those with larger anions **6** and **7**, adopt a doubly-stranded polymeric structure, in which the anions act as bidentate ligands. Supramolecular isomerism is observed for the $CF_3SO_3^-$ counteranion. When complex **5** is recrystallized in petroleum ether, the ligands and the silver ion form $Ag_4(\mathbf{L}^{\mathbf{1\text{-}Me}})_4$ macrometallocycles that are connected into a double-stranded polymer through the anions. When **4** is recrystallized in diethyl ether, a one-dimensional chain, $[Ag\text{-}ligand\text{-}]_\infty$, is obtained. The existence of C(H)···F or $C(H_2)$···F hydrogen-bonds is identified by short contacts in the range 2.998(4) – 3.203(4) Å and IR absorptions near 521

cm^{-1}. The short Ag···Ag contacts (2.9836(5) – 3.1593(3) Å) in the two fluorocarboxylate complexes, **6** and **7**, indicate a significant metal–metal bonding contribution.

Acknowledgements. This work was supported by the Natural Sciences and Engineering Research Council of Canada (F.B.). M.O.A. would like to thank the Programme Canadien de Bourse de la Francophonie for a graduate scholarship. The authors also thank Dr. M. Simard and F. Bélanger-Gariépy for collecting the X-ray intensities and H. Dinel for performing the elemental analyses.

Supplementary Material Available: Table S1 of the comparison of the bond distances and angles involving the silver(I) ions. Figure S1 and X-ray crystallographic information files (CIF) for compounds ($\mathbf{L}^{\mathbf{1\text{-}Ph}}$, **1**-**7**). This material is available free of charge via the Internet at http://pubs.acs.org.

2.1.6 References

(1) (a) Leininger, S.; Olenyuk, B.; Stang, P. J.; *Chem. Rev.* **2000**, *100*, 853. (b) Holliday, B. J.; Mirkin, C. A. *Angew. Chem. Int. Ed.* **2001**, *40*, 2022. (c) McCleverty, J. A.; Ward, M. D. *Acc. Chem. Res.* **1998**, *31*,842.

(2) For example: (a) Withersby, M. A.; Blake, A. J.; Champness, N. R.; Cooke, P. A.; Hubberstey, P.; Li, W. S.; Schröder, M. *Inorg. Chem.* **1999**, *38*, 2259. (b) Blake, A. J.; Champness, N. R.; Cooke, P. A.; Nicolson, J. E. B.; Wilson, C. *J. Chem. Soc., Dalton Trans.* **2000**, 3811. (c) Withersby, M. A.; Blake, A. J.; Champness, N. R.; Hubberstey, P.; Li, W. S.; Schröder, M. *Angew. Chem. Int. Ed.* **1997**, *36*, 2327. (d) Noro, S.; Kitaura, R.; Kondo, M.; Kitagawa, S.; Ishii, T.; Matsuzaka, H.; Yamashita, M. *J. Am. Chem. Soc.* **2002**, *124*, 2568. (e) Chatterton, N. P.; Goodgame, D. M. L.; Grachvogel, D. A.; Hussain, I.; White, A. J. P.; Williams, D. J. *Inorg. Chem.* **2001**, *40*, 312.

(3) Bu, X. H.; Chen, W.; Du, M.; Biradha, K.; Wang, W. Z.; Zhang, R. H. *Inorg. Chem.* **2002**, *41*, 437.

(4) (a) Bu, X. H.; Chen, W.; Hou, W. F.; Du, M.; Zhang, R. H.; Brisse, F. *Inorg. Chem.* **2002**, *41*, 3477. (b) Bu, X. H.; Chen, W.; Lu, S. L.; Zhang, R. H.; Liao, D. Z.; Bu, W. M.; Shionoya, M.; Brisse, F.; Ribas, J. *Angew. Chem. Int. Ed.* **2001**, *40*, 3201. (c) Awaleh, M. O.; Badia, A.; Brisse, F. *Inorg. Chem.* **2005**, *44*, 7833.

(5) (a) Moulton, B.; Zaworotko, M. J. *Chem . Rev.* **2001**, *101*, 1629. (b) Gudbjartson, H.;

Biradha, K.; Poirier, K. M.; Zaworotko, M. J. *J. Am. Chem. Soc.* **1999**, *121*, 2599.

(6) Oh, M.; Carpenter, G. B.; Sweigart, D. A. *Angew. Chem. Int. Ed.* **2002**, *41*, 3650.

(7) Enraf-Nonius. CAD-4 Software, Version 5.0. Enraf-Nonius; Delft, Holland, 1989.

(8) SAINT Release 6.06, Integration Software for Single Crystal Data; Bruker AXS Inc.: Madison, WI, 1999.

(9) Sheldrick, G. M. SADABS Bruker Area Detector Absorption Corrections; Bruker AXS Inc.: Madison, WI, 1996.

(10) XPREP Release 5.10; X-ray Data Preparation and Reciprocal Space Exploration Program. Bruker AXS Inc., Madison, WI, 1997.

(11) SHELXTL Release 5.10, The Complete Software Package for Single-Crystal Structure Determination; Brucker AXS Inc.: Madison, WI, 1997.

(12) (a) Sheldrick, G. M. SHELXS97, Program for the Solution of Crystal Structures; University of Göttingen: Göttingen, Germany, 1997. (b) Sheldrick, G.M. SHELXL97, Program for the Refinement of Crystal Structures; University of Göttingen: Göttingen, Germany, 1997.

(13) Hartley, F. R.; Murray, S. G.; Levason, W.; Soutter, H. E.; McAuliffe, C. A. *Inorg. Chim. Acta* **1979**, *35*, 265.

(14) Black, J. R.; Champness, N. R.; Levason, W.; Reid, G. *J. Chem. Soc., Chem. Comm.* **1995**, 1277.

(15) Wang, Q. M.; Mak, T. C. W. *J. Am. Chem. Soc.* **2001**, *123*, 7594.

(16) Jung, O. S.; Kim, Y. J.; Lee, Y. A.; Park, K. M.; Lee, S. S. *Inorg.Chem.* **2003**, 42, 844.

(17) Vij, A.; Connors, P. J.; Rice, B. L.; Kirchmeier, R. L.; Shreeve, J. M. *Zeit. Anorg. Chem.* **1995**, *621*, 1865.

(18) Angaridis, P.; Cotton, F. A.; Petrukhina, M. A. *Inorg. Chim. Acta* **2001**, *324*, 318.

(19) Cotton, F. A.; Donahue, J. P.; Lin, C.; Murillo, C. A. *Inorg Chem.* **2001**, *40*, 1234.

(20) Wang, Q. M.; Guo, G. C.; Mak, T. C. W. *J. Cluster Sci.* **2002**, *13*, 63.

(21) Bondi, A. J. *J. Phys. Chem.* **1964**, *68*, 441.

(22) Schultheiss, N.; Powell, D. R.; Bosch, E. *Inorg. Chem.* **2003**, *42*, 5304.

(23) Xie, Y. B.; Bu, X. H. *J. Cluster Sci.* **2003**, *14*, 471.

(24) Bosch, E.; Barnes, C. L. *Inorg. Chem.* **2002**, *41*, 2543.

(25) Ahmed, L. S.; Dilworth, J. R.; Miller, J. R.; Wheatly, N. *Inorg. Chim. Acta* **1998**, *278*, 229 and references therein.

(26) Niu, Y.; Hou, H.; Zhu, Y. *J. Cluster Sci.* **2003**, *14*, 483.

(27) Reger, D. L.; Semenius, R. F.; Silaghi-Dumitrescu, I.; Smith, M. D. *Inorg. Chem.* **2003**, *42*, 3751.

(28) Nakamoto, K. Infrared Spectra of Inorganic and Coordination Compounds. 3rd ed.; Wiley-VCH: New York, 1978.

(29) Rosenthal, M. R. *J. Chem. Ed.* **1973**, *50*, 331 and references therein.

(30) Clark, H. C.; O'Brien, R. J. *Inorg. Chem.* **1963**, *2*, 1020 and references therein.

(31) Deacon, G. B.; Phillips, R. J. *Coord. Chem. Rev.* **1980**, *33*, 227.

(32) Szłyk, E.; Szymańska, I.; Surdykowski, A.; Głowiak, T.; Wojtczak, A.; Goliński, A. *J. Chem. Soc., Dalton. Trans.* **2003**, 3404.

(33) Johnston, D. H.; Shriver, D. F. *Inorg. Chem.* **1993**, *32*, 1045.

(34) Lawrance, G. A. *Chem. Rev.* **1986**, *86*, 17 and references therein.

(35) Zhong, J. C.; Munakata, M.; Kuroda-Sowa, T.; Maekawa, M.; Suenaga, Y.; Konaka, H. *Inorg. Chem.* **2001**, *40*, 3191.

2.2 Coordination networks with flexible ligands based on silver(I) salts. Complexes of 1,3-bis(phenylthio)propane with silver(I) salts of PF_6^-, CF_3COO^-, $CF_3CF_2COO^-$, $CF_3CF_2CF_2COO^-$, *p*-TsO^-, and $CF_3SO_3^-$.[†]

2.2.1 Abstract

The synthesis and characterization of nine coordination networks based on 1,3-bis(phenylthio)propane, $L^{3\text{-Ph}}$, and silver(I) salts of PF_6^- (**1**), CF_3COO^- (**2**), $CF_3CF_2COO^-$ (**3**), $CF_3CF_2CF_2COO^-$ (**4**), *p*-TsO^- (**5**, **6**), and $CF_3SO_3^-$ (**7**, **8**, **9**) are reported. Only **1** and other "isostructural" complexes with weakly coordinating anions such as ClO_4^- and SbF_6^- are of the host-guest type. In all the other complexes, the anions and the acetone molecules, when present, are coordinated to the metal. Most of the complexes studied here form a 2D-coordination network. Only **4** and **5** adopt a polymer-like chain structure. The packing of the chains of **4** is pseudo-hexagonal compact, while that of **5** is of the centered type. In complex **1**, the silver atom is tetrahedrally coordinated to the sulfur atoms of four different ligands. The PF_6^- anions and acetone molecules, sandwiched between the silver-ligand cationic sheets, are held through electrostatic and van der Waals interactions. In each of the three perfluorocarboxylates (**2-4**), two silver atoms are joined by the anions in a diatomic bridging mode. The Ag···Ag distances are sufficiently short to indicate weak metal···metal interactions. The dimeric units in **2** and **3** are interconnected through the ligands, thereby generating a 2D-network of neutral sheets, while, in **4**, the dimeric units are bound to four ligands and a 1D-coordination polymer is generated. In the case of sulfonate anions (*p*-TsO^- and $CF_3SO_3^-$), the crystallization solvent influences the structure adopted. Thus, in **5**, **7**, and **9** obtained from petroleum ether, or other nonpolar solvents, two silver atoms are bound in a double-bridge fashion, while a monobridge mode is noted for **6** and **8**, both recrystallized from diethylether. In **8**, both bridging types are observed.

The thermogravimetric investigation in the room temperature – 450 °C interval of complexes **1**, **3**, and **7**, which incorporate acetone molecules in their crystal structures, reveals a two-step weight loss for **1** (the acetone molecules are lost first followed by the ligands leaving behind the silver salt), while complexes **3** and **7** decompose in a single step to metallic silver.

[†] Awaleh, M. O.; Badia, A.; Brisse, F. *Inorg. Chem.* **2005**, *44*, 7833-7845.

2.2.2 Introduction

In the last two decades, there has been considerable activity in the design and synthesis of solid frameworks.[1] The self-assembly of metal-organic coordination polymers has attracted a great deal of attention because of their potential applications as functional materials.[2]

The properties of coordination polymer materials are to some extent dependent on their network topology. Thus, it is of interest to understand and control the subtle factors that influence the formation of these supramolecular networks. Moreover, the strategy consisting of varying the coordination site and/or the size and shape of the ligand is usually employed in crystal engineering in order to synthesize new coordination polymers. The metal centers are linked with rigid bridging ligands[3] or less frequently by flexible building blocks.[4] However, for a given ligand, the structure of the resulting coordination polymer is difficult to predict because of factors affecting the framework formation, such as the solvent,[5] the counteranion[6] and the metal-to-ligand ratio.[7] The ability of the sulfur atom, as a soft base, to coordinate to the silver atom, a soft acid, has been exploited in this study. We have previously attempted to analyze the effects of the counteranions and the length of the spacer on the topology of the polymer coordination on the basis of the mutual attraction between the soft silver atom and the soft sulfur atom.[4b, 7] We have reported earlier on the structures of several silver(I) complexes with the bis(phenylthio)methane ligand[8]. In an effort to rationalize further structural effects of the ligand spacer and the counteranion, we have now synthesized and characterized a number of complexes, all based on the 1,3-bis(phenylthio)propane ligand, $L^{3\text{-Ph}}$, but with different classes of anions: weakly coordinating ones such as PF_6^- (**1**), perfluorocarboxylates: CF_3COO^- (**2**), $CF_3CF_2COO^-$ (**3**), $CF_3CF_2CF_2COO^-$ (**4**), and sulfonates: *p*-TsO^- (**5**, **6**), $CF_3SO_3^-$ (**7**, **8**, **9**). The crystal structures of **1**, **3** and **7** incorporate a molecule of solvent, either as a guest or as a coordinating molecule. The ease of release of these molecules is examined by thermogravimetric analysis.

In this study, supramolecular isomerism was observed for complexes **5**, **6** (with *p*-TsO^-), and **7**-**9** (with $CF_3SO_3^-$). The isomerism of supramolecular networks, which has been observed in similar systems, is influenced by several factors, such as the metal-to-ligand ratio[9] or the guest molecule.[10] The isomerism reported here occurred as a consequence of the solvent used for recrystallization.

2.2.3 Experimental Section

Materials and General Methods. Except for the ligand, all the reagents required for the syntheses were commercially available and employed without further purification. The elemental analyses were performed by the Laboratoire d'analyse élémentaire (Université de Montréal), the IR spectra (KBr pellets) were recorded on a Perkin-Elmer 1750 FTIR spectrometer (4000-450 cm^{-1}). ^{1}H (400 MHz and 300 MHz), $^{13}C\{^{1}H\}$ (100.56 MHz), and ^{19}F (376.31 MHz) solution NMR spectra were recorded at 25 °C, either on a Bruker ARX400, AMX300, or AV300 spectrometer. ^{1}H and ^{13}C chemical shifts are reported in parts per million and are referenced to residual solvent signals of the following deuterated solvents: DMSO ($\delta_{1H} = 2.50$) and acetone ($\delta_{1H} = 2.05$; $\delta_{13C} = 29.8$). The chemical shifts for ^{19}F were referenced to $C_6H_5CF_3$ (-63.9 ppm). The weight loss experiments were carried out, under a nitrogen atmosphere, on a TG Instrument 2950 TGA HR V5.3C thermal analyzer at a scan rate of 10 °C min^{-1}.

Syntheses. The ligand 1,3-bis(phenylthio)propane, $\mathbf{L^{3\text{-}Ph}}$, was synthesized by following a literature method.[11] Yield: 82%. Anal. Found: C, 69.36; H, 6.35. Calcd for $C_{15}H_{16}S_2$: C, 69.18; H, 6.19. ^{1}H NMR (acetone-d_6, 300 MHz): δ 2.02 (qt, 2H, -S-CH_2-C**H**$_2$-CH_2-S-), 3.08 (t, 4H, -S-C**H**$_2$-CH_2- CH_2-S-), 7.15-7.36 (*m*, 10H, C_6H_5-).

$^{13}C\{^{1}H\}$ NMR (acetone-d_6, 100.56 MHz): 34.2 (S-**C**-C), 31.8 (S-C-**C**), 126.2-136.7 (**C**$_6$H$_5$).

IR (KBr, cm^{-1}): 3052m, 2917m, 2849w, 2668w, 2604w, 1943w, 1871w, 1792w, 1583m, 1479m, 1438m, 1342w, 1297m, 1255m, 1201w, 1183w, 1155w, 1089m, 1069w, 1024m, 1000w, 957w, 895w, 836w, 736m, 689m.

$\{[Ag_2(L^{3\text{-}Ph})_4](PF_6)_2(CH_3COCH_3)_2\}_\infty$ (1). To a solution of $AgPF_6$ (290 mg, 1.15 mmol) in acetone (10 mL) was added a solution of $\mathbf{L^{3\text{-}Ph}}$ (0.25 mL, 1.08 mmol) in diethyl ether (5 mL). The mixture was kept under reflux at 50 °C for 30 min. Evaporation of the solvent in the dark and at room temperature produced single crystals suitable for X-ray analysis. Yield: 70% based on $AgPF_6$. Anal. Found: C, 47.83; H, 4.33. Calcd for $C_{66}H_{76}Ag_2F_{12}O_2S_8P_2$: C, 47.65; H, 4.60. ^{1}H NMR (DMSO-d_6, 300 MHz): δ 2.10 (qt, 2H, -S-(CH_2)-(C**H**$_2$)-), 3.31 (t, 4H, -S-(C**H**$_2$)-), 7.34-7.52 (*m*, 10H, C$_6$**H**$_5$-).

$^{19}F\{^{1}H\}$ NMR (DMSO-d_6, 376.31 MHz): -71.8 and -74.3, (d, F-P).

IR (KBr, cm^{-1}): 3444w, 3072w, 3056w, 3018w, 3002w, 2916w, 2848w, 2344w, 1943w, 1868w, 1794w, 1704w, 1637m, 1583m, 1479s, 1438s, 1384w, 1303m, 1146m, 1086m, 1069w, 1025m, 1000w, 843vs, 737s, 690s, 661w, 616w, 560s, 501m.

$[Ag_2L^{3\text{-Ph}}(CF_3CO_2)_2]_\infty$ (2). A solution of $AgCF_3CO_2$ (217 mg, 0.98 mmol) in acetone (10 mL) was stirred with a solution of $L^{3\text{-Ph}}$ (0.20 mL, 0.87 mmol) in diethyl ether (10 mL). The mixture was refluxed at 50 °C for 70 min. The resulting solution was kept for 3 days in the dark at room temperature to obtain single crystals suitable for X-ray analysis. Yield: 70% based on $AgCF_3CO_2$. Anal. Found: C, 32.68; H, 2.18. Calcd for $C_{19}H_{16}Ag_2F_6O_4S_2$: C, 32.50; H, 2.30. ^{1}H NMR (acetone-d_6, 300 MHz): δ 2.10 (qt, 2H, -S-(CH_2)-($\mathbf{CH_2}$)-), 3.28 (t, 4H, -S-($\mathbf{CH_2}$)-), 7.28-7.55 (*m*, 10H, $\mathbf{C_6H_5}$-).

^{19}F{^{1}H} NMR (acetone-d_6, 376.31 MHz): –74.15 (s, F-C).

IR (KBr, cm^{-1}): 3440w, 2914w, 2853w, 1685vs, 1583m, 1479s, 1436s, 1410w, 1208s, 1025m, 838s, 804s, 724s, 689m, 598w, 518w.

$[Ag_2L^{3\text{-Ph}}(CF_3CF_2CO_2)_2(CH_3COCH_3)]_\infty$ (3). A 10 mL volume of acetone was added to 360 mg (1.33 mmol) of $AgCF_3CF_2CO_2$. The mixture was stirred with a solution of $L^{3\text{-Ph}}$ (0.20 mL, 0.87 mmol) in diethyl ether (5 mL). The mixture was kept under reflux at 60 °C for 140 min. The resulting solution was layered on diethyl ether and then stored at room temperature in the dark. Several days later relatively large colorless crystals appeared. Yield: 35% based on $AgCF_3CF_2CO_2$. One such crystal was cut into a platelet and mounted for X-ray analysis. Anal. Found: C, 33.84; H, 2.61. Calcd for $C_{24}H_{22}Ag_2F_{10}O_5S_2$: C, 33.51; H, 2.58. ^{1}H NMR (DMSO-d_6, 300 MHz): 2.05 (qt, 2H, -S-(CH_2)-($\mathbf{CH_2}$)-), 3.19 (t, 4H, -S-($\mathbf{CH_2}$)-), 7.24-7.45 (*m*, 10H, $\mathbf{C_6H_5}$-).

^{19}F{^{1}H} NMR (DMSO-d_6, 376.31 MHz): –84.1 (CF_3) and –119.2 (CF_3CF_2).

IR (KBr, cm^{-1}): 3434w, 3075w, 2927w, 2347w, 1679vs, 1585w, 1481m, 1438m, 1411w, 1384w, 1329m, 1210m, 1159s, 1030s, 817m, 734m, 690m, 587w, 541w.

$[AgL^{3\text{-Ph}}(CF_3CF_2CF_2CO_2)]_\infty$ (4). A solution of $AgCF_3CF_2CF_2CO_2$ (252 mg, 0.78 mmol) in acetone (10 mL) was stirred with a solution of $L^{3\text{-Ph}}$ (0.25 mL, 1.08 mmol) in diethyl ether (5 mL). The mixture was refluxed at 60 °C for 70 min. The resulting solution was layered on hexane at room temperature and left in the dark. After 3 days, single crystals suitable for an X-ray analysis were obtained. Yield: 35% based on $AgCF_3CF_2CF_2CO_2$. Anal. Found: C, 39.44; H, 2.34. Calcd for $C_{19}H_{16}AgF_7O_2S_2$: C, 39.26; H, 2.77. ^{1}H NMR (acetone-d_6, 300 MHz): δ 2.05 (qt, 2H, -S-(CH_2)-($\mathbf{CH_2}$)-), 3.21 (t, 4H, -S-(CH_2)-), 7.22-7.47 (*m*, 10H, $\mathbf{C_6H_5}$-). ^{19}F{^{1}H} NMR (acetone-d_6, 376.31 MHz): –81.9 ($\mathbf{CF_3}$), –116.6 ($CF_3\mathbf{CF_2}CF_2$), –127.8 ($CF_3CF_2\mathbf{CF_2}$). IR (KBr, cm^{-1}): 3430w, 3057w, 2922w, 2345w, 1942w, 1681s, 1583w,

1480m, 1439m, 1411w, 1384w, 1340m, 1274w, 1218vs, 1157w, 1116s, 1085w, 1025m, 1144s, 1088vs, 1025m, 966w, 813m, 737m, 689m, 590w.

$[AgL^{3\text{-}Ph}(p\text{-}TsO)]_\infty$ (5). A solution of Ag(*p*-TsO) (303 mg, 1.08 mmol) in acetone (5 mL) was stirred with a solution of $L^{3\text{-}Ph}$ (0.20 mL, 0.87 mmol) in diethyl ether (5 mL). This mixture was refluxed at 60 °C for 150 min. This solution was filtered and layered on petroleum ether at room temperature. After 2 days in the dark, the mixture yielded single crystals suitable for X-ray analysis. These crystals were then stored in a freezer in order to avoid their eventual decomposition. Yield: 65% based on $Ag(C_7H_7O_3S)$. Anal. Found: C, 48.55; H, 4.15. Calcd for $C_{22}H_{23}AgO_3S_3$: C, 48.98; H, 4.30. ^{1}H NMR (acetone-d_6, 400 MHz): δ 1.96 (qt, 2H, -S-(CH_2)-(CH_2)-), 2.42 (*s*, 3H, CH_3-C_6H_4-SO_3), 3.17 (t, 4H, -S-(CH_2)-), 7.30-7.40 (m, 10H, C_6H_5-), 7.76-7.79 (*m*, 4H, CH_3-C_6H_4-SO_3).

IR (KBr, cm^{-1}): 3057w, 2919w, 1583m, 1480m, 1438m, 1390w, 1189vs, 1131m, 1044m, 1025w, 1014m, 816m, 737s, 690s, 565m.

$[AgL^{3\text{-}Ph}(p\text{-}TsO)]_\infty$ (6). The synthesis of this complex is identical to that of **5** except that **6** was recrystallized by diffusion of diethyl ether into the solution at room temperature.

The mixture was kept in the dark for two days to obtain single crystals suitable for X-ray analysis. Yield: 65% based on Ag(*p*-TsO). Anal. Found: C, 48.56; H, 4.15. Calcd for $C_{22}H_{23}AgO_3S_3$: C, 48.98; H, 4.30.^{1}H NMR (acetone-d_6, 400 MHz): δ 2.045 (qt, 2H, -S-(CH_2)-(CH_2)-), 2.40 (*s*, 3H, CH_3-C_6H_4-SO_3), 3.20 (t, 4H, -S-(CH_2)-), 7.19-7.46 (m, 10H, C_6H_5-), 7.76- 8.01 (*m*, 4H, CH_3-C_6H_4-SO_3). IR (KBr, cm^{-1}): 3439m, 2918w, 1583m, 1480m, 1438m, 1384s, 1190vs, 1131m, 1044m, 1025w, 1015m, 815m, 738s, 690s, 565m.

$[Ag_2L^{3\text{-}Ph}(CF_3SO_3)_2(CH_3COCH_3)]_\infty$ (7). A solution of $AgCF_3SO_3$ (618 mg, 2.40 mmol) in acetone (5 mL) was stirred with a solution of $L^{3\text{-}Ph}$ (0.20 mL, 0.87 mmol) in diethyl ether (5 mL). The mixture was refluxed at 60 °C for 90 min. The resulting solution was layered on petroleum ether and kept at room temperature in the dark. After 4 days, single crystals suitable for X-ray analysis were obtained. Yield: 40% based on $AgCF_3SO_3$. Anal. Found: C, 28.29; H, 2.27. Calcd for $C_{20}H_{22}Ag_2F_6O_7S_4$: C, 28.86; H, 2.66. ^{1}H NMR (DMSO-d_6, 300 MHz): δ 2.11 (qt, 2H, -S-(CH_2)-(CH_2)-), 3.34 (t, 4H, -S-(CH_2)-), 7.36-7.57 (*m*, 10H, C_6H_5-). ^{19}F{^{1}H} NMR (DMSO-d_6, 376.31 MHz): –79.1 (s, F-C). IR (KBr, cm^{-1}): 3056w, 2917w, 1583m, 1480m, 1438m, 1258vs, 1178s, 1089w, 1069w, 1033s, 837w, 769w, 737s, 690s, 642s, 580m, 519m.

$[Ag_2L^{3\text{-}Ph}(CF_3SO_3)_2]_\infty$ (8). To a solution of $AgCF_3SO_3$ (275 mg, 1.07 mmol) in acetone

(5 mL) was added a solution of $L^{3\text{-Ph}}$ (0.20 mL, 0.87 mmol) in diethyl ether (5 mL). The mixture was stirred at 50 °C for 40 min, then layered on diethyl ether and left to stand in the dark at room temperature. Crystals suitable for an X-ray study appeared after 3 weeks. Yield: 38% based on $AgCF_3SO_3$. Anal. Found: C, 26.78; H, 2.15. Calcd for $C_{17}H_{16}Ag_2F_6O_6S_4$: C, 26.37; H, 2.08. ^{1}H NMR (acetone-d_6, 300 MHz): 2.25 (qt, 2H, -S-(CH_2)-(CH_2)-), 3.18 (t, 4H, -S-(CH_2)-), 7.21-7.41 (*m*, 10H, C_6H_5-).

^{19}F{^{1}H} NMR (acetone-d_6, 376.31 MHz): –79.2 (s, F-C).

IR (KBr, cm^{-1}): 3436m, 2923w, 1630m, 1583w, 1481m, 1438m, 1385s, 1260vs, 1178m, 1089m, 1034s, 874w, 804w, 739m, 691m, 645m, 582w, 520w.

$[Ag_2L^{3\text{-Ph}}(CF_3SO_3)_2]_\infty$ (9). To generate different structures the molar ratio of silver salt to ligand was modified. To a solution of $AgCF_3SO_3$ (614 mg, 2.40 mmol) in acetone (5 mL) was added a solution of $L^{3\text{-Ph}}$ (0.30 mL, 1.30 mmol) in diethyl ether (5 mL). The mixture was stirred at 60 °C for 160 min, then layered on hexane and left to stand in the dark at room temperature. Crystals suitable for an X-ray study appeared after 3 weeks. Yield: 81% based on $AgCF_3SO_3$. These crystals had a clearly different morphology from those of **8**. Anal. Found: C, 26.06; H, 1.91. Calcd for $C_{17}H_{16}Ag_2F_6O_6S_4$: C, 26.37; H, 2.08. ^{1}H NMR (acetone-d_6, 300 MHz): 2.35 (qt, 2H, -S-(CH_2)-(CH_2)-), 3.35 (t, 4H, -S-(CH_2)-), 7.31-7.55 (*m*, 10H, C_6H_5-). ^{19}F{^{1}H} NMR (acetone-d_6, 376.31 MHz): –78.8 (s, F-C).

IR (KBr, cm^{-1}): 3434m, 3061w, 2924w, 1694w, 1623m, 1476w, 1442w, 1257vs, 1172s, 1030s, 805w, 742m, 687m, 636s, 576w, 521m, 496w.

$\{[Ag_2(L^{3\text{-Ph}})_4](ClO_4)_2(CH_3COCH_3)_2\}_\infty$ (10), $\{[Ag_2(L^{3\text{-Ph}})_4](SbF_6)_2(CH_3COCH_3)_2\}_\infty$ (11). Other complexes related to **1** were synthesized[12] using weakly coordinating anions: ClO_4^- (**10**), SbF_6^- (**11**). Their syntheses follow the procedure described for **1**. These will not be fully described as the acetone molecules were too disordered to be precisely located.

Caution! Although we met no problems in handling perchlorate salts, great care should be taken due to their potential explosive nature.

Crystal Structure Determinations. X-ray diffracted intensities were measured on a Bruker AXS Platform diffractometer equipped with a SMART 2K CCD area detector using monochromatic CuKα (λ = 1.54178 Å) radiation. The X-ray intensity data were processed with the program SAINT.[13] An empirical absorption correction, based on multiple measurements of equivalent reflections, was applied using the program SADABS.[14] The space group was confirmed by the XPREP[15] routine in the program SHELXTL.[16] The

structures were solved by direct methods and refined by full-matrix least-squares and difference Fourier techniques.[17] All non-hydrogen atoms were refined anisotropically, while the hydrogen atoms were introduced at calculated positions using a riding model and refined isotropically. The thermal parameters of the fluorine atoms of the PF_6^- counter anions in complex **1** were slighty higher than those of the other atoms in the structure indicating a slight disorder for this group. Because the acetone molecules were also disordered their carbon atoms were refined isotropically. The occupancy factors of the two disordered pentafluoropropionate anions in complex **3** were refined. One anion is split over two sites, with occupancies of 61 and 39%, while the other occupies four sites in the proportions of 39, 15, 27 and 19%. The C-F distances in both anions were constrained to be equal (SADI[16]). The thermal parameters of all disordered atoms were constrained such that the corresponding atoms of the major and the minor entities kept the same values (EADP[16]). Because of the correlation between the temperature factor and the occupancy factor, the former was refined isotropically. Finally, the occupancy factor was fixed and the model was refined anisotropically with the ISOR[16] constraints imposed on the fluorine atoms. The data collection for **8** was limited to $\theta = 55^{\circ}$, since the crystal did not diffract at higher angles. The solvent molecules in **10** and **11**, present in a very disordered state, prevented us from establishing their exact position within the structures. However, the main constituents of the structures were found without ambiguity. Crystal data, data collection and structure refinement parameters are listed in Table 2.2.1.

Table 2.2.1. Crystal data and X-ray data collection parameters.

	1	2	3	4	5
formula	$C_{66}H_{76}Ag_2F_{12}O_2S_8P_2$	$C_{19}H_{16}Ag_2F_6O_4S_2$	$C_{24}H_{22}Ag_2F_{10}O_5S_2$	$C_{19}H_{16}AgF_7O_2S_2$	$C_{22}H_{23}AgO_3S_3$
mol wt	1663.51	702.18	860.28	581.31	539.45
cryst size (mm)	0.35×0.25×0.15	0.31×0.12×0.03	0.23×0.12×0.03	0.43×0.11×0.04	0.21×0.13×0.10
cryst system	monoclinic	monoclinic	monoclinic	monoclinic	monoclinic
space group	$P2_1/c$	$P2_1/c$	$C2/c$	$C2/c$	$P2_1/n$
a (Å)	26.7293(3)	26.1193(2)	25.5907(3)	17.1456(2)	15.0658(2)
b (Å)	13.0101(1)	11.2175(1)	8.4233 (1)	8.3145(1)	8.8692(1)
c (Å)	20.9805(2)	7.3670(1)	29.4683 (3)	30.1588(3)	16.2685(2)
α (deg)	90	90	90	90	90
β (deg)	95.253(1)	91.709(1)	107.886(1)	105.543(1)	93.760(1)
γ (deg)	90	90	90	90	90
V (Å^3)	7265.34(12)	2236.59(4)	6045.13(12)	4142.12(8)	2169.14(5)
Z	4	4	8	8	4
D(calcd) (g cm^{-3})	1.521	2.085	1.890	1.864	1.652
F(000)	3392	1368	3376	2304	1096
Temp (K)	220(2)	220(2)	220(2)	100(2)	220(2)
μ, (mm^{-1})	7.514	16.501	12.574	10.420	10.329
θ_{max} (deg)	72.98	72.91	72.94	72.89	72.90
R1[a] [$I > 2\sigma(I)$]	0.0622	0.0446	0.0527	0.0367	0.0452
Rw[b] [$I > 2\sigma(I)$]	0.1746	0.1099	0.1357	0.0878	0.1264
R [all data]	0.0727	0.0495	0.0545	0.0426	0.0511
Rw [all data]	0.1830	0.1129	0.1378	0.0902	0.1309
S[c]	1.072	1.007	1.053	0.998	1.055

	6	7	8	9
formula	$C_{22}H_{23}AgO_3S_3$	$C_{20}H_{22}Ag_2F_6O_7S_4$	$C_{8.5}H_8AgF_3O_3S_2$	$C_{17}H_{16}Ag_2F_6O_6S_4$
mol wt	539.45	832.36	387.14	774.28
cryst size (mm)	0.26×0.24×0.17	0.30×0.07×0.05	0.17×0.05×0.02	0.21×0.12×0.09
cryst system	monoclinic	monoclinic	monoclinic	monoclinic
space group	$P2_1/c$	$P2_1/n$	$C2/c$	$P2_1/n$
a (Å)	14.6787(3)	8.4179(2)	28.9764(10)	8.1416(1)
b (Å)	9.8460(2)	24.1660(4)	4.8104(2)	23.6395(2)
c (Å)	15.7897(4)	13.9928(2)	20.3261(7)	12.3921(1)
α (deg)	90	90	90	90
β (deg)	99.383(2)	93.960(1)	119.012(1)	90.757(1)
γ (deg)	90	90	90	90
V (Å^3)	2251.50(9)	2839.72(9)	2477.70(16)	2384.82(4)
Z	4	4	8	4
D(calcd) (g cm^{-3})	1.591	1.947	2.076	2.157
F(000)	1096	1640	1512	1512
Temp (K)	220(2)	220(2)	220(2)	100(2)
μ, (mm^{-1})	9.952	14.538	16.569	17.214
θ_{max} (deg)	72.85	72.77	55.03	72.75
R1[a] [$I > 2\sigma(I)$]	0.0461	0.0561	0.0367	0.0476
Rw[b] [$I > 2\sigma(I)$]	0.1157	0.1366	0.0727	0.1292
R [all data]	0.0624	0.0669	0.0608	0.0727
Rw [all data]	0.1226	0.1433	0.0778	0.1507
S[c]	0.975	0.975	0.898	1.097

[a] $R = \Sigma \, ||F_o| - |F_c|| / \Sigma \, |F_o|$. [b] $R_w = [\Sigma \, w (F_o^2 - F_c^2)^2 / \Sigma \, w(F_o^2)^2]^{1/2}$.
[c] $S = [\Sigma \, w(F_o^2 - F_c^2)^2 / (m-n)]^{1/2}$ (m is the number of reflections and n the number of parameters).

2.2.4 Results and Discussion

Crystal structures. **$\{[Ag_2(L^{3\text{-Ph}})_4](PF_6)_2(CH_3COCH_3)_2\}_\infty$ (1).** Complex **1** forms a two-dimensional coordination network, in which each crystallographically independent Ag(I) is linked in a tetrahedral manner to a sulfur atom of four different $L^{3\text{-Ph}}$ ligands. The other

sulfur atom of each ligand is bound to a neighboring Ag(I) ion thus forming a cationic sheet parallel to the (001)-plane (Figure 2.2.1a). The Ag–S distances, 2.538(1) – 2.598(1) Å, fall within the normal range of the silver(I) – thiol complexes. The silver atoms adopt a distorted tetrahedral environment (S–Ag(1)–S: 104.4(1) – 116.5(1)°; S-Ag(2)-S: 99.0(1) – 128.6(1)°). The PF_6^- anions and the acetone molecules are inserted between the layers. The distance between sheets is half the *c*-dimension of the unit cell (10.49 Å). The sheets are stacked parallel to the *ab*-plane. The repeating unit in **1** is a 24-membered macrometallocycle $Ag_4(\mathbf{L}^{3\text{-Ph}})_4$. The S···S distances of the ligands are different and have values of: 5.525(1), 5.510(1), 5.027(1), and 5.535(1) Å, respectively. This complex forms a noninterpenetrating framework and the phenyl groups are located on both sides of the layers in a manner comparable to the 1,4-bis(phenylthio)butane ligand.[7] In the packing of the structural units, the aromatic rings are concentrated in a plane at *c*/2 that also includes the PF_6^- anions and the acetone molecules (Figure 2.2.1b). The weakly coordinating counterions such as tetrafluoroborate[18] and hexafluorophosphate are situated between the cationic sheets instead of being coordinated to the metal. However, since **1** also accommodates acetone molecules between layers, a thermogravimetric investigation was undertaken in order to establish how strongly the acetone molecules are held within the structure (see below).

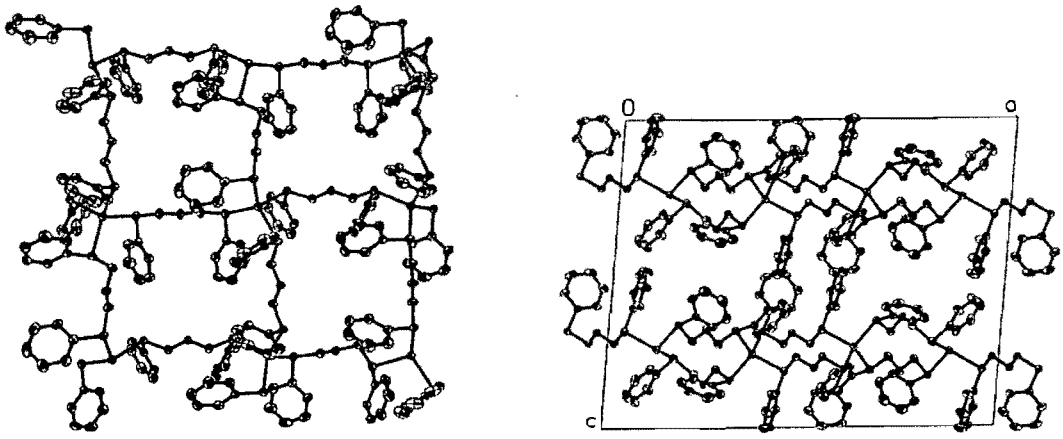

(a) (b)

Figure 2.2.1. (a) The cationic sheet of **1** parallel to (001) (The anions, the acetone and the H atoms are omitted for clarity.) (b) Packing of **1** shown as a projection of the cationic sheets onto the *ac*-plane.

$\{[Ag_2(L^{3\text{-}Ph})_4](ClO_4)_2(CH_3COCH_3)_2\}_\infty$ (10), $\{[Ag_2(L^{3\text{-}Ph})_4](SbF_6)_2(CH_3COCH_3)_2\}_\infty$ (11). Complexes **1**, **10** and **11** have comparable unit cell dimensions, space groups, and stoichiometries.[12] The structure consists of $Ag_2(L^{3\text{-}Ph})_4$ layers (silver(I) and ligands) between which are inserted the anions and the guest molecules. These cationic sheets are practically identical to **1** (Figure S1a-d, Annexe II). Furthermore, as we report above for the PF_6^- anion, the acetone molecules present in **10** and **11** are in a very disordered state. Hence, the above three compounds **1**, **10**, and **11**, may be considered as being isostructural. Related structures, $[Ag(PhSCH_2CH_2CH_2SPh)_2]^+$ with the BF_4^- anion and water and $[Ag(PhSeCH_2CH_2CH_2SePh)_2]^+$ with BF_4^- and CH_2Cl_2, were reported by Black *et* al.[18,19] The authors indicate a 3D-network, but their compounds are in fact "isostructural" with **1**, **10**, and **11**, although the guest is now water (Figure S1d, Annexe II) or CH_2Cl_2. Common to all these structures is the fact that the anions have a slight oscillating disorder and the guest is, in most cases, very disordered. This is a typical occurrence in host-guest (intercalation) compounds. In contrast, it is worth pointing out that the structures observed when the shorter bis(phenylthio)methane ligand is combined with the same anions, a 1D-coordination polymer is observed instead of the layered structure.[8] Furthermore, XY_4^- anions, as well as CF_3COO^- and $CF_3SO_3^-$, are coordinated to the Ag(I) ions. In order to study the effect of the anion upon the network, complexes with more strongly coordinating counteranions such as trifluoroacetate and trifluoromethanesulfonate were studied.[20]

$[Ag_2L^{3\text{-}Ph}(CF_3COO)_2]_\infty$ (2). Two silver atoms are joined in a bridging mode by two trifluoroacetate groups, thus giving rise to a $Ag_2(O_2CCF_3)_2$ dimer[21a] (Scheme 1). These dimers are linked together by the ligands, through μ_2-S bridge, so as to form a chain parallel to the *b*-axis (Figure S2, Annexe II).

Scheme 1

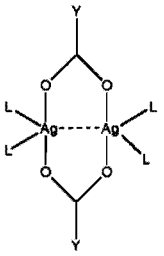

Y: CF_3 (**2**), CF_3CF_2 (**3**) and $CF_3CF_2CF_2$ (**4**)

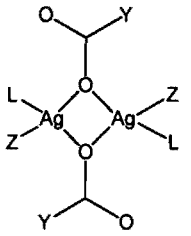

Y: CF_3CF_2, Z: acetone (**3**)

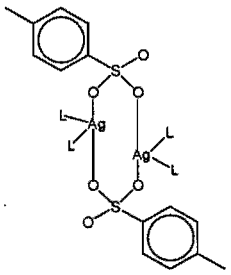

(**5**)

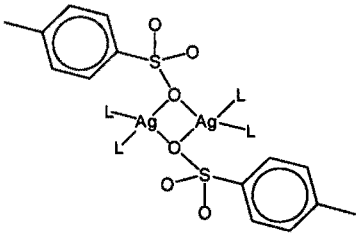

(**6**)

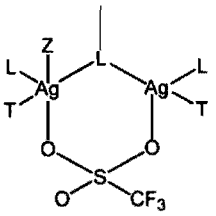

(**7**)

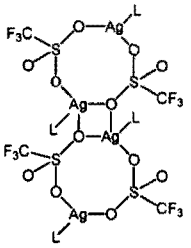

(**8**)

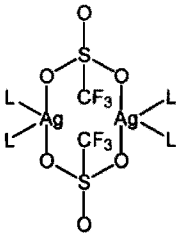

(**9**)

Z = acetone; L = 1,3-bis(phenylthio)propane; T = $CF_3SO_3^-$

Since each sulfur is bound to two silver ions, the chains are interconnected and form a 2D-coordination network (Figure 2.2.2a). Each Ag(I) ion is linked to two sulfur atoms from two distinct ligands (Ag–S: 2.478(1) and 2.697(1) Å), and to two oxygen atoms from two distinct trifluoroacetate groups (Ag–O: 2.268(3) and 2.348(3) Å). There is a further weak bond between the silver atoms of the dimer (Ag···Ag: 3.2459(5) Å). Thus, the coordination around the silver atom is a distorted triangular bipyramid (S–Ag–S: 155.6(1), O–Ag–O: 110.2(2), 112.1(1) and 133.0(1)°).

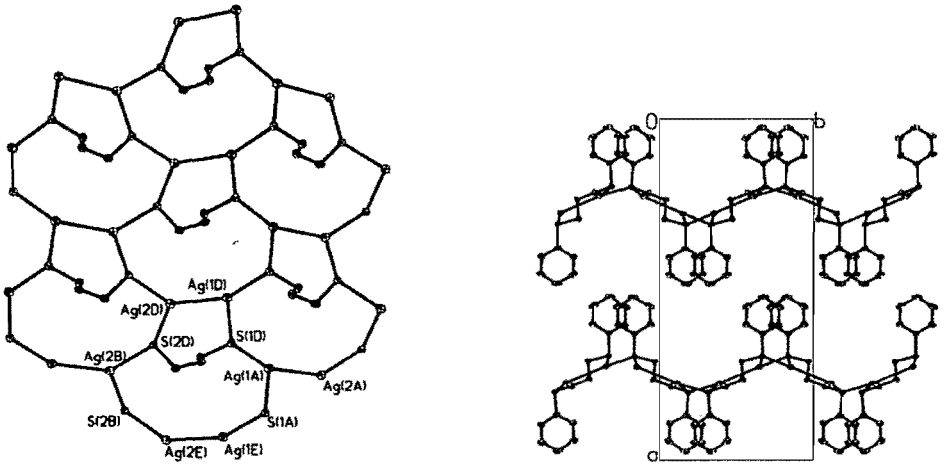

(a) (b)

Figure 2.2.2. (a) Repeat unit of **2** showing the 7-and 11-membered metallomacrocycles associated in a sheetlike structure. (The phenyl and the trifluoroacetate groups, as well as the H atoms, are omitted for clarity) (b) Sheets, perpendicular to the *a*-axis, shown edge-on in this packing of **2**. Note the "in-phase" disposition of consecutive layers.

The Ag···Ag interaction is somewhat longer than that observed in trifluoroacetate-bridged silver-silver systems (3.16 Å[22]) or from our own results,[8] but significantly shorter than the sum of the van der Waals radii (3.40 Å).[23] The S···S distance for all the ligands is 4.938(1) Å. The repeat unit of this complex is formed by two rings sharing a side that are an 11-membered, $Ag_4\mathbf{L}^{3\text{-Ph}}S_2$, and a 7-membered, $Ag_2\mathbf{L}^{3\text{-Ph}}$ metallomacrocycle (Figure 2.2.2a). These rings constitute a puckered 2D-network of $[Ag_2\mathbf{L}^{3\text{-Ph}}(CF_3COO)_2]_\infty$, sheets parallel to the (100)-plane and separated by *a*/2 (Figure 2.2.2b). In addition, the topology of this complex is that of a wire netting, where the repeat unit is a chairlike 6-membered ring reminiscent of that adopted by some elements such as arsenic, antimony and bismuth[24, 25] (Figure S3, Annexe II).

$[Ag_2\mathbf{L}^{3\text{-Ph}}(CF_3CF_2CO_2)_2(CH_3COCH_3)]_\infty$ (3). In this complex, which incorporates an acetone molecule, there are two kinds of silver atoms. On one hand, Ag(1) atoms are coordinated to two sulfurs from two distinct ligands (Ag–S: 2.500(1) and 2.625(1) Å) and to two oxygens from two different pentafluoropropionates (Ag–O: 2.345(4) and 2.359(4) Å). In addition, two neighboring Ag(I) atoms are connected in a diatomic bridging mode by two pentafluoropropionates to form a $Ag_2(O_2CCF_2CF_3)_2$ dimer (Chart 1). These silver atoms are weakly bound, as the Ag(1)···Ag(1) distance is only 3.0502(7) Å.

The coordination of Ag(1) is that of a distorted square-based pyramid (S–Ag(1)–Ag(1) = 150.6(1)°; O–Ag(1)–O = 103.6(1), 123.7(2), and 123.8(2)°). On the other hand, the other silver atom, Ag(2), is coordinated to the oxygen of the acetone molecule (Ag(2)–O: 2.333(4) Å), to two other oxygen atoms, each from a different pentafluoropropionate (Ag(2)–O: 2.354(4), 2.408(4) Å) and to a sulfur atom also bound to Ag(1), (Ag(2)–S: 2.488(1) Å). This second silver atom, Ag(2), has the environment of a distorted tetrahedron (S–Ag(2)–O = 125.8(1), 115.8(1)°; O–Ag(2) –O = 110.4(2), 78.6(2)°). Two adjacent Ag(2) atoms are coupled in a monatomic bridging mode by two pentafluoropropionates, thus building the $Ag_2(O_2CCF_2CF_3)_2$ dimer (Chart 1). However, the long Ag(2)···Ag(2) distance, 3.6854(8) Å, signals the absence of any interaction between the Ag(2) ions.[23] There are two distinct repeat units in this complex, unit **A** (Figure 2.2.3a) and unit **B** (Figure 2.2.3b, Figure S4, Annexe II). In unit **A**, two pentafluoropropionate groups bring adjacent silver atoms together in a dibridging mode. Two of these are linked into a 14-membered-ring, the $Ag_4(\mathbf{L}^{3\text{-Ph}})_2$ repeat unit **A**, by two ligand molecules. The **A** units share Ag···Ag edges and, in doing so, give rise to a ribbon. The **B** units, whose pairs of neighboring silver atoms are tied in a monoatomic bridging mode by pentafluoropropionate groups, consist of 20-membered-rings. They, in turn, share edges yielding another ribbon. Neighboring **A** and **B** ribbons share their ligand edges resulting in a 2D-sheet (Figure 2.2.3c). The neutral sheets are stacked parallel to the (100)-plane (Figure 2.2.3d). The S···S distances in all the ligands of complex **3** are 5.621(3) Å long.

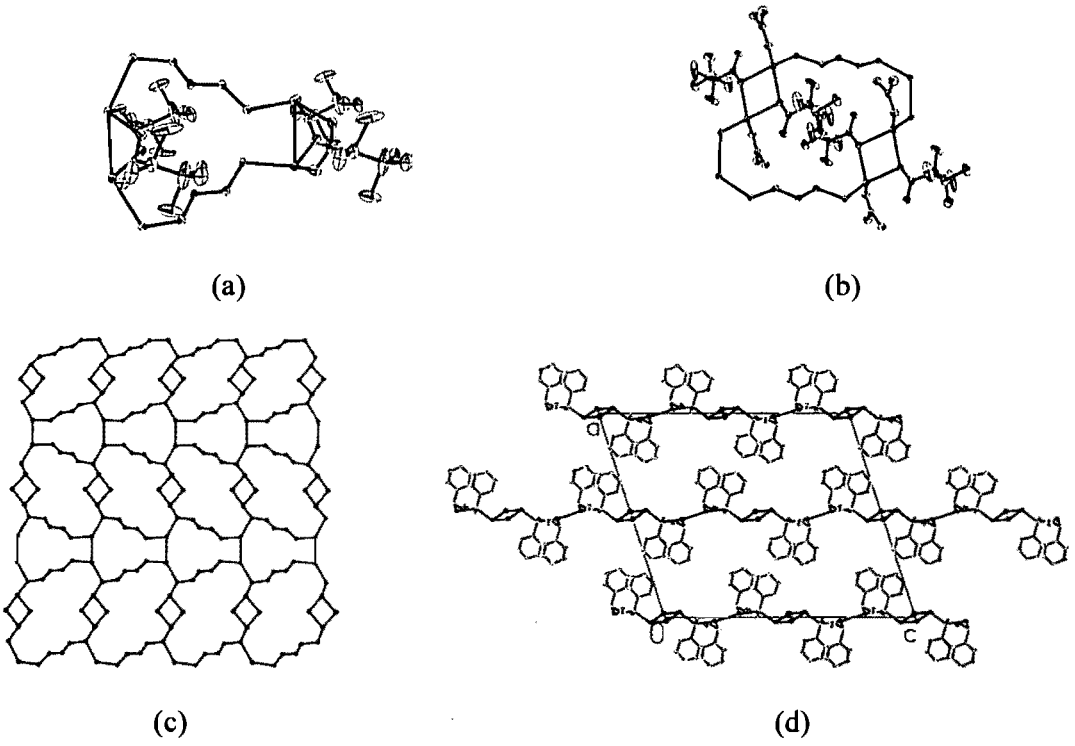

Figure 2.2.3. (a). **A** repeat unit of complex **3**. (Phenyl group and H atoms are omitted for clarity.) (b) View of the **B** repeat unit. (c) Association of the **A** and **B** units into ribbons, which in turn combine into the 2D-network of **3**. (d) Packing of complex **3**. The layers are shown edge-on.

$[AgL^{3\text{-}Ph}(CF_3CF_2CF_2CO_2)]_\infty$ (4). Here, two adjacent silver atoms are brought together in a diatomic bridging mode by two heptafluorobutyrate anions (Chart 1) resulting in $Ag_2(O_2CCF_2CF_2CF_3)_2$ dimers, which are connected by two ligands to generate a double chain parallel to the *b*-axis (Figure 2.2.4a, b). The packing of the chains, projected end on onto the *ac*-plane, is of the distorted hexagonal-type (Figure 2.2.4c). Each silver atom is linked to two oxygen atoms (Ag–O: 2.330(2) and 2.417(2) Å), from different heptafluorobutyrate groups, to two sulfur atoms from distinct ligands (Ag–S: 2.5027(8) and 2.5913(8) Å) and to another silver atom (3.1594(4) Å). Hence, the silver atom has a 5-fold coordination (O–Ag–O = 119.4(1)°, O–Ag–S = 110.2(1), 117.1(1)° and S–Ag–Ag = 149.5(1)°). The short silver-silver distance indicates again a weak metal-metal interaction.[22, 27] The repeat unit of complex **4** is a 14-membered metallomacrocycle, $Ag_4(L^{3\text{-}Ph})_2$, which is identical to that of unit **A** of complex **3**. However, contrary to **3**, complex **4** forms a 1D-coordination polymer. It seems that the increased length and bulk of the counteranion prevent the formation of **B** units as in complex **3**.

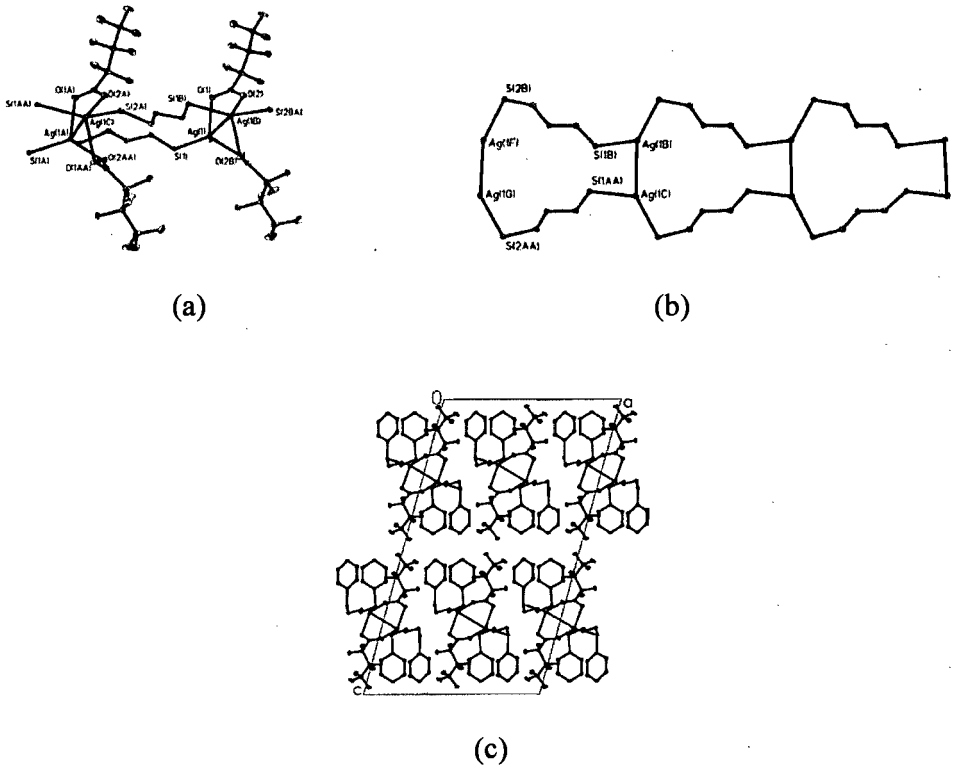

Figure 2.2.4. (a) View of the repeat unit of **4** and (b) their association into a 1D-chain extending parallel to the *b*-axis. (The phenyl and heptafluorobutyrate groups and the H atoms are omitted for clarity). (c) Packing projection of complex **4**, showing the chains perpendicular to the *ac*-plane.

It is worth noting that the fluorocarbon chain length of the counteranion modifies the supramolecular networks. Indeed, complexes **2** ($CF_3CO_2^-$) and **3** ($CF_3CF_2CO_2^-$) form 2D-networks, whereas complex **4** ($CF_3CF_2CF_2CO_2^-$) is a 1D-coordination polymer. This fact shows the influence of the size of the counteranion upon the supramolecular architecture. The S···S distances in all ligands of complexes **3** and **4** are respectively 5.621(3) Å and 5.537(1) Å. These distances are significantly longer than that in complex **2**, 4.938(1) Å. This difference may be explained by the fact that the heptafluorobutyrate and the pentafluoropropionate anions are more flexible than the trifluoroacetate, thus allowing complexes **3** and **4** to be less strained than complex **2**. This fact reveals that the structure of coordination polymers based on flexible ligands depends not only on their flexibility[7] but also on the size of the counteranion, when the latter is part of the network. The carboxylate planes in each dimer form a dihedral angle of about 120° and the averaged C–O distances remain fairly constant (1.228, 1.216 and 1.236 Å in **2-4**, respectively). However, the average Ag–O distance increases from 2.290 for **2**, to 2.351 for 3, and 2.374 Å for **4**.

This observation seems to point to a correlation between Ag–O distance and the increasing electron withdrawing power related to the number of fluorine atoms in the anions, increasing from acetate to butyrate. Here again, when the shorter bis(phenylthio)methane ligand is used with perfluorocarboxylate anions, no 2D-networks are reported, but double-stranded 1D-chains are noted.[8]

$[AgL^{3\text{-Ph}}(p\text{-TsO})]_\infty$ (5). In this complex, two silver atoms and two *p*-tosylate groups form a dimer in a bridging mode through two of the latter's oxygen atoms. The dimers are interconnected by the ligand molecules, giving rise to a double chain extending parallel to the *b*-axis (Figure 2.2.5a-c). Hence, the structure of this complex may be described as a ladderlike 1D-coordination polymer. The repeat unit of this double chain may be seen as the combination of a 20-membered, $Ag_4(\mathbf{L}^{3\text{-Ph}})_2O_4S_2$, and an 8-membered $Ag_2O_4S_2$, metallomacrocycles. The silver(I) ion adopts a distorted tetrahedral coordination: the Ag–S distances are 2.496(1) and 2.578(1) Å, while the Ag–O distances are 2.472(4) and 2.348(4) Å. The bond angles are O–Ag–O = 109.2(2) and O–Ag–S = 131.5(1), 103.5(1), and 88.2(2)°. The S···S separation in every ligand is 5.548(1) Å indicative of a fully extended conformation. The Ag···Ag distance, which is 3.7503(5) Å, excludes any metal-metal interaction[23] (Chart 1). The projection of the structure onto the *ac*-plane reveals that each double chain is surrounded by four others in a centered-type of packing (Figure 2.2.5c).

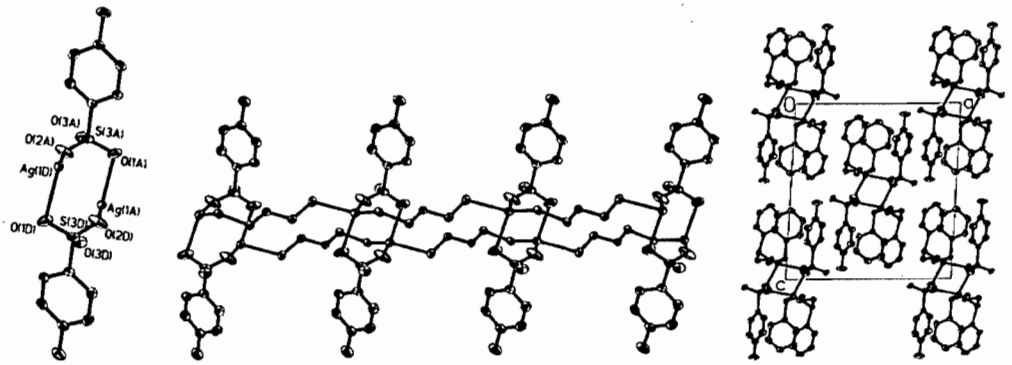

(a) (b) (c)

Figure 2.2.5. (a) Repeat unit of **5** showing the 8-membered $Ag_2O_4S_2$. (b) 20-membered $Ag_4(\mathbf{L}^{3\text{-Ph}})_2O_4S_2$ metallomacrocycles as part of the 1D-chain extending in the *b*-direction. (The phenyl groups and the H atoms are omitted for clarity.) (c) Packing of the chains of **5** seen along the chain axis.

$[AgL^{3\text{-Ph}}(p\text{-TsO})]_\infty$ (6). Complex **6** was obtained in the same manner as **5**, except that the recrystallization solvent was diethyl ether instead of petroleum ether used for **5**. As a

consequence, a totally different structure is observed. The repeat unit of **6** consists of a 28-membered, $Ag_6(L^{3\text{-Ph}})_4$, metallomacrocycle. Taking part in that large ring are four 4-membered, Ag_2O_2, diamond shaped rings (Figure 2.2.6a). In this diamond-shaped ring two silver atoms are bridged by two oxygen atoms, each from a different *p*-tosylate anion (Scheme 1). The distorted tetrahedral coordination of silver is completed with two S atoms from different ligands. The larger rings share edges and form puckered layers parallel to the *bc*-plane (Figure 2.2.6b). The projection of the layers onto the *ab*-plane clearly shows the disposition of the aromatic rings on either side of the layer (Figure 2.2.6c). Each silver is bound to two sulfur atoms (Ag–S: 2.461(1) and 2.468(1) Å) from different ligands and to two oxygen atoms from distinct *p*-tosylate groups (Ag–O: 2.400(3) and 2.491(3) Å). The bond angles are as follows: O–Ag–O = 74.9(1)°; S–Ag–S = 150.3(1)°; O–Ag–S 113.8(1) and 92.9(1)°. The S···S separation for all ligands is 4.954(3) Å, establishing the existence of *gauche* torsion angles in the aliphatic sequence of the ligand in this form of the complex.

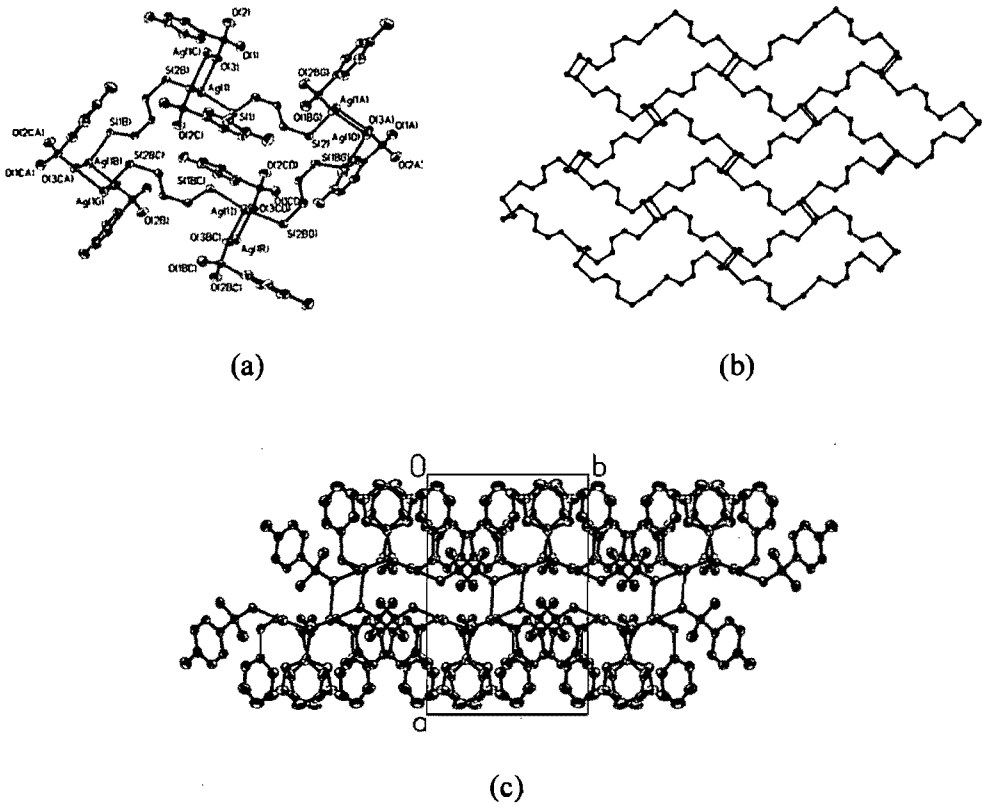

Figure 2.2.6. (a) Atomic numbering and the repeat unit of **6** showing the 4-membered Ag_2O_2 and the 28-membered, $Ag_6(L^{3\text{-Ph}})_4$ metallomacrocycles. (The phenyl groups and the H atoms are omitted for clarity.) (b) A view of the 2D-polymer coordination of **6** parallel to (100)-plane. (c) Double-layer sheet of complex **6** shown edge on.

$[Ag_2L^{3\text{-}Ph}(CF_3SO_3)_2(CH_3COCH_3)]_\infty$ (7). Here adjacent silver ions are linked by the triflate anion and by the S of a ligand in a μ_2-S bridging mode (Scheme 1). Adjacent silver ions are linked by the trifluoromethanesulfonate into a chain parallel to the [202]-direction and every second silver atom is attached an acetone molecule (Figure S5, Annexe II). These chainlike structures are then interconnected by ligand molecules, thus yielding a 2D-network whose repeat unit is a 16-membered metallomacrocycle, $Ag_4(L^{3\text{-}Ph})_2S_2$ (Figure 2.2.7a, b). The $[Ag_2L^{3\text{-}Ph}(CF_3SO_3)_2(CH_3COCH_3)]_\infty$ sheets are parallel to the (010)-plane (Figure 2.2.7c). It is worth noting that there are two distinct silver atoms (Figure S6a, Annexe II). On one hand, Ag(1) has the environment of a distorted tetrahedron (Ag(1)-S = 2.516(1) and 2.590(1) Å; Ag(1)-O = 2.356(4) and 2.463(5) Å; S–Ag(1)–S = 124.6(1)°; O–Ag(1)–S = 131.4(1), 103.9(1), and 83.1(1)°). The other silver atom, Ag(2), is coordinated to two sulfur atoms from two distinct ligands (Ag(2)–S: 2.602(1) and 2.631(1) Å), to two oxygen atoms from two distinct trifluoromethanesulfonates (Ag(2)–O: 2.518(5) and 2.393(4) Å) and to the oxygen atom of an acetone molecule (Ag(2)–O: 2.486(4) Å). Thus, Ag(2) adopts a distorted triangular bipyramid coordination (O–Ag(2)–O : 170.6(2)°, O–Ag(2)–S : 128.1(1), 106.3(1), and 124.8(1)°). Since the S···S separation in all ligands is 5.609 (2) Å, they are in the all-trans conformation.

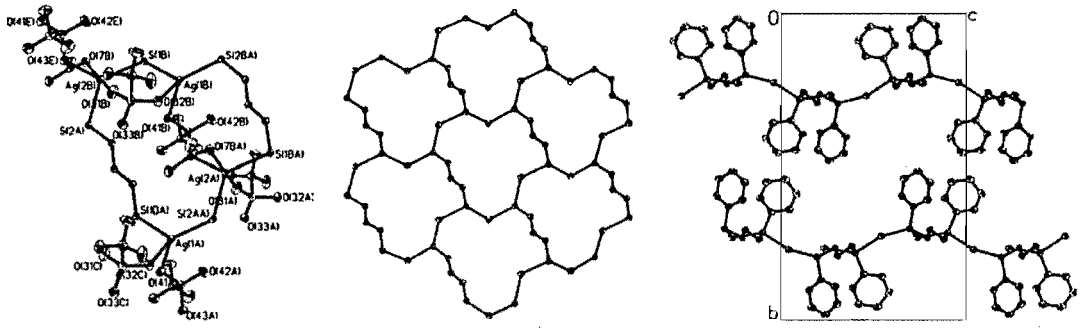

(a) (b) (c)

Figure 2.2.7. (a) Atomic numbering and structure showing the two distinct environments of the silver atom in complex 7. (b) View of the 2D-sheet parallel to the (010)-plane. (The phenyl groups and the H atoms are omitted for clarity). (c) Packing of 7 illustrating the "in-phase" relative disposition of the sheets. The anions are omitted for clarity.

$[Ag_2L^{3\text{-}Ph}(CF_3SO_3)_2]_\infty$ (**8**). Complex **8** was synthesized with a ligand-to-silver salt ratio different from that used for 7. The recrystallization solvent was diethyl ether as opposed to petroleum ether in the case of 7. In the structure of **8**, the asymmetric unit contains only

half the above composition. Hence, the central carbon of the ligand is on a crystallographic two-fold axis. Each silver atom is linked to three oxygen atoms from three different trifluoromethanesulfonates (Ag–O: 2.415(4), 2.459(4) and 2.481(4) Å) to build a chain along the *b*-axis formed by the alternation of two adjacent Ag_2O_2 and $Ag_2O_4S_2$ rings (Figure 2.2.8a). In turn, these chains are linked through the ligands along the *c*-axis so as to generate a 2D-coordination network (Ag-S: 2.445(2) Å) (Figure 2.2.8b). The silver atom adopts a distorted tetrahedral coordination where the bond angles range from 77.4(1) to 141.0(1)°. The S···S separation for all the ligands is 5.418(3) Å. The repeat unit of this complex is a 21-membered metallomacrocycle. The complex forms layers parallel to the (100)-plane spaced at *a*/2 intervals. The complex adopts a zigzag-like 2D-coordination polymer (Figure 2.2.8c).

Both the monatomic bridge and the double-bridge modes are observed in this compound obtained from diethyl ether. When petroleum ether was used, only the double-bridged mode was noted (complex 7) (Scheme 1).

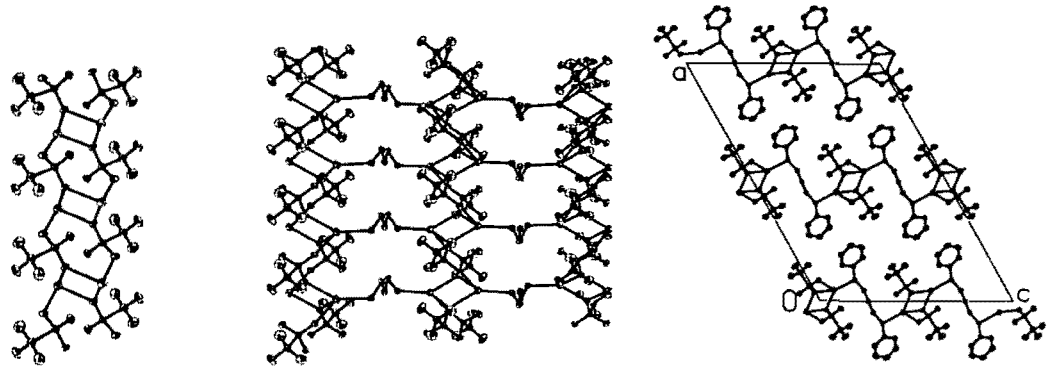

(a) (b) (c)

Figure 2.2.8. (a) 1D-chain of complex **8** is made up of two adjacent rings: the square Ag_2O_2; the puckered $Ag_2O_4S_2$. (b) The 2D-sheet structure of **8** obtained with the ligand linking the chains. The sheet is parallel to (100). The phenyl and triflate groups and the H atoms are omitted for clarity. (c) Packing diagram, showing the sheets parallel to the *bc*-plane. The chains (a) are parallel to the *b*-axis.

$[Ag_2L^{3\text{-}Ph}(CF_3SO_3)_2]_\infty$ (9). Although it does not contain acetone, this third complex, with the trifluoromethanesulfonate anion, bears a very strong topological relationship with 7 (Figure S7, Annexe II). The two silver atoms, although crystallographically distinct, have the same kind of environment. Ag(1) and Ag(2) are connected, in a dibridging mode, by the oxygen atoms from two CF_3SO_3 anions (Figure 2.2.9a, Chart 1). Each silver is, in turn, bound to another one through a μ_2-S bridge (Figure 2.2.9a, Figure S6b, Annexe II). Thus, a

metallomacrocycle of composition $Ag_4(L^{3\text{-}Ph})_2S_2$ is obtained. This metallomacrocycle is identical to that observed for **7**, although the anions are connected to the silver ions in different ways. Nethertheless, there is also an acetone molecule bound to one of the silver ions of **7**. The projection of the 2D-network on the *bc*-plane is shown in Figure 2.2.9b. The backbone undulations from one layer to the next are "out-of-phase", while they are "in-phase" for **7** (Figure 2.2.7c, Figure S8, Annexe II). The S1··S2 distance of 5.538(2) Å indicates that the ligands are in the fully extended conformation. The two Ag(1) and Ag(2) ions, forming a dimer with a triflate and a μ_2-S bridge do not interact since they are separated by 4.8535(5) Å. Interestingly, the bis(phenylthio)methane silver(I) complexes with the triflate anion are also polymorphic due to the influence of the solvent. Contrary to what is reported here, the complexes do not associate in 2D-networks, but form 1D-coordination polymers.

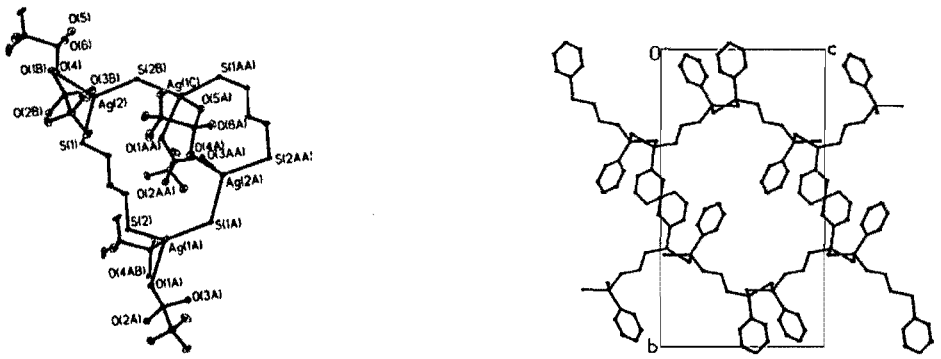

(a) (b)

Figure 2.2.9. (a) The repeat unit of **9** is very similar to that of **7**. (b) A side view of the 2D-network. Notice the "out-of-phase" disposition of consecutive planes as compared to the "in-phase" disposition in Figure 2.2.7c. The anions and the H atoms have been omitted for clarity.

Supramolecular Isomerism of the Networks. As noted in the above crystal structure reports, the choice of the recrystallization solvent for complexes with the sulfonate anions influences the coordination of the silver and consequently the resulting network. Two complexes were obtained with the *p*-tosylate anion (**5** and **6**). Complex **5**, characterized by the presence of a double-bridge coordination, was recrystallized in petroleum ether, while diethyl ether was used for **6** which is characterized by a monatomic bridge coordination.

Three distinct complexes were synthesized with the trifluoromethanesulfonate anion (**7-9**).

The situation described above is also observed for these complexes with the trifluoromethanesulfonate anion. Thus, complex **7**, obtained from a petroleum ether solution and complex **9**, from an hexane solution, both give rise to a double-bridge mode, while the diethyl ether solution yielded complex **8**, which has a monatomic bridge mode (as well as a double-bridge mode) (Chart 1). It is concluded that, in the case of anions containing the sulfonate group, supramolecular isomerism is solvent driven: the diethyl ether solvent promotes the formation of a monatomic-bridge mode whereas the petroleum ether (a nonpolar solvent) favors a double-bridge mode. This is confirmed by the fact that when recrystallizing [Ag$\mathbf{L}^{3\text{-Ph}}$(*p*-TsO)] or [$Ag_2\mathbf{L}^{3\text{-Ph}}(CF_3SO_3)_2$] from pentane or heptane (nonpolar solvents), one gets crystals whose unit-cell dimensions are identical with those of **5** or **7**, respectively.

Metal-Metal Bonds. The complexes synthesized with trifluoroacetate, pentafluoropropionate and heptafluorobutyrate present short silver-silver contacts. The observed distances, listed in Table 2.2.2 are compared with others reported in an earlier work.[8] All these distances are shorter than the sum of the van der Waals radii of two silver atoms (3.40Å[23]) and slightly longer than 2.89 Å, which is twice the metallic radius of silver.[23] There is therefore a weak interaction between the metal atoms comparable to that reported by Wang and Mak.[27] Although the larger number of fluorine atoms seems to affect the average Ag-O distances, it does not reinforce or weaken the Ag···Ag interactions. Interestingly, complexes with the *p*-tosylate and the trifluoromethanesulfonate anion, which both form bridged dimers, do not have metal-metal interactions as the Ag···Ag distances are 3.750(1) and 3.745(1) Å respectively.

Table 2.2.2. Comparison of the short Ag···Ag contacts (Å) observed with the corresponding values reported for bis(phenylthio)methane complexes.[8]

Anion	Complex [a]$\mathbf{L}^{1\text{-Ph}}$	Ag···Ag contacts	Complex [b]$\mathbf{L}^{3\text{-Ph}}$	Ag···Ag contacts
CF_3COO^-	-		**2**	3.2459(5)
$CF_3CF_2COO^-$			**3**	3.0502(7)
$CF_3CF_2CF_2COO^-$	**6**[c]	3.1593(3)	**4**	3.1594(4)
p-TsO^-	-		**5**	3.7503(5)
$CF_3SO_3^-$	**5**[c]	4.711(2), 5.524(1)	**8**	3.745(1)
			9	4.854(1)
$^-OOCCF_2CF_2COO^-$	**7**[c]	2.9836(5)		
		3.0168(5)		

[a]$\mathbf{L}^{1\text{-Ph}}$ = bis(phenylthio)methane, reference 8. [b]$\mathbf{L}^{3\text{-Ph}}$ = 1,3-bis(phenylthio)propane.
[c]Number as assigned in ref 8.

Infrared spectroscopy. The peaks observed at 1685 and 1410 cm^{-1} in the IR spectrum of complex **2** are assigned to the characteristic antisymmetric and symmetric stretching bands of the carboxylate group, respectively. Furthermore, the value of 275 cm^{-1} [$\nu_{asym}(CO_2)$ - $\nu_{sym}(CO_2)$] obviously points to the occurrence of the dibridging mode,[28] in agreement with the established crystal structure (see Table 2.2.3a). This observation also applies to **3** and **4**. Although the crystal structure of **3** reveals the presence of dimers with either the diatomic or the monoatomic bridging modes, only the former is identified from its FTIR spectrum. The IR spectra of complexes **5** and **6** are similar. Thus, the different coordinations of the silver atom, in monoatomic (**5**) and diatomic (**6**) bridging modes cannot be established by means of IR data. The unambiguous assignment of the vibration modes of the $CF_3SO_3^-$ anion in complexes **7-9** is quite difficult because of the mixing of CF_3 and SO_3 vibrations in the stretching-mode region between 1000 and 1300 cm^{-1}.[29] However, according to Lawrance,[30] the trifluoromethanesulfonate anion in $AgCF_3SO_3$ has absorption bands at 1270 and 1043 cm^{-1}. These have been assigned to the $\nu[SO_3(E)]$ and $\nu[SO_3(A_1)]$ vibrations.[30] We have compuled in Table 2.2.3b, the $\nu[SO_3(E)]$ and $\nu[SO_3(A_1)]$ vibrations of the triflate bearing complexes (**7-9**) as well as those of $AgCF_3SO_3$ and those of a silver triflate coordination polymer. One can observe that the three complexes **7-9** have strikingly similar IR frequencies even if the triflate anions in these complexes have different coordination modes (μ^2 in **7** and **9**, $\mu^1 + \mu^2$ in **8**). Thus, we can not differentiate the coordination modes of the triflates by means of infrared spectroscopy.

In complex **1**, the peaks at 843 and 560 cm^{-1} are assigned respectively to $\nu_3(T_{1u})$ and $\nu_4(T_{1u})$ vibrations of the PF_6^- anion.[33-35] The peaks observed in **10** at 1137 and 1073 cm^{-1} are assigned respectively to $\nu_4(E)$ and $\nu_1(A_1)$ vibrations of the ClO_4^- anion.[36] The IR spectrum of complex **11** shows a band at 664 cm^{-1} that is assigned to $\nu_3(T_{1u})$ vibration of the SbF_6^- anion.[34,37]

Table 2.2.3a. Comparison of FTIR frequencies (cm^{-1}), COO vibrations ($\Delta = [\nu_{asym}(CO_2) - \nu_{sym}(CO_2)]$).

	Complex	ν_{asym} (CO_2)	ν_{sym} (CO_2)	Δ
2	$[Ag_2L^{3\text{-Ph}}(CF_3COO)_2]$	1685	1410	275
3	$[Ag_2L^{3\text{-Ph}}(CF_3CF_2COO)_2(CH_3COCH_3)]$	1679	1411	268
4	$[AgL^{3\text{-Ph}}(CF_3CF_2CF_2COO)]$	1681	1411	270
	$[Ag_2(CF_3COO)_2(dppm)]$[a]	1670	1407	263
	$[Ag_2(CF_3CF_2COO)_2(dppm)]$[a]	1672	1406	266
	$[Ag_2(CF_3CF_2CF_2COO)_2(dppm)]$[a]	1670	1396	274

Table 2.2.3b. Comparison of FTIR frequencies (cm^{-1}), SO_3 vibrations.

Complex	ν_{asym} (SO_3)	ν_{sym} (SO_3)
7	1258	1033
8	1260	1034
9	1257	1030
$Ag_2(\mathbf{L})(CF_3SO_3)_2$[b]	1257	1035
$AgCF_3SO_3$[c]	1270	1043

[a]Reference 28. [b]Reference 32 (**L**: dibenzo[*b*, *def*]chrysene). [c]Reference 31.

Thermogravimetric Investigation. Three complexes incorporate acetone molecules in their structures. However, the crystallographic results reveal two types of associations. In **1**, acetone and PF_6^- are inserted between layers while in **3** and **7** acetone is part of the network through its coordination to silver atoms. A different thermal behavior is therefore expected. Another question is whether the acetone molecule in **1** is necessary for the stability of the structure. The thermograms of $\{[Ag_2(L^{3\text{-Ph}})_4](PF_6)_2(CH_3COCH_3)_2]\}_\infty$ (**1**) and $[Ag_2L^{3\text{-Ph}}(CF_3CF_2CO_2)_2(CH_3COCH_3)]_\infty$ (**3**) are shown in Figure 2.2.10a,b, respectively. The TGA curve of complex **1** exhibits a two-step degradation. The first step, which occurs in the interval of 85-100 °C corresponds to the departure of 2 moles of acetone/mol of $[C_{60}H_{64}S_8Ag_2(PF_6)_2(CH_3COCH_3)_2]$

(expt/theor = 7.12/6.98%). The second step, which occurs between 150-280 °C, corresponds to the loss of the ligand $\mathbf{L}^{\mathbf{3\text{-}Ph}}$, (expt/theor = 66.32/62.62%). The remaining white residue is $AgPF_6$. Hence, very soon after the loss of acetone, the $[Ag_2(\mathbf{L}^{\mathbf{3\text{-}Ph}})_4]_\infty$ layer structure starts to disintegrate with the loss of the four ligand molecules. Not surprisingly, all three complexes, **1** (PF_6^-), **10** (ClO_4^-)[12] and **11** (SbF_6^-),[12] in which the anions and the acetone molecules are sandwiched between the layers, have the same thermal decomposition pattern (Figures S9, S10, Annexe II). The residues are $AgClO_4$ and $AgSbF_6$ for **10** and **11** respectively.

In the case of **3** and **7**, the acetone molecules are more strongly held, through coordination bonds to the silver atoms. However, the decomposition of the complexes, which start at about 180 °C, is a one-step process completed at 300 and 320 °C for **3** (Figure 2.2.10b) and **7** (Figure S11, Annexe II), respectively. The weight loss corresponds to the departure of the acetone molecules, the ligands and the anions (expt/theor = 76.62/74.92% for **3**, expt/theor = 74.30/74.08% for **7**). The collapse of the network is total, as the remaining black residue is silver. In a study on chemical vapor deposition of silver films,[38] it was reported for example, that the silver(I) heptafluorocarboxylate complex decomposes between 250 and 380 °C, and the residue consists of metallic silver. The decomposition of complex **3**, which incorporates the pentafluoropropionate anion, ends at a lower temperature, 300 °C. Thus, it could be used as a material for the vapor deposition of silver film because of its low temperature decomposition. This suggestion could be confirmed by a volatility study.

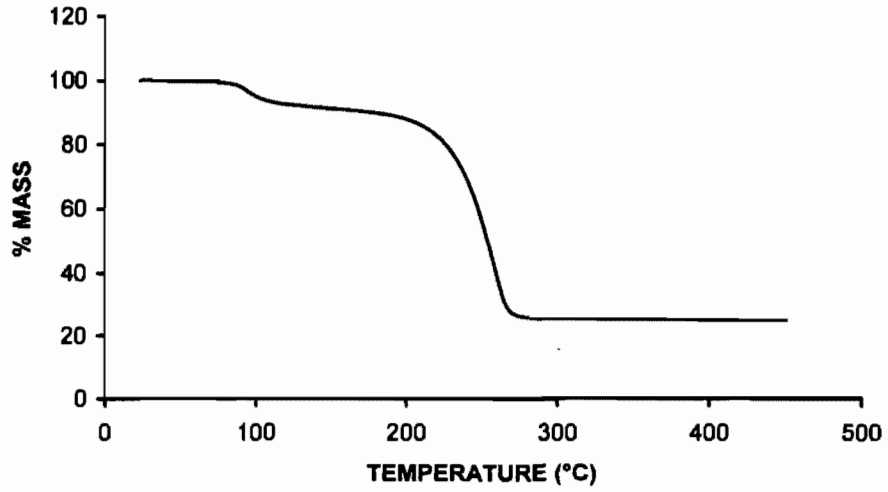

(a) Complex **1**

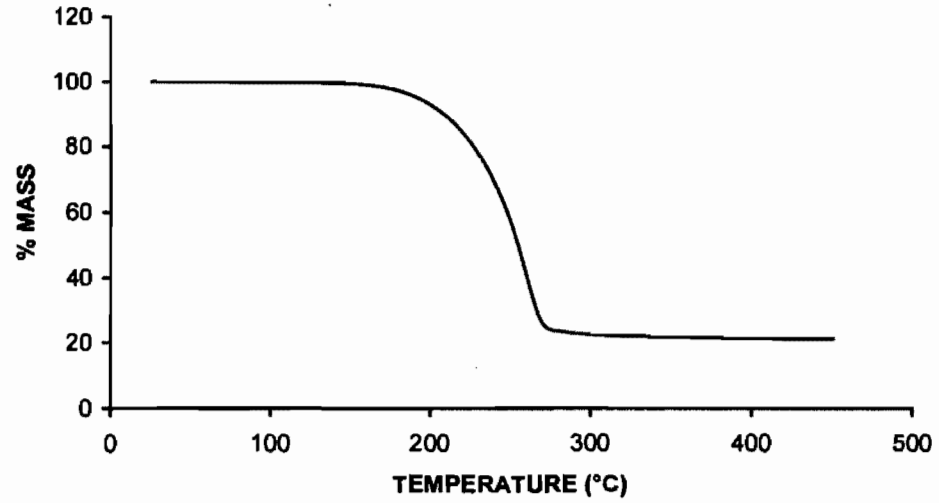

(b) Complex **3**

Figure 2.2.10. TGA curves recorded at a heating rate of 10 °C min^{-1}. (a) Two-step decomposition of **1** is shown. The acetone is lost first, followed by the loss of the ligand. (b) Acetone, the ligand, and the anion of **3** are eliminated in a single step between 180 and 300 °C.

2.2.5 Conclusions

We have synthesized and characterized eleven different coordination polymers involving Ag(I) and the 1,3-bis(phenylthio)propane ligand. The type of anion and, in some cases, the recrystallization solvent is responsible for the remarkable diversity in the structures observed. However, some common features emerge:

(1) With weakly coordinating, nearly spherical anions (XY_4^- and XY_6^-), comparable cationic layer structures are formed between Ag(I) and the ligand. The anions and acetone molecules, inserted between the sheets, have only van der Waals interactions with the layers.

(2) All perfluorocarboxylates form dimeric units with moderately short metal-metal distances indicating weak Ag···Ag interactions. These units, in turn, develop into 2D-coordination networks, except for **4**, which forms a 1D-coordination polymer.

(3) Solvent-driven supramolecular isomerism is observed with the sulfonate anions (*p*-TsO^- and $CF_3SO_3^-$). Four of the five complexes adopt a 2D-structure of neutral sheets in which the anions are coordinated to the metal centers. As for the polymorphic *p*-tosylates, **6** adopts the 2D-layer structure while the other, **5**, forms a linear coordination polymer. All three triflates, **7- 9**, have the same metal-to-ligand ratio (2:1), although **7** includes an extra acetone molecule. Complexes **7-9** all adopt a 2D-structure, those of **7** and **9** being almost identical. The type of silver environment in the polymorphs is associated with the polarity of the recrystallization solvent.

(4) All complexes with the 1,3-bis(phenylthio)propane (except **4** and **5**) form a 2D-network. However, the structures generated with the shorter bis(phenylthio)methane complexes were all of the 1D-coordination polymer class, and no 2D-networks were formed. Furthermore, it was found that the XY_4^- anions were coordinated to the silver(I) ions. Clearly, the length of the ligand affects the outcome.

Acknowledgements. Financial support from the Natural Sciences and Engineering Research Council of Canada (F.B.) and a graduate scholarship from the Programme Canadien de Bourse de la Francophonie (M.O.A.) are gratefully acknowledged. The authors aloso thank Dr. M. Simard and F. Bélanger-Gariépy for the X-ray data collections, and H. Dinel for elemental analyses.

Supplementary Material Available: Table of bond distances and angles involving the silver atoms (Table S1), Figures S1 – S11 and X-ray crystallographic information files (CIF) for compounds **1-9**. This material is available free of charge via the Internet at http://pubs.acs.org

2.2.6 References

(1) (a) Hagrman, P. J.; Hagrman, D.; Zubieta, J. *Angew. Chem. Int. Ed.* **1999**, *38*, 2638. (b) Khlobystov, A. N.; Blake, A. J.; Champness, N. R.; Lemenovskii, D. A.; Majouga, A. G.; Zyk, N. V.; Schröder, M. *Coord. Chem. Rev.* **2001**, *222*, 155. (c) Batten, S. R.; Robson, R. *Angew. Chem. Int. Ed.* **1998**, *37*, 1461. (d) Swiegers, G. F.; Malefetse, T. J. *Chem. Rev.* **2000**, *100*, 3483.

(2) (a) Stumpf, H. O.; Ouahab, L.; Pei, Y.; Grandjean, D.; Kahn, O. *Science* **1993**, *261*, 447. (b) Yaghi, O. M.; Li, G.; Li, H. *Nature* **1995**, *378*, 703.

(3) (a) Blake, A. J.; Champness, N. R.; Hubberstey, P.; Li, W. S.; Withersby, M. A.; Schröder, M. *Coord. Chem. Rev.* **1999**, *183*, 117. (b) Sharma, C. V. K.; Broker, G. A.; Huddleston, J. G.; Baldwin, J. W.; Metzger, R. M.; Rogers, R. D. *J. Am. Chem. Soc.* **1999**, *121*, 1137. (c) Abrahams, B. F.; Batten, S. R.; Hoskins, B. F.; Robson, R. *Inorg. Chem.* **2003**, *42*, 2654. (d) Abrahams, B. F.; Jackson, P. A.; Robson, R. *Angew. Chem. Int. Ed.* **1998**, *37*, 2656.

(4) (a) Goodgame, D. M. L.; Grachvogel, D. A.; Hussain, I.; White, A. J. P.; Williams, D. J. *Inorg. Chem.* **1999**, *38*, 2057. (b) Bu, X. H.; Chen, W.; Lu, S. L.; Zhang, R. H.; Liao, D. Z.; Bu, W. M.; Shionoya, M.; Brisse, F.; Ribas, J. *Angew. Chem. Int. Ed.* **2001**, *40*, 3201.

(5) (a) Withersby, M. A.; Blake, A. J.; Champness, N. R.; Cooke, P. A.; Hubberstey, P.; Li, W. S.; Schröder, M. *Inorg. Chem.* **1999**, *38*, 2259. (b) Blake, A. J.; Champness, N. R.; Cooke, P. A.; Nicolson, J. E. B.; Wilson, C. *J. Chem. Soc., Dalton Trans.* **2000**, 3811.

(6) For example: (a) Withersby, M. A.; Blake, A. J.; Champness, N. R.; Hubberstey, P.; Li, W. S.; Schröder, M. *Angew. Chem. Int. Ed.* **1997**, *36*, 2327. (b) Noro, S.; Kitaura, R.; Kondo, M.; Kitagawa, S.; Ishii, T.; Matsuzaka, H.; Yamashita, M. *J. Am. Chem. Soc.* **2002**, *124*, 2568. (c) Chatterton, N. P.; Goodgame, D. M. L.; Grachvogel, D. A.; Hussain, I.; White, A. J. P.; Williams, D. J. *Inorg. Chem.* **2001**, *40*, 312.

(7) Bu, X. H.; Chen, W.; Hou, W. F.; Du, M.; Zhang, R. H.; Brisse, F. *Inorg. Chem.* **2002**, *41*, 3477.

(8) Awaleh, M. O; Badia, A.; Brisse, F. *Cryst. Growth Des.* **2005**, 5, 1897.

(9) Oh, M.; Carpenter, G. B.; Sweigart, D. A. *Angew. Chem. Int. Ed.* **2002**, *41*, 3650.

(10) (a) Moulton, B.; Zaworotko, M. J. *Chem . Rev.* **2001**, *101*, 1629. (b) Gudbjartson, H.; Biradha, K.; Poirer, K. M.; Zaworotko, M. J. *J. Am. Chem. Soc.* **1999**, *121*, 2599. (c) Kasai, K.; Aoyagi, M.; Fujita, M. *J. Am. Chem. Soc.* **2000**, *122*, 2140.

(11) Hartley, F. R.; Murray, S. G.; Levason, W.; Soutter, H. E.; McAuliffe, C. A. *Inorg. Chim. Acta* **1979**, *35*, 265.

(12) $\{[Ag_2(L^{3\text{-}Ph})_4](ClO_4)_2(CH_3COCH_3)_2\}_\infty$ **10**. $C_{66}H_{76}Ag_2O_{10}Cl_2S_8$. Formula weight: 1572.47. Synthesized with the same procedure as **1** with $AgClO_4.H_2O$ (178 mg, 0.79 mmol) and $L^{3\text{-}Ph}$ (0.35 mL, 1.52 mmol). Yield 65% based on $AgClO_4.H_2O$.

A TGA curve indicated a two-step decomposition (Figure S9, Annexe II). First, two acetone molecules were released between 95 and 110 °C, (exp./th. = 7.19/7.38%). In a second step that take place between 180 and 310 °C, the ligands were eliminated (exp./th. = 68.56/66.24%). The residue consisted of $AgClO_4$. This result is coherent with the analytical results. Anal. Found: C, 49.94; H, 4.53. Calcd for $C_{66}H_{76}Ag_2O_{10}Cl_2S_8$: C, 50.41; H, 4.87. ^{1}H NMR (DMSO-d_6, 400 MHz): δ 1.81 (qt, 2H, -S-(CH_2)-(CH_2)-), 3.06 (t, 4H, -S-(CH_2)-), 7.27-7.69 (*m*, 10H, C_6H_5-). IR (KBr, cm^{-1}): 3447m, 3057w, 2916w, 1634s, 1583m, 1479s, 1438s, 1297w, 1137s, 1073vs, 1025m, 934w, 737s, 689s, 474w. Crystal data: monoclinic, $P2_1/c$, a = 26.3970(1), b = 12.8558(2), c = 20.9301(3) Å, β = 94.47(1)°, V = 7081.42(8) Å^3, Z = 4, μ(CuKα) = 7.15 mm^{-1}, R1 (I > 2 σ(I)) = 0.0597, Rw = 0.1550, R1 (all data) = 0.0808, Rw = 0.1674, S = 0.947. The perchlorate anions, the acetone molecules and half of the ligands are disordered.

$\{[Ag_2(L^{3\text{-}Ph})_4](SbF_6)_2(CH_3COCH_3)_2\}_\infty$ **11**. $C_{66}H_{76}Ag_2F_{12}O_2S_8Sb_2$. Formula weight = 1845.07. Synthesized with the same conditions as 1 with $AgSbF_6$ (164 mg, 0.48 mmol) and $L^{3\text{-}Ph}$ (0.35 mL, 1.52 mmol). Yield 74% based on $AgSbF_6$. Anal. Found: C, 42.88; H, 3.89. Calcd for $C_{66}H_{76}Ag_2F_{12}O_2S_8Sb_2$: C, 42.96; H, 4.15. ^{1}H NMR (DMSO-d_6, 400 MHz): δ 1.84 (qt, 2H, -S-(CH_2)-(CH_2)-), 3.07 (t, 4H, -S-(CH_2)-), 7.28-7.59 (*m*, 10H, C_6H_5-).

IR (KBr, cm^{-1}): 3435w, 3057m, 2918m, 1583s, 1480s, 1438s, 1334w, 1301w, 1257w, 1158w, 1089m, 1069w, 1024s, 737vs, 691vs, 664vs, 491m. Crystal data: monoclinic, $P2_1/c$, a = 27.1584(2), b = 13.0497(2), c = 20.5848(3) Å, β = 97.79(1)°,

V = 7227.72(9) Å^3, Z = 4, μ(CuKα) = 12.87 mm^{-1}, R1 (I > 2 σ(I)) = 0.0528, Rw = 0.1454, R1 (all data) = 0.0695, Rw = 0.1529, S = 1.045. The fluorine atoms have a slight oscillating disorder while the acetones are much more disordered. The silver atoms and the ligands form cationic sheets of composition $Ag_2(L^{3\text{-}Ph})_4$. The non-coordinating anions and the guest molecules occupy the voids between parallel sheets. The TGA curve shown in Figure S10, Annexe II, reveals the same decomposition pattern noted for **1** and **10**. The acetone molecules leave first, at a temperature between 75 and 90 °C (exp./th. = 6.59/6.29%), followed by loss of the ligands, between 160 and 310 °C, (exp./th. = 60.41/56.45%) which leaves a residue of $AgSbF_6$.

(13) SAINT Release 6.06, Integration Software for Single Crystal Data; Bruker AXS Inc.: Madison, WI, 1999.

(14) Sheldrick, G. M. SADABS Bruker Area Detector Absorption Corrections; Bruker AXS Inc.: Madison, WI, 1996.

(15) XPREP Release 5.10; X-ray Data Preparation and Reciprocal Space Exploration Program. Bruker AXS Inc., Madison, WI, 1997.

(16) SHELXTL Release 5.10, The Complete Software Package for Single-Crystal Structure Determination; Brucker AXS Inc.: Madison, WI, 1997.

(17) (a) Sheldrick, G. M. SHELXS97, Program for the Solution of Crystal Structures; University of Göttingen: Göttingen, Germany, 1997. (b) Sheldrick, G. M. SHELXL97, Program for the Refinement of Crystal Structures; University of Göttingen: Göttingen, Germany, 1997.

(18) Black, J. R.; Champness, N. R.; Levason, W.; Reid, G. *J. Chem. Soc., Chem. Comm.* **1995**, 1277.

(19) Black, J. R.; Champness, N. R.; Levason, W.; Reid, G. *J. Chem. Soc., Dalton Trans.* **1995**, 3439.

(20) Jung, O. S.; Kim, Y. J.; Lee, Y. A.; Park, K. M.; Lee, S. S. *Inorg. Chem.* **2003**, *42*, 844.

(21) (a) Griffin, R. G.; Ellett, Jr., J. D.; Mehring, M.; Bullitt, J. G.; Waugh, J. S. *J. Chem. Phys.* **1972**, *57*, 2147. (b) Blakeslee, A. E.; Hoard, J. L. *J. Am. Chem. Soc.* **1956**, *78*, 3029.

(22) Bosch, E.; Barnes, C. L. *Inorg. Chem.* **2002**, *41*, 2543.

(23) Porterfield, W. W. *Inorganic Chemistry: A Unified Approach*, Addison-Wesley; Reading, MA, 1994, pp.168, 180.

(24) Brandys, M. C.; Puddephatt, R. J.; *J. Am. Chem. Soc.* **2002**, *124*, 3946.

(25) Wells, A. F. *Structural Inorganic Chemistry*; Oxford University Press: Oxford, 1975.

(26) Ara, I.; El Bahij, F.; Lachkar, M. F. *Acta Crystallogr.* **2003**, *C59*, m265.

(27) Wang, Q. M.; Mak, T. C. W. *J. Am. Chem. Soc.* **2001**, *123*, 7594.

(28) Szlyk, E.; Szymanska, I.; Surdykowski, A.; Glowiak, T.; Wojtczak, A.; Golinski, A. *J. Chem. Soc. Dalton Trans.* **2003**, 3404 and references therein.

(29) Johnston, D. H.; Shriver, D. F. *Inorg. Chem.* **1993**, *32*, 1045.

(30) Lawrance, G. A. *Chem. Rev.* **1986**, *86*, 17 and references therein.

(31) Batchelor, R. J.; Ruddick, J. N. R.; Sams, J. R.; Aubke, F. *Inorg. Chem.* **1977**, *16*, 1414 and references therein.

(32) Zhong, J. C.; Munakata, M.; Kuroda-Sowa, T.; Maekawa, M.; Suenaga, Y.; Konaka, H. *Inorg. Chem.* **2001**, *40*, 3191.

(33) Matsumoto, K.; Hagiwara, R.; Ito, Y.; Tamada, O. *Solid State Sci.* **2002**, *4*, 1465.

(34) Reger, D. L.; Semeniuc, R. F.; Rassolov, V.; Smith, M. D. *Inorg. Chem.* **2004**, *43*, 537.

(35) Jung, O. S.; Kim, Y. J.; Lee, Y. A.; Chae, H. K.; Jang, H. G.; Hong , J. *Inorg. Chem.* **2001**, *40*, 2105.

(36) Rosenthal, M. R. *J. Chem. Educ.* **1973**, *50*, 331 and references therein.

(37) Chen, Y. D.; Zhang, L. Y; Shi, L. X; Chen, Z. N. *Inorg. Chem.* **2004**. *43*, 7493.

(38) Edwards, D. N.; Harker, R. M.; Mahon, M. F.; Molloy, K. C. *Inorg. Chim. Acta* **2002**, *328*, 134.

Chapitre 3. Réseaux métallosupramoléculaires d'argent(I) construits avec le bis(méthylthio)méthane $L^{1\text{-}Me}$.

3.1 Influence of the anion on the structure of bis(methylthio)methane supramolecular coordination complexes.[†]

3.1.1 Abstract

A series of coordination networks has been synthesized by self-assembly of the small bis(methylthio)methane building block and AgX (X = NO_3^- (**1**), ClO_4^- (**2, 3**), *p*-TsO^- (**4**), CF_3COO^- (**5**), $CF_3CF_2CF_2COO^-$ (**6**), $CF_3SO_3^-$ (**7**), $C_6H_5COO^-$ (**8**), $CH_3SO_3^-$ (**9**), $HOOCCF_2CF_2COO^-$ (**10**)) in order to rationalize the effect of the size of the anions and the ligands upon the structure adopted by the supramolecular coordination network. In complexes **1-7**, each silver(I) is coordinated with sulfur atoms from three different ligands. They form very similar two-dimensional solid-state organizations. The structures consist of layers, made up of Ag and bis(methylthio)methane ligands only, in which the anions complete the tetrahedral coordination of the silver atoms. Upon closer inspection, the neutral 2D networks may be sorted into two distinct classes. Group 1 incorporates the smallest anions, NO_3^- and ClO_4^-, whereas the more elongated anions, *p*-TsO^-, CF_3COO^-, $CF_3CF_2CF_2COO^-$, and $CF_3SO_3^-$, are found in group 2. The main difference between these groups is in the organization of the neutral layers. In group 1, the repeat unit consists of a large 14-membered metallomacrocycle, whereas in group 2, the metallomacrocycle consists of 10-membered rings. The two polymorphs of the perchlorate complexes are structurally comparable. Dimeric units are the basis for the other three complexes. In the benzoate **8**, the dimers are formed with two anions. They are linked by ligand molecules to form a 1D polymeric chain that adopts a distorted hexagonal packing. The silver atoms have a distorted triangular bipyramidal coordination and the Ag···Ag distance is 2.911 Å. In complex **9**, two ligands each bridge a pair of silver atoms to form a dimer (Ag···Ag = 3.243 Å). A neutral 1D coordination polymer is obtained when anions connect, in a dibridging mode, the silver atoms of adjacent dimers $[Ag(CH_3SCH_2SCH_3)]_2$. Weak hydrogen interactions between chains result in a 3D network. The silver coordination is triangular bipyramidal. Complex **10** is also a 1D coordination polymer with a centrosymmetric dimer. Two ligands and two anions are coordinated to the silver atoms. The Ag···Ag contact is

[†] Awaleh, M. O.; Badia, A.; Brisse, F. *Cryst. Growth Des.* **2006**, *6*, 2674-2685.

3.067 Å. The 1D coordination polymer is obtained through H-bonding between carboxylate groups. The stoichiometries of the complexes were independent of the initial metal-to-ligand ratios and were not influenced by the solvent of recrystallization.

3.1.1 Introduction

Metal-organic coordination polymers are attracting a great deal of attention because of their potential as functional materials.[1] In metal-organic crystal engineering one takes advantage of the coordinating ability of metal centers and organic ligands in order to build new coordination polymers. The main goal in metal-organic crystal engineering is to predict the topology of supramolecular architectures in order to synthesize extended solid-state materials with desired properties. However, there still remain many obstacles to overcome before the synthesis of coordination polymers with a desired topology is possible. Many parameters are involved in the formation of the metal-organic framework (MOF), such as the metal and its coordinating possibilities, the nature of the counteranion, the metal-to-ligand ratio, the flexibility of the organic building blocks, the number and the orientation of the coordinating sites in the organic spacers, and the solvent of recrystallization among others.[2]

Neverthless, to gain more information about those subtle factors, not yet well-understood, we have undertaken a study on the effect of one parameter at a time upon the topology of the networks by carrying out a systematic examination of a series of supramolecular coordination polymers using the same building block, the same metal centre, the same experimental conditions and varying only one or two parameters at time.[3]

A study of inorganic-organic supramolecular architectures was undertaken with dithiolate ligands, $\mathbf{L^{n\text{-}R}}$ = **R**-S$(CH_2)_n$-S-**R**, where n is the number of CH_2 groups and **R** is the phenyl group, used as building blocks.[4-9] These ligands were selected for the following reasons: (i) the dithiolate building blocks afford two coordination sites to metal centres, which is the minimum number of connecting sites required to expand the coordination sphere of the metal centers into extended solid-state networks; (ii) the variation of the aliphatic segment between the S atoms,[10] hence the distance separating silver centers and the number of possible conformations, can allow us to study the influence of the flexibility of the building block upon the coordination polymers; (iii) whether the bulk of the **R** substituent hinders the coordinating ability of the S atoms. This may affect the coordination

sphere of the metal centre and consequently the expansion of the latter into the coordination polymers.

On the other hand, the role of anions in supramolecular chemistry is of great interest because of its application in ion-pair recognition and especially in anion-exchange.[11] In this context, we have paid attention to the role of the counteranions upon the supramolecular architectures when the diarylthioether ligands are used as building blocks.[4-9] The main reason for our interest in the role of the anions upon the topology is to synthesize materials with useful properties such as anion-exchange.

We have classified[8] the anions as follows: (i) spherical anions that are mainly noncoordinanting (PF_6^-, SbF_6^-, BF_4^-); (ii) moderately coordinating sulfonates (*p*-TsO^-, $CF_3SO_3^-$, $CH_3SO_3^-$, $C_{10}H_7SO_3^-$); (iii) strongly coordinating carboxylate anions ($CF_3CO_2^-$, $C_6H_5CO_2^-$, $CF_3CF_2CO_2^-$, $CF_3CF_2CF_2CO_2^-$, $^-OOCCF_2CF_2COO^-$); (iv) the small planar NO_3^- anion that is a fairly coordinating one with versatile coordination modes and the perchlorate (ClO_4^-) that is a weakly coordinating anion.

From this systematic investigation of the supramolecular architectures based on the self-assembly of the bidentate thiolate building blocks and Ag(I) centers, we concluded that the initial metal-to-ligand ratio does not play any role upon the resulting structures.

In addition, we have shown that two parameters play a major role upon the structures of coordination polymers: the length of the organic spacers and the coordinating ability of the counteranions. We have evidence that the noncoordinating anions lead systematically to cationic coordination polymer when the lengths of the building blocks are of the intermediate size (n = 3-5). These materials may present anion-exchange properties.[5,6]

However, it is difficult to rationalize the topology obtained with the moderately or strongly coordinating anions, because they have shown rich coordination modes. For example, the moderately coordinating sulfonate counteranion displayed solvent-induced supramolecular isomerism, thus the influence of the solvent of recrystallization upon the supramolecular coordination polymers adds to that of the anions and the length of the ligands making the prediction of the resulting structures less certain.

Finally, the strongly coordinating perfluorocarboxylate anions yield complexes with a variety of coordination networks. These usually incorporate silver dimers exhibiting weak argentophilic interactions.

Thus, we conclude that it is necessary to focus attention on the influence of the coordinating anions upon the formation of coordination polymer, since the noncoordinating anions usually favour the formation of cationic networks. The coordinating anions lead to neutral frameworks of unpredicatable topologies. For this purpose we have chosen a small ligand, the bis(methylthio)methane, $\mathbf{L^{1\text{-}Me}}$, that presents three advantages: (i) it is a small flexible dithioether ligand so that the length parameter, which often interferes with the effect of the anions, is minimized; (ii) the conformational degrees of freedom of this ligand are limited; (iii) the small methyl group substituent on the ligand may allow for more ligands to approch the silver(I) centers, affording a higher dimensional coordination polymer.

Combined with this ligand, we have selected the following coordinating anions (weakly, moderately and strongly): ClO_4^-, NO_3^-, $CF_3SO_3^-$, $CH_3SO_3^-$, $CF_3CO_2^-$, $C_6H_5CO_2^-$, $CF_3CF_2CF_2CO_2^-$ and $^-OOCCF_2CF_2COO^-$. As coordinating anions, they are expected to occupy at least one coordination site on the metal center. On the basis of their sizes, these anions belong to three categories: (i) small anions (ClO_4^-, NO_3^-); (ii) medium-sized anions ($CH_3SO_3^-$, $CF_3CO_2^-$, $C_6H_5CO_2^-$). Because the perfluorocarboxylates have shown similar topologies, we include the longer heptafluorobutyrate anion, $CF_3CF_2CF_2CO_2^-$, in this group; and (iii) the tetrafluorosuccinate, $^-OOCCF_2CF_2COO^-$, which is in a class by itself as it is a dicarboxylate. One of the reasons for including the tetrafluorosuccinate anion was to increase the dimensionality of the coordination polymer, because we expected that the dianion would act as an interconnecting agent.[7] However, when attempts to form a 2D-network using silver salts of dicarboxylate and $\mathbf{L^{1\text{-}Ph}}$ failed, we suspected that the presence of the phenyl group on the ligand prevented it. We are testing this hypothesis by self-assembling the $\mathbf{L^{1\text{-}Me}}$ ligand with the tetrafluorosuccinate anion.

A survey of the Cambridge Structural Database (CSD) revealed that there are only ten complexes of the bis(methylthio)methane, $\mathbf{L^{1\text{-}Me}}$, whose crystal structures have been established.[12] Seven of them contain Ru, Rh, Mn or Sn centers and only three complexes

contain the d^{10} metals.[13] One incorporates the $AgBF_4$ salt, whereas in the other two, the S atoms are replaced by Se and Ag(I) is replaced by Cu(I).

It is not unusual for this class of complexes to demonstrate polymorphism. For example, here, complexes **2** and **3** are polymorphs. This property was reported earlier in another series of complexes with the $\mathbf{L^{3\text{-}Ph}}$ ligand.[6]

In an attempt to acquire a large variety of complexes, we have followed, besides the standard self-assembly method, a synthetic approach based on anion-exchange.[14]

3.1.3 Experimental Section

Materials and General Methods. Except for bis(methylthio)methane, all the reagents required for the syntheses were commercially available and employed without further purification. The elemental analyses were performed by the Laboratoire d'Analyse Élémentaire (Université de Montréal), and IR spectra were recorded on a Perkin-Elmer 1750 FTIR spectrometer (4000-450 cm^{-1}) with samples prepared as KBr pellets. NaCl plates were used for liquid spcimens. ^1H and ^{19}F NMR spectra were recorded on Bruker AV400 and AV300 spectrometers at 25 °C. ^1H chemical shifts are reported in parts per million and are referenced to residual solvent signals of deuterated DMSO (δ_{1H} = 2.50). The chemical shifts are referenced to $C_6H_5CF_3$ (-63.9 ppm) for ^{19}F spectra.

Syntheses. The ligand bis(methylthio)methane, $\mathbf{L^{1\text{-}Me}}$, was synthesized by following a literature method.[15] Yield: 41%. Anal. Found: C, 33.45; H, 7.32. Calcd for $C_3H_8S_2$: C, 33.29; H, 7.45. ^1H NMR (DMSO-d_6, 400 MHz): δ 2.16 (*s*, 6H, CH_3-S-CH_2-S-CH_3), 3.71 (*s*, 2H, CH_3-S-CH_2-S-CH_3). IR (KBr, cm^{-1}): 2973m, 2915s, 2855m, 2828m, 2756w, 2588w, 2380w, 2269w, 2181w, 2128w, 2076w, 2034w, 1671w, 1435m, 1422m, 1384m, 1316m, 1203s, 1154m, 1123w, 985m, 958m, 805m, 745s, 693s, 648w.

Caution! Although we met no problems in handling perchlorate salts, great care should be taken due to their potentially explosive nature.

$\mathbf{[Ag_2(L^{1\text{-}Me})_2(NO_3)_2]_\infty}$ **1.** A solution of $AgNO_3$ (270 mg, 1.59 mmol) in methanol (5 mL) was mixed with a solution of $\mathbf{L^{1\text{-}Me}}$ (0.30 mL, 2.93 mmol) in diethyl ether (5 mL) at room temperature to yield a white microcrystalline precipitate. After filtration, the solid was dissolved in acetone and recrystallized by diffusion of petroleum ether into the solution. Several days later, single crystals suitable for X-ray analysis were obtained. Yield: 81% based on $AgNO_3$. Anal. Found: C, 12.92; H, 2.47; N, 4.89. Calculated for $C_6H_{16}S_4Ag_2N_2O_6$: C, 12.96; H, 2.90; N, 5.04. ^1H NMR (DMSO-d_6, 400 MHz): δ 2.14 (*s*,

6H, CH_3-S-CH_2-S-CH_3), 3.78 (*s*, 2H, CH_3-S-CH_2-S-CH_3). IR (KBr, cm^{-1}): 3466m, 2971w, 2915w, 2854vw, 2764w, 2426w, 1766w, 1631w, 1383br, 1203w, 985w, 833m, 825m, 745w, 717w, 694w, 669vw.

$[Ag_2(L^{1\text{-}Me})_2(ClO_4)_2]_\infty$ 2. $AgClO_4.H_2O$ (376 mg, 1.67 mmol) was dissolved in 5 mL of acetone. The solution was stirred with a solution of $L^{1\text{-}Me}$ (0.35 mL, 3.42 mmol) in diethyl ether (5 mL). A white precipitate is obtained. After filtration, the solid was dissolved in acetone and recrystallized by diffusion of petroleum ether into the solution. Crystals appeared after several days. Yield: 73% based on $AgClO_4.H_2O$. Anal. Found: C, 11.59; H, 2.27. Calculated for $C_6H_{16}Ag_2Cl_2O_8S_4$: C, 11.42; H, 2.56. ^1H NMR (DMSO-d_6, 300 MHz): δ 2.11 (*s*, 6H, CH_3-S-CH_2-S-CH_3), 3.79 (*s*, 2H, CH_3-S-CH_2-S-CH_3).

IR (KBr, cm^{-1}): 3447m, 2974m, 2915m, 2854w, 2828w, 2187w, 2013w, 1626m, 1435m, 1423m, 1384w, 1318w, 1203m, 1092br, 985m, 959m, 941m, 805m, 745m, 693m, 636s, 627s.

$[Ag_2(L^{1\text{-}Me})_2(ClO_4)_2]_\infty$ 3. A solution of $AgCF_3SO_3$ (382 mg, 1.49 mmol) in acetone (5 mL) was mixed with a solution of $L^{1\text{-}Me}$ (0.30 mL, 2.93 mmol) in diethyl ether (5 mL) at room temperature, resulting in a white microcrystalline precipitate that was filtered. To 150 mg of the precipitate, was added an aqueous solution (5 mL) of $LiClO_4$ (150 mg, 1.41 mmol). The mixture was stirred for 2 hours at room temperature and then filtered. The solid was dissolved in acetone and recrystallized by diffusion of petroleum ether. Single crystals suitable for X-ray analysis were obtained within a week. Yield: 61% based on $[Ag_2(L^{1\text{-}Me})_2(ClO_4)_2]$. Anal. Found: C, 11.07; H, 2.22. Calculated for $C_6H_{16}Ag_2Cl_2O_8S_4$: C, 11.42; H, 2.56. ^1H NMR (DMSO-d_6, 300 MHz): δ 2.10 (*s*, 6H, CH_3-S-CH_2-S-CH_3), 3.78 (*s*, 2H, CH_3-S-CH_2-S-CH_3). IR (KBr, cm^{-1}): 3450m, 2974w, 2915m, 2855w, 2829w, 2012w, 1627m, 1435m, 1423m, 1384w, 1317w, 1203m, 1093br, 985m, 958w, 941w, 805w, 744m, 693m, 636s, 627s.

$[Ag_2(L^{1\text{-}Me})_2(p\text{-}TsO)_2]_\infty$ 4. This complex was synthesized following the procedure described for **2** using Ag(*p*-TsO) (175 mg, 0.63 mmol) and $L^{1\text{-}Me}$ (0.30 mL, 2.93 mmol). Yield: 75% based on $Ag(C_7H_7O_3S)$. Anal. Found: C, 31.04; H, 3.70. Calculated for $C_{20}H_{30}S_6Ag_2O_6$: C, 31.01; H, 3.90. ^1H NMR (DMSO-d_6, 400 MHz): δ 2.11 (*s*, 6H, CH_3-S-CH_2-S-CH_3), 3.74 (*s*, 2H, CH_3-S-CH_2-S-CH_3), 2.309 (*s*, 3H, $CH_3C_6H_4SO_3$), 7.12-7.48 (m, 4H, $CH_3C_6H_4SO_3$). IR (KBr, cm^{-1}): 3468m, 2964w, 2915w, 2426w, 1632w, 1384w, 1261vs, 1185m, 1129m, 1108w, 1044w, 1014w, 814m, 745w, 691w, 570w.

$[AgL^{1\text{-}Me}(CF_3CO_2)]_\infty$ 5. This complex was synthesized in the same manner as **2** using $AgCF_3CO_2$ (217 mg, 0.98 mmol) and $L^{1\text{-}Me}$ (0.30 mL, 2.93 mmol). It is only after several weeks that very small crystals appeared. Although they were of a poor quality they were the only ones we could use for an X-ray analysis. Yield: 37% based on $AgCF_3CO_2$. Anal. Found: C, 18.42; H, 2.48. Calculated for $C_5H_8S_2AgF_3O_2$: C, 18.25; H, 2.45. ^{1}H NMR (DMSO-d_6, 300 MHz): δ 2.14 (*s*, 6H, CH_3-S-CH_2-S-CH_3), 3.73 (*s*, 2H, CH_3-S-CH_2-S-CH_3). ^{19}F NMR (DMSO-d_6, 376.31 MHz): δ –74.1. IR (KBr, cm^{-1}): 3437m, 2915w, 1683vs, 1434m, 1384w, 1307w, 1209vs, 1133vs, 957w, 839s, 804s, 724s, 690w, 599w, 518w.

$[AgL^{1\text{-}Me}(CF_3CF_2CF_2CO_2)]_\infty$ 6. This complex was synthesized in the same manner as **2** using $CF_3CF_2CF_2CO_2Ag$ (252 mg, 0.78 mmol) and $L^{1\text{-}Me}$ (0.30 mL, 2.93 mmol).

Yield: 63% based on $CF_3CF_2CF_2CO_2Ag$. Anal. Found: C, 19.62; H, 1.30. Calculated for $C_7H_8AgF_7O_2S_2$: C, 19.59; H, 1.88. ^{1}H NMR (DMSO-d_6, 400 MHz): δ 2.12 (*s*, 6H, CH_3-S-CH_2-S-CH_3), 3.76 (*s*, 2H, CH_3-S-CH_2-S-CH_3). ^{19}F{^{1}H} NMR (DMSO-d_6, 376.31 MHz): –81.9 (CF_3), –116.6 ($CF_3CF_2CF_2$), –127.8 ($CF_3CF_2CF_2$). IR (KBr, cm^{-1}): 3444m, 2916w, 2855vw, 1683vs, 1382m, 1342s, 1274m, 1220s, 1157m, 1084m, 968s, 936m, 814m, 765w, 743m, 719m, 693w, 639w, 587w, 528w.

$[Ag_2(L^{1\text{-}Me})_2(CF_3SO_3)_2]_\infty$ 7. An aqueous solution (5 mL) of $NaCF_3SO_3$ (150 mg, 0.87 mmol) was added to a suspension of microcrystalline complex **2**, $[Ag_2(L^{1\text{-}Me})_2(ClO_4)_2]$ (150 mg, 0.24 mmol). The mixture was stirred for 4 h at room temperature and then filtered. The precipitate was dissolved in acetone and recrystallized by diffusion of petroleum ether into the solution. Crystals suitable for X-ray analysis were obtained in two days. Yield: 68% based on $[Ag_2(L^{1\text{-}Me})_2(CF_3SO_3)_2]$. Anal. Found: C, 13.20; H, 2.50. Calculated for $C_8H_{16}S_6Ag_2F_6O_6$: C, 13.16; H, 2.21. ^{1}H NMR (DMSO-d_6, 300 MHz): δ 2.09 (*s*, 6H, CH_3-S-CH_2-S-CH_3), 3.73 (*s*, 2H, CH_3-S-CH_2-S-CH_3). ^{19}F NMR (DMSO-d_6, 376.31 MHz): δ –78.2. IR (KBr, cm^{-1}): 3431m, 2971w, 2915m, 2855w, 1630m, 1435m, 1424m, 1384w, 1260vs, 1203s, 1178s, 1101w, 1033s, 986w, 958w, 805m, 769w, 745m, 692m, 643s, 581m, 518m.

$[AgL^{1\text{-}Me}(C_6H_5CO_2)]_\infty$ 8. This complex was synthesized in the same manner as **2** using $C_6H_5CO_2Ag$ (175 mg, 0.76 mmol) and $L^{1\text{-}Me}$ (0.30 mL, 2.93 mmol). Yield: 81% based on $C_6H_5CO_2Ag$. Anal. Found: C, 35.77; H, 3.73. Calculated for $C_{10}H_{13}S_2AgO_2$: C, 35.62; H, 3.89. ^{1}H NMR (DMSO-d_6, 400 MHz): δ 2.11 (*s*, 6H, CH_3-S-CH_2-S-CH_3), 3.73 (*s*, 2H,

CH_3-S-CH_2-S-CH_3), 7.33-7.94 (m, 5H, $C_6H_5CO_2$). IR (KBr, cm^{-1}): 3434m, 2967w, 2917w, 1645m, 1540s, 1381s, 1261w, 1064w, 1025w, 834w, 804w, 742w, 708m, 689w, 676w, 664w.

$[AgL^{1\text{-}Me}(CH_3SO_3)]_\infty$ 9. This complex was synthesized in the same manner as **2** using $AgCH_3SO_3$ (486 mg, 2.39 mmol) and $\mathbf{L^{1\text{-}Me}}$ (0.30 mL, 2.93 mmol). Yield: 31% based on $AgCH_3SO_3$. Anal. Found: C, 15.23; H, 3.70. Calculated for $C_4H_{11}S_3AgO_3$: C, 15.44; H, 3.56. ^1H NMR (DMSO-d_6, 400 MHz): δ 2.14 (*s*, 6H, CH_3-S-CH_2-S-CH_3), 3.75 (*s*, 2H, CH_3-S-CH_2-S-CH_3), 2.831 (*s*, 3H, CH_3-SO_3). IR (KBr, cm^{-1}): 3458m, 2964w, 2915w, 1635m, 1424w, 1261m, 1201m, 1100w, 1050m, 873w, 787m, 744w, 693w, 618w, 560w.

$[AgL^{1\text{-}Me}(HOOCCF_2CF_2COO)]_\infty$ 10. Complex **10** was synthesized by the self-assembly of $\mathbf{L^{1\text{-}Me}}$ and the reaction product of tetrafluorosuccinic acid and Ag_2CO_3. Tetrafluorosuccinic acid (245 mg, 1.30 mmol) and silver carbonate (156 mg, 0.56 mmol) were combined in 5 mL of acetone and stirred at room temperature for 2 hours. The filtrate was then mixed with a solution of $\mathbf{L^{1\text{-}Me}}$ (0.30 mL, 2.93 mmol) in diethyl ether (5 mL) and then the mixture was refluxed at 50 °C for 1 hour. The resulting solution was filtered and recrystallized by diffusion of petroleum ether into the solution. Single crystals suitable for X-ray analysis were found after two weeks. Yield: 68% based on $HOOC(CF_2)_2COOH$. Anal. Found: C, 20.56; H, 2.30. Calcd for $C_7H_9AgF_4O_4S_2$: C, 20.75; H, 2.24. ^1H NMR (DMSO-d_6, 300 MHz): δ 2.09 (*s*, 6H, CH_3-S-CH_2-S-CH_3), 3.73 (*s*, 2H, CH_3-S-CH_2-S-CH_3). $^{19}F\{^1H\}$ NMR (DMSO-d_6, 376.31 MHz): −118.7 (CF_2CF_2). IR (KBr, cm^{-1}): 3440m, 2920w, 1784s, 1680m, 1641w, 1372w, 1165s, 1140m, 988m, 875m, 778s, 630s, 555w.

Structure Determination. X-ray intensity data was recorded on a Bruker AXS Platform diffractometer equipped with a SMART 2K CCD area detector using graphite-monochromatized Cu Kα (λ = 1.54178 Å) for **1-5** and **9**. For **6 – 8** and **10**, the X-ray intensity data was obtained on an SMART 6K CCD equipped with a rotating anode (Cu Kα). The program SAINT[16] was used for the data reduction. An empirical absorption correction, based on multiple measurements of equivalent reflections, was applied using the program SADABS.[17] The space group was confirmed by the XPREP[18] routine in the program SHELXTL.[19] The structures were solved by direct methods and refined by full-matrix least-squares and difference Fourier techniques, based on F^2, using SHELXL-97.[20] All non-hydrogen atoms were refined anisotropically, while the isotropic hydrogen atoms were introduced at calculated positions using a riding model. In the case of **5**, all crystals

were of a poor quality and attempts to grow more suitable crystals failed. A large residual electron density was noted at 0.99 Å from Ag(I). We were not able to remeasure the X-ray data using the Mo Kα radiation as the crystal had been damaged. The H atom on the succinate in complex **10** was found on a Fourier difference map and was included in a fixed position. Complexes **2**, **5** and **6** belong to the chiral $Pca2_1$ space group. The Flack parameter,[21] which took the values of 0.030(11), 0.06(3), and 0.043(13) for **2**, **5**, and **6** respectively, confirmed that the reported structures are of the correct hand. The crystal data, intensity data collection parameters, and structure refinement parameters are listed in Table 3.1.1.

Table 3.1.1. Crystal data and X-ray data collection parameters.

	1	**2**	**3**	**4**	**5**
Formula	$C_6H_{16}Ag_2N_2O_6S_4$	$C_6H_{16}Ag_2Cl_2O_8S_4$	$C_6H_{16}Ag_2Cl_2O_8S_4$	$C_{20}H_{30}Ag_2O_6S_6$	$C_5H_8AgF_3O_2S_2$
Mol wt	556.19	631.07	631.07	774.54	328.10
Cryst. size	0.14x0.10x0.04	0.14x0.09x0.05	0.33x0.10x0.04	0.32x0.12x0.04	0.19x0.12x0.08
Space group	*Pbca*	*Pca*2_1	*P*$2_1/c$	*Pbca*	*Pca*2_1
a (Å)	8.9793(2)	20.8995(1)	18.0705(2)	10.9920(1)	10.4756(2)
b (Å)	16.7321(4)	8.8901(1)	11.3354(1)	8.7129(1)	10.8952(2)
c (Å)	21.4072(5)	9.4567(1)	8.5295(1)	28.4137(3)	8.9067(1)
α (deg)	90	90	90	90	90
β (deg)	90	90	93.634(1)	90	90
γ (deg)	90	90	90	90	90
Volume (Å^3)	3216.27(13)	1757.04(3)	1743.66(3)	2721.24(5)	1016.56(3)
Z	8	4	4	4	4
D(calc) (g cm^{-3})	2.297	2.386	2.404	1.891	2.150
F(000)	2176	1232	1232	1552	640
Temp (K)	100(2)	100(2)	150(2)K	100(2)	293(2)K
μ, (mm^{-1})	24.625	25.439	25.634	16.149	19.948
θ_{max} (deg)	72.77	72.75	72.83	72.85	72.91
R1[a][$I > 2\sigma(I)$]	0.0531	0.0451	0.0378	0.0311	0.0682
Rw[b][$I > 2\sigma(I)$]	0.1247	0.1122	0.0884	0.0776	0.1595
R [all data]	0.0688	0.0457	0.0428	0.0347	0.0695
Rw [all data]	0.1300	0.1124	0.0906	0.0793	0.1607
S[c]	0.996	1.017	0.994	1.013	1.115

	6	**7**	**8**	**9**	**10**
Formula	$C_7H_8AgF_7O_2S_2$	$C_8H_{16}Ag_2F_6O_6S_6$	$C_{10}H_{13}AgO_2S_2$	$C_4H_{11}S_3AgO_3$	$C_7H_9AgF4O_4S_2$
Mol wt	429.12	730.31	337.19	311.18	405.13
Cryst. size	0.39x0.12x0.07	0.16x0.06x0.02	0.14x0.04x0.01	0.14x0.04x0.04	0.20x0.04x0.02
Space group	*Pca*2_1	*P*$2_1/c$	*P*-1	*P*$2_1/n$	*P*-1
a (Å)	10.7139(1)	9.0925(1)	6.8647(1)	9.6279(5)	6.7508(2)
b (Å)	13.4083(2)	21.699(3)	7.6822(1)	7.4958(4)	8.3046(3)
c (Å)	8.9523(1)	11.0192(2)	12.3591(2)	13.5720(7)	10.8924(4)
α (deg)	90	90	78.926(1)	90	87.974(2)
β (deg)	90	90.147(1)	87.441(1)	91.702(2)	83.849(2)
γ (deg)	90	90	74.335(1)	90	83.473(2)
Volume (Å^3)	1286.04(3)	2171.15(6)	615.86(2)	979.04(9)	602.99(4)
Z	4	4	2	4	2
D(calc) (g cm^{-3})	2.216	2.234	1.818	2.111	2.231
F(000)	832	1424	336	616	396
Temp (K)	200(2)	150(2)K	150(2)	200(2)	150(2)
μ, (mm^{-1})	16.444	20.590	16.126	22.221	22.221
θ_{max} (deg)	72.75	68.98	68.80	69.06	68.99
R1[a][$I > 2\sigma(I)$]	0.0459	0.0244	0.0305	0.0262	0.0337
Rw[b][$I > 2\sigma(I)$]	0.1087	0.0643	0.798	0.0732	0.0919
R [all data]	0.0485	0.0269	0.0315	0.0270	0.0356
Rw [all data]	0.1100	0.0658	0.0806	0.0737	0.0946
S[c]	1.041	1.031	0.987	1.080	0.808

[a] $R = \Sigma \, | \, |F_o| - |F_c| \, | / \Sigma |F_o|$. [b] $R_w = [\Sigma w(F_o^2 - F_c^2)^2 / \Sigma w(F_o^2)^2]^{1/2}$.
[c] $S = [\Sigma w(F_o^2 - F_c^2)^2 / (m-n)]^{1/2}$ (m is the number of reflections and n the number of parameters).

3.1.4 Results and Discussion

Synthesis of the complexes. Except for **3**, **7**, and **10**, all the complexes were obtained as polymeric compounds *via* the self-assembly of bis(methylthio)methane, $L^{1\text{-}Me}$, with a number of silver(I) salts. Direct mixing of solutions of the organic ligand and the silver salts gave rise to white microcrystalline solids, which were identical to the corresponding

single-crystals obtained by recrystallization from petroleum ether, as confirmed by elemental analysis. Neither the white microcrystalline solids nor the single crystals are soluble in water or in nonpolar solvents (pentane, hexane). These were however found to be soluble in polar solvents (acetone, DMSO). The crystals for all those complexes are relatively stable in air, although a noticeable darkening becomes evident after about six weeks. The self-assembly of the bis(methylthio)methane and silver salts gave rise to complexes which have been found to not be dependent on the recrystallization solvent because the same crystals were obtained whatever the solvent of recrystallization used (pentane, hexane, heptane, petroleum ether). In addition, all attempts to form complexes with different stoichiometries failed. The various ligand:metal ratios investigated (up to 1:10) always resulted in identical crystals.

Complex **3**, $[Ag_2(\mathbf{L}^{1\text{-}Me})_2(ClO_4)_2]_{\infty}$,, was obtained by an anion-exchange process by first reacting bis(methylthio)methane and silver trifluoromethanesulfonate. The direct self-assembly of the triflate silver salt and $\mathbf{L}^{1\text{-}Me}$ leads to a microcrystalline solid that forms a three-dimensional channel-like cationic framework in which the triflate anions are located.[9] This microcrystalline solid was soaked for 2 h in an aqueouse solution of $LiClO_4$, and the anion-exchange was monitored by infrared spectroscopy every 40 min. Once the exchange of the triflate by the perchlorate was completed (as confirmed by IR spectroscopy), the resulting product was dissolved in acetone and then recrystallized from petroleum ether to obtain crystals suitable for X-ray structure determination.

Complex **7**, $[Ag_2(\mathbf{L}^{1\text{-}Me})_2(CF_3SO_3)_2]_{\infty}$, was obtained by an anion-exchange process involving complex **2**. Crystals of **2** were immersed in an aqueous solution of $NaCF_3SO_3$. Stirring of this mixture for 4 h led to the complete replacement of the perchlorate anions by the triflate ones. This anion-exchange process was monitored by infrared spectroscopy: samples were collected every hour, and their infrared spectra recorded. The IR of $[Ag_2(\mathbf{L}^{1\text{-}Me})_2(ClO_4)_2]_{\infty}$, **2**, shows an intense broad band at 1092 cm^{-1}, the $\nu_1(A_1)$ vibration, which is characteristic of the ClO_4^- anion.[22,23] The infrared spectra (see the Supporting Information, Figure S1, Annexe III) show the gradual disappearance of the perchlorate band at

1092 cm^{-1} and the simultaneous appearance and growth of the two characteristic bands of trifluoromethanesulfonate: $\nu[SO_3(E)]$ at 1270 cm^{-1} and $\nu[SO_3(A_1)]$ at 1030 cm^{-1}.[24,25] After 4 hours, the band at 1092 cm^{-1} has completely disappeared, indicating that the anion

exchange was complete. The resulting product of this anion-exchange process was dissolved in acetone and then recrystallized from petroleum ether to yield single crystals of 7 suitable for X-ray analysis. Further details about the anion exchange of complexes formed by $\mathbf{L}^{\mathbf{l\text{-}Me}}$ with silver(I) salts of weakly or noncoordinating anions will be provided in a future report.[9]

Description of the structures of the complexes. The supramolecular coordination polymers obtained by the direct self-assembly of the small bis(methylthio)methane, $\mathbf{L}^{\mathbf{l\text{-}Me}}$and the silver(I) centres bearing coordinating counteranions or obtained by a synthetic approach on the basis of anion-exchange have shown to be independent from the metal-to-ligand ratio as well as from the solvent of recrystallization. Thus, the only parameters that vary here are the size and the shape of the coordinating anions.

Of the 10 complexes synthesized, seven form 2D coordination networks, while the other three generate 1D coordination polymers. The two topologically identical perchlorate complexes **2** and **3**, which are obtained respectively by direct self-assembly and by anion-exchange process, are polymorphs.

General description of the 2D-networks. It is observed that complexes **1-7** adopt very similar solid-state organizations. The basic framework consists of a 2D coordination network based on $(AgL^{l\text{-}Me})_{\infty}$ layers in which each silver atom is surrounded by three sulfurs, whereas the anions are coordinated to Ag atoms through one of their oxygen atoms. In this respect, these structures may be considered as topologically comparable. We may distribute them in two slightly different groups depending on the size and shape of the anions. In group 1, which contains the smaller coordinating anions, NO_3^- and ClO_4^-, the repeat unit is a 14-membered ring. Group 2 contains the larger anions (**4-7**) which act here as monodentate ligands. The repeat unit for this group is a simple 10-membered macrometallocycle, $Ag_3(L^{l\text{-}Me})_2S$.

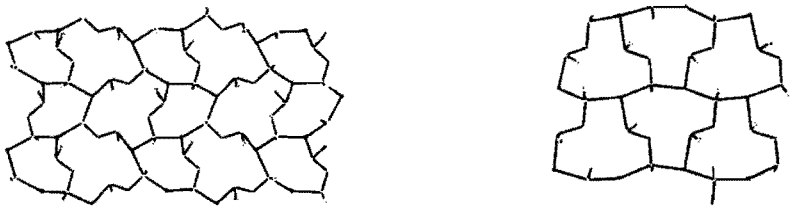

(a) (b)

Figure 3.1.1. (a) All group 1 compounds have this 2D structure. (b) All group 2 compounds form this 2D-network. The anions and the hydrogen atoms are omitted for clarity.

The repeat unit of the group 1 complexes consists of 14-membered macrometallocycles which may be seen as the fusion of an 8- and a 12-membered ring. The repeat units of the layers of the complexes in groups 1 and 2 are compared in Figure 3.1.1a and 3.1.1.b as projections of the 2D planes. Side views of the unit-cell content of the group 1 complexes are compared in Figures 3.1.2 and Figures S2-S4 (Annexe III). The anions coordinated to the silver occupy the space between the 2D sheets. The layer spacing increases from 8.366 to 9.457 Å going from **1** to **2**, thus reflecting the larger size of the perchlorate anion. The inter-layer distance is 9.035 Å for **3**. The larger anions all form complexes of group 2. The layers (Figure 3.1.1b) are constituted of nearly identical repeat units (see Supporting Information, Figures S5-S8, Annexe III).

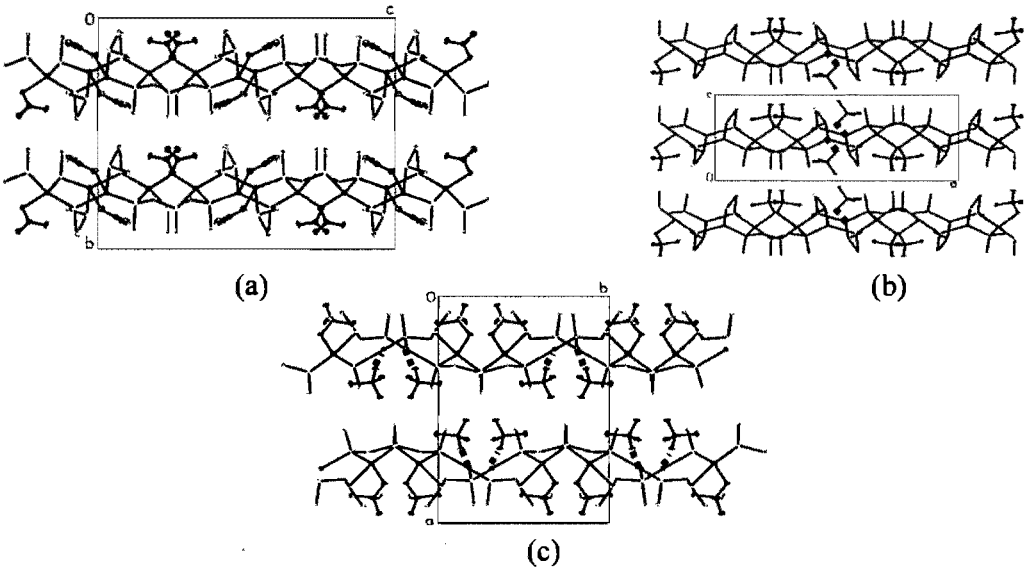

Figure 3.1.2. Packing of the Group 1 complexes. (a) View down the *a*-axis of **1**. The nitrate anions, coordinated to the silver atoms in a monoatomic mode, are located between the sheets. (b) The *ac*-plane projection of **2**. (c) The *ab*-plane projection of the other perchlorate, **3**. The perchlorates in **2** and **3** are also coordinated to the silver atom in a monoatomic mode and are located between the sheets.

The crystal structures of the group 2 complexes are compared in Figure 3.1.3. Of the group 2 structures, those of **5** and **6** may be considered "isostructural", this is best appreciated when comparing Figures 3.1.3c and 3.1.3d. The larger *b*-dimension of the unit cell in **6** is clearly related to the larger anion.

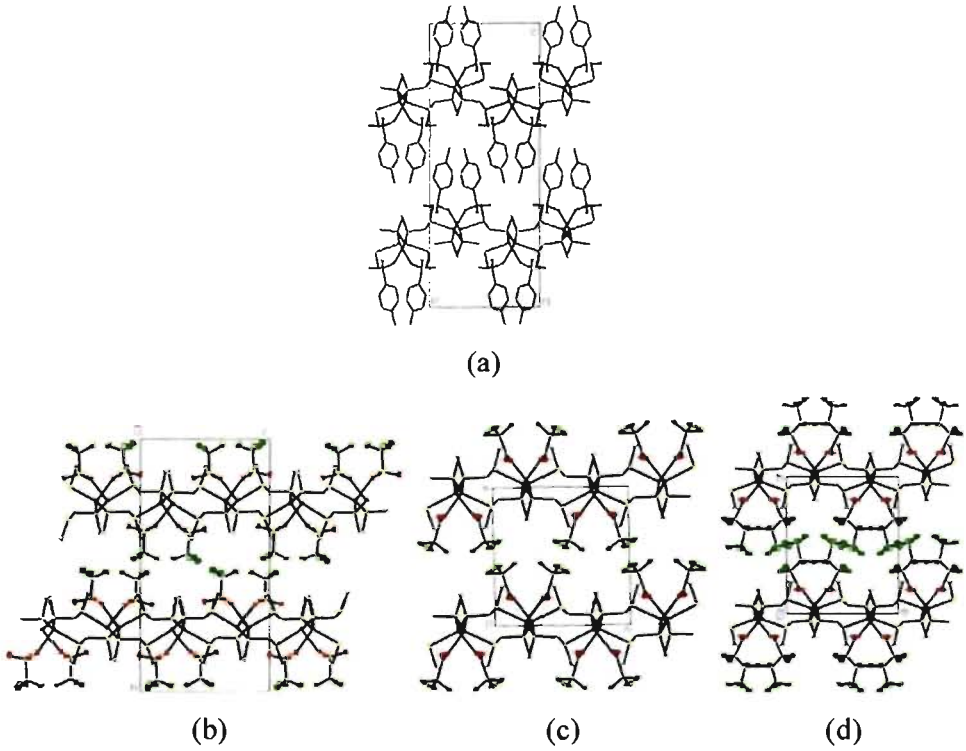

Figure 3.1.3. (a) Packing of **4**; paratoluenesulfonate anions are located between the neutral sheets, and there is no π-π stacking between the phenyl groups of the anions. (b) Packing of **7**. (c) Packing of **5**; the trifluoro acetates are within the layers. (d) Packing of **6**; the heptafluorobutyrate anions are also located between the neutral sheets. Because of the bulkiness of the anion, the *b*-dimension is longer in **6** than in **5**.

In both groups, the coordination of Ag is four $3S(L^{1\text{-}Me})$ + 1O(A) (Figure 3.1.4 and S9, Annexe III). The bond distances describing the coordination of the Ag(I) are compared in Tables 3.1.2 and S1 (Annex III). In the group 1 complexes, **1** and **2**, there are two distinct anions coordinated to the silver atoms. One anion is fairly strongly coordinated, whereas the other is at a longer distance. In the case of **3**, the two anions are weakly coordinated to the Ag(I) atoms. In complexes **4-6** (group 2), the Ag-O distances are short, in the 2.305-2.343 Å range. The complexes of group 1 have a triangular coordination of sulfur atoms. The fourth ligand, an oxygen atom, is more or less perpendicular to the AgS_3 group. The coordination in group 2 is tetrahedral, although fairly distorted. The sums of the bond angles around the silver centers in complexes **1-7** are compared in Table 3.1.2. With the exception of complex **7**, these sums are clearly higher, for group 1 complexes, indicating an almost planar AgS_3 group. A plot of the Ag-O distances as a function of the sum of the bond angles around the silver centers is shown in Figure S14 (Annexe IV).

It clearly differentiates between the tetrahedral and the triangular-plus-one coordinations.

Table 3.1.2. Comparison of the bond distances (Å) around the silver atom in complexes **1-10**.

Bond	**1**	**2**	**3**	**4**	**5**	**6**	**7**
Ag-O	2.571(5)	2.461(5)	2.633(4)	2.343(2)	2.305(6)	2.306(4)	2.487(2)
Ag-S	2.525(2)	2.545(2)	2.527(1)	2.533(1)	2.539(3)	2.567(2)	2.563(1)
Ag-S	2.542(2)	2.546(2)	2.538(1)	2.543(1)	2.577(2)	2.594(2)	2.567(1)
Ag-S	2.552(2)	2.581(2)	2.570(1)	2.583(1)	2.584(3)	2.601(2)	2.570(1)
Ag-O	2.377(5)	2.619(5)	2.574(4)				2.473(2)
Ag-S	2.532(2)	2.503(2)	2.498(1)				2.569(1)
Ag-S	2.550(2)	2.528(2)	2.557(1)				2.578(1)
Ag-S	2.621(2)	2.557(1)	2.667(1)				2.580(1)
SUM1[a]	359.9	359.0	356.5	333.4	337.2	331.8	350.7
SUM2[a]	338.1	350.3	352.7	352.5			

Bond	**8**	**9**	Bond	**10**	$\mathbf{L^{1\text{-}Ph}}$
Ag-O	2.267(2)	2.440(3)	Ag-O	2.627(2)	2.280(2)
Ag-O	2.413(2)	2.461(3)	Ag-O	2.786(8)	2.314(2)
Ag-S	2.563(1)	2.489(1)	Ag-O	2.859(8)	
Ag-S	2.629(1)	2.519(1)	Ag-S	2.479(1)	2.583(1)
Ag-Ag	2.9111(4)	3.2430(5)	Ag-S	2.479(1)	2.654(1)
			Ag-Ag	3.0670(5)	2.9836(5)

[a]SUM1 and [a]SUM2 (deg) refer to the sum of the S-Ag-S bond angles around the silver centers. The SUM value is 360° in a triangular (planar) environment and 328.5° for the tetrahedral coordination.

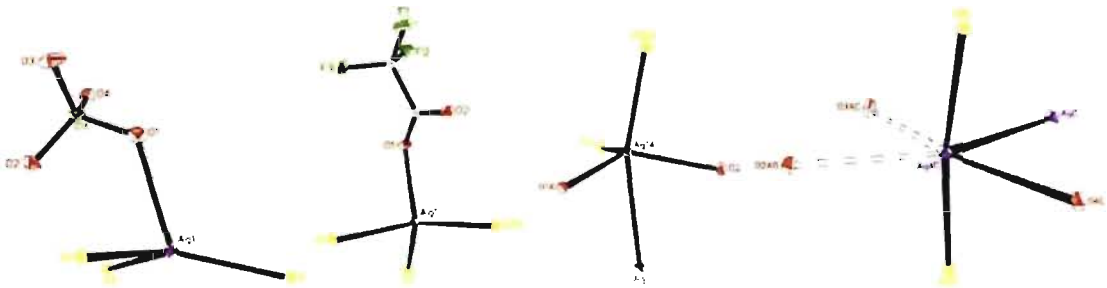

(a) (b) (c) (d)

Figure 3.1.4. Comparison of the coordination environment of the silver centers. (a) Triangular-plus-one coordination in complex **2** of group 1. (b) Tetrahedral in complex **5** of group 2. (c) Distorted triangular bipyramidal in **8**. (d) Octahedral in complex **10**, see Figure 3.1.8b.

Specific comments about the structures of the group 1 complexes.

$[Ag_2(L^{1\text{-}Me})_2(NO_3)_2]_\infty$ 1. The repeat unit of this complex is the juxtaposition of a 12-membered, $Ag_3(L^{1\text{-}Me})_3$, and an 8-membered, $Ag_3L^{1\text{-}Me}S_2$, metallomacrocycle (Figure 3.1.1a). The association of the rings generates a neutral, puckered 2Dnetwork of $[Ag_2(L^{1\text{-}Me})_2(NO_3)_2]_\infty$ parallel to the (010)-plane (Figure 3.1.1a). The nitrate anion, a coordinating anion,[22] completes the coordination sphere of the silver atom in a tetrahedral fashion (Figure 3.1.2a).

$[Ag_2(L^{1\text{-}Me})_2(ClO_4)_2]_\infty$ 2. In complex **2**, the perchlorates complete the coordination sphere of the silver atoms (Figure 3.1.2a), as does the nitrate in complex **1**. In this complex, the perchlorates are more strongly coordinated to one type of silver atom (Ag(1)-O = 2.461(5) Å) and weakly coordinated to the other type of silver (Ag(2)-O = 2.619(5) Å).

We speculate that the resemblance of the nitrate and perchlorate-containing networks may be due to the comparable bulk of these anions.

$[Ag_2(L^{1\text{-}Me})_2(ClO_4)_2]_\infty$ 3. Here, there are again two crystallographically different silver atoms and two perchlorates in the 2D network. The perchlorates also have significantly different Ag-O distances. Ag(1)-O = 2.574(4) Å and Ag(2)-O = 2.633(4) Å. Since the topology of the supramolecular architectures obtained with the small group 1 anions, NO_3^- and ClO_4^-, is similar we decided to try to synthesize complexes with another small anion, such as NO_2^-. Neither the direct self-assembly nor the anion-exchange process yielded a complex with NO_2^-. However, complex **3**, with perchlorate, was successfully obtained by the anion-exchange process. This complex **3**, which is a polymorph of **2**, has a coordination network with the same topology as that of complexes **1** and **2**.

Specific comments about the structures of group 2 complexes.

$[AgL^{1\text{-}Me}(p\text{-}TsO)]_\infty$ 4. In complex **4**, each silver atom is surrounded by sulfurs from three different ligands, whereas each sulfur joins two silver atoms. This results in a 2D coordination network parallel to the *ab*-plane (Figure 3.1.1b and S5a, Annex III). The repeat unit is a 10-membered $Ag_3(L^{1\text{-}Me})_2S$ ring. The paratosylate (a coordinating anion for the dithioether spacers[6]) completes the coordination sphere of the silver atom through one of its oxygen atoms. In addition, as this anion is bulkier than the nitrate, a larger distance between the layers is required to accommodate this elongated anion (Figure 3.1.3a). However, there are no π-π interaction between the rings of adjacent tosylates as their mean planes form an 88° angle.

$[AgL^{1\text{-}Me}(CF_3CO_2)]_\infty$ 5 and **$[Ag(L^{1\text{-}Me})_2(CF_3CF_2CF_2CO_2)]_\infty$ 6.** Panels c and d of Figure 3.1.3 clearly show the relation between these two complexes, which may be considered isostructural. Except for the *b*-dimension, their unit cells are very similar, and so are their structures. The intermediate pentafluorocarboxylate was also synthesized, as we expected that its structure would fit in between those of **5** and **6**. Surprisingly, the 2D layer structure was not observed. Instead, a very unusual clusterlike structure was noted and will be reported later.

$[AgL^{1\text{-}Me}(CF_3SO_3)]_\infty$ 7. With $L^{1\text{-}Me}$, the trifluoromethanesulfonate complex behaves as the trifluoroacetate, they both form a 2D network of group 2 complexes. This situation is to be paralleled to that noted with the $L^{1\text{-}Ph}$ ligand, in which both the trifluoromethanesulfonate and the trifluoroacetate adopt the same structure, although in this work, it is that of a 1D coordination polymer.[7]

The fluorine atoms of the perfluorocarboxylates usually occupy the space between adjacent layers. Hence, they may be subject to repulsive dipole-dipole interactions or attractive C-F···H very weak interactions that may increase the dimensionality of the networks.[7] Thus, we were interested in the use of carboxylate anions without fluorine atoms such as the $CH_3CO_2^-$ or $C_6H_5CO_2^-$ in order to see if coordination networks similar to those of group 2 would be obtained. This led us to synthesize complex **8**, by reacting $L^{1\text{-}Me}$ with silver benzoate.

1D coordination polymers. **$[AgL^{1\text{-}Me}(C_6H_5CO_2)]_\infty$ 8.** In this complex, two adjacent silver atoms are bound in a diatomic bridging mode by two benzoate groups to form the $[(C_6H_5COO)Ag]_2$ dimer. Each dimer is linked to two others by four bis(methylthio)methane building blocks, so as to generate a ladderlike 1D coordination polymer extending parallel to the *a*-axis (Figure 3.1.5).

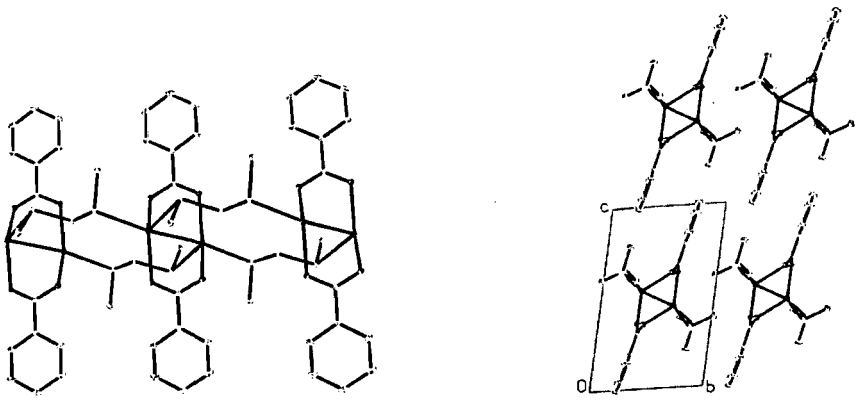

(a) (b)

Figure 3.1.5. (a) One-dimensional coordination polymer $[AgL^{1\text{-}Me}(C_6H_5CO_2)]_\infty$ (**8**), shown parallel to the *a*-axis. (b) Projection down the *a*-axis showing the packing of this double-stranded 1D coordination polymer.

The repeating unit of this complex is a 10-membered metallomacrocycle, $Ag_4(\mathbf{L}^{1\text{-}Me})_2$. On the other hand, this structure may also be described as a corrugated ribbon of adjacent 10-membered rings, $Ag_4(\mathbf{L}^{1\text{-}Me})_2$, sharing Ag···Ag edges, whereas the two benzoate groups coordinated to the silver atoms are in a direction nearly perpendicular (88°) to the ribbon axis. It is worth noting that the same topology was noted for the self-assembly of the bis(phenylthio)methane, $\mathbf{L}^{1\text{-}Ph}$, and the 1,3- bis(phenylthio)propane, $\mathbf{L}^{3\text{-}Ph}$, spacers with the heptafluorobutyrate anion (Figures S10 and S11, Annex III),[6,7] although a 2D structure occurs with $\mathbf{L}^{1\text{-}Me}$ and the same anion (group 2 complex). The structure of **8** is further reinforced by stacking interactions between aromatic rings from consecutive layers (d_c-d_c = 3.931 Å and d-d = 3.594 Å) (Figure 3.1.6).

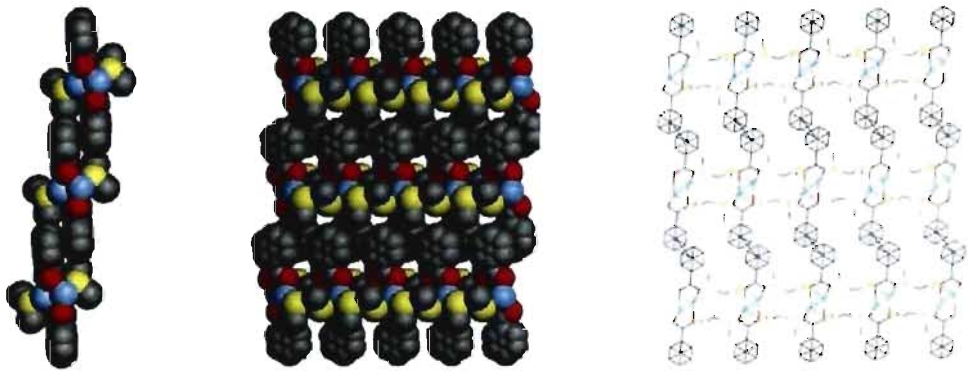

(a) (b) (c)

Figure 3.1.6. (a, b) π- π stacking nearly perpendicular to the *b*-axis. (c) π- π stacking shown parallel to the *ac*-plane for complex **8**. (silver atoms: blue; oxygen atoms: red; carbon atoms: grey and sulphur atoms: yellow).

In this complex, the silver atom is linked to two sulfur atoms from two different ligands, to two oxygen atoms from distinct carboxylate groups and (weakly) to an adjacent silver atom (Ag···Ag: 2.9114(4) Å) so that its environment is that of a distorted trigonal bipyramid. The actual bond distances and angles around the silver atom are given in Table S1 (Annexe III). The silver-silver distance of 2.9114(4) Å is less than the sum of the van der Waals radii of two silver atoms, 3.44 Å, but slightly longer than twice the metallic radius of silver, 2.89 Å,[26] indicating a silver-silver interaction.[27-29] However, it is not clear whether this short silver-silver distance is due to a genuine metal-metal interaction or a geometrical constraint.[30]

A 1D-coordination polymer is noted with the benzoate anion, $C_6H_5CO_2^-$ as opposite to the 2D coordination networks obtained with the perfluorocarboxylate. This situation is likely favored by the secondary π-π stacking between the benzoate groups from adjacent chains that lead to a two-dimensional network. This fact shows clearly the influence of the shape of the coordinating anions upon the supramolecular network.

On the other hand, the counteranions bearing sulfonate group such as the trifluoromethanesulfonate, $CF_3SO_3^-$, and the paratoluenesulfonate, $C_7H_7SO_3^-$, display comparable coordination networks (group 2). It was of interest that those two anions with different size show similar topology where their sulfonate group completed only the coordination sphere of the metal centre via one oxygen atom, whereas the remaining part of these anions lay between neighboring layers. Thus, we chose to react the $\mathbf{L}^{\mathbf{1\text{-}Me}}$ spacer with

silver(I) methanesulfonate, which is more similar to the triflate than the paratoluenesulfonate, in order to see if a similar 2D coordination network would form.

$[AgL^{1\text{-}Me}(CH_3SO_3)]_\infty$ 9. In this complex, two centrosymmetrically-related silver atoms are bound by two bis(methylthio)methane ligands in a dibridging fashion, thus yielding a $[Ag(CH_3SCH_2SCH_3)]_2$ dimer (Figure 3.1.7a). In this dimer, the Ag-Ag distance of 3.2430(5) Å is slightly shorter than the sum of the van der Waals radii of two silver atoms, 3.44 Å, indicating a very weak silver-silver interaction.[27-29] Each dimer is bound by four methanesulfonate anions in a dibridging mode to two other dimers so as to build a 1D coordination polymer extending parallel to the *b*-axis (Figure 3.1.7b). In other words, the chains are made up of $[Ag(OSO)_2Ag]$ rings sharing Ag atoms. The $[Ag(CH_3SCH_2SCH_3)]_2$ dimers are almost perpendicular to the ribbon that constitutes the polymeric chain. The oxygen and the sulfur atoms of each of the four $CH_3SO_3^-$ anions and the two silver atoms to which they are coordinated are nearly coplanar. This group of atoms is inclined 84(1)° to the plane of the dimers. The silver atom is coordinated by two oxygen atoms from distinct methanesulfonate anions (Ag-O = 2.440(3) and 2.461(3) Å), by two sulfur atoms from different bis(methylthio)methane ligands (Ag-S = 2.4891(8) and 2.5193(8) Å) and (weakly) by an adjacent silver atom (Ag-Ag = 3.2430(5) Å). The silver atom therefore adopts a distorted trigonal bipyramid environment (Ag-Ag-O = 169.6(1)°; O-Ag-O = 104.8(1)°; O-Ag-S = 96.8(1) and 95.4(1)°).

There are weak hydrogen-bond interactions between the sulfonate oxygen atoms that are not engaged with the silver (I) centre of one polymer, and a methylene hydrogen of the building block of another chain ($C\cdots O(2)^{i}$: 3.267 Å and $C-H\cdots O(2)^{i}$ = 165.5° and $C\cdots O(2)^{ii}$ = 3.346 Å and $C-H\cdots O(2)^{ii}$ = 110.4°; symmetry codes (i):1-x,-y,-z and (ii): 1-x, 1-y,-z). Consequently, the $[AgL_2{}^{1\text{-}Me}(CH_3SO_3)]_\infty$ 1D coordination polymer is surrounded by six other chains, thus building a 3D neutral network (Figure 3.1.7c). Each chain has six neighbours in a hexagonal environment. This complex with CH_3SO_3 did not give the structure expected on the basis of its size. This could be attributed to the existence of weak hydrogen bond interactions.

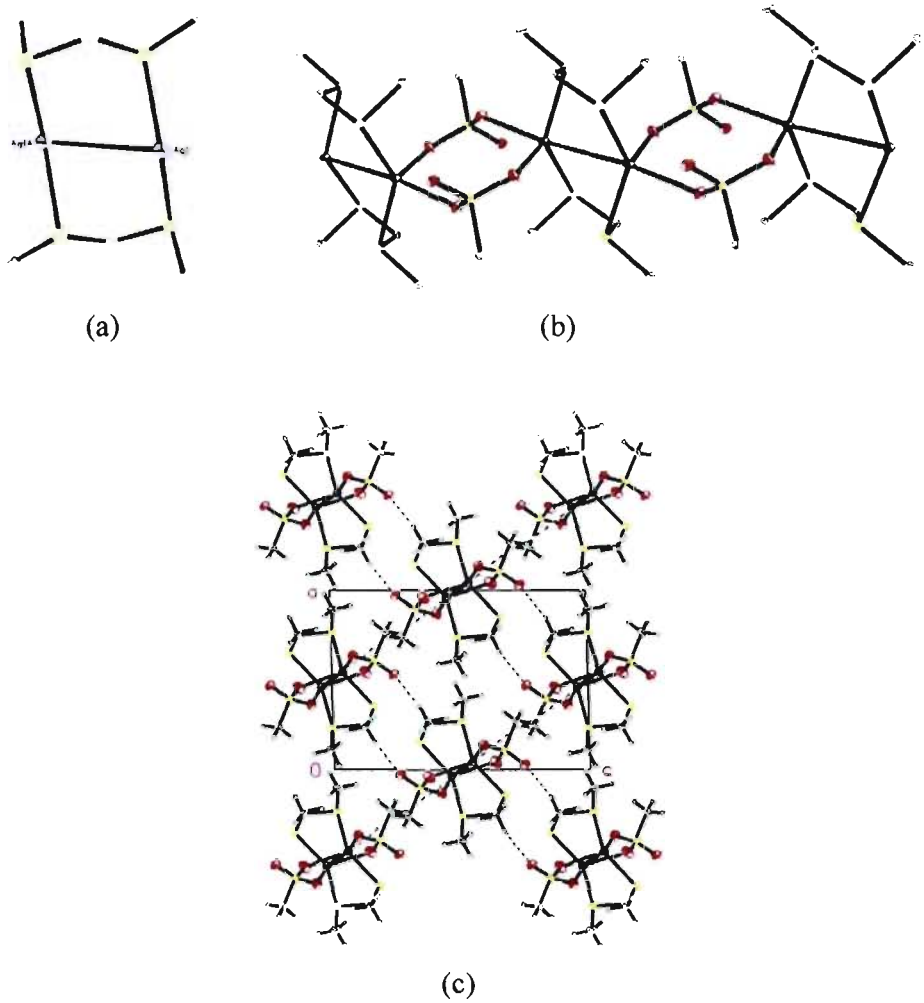

Figure 3.1.7. (a) $[Ag(CH_3SCH_2SCH_3)]_2$ dimer of **9**. (b) The 1D coordination polymer of **9**, extending parallel to the *b*-axis, consists of a repetition of dimers linked by two CH_3SO_3 molecules. (c) Projection on the *ac*-plane of the 1D coordination polymer **9**. The 1D chains form a 3D-network through hydrogen bonds (shown as dashed lines) between the oxygen atoms of the methanesulfonate and the H atoms of the methylene group of the bis(methylthio)methane spacer. ($C\cdots O(2)^{i}$=3.267 Å and $C–H\cdots O(2)^{i}$= 165.5° and $C\cdots O(2)^{ii}$ = 3.346 Å and $C–H\cdots O(2)^{ii}$ = 110.4°; symmetry codes (**i**): 1-x,-y,-z and (**ii**): 1-x,1-y,-z). The 1D chains are shown perpendicular to the *ac*-plane.

$[AgL^{1\text{-}Me}(HOOCCF_2CF_2COO)]_\infty$ 10. With its two carboxylate groups, this anion was expected to increase the dimensionality of the network. For example, we could expect that the 2D networks of **5** and **6** would form a 3D network where the dicarboxylate anion links the layers. Unfortunately, the expected 3D structure was not obtained. Two ligands and two silver atoms form a centrosymmetric dimeric unit comparable to that observed in **9** (Figure 3.1.8a). Each unit is also coordinated by two succinate anions via a moderate Ag-O (2.628(2) Å) and a weak Ag-O coordination bond: Ag-O4#1 = 2.786(8) and

Ag-O(2)#2 = 2.859(8) Å (see the Supporting Information, Table-S1, Annex III). Brammer *et* al. reported slightly longer Ag-O distances of 2.890(2) and 2.865(5) Å in coordination compounds based on the trifluroacetate salts of 2,6-dimethylpyrazine (2,6-DMP) and 2,5-dimethylpyrazine (2,5-DMP), respectively.[31]

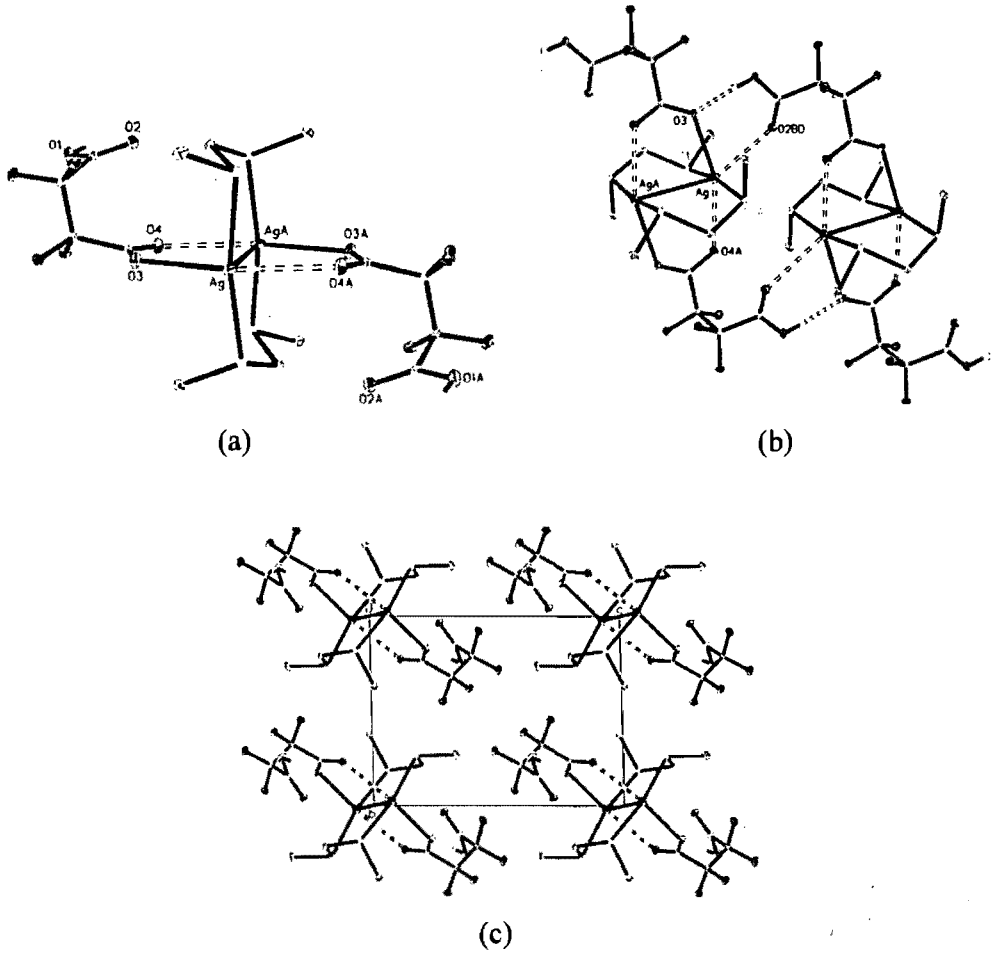

Figure 3.1.8. Complex **10**. (a) The dimer and its environment. (b) Association of two units to show bond formation and the short contacts involved in the 1D coordination polymer. (c) Projection of the 1D chains along the *a*-axis.

A 1D-coordination polymer is obtained as the other end of the succinate forms a hydrogen bond with the carboxylate oxygen atom of a neighboring unit. In other words, consecutive $[AgL^{1\text{-}Me}(OOCCF_2CF_2COOH)]_2$ units form a one-dimensional coordination polymer, extending parallel to the *a*-axis, by means of very strong hydrogen-bond interaction (O(1)···O(3) = 2.514 Å and O(1)–H···O(3)^{i} = 176°; symmetry code (i): 1+x,y,z) (Figure 3.1.8 b,c). The 1D coordination polymer is shown projected down the *a*-axis

(Figure 3.1.8 c and Figure S12, Annexe III). Each chain, surrounded by six others, adopts the hexagonal type of packing.

The succinate anion is in the *gauche* conformation, as is the related complex with the $\mathbf{L}^{\mathbf{1\text{-}Ph}}$ ligand.[7]

The environment around the silver atom may be best described as that of a very distorted octahedron (S-Ag-S = 169.3(1)°; O-Ag-O = 69.8(1), 79.6(1), 82.5(1) and 128.1(1)°). In the $[Ag\mathbf{L}^{\mathbf{1\text{-}Me}}(OOCCF_2CF_2COOH)]_2$ subunit, the dihedral angle between the two 8-membered rings $Ag_2S_4C_4$ and $Ag_2O_4C_2$ is 81.6(1)°.

The silver-silver distance of 3.0670(5) Å indicates a weak silver-silver interaction.[27-29] We noted the presence of such weak silver-silver interactions when bis(phenylthio)ether organic spacers were self-assembled with perfluorocarboxylate counter-anions.[6-8] In those coordination networks, two adjacent silver atoms often form a dimer with two perfluorocarboxylate groups. However, here the carboxylate groups of tetrafluorosuccinate do not form dimers. The tetrafluorosuccinate is coordinated to only one silver atom (Ag-O = 2.628(2) Å). There is another longer Ag-O distance at 2.787(2) Å and Ag-S interactions at 2.4788(8) and 2.4793(8) Å. In the corresponding complex with $\mathbf{L}^{\mathbf{1\text{-}Ph}}$, the Ag-O distances are much shorter (2.314(2) and 2.280(2) Å), whereas there is a relatively shorter Ag···Ag interaction at 2.9836(5) Å.

Our strategy to increase the dimensionality of the network using the tetrafluorosuccinate failed. However, the 1D coordination polymer obtained here is different from that resulting from the self-assembly of $\mathbf{L}^{\mathbf{1\text{-}Ph}}$ and the tetrafluorosuccinate anion.

Influence of the R substituent. Although the strength of the anion was found to be an important factor, the type of structure adopted also depends on the geometry (shape and dimension or anisotropy) of the anion. The bulkiness of the anion is one factor and so is that of the ligand. This latter parameter concerns the size of the R substituent on the sulfur atoms. In nearly all the coordination polymers reported so far, the R substituent was a phenyl group. Bu and coworkers reported the existence of a 1D coordination polymer in the self-assembly of bis(*tert*-butylthio)methane, $\mathbf{L}^{\mathbf{1\text{-}tBu}}$, with silver perchlorate.[32] The structure adopted was topologically identical to that reported with $\mathbf{L}^{\mathbf{1\text{-}Ph}}$ and ClO_4^- and other weakly coordinating anions.[7] Thus, it is expected that with the smaller methyl group as

substituent on the ligand, more ligands could approach the metal center, hence allows for an increase in the dimensionality of the resulting coordination polymers.

In the series of $\mathbf{L}^{1\text{-}\mathbf{R}}$ complexes, **R** = CH_3, Ph, or *t*-Bu, obtained with the silver(I) perchlorate anion, a single 1D coordination chain formed when **R** = Ph and *t*-Bu, whereas the smallest **R** substituent, CH_3, yielded a 2D coordination network. Clearly the size of **R** has a dominant effect. The bulkiness of the Ph and *t*-Bu substituents prevents the formation of a 2D network. However, 2D coordination networks may be obtained when a longer ligand, such as $\mathbf{L}^{3\text{-}\mathbf{Ph}}$, is used. In this case, the phenyl groups are positioned farther apart, thereby minimizing their interactions. On the other hand, it is interesting to compare the structures of two succinates in which only the substituents on the ligand differ: complex **10** with R = Me and another complex with $\mathbf{L}^{1\text{-}\mathbf{Ph}}$, where **R** = Ph. Both succinates form double-stranded chains although with completely different organizations of the anions and the ligands (see the Supporting Information, Figure S12, Annexe III).

Comments on Ag-O distances. In the above descriptions of the Ag(I) coordination, we are faced with deciding whether a given oxygen atom is part, or not, of the metal coordination. The range of Ag-O distances observed here in these coordination networks and polymers is fairly wide. The distribution ranges from a low of 2.267(2) Å in **8** to a high value of 2.633(4) Å in **3** and possibly up to 2.859(8) Å in **10**. An analysis of the Ag-O distances of Ag(I) containing coordination complexes using the Cambridge Structural Database was undertaken for each of the main coordination numbers, 4, 5 and 6. The distributions are shown in Figure S13 of the supporting information (Annex III). It is interesting to observe that indeed the distribution of the Ag-O distances is fairly wide whatever the coordination number. In this respect, one should appreciate the fact that the oxygens are not the only coordinating atoms around silver. Hence, it seems that the relative interplay or interactions between these atoms skew the distributions. Overall, there seems to be a trend in the mean and the median values as the coordination number increases. These quantities are 2.450, 2.478, 2.493 Å and 2.450, 2.468 and 2.491 Å for coordination numbers 4, 5, and 6, respectively. The three distributions overlap so much that there is no clear cut value of the Ag-O distance that would clearly relate to a given coordination. A recent study of the distribution of the Ag-S distances has been reported by Silva *et* al.[33] They also found that the average Ag-S distance increases with the coordination number. However, their proposed ranges for each coordination number do overlap significantly.

In the case of **10**, we consider here that the dimer consists of two dibridging succinate groups as well as two ligands (Figure 3.1.8a). However, the two Ag-O distances, 2.627(2) and 2.786(2) Å, are relatively long. If these distances were excluded, the Ag(I) coordination would change from 6 to 4. Furthermore, depending on our choice of coordination, **10** could be considered as being made up of individual units hydrogen bonded to one another, or it could be seen as a 1D coordination polymer if the O(2) atom is considered as being coordinated to Ag(I) with an Ag-O(2) distance of 2.859(8) Å (Figure 3.1.8b).

In this respect, we found that whenever structures are topologically identical, the coordination number is assigned on that relationship rather than the actual Ag-O distances. For example, there are two crystalographically different perchlorates groups in both **2** and **3**. We describe these structures as being topologically identical. However, the distances between a perchlorate oxygen and silver(I) are 2.461(5) and 2.619(5) Å in **2** and 2.574(4) and 2.633(4) Å in **3**, one could consider that only one perchlorate is silver coordinated in **2** and that none are in **3**. Hence, the description of the silver coordination would differ.

In a related series of coordination polymers based on the $\mathbf{L}^{\mathbf{4\text{-}Ph}}$ ligand,[8] we considered as being topologically identical two complexes containing the pentafluoropropionate and the heptafluorobutyrate anions. Thus, we said that the Ag(I) has in both cases a distorted triangular bipyramid coordination although, in the heptafluoro complex the Ag-S distance was 3.050(2) Å when compared to that in the pentafluoro propionate, 2.899(1) Å.

3.1.5 Conclusions

To rationalize the influence of the coordinating anions upon the structure of the supramolecular coordination polymers, we have selected a small flexible ligand, the bis(methylthio)methane.

We have shown that the size of the anions have a marked influence upon the coordination polymers. For complexes with the small anions (group 1) two-dimensional coordination networks with identical topologies have been found. Half of the anions are more strongly bonded to the silver centers than the other half. The layers are made up of 14-membered rings. For group 2 complexes, those with the longer anions, topologically identical layered structures made up of 10-membered rings are observed. The side chains of the anions extend between layers (paratoluenesulfonate **4**, trifluoromethanesulfonate **7**,

perfluorocarboxylates **5** and **6**). The other three complexes (**8-10**) form 1D coordination polymers. The benzoate **8** however, forms a 1D chain with a stacking of the aromatic rings.

Another type of 1D coordination polymer is observed for the methanesulfonate **9**. Each chain is surrounded by six others. They are bound to one another via weak C-H···O interactions. A 3D network may be considered when these interactions are taken into account. An intricate 1D polymeric structure (**10**) is found with the tetrafluorosuccinate salt. All three 1D chains have a centrosymmetric dimer. However, the Ag···Ag distances are not particularly short, with values of 2.911, 3.243, and 3.067 Å for **8**, **9**, and **10**, respectively.

Finally, we have shown that the bulk of the substituent on the ligand affects the type of structures. With the perchlorate anion, the ligand with the smaller CH_3 substituent allows for a 2D coordination network while 1D coordination polymers are noted when the substituent is either Ph or *t*-Bu.

In most of the supramolecular polymers reported here, the organic building block expanded the networks by linking adjacent metal centers, while the anions completed the coordination sphere of the silver atoms. Thus, to synthesize functionalized materials with zeolitic properties, one strategy would consist in liberating the coordination site occupied by the anions and by replacing them with noncoordinating ones such as BF_4^-, PF_6^-, or SbF_6^-. This approach leads to the formation of 1D, 2D, or 3D microporous frameworks, which present anion-exchange properties that will be reported in the future.

Acknowledgements. This work was supported by the Natural Sciences and Engineering Research Council of Canada (F.B.). M.O.A. thanks the Organisation Internationale de la Francophonie and the Programme des bourses d'excellence de la Francophonie du Canada for a graduate scholarship. The authors also thank Dr. M. Simard, Dr T. Maris, and F. Bélanger-Gariépy for helpful discussions.

Supplementary Material Available: Table of the bond distances and angles involving the silver atoms, Figures S1-S14 and X-ray crystallographic information files (CIF) for compounds (1-10). This material is available free of charge via the Internet at http://pubs.acs.org

3.1.6 References

(1) For example: (a) Stumpf, H. O.; Ouahab, L.; Pei, Y.; Grandjean, D.; Kahn, O. *Science* **1993**, *261*, 447. (b) Gardner, G. B.; Venkataraman, D.; Moore, J. S.; Lee, S. *Nature* **1995**, *374*, 792. (c) Yaghi, O.M.; Li, G.; Li, H. *Nature* **1995**, *378*, 703. (d) Bruce, D. W. *Acc. Chem. Res.* **2000**, *33*, 831 (e) Moulton, B.; Lu, J.; Hajndl, R.; Hariharan, S.; Zaworotko, M.J. *Angew. Chem. Int. Ed.* **2002**, *41*, 2821. (f) McCleverty, J. A.; Ward, M. D., *Acc. Chem. Res.* **1998**, *31*, 842. Noro, S.; Kitaura, R.; Kondo, M.; Kitagawa, S.; Ishii, T.; Matsuzaka, H.; Yamashita, M. *J. Am. Chem. Soc.* **2002**, *124*, 2568.

(2) (a) Withersby, M. A.; Blake, A. J.; Champness, N. R.; Cooke, P. A.; Hubberstey, P.; Li, W. S.; Schröder, M. *Inorg. Chem.* **1999**, *38*, 2259. (b) Blake, A. J.; Champness, N. R.; Cooke, P. A.; Nicolson, J. E. B.; Wilson, C. *J. Chem. Soc., Dalton Trans.* **2000**, 3811. (c) Withersby, M. A.; Blake, A. J.; Champness, N. R.; Hubberstey, P.; Li, W. S.; Schröder, M. *Angew. Chem. Int. Ed.* **1997**, *36*, 2327. (d) Noro, S.; Kitaura, R.; Kondo, M.; Kitagawa, S.; Ishii, T.; Matsuzaka, H.; Yamashita, M. *J. Am. Chem. Soc.* **2002**, *124*, 2568. (e) Feazell, R. P.; Carson, C. E.; Klausmeyer, K. K. *Inorg. Chem.* **2006**, *45*, 2635. (f) Feazell, R. P.; Carson, C. E.; Klausmeyer, K. K. *Inorg. Chem.* **2006**, *45*, 2627. (g) Feazell, R. P.; Carson, C. E.; Klausmeyer, K. K. *Inorg. Chem.* **2006**, *45*, 935.

(3) Reger, D. L.; Semeniuc, R. F.; Rassolov, V.; Smith, M. D. *Inorg. Chem.* **2004**, *43*, 537.

(4) Bu, X. H.; Chen, W.; Lu, S. L.; Zhang, R. H.; Liao, D. Z.; Bu, W. M.; Shionoya, M.; Brisse, F.; Ribas, J. *Angew. Chem. Int. Ed.* **2001**, *40*, 3201.

(5) Bu, X. H.; Chen, W.; Hou, W. F.; Du, M.; Zhang, R. H.; Brisse, F. *Inorg. Chem.* **2002**, *41*, 3477.

(6) Awaleh, M.O; Badia, A.; Brisse, F. *Inorg. Chem.* **2005**, *44*, 7833.

(7) Awaleh, M.O; Badia, A.; Brisse, F. *Cryst. Growth Des.* **2005**, *5*, 1897.

(8) Awaleh, M.O; Badia, A.; Brisse, F.; Bu, X. H. *Inorg. Chem.* **2006**, *45*, 1560.

(9) Awaleh, M.O; Badia, A.; Brisse, F.; *Inorg. Chem.* **2006**, *To be submitted.*

(10) (a) Awaleh, M. O.; Badia, A.; Brisse, F. *Acta Crystallogr.* **2005**, *E61*, o2479.
(b) Awaleh, M. O.; Badia, A.; Brisse, F. *Acta Crystallogr.* **2005**, *E61*, o2476.
(d) Awaleh, M. O.; Badia, A.; Brisse, F. *Acta Crystallogr.* **2005**, *E61*, o2473.

(11) (a) Reed, C. A. *Acc. Chem. Res.* **1998**, *31*, 133. (b) Turner, B.; Shterenberg, A.; Kapon, M.; Suwinska, K.; Eichen, Y. *J. Chem. Soc., Chem. Comm.* **2001**, 13. (c) Beer, P. D.; Gale, P. A.; *Angew. Chem. Int. Ed.* **2001**, *40*, 486. (d) Gale, P. A. *Coord. Chem. Rev.* **2000**, *199*, 181. (e) Wu, H. P.; Janiak, C.; Rheinwald, G.; Lang, H. *J. Chem. Soc., Dalton Trans.* **1999**, 183. (f) Janiak, C.; Uehlin, L.; Wu, H. P.; Klüfers, P.; Piotrowski, H.; Scharmann, T. G. *J. Chem. Soc., Dalton Trans.* **1999**, 3121. (g)Yaghi, O. M.; Li, H.; Groy, T. L. *Inorg. Chem.* **1997**, *36*, 4292. (h) Robson, R.; Hoskins, B. F. *J. Am. Chem. Soc.* **1990**, *112*, 1546. (i) Yang, G.; Raptis, R. G. *J. Chem. Soc., Chem. Comm.* **2004**, 2058. (j) Khlobystov, A. N.; Champness, N. R.; Roberts, C. J.; Tendler, S. J. B.; Thompson, C.; Shroder, M. *CrysEngComm.* **2002**, *4*, 426. (k) Jung, O. K.; Kim, Y. J.; Lee, Y. A.; Park, J. K.; Chae, H. K. *J. Am. Chem. Soc.* **2000**, *122*, 9921. (l) Jung, O. S.; Kim, Y. J.; Lee, Y. A.; Park, K. M.; Lee, S. S. *Inorg. Chem.* **2003**, *42*, 844. (m) Jung, O. S.; Kim, Y. J.; Lee, Y. A.; Chae, H. K.; Jang, H. G.; Hong, J. *Inorg. Chem.* **2001**, *40*, 2105.

(12) (a) Sherlock, S. J.; Cowie, M.; Singleton, E.; Steyn, M. M. D. V. *Organometallics* **1988**, *7*, 1663. (b) Hilts, R. W.; Sherlock, S. J.; Cowie, M.; Singleton, E.; Steyn, M. M. D. V. *Inorg. Chem.* **1990**, *29*, 3161. (c) Connolly, J.; Goodban, G. W.; Reid, G.; Slawin, A. M. Z. *J. Chem. Soc., Dalton Trans.* **1998**, 2225. (d) Genge, A. R. J.; Levason, W.; Reid, G. *J. Chem. Soc., Dalton Trans.* **1997**, 4479. (e) Valderrama, M.; Contreras, R.; Arancibia, V.; Boys, D. *J. Organomet. Chem.* **2001**, *620*, 256.

(13) Black, J. R.; Champness, N. R.; Levason, W.; Reid, G. *Inorg. Chem.* **1996**, *35*, 4432.

(14) Du, M.; Guo, Y. M.; Chen, S. T.; Bu, X. H. *Inorg. Chem.* **2004**, *43*, 1287.

(15) Hartley, F. R.; Murray, S. G.; Levason, W.; Soutter, H. E.; McAuliffe, C. A. *Inorg. Chim. Acta* **1979**, *35*, 265.

(16) SAINT Release 6.06, Integration Software for Single Crystal Data; Bruker AXS Inc.: Madison, WI, 1999.

(17) Sheldrick, G.M. SADABS Bruker Area Detector Absorption Corrections; Bruker AXS Inc.: Madison, WI, 1996.

(18) XPREP Release 5.10; X-ray Data Preparation and Reciprocal Space Exploration Program. Bruker AXS Inc., Madison, WI, 1997.

(19) SHELXTL Release 5.10, The Complete Software Package for Single-Crystal Structure Determination; Brucker AXS Inc.: Madison, WI, 1997.

(20) (a) Sheldrick, G.M. SHELXS97, Program for the Solution of Crystal Structures;

University of Göttingen: Göttingen, Germany, 1997. (b) Sheldrick, G.M. SHELXL97, Program for the Refinement of Crystal Structures; University of Göttingen: Göttingen, Germany, 1997.

(21) Flack, H. D.; Schwarrzenbach, D. *Acta Crystallogr., Sect. A* **1988**, *44*, 499.

(22) (a) Jung, O. S.; Kim, Y. J.; Lee, Y. A.; Park, K. M.; Lee, S. S. *Inorg. Chem.* **2003**, *42*, 844. (b) Jung, O. S.; Kim, Y. J.; Park, K. M.; Cho, S. N. *J. Mol. Struct.* **2003**, *657*, 207. (c) Jung, O. S.; Kim, Y. J.; Lee, Y. A.; Chae, H. K.; Jang, H. G.; Hong, J. *Inorg. Chem.* **2001**, *40*, 2105.

(23) Reger, D. L.; Semeniuc, R. F.; Rassolov, V.; Smith, M. D. *Inorg. Chem.* **2004**, *43*, 537.

(24) Lawrance, G. A. *Chem. Rev.* **1986**, *86*, 17 and references therein.

(25) Batchelor, R. J.; Ruddick, J. N. R.; Sams, J. R.; Aubke, F. *Inorg. Chem.* **1977**, *16*, 1414 and references therein.

(26) Porterfield, W. W. *Inorganic Chemistry: A Unified Approach*, Addison-Wesley, 1994, p.168, 180.

(27) Schultheiss, N.; Powell, D. R.; Bosch, E. *Inorg. Chem.* **2003**, *42*, 5304.

(28) Bosch, E.; Barnes, C. L. *Inorg. Chem.* **2002**, *41*, 2543.

(29) Ahmed, L. S.; Dilworth, J. R.; Miller, J. R.; Wheatly, N. *Inorg. Chim. Acta* **1998**, *278*, 229 and references therein.

(30) Riley, P. J.; Reid, J. L.; Côté, A. P.; Shimizu, G. K. H. *Can. J. Chem.* **2002**, *80*, 1584.

(31) Brammer, L.; Burgard, M. D.; Eddleston, M. D.; Rodger, C. S.; Rath, N. P.; Adams, H. *CrystEngComm.* **2002**, *4(44)*, 239.

(32) Li, J. R.; Zhang, R, H.; Bu, X. H. *Cryst. Growth Des.* **2003**, *3*, 829.

(33) Silva, R. M.; Smith, M. D.; Gardinier, J. R. *Inorg. Chem.* **2006**, *45*, 2132.

3.2. Complexes métallosupramoléculaires d'argent (I): Synthèse, caractérisation et propriétés d'échange anioniques.

3.2.1 Introduction

Les réseaux métallosupramoléculaires résultent de l'autoassemblage de sels de métaux de transition et de ligands organiques. Pour ce faire, les ligands doivent pouvoir se coordonner facilement aux centres métalliques.[1]

L'intérêt de l'étude de ces matériaux est d'identifier les paramètres qui influencent leurs topologies.[2] Ces paramètres peuvent être mis à profit afin de générer des matériaux métallosupramoléculaires avec des architectures désirées et, par voie de conséquence des propriétés modulables.[3]

Nous nous sommes intéressés à l'influence de la coordinabilité des anions sur la topologie des réseaux générés par autoassemblage de ligands dithiolatés flexibles et de sels d'argent (I).[4-8] Le but de cette étude était d'élaborer des matériaux métalloorganiques présentant des propriétés d'échange anioniques.[9]

L'application potentielle de ces matériaux est d'actualité. Par exemple, Rogers *et al.* ont synthétisé un polymère de coordination cationique en associant le nitrate d'argent et la pyrimidine. Le résultat de cette réaction est une structure en canaux où sont placés les anions nitrates. Cette métallosupramolécule a été utilisée pour échanger les nitrates avec des anions radioactifs comme le pertechnate, TcO_4^-.[10] Ce type de matériaux ouvre ainsi des perspectives technologiques importantes pour disposer de certains déchets radioactifs.[11-12]

Les métallosupramolécules susceptibles de présenter des propriétés d'échange anioniques sont souvent constituées de réseaux cationiques, dont la charge est compensée par l'anion qui est non coordonnant ou faiblement coordonnant.[13]

Dans le chapitre 3.1, nous avons décrit l'existence de réseaux élaborés à l'aide du bis(méthylthio)méthane, $\mathbf{L^{1\text{-}Me}}$ et des sels d'argent avec divers contre-ions.[8] Les anions sont coordonnés à l'argent dans l'ensemble de ces composés. L'utilisation de sels d'argent(I) avec des contre-ions non coordonnants ou faiblements coordonnants pourrait permettre la formation de réseaux cationiques, susceptible de présenter des propriétés d'échange. Cette approche nous a permis d'obtenir quatre réseaux cationiques. Nous rapportons ici les métallosupramolécules cationiques formés par autoassemblage du ligand $\mathbf{L^{1\text{-}Me}}$ et de sels d'argent AgX (X = BF_4^-; PF_6^-; SbF_6^-; $CF_3SO_3^-$). De plus, nous explorons les propriétés

d'échange anioniques de ces réseaux. Les échanges ont été suivis par analyse élémentaire, spectroscopie infrarouge et diffraction de rayons X sur poudre.

3.2.2 Partie expérimentale.

À l'exception du ligand, tous les réactifs proviennent de sources commerciales et ont été utilisés tels que reçus. Les analyses élémentaires ont été effectuées au Laboratoire d'Analyse Élémentaire de l'Université de Montréal. Les spectres infrarouges ont été enregistrés à la température ambiante à l'aide d'un spectromètre Perkin-Elmer 1750 FTIR (4000 à 400 cm^{-1}). Lors de ces mesures, des pastilles de KBr ont été préparées pour les composés **1 - 4** alors que des plaques de NaCl furent utilisées pour le ligand qui est liquide à la température ambiante. Les spectres RMN ^{1}H (400 MHz et 300 MHz), ^{19}F (376.31 MHz) ont été enregistrés à température ambiante à l'aide des spectromètres Bruker AV400 et AV300. Le signal résiduel du solvant DMSO deutéré a été utilisé pour calibrer les spectres de RMN ^{1}H ($\delta_{1H} = 2.50$).

Synthèses. Le ligand bis(méthylthio)méthane, $\mathbf{L^{1\text{-}Me}}$ a été synthétisé selon une procédure publiée.[14] Rendement: 41%. Analyse élémentaire, calculé pour $C_3H_8S_2$: C, 33.29; H, 7.45. Obtenu: C, 33.45; H, 7.32. RMN ^{1}H (DMSO-d_6, 300 MHz): δ 2.16 (*s*, 6H, CH_3-S-CH_2-S-CH_3), 3.72 (*s*, 2H, CH_3-S-CH_2-S-CH_3). IR (KBr, cm^{-1}): 2973m, 2915F, 2855m, 2828m, 2756f, 2588f, 2380f, 2269f, 2181f, 2128f, 2076f, 2034f, 1671f, 1435m, 1422m, 1384m, 1316 m, 1203m, 1154m, 1123f, 985m, 958m, 805m, 745F, 693m, 648f.

$[Ag_3(L^{1\text{-}Me})_6(CF_3SO_3)_3]_\infty$ (1). Un solide cristallin blanc se forme lorsqu'une solution de $AgCF_3SO_3$ (382 mg, 1.49 mmol) dans l'acétone (5 mL) est ajoutée à la température ambiante à une solution de $\mathbf{L^{1\text{-}Me}}$ (0.30 mL, 2.93 mmol) dans le diéthyl éther (5 mL).

Ce solide a été recristallisé par diffusion d'éther de pétrole dans une solution saturée du composé dans l'acétone. Des cristaux ont été obtenus après quelques jours. Rendement: 93%. Analyse élémentaire calculé pour $C_{21}H_{48}Ag_3F_9O_9S_{15}$: C, 17.76; H, 3.41. Obtenu: C, 17.94; H, 3.33. RMN ^{1}H (DMSO-d_6, 300 MHz): δ 2.09 (*s*, 6H, CH_3-S-CH_2-S-CH_3), 3.73 (*s*, 2H, CH_3-S-CH_2-S-CH_3). RMN ^{19}F (DMSO-d_6, 376.31 MHz): δ -78.3. IR (KBr, cm^{-1}): 3468m, 2915m, 1627m, 1434m, 1422m, 1384m, 1270F, 1202m, 1175F, 1030F, 805m, 766m, 745m, 694m, 647m, 579m, 520m.

$[Ag(L^{1\text{-}Me})_2(PF_6)]_\infty$ (2). Ce complexe a été synthétisé de la même manière que le complexe **1** en utilisant 174 mg de $AgPF_6$ (0.69 mmol) et 0.35 mL de $\mathbf{L^{1\text{-}Me}}$ (3.42 mmol).

Rendement: 84%. Analyse élémentaire, calculé pour $C_6H_{16}AgPF_6S_4$: C, 15.36; H, 3.44. Obtenu: C, 15.01; H, 3.42. RMN ^{1}H (DMSO-d_6, 300 MHz): δ 2.1723 (*s*, 6H, CH_3-S-CH_2-S-CH_3), 3.830 (*s*, 2H, CH_3-S-CH_2-S-CH_3). RMN ^{19}F (DMSO-d_6, 376.31 MHz): δ -69.3, -71.8 (d, F–P). IR (KBr, cm^{-1}): 3435m, 2972f, 2914m, 2853f, 2450f, 1630m, 1435m, 1422m, 1384f, 1309F, 1274f, 1203m, 1149F, 1123w, 835F, 745m, 693m, 560F, 517m, 503m.

$[Ag(L^{1\text{-}Me})_2(SbF_6)(Et_2O)_{0.5}]_\infty$ (3). Ce composé a été préparé de la même manière que le complexe **1** en utilisant 284 mg de $AgSbF_6$ (0.83 mmol) et 0.30 mL de $L^{1\text{-}Me}$ (2.93 mmol). Rendement: 76%. Analyse élémentaire, calculé pour $C_8H_{21}O_{0.5}AgSbF_6S_4$: C, 16.09; H, 3.54. Obtenu: C, 15.81; H, 3.39. RMN ^{1}H (DMSO-d_6, 400 MHz): δ 2.09 (*s*, 6H, CH_3-S-CH_2-S-CH_3), 3.73 (*s*, 2H, CH_3-S-CH_2-S-CH_3).

RMN ^{19}F (DMSO-d_6, 376.31 MHz): δ -137.5 – -102.9 (m, F–Sb).

IR (KBr, cm^{-1}): 3449m, 2973m, 2915m, 2855f, 2829f, 2104f, 1628m, 1524m, 1435m, 1423m, 1384m, 1317f, 1258f, 1203m, 1124f, 1084m, 1035f, 985m, 958f, 805f, 745m, 664F.

$[Ag(L^{1\text{-}Me})_{2.5}(BF_4)]_\infty$ (4). Ce complexe a été synthétisé de la même manière que le complexe **1** en utilisant 235 mg de $AgBF_4$ (1.21 mmol) et 0.40 mL de $L^{1\text{-}Me}$ (3.91 mmol). Rendement: 36%. Analyse élémentaire, calculé pour $C_{7.5}H_{20}AgBF_4S_5$: C, 19.36; H, 4.33. Obtenu: C, 19.68; H, 4.55. RMN ^{1}H (DMSO-d_6, 300 MHz): δ 2.09 (*s*, 6H, CH_3-S-CH_2-S-CH_3), 3.73 (*s*, 2H, CH_3-S-CH_2-S-CH_3). RMN ^{19}F (DMSO-d_6, 376.31 MHz): δ -148.2.

IR (KBr, cm^{-1}): 3468m, 2973m, 2914F, 2828f, 1624f, 1435m, 1422m, 1384f, 1251F, 1203F, 1177F, 1074F, 985m, 958w, 805m, 768m, 745F, 693F, 652F, 579m, 519m.

Procédure d'échange anionique. 150 mg du complexe $[Ag_n(L^{1\text{-}Me})_m(X)_n]_\infty$, X étant l'anion sortant, est placé dans une solution aqueuse (5 mL) du sel LiY ou NaY (150 mg), Y étant l'anion entrant. Le tout est agité vigoureusement. Toutes les 40 min environ, un échantillon de 10 mg est prélevé, filtré et séché à l'air avant l'enregistrement de son spectre infrarouge. Quand l'échange anionique est estimé être terminé, sur la base des spectres infrarouges, l'agitation est arrêtée. Une fois le solide filtré est séché à l'air, on en enregistre le diagramme de poudre et fait l'analyse élémentaire.

Études cristallographiques. Les données cristallographiques des complexes 1, 3 et 4 ont été collectées avec un diffractomètre Brucker AXS équipé d'un détecteur CCD Smart 2K. La radiation Kα utilisée est celle générée par une anode de cuivre monochromatisée par un

cristal de graphite (λ = 1.54178 Å). Les intensités diffractées par le complexe 2 ont été enregistrées sur un diffractomètre à anode tournante Nonius FR591 équipé d'un détecteur CCD Smart 6K avec la radiation du cuivre.

Le programme SAINT a été utilisé pour l'intégration et la réduction des données.[15] Les intensités *I(hkl)* enregistrées ont été corrigées des effets de Lorentz, de polarisation ainsi que des phénomènes d'absorption grâce au programme SADABS.[16] La procédure XPREP[17] du logiciel SHELXTL[18] a été employée pour l'analyse des intensités diffractées afin d'en tirer la symétrie de Laue, les conditions d'existence des réflexions *hkl* et les groupes d'espaces possible. Les structures ont été résolues par les méthodes directes et les affinements sont effectués par la méthode des moindres carrés sur $F(hkl)^2$ à l'aide de la suite de logiciels SHELXL-97.[19] Excepté si mentionné, tous les atomes semi-lourds ont été affinés anisotropiquement. Les facteurs thermiques des atomes d'hydrogène, placés à des positions idéalisées, ont été affinés isotropiquement. Lors de l'affinement, ces atomes d'hydrogène sont replacés de façon à suivre le mouvement des atomes parents.

Pour le complexe **1**, la procédure XPREP[17] du logiciel SHELXTL[18] a proposé trois groupes d'espaces compatibles avec les données: *C*2, *Cm* et *C*2/*m*. Comme nos produits de départs ne sont pas chiraux, nous avons essayé de résoudre la structure dans les groupes d'espaces *Cm* et *C*2/*m*. Aucun de ces deux groupes d'espace n'a donné une structure raisonnable. La structure a été résolue et affinée dans le groupe spatial *C*2, qui s'est avéré être le bon groupe d'espace. Le paramètre de Flack,[20] avec une valeur de 0.008(5), confirme que nous avons la bonne structure absolue.

Dans le complexe **2**, l'anion PF_6^- est désordonné. L'atome de phosphore, situé sur un axe cristallographique d'ordre 2, a été affiné anisotropiquement. Les atomes de fluor de cet anion, distribués statistiquement sur trois positions avec les facteurs d'occupation 40, 35 et 25% ont été affinés isotropiquement. Lors de l'affinement, les distances P-F ont été contraintes à être égales pour les trois orientations du groupe.

Les molécules de solvant (diéthyl ether) du complexe **3** sont sévèrement désordonnées. La correction des données par la procédure SQUEEZE du logiciel PLATON[22] (80 électrons/maille) correspond à la présence d'une demi-molécule de diéthyl éther par unité asymétrique (84 électrons/maille). La procédure BYPASS[21] du logiciel PLATON[22] a été utilisée pour supprimer des données brutes la contribution des molécules de solvant très désordonnées. Le modèle final qui ne contient pas les molécules de solvant a

été affiné. Cependant, les molécules de solvant ont été prises en compte pour le calcul des données cristallographiques.

Dans le complexe **4**, un des ligands bis(méthylthio)méthane est désordonné. Il est distribué statistiquement sur deux sites avec les facteurs d'occupation de 72 et de 28% respectivement. Les distances Ag-S et S-C des parties majeure et mineure ont été contraintes à être égales (avec l'instruction SADI).[19] Les facteurs thermiques des atomes ont été soumis à des contraintes pour que les ellipsoïdes soient normaux (avec l'instruction EADP).[19] Dans ce complexe **4**, l'anion tétrafluoroborate est aussi désordonné. Il est réparti statistiquement sur deux positions avec les facteurs d'occupation de 68 et de 32% respectivement. L'instruction SADI du logiciel SHELXS-97[19] a été appliquée aux entités majeure et mineure de cet anion de façon à ce qu'il garde sa géométrie tétraédrique. Les facteurs thermiques anisotropiques des atomes de BF_4^- ont été soumis à des contraintes pour que les ellipsoïdes soient normaux (avec l'instruction EADP).[19]

Les données cristallographiques des complexes **1-4** sont présentées dans le tableau 3.2.1. Nous avons placé en annexe IV (tableau S1) les longueurs des liaisons et les angles de valences des complexes **1-4**, ainsi que d'autres détails des études structurales.

Les diagrammes de poudre ont été enregistrés sur un diffractomètre de rayons X Brucker D8 Advance avec la radiation Kα du cuivre (λ = 1.54178 Å) à 25 °C avec un temps de mesure par pas de 0.02 $(2\theta)^\circ$ s^{-1}.

Tableau 3.2.1. Données cristallographiques des composés 1, 2, 3 et 4.

	1	2	3	4
formule	$C_{21}H_{48}Ag_3F_9O_9S_{15}$	$C_6H_{16}S_4AgPF_6$	$C_8H_{21}S_4O_{0.5}AgSbF_6$	$C_{7.5}H_{20}S_5AgBF_4$
masse moléculaire	1420.10	469.27	597.13	465.21
système	Monoclinique	Monoclinique	Monoclinique	Monoclinique
groupe d'espace	*C*2	*C*2/*c*	*C*2/*c*	*C*2/*c*
a, Å	17.3226(2)	8.2468(4)	13.2985(4)	16.7916(9)
b, Å	9.2820(1)	19.101(1)	16.1208(4)	9.1090(4)
c, Å	29.838893)	10.1381(5)	8.9804(3)	22.670(1)
α, deg	90	90	90	90
β, deg	93.726(1)	107.065(2)	95.883(2)	99.676(4)
γ, deg	90	90	90	90
volume, $Å^3$	4787.59(9)	1526.67(13)	1915.1(1)	3418.2(3)
Z	4	4	4	8
D(calc), g cm^{-1}	1.970	2.042	2.071	1.808
temp, K	100(2)	200(2)	100(2)	100(2)
λ	1.54178 Å	1.54178 Å	1.54178 Å	1.54178 Å
μ, mm^{-1}	16.567	17.161	23.835	15.393
F(000)	2832	928	1072	1864
θ_{max}, (deg)	72.88	69.01	72.78	72.85
R^a [$I > 2\sigma(I)$]	0.0298	0.0399	0.0379	0.0580
Rw^b [$I > 2\sigma(I)$]	0.0700	0.1124	0.1135	0.1528
R [all data]	0.0313	0.0412	0.0394	0.0601
*R*w [all data]	0.0707	0.1146	0.1148	0.1549
S^c	1.004	1.076	0.961	0.932

$^aR = \Sigma \, || F_o | - | F_c || / \Sigma \, | F_o |$. $^bR_w = [\, \Sigma \, w(F_o^2 - F_c^2)^2 / \Sigma \, w(F_o^2)^2]^{1/2}$.
$^cS = [\, \Sigma \, w(F_o^2 - F_c^2)^2 / (m\text{-}n)]^{1/2}$ (m est le nombre de réflexions et n est le nombre de paramètres).

3.2.3 Résultats

Synthèse des réseaux de coordination. Les composés de coordination **1-4** sont des solides blancs constitués de très petits cristaux. Afin de faire croître des cristaux plus gros, nous avons dissout chacun de ces complexes dans l'acétone. Ils ont ensuite été recristallisés à partir de l'éther de pétrole. L'analyse élémentaire et la mesure des mailles ont confirmé que les cristaux sont identiques aux solides cristallins correspondants.

Les composés **1-4** sont insoluble dans l'eau et les solvants non polaires (pentane, hexane, heptane ou éther de pétrole) mais ils sont solubles dans les solvants polaires comme l'acétone ou le diméthylsulfoxyde. La stoichiomètrie des composés est

indépendante des rapports métal-ligand des produits de départ. En effet, malgré la variation du rapport métal-ligand (1:10 à 10:1), des cristaux identiques ont toujours été obtenus, confirmé par la mesure des mailles cristallines. Par ailleurs, des cristaux identiques ont été obtenus avec différents solvants de recristallisation (éther de pétrôle, heptane, hexane ou pentane). De ce fait, nous pouvons dire que ces complexes sont obtenus indépendement des rapports métal-ligand des produits de départ ou du solvant de recristallisation.[8]

Études structurales.

$[Ag_3(L^{1\text{-}Me})_6(CF_3SO_3)_3]_\infty$ (1). L'autoassemblage du bis(méthylthio)méthane, $L^{1\text{-}Me}$, avec le triflate d'argent conduit au complexe **1** dont la structure consiste en un réseau de coordination cationique tridimensionnel. Ce réseau forme des canaux dans lesquels se trouvent les anions triflates (Figure 3.2.1). Les canaux de section "circulaire" sont parallèles à l'axe cristallographique *b*. Comme dans ce complexe les anions triflates équilibrent seulement la charge du réseau cationique, ils pourraient être remplacés par d'autres anions. C'est pourquoi nous avons décidé d'étudier les propriétés d'échanges anioniques de ce complexe. Nous reviendrons sur les propriétés d'échange de ce composé dans la partie traitant les échanges.

Le complexe a trois atomes d'argent cristallographiquement différents. Chaque atome d'argent est coordonné à quatre atomes de soufre provenant de ligands différents. Les distances Ag-S, dans l'intervalle 2.526(1)-2.698(8) Å, se comparent bien à celles que nous avons observé pour les réseaux formés avec des ligands dithiolatés semblables.[4-8]

Les atomes d'argent adoptent une coordination tétraédrique déformée où les angles S-Ag-S sont dans l'intervalle 94.2(1)-127.0(1)° (Tableau S1, Annexe IV).

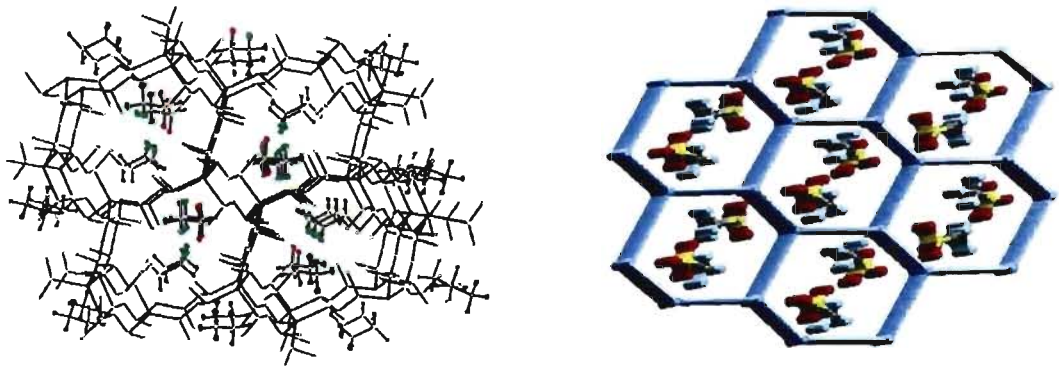

(a) (b)

Figure 3.2.1. (a) Projection le long de l'axe cristallographique *b* du réseau cationique 3D, $[Ag_3(\mathbf{L}^{\mathbf{1\text{-}Me}})_6(CF_3SO_3)_3]_\infty$. (Les atomes d'hydrogène ont été omis pour plus de clarté). Dans (b) les coins des hexagones représentent les atomes d'argent tandis que les côtés schématisent les ligands.

Black et *al.* ont signalé l'existence d'un réseau cationique tridimensionnel, similaire à celui du complexe **1**, en combinant le même ligand $\mathbf{L}^{\mathbf{1\text{-}Me}}$ avec le sel de cuivre $[Cu(MeCN)_4]PF_6$.[23] Les anions hexafluorophosphates sont localisés dans les canaux.[23] Ceci nous a incité à autoassembler le bis(méthylthio)méthane et $AgPF_6$ (complexe **2** ci-dessous).

$[Ag(\mathbf{L}^{\mathbf{1\text{-}Me}})_2(\mathbf{PF_6})]_\infty$ (2). Malheureusement, la structure à canaux attendue n'a pas été obtenue. Il s'est plutôt formé un polymère de coordination cationique, qui se propage parallèlement à l'axe cristallographique *c* (Figure 3.2.2a).

Dans ce complexe, deux atomes d'argent adjacents, liés par deux ligands $\mathbf{L}^{\mathbf{1\text{-}Me}}$, forment le dimère $[Ag(\mathbf{L}^{\mathbf{1\text{-}Me}})]_2$ (Figure 3.2.2a). Les dimères $[Ag(\mathbf{L}^{\mathbf{1\text{-}Me}})]_2$ voisins ont leurs atomes d'argent en commun. Les anions hexafluorophosphates ne font que compenser la charge des ions métalliques du polymère de coordination.

Comme le montre la figure 3.2.2b, les chaînes du complexe **2** ont un packing de type hexagonal. Chaque atome d'argent est coordonné à quatre atomes de soufre provenant de quatre ligands (Ag-S: 2.595 (1) - 2.612 (1) Å). Puisque les angles S-Ag-S sont dans l'intervalle 102.9(1) - 119.4(1)° (Tableau S1, Annexe IV), les atomes d'argent ont un environnement tétraédrique déformé.

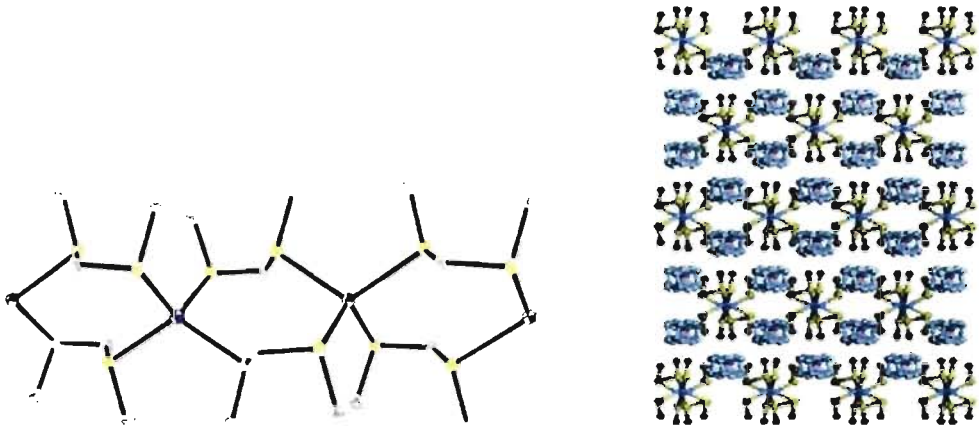

(a) (b)

Figure 3.2.2. (a) Le polymère de coordination cationique **2**. (b) Projection le long de l'axe de chaîne du complexe 1D $[Ag(\mathbf{L}^{1\text{-}Me})_2(PF_6)]_\infty$. Les chaînes sont en jaune alors que les anions PF_6^- désordonnés sont en bleu. (Les atomes d'hydrogène ont été omis pour plus de clarté).

Comme les anions PF_6^- et SbF_6^- ont la même géométrie octaédrique, ils devraient avoir des structures identiques. C'est pourquoi, nous avons entrepris la synthèse du complexe **3**, en combinant le bis(méthylthio)méthane et $AgSbF_6$.

$[Ag(\mathbf{L}^{1\text{-}Me})_2(SbF_6)(Et_2O)_{0.5}]_\infty$ (3). Comme le montre la figure 3.2.3, le complexe **3** est un polymère de coordination cationique similaire à celui du complexe **2**. Les anions SbF_6^- ne font que compenser la charge des ions métalliques. Il est à noter que contrairement au complexe **2**, les anions SbF_6^- du complexe **3** ne sont pas désordonnés. Par ailleurs, ce complexe incorpore des molécules de diéthyléther désordonnées. Une projection de ce complexe le long de l'axe cristallographique *c* est illustrée à la figure 3.2.3b. Nous constatons que les chaînes du polymère de coordination $[Ag(\mathbf{L}^{1\text{-}Me})_2]_\infty$ et les anions hexafluoroantimonate forment des canaux hexagonaux. Les molécules de diéthyléther désordonnées occupent ces canaux (Figure 3.2.3b) alors que les anions SbF_6^- sont placés à mi-chemin entre chaque paire de chaînes. Les atomes d'argent ont une géométrie tétraédrique déformée (S-Ag-S: 102.7(1) - 122.4(1)°) (Tableau S1, Annexe IV).

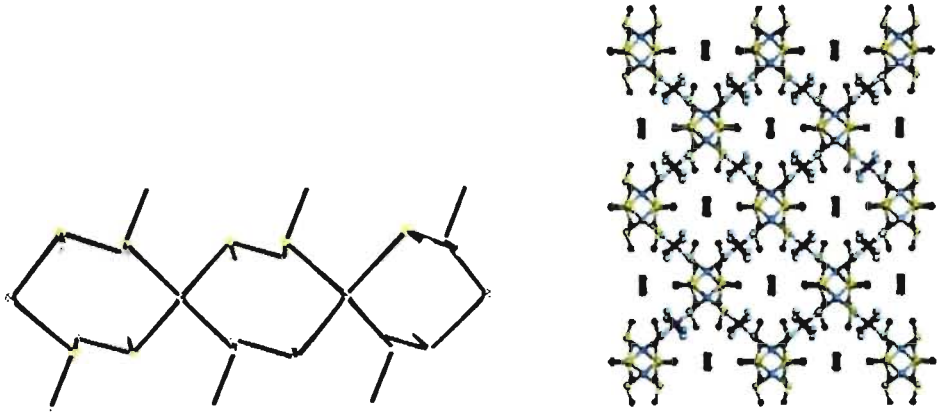

(a) (b)

Figure 3.2.3. (a) Le polymère de coordination cationique **3**. (b) Projection le long de l'axe de chaîne du complexe $[Ag(\mathbf{L}^{\mathbf{1\text{-}Me}})_2(SbF_6)(Et_2O)_{0.5}]_\infty$. Les chaînes sont en jaune. Les anions SbF_6^- sont placés entre les chaînes voisines. Les molécules Et_2O occupent les centres des canaux hexagonaux. (Les atomes d'hydrogène ont été omis pour plus de clarté).

Black et al. ont signalé l'existence d'un polymère cationique similaire à ceux des complexes **2** et **3**, obtenu par autoassemblage du bis(méthylséléno)méthane et du sel $AgBF_4$.[23] C'est ce qui nous a donné l'idée de faire réagir le bis(méthylthio)méthane et $AgBF_4$ (complexe **4**).

$[Ag(\mathbf{L}^{\mathbf{1\text{-}Me}})_{2.5}(\mathbf{BF_4})]_\infty$ (4). Malheureusement, le polymère de coordination cationique attendu n'a pas été obtenu. Il s'est plutôt formé un réseau de coordination bidimensionnel cationique parallèle au plan *ab* (Figure 3.2.4a). Dans ce complexe, chaque atome d'argent est coordonné à quatre atomes de soufre provenant de quatre ligands $\mathbf{L}^{\mathbf{1\text{-}Me}}$ différents. Trois de ces ligands sont impliqués dans la formation du réseau à deux dimensions tandis que le quatrième ligand ne fait que compléter la sphère de coordination de l'argent (Figure 3.2.4a, b). En d'autres termes, un atome de soufre de ce quatrième ligand est coordonné avec un argent alors que l'autre soufre, non coordonné, se trouve entre des feuillets cationiques adjacents (Figure 3.2.4b, c). L'unité de répétition de ce réseau 2D cationique est le métallamacrocycle $Ag_6(\mathbf{L}^{\mathbf{1\text{-}Me}})_6$ (Figure 3.2.4a). Les atomes d'argent ont une coordination tétraédrique (S-Ag-S: 104.3(1) ; 105.3(1) ; 106.2(1) ; 103.7(1)°) (Tableau S1, Annexe IV). Les anions désordonnés BF_4^-, situés entre les feuillets cationiques, ne font que compenser la charge des ions métalliques (Figure 3.2.4c).

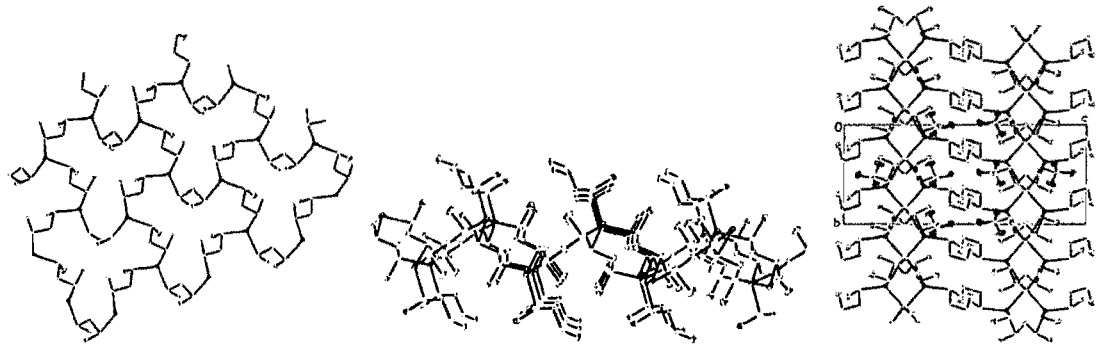

(a) (b) (c)

Figure 3.2.4. (a) Le réseau cationique 2D du complexe **4** parallèle au plan ab (le quatrième ligand qui complète la sphère de coordination de l'argent a été omis pour plus de clarté). (b) Le même réseau 2D montré avec le quatrième ligand situé alternativement en haut et en bas du plan du réseau. (c) Projection le long de l'axe cristallographique a du complexe **4**.
Les anions sont localisés entre les feuillets cationiques. (Les atomes d'hydrogène ont été omis pour plus de clarté).

Propriété d'échange anionique.

Échanges à partir du complexe $[Ag_3(L^{1\text{-}Me})_6(CF_3SO_3)_3]_\infty$

Les échanges ont été suivis par spectroscopie infrarouge, analyse élémentaire et diffraction de rayons X sur poudre. Par exemple, quand le complexe **1**, $[Ag_3(L^{1\text{-}Me})_6(CF_3SO_3)_3]_\infty$, a été placé dans une solution aqueuse de $LiClO_4$ et le tout agité durant deux heures, les anions triflates du complexe **1** ont été complètement remplacés par les anions perchlorates.

Les spectres infrarouges enregistrés sur des échantillons collectés à différent moments durant le processus d'échange sont illustrés à la figure 3.2.5. On remarque que durant ce processus, les fréquences de vibration caractéristiques des anions triflates ($\nu[SO_3(E)]$: 1270 cm^{-1} et $\nu[SO_3(A_1)]$: 1030 cm^{-1})[24] diminuent alors qu'en même temps l'intensité de la fréquence de vibration caractéristique du perchlorate, ($\nu_1(A_1)$: 1092 cm^{-1})[25], augmente.

Le spectre infrarouge enregistré avec un échantillon collecté après deux heures d'échange montre bien la disparition complète des fréquences de vibration caractéristiques des anions triflates et que seule la fréquence de vibration du perchlorate est présente. Sur la base de ces résultats, on peut considérer que l'échange a été complété après deux heures.
D'autre part, le RMN de fluor du produit resultant de l'échange a confirmé la non présence des anions triflates. L'analyse élémentaire a été utilisée pour confirmer que l'échange a été

complété. L'analyse élémentaire de l'échantillon collecté après deux heures d'échange confirme que le produit final est le composé $[Ag_3(\mathbf{L}^{\mathbf{1\text{-}Me}})_6(ClO_4)_3]_\infty$, montrant que l'échange a été complété durant cette période (Tableau 3.2.2). De plus, nous avons enregistré les spectres de poudre des produits avant et après l'échange pour déterminer si la structure du produit de départ est maintenue au cours de l'échange.

Le spectre de poudre du produit résultant de l'échange est très comparable à celui du produit de départ, le complexe **1** (Figure 3.2.6). Ainsi, nous pouvons considérer que les triflates du complexe **1** ont été remplacés par les perchlorates sans que le réseau de **1** change durant le processus.

De la même manière les anions triflates du complexe **1**, $[Ag_3(\mathbf{L}^{\mathbf{1\text{-}Me}})_6(CF_3SO_3)_3]_\infty$, peuvent être remplacés par les tétrafluoroborates ou les nitrates (Figure S1-S4, Annexe IV et Tableau 3.2.2). On a ainsi obtenu les complexes $[Ag_3(\mathbf{L}^{\mathbf{1\text{-}Me}})_6(ClO_4)_3]_\infty$, $[Ag_3(\mathbf{L}^{\mathbf{1\text{-}Me}})_6(BF_4)_3]_\infty$ et $[Ag_3(\mathbf{L}^{\mathbf{1\text{-}Me}})_6(NO_3)_3]_\infty$.

Toutefois, les triflates du complexe **1** n'ont pas pu être échangés avec les anions PF_6^- et SbF_6^-. En effet, quand nous avons placé du solide de **1** dans une solution aqueuse de $NaPF_6$ ou de $NaSbF_6$ et le tout agité durant plus de 72 heures, le spectre infrarouge du produit collecté était identique à celui du complexe **1**. Ceci démontre que l'anion $CF_3SO_3^-$ n'a pas pu être remplacé durant cette période par PF_6^- et SbF_6^-.

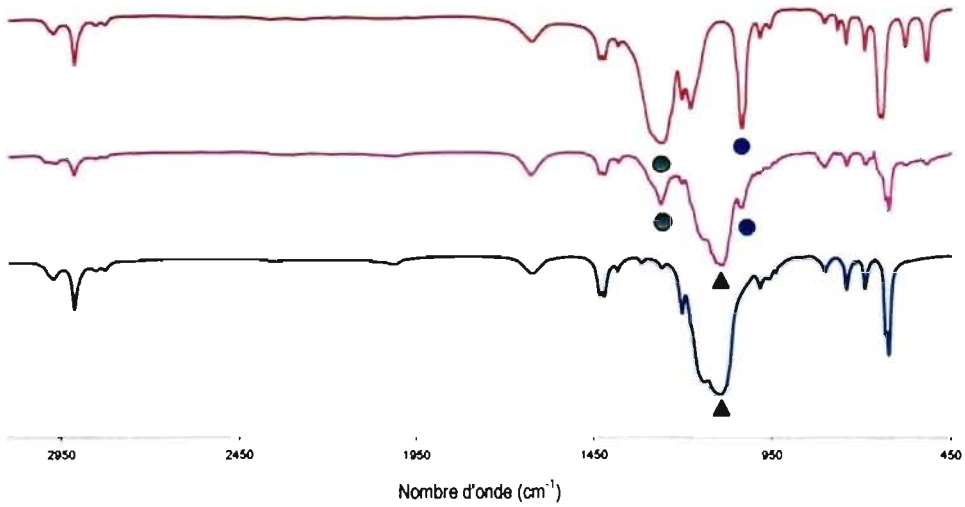

Figure 3.2.5. Évolution des spectres infrarouges durant l'échange des anions triflates du complexe **1**, $[Ag_3(L^{1\text{-}Me})_6(CF_3SO_3)_3]_\infty$, avec les anions perchlorates. Le spectre rouge est celui du complexe **1**, $[Ag_3(L^{1\text{-}Me})_6(CF_3SO_3)_3]_\infty$, comme préparé (Les bandes de vibrations caractéristiques du triflate sont $\nu[SO_3(E)]$: 1270 cm^{-1} (●), et $\nu[SO_3(A_1)]$: 1030 cm^{-1} (●)). Le spectre en violet est celui du complexe **1** agité avec une solution aqueuse de $LiClO_4$ durant 40 min, montrant la décroissance de l'intensité des bandes caractéristique du triflate et l'augmentation de l'intensité de la bande caractéristique du perchlorate (▲: 1092 cm^{-1}, $\nu_1(A_1)$). Le spectre bleu est celui du produit résultant de l'échange après deux heures et correspond au composé $[Ag_3(L^{1\text{-}Me})_6(ClO_4)_3]_\infty$.

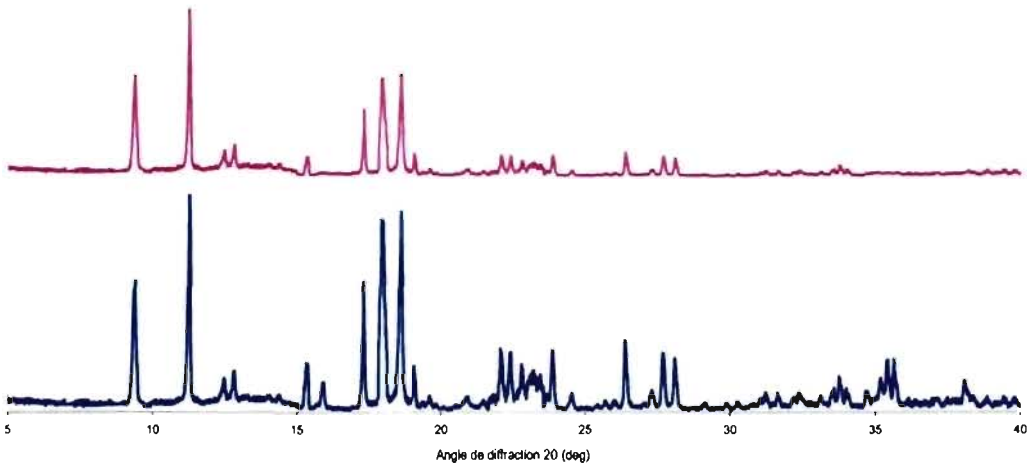

Figure 3.2.6. En bleu: Diagramme de poudre du complexe **1** comme synthétisé. En violet: Diagramme de poudre du produit résultant de l'échange **1** + $LiClO_4$.

Tableau 3.2.2. Analyses élémentaires des complexes obtenus par échange d'anions.

	Calculé			Observé		
	C %	H %	N %	C %	H %	N %
$[Ag_3(\mathbf{L}^{1\text{-}Me})_6(CF_3SO_3)_3]_\infty$	17.76	3.41		17.94	3.33	
$[Ag_3(\mathbf{L}^{1\text{-}Me})_6(ClO_4)_3]_\infty$	17.01	3.81		17.31	3.49	
$[Ag_3(\mathbf{L}^{1\text{-}Me})_6(BF_4)_3]_\infty$	17.53	3.92		17.02	3.12	
$[Ag_3(\mathbf{L}^{1\text{-}Me})_6(NO_3)_3]_\infty$	18.65	4.17	3.63	17.91	4.34	3.88
$[Ag(\mathbf{L}^{1\text{-}Me})_2(PF_6)]_\infty$	15.36	3.44		15.01	3.42	
$[Ag(\mathbf{L}^{1\text{-}Me})_2(ClO_4)]_\infty$	17.01	3.81		16.95	3.57	
$[Ag(\mathbf{L}^{1\text{-}Me})_2(BF_4)]_\infty$	17.53	3.92		17.32	3.27	
$[Ag(\mathbf{L}^{1\text{-}Me})_2(NO_3)]_\infty$	18.65	4.17	3.63	19.42	3.87	3.63
$[Ag(\mathbf{L}^{1\text{-}Me})_2(SbF_6)(Et_2O)_{0.5}]_\infty$	16.09	3.54		15.81	3.39	
$[Ag(\mathbf{L}^{1\text{-}Me})_2(ClO_4)(Et_2O)_{0.5}]_\infty$	20.85	4.59				
$[Ag(\mathbf{L}^{1\text{-}Me})_2(ClO_4)]_\infty$	17.01	3.81		17.22	3.63	
$[Ag(\mathbf{L}^{1\text{-}Me})_2(BF_4)]_\infty$	17.53	3.92		17.19	3.28	
$[Ag(\mathbf{L}^{1\text{-}Me})_2(NO_3)]_\infty$	18.65	4.17	3.63	19.77	4.02	3.47

Échanges à partir du complexe $[Ag(L^{1\text{-}Me})_2(PF_6)]_\infty$

Le polymère de coordination **2**, $[Ag(\mathbf{L}^{1\text{-}Me})_2(PF_6)]_\infty$, présente aussi des propriétés d'échange anioniques. À la figure 3.2.7 sont montrés les spectres infrarouges enregistrés sur des échantillons collectés à différent temps durant le processus d'échange des anions hexafluorophosphate du complexe **2** avec des anions perchlorates.

Le spectre infrarouge du produit collecté après deux heures d'agitation du complexe **2**, $[Ag(\mathbf{L}^{1\text{-}Me})_2(PF_6)]_\infty$, dans une solution aqueuse de $LiClO_4$, montre que la fréquence de vibration caractéristique de l'anion hexafluorophosphate ($\nu_3(T_{1u})$: 835 cm^{-1})[26] disparaît totalement et que seule la fréquence de vibration caractéristique du perchlorate est présente ($\nu_1(A_1)$: 1092 cm^{-1}) (Figure 3.2.7).[25] Le RMN de fluor du produit resultant de l'échange a affirmé la non présence des anions hexafluorophosphate. L'analyse élémentaire de l'échantillon collecté après deux heures d'échange confirme que le produit final est le

composé $[Ag(\mathbf{L}^{1\text{-}Me})_2(ClO_4)]_\infty$ (Tableau 3.2.2). It faut remarquer que la structure et la stoichiométrie de ce complexe perchloraté sont différentes de ce qui a été observé plutôt en partant du complexe avec le triflate.

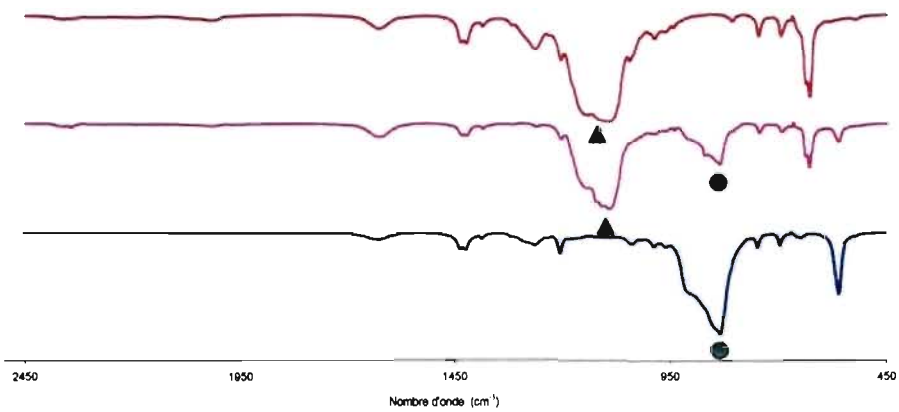

Figure 3.2.7. Évolution des spectres infrarouges durant l'échange des anions hexafluorophosphate du complexe **2**, $[Ag(L^{1\text{-}Me})_2(PF_6)]_\infty$, avec les anions perchlorates.
Le spectre bleu est celui du complexe **2**, $[Ag(L^{1\text{-}Me})_2(PF_6)]_\infty$, comme préparé (vibration caractéristique du l'hexafluorophosphate (● : 835 cm^{-1}, $\nu_3(T_{1u})$). Le spectre en violet est celui du complexe **2**, agité dans une solution aqueuse de $LiClO_4$ durant 40 min, montrant la décroissance de l'intensité de la bande caractéristique de l'hexafluorophosphate et l'augmentation de l'intensité de la bande caractéristique du perchlorate (▲ :1092 cm^{-1}, $\nu_1(A_1)$). Le spectre rouge est celui du produit résultant de l'échange après deux heures et correspond au composé $[Ag(L^{1\text{-}Me})_2(ClO_4)]_\infty$.

Comme illustrée à la figure 3.2.8, le diagramme de diffraction du produit final de l'échange, $[Ag(\mathbf{L}^{1\text{-}Me})_2(ClO_4)]_\infty$, est semblable à celui du produit de départ, le complexe **2** $[Ag(\mathbf{L}^{1\text{-}Me})_2(PF_6)]_\infty$. Ceci montre que le polymère de coordination **2** retient sa structure durant cet échange. De la même manière, les anions PF_6^- du complexe **2** peuvent être remplacés par les tétrafluoroborates et les nitrates, $[Ag(\mathbf{L}^{1\text{-}Me})_2(BF_4)]_\infty$ et $[Ag(\mathbf{L}^{1\text{-}Me})_2(NO_3)]_\infty$ respectivement (Figures S5-S8, Annexe IV et Tableau 3.2.2). Toutefois, les anions PF_6^- du composé **2** ne peuvent être échangés ni avec SbF_6^- ni avec $CF_3SO_3^-$. En effet, le spectre infrarouge du produit collecté après 72 heures d'agitation du complexe **2** dans une solution aqueuse de $NaSbF_6$ ou de $NaCF_3SO_3$, a été presque identique à celui du produit de départ, c'est à dire le complexe **2**.

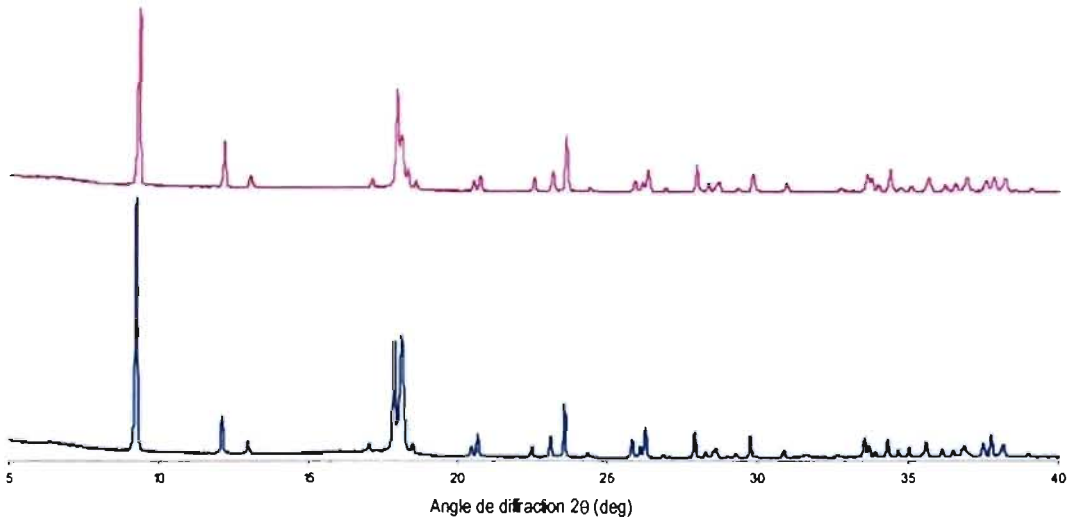

Figure 3.2.8. En bleu: Diagramme de poudre du complexe **2** comme synthétisé. En violet: Diagramme de poudre du produit résultant de l'échange **2** + $LiClO_4$.

Échanges à partir du complexe $[Ag(L^{1\text{-}Me})_2(SbF_6)(Et_2O)_{0.5}]_\infty$

Le polymère de coordination **3**, $[Ag(\mathbf{L}^{1\text{-}Me})_2(SbF_6)(Et_2O)_{0.5}]_\infty$, exhibe aussi des propriétés d'échange. Nous avons immergé dans une solution aqueuse de $LiClO_4$ le complexe **3** et le tout a été agité durant environ deux heures. Les spectres infrarouges des échantillons collectés à différents intervalles ont montré la diminution de l'intensité de l'absorption caractéristique du SbF_6^- ($\nu_3(T_{1u})$: 664 cm^{-1})[27,28] concomitant à l'augmentation de l'intensité de l'absorption caractéristique du perchlorate, ($\nu_1(A_1)$: 1084 cm^{-1})[25] (Figure 3.2.9). L'échange se complète en un peu plus de deux heures. Le RMN de fluor du produit resultant de l'échange a affirmé la non présence des anions SbF_6^-. L'analyse élémentaire du produit final de l'échange s'est révélé être $[Ag(\mathbf{L}^{1\text{-}Me})_2(ClO_4)]_\infty$ (Tableau 3.2.2). On doit remarquer que Et_2O n'est plus présent. Ce complexe a la même stoichiométrie que celui obtenu précédemment à partir de PF_6^-.

Le diagramme de poudre du produit final est similaire à celui du produit de départ, le complexe **3** (Figure 3.2.10). De ce fait, on pourrait considérer que le composé **3** retient sa structure durant cet échange. De même les anions hexafluoroantimonate du composé **3** peuvent aussi être échangés avec les tétrafluoroborates ou les nitrates,

$[Ag(\mathbf{L}^{1\text{-}Me})_2(BF_4)]_\infty$ et $[Ag(\mathbf{L}^{1\text{-}Me})_2(NO_3)]_\infty$ respectivement (Figures S9-S12, Annexe IV et Tableau 3.2.2). Néanmoins, les anions SbF_6^- de ce composé ne peuvent pas être échangés avec les anions PF_6^- ou $CF_3SO_3^-$.

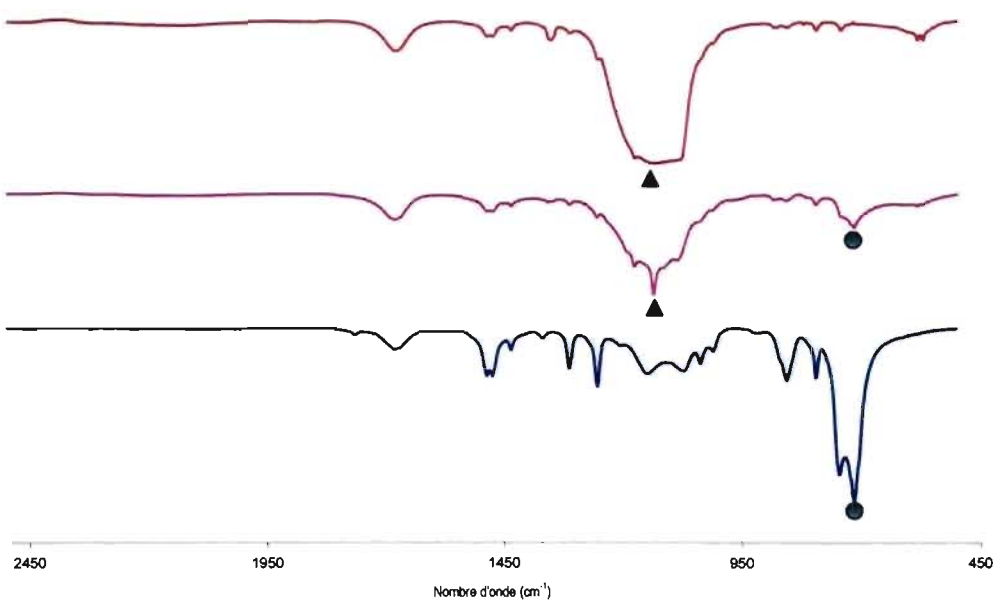

Figure 3.2.9. Évolution des spectres infrarouges durant l'échange des anions hexafluoroantimonate du complexe **3**, $[Ag(L^{1\text{-}Me})_2(SbF_6)(Et_2O)_{0.5}]_\infty$, avec les anions perchlorates. Le spectre bleu est celui du complexe **3**, comme préparé (vibration caractéristique du l'hexafluoroantimonate (● : 664 cm^{-1}, $\nu_3(T_{1u})$)).
Le spectre en violet est celui du complexe **3**, agité dans une solution aqueuse de $LiClO_4$ durant 40 min, montrant la décroissance de l'intensité de la bande caractéristique de l'hexafluoroantimonate et l'augmentation de l'intensité de la bande caractéristique du perchlorate (▲ : 1084 cm^{-1}, $\nu_1(A_1)$). Le spectre rouge est celui du produit résultant de l'échange après deux heures et correspond au composé $[Ag(L^{1\text{-}Me})_2(ClO_4)]_\infty$.

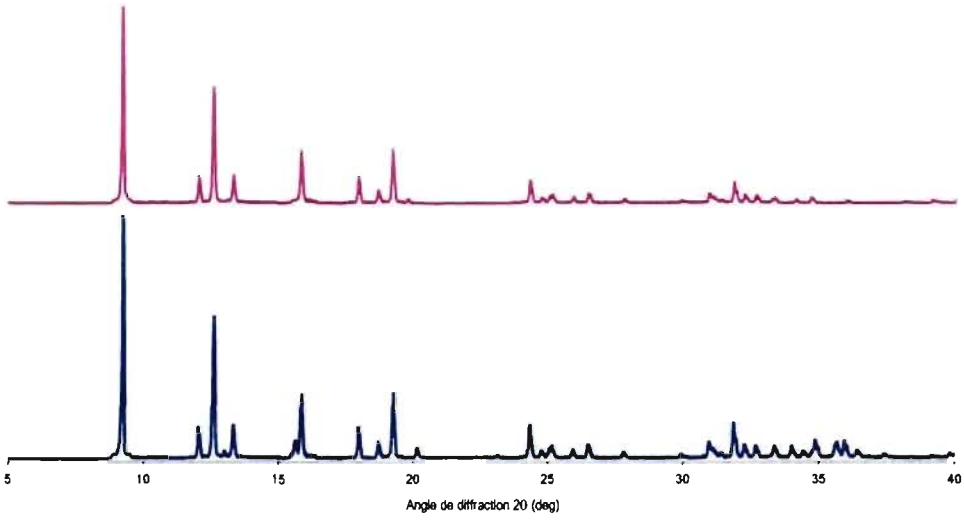

Figure 3.2.10. En bleu: Diagramme de poudre du complexe **3** comme synthétisé. En violet: Diagramme de poudre du produit résultant de l'échange **3** + $LiClO_4$.

3.2.4 Discussion

Nous avons rapporté dans le chapitre 3.1 des réseaux de coordination obtenus par auto-assemblage du petit ligand $\mathbf{L}^{\mathbf{1\text{-}Me}}$ et de divers sels d'argent.[8] Dans la plupart de ces composés, le ligand $\mathbf{L}^{\mathbf{1\text{-}Me}}$ propage les centres métalliques alors que les anions complètent la sphère de coordination de l'argent.[8] On concluait que les complexes du petit ligand $\mathbf{L}^{\mathbf{1\text{-}Me}}$ et des sels d'argent dont les anions sont peu ou non coordonnants étaient susceptibles de former des composés métallosupramoléculaires cationiques ayant des propriétés d'échange anioniques. Bien que le triflate puisse être considéré comme moyennement coordonnant, sa combinaison avec $\mathbf{L}^{\mathbf{1\text{-}Me}}$ donne un réseau cationique tridimensionnel alors que les structures avec les anions octaédriques PF_6^- et SbF_6^- sont constituées de doubles chaînes cationiques (Figures 3.2.1, 3.2.2 et 3.3.3).

Avec l'anion tétrafluoroborate, un réseau bidimensionnel cationique a été obtenu (Figure 3.2.4). Nous avons observé que les anions BF_4^- localisés entre les feuillets cationiques du composé **4** ne pouvaient être échangés avec aucun des anions suivants: NO_3^-; ClO_4^-; PF_6^-; SbF_6^-; $CF_3SO_3^-$. Il se pourrait que les ligands $\mathbf{L}^{\mathbf{1\text{-}Me}}$ désordonnés, localisés entre les feuillets cationiques du composé **4**, empêchent les anions tétrafluoroborates aussi désordonnés d'être échangés (Figure 3.2.4).

Par contre, le réseaux cationique tridimensionnel (composé **1**) et unidimensionnels (composés **2** et **3**) exhibent des propriétés d'échanges. Nous avons observé que les anions

$CF_3SO_3^-$ (86.9 Å^3)[29a] dans le composé **1**, PF_6^- (73.0 Å^3)[29a] et SbF_6^- (88.7 Å^3)[29a], respectivement dans les composés **2** et **3**, peuvent être échangés avec des anions plus petits comme ClO_4^- (54.4 Å^3)[29a], BF_4^- (53.4 Å^3)[29a] et NO_3^- (40.2 Å^3).[29b] Toutefois, les anions $CF_3SO_3^-$, PF_6^- et SbF_6^- ne s'échangent pas entre eux. Cette situation pourrait être attribuée aux tailles relativement comparables de ces anions.

Réversibilité des échanges

Récemment, Shu *et al.* ont rapporté des polymères de coordination d'argent qui présentent des propriétés d'échanges anioniques réversibles.[30]

Nous avons décidé d'investiguer la réversibilité des échanges anioniques des composés **1-3**. Quand nous échangeons les triflates du **1**, $[Ag_3(\mathbf{L}^{\mathbf{1\text{-}Me}})_6(CF_3SO_3)_3]_\infty$, par des anions perchlorates, nous obtenons le composé isostructural $[Ag_3(\mathbf{L}^{\mathbf{1\text{-}Me}})_6(ClO_4)_3]_\infty$.
Après l'avoir filtré et séché, nous l'avons placé dans une solution aqueuse de $NaCF_3SO_3$ et le tout a été agité pendant un peu plus de deux heures. Le spectre infrarouge du produit résultant de cet échange est identique à celui du composé **1**, $[Ag_3(\mathbf{L}^{\mathbf{1\text{-}Me}})_6(CF_3SO_3)_3]_\infty$.
Ceci montre que l'échange des anions triflates dans **1** avec les perchlorates est réversible. Une analyse élémentaire confirme aussi cette réversibilité.[31]

Il est à noter que nous avons suivi la réversibilité des échanges principalement par spectroscopie infrarouge. Par la même procédure, nous avons observé que les triflates dans **1** s'échangeaient de manière réversible avec les nitrates et les tétrafluoroborates. Les complexes **2** et **3** présentent aussi des échanges réversibles établis par spectroscopie infrarouge seulement.

Nous n'avons pas enregistré les digrammes de poudre résultants de ces échanges réversibles. Il serait intéressant de le faire afin de s'assurer que la structure se maintient durant cet échange inverse. Il serait aussi intéressant de faire les analyses élémentaires de tous les produits résultants de ces échanges inverses, afin de confirmer la réversibilité de ces échanges.

Comme ces complexes sont insolubles dans l'eau, nous pouvons penser que l'échange anionique des composés **1-3** pourrait être un processus qui se passe à l'état solide.[32] D'un autre côté, nous avons voulu voir si ces échanges pouvaient être un phénomène basé sur une dissolution suivie d'une recristallisation.[33]

Pour tester cette hypothèse, nous avons choisi un solvant où les complexes sont solubles. Nous avons dissout 150 mg du composé **1**, $[Ag_3(\mathbf{L}^{\mathbf{1\text{-}Me}})_6(CF_3SO_3)_3]_\infty$, dans

5 mL d'acétone puis nous avons ajouté 150 mg de $LiClO_4$. La solution résultante a été recristallisé par diffusion d'éther de pétrole. Cette procédure nous a permis d'avoir des cristaux. Ces derniers se sont révélés être le complexe $[Ag_2(L^{1\text{-}Me})_2(ClO_4)_2]_\infty$ que nous avons synthétisé en combinant directement $L^{1\text{-}Me}$ et $AgClO_4$ (Figure S15, Annexe IV) (Chapitre 3.1).[8] Le fait que nous n'avons pas obtenu le composé $[Ag_3(L^{1\text{-}Me})_6(ClO_4)_3]_\infty$, résultant de l'échange des triflates du complexe **1** avec les perchlorates montre que nos échanges anioniques ne sont pas régis par un phénomène basé sur une dissolution suivie d'une recristallisation. De même, quand nous avons utilisé la même procédure avec les complexes **2** et **3**, les cristaux formés ont été identifiés comme étant le complexe $[Ag_2(L^{1\text{-}Me})_2(ClO_4)_2]_\infty$ (Figure S15, Annexe IV).[8]

Sur la base de ces résultants et le fait que nos composés sont insolubles dans l'eau, nous pensons que les échanges exhibés par les complexes **1-3** sont des phénomènes qui se passent à l'état solide.

Il est à noter que nous avons deux types de structures avec les anions triflates. La combinaison directe de $L^{1\text{-}Me}$ avec le triflate d'argent donne le réseau cationique tridimensionnel (complexe **1**) $[Ag_3(L^{1\text{-}Me})_6(CF_3SO_3)_3]_\infty$, avec un bon rendement. Pour ce même anion, nous avons rapporté dans le chapitre 3.1, un complexe d'une autre stoechiométrie formant un réseau neutre bidimensionnel. Ce produit est obtenu par un processus d'échange anionique, $[Ag_2(L^{1\text{-}Me})_2(CF_3SO_3)_2]_\infty$ (Figure S16, Annexe IV).[8] Dans ce dernier, le triflate complète la sphère de coordination du métal (Figure S16, Annexe IV). Quand, nous avons dissout le réseau bidimensionnel $[Ag_2(L^{1\text{-}Me})_2(CF_3SO_3)_2]_\infty$ dans l'acétone et recristallisé par diffusion d'éther de pétrole, nous obtenons le réseau tridimensionnel, $[Ag_3(L^{1\text{-}Me})_6(CF_3SO_3)_3]_\infty$. Du fait que la réaction directe de $L^{1\text{-}Me}$ et $AgCF_3SO_3$ donne le réseau 3D et que la recristallisation du réseau 2D donne aussi le réseau 3D, nous pensons que la structure 3D est la phase la plus stable.

3.2.5 Conclusions

Des réseaux cationiques à une, deux ou trois dimensions ont été synthétisés par autoassemblage du ligand bis(méthylthio)méthane $L^{1\text{-}Me}$ avec les sels d'argent suivants: $AgPF_6$, $AgSbF_6$, $AgBF_4$ et $AgCF_3SO_3$.

Le réseau cationique 2D obtenu avec BF_4^-, ne montre pas de propriété d'échange anionique, tandis que les réseaux cationiques 1D et 3D exhibent des propriétés d'échange réversibles avec les petits anions comme le perchlorate, le nitrate et le tétrafluoroborate.

L'étude des échanges anioniques mérite d'être approfondie. Par exemple, quand les triflates du composé **1**, $[Ag_3(\mathbf{L}^{\mathbf{l\text{-}Me}})_6(CF_3SO_3)_3]_\infty$, ont été échangés avec des perchlorates, le composé isostructural $[Ag_3(\mathbf{L}^{\mathbf{l\text{-}Me}})_6(ClO_4)_3]_\infty$ a été obtenu. Comme les anions ClO_4^- du composé $[Ag_3(\mathbf{L}^{\mathbf{l\text{-}Me}})_6(ClO_4)_3]_\infty$ peuvent être échangés en retour avec des anions $CF_3SO_3^-$, ce qui montre la réversibilité des échanges, il serait intéressant de tester si les ClO_4^- du composé $[Ag_3(\mathbf{L}^{\mathbf{l\text{-}Me}})_6(ClO_4)_3]_\infty$ peuvent être échangés avec les anions PF_6^- et SbF_6^-, puisque ces anions ont des tailles semblables à celle du triflate.

3.2.6 Références

(1) (a) Eddaoudi, M.; Moler, D. B.; Li, H.; Chen, B.; Reineke, T. M.; O'Keefe, M. Yaghi, O. M. *Acc. Chem. Res.* **2001**, *34*, 319. (b) Moulton, B.; Zaworotko, M. J. *Chem . Rev.* **2001**, *101*, 1629. (c) Khlobystov, A. N.; Blake, A. J.; Champness, N. R.; Lemenovskii, D. A.; Majouga, A. G.; Zyk, N. V.; Schröder, M. *Coord. Chem. Rev.* **2001**, *222*, 155.

(2) (a) Withersby, M. A.; Blake, A. J.; Champness, N. R.; Cooke, P. A.; Hubberstey, P.; Li, W. S.; Schröder, M. *Inorg. Chem.* **1999**, *38*, 2259. (b) Blake, A. J.; Champness, N. R.; Cooke, P. A.; Nicolson, J. E. B.; Wilson, C. *J. Chem. Soc., Dalton Trans.* **2000**, 3811. (c) Withersby, M. A.; Blake, A. J.; Champness, N. R.; Hubberstey, P.; Li, W. S.; Schröder, M. *Angew. Chem. Int. Ed.* **1997**, *36*, 2327. (d) Noro, S.; Kitaura, R.; Kondo, M.; Kitagawa, S.; Ishii, T.; Matsuzaka, H.; Yamashita, M. *J. Am. Chem. Soc.* **2002**, *124*, 2568.

(3) (a) Yaghi, O.M.; Li, G.; Li, H. *Nature* **1995**, *378*, 703. (b) Gardner, G. B.; Venkataraman, D.; Moore, J. S.; Lee, S. *Nature* **1995**, *374*, 792. (c) Abrahams, B. F.; Hoskins, B. F.; Michall, D. M.; Robson, R. *Nature* **1994**, *369*, 727. (d) Stumpt, H. O.; Ouahab, L.; Pei, Y.; Grandjean, D.; Kahn, O. *Science* **1993**, *261*, 447.

(4) Bu, X. H.; Chen, W.; Hou, W. F.; Du, M.; Zhang, R. H.; Brisse, F. *Inorg. Chem.* **2002**, *41*, 3477.

(5) Awaleh, M. O; Badia, A.; Brisse, F. *Inorg. Chem.* **2005**, *44*, 7833.

(6) Awaleh, M. O; Badia, A.; Brisse, F. *Cryst. Growth Des.* **2005**, *5*, 1897.

(7) Awaleh, M. O; Badia, A.; Brisse, F.; Bu, X. H. *Inorg. Chem.* **2006**, *45*, 1507.

(8) Awaleh, M. O.; Badia, A.; Brisse, F. *Cryst. Growth Des.* **2006**, *6*, 2674.

(9) (a) Jung, O. S.; Kim, Y. J.; Lee, Y. A.; Park, K. M.; Lee, S. S. *Inorg. Chem.* **2003**, *42*, 844. (b) Jung, O. S.; Kim, Y. J.; Lee, Y. A.; Chae, H. K.; Jang, H. G.; Hong, J. *Inorg. Chem.* **2001**, *40*, 2105. (c) Yaghi, O. M.; Li, H. *J. Am. Chem. Soc.* **1996**, *118*, 295.

(10) Sharma, C. V. K.; Griffin. S. T.; Rogers, R. D. *J. Chem. Soc., Chem. Comm.* **1998**, 215.

(11) Rogers, R. D.; Zhang, J.; Griffin, S. T. *Sep. Sci. Technol.* **1997**, *32*, 699.

(12) Rogers, R. D. ; Bond, A. H.; Zhang, J.; Bauer, C. B. *Appl. Radiat. Isot.* **1996**, *47*, 497.

(13) (a) Yaghi, O. M.; Li, H. *J. Am. Chem. Soc.* **1995**, *117*, 10401. (b) Du, M.; Zhao, X. J.; Guo, J. H.; Batten, S. R. *J. Chem. Soc., Chem. Comm.* **2005**, 4836. (c) Muthu, S.; Yip, J. H. K.; Vittal, J. J. *J. Chem. Soc., Dalton. Trans.* **2002**, 4561. (d) Jung, O. S.; Kim, Y. J.; Lee, Y. A.; Park, J. K.; Chae, H. K. *J. Am. Chem. Soc.* **2000**, *122*, 9921.

(14) Hartley, F. R.; Murray, S. G.; Levason, W.; Soutter, H. E.; McAuliffe, C. A. *Inorg. Chim. Acta* **1979**, *35*, 265.

(15) SAINT Release 6.06, Integration Software for Single Crystal Data; Bruker AXS Inc.: Madison, WI, **1999**.

(16) Sheldrick, G.M. SADABS Bruker Area Detector Absorption Corrections; Bruker AXS Inc.: Madison, WI, **1996**.

(17) XPREP Release 5.10; X-ray Data Preparation and Reciprocal Space Exploration Program. Bruker AXS Inc., Madison, WI, **1997**.

(18) SHELXTL Release 5.10, The Complete Software Package for Single-Crystal Structure Determination; Brucker AXS Inc.: Madison, WI, **1997**.

(19) (a) Sheldrick, G.M. SHELXS97, Program for the Solution of Crystal Structures; University of Göttingen: Göttingen, Germany, **1997**. (b) Sheldrick, G.M. SHELXL97, Program for the Refinement of Crystal Structures; University of Göttingen: Göttingen, Germany, **1997**.

(20) Flack, H. D.; Schwarzenbach, D. *Acta Crystallogr. Sect. A* **1988**, *44*, 499.

(21) Sluis, P. van der.; Spek, A. L. *Acta Crystallogr. Sect. A* **1990**, *46*, 194.

(22) Spek, A. L. *J. Appl Crystallogr.* **2003**, *36*, 7.

(23) Black, J. R.; Champness, N. R.; Levason, W.; Reid, G. *Inorg. Chem.* **1996**, *35*, 4432.

(24) (a) Lawrance, G. A. *Chem. Rev.* **1986**, *86*, 17 and references therein.; (b) Batchelor, R. J.; Ruddick, J. N. R.; Sams, J. R.; Aubke, F. *Inorg. Chem.* **1977**, *16*, 1414. and references therein.

(25) Rosenthal, M. R. *J. Chem. Educ.* **1973**, *50*, 331 and references therein.

(26) (a) Matsumoto, K.; Hagiwara, R.; Ito, Y.; Tamada, O. *Solid State Sci.* **2002**, *4*, 1465. (b) Reger, D. L.; Semeniuc, R. F.; Rassolov, V.; Smith, M. D. *Inorg. Chem.* **2004**, *43*, 537. (c) Jung, O. S.; Kim, Y. J.; Lee, Y. A.; Chae, H. K.; Jang, H. G.; Hong , J. *Inorg. Chem.* **2001**, *40*, 2105.

(27) Nakamoto, K. *Infrared Spectra of Inorganic and Coordination Compounds,* 3rd ed.; Wiley-VCH: New York, 1978.

(28) Bernhardt, E.; Bach, C.; Bley, B.; Wartchow, R.; Westphal, U.; Sham, I. H. T.; Ahsen, B. V.; Wang, C.; Willner, H.; Thompson, R. C.; Aubke, F. *Inorg. Chem.* **2005**, *44*, 4189.

(29) (a) Yamada, M.; Hagiwara, H.; Torigoe, H.; Matsumoto, N.; Kojima, M.; Dahan, F.; Tuchagues, J. P.; Re, N.; Iijima, S. *Chem. Eur. J.* **2006**, *12*, 4536. (b) Le volume moléculaire du nitrate a été calculé en utilisant le programe Spartan dans les mêmes conditions que les auteurs de la référence 30a ont calculé avec le même programme les volumes moléculaires des anions BF_4^-; ClO_4^-; PF_6^-; SbF_6^- et $CF_3SO_3^-$.

(30) Shu, M.; Tu, C.; Xu, W.; Jin, H.; Sun, J. *Cryst. Growth Des.* **2006**, *6*, 1890.

(31) Produit final de l'échange $[Ag_3(L^{1\text{-}Me})_6(CF_3SO_3)_3]_\infty$: analyse élémentaire calculée pour $C_{21}H_{48}Ag_3F_9O_9S_{15}$: C, 17.76; H, 3.41. Obtenu: C, 18.01; H, 3.35.

(32) (a) Fan, J.; Sun, W. Y.; Okamura, T. A.; Zheng, Y. Q.; Sui, B.; Tang, W. X.; Ueyama, N. *Cryst. Growth Des.* **2004**, *4*, 579. (b) Fan, J.; Gan, L.; Kawaguchi, H.; Sun, W. Y.; Yu, K. B.; Tang, W. X. *Chem. Eur. J.* **2003**, *9*, 3965. (c) Yaghi, O. M.; Li, H.; Davis, C.; Richardson, D.; Groy, T. L. *Acc. Chem. Res.* **1998**, *31*, 474.

(33) Khlobystov, A. N.; Champness, N. R.; Roberts, C. J.; Tendler, S. J. B.; Thompson, C.; Schröder, M. *CrystEngComm.* **2002**, *4*, 426.

3.3 One-dimensional coordination polymers incorporating silver(I) perfluorocarboxylate cuboctahedral clusters and the bis(methylthio)methane ligand.[†]

3.3.1 Abstract

Two topologically comparable complexes, $[Ag_6(CF_3CO_2)_3(\mathbf{L}^{1\text{-}Me})_3(SCH_3)_3]_\infty$ (**1**) and $[Ag_6(CF_3CF_2CO_2)_3(\mathbf{L}^{1\text{-}Me})_2(SCH_3)_3(H_2O)]_\infty$, (**2**) were prepared and characterized by single crystal diffractometry. The structures consist of $Ag_{12}S_6$ clusters linked by bis(methylthio)methane ligands, $L^{1\text{-}Me}$, thus forming 1D-coordination polymers. The twelve Ag atoms of the cluster are situated at the corners of a distorted cuboctahedron. The sulfur atoms of the six μ_4-SCH_3 entities occupy a position at about 0.8 Å above the center of each of the square faces of the polyhedron. The cleavage of the C-S bond of some of the ligands occurs during the syntheses, producing the $^-SCH_3$ anions. The coordination of the silver atoms varies from 5 to 7. The Ag···Ag contacts range from 2.9250(5) to 3.3615(6) Å and from 2.961(1) to 3.380(1) Å for **1** and **2**, respectively. A polymeric ribbon is obtained when four ligands link a given cluster to two others. The chains of **1**, held by van der Waals forces only, pack in a hexagonal manner. The two water molecules in **2** (Ag-OH_2 = 2.385(7) Å) are coordinated to silver atoms of the cluster. They are also strongly hydrogen bonded to the oxygen atoms of two pentafluoropropionate groups, one within the cluster (O···O = 2.741(1) Å), the other in an adjacent chain (O···O = 2.818(1) Å). The chains, thus H-bonded to one another, generate a 2D-coordination network.

3.3.2 Introduction

The synthesis and characterization of metal organic frameworks (MOFs) has been an active research area since the discovery of the first coordination polymers in the mid 1990s.[1, 2]

A remarkable feature of metal-organic compounds is that the properties of the metal inorganic centre can be expanded through the organic building block. Hence, the interest in hybrid inorganic-organic extended solid state resides in the fact that their new physical properties, such as gas-storage,[3] anion-exchange,[4] non-linear optic[5] or magnetism,[6] often differ from those of the parent organic or inorganic compounds. Since to some extent, it is possible to design an organic connector, in which the connecting sites have a good

---

[†] Awaleh, M. O.; Badia, A.; Brisse, F. *Inorg. Chem.* **2007**. *In Press.*

coordinating ability with the chosen metal, one may be able to tailor the physical properties of the resulting coordination polymer materials. However, even if the major goal in crystal engineering is to predict the resulting MOFs of a given system,[7] there still remains a long way to go before the synthesis of coordination polymers with predictable topologies is achieved, because it is difficult to simultaneously control the many factors that influence the crystallization process.[8]

We are currently using flexible symmetrical thiol ligands as organic building blocks to propagate the coordination sphere of d^{10} metal centres, Ag(I) and Au(I), *via* metal-directed self-assembly[9] in order to investigate the influence of the experimental parameters, such as the type of anions, the size and shape of the organic connectors, the metal-to-ligand ratio, and the recrystallization solvent, among others, upon the supramolecular architectures.[10-17] It has been reported that the silver(I) centres have a propensity to form metallomacrocycle clusters when they are combined with asymmetrical thiol ligands as opposed to gold(I), which privileges supramolecular arrangements.[9] However, the flexible symmetrical thioether spacers promote supramolecular arrangements for Ag(I), from one to three dimensional coordination polymers/networks are formed in which the metal centers are propagated by the organic ligands.[10-20] In the gold(I) complexes the Au(I)-Au(I) aurophilic interaction[21-27] allows for the expansion of the discrete molecules into 1D or 2D networks.[17]

We recently reported MOFs based on the self-assembly of the small bis(methylthio)methane, $\mathbf{L^{1\text{-}Me}}$, building block and silver(I) salts, wherein the anions have a marked influence upon the resulting coordination polymers or networks.[15] The combination of trifluoroacetate or heptafluorobutyrate and $\mathbf{L^{1\text{-}Me}}$ led to the formation of "isostructural" two-dimensional frameworks, in which the anions complete the coordination sphere of the silver(I) centers. Hence, the self-assembly of $\mathbf{L^{1\text{-}Me}}$ with pentafluoropropionate, an anion of intermediate size, was expected to be isostructural. Surprisingly, this latter complex was found to form a 1D-coordination polymer consisting of ligand-linked clusters rather than the expected structure. We serendipitously obtained another cluster-bearing structure when this small ligand was combined with silver(I) trifluoroacetate. However, no cluster could be obtained with the longer heptafluorobutyrate.

Here, we wish to report the structures of two unusual atlas-sphere thiolate-silver clusters, $[Ag_6(CF_3CO_2)_3(\mathbf{L^{1\text{-}Me}})_3(SCH_3)_3]_\infty$ **(1)** and $[Ag_6(CF_3CF_2CO_2)_3(\mathbf{L^{1\text{-}Me}})_2(SCH_3)_3(H_2O)]_\infty$ **(2)**.

3.3.3 Experimental Section

Materials and General Methods. The ligand was synthesized following a published report.[28] The elemental analyses were performed by the Laboratoire d'Analyse Élémentaire (Université de Montréal), and IR spectra were recorded on a Perkin-Elmer 1750 FTIR (4000-450 cm^{-1}) spectrometer with solid samples prepared as KBr pellets for the complexes, while NaCl plates were used for the liquid ligand. The ^1H (300 MHz) NMR spectra in solution were recorded on a Bruker AV300 at 25 °C. ^1H chemical shifts are reported in parts per million and are referenced to residual solvent signals of deuterated DMSO (δ_{1H} = 2.50). No NMR spectra are reported for **1** and **2** since these complexes could not be solubilized. The GC/MS analyses were made on an Agilent Technologies 6890 Network GC system equipped with an HP-5MS capillary column and a 5973 MS selective detector.

Syntheses. Bis(methylthio)methane, $L^{1\text{-}Me}$. Oil. Yield: 41%. Anal. Found: C, 33.45; H, 7.32. Calcd for $C_3H_8S_2$: C, 33.29; H, 7.45. ^1H NMR (DMSO-d_6, 300 MHz): δ 2.16 (*s*, 6H, CH_3-S-CH_2-S-CH_3), 3.71 (*s*, 2H, CH_3-S-CH_2-S-CH_3). IR (KBr, cm^{-1}): 2973m, 2915s, 2855m, 2828m, 2756w, 2588w, 2380w, 2269w, 2181w, 2128w, 2076w, 2034w, 1671w, 1435m, 1422m, 1384m, 1316m, 1203s, 1154m, 1123w, 985m, 958m, 805m, 745s, 693s, 648w.

$[Ag_6(CF_3CO_2)_3(L^{1\text{-}Me})_3(SCH_3)_3]_\infty$ (1). $Ag(CF_3CO_2)$ (217 mg, 0.98 mmol) was dissolved in 5 mL of acetone. This mixture was stirred with a solution of bis(methylthio)methane (0.30 mL, 2.93 mmol) in diethyl ether (5 mL) at room temperature for 2 h and then filtered. The filtrate was left standing at room temperature for several months in closed container until single crystals suitable for X-ray analysis appeared (Yield 32%). Analysis, found: C 14.61, H 2.31; calculated for $C_{18}H_{33}O_6F_9S_9Ag_6$: C 14.89, H 2.29. IR (KBr, cm^{-1}): 3430w, 3047w, 2997w, 2924w, 2834w, 1678vs, 1411s, 1330vs, 1206vs, 1158vs, 1029s, 980w, 836w, 817s, 778w, 731s, 693w, 651w, 585m, 539w, 515w.

$[Ag_6(CF_3CF_2CO_2)_3(L^{1\text{-}Me})_2(SCH_3)_3(H_2O)]_\infty$ (2). This complex was synthesized in the same manner as **1** using $Ag(CF_3CF_2CO_2)$ (350 mg, 1.29 mmol) and $L^{1\text{-}Me}$ (0.30 mL, 2.93 mmol). About four months later, single crystals suitable for X-ray analysis were deposited (Yield: 37 %). Analysis, found: C 14.62, H 2.11; $C_{18}H_{27}O_7F_{15}S_7Ag_6$: C 14.30, H 1.80. IR

(KBr, cm^{-1}): 3431br, 3098w, 2916w, 2863w, 1670vs, 1437s, 1370m, 1323w, 1218vs, 1148vs, 840s, 807s, 725s, 598m, 516m.

X-ray diffraction. The X-ray intensity data were collected on a SMART 6K CCD equipped with a rotating anode (Cu Kα, λ = 1.54178 Å) and an area detector using the Mirror Montel 200 Optics as monochromator. The unit-cell refinement and data reduction were obtained with the program SAINT[29]. An empirical absorption correction, based on the multiple measurements of equivalent reflections, was applied using the program SADABS.[30] The space groups were confirmed by the XPREP[31] routine in the program SHELXTL.[32] The structures were solved by direct methods and difference-Fourier techniques with SHELXS-97.[33] The structure refinements were carried out based on F^2 by full-matrix least-squares.[32] In complex **1**, two trifluoroacetate groups were found to be disordered over three different orientations in the ratios 40/36/24 and 60/20/20, respectively. The C-F distances of those anions were constrained to be equal (SADI[33]). The thermal parameters of all disordered atoms were constrained such that the corresponding atoms of the major and the minor entities kept the same values (EADP[33]). In complex **2**, some of the CF_3 groups were slightly disordered as their thermal ellipsoids were larger than those of the other atoms. These atoms were constrained such that they had approximately the same thermal ellipsoids as the corresponding non disordered atoms using the EADP instruction of SHELXS-97.[33] The H atoms on the water molecule of complex **2** were found on a Fourier-difference map and were included in the refinement at their fixed positions. Crystal data and data collection parameters are listed in Table 3.3.1.

Table 3.3.1. Crystal data and X-ray data collection parameters.

	1	**2**
Formula	$C_{18}H_{33}Ag_6F_9O_6S_9$	$C_{18}H_{27}Ag_6F_{15}O_7S_7$
Mol wt	1452.20	1512.02
Crystal size (mm)	0.16x0.04x0.04	0.20x0.11x0.08
Space group	$P2_1/c$	P-1
a (Å)	13.2763(2)	13.0172(8)
b (Å)	20.7631(4)	13.2443(8)
c (Å)	15.7275(3)	14.9673(9)
α (deg)	90	87.15(1)
β (deg)	109.47(1)	64.59(1)
γ (deg)	90	63.44(1)
Volume (Å^3)	4087.41(13)	2052.3(2)
Z	4	2
D(calc) (g cm^{-3})	2.360	2.443
F(000)	2784	1436
Temp (K)	200(2)	153(2)
μ, (mm^{-1})	27.585	26.820
θ_{max} (deg)	68.96	68.88
$R1$[a] [$I > 2\sigma(I)$]	0.0351	0.0507
Rw[b] [$I > 2\sigma(I)$]	0.0928	0.1249
R [*all data*]	0.0374	0.0865
Rw [*all data*]	0.0942	0.1466
S[c]	1.040	0.944

[a] $R = \Sigma \, || F_o | - | F_c || / \Sigma \, | F_o |$. [b] $R_w = [\, \Sigma \, w(F_o^2 - F_c^2)^2 / \Sigma \, w(F_o^2)^2]^{1/2}$.
[c] $S = [\, \Sigma \, w(F_o^2 - F_c^2)^2 / (\text{m-n})]^{1/2}$ (m is the number of reflections and n the number of parameters).

3.3.4 Results and Discussion

Crystals of complexes of **1** and **2** are quite difficult to obtain. It usually takes 4 to 5 months to grow them as small single crystals. It is worth signaling that **1** has a polymorph. However, it does not coexist, at the time of crystallization, with its other form.

$[Ag_6(CF_3CO_2)_3(L^{1\text{-}Me})_3(SCH_3)_3]$ (1). The content of the asymmetric unit and the atomic numbering of **1** are shown in Figure 3.3.1a. In this structure, the two centrosymmetrically related units generate a twelve-silver nuclear complex, $[Ag_{12}(CF_3CO_2)_6(L^{1\text{-}Me})_6(SCH_3)_6]$ which may be best described as an atlas-sphere cluster (Figure 3.3.1b). These clusters are linked through the bis(methylthio)methane spacers and form a 1D-coordination polymer.

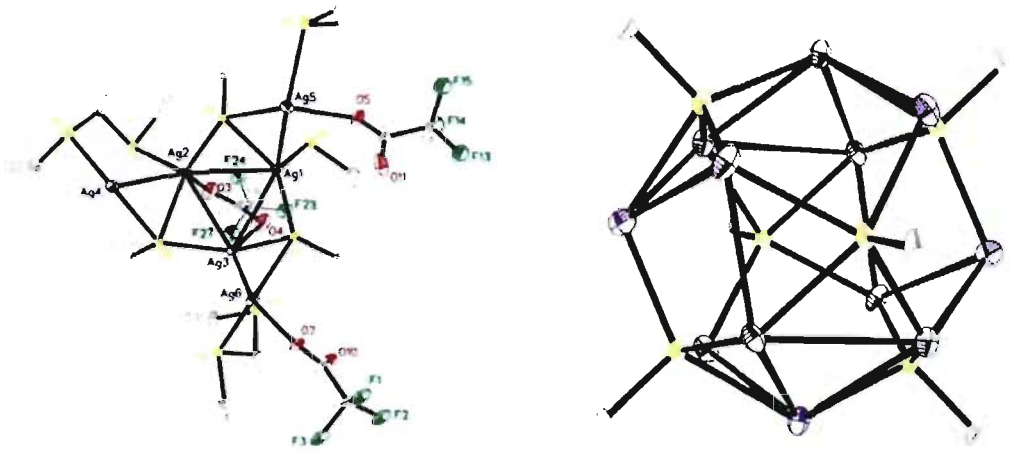

(a) (b)

Figure 3.3.1. (a) The asymmetric unit and atomic numbering of **1** (H atoms as well as the minors parts of the disordered fluorine atoms have been omitted for clarity). (b) The atlas-sphere cluster of **1**. The μ_4-S bridges four silver atoms (H atoms, trifluoroacetate groups and the bis(methylthio)methane have been omitted for clarity).

The structural analysis reveals the presence of the $^{-}SCH_3$ entity that links four silver (I) ions in a μ_4-bridging mode (Figure 3.3.1b). This type of bridging is not unusual. For example, Su *et al.* reported a one-dimensional coordination polymer where the $^{-}SC_2H_4NH_3^{+}$ zwitterion demonstrated the μ_4 bridging mode connecting four Ag(I) centers.[34] Similarly, Jeannin *et al.* reported that the action of an alkylthioalkyne on iron carbonyl produced a cluster containing the μ-SC_2H_5 entity.[35]

In the cluster of complex **1**, there are two types of sulfur atoms, each type being associated with a distinct coordination mode. The sulfur atom of the bis(methylthio)methane building block, $\mathbf{L}^{\mathbf{l\text{-}Me}}$, is only coordinated to one silver center, while the S atom of the $^{-}SCH_3$ unit is involved in four coordinations toward Ag(I) atoms in a square pyramidal fashion, $Ag_4(\mu_4\text{-}SCH_3)$.

The cluster may be described as made up of three sections. A central layer consists of an almost planar ring of eight atoms $(Ag\text{-}S\text{-})_4$, that has above and below it two square based pyramids $Ag_4(\mu_4\text{-}SCH_3)$. These pyramids are connected to the central eight-membered ring through Ag-Ag and Ag-S bonds. This description applies to any pair of diametrically opposed $^{-}SCH_3$ groups (Figure 3.3.1b).

Alternatively, the clusters may be described in terms of a distorted cuboctahedron. The notation 3^24^2 describing a perfect cuboctahedron indicates that two triangular faces and

two square faces meet at each corner. The silver atoms occupy the corners of the polyhedron while the sulphur atoms of the (μ_4-SCH_3) units are located above each of the square faces (Scheme 1).

Scheme 1[a]

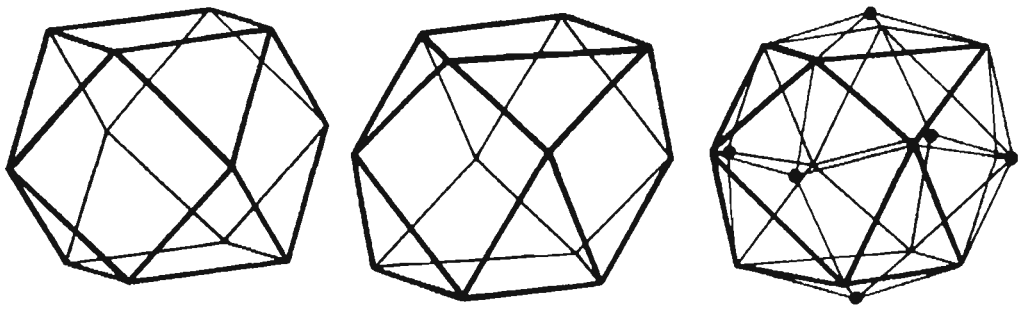

(a) (b) (c)

[a] (a) A perfect cuboctahedron with square and equilateral triangular faces. (b) The distorted cuboctahedron made of the 12 Ag atoms in **1**. There is an Ag atom at each corner of the polyhedron. (c) The $Ag_{12}S_6$ cluster in **1**. The black circles above each of the distorted square faces represent the sulfur atoms.

The 1D-coordination polymer is obtained as each bis(methylthio)methane spacer joins the Ag(1) and Ag(5) atoms of adjacent clusters (Figure 3.3.2).

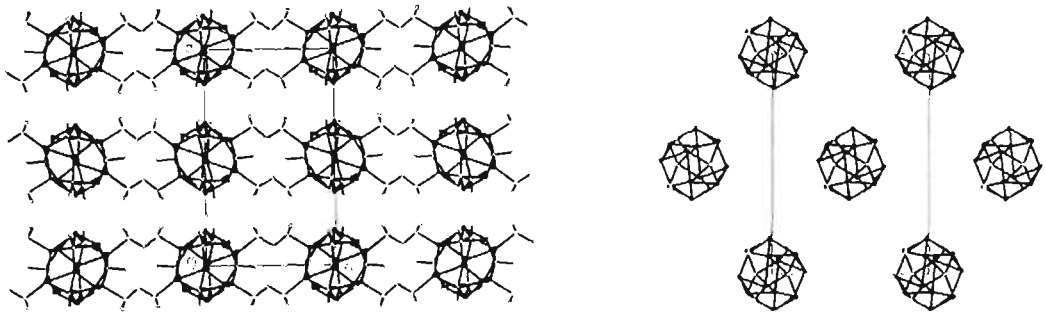

(a) (b)

Figure 3.3.2. (a) The clusters in **1** are interconnected through the bis(methylthio)methane spacers forming chains parallel to the *a*-axis (The trifluoroacetate groups, and the H atoms have been omitted for clarity). (b) Packing diagram of **1**, viewed down the chain axis (the *a*-axis), showing the hexagonal packing of cylindrical rods.

The Ag-S distances, ranging from 2.605(1) to 2.656(1) Å, are in the normal interval for silver dithioether complexes (2.434(2)-2.697(1) Å) (Table S3, Annexe V).[15, 36] The Ag-S distances for the μ_4-SCH_3 unit are shorter as they vary from 2.466(1) to 2.581(1) Å and are in the normal range for $Ag_4(\mu_4\text{-}SR)$.[34, 35, 37] The trifluoroacetate anions adopt two coordination modes (Figure 3.3.1a). In one case, the anion completes the coordination sphere of the metal centre (Scheme 2a) and in the other, it bridges two silver atoms resulting in the Ag(2)-O(3)-C(5)-O(4)-Ag(3) five-membered ring (Scheme 2b).

Scheme 2

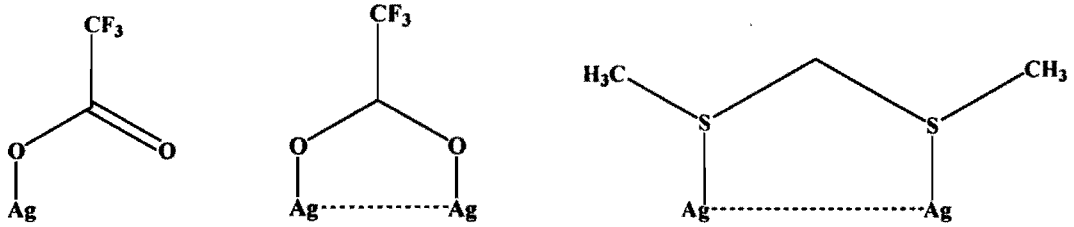

(a) (b) (c)

The bis(methylthio)methane organic connector plays two distinct roles. First, one $\mathbf{L}^{\mathbf{1\text{-}Me}}$ bridges two silver(I) centres through its sulphur atoms producing a five-membered ring, Ag(2)-S(1)-C(11)-S(2)-Ag(4) (Figure 1 and Scheme 2c).

This kind of coordination was observed when $\mathbf{L}^{\mathbf{1\text{-}Me}}$ was self-assembled with the methylsulfonate or the succinate silver(I) salts.[15] Secondly, four $\mathbf{L}^{\mathbf{1\text{-}Me}}$ spacers link one $[Ag_{12}(CF_3CO_2)_6(\mathbf{L}^{\mathbf{1\text{-}Me}})_6(SCH_3)_6]$ cluster to two others to form a one-dimensional coordination polymer parallel to the *a*-axis (Figure 3.3.2a). The solid-state organization of this metal-organic coordination polymer may be best described as a hexagonal packing of cylindrical rods (Figure 3.3.2b).

In this complex, the silver atoms present different coordination modes, from 5 to 7. Atom Ag(6) has coordination 5, while Ag(1), Ag(4), and Ag(5) have a coordination of six. The Ag(2) and Ag(3) atoms have coordination 7 (Figure S1, Annexe V). The silver-silver distances, which range from 2.9250(5) to 3.3615(6) Å, are shorter than the sum of the van der Waals radii, 3.44 Å,[38] and the shorter distance, 2.9250(5) Å, is slightly longer than 2.89 Å, which is twice the metallic radius of silver (Table S1, Annexe V).[38] According to the literature there may be some weak interactions between the metal centres.[39-41]

$[Ag_6(CF_3CF_2CO_2)_3(L^{1\text{-}Me})_2(SCH_3)_3(H_2O)]_\infty$ (2). The X-ray analysis of **2** reveals the existence of a $Ag_{12}S_6$ cluster comparable to that of **1**. These two clusters are nearly identical except for the presence of two water molecules in **2**. The repeat unit of this complex consists of $[Ag_{12}(CF_3CF_2CO_2)_6(L^{1\text{-}Me})_4(SCH_3)_6(H_2O)_2]$ (Figure 3.3.3). In this complex, $L^{1\text{-}Me}$, $CF_3CF_2CO_2^-$, H_2O, and μ_4-SCH_3 groups are all bound to silver atoms. The silver-silver distances in **2**, which range from 2.961(1) to 3.380(1) Å, indicate, as for **1**, the presence of some weak argentophilicity (Table S1, Annexe V).[39-41]

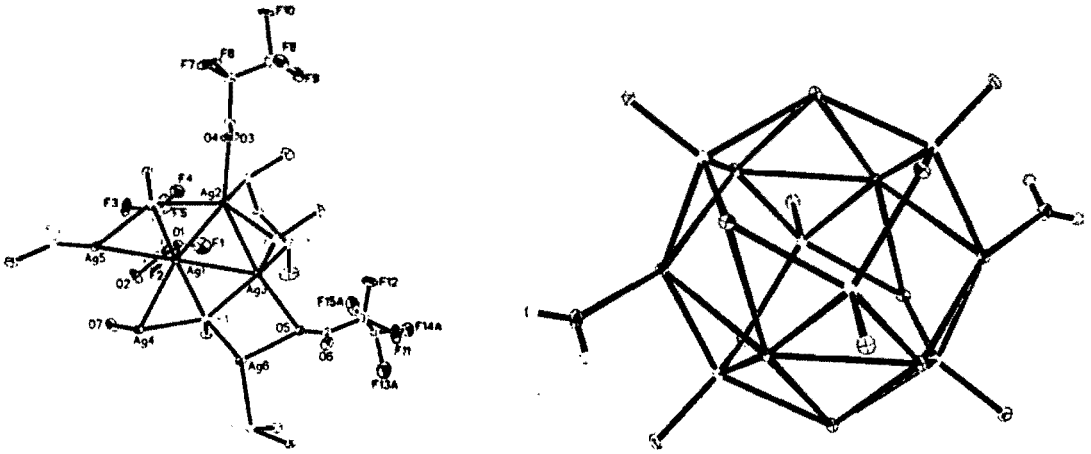

(a) (b)

Figure 3.3.3. Complex **2**. (a) The content of the asymmetric unit and atomic numbering. (b) The centrosymmetric cluster with the two water molecules coordinated to the Ag(4) atoms. The description of **2** follows that of **1**.

The description of **2** follows that of **1**. The disordered pentafluoropropionate group displays a monodentate bridging mode and a dibridging mode in associating two metal centers. The bis(methylthio)methane ligand has two kinds of coordination modes. On the one hand, $L^{1\text{-}Me}$ dibridges two silver(I) centers (Scheme 2c). Secondly, four $L^{1\text{-}Me}$ organic connectors join one $[Ag_{12}(CF_3CF_2CO_2)_6(L^{1\text{-}Me})_4(SCH_3)_6(H_2O)_2]$ cluster to two others, thus developing into a one dimensional coordination polymer parallel to the *a*-axis (Figure 3.3.4a). The two water molecules are centrosymmetrically related. The O(7) water molecule (Ag(4)-O(7) = 2.385(7) Å) completes the coordination sphere of the Ag(4) atom. In turn, this water molecule is strongly hydrogen bonded to the oxygen atoms of two pentafluoropropionates. The first H-bond between O(7) and the O(2) atom of a pentafluoropropionate is characterized by: O(2)- O(7): 2.741(1) Å; and O(7)-H···O(2):

167.3°. The second H-bond interaction takes place between the water molecule of a cluster and the $CF_3CF_2CO_2^-$ group in an adjacent coordination polymer (O(7)-O(2)#2: 2.818(1) Å; O(7)-H···O(2): 160.9°; symmetry code: #2: -x+1, -y, -z+2) (Table S2, Annexe V). Thus, this second H-bond linking polymeric chains gives rise to a two-dimensional coordination polymer parallel to the (001)-plane (Figure 3.3.4b).

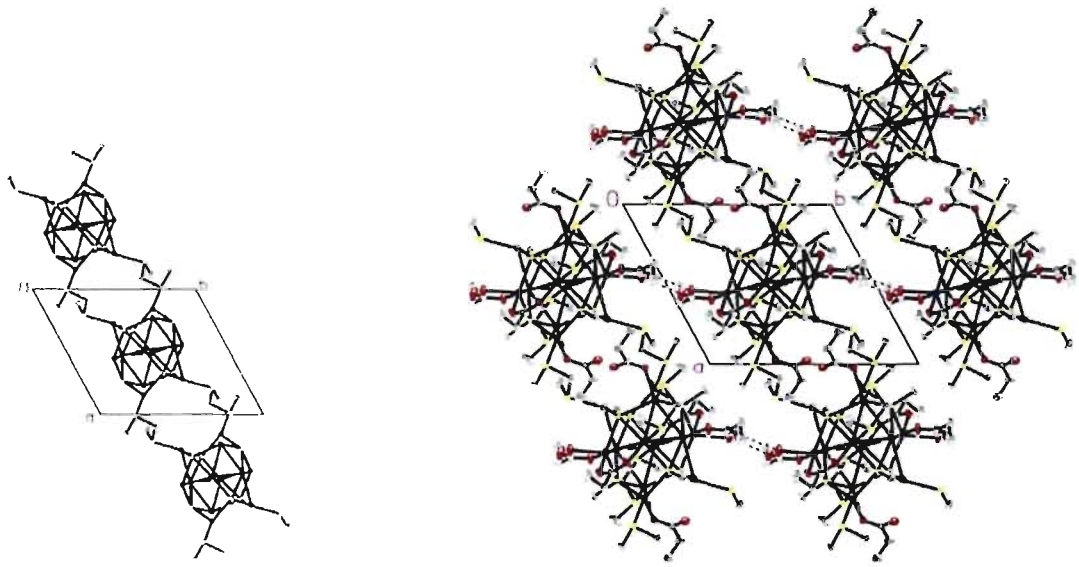

(a) (b)

Figure 3.3.4. Complex **2**. (a) The 1D-association of clusters resulting in chains parallel to the *a*-axis. (b) Disposition of the chains on the *ab*-plane showing the H-bonding and revealing the hexagonal environment of the clusters.

The Ag-S distances for the μ_4-SCH_3 unit range from 2.443(2) to 2.553(3) Å which are in the normal interval for $Ag_4(\mu_4\text{-SR})$ (2.577(5) - 2.690(5) Å).[34, 35, 37] The Ag-S separation (2.429(2)-2.691(3) Å) when the bis(methylthio)methane is coordinated to the Ag(I) ions compares well to those in the silver dithioether coordination polymers (2.434(2)-2.697(1) Å) (Table S3).[15, 36] It is of interest to note that there exist Cu(I) complexes whose structures are related to ours. The crystal structures of two Cu(I) complexes containing the $Cu_{12}S_6$ cluster and quadruply bridging zwitterionic thiolate ligands were reported by Prichard *et al.*[42] The similarities stop here as the $Cu_{12}S_6$ clusters, bridged to one another through Br or Cl atoms coordinated to Cu(I) atoms, form a 2-dimensional network.

Supramolecular isomerism and topology. We have just described two 1D-coordination polymers, **1** and **2**, which are topologically identical. Polymer **1** is a supramolecular polymorph of the 2D-coordination network $[AgL^{1\text{-}Me}(CF_3CO_2)]_\infty$. This latter complex is, in turn, topologically related to the heptafluorocarboxylate, $[AgL^{1\text{-}Me}(CF_3CF_2CF_2CO_2)]_\infty$ (Figure S3, Annexe V). The relationship between these four silver(I) complexes of bis(methylthio)methane and the three perfluorocarboxylate anions is summarized in Table 3.3.2. It was the attempt to synthesize the analogous pentafluropropionate that led to the discovery of complexes **1** and **2**. Attempts to synthesize the related heptafluorobutyrate incorporating the $Ag_{12}S_6$ cluster were unsuccessful.

Table 3.3.2. Summary of the structures observed for some complexes of silver(I) salts and bis(methylthio)methane.

Trifluoroacetate	Pentafluoropropionate	Heptafluorobutyrate
Clusters in 1D-coordination polymer		
$[Ag_6(CF_3CO_2)_3(L^{1\text{-}Me})_3(SCH_3)_3]_\infty$	$[Ag_6(CF_3CF_2CO_2)_3(L^{1\text{-}Me})_2(SCH_3)_3(H_2O)]_\infty$	not observed
2D-coordination network		
$[AgL^{1\text{-}Me}(CF_3CO_2)]_\infty$	not observed	$[AgL^{1\text{-}Me}(CF_3CF_2CF_2CO_2)]_\infty$

Comment on μ_4-SCH$_3$. The μ_4-SCH_3 entities bridging four adjacent silver(I) centers were observed in **1** and **2**. Each of those species comes from the C-S cleavage of the $CH_3SCH_2SCH_3$ organic building block, $\mathbf{L^{1\text{-}Me}}$. In addition, the GCMS of the $CH_3SCH_2SCH_3$ ligand, $\mathbf{L^{1\text{-}Me}}$, shows a mean peak at 108, which corresponds to the $\mathbf{L^{1\text{-}Me}}$, and another one at 61, that matches the $CH_3SCH_2^+$ entity. Hence, the GCMS shows the natural weakness of the C-S bond. The cleavage of dithiolates is not uncommon. For example, Jeannin *et al.* described the structure of the $[Fe_4(CO)_{12}(\mu_4\text{-}S)(\mu\text{-}SC_2H_5)_2]$ cluster obtained by the self-assembly process of $[Fe_3(CO)_{12}]$ and $CH_3\text{-}C{\equiv}C\text{-}SC_2H_5$.[35] The unsymmetrical $CH_3\text{-}C{\equiv}C\text{-}SC_2H_5$ building block undergoes a C-S cleavage during the synthesis of that complex. Prichard *et al.* indicated that zwitterionic ligands were a requisite for their $Cu_{12}S_6$ cluster to form.[42] However, this is not a requirement for the syntheses of

$Ag_{12}S_6$ clusters. That a cleavage is noted in two $\mathbf{L^{1\text{-}Me}}$ complexes is surprising, since there are many structures containing the dithiolate family of ligands, $\mathbf{L^{n\text{-}R}}$, but none involving the presence of a cluster. It could be that the small size of the ligand (**n** = 1 and **R** = Me) is the controlling factor. However, as **1** has a polymorph that does not contain a cluster, it is not clear how the same $\mathbf{L^{1\text{-}Me}}$ ligand is at times the subject of C-S cleavage while at others it retains its structure.

3.3.5 Conclusions

Unusual 1D-coordination polymers are observed in complexes of bis(methylthio)methane and silver(I) trifluoroacetate as well as silver(I) pentafluoropropionate. In both complexes, an $Ag_{12}S_6$ cluster is formed with a fragment of the ligands and the silver(I) centers. The clusters incorporate the $^{-}SCH_3$ anion, in a μ_4-SCH_3 coordination, which is obtained through the breakup of some of the ligand molecules.

The clusters are associated through the bis(methylthio)methane ligands in a double chain 1D-coordination polymer. The pentafluoropropionate complex incorporates silver-coordinated water molecules. These form hydrogen bonds that connect adjacent chains in a 2D-coordination network.

The cluster-containing complex is more difficult to synthesize than its polymorphic form. It is interesting to note that no cluster could be obtained with the longer heptafluorobutyrate. Although numerous complexes containing the $\mathbf{L^{n\text{-}R}}$ ligand (**n** = 1-10 and **R** = Me, Et, Ph, *t*Bu, Benz) have been reported, it is only with the smallest one, $\mathbf{L^{1\text{-}Me}}$, that clusters can be formed, albeit with difficulty.

Acknowledgement. This project was funded by the Natural Sciences and Engineering Research Council of Canada (F.B.). M.O.A. would like to thank the Agence Canadienne de Développement International (ACDI) and the Programme Canadien de Bourse de la Francophonie (PCBF) for a graduate scholarship.

Supplementary Material Available: X-ray crystallographic information files (CIF) for compounds **1**, and **2** and Figures S1-S3. Table of the silver-silver distances, the characteristics of the hydrogen bonds and selected bond distances and angles in **1** and **2**. This material is available free of charge via the Internet at http://pubs.acs.org

3.3.6 References

(1) Abrahams, B. F.; Hoskins, B. F.; Liu, J.; Robson, R. *J. Am. Chem. Soc.* **1991**, *113*, 3045.

(2) (a) Eddaoudi, M.; Moler, D. B.; Li, H.; Chen, B.; Reineke, T. M.; O'Keeffe, M. Yaghi, O. M. *Acc. Chem. Res.* **2001**, *34*, 319. (b) Rosi, N. L.; Eddaoudi, M.; Kim, J.; O'Keeffe, M.; Yaghi, O. M. *CrystEngComm.* **2002**, *4*, 401. (c) Yaghi, O. M.; O'Keeffe, M.; Ockwig, N. W.; Chae, H. K.; Eddaoudi, M.; Kim, J. *Nature* **2003**, *423*, 705. (d) Moulton, B.; Zaworotko, M. J. *Chem. Rev.* **2001**, *101*, 1629. (e) Ockwig, N. W.; Delgado-Friedrichs, O.; O'Keeffe, M.; Yaghi, O. M. *Acc. Chem. Res.* **2005**, *38*, 176. (f) Khlobystov, A. N.; Blake, A. J.; Champness, N. R.; Lemenovskii, D. A.; Majouga, A. G.; Zyk, N. V.; Schröder, M. *Coord. Chem. Rev.* **2001**, *222*, 155. (g) Swiegers, G. F.; Malefetse, T. J. *Chem. Rev.* **2000**, *100*, 3483.

(3) (a) Rowsell, J. L. C.; Eckert, J.; Yaghi, O. M. *J. Am. Chem. Soc.* **2005**, *127*, 14904. (b) Zheng, N.; Yassar, A.; Antoun, T.; Yaghi, O. M. *J. Am. Chem. Soc.* **2005**, *127*, 12752. (c) Rowsell, J. L. C.; Spencer, E.C.; Eckert, J.; Howard, J. A. K.; Yaghi, O. M. *Science* **2005**, *309*, 1350. (d) Rowsell, J. L. C.; Yaghi, O. M. *Ang. Chem. Int. Ed.* **2005**, *44*, 4670.

(4) (a) Jung, O. K.; Kim, Y. J.; Lee, Y. A.; Park, J. K.; Chae, H. K. *J. Am. Chem. Soc.* **2000**, *122*, 9921. (b) Jung, O. S.; Kim, Y. J.; Lee, Y. A.; Park, K. M.; Lee, S. S. *Inorg. Chem.* **2003**, *42*, 844. (c) Jung, O. S.; Kim, Y. J.; Lee, Y. A.; Chae, H. K.; Jang, H. G.; Hong, J. *Inorg. Chem.* **2001**, *40*, 2105. (d) Yaghi, O. M.; Li, H. *J. Am. Chem. Soc.* **1996**, *118*, 295. (e)Yaghi, O. M.; Li, H. *J. Am. Chem. Soc.* **1995**, *117*, 10401.

(5) (a) Han, H.; Song, Y.; Hou, H.; Fan, Y.; Zhu, Y. *J. Chem. Soc., Dalton Trans.* **2006**, 1972. (b) Li, L.; Yang, H.; Song, Y.; Hou, H.; Fan, Y. *Inorg. Chim. Acta* **2006**, *359*, 2135. (c) Anthony, S. P.; Radhakrishnan, T. P. *Cryst. Growth Des.* **2004**, *4*, 1223.

(6) (a) Batten, S. R.; Murray, K. S. *Coord. Chem. Rev.* **2003**, *246*, 103. (b) Guo, X.; Zhu, G.; Li, Z.; Chen, Y.; Li, X.; Qiu, S. *Inorg. Chem.* **2006**, *45*, 4065. (c) Lin, P.; Clegg, W.; Harrington, R. W.; Henderson, R. A.; Fletcher, A. J.; Bell, J.; Thomas, K. M. *Inorg. Chem.* **2006**, *45*, 4284.

(7) Reger, D. L.; Watson, R. P.; Gardinier, J. R.; Smith, M. D. *Inorg. Chem.* **2004**, *43*, 6609.

(8) (a) Withersby, M. A.; Blake, A. J.; Champness, N. R.; Cooke, P. A.; Hubberstey, P.; Li, W. S.; Schröder, M. *Inorg. Chem.* **1999**, *38*, 2259. (b) Blake, A. J.; Champness, N. R.;

Cooke, P. A.; Nicolson, J. E. B.; Wilson, C. *J. Chem. Soc., Dalton Trans.* **2000**, 3811. (c) Withersby, M. A.; Blake, A. J.; Champness, N. R.; Hubberstey, P.; Li, W. S.; Schröder, M. *Angew. Chem. Int. Ed.* **1997**, *36*, 2327. (d) Noro, S.; Kitaura, R.; Kondo, M.; Kitagawa, S.; Ishii, T.; Matsuzaka, H.; Yamashita, M. *J. Am. Chem. Soc.*, **2002**, *124*, 2568.

(9) Nomiya, K.; Yokoyama, H.; Noguchi, R.; Machida, K. *Chemistry Letters* **2002**, 922.

(10) Bu, X. H.; Chen, W.; Lu, S. L.; Zhang, R. H.; Liao, D. Z.; Bu, W. M.; Shionoya, M.; Brisse, F.; Ribas, J. *Angew. Chem. Int. Ed.* **2001**, *40*, 3201.

(11) Bu, X. H.; Chen, W.; Hou, W. F.; Du, M.; Zhang, R. H.; Brisse, F. *Inorg. Chem.* **2002**, *41*, 3477.

(12) Awaleh, M. O.; Badia, A.; Brisse, F. *Inorg. Chem.* **2005**, *44*, 7833.

(13) Awaleh, M. O.; Badia, A.; Brisse, F. *Cryst. Growth Des.* **2005**, *5*, 1897.

(14) Awaleh, M. O.; Badia, A.; Brisse, F.; Bu, X. H. *Inorg. Chem.* **2006**, *45*, 1560.

(15) Awaleh, M. O.; Badia, A.; Brisse, F. *Cryst. Growth Des.* **2006**, *6*, 2674.

(16) Awaleh, M. O.; Badia, A.; Brisse, F. *CrystEngComm.* **2007**, *submitted.*

(17) Awaleh, M. O.; Baril-Robert, F.; Reber, C., Badia, A.; Brisse, F. *Cryst. Growth Des.* **2007**, *Submitted.*

(18) Black, J. R.; Champness, N. R.; Levason, W.; Reid, G. *J. Chem. Soc., Chem. Comm.* **1995**, 1277.

(19) Black, J. R.; Champness, N. R.; Levason, W.; Reid, G. *J. Chem. Soc., Dalton Trans.* **1995**, 3439.

(20) Bu, X. H.; Hou, W. F.; Du, M.; Chen, W.; Zhang, R. H. *Cryst. Growth Des.* **2002**, *2*, 303.

(21) Pyykkö, P.; Zhao, Y. *Angew. Chem.* **1991**, *103*, 622.

(22) Sladek, A.; Schmidbaur, H. *Inorg. Chem.* **1996**, *35*, 3268 and references therein.

(23) Li, J.; Pyykkö, P. *Chem. Phys. Lett.* **1992**, *197*, 586.

(24) Schmidbaur, H. *Pure Appl. Chem.* **1993**, *65*, 691.

(25) Li, J.; Pyykkö, P. *Inorg. Chem.* **1993**, *32*, 2630.

(26) King, C.; Wang, J. C.; Khan, Md. N. I.; Flacker, J. P., Jr. *Inorg. Chem.* **1989**, *28*, 2145.

(27) Schmidbaur, H. *Chem. Soc. Rev.* **1995**, 391.

(28) Hartley, F. R.; Murray, S. G.; Levason, W.; Soutter, H. E.; McAuliffe, C. A. *Inorg. Chim. Acta* **1979**, *35*, 265.

(29) SAINT Release 6.06, Integration Software for Single Crystal Data; Bruker AXS Inc.: Madison, WI, 1999.

(30) Sheldrick, G.M. SADABS Bruker Area Detector Absorption Corrections; Bruker AXS Inc.: Madison, WI, 1996.

(31) XPREP Release 5.10; X-ray Data Preparation and Reciprocal Space Exploration Program. Bruker AXS Inc., Madison, WI, 1997.

(32) SHELXTL Release 5.10, The Complete Software Package for Single-Crystal Structure Determination; Brucker AXS Inc.: Madison, WI, 1997.

(33) (a) Sheldrick, G.M. SHELXS97, Program for the Solution of Crystal Structures; University of Göttingen: Göttingen, Germany, 1997. (b) Sheldrick, G.M. SHELXL97, Program for the Refinement of Crystal Structures; University of Göttingen: Göttingen, Germany, 1997.

(34) Su, W.; Cao, R.; Hong, M.; Chen, J.; Lu, J. *J. Chem. Soc., Chem. Comm.* **1998**, 1389.

(35) Jeannin, S.; Jeannin, Y.; Robert, F.; Rosenberger, C. *C. R. Acad. Sci. Paris.* **1992.** *Serie II t.314,* 1165.

(36) Silva, R. M.; Smith, M. D.; Gardinier, J. R. *Inorg. Chem.* **2006**, *45*, 2132.

(37) Wolf, T. E.; Berg, J. M.; Power, P. P.; Hodgson, K. O.; Holm, R. H. *Inorg. Chem.* **1980**, *19*, 430.

(38) Porterfield, W. W. *Inorganic Chemistry: A Unified Approach*, Addison-Wesley, 1994, p.168, 180

(39) Ahmed, L. S.; Dilworth, J. R.; Miller, J. R.; Wheatly, N. *Inorg. Chim. Acta* **1998**, *278*, 229 and references therein.

(40) Wang, Q. M.; Mak, T. C. W. *J. Am. Chem. Soc.* **2001**, *123*, 7594.

(41) Bosch, E.; Barnes, C. L. *Inorg. Chem.* **2002**, *41*, 2543.

(42) Prichard, R. G.; Parish, R. V.; Salehi, Z. *J. Chem. Soc., Dalton Trans.* **1999**, 243.

CHAPITRE 4. Réseaux de coordination élaborés avec des ligands dithiolatés $L^{n\text{-}Ph}$, n pair, et analyse thermogravimétrique.

4.1 Synthesis and characterization of silver(I) coordination networks bearing flexible thioethers: anion *versus* ligand dominated structures.[†]

4.1.1 Abstract

This report describes the synthesis and X-ray characterization of a series of $L^{n\text{-}Ph}AgX$ complexes wherein $L^{n\text{-}Ph}$ = $PhS(CH_2)_nSPh$ (n = 2, 4, 6, 10) and X = $CF_3SO_3^-$, CF_3COO^-, $CF_3CF_2COO^-$, $CF_3CF_2CF_2COO^-$, NO_3^- and ClO_4^-. This study was undertaken in order to rationalize the structure of the coordination networks formed as a function of the anion coordinating strength and the ligand structure. The following complexes were examined: with $L^{2\text{-}Ph}$, $CF_3SO_3^-$ (**1**), CF_3COO^- (**2**), ClO_4^- (**3**); $L^{4\text{-}Ph}$, $CF_3SO_3^-$ (**4**), CF_3COO^- (**5**), $CF_3CF_2COO^-$ (**6**), $CF_3CF_2CF_2COO^-$ (**7**); $L^{6\text{-}Ph}$, CF_3COO^- (**8**), $CF_3CF_2COO^-$ (**9**), $CF_3CF_2CF_2COO^-$ (**10**); and $L^{10\text{-}Ph}$, NO_3^- (**11**). The anions selected are classified in three groups of increasing coordinating strength: perchlorates, fluorosulfonates, and perfluorocarboxylates. Except in two cases, (**1** and **8**) all complexes form 2D-coordination networks. The 2D-network in **1** ($L^{2\text{-}Ph}$, $CF_3SO_3^-$) is made up of Ag(I) and $L^{2\text{-}Ph}$, while the anion is only a terminal co-ligand that completes the trigonal coordination around Ag(I). In **4** ($L^{4\text{-}Ph}$, $CF_3SO_3^-$), a 1D-coordination polymer, $[Ag\text{-}L^{4\text{-}Ph}\text{-}]_\infty$ is observed where the anions are coordinated to Ag(I) in a trigonal fashion. The perfluorocarboxylates form tetrameric units in a zigzag shape, but only with the $L^{4\text{-}Ph}$ ligand. In these (**6** and **7**), the silver-silver distances are very short, especially those of the central bond, indicating the presence of weak Ag-Ag interactions. Dimers, with short silver-silver distances, are observed with ligands $L^{2\text{-}Ph}$ and $L^{6\text{-}Ph}$ and perfluorocarboxylates. In **8**, ($L^{6\text{-}Ph}$, CF_3COO^- H_2O), a 3D channel-like structure is built through water molecules that connect adjacent layers. An unusual stoichiometry is noted in **3** ($L^{2\text{-}Ph}$, ClO_4^-, acetone); Ag:L is 4:2.5. In **11** ($L^{10\text{-}Ph}$ and NO_3^-), the nitrate acts as a bidentate ligand and an $[Ag\text{-}NO_3\text{-}]_\infty$ chain is formed. Adjacent chains are linked by the $L^{10\text{-}Ph}$ ligands into a 2D coordination network.

[†] Awaleh, M. O.; Badia, A.; Brisse, F, Bu, X. H. *Inorg. Chem.* **2006**, *45*, 1560-1574.

4.1.2 Introduction

The self-assembly of metal-organic coordination polymers is attracting great attention because of their potential as functional materials.[1] The properties of materials composed of coordination networks depend on their network topology. Thus, it is pertinent to understand and control the subtle factors that influence the formation of the supramolecular networks. However, in metal-organic crystal engineering, predicting the coordination polymer topology when flexible ligands are used is more difficult due to the numerous factors affecting the formation of the supramolecular framework. For a given metal and a specific set of ligands, these factors include the recrystallization solvent used,[2] the nature of the counteranions,[3] and the metal-to-ligand ratio.[4] On the other hand, the anion coordination chemistry is a promising area because of its application in anion template assembly, ion-pair recognition, and the role of anions in supramolecular chemistry.[5, 6] Besides their size and geometry, the coordinating ability of anions is also very important. An important question is whether the topology of a compound is determined primarily by the nature of the ligand or the coordinating character of the anion. To understand the influence of the anion, especially its coordinating ability, we have explored several anions of different size and coordination strength.[7] These may be classified as follows: spherical anions that are noncoordinating[8] or weakly coordinating (group 1: PF_6^-, SbF_6^-, ClO_4^-, BF_4^-), moderately coordinating sulfonate anions (group 2: *p*-TsO^-, $CF_3SO_3^-$), and coordinating perfluorocarboxylate anions (group 3: $CF_3CO_2^-$, $CF_3CF_2CO_2^-$, $CF_3CF_2CF_2CO_2^-$, $^-OOCCF_2CF_2COO^-$). The planar NO_3^- anion is in a class by itself as it is small in size but fairly coordinating and potentially bidentate.

The structures of previously reported networks were found to be influenced by the nature of the counteranion, the metal-to-ligand ratio, the length (size) of the ligand, as well as the recrystallization solvent.[4, 7] In a study of coordination networks based on bis(phenylthio)methane,[7a] 1D-coordination polymers were obtained regardless of the coordination strength of the anion. However, simple [Ag-ligand-]$_\infty$ chains were produced in the presence of weakly coordinating anions (BF_4^-, ClO_4^-). In these cases, the anions only complete the coordination sphere of Ag(I). When stronger anions were involved, three different double-stranded chains were noted, and both the anions and the ligands were involved in the formation of 1D-coordination polymers with Ag(I). A comparable distinction could be made with the slightly longer ligand, 1,3-bis(phenylthio)propane.[7b]

The noncoordinating anions of group 1 were observed as guests in the $(Ag\text{-ligand})_\infty$ layer structures. On the other hand, a variety of 2D-coordination networks that included all the structural units were observed for the medium and strongly coordinating anions of groups 2 and 3.

It has been noted on many occasions that chemically symmetrical molecules containing a central aliphatic segment with an even number of methylenes often have a crystallographic centre of symmetry in the middle of the central CH_2-CH_2 bond. For example, the free ligands $\mathbf{L}^{4\text{-Ph}}$, $\mathbf{L}^{6\text{-Ph}}$, $\mathbf{L}^{8\text{-Ph}}$, and $\mathbf{L}^{10\text{-Ph}}$, which all contain an aliphatic sequence with an even number of CH_2 groups, are in the fully extended conformation.[9] Thus, we have extended our previous work by investigating supramolecular networks based on diarylthioether spacers with an even number of carbon atoms in the aliphatic part. Herein, we report the synthesis and characterization of a number of silver coordination polymers obtained by varying the counteranion as well as the length of the spacer. We previously reported that perfluorocarboxylate anions formed supramolecular networks containing weak Ag-Ag interactions[7] with bis(phenylthio)methane and 1,3-bis(phenylthio)propane building blocks. This present study was thus undertaken in order to identify new supramolecular architectures involving silver-silver short interactions. The building blocks used are depicted in Scheme 1.

Scheme 1

$\mathbf{L}^{n\text{-Ph}}$ =

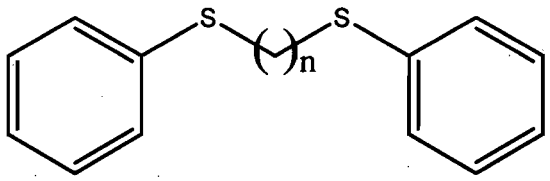

n = 2 : 1,2-bis(phenylthio)ethane ($\mathbf{L}^{2\text{-Ph}}$); n = 4 : 1,4-bis(phenylthio)butane ($\mathbf{L}^{4\text{-Ph}}$)
n = 6 : 1,6-bis(phenylthio)hexane ($\mathbf{L}^{6\text{-Ph}}$); n = 10 : 1,10-bis(phenylthio)decane ($\mathbf{L}^{10\text{-Ph}}$)

4.1.3 Experimental Section

Materials and General Methods. Except for the ligands, all of the reagents required for the syntheses were commercially available and employed without further purification. Elemental analyses were performed by the Laboratoire d'Analyse Élémentaire (Université

de Montréal). IR spectra were recorded on a Perkin-Elmer 1750 FTIR (4000-450 cm^{-1}) spectrometer with samples prepared as KBr pellets. ^1H (400 MHz and 300 MHz) and ^{19}F (376.31 MHz) solution NMR spectra were recorded on Bruker AV400 and AV300 spectrometers at 25 °C. ^1H chemical shifts are reported in parts per million and are referenced to residual solvent signals of the following deuterated solvents: DMSO (δ_{1H} = 2.50) and acetone (δ_{1H} = 2.05). The chemical shifts are referenced to $C_6H_5CF_3$ (-63.9 ppm) for ^{19}F.

Caution! Although we met no problems in handling perchlorate salts, great care should be taken due to their potentially explosive nature.

Syntheses. The ligands $\mathbf{L^{n\text{-}Ph}}$ (n = 2, 4, 6, 10) were synthesized according to the method previously reported in the literature,[10] and their characterizations are detailed in the Supporting information section.

$[Ag_2L^{2\text{-}Ph}(CF_3SO_3)_2]_\infty$ (1). To a solution of $AgCF_3SO_3$ (265 mg, 1.03 mmol) in acetone (5 mL) was added a solution of $\mathbf{L^{2\text{-}Ph}}$ (109 mg, 0.44 mmol) in diethyl ether (5 mL). The reaction mixture was refluxed at 50 °C for 90 min, then filtered while hot. The complex was recrystallized by diffusion a hot diethyl ether into the solution in a closed vessel stored in the dark. After a few days, single crystals suitable for X-ray analysis were obtained. Yield: 65% based on $AgCF_3SO_3$. Anal. Found: C, 25.61; H, 2.02. Calcd for $C_{16}H_{14}Ag_2F_6O_6S_4$: C, 25.28; H, 1.86. ^1H NMR (acetone-d_6, 300 MHz): δ 3.29 (*s*, 4H, -S-$(CH_2)_2$-S-), 7.41-7.63 (*m*, 10H, C_6H_5-). ^{19}F NMR (acetone-d_6, 376.31 MHz): δ -79.1. IR (KBr, cm^{-1}): 3442m, 3057w, 3003w, 2935w, 1611w, 1581m, 1510w, 1479m, 1428m, 1384w, 1254vs, 1178s, 1085w, 1070w, 1033s, 1000w, 906w, 829w, 769w, 735s, 715w, 690m, 652s, 643s, 577w, 517m, 488w, 477w.

$[Ag_2L^{2\text{-}Ph}(CF_3CO_2)_2]_\infty$ (2). The complex was synthesized in the same manner as **1** with $AgCF_3CO_2$ (232 mg, 1.05 mmol) and $\mathbf{L^{2\text{-}Ph}}$ (113 mg, 0.46 mmol). Yield: 40% based on $AgCF_3CO_2$. Anal. Found: C, 31.40; H, 2.29. Calcd for $C_{18}H_{14}Ag_2F_6O_4S_2$: C, 31.42; H, 2.05. ^1H NMR (acetone-d_6, 300 MHz): δ 3.31 (*s*, 4H, -S-$(CH_2)_2$-S-), 7.39-7.69 (*m*, 10H, C_6H_5-). ^{19}F NMR (acetone-d_6, 376.31 MHz): δ –74.1. IR (KBr, cm^{-1}): 3438m, 3077w, 3056w, 2935w, 1661vs, 1580m, 1479m, 1436m, 1384w, 1331w, 1209s, 1136s, 1086w, 1024m, 894w, 840m, 807m, 734s, 725m, 690m, 578w, 517w, 477w.

$[Ag_4(L^{2\text{-}Ph})_{2.5}(ClO_4)_4(CH_3COCH_3)_2]_\infty$ (3). The complex was synthesized in the same manner as **1** with $AgClO_4.H_2O$ (202 mg, 0.89 mmol) and $\mathbf{L^{2\text{-}Ph}}$ (80 mg, 0.32 mmol).

Yield: 71% based on $AgClO_4.H_2O$. Anal. Found: C, 31.10; H, 3.07. Calcd for $C_{41}H_{47}Ag_4Cl_4O_{18}S_5$: C, 31.54; H, 3.03. ^{1}H NMR (DMSO-d_6, 300 MHz): δ 3.41 (*s*, 4H, -S-$(CH_2)_2$-S-), 7.43-7.66 (*m*, 10H, C_6H_5-). IR (KBr, cm^{-1}): 3435m, 3056w, 1709m, 1687m, 1580m, 1479m, 1439m, 1363m, 1262w,1207w, 1091br, 1023s, 916m, 734s, 690s, 626s, 477m.

$[AgL^{4\text{-Ph}}(CF_3SO_3)]_\infty$ (4). A solution of $AgCF_3SO_3$ (241 mg, 0.94 mmol) and $L^{4\text{-Ph}}$ (134 mg, 0.49 mmol) in diethyl ether (20 mL) was kept under reflux at 60 °C for 90 min and then filtrate. Petroleum ether was slowly diffuse into the filtrate in the dark to obtain colourless single crystals suitable for X-ray analysis. Yield: 63% based on $AgCF_3SO_3$. Anal. Found: C, 38,46; H, 3.62. Calcd for $C_{17}H_{18}AgF_3O_3S_3$: C, 38.42; H, 3.41. ^{1}H NMR (acetone-d_6, 300 MHz): δ 1.94 (qt, 4H, -S-CH_2-$(CH_2)_2$- CH_2-S-), 3.21 (t, 4H, -S-CH_2-$(CH_2)_2$- CH_2-S-), 7.39-7.68 (*m*, 10H, C_6H_5-). ^{19}F NMR (acetone-d_6, 376.31 MHz): -79.1.

IR (KBr, cm^{-1}): 3468w, 3057w 2994w 2941w, 2926w, 2861w, 2346w, 1978w, 1955w, 1869w, 1803w, 1734w, 1579w, 1452m, 1480m, 1440m, 1417w, 1384w, 1315m, 1257vs, 1220s, 1204s, 1151s, 1167s, 1113m, 1094m, 1070m, 1028, 916w, 875w, 759w, 730m, 746s, 730m, 713w, 705w, 688s, 629s, 573w, 515m, 493m

$[Ag_2(L^{4\text{-Ph}})_{0.5}(CF_3CO_2)_2]_\infty$ (5). This complex was synthesized in the same manner as **4** with $AgCF_3CO_2$ (259 mg, 1.17 mmol) and $L^{4\text{-Ph}}$ (153 mg, 0.56 mmol). Yield: 38% based on $AgCF_3CO_2$. Anal. Found: C, 24.92; H, 1.65. Calcd for $C_{12}H_9Ag_2F_6O_4S_1$: C, 24.89; H, 1.57. ^{1}H NMR (acetone-d_6, 300 MHz): δ 1.87 (qt, 4H, -S-CH_2-$(CH_2)_2$-CH_2-S-), 3.16 (t, 4H, -S-CH_2-$(CH_2)_2$-CH_2-S-), 7.29-7.59 (*m*, 10H, C_6H_5-).

^{19}F NMR (acetone-d_6, 376.31 MHz): δ -74.2. IR (KBr, cm^{-1}): 3447m, 3057w, 2947w, 2927w, 2854w, 1685vs, 1586w, 1479m, 1437m, 1384w, 1312w, 1208vs, 1136s, 1094w, 1071w, 1023w, 893w, 840w, 804w, 731s, 702, 689m, 481w, 461w.

$[Ag_2L^{4\text{-Ph}}(CF_3CF_2CO_2)_2]_\infty$ (6). Complex **6** was synthesized in the same manner as **4** with $AgCF_3CF_2CO_2$ (270 mg, 0.99 mmol) and $L^{4\text{-Ph}}$ (209 mg, 0.76 mmol). Yield: 57% based on $AgCF_3CF_2CO_2$. Anal. Found: C, 32.19; H, 2.04. Calcd for $C_{22}H_{18}Ag_2F_{10}O_4S_2$: C, 32.37; H, 2.22. ^{1}H NMR (acetone-d_6, 300 MHz): δ 1.84 (qt, 4H, -S-CH_2-$(CH_2)_2$-CH_2-S-), 3.09 (t, 4H, -S-CH_2-$(CH_2)_2$-CH_2-S-), 7.26-7.48 (*m*, 10H, C_6H_5-). ^{19}F NMR (acetone-d_6, 376.31 MHz): δ -84.0 (CF_3), -119.3 (CF_3CF_2). IR (KBr, cm^{-1}): 3441w, 3074w, 2947w, 2928w 2854w, 1679s, 1480w, 1413m, 1330s, 1213s, 1071w, 1032s, 874w, 818s, 779m, 732s, 688m, 646w, 586m, 541m, 518w, 496w, 460w.

$[Ag_2L^{4\text{-}Ph}(CF_3CF_2CF_2CO_2)_2]_\infty$ (7). The complex was synthesized in the same manner as **4** with $AgCF_3CF_2CF_2CO_2$ (226 mg, 0.70 mmol) and $L^{4\text{-}Ph}$ (206 mg, 0.75 mmol). Yield: 67% based on $AgCF_3CF_2CF_2CO_2$. Anal. Found: C, 31.42; H, 2.38. Calcd for $C_{24}H_{18}S_2Ag_2F_{14}O_4$: C, 31.46; H, 1.98. ^{1}H NMR (acetone-d_6, 300 MHz): δ 1.85 (qt, 4H, -S-CH_2-$(CH_2)_2$-CH_2-S-), 3.12 (t, 4H, -S-CH_2-$(CH_2)_2$-CH_2-S-), 7.27-7.55 (*m*, 10H, C_6H_5-).

^{19}F NMR (acetone-d_6, 376.31 MHz): δ -81.9(CF_3), -116.7 ($CF_3CF_2CF_2$), -127.7 ($CF_3CF_2CF_2$). IR (KBr, cm^{-1}): 3422m, 2928m, 1667vs, 1481m, 1440m, 1407w, 1339m, 1223vs, 1156w, 1117m, 1079w, 1024w, 963m, 931m, 810m, 742m, 731m, 717m, 689m, 643w, 527w, 482w.

$\{[Ag_2L^{6\text{-}Ph}(CF_3CO_2)_2.H_2O].H_2O\}_\infty$ (8). A 5 mL portion of chloroform was added to 124 mg (0.41 mmol) of $L^{6\text{-}Ph}$. To this mixture was added a solution of $AgCF_3CO_2$ (217 mg, 0.98 mmol) in acetone (5 mL). It was then refluxed at 60 °C for 140 min. The resulting solution was layered on diethyl ether and then stored at room temperature in the dark. Several days later, colorless crystals appeared. Yield: 35 % based on $AgCF_3CO_2$. Found: C, 33.84; H, 3.63. Calcd for $C_{22}H_{26}Ag_2F_6O_6S_2$: C, 33.86; H, 3.36. ^{1}H NMR (acetone-d_6, 400 MHz): δ 1.47 (qt, 4H, -S-$(CH_2)_2$-$(CH_2)_2$-$(CH_2)_2$-S-), 1.65 (qt, 4H, -S-CH_2-CH_2-$(CH_2)_2$-CH_2-CH_2-S-), 3.01 (t, 4H, -S-CH_2-$(CH_2)_4$-CH_2-S-), 7.18-7.42 (*m*, 10H, C_6H_5-).

^{19}F NMR (acetone-d_6, 376.31 MHz): -74.2. IR (KBr, cm^{-1}): 3450br, 3055w, 2934w, 1684vs, 1580w, 1478w, 1436m, 1383w, 1207s, 1136s, 1086w, 1024m, 841m, 804m, 735s, 690m, 477w.

$[Ag_2L^{6\text{-}Ph}(CF_3CF_2CO_2)_2]_\infty$ (9). The complex was synthesized in the same manner as **8** with $AgCF_3CF_2CO_2$ (231 mg, 0.85 mmol) and $L^{6\text{-}Ph}$ (156 mg, 0.52 mmol). Yield: 68% based on $AgCF_3CF_2CO_2$. Anal. Found: C, 33.98; H, 2.67. Calcd for $C_{24}H_{22}Ag_2F_{10}O_4S_2$: C, 34.14; H, 2.63. ^{1}H NMR (acetone-d_6, 400 MHz): δ 1.47 (qt, 4H, -S-$(CH_2)_2$-$(CH_2)_2$-$CCH_2)_2$-S-), 1.65 (qt, 4H, -S-CH_2-CH_2-$(CH_2)_2$-CH_2-CH_2-S-), 3.03 (t, 4H, -S-CH_2-$(CH_2)_4$-CH_2-S-), 7.14-7.34 (*m*, 10H, C_6H_5-). ^{19}F NMR (acetone-d_6, 376.31 MHz): -84.0 (CF_3), -119.4 (CF_3CF_2). IR (KBr, cm^{-1}): 3459m, 3058w, 2943w, 2924m, 2853w, 1682vs, 1584w, 1480m, 1458w, 1438w, 1411m, 1320s, 1214s, 1164vs, 1091w, 1070w, 1030s, 893w, 820m, 780w, 732s, 703w, 689m, 587w, 540w, 480w.

$[Ag(L^{6\text{-}Ph})_{0.5}(CF_3CF_2CF_2CO_2)]_\infty$ (10). The complex was synthesized in the same manner as **8** but using $AgCF_3CF_2CF_2CO_2$ (265 mg, 0.83 mmol) and $L^{6\text{-}Ph}$ (198 mg, 0.65 mmol). Yield: 79% based on $AgCF_3CF_2CF_2CO_2$. Anal. Found: C, 33.04; H, 2.62. Calcd for

$C_{13}H_{11}AgF_7O_2S$: C, 33.07; H, 2.35. ^{1}H NMR (acetone-d_6, 400 MHz): δ 1.48 (qt, 4H, -S-$(CH_2)_2$-$(CH_2)_2$-$(CH_2)_2$-S-), 1.69 (qt, 4H, -S-CH_2-CH_2-$(CH_2)_2$-CH_2-CH_2-S-), 3.02 (t, 4H, -S-CH_2-$(CH_2)_4$-CH_2-S-), 7.17-7.36 (*m*, 10H, C_6H_5-).

^{19}F NMR (acetone-d_6, 376.31 MHz): -81.9 (CF_3), -116.6 ($CF_3CF_2CF_2$), -127.8 ($CF_3CF_2CF_2$). IR (KBr, cm^{-1}): 3446m, 3058w, 2944w, 2925w, 2854w, 1683vs, 1584w, 1481m, 1458w, 1439w, 1407m, 1339m, 1221s, 1159w, 1118m, 1084m, 1023w, 968m, 933m, 812m, 741m, 731s, 720w, 688m, 649w, 593w, 527w, 481w.

$[AgL^{10\text{-}Ph}(NO_3)]_\infty$ (11). To a solution of $AgNO_3$ (252 mg, 1.48 mmol) in methanol (5 mL) was added a solution of $L^{10\text{-}Ph}$ (361 mg, 1.01 mmol) in diethyl ether (5 mL). The mixture was refluxed at 50 °C for 120 min and then filtered. After cooling, the filtrate was recrystallized by diffusion of diethyl ether into the solution at room temperature and kept in the dark. After a few days crystals suitable for X-ray analysis were deposited. Yield: 65% based on $AgNO_3$. Anal. Found: C, 49.92; H, 5.43; N, 2.43. Calcd for $C_{22}H_{30}AgNO_3S_2$: C, 50.00; H, 5.72; N, 2.65.. ^{1}H NMR (acetone-d_6, 400 MHz): δ 1.31 (*m*, 8H, -S-$(CH_2)_3$-$(CH_2)_4$-$(CH_2)_3$-S-), 1.47 (qt, 4H, -S-$(CH_2)_2$-CH_2-$(CH_2)_4$-CH_2-$(CH_2)_2$-S-), 1.61 (qt, 4H, -S-CH_2-CH_2-$(CH_2)_6$-CH_2-CH_2-S-), 3.01 (t, 4H, -S-CH_2-$(CH_2)_8$-CH_2-S-), 7.18-7.40 (m, 10H, C_6H_5-). IR (KBr, cm^{-1}): 3435m, 2922s, 2851s, 1749w, 1630w, 1581w, 1480m, 1465m, 1438m, 1384s, 1352vs, 1333s, 1232w, 1155w, 1084w, 1067w, 1037w, 1025w, 998w, 892w, 881w, 764w, 743m, 733s, 687s, 498w, 477w, 465w.

X-Ray crystallography. Crystal Structure Determinations. X-ray diffracted intensities were measured on a Bruker AXS Platform diffractometer equipped with a SMART 2K CCD area detector using monochromatic Cu Kα (λ = 1.54178 Å) radiation. The X-ray intensity data were processed with the program SAINT.[11] An empirical absorption correction, based on multiple measurements of equivalent reflections, was applied using the program SADABS.[12] The space group was confirmed by the XPREP[13] routine in the program SHELXTL.[14] The structures were solved by direct-methods and refined by full-matrix least squares and difference Fourier techniques.[15]

All non-hydrogen atoms were refined anisotropically, while the hydrogen atoms were introduced at calculated positions using a riding model and refined isotropically.

In complex 7, one heptafluorobutyrate anion was found to be disordered. This anion was split over two sites with occupancies of 67 and 33%. The C-F and C-C distances in the major and minor entities of this anion were constrained to be equal (SADI[15]). The thermal

parameters of all disordered atoms were constrained such that the corresponding atoms of the major and the minor entities kept the same values (EADP[15]).

The trifluoro group of **8** was found to be in four different orientations in the ratio 38/28/20/14. The C-F distances were constrained to be equal, while the thermal parameters were constrained such that they kept the same values in each orientation. In addition, the OW(4) water molecule is split over two centrosymmetrically related nearby sites. The thermal parameters of the phenyl group of $\mathbf{L^{6\text{-}Ph}}$ in complex **10** were found to be high because of disorder. Thus, the thermal displacement parameters of the phenyl group were restrained to be equal within an effective standard deviation and to not deviate much from a spherical shape (use of the DELU[15] and ISOR[15] instructions). Crystal data and data collection parameters are listed in Table 4.1.1.

Table 4.1.1. Crystal data and X-ray data collection parameters.

	1	2	3	4	5
Formula	$C_{16}H_{14}Ag_2F_6O_6S_6$	$C_{18}H_{14}Ag_2F_6O_4S_2$	$C_{41}H_{47}Ag_4Cl_4O_{18}S_5$	$C_{17}H_{18}AgF_3O_3S_3$	$C_{12}H_9Ag_2F_6O_4S$
mol wt	760.25	688.15	1561.37	531.36	578.99
cryst size (mm)	0.27 × 0.11 × 0.07	0.25 × 0.14 × 0.10	0.24 × 0.06 × 0.05	0.34 × 0.17 × 0.13	0.25 × 0.11 × 0.07
cryst system	Monoclinic	Monoclinic	Triclinic	Triclinic	Monoclinic
space group	$P2_1/c$	$C2/c$	P-1	P-1	$P2_1/c$
a (Å)	8.3209(1)	30.2872(3)	13.2480(2)	9.7996(2)	13.1732(2)
b (Å)	10.8072(1)	8.8790(1)	14.2262(2)	10.1521(2)	13.8286(2)
c (Å)	25.6612(3)	18.0509(2)	14.7858(3)	11.7852(2)	8.7495(1)
α (deg)	90	90	92.851(1)	78.469(1)	90
β (deg)	96.494(1)	120.43	101.993	66.297(1)	92.608(1)
γ (deg)	90	90	101.449	68.346(1)	90
volume (Å^3)	2292.79(4)	4185.74(8)	2659.54(8)	995.97(3)	1592.22(4)
Z	4	8	2	2	4
D(calc) (g cm^{-3})	2.202	2.184	1.950	1.772	2.415
F(000)	1480	2672	1546	532	1108
Temp (K)	100(2)	100(2)	100(2)	220(2)	220(2)
μ, (mm^{-1})	17.882	17.616	15.927	11.457	21.771
θ_{max} (deg)	72.64°	72.79°	72.88	72.80°	72.92°
R1[a] [$I > 2\sigma(I)$]	0.0257	0.0457	0.0417	0.0320	0.0385
Rw[b] [$I > 2\sigma(I)$]	0.0630	0.1225	0.1011	0.0843	0.1020
R [*all data*]	0.0295	0.0468	0.0501	0.0352	0.0432
Rw [*all data*]	0.0641	0.1236	0.1041	0.0892	0.1048
S[c]	1.003	1.130	1.000	1.078	1.000

	6	7	8	9	10
Formula	$C_{22}H_{18}Ag_2F_{10}O_4S_2$	$C_{24}H_{18}Ag_2F_{14}O_4S_2$	$C_{22}H_{22}Ag_2F_6O_4S_2.(H_2O)_2$	$C_{24}H_{22}Ag_2F_{10}O_4S_2$	$C_{13}H_{11}AgF_3O_2S$
mol wt	816.22	916.24	780.29	844.28	472.15
cryst size (mm)	0.25 × 0.12 × 0.09	0.22 × 0.15 × 0.06	0.23 × 0.16 × 0.06	0.43 × 0.09 × 0.07	0.13 × 0.07 × 0.02
cryst system	Triclinic	Triclinic	Monoclinic	Triclinic	Triclinic
space group	P-1	P-1	$C2/c$	P-1	P-1
a (Å)	9.7118(5)	9.5464(1)	19.1312(2)	10.2786(1)	5.0167(3)
b (Å)	11.3140(6)	11.2508(2)	17.8749(2)	13.0241(1)	12.0797(5)
c (Å)	14.0734(6)	14.8801(2)	8.8084(1)	13.3040(1)	13.1304(5)
α (deg)	111.128(3)	88.094(1)	90	116.366(1)	95.093(3)
β (deg)	91.177(3)	81.725(1)	117.088(1)	111.193(1)	91.816(3)
γ (deg)	107.772(3)	70.387(1)	90	92.934(1)	98.354(3)
volume (Å^3)	1358.67(12)	1489.60(4)	2681.78(5)	1439.23(2)	783.35(6)
Z	2	2	4	2	2
D(calc) (g cm^{-3})	1.995	2.043	1.933	1.948	2.002
F(000)	796	892	1544	828	462
Temp (K)	220(2)	100 (2)	100 (2)	100(2)	100(2)
μ, (mm^{-1})	13.914	12.983	13.893	13.161	1.500
θ_{max} (deg)	73.08°	72.96°	72.83	72.97	26.12
R1[a] [$I > 2\sigma(I)$]	0.0450	0.0535	0.0372	0.0359	0.0455
Rw[b] [$I > 2\sigma(I)$]	0.1144	0.1408	0.1013	0.0936	0.1135
R [*all data*]	0.0569	0.0598	0.0384	0.0370	0.0481
Rw [*all data*]	0.1280	0.1447	0.1028	0.0945	0.1157
S[c]	0.973	1.033	1.042	1.044	1.038

	11
Formula	$C_{22}H_{30}AgNO_3S_2$
mol wt	528.46
cryst size (mm)	0.12 × 0.08 × 0.04
cryst system	Monoclinic
space group	$P2_1/n$
a (Å)	5.5556(1)
b (Å)	18.6523(4)
c (Å)	21.9144(5)
α (deg)	90
β (deg)	90.723(2)
γ (deg)	90
volume (Å^3)	2270.69(8)
Z	4
D(calc) (g cm^{-3})	1.546
F(000)	1088
Temp (K)	100(2)
μ, (mm^{-1})	9.023
θ_{max} (deg)	72.81
R1[a] [$I > 2\sigma(I)$]	0.0454
Rw[b] [$I > 2\sigma(I)$]	0.1114
R [*all data*]	0.0575
Rw [*all data*]	0.1156
S[c]	0.971

[a] $R = \Sigma \, || F_o | - | F_c || / \Sigma \, | F_o |$. [b] $R_w = [\Sigma \, w(F_o^2 - F_c^2)^2 / \Sigma \, w(F_o^2)^2]^{1/2}$.
[c] $S = [\Sigma \, w(F_o^2 - F_c^2)^2 / (m-n)]^{1/2}$ (m is the number of reflections and n the number of parameters).

Table 4.1.2. Comparison of the bond distances (Å) describing the coordination of the silver atoms in complexes **1-11**.

1	Ag(1)–S: 2.482(1), 2.511(1), Ag(1)–O: 2.385(2); Ag(2)-S: 2.493(1), 2.526(1), Ag(2)-O: 2.372(2)
2	Ag(1)–S: 2.495(1), 2.834(1); Ag(1)–O: 2.279(3), 2.304(2); Ag(1)···Ag(1): 3.0813(5); Ag(2)–S: 2.498(1), 2.920(1); Ag(2)–O: 2.242(3), 2.304(3); Ag(2)···Ag(2): 3.3813(6).
3	Ag(1)–S: 2.625(1), 2.636(1), 2.642(1), 2.658(1); Ag(2)–S: 2.493(1), 2.507(1); Ag(2)-O: 2.549(4); Ag(3)–S: 2.493(1), 2.509 (1); Ag(3)–O: 2.538(4), 2.586(4) Ag(4)–O: 2.302(3), 2.350(4); Ag(4)–O: 2.476(4); Ag(4)–S: 2.452(1).
4	Ag–S: 2.475(1), 2.502(1); Ag–O: 2.323(2).
5	Ag(1)–S: 2.528(1), 2.589(1); Ag(1)–O: 2.346(3); Ag(1)···Ag(2): 3.3212(6); Ag(2)–O: 2.234(3), 2.271(3), 2.485(3); Ag(2)···Ag(2): 3.1688(7).
6	Ag(1)–S: 2.697(1); Ag(1)–O: 2.247(4), 2.334(4), 2.419(4); Ag(1)···Ag(2): 3.1048(6); Ag(1)···Ag(1): 2.9137(8). Ag(2)–O: 2.291(4); Ag(2)···Ag(1): 3.1048(6).
7	Ag(1)–S: 2.654(2); Ag(1)···Ag(1): 2.8669(9) Å); Ag(1)···Ag(2): 3.1594(6); Ag(1)–O: 2.268 (4), 2.359(4), 2.372(4); Ag(2)–O: 2.313(4); Ag(2)–S: 2.464(2), 2.525 (2); 3.050(2); Ag(2)···Ag(1): 3.1594(6).
8	Ag–S: 2.534(1), 2.576(1); Ag–O: 2.496(4), Ag–OW(3): 2.417(2).
9	Ag(1)–O: 2.340(2), 2.352(2), 2.418(2); Ag(1)–S: 2.536(1); Ag(1)···Ag(1): 3.0052(4); Ag(2)–O: 2.419(2), 2.558(2); Ag(2)–S: 2.510(1), 2.549(1).
10	Ag–O: 2.256(3), 2.284(3); Ag–S: 2.644(1), 2.872(1); Ag···Ag: 2.9730(5).
11	Ag–O: 2.461(3), 2.491(3); Ag–S: 2.494(1), 2.512(1).

4.1.4 Results

Crystal Structures. The bond distances describing the coordination of the silver atoms in complexes **1-11** are compared in Table 4.1.2.

$[Ag_2L^{2\text{-Ph}}(CF_3SO_3)_2]_\infty$ **(1)**. The repeat unit of **1** consists of a 14-membered $Ag_4(L^{2\text{-Ph}})_2S_2$ macrocycle (Figure 4.1.1a). There are two crystallographically distinct silver atoms with comparable environments in the macrocycle. These silver atoms, Ag(1) and Ag(2), are associated via a μ_2-S bridge formed by the ligand, resulting in a polygonal mesh parallel to the (001)-plane (Figure 4.1.1b). The triflate is only a terminal co-ligand which completes the coordination sphere of the silver atoms (Figure 4.1.1a). The triflate, as well as the phenyl groups, are located on both sides of the corrugated layer (Figure 4.1.1c). Each silver atom, linked to two sulfur atoms from distinct ligands and to an oxygen from the triflate, adopts a distorted trigonal environment. The sum of the bond angles around Ag(1) and Ag(2) are 359.4 and 360.0°, respectively. In this complex, the 1,2-bis(phenylthio)ethane ligand is in the same trans conformation, S-C-C-S: -178.6(2)°, as the free ligand.[9a] In addition, the S···S distance in the ligand is 4.342(1) Å, which is equivalent to that of the free ligand 4.4312(7) Å.[9a]

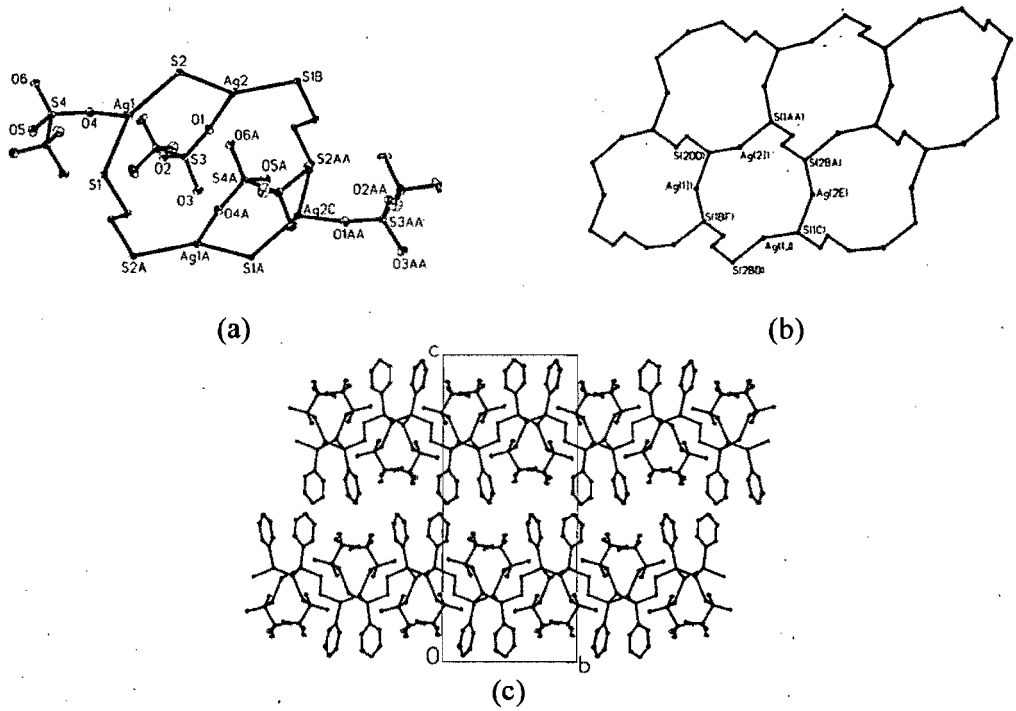

Figure 4.1.1. (a) The repeat unit of complex **1**, $Ag_4(L^{2\text{-Ph}})_2S_2$. The 2D-network of **1** parallel to the (001)-plane (the phenyl groups and the hydrogen atoms are omitted for clarity). (c) In this packing of **1,** the layers are shown edge-on.

$[Ag_2L^{2\text{-}Ph}(CF_3CO_2)_2]_\infty$ (**2**). Complex **2**, containing the trifluoroacetate anion, has two kinds of silver atoms: Ag(1) and Ag(2). Adjacent silver atoms of the same species are joined in a bridging fashion by two trifluoroacetate groups, thus giving rise to $(Ag(1)O_2CCF_3)_2$ and $(Ag(2)O_2CCF_3)_2$ dimers which are identical to those found in the structure of the trifluoroacetate silver salt[16] (Scheme 2b and Figure S1, Annexe VI).

Scheme 2. Different coordination modes of the perfluorocarboxylate anions.

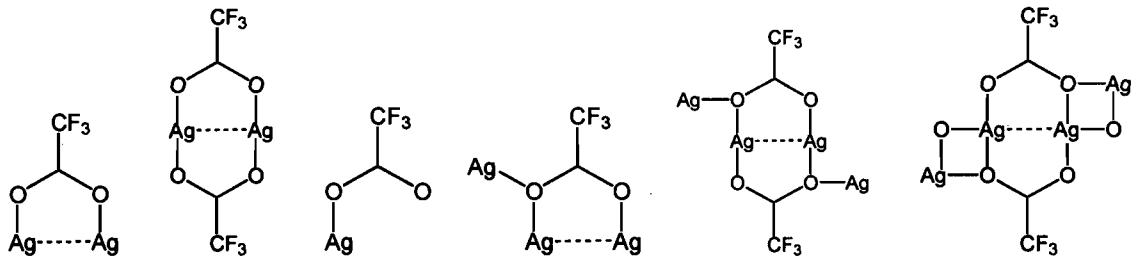

Two consecutive dimers are connected, via a μ_2-S bridge, by $L^{2\text{-}Ph}$ building blocks, thus generating a 2-D coordination network (Figure S2, Annexe VI). The repeat unit of this complex is a 10-membered $Ag_2(L^{2\text{-}Ph})_2$ metallomacrocycle (Figure 4.1.2a and Figure S3a, Annexe VI). The repeat units share their ligand edges and, in doing so, give rise to a ribbon parallel to the *b*-axis (Figure S3b, Annexe VI). The ribbons are interconnected by silver-silver interactions, 3.0813(5) Å, of the $(Ag(1)O_2CCF_3)_2$ dimers so as to form a 2D-coordination network parallel to the *bc*-plane (Figure 4.1.2c and Figure S5, Annexe VI).

In another description of the structure, there are two distinct repeat units in this complex, unit **A** and unit **B**.

In unit **A**, two silver atoms are linked by two ligands in order to form a 10-membered $Ag_2(L^{2\text{-}Ph})_2$ metallomacrocycle (Figure 2a and Figure S3a, Annexe VI). The **A** units share their ligand edges, thus forming a ribbon parallel to the *b*-axis (Figure S3b, Annexe VI). The **B** unit is formed by 10-membered Ag_6S_4 metallomacrocycles (Figure 4.1.2b and Figure S4a, Annexe VI). The units also share Ag···Ag edges in order to form a ribbon (Figure S4b, Annexe VI). Alternating **A** and **B** ribbons share their silver and their sulfur atoms, resulting in a 2D-neutral sheet perpendicular to the *a*-axis (Figure 4.1.2c and Figure S5, Annexe VI).

Each Ag(1) is linked to the sulfur atoms of two ligands, to two oxygen atoms from distinct trifluoroacetate groups, and to another silver atom producing a very distorted trigonal bipyramid. The other silver atom, Ag(2), has a tetrahedral coordination. It is surrounded by the sulfur atom of two ligands, and is linked to two oxygen atoms from different trifluoroacetate groups. The Ag(2)···Ag(2) contact distance is 3.3813(6) Å, a distance slightly shorter than the sum of the van der Waals radius of two silver atoms, 3.44 Å.[17] The two Ag-S distances, 2.834(1) and 2.920(1) Å, are slightly longer than the "normal" silver-thiol distance. Such longer Ag–S distances are not unusual in Ag(I) complexes where the thiol is linked to adjacent silver atoms via a μ_2-S bridge. For example, Ag–S bonds of 2.912 (5) and 2.959(5) Å are reported for the mercaptopyridine[18] and 2.936(2) Å in $[Ag_2(hfpd)_2([14]aneS_4)]_\infty$,[19] and 2.886 (1) Å for the S, S'-bis(8-quinolyl)-4-oxa-1,7-dithiaheptane(OETQ).[20]

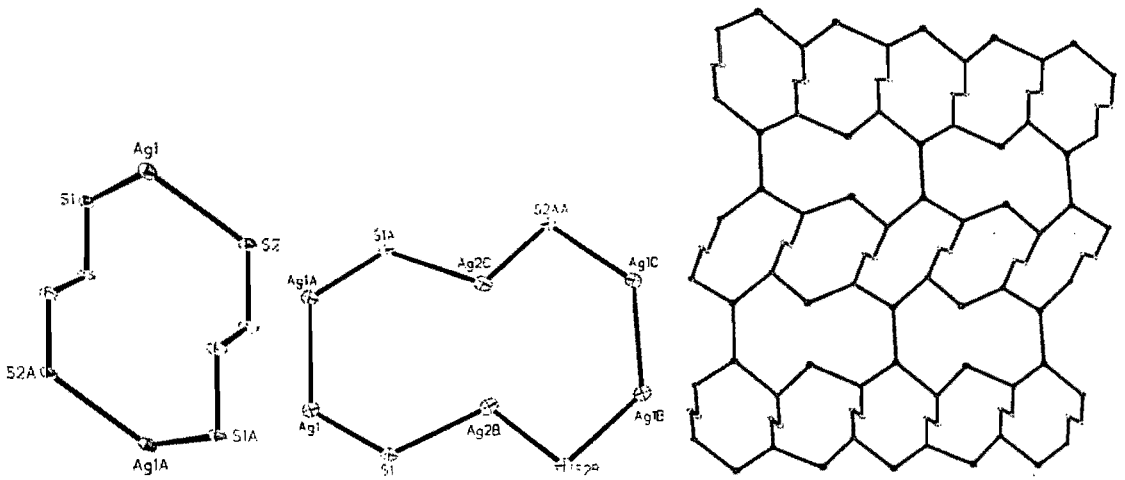

(a) (b) (c)

Figure 4.1.2. (a) The **A** repeat unit of complex **2**, $Ag_2(\mathbf{L}^{2\text{-Ph}})_2$. (b) The **B** repeat unit, Ag_6S_4. (c) The **A** units share their ligand edges forming a ribbon parallel to the *b*-axis. The **B** units share their Ag-Ag edges, giving rise to a ribbon alongside the *b*-axis. Neighbouring **A** and **B** ribbons share their silvers as well as their sulfur atoms, resulting in a neutral 2D-network parallel to (100)-plane. The phenyl groups, the trifluoroacetate groups and the hydrogen atoms are omitted for clarity.

$[Ag_4(\mathbf{L}^{2\text{-Ph}})_{2.5}(ClO_4)_4(CH_3COCH_3)_2]_\infty$ (3). In this complex, there are four types of silver atoms, Ag(1), Ag(2), Ag(3) and Ag(4), four perchlorate groups, and the ligand which is present in both the cis and the trans conformations. Two ligands in the cis-conformation are connected to the Ag(1) silver atom in a chelating mode so as to form $Ag(\mathbf{L}^{2\text{-Ph}})_2$

(Ag(1)($\mathbf{L}^{2\text{-Ph}}$)$_2$) metallomacrocycles. Each of the ligands' sulfur atoms are also bound to either Ag(2) or Ag(3). In doing so, chains of alternating $Ag(1)_2Ag(2)_2S_4$ and $Ag(1)_2Ag(3)_2S_4$ metallomacrocycles extending along the *c*-axis are obtained (Figure 4.1.3).

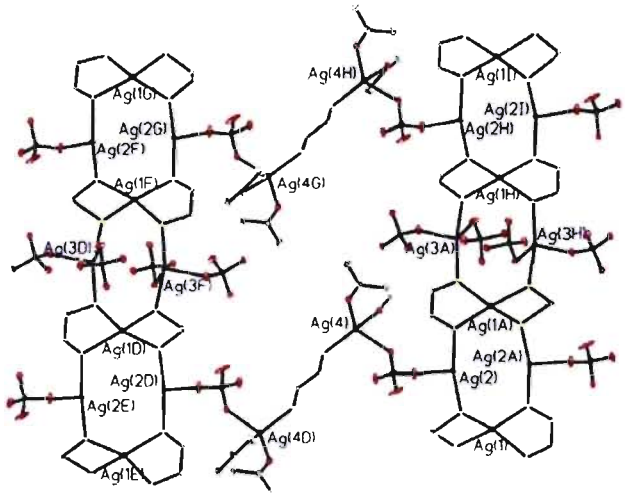

Figure 4.1.3. The four different silver atoms in **3**. The $Ag_4(\mathbf{L}^{2\text{-Ph}})_4$ rings are interconnected and build a double-chain parallel to the *c*-axis. Adjacent double-chains form a 2D-coordination network through linkage with the ligand *via* the perchlorate anions. The resulting network is parallel to the (220)-plane. The phenyl groups and the hydrogen atoms are omitted for clarity.

Two perchlorates complete the tetrahedral coordination of the Ag(3) atoms, while the coordination of Ag(2) is trigonal, with only one perchlorate group present. The chains, which run parallel to the *c*-axis, are associated in a 2D-coordination network with the help of the ligand in its trans conformation. The ligand thus binds two centrosymetrically related Ag(4) atoms themselves bound to the oxygen of a perchlorate which, in turn, is coordinated to Ag(2). The other two ligands that complete the tetrahedral coordination of Ag(4) are the oxygen atoms of two acetone molecules. In other words, this perchlorate bridges Ag(2) and Ag(4) in a μ-O,O'coordination mode. A 2D-network parallel to the (220)-plane is thus generated (Figure 4.1.3).

In terms of coordination, Ag(1) is connected to four sulfur atoms from two distinct ligands forming a distorted tetrahedral environment. Ag(2) is surrounded by three atoms in a trigonal arrangement: two sulfur atoms from different ligands and the oxygen atom of a perchlorate. This coordination is very distorted since the angles deviate strongly from 120°; S–Ag(2)–S,: 153.7(1); S–Ag(2)–O, 102.1(1) and 99.6(1)°; Σ_{Ag} = 355.4°. Ag(3) is

tetrahedrally surrounded by two sulfur atoms from different ligands and by two oxygen atoms from distinct perchlorates. Finally, Ag(4) is surrounded by two oxygen atoms from acetone molecules, the oxygen atom from a perchlorate, and the sulfur atom from a ligand yielding a distorted tetrahedral coordination.

$[AgL^{4\text{-}Ph}(CF_3SO_3)]_\infty$ (4). In its crystal structure, **4** forms a 1D-coordination polymer extending parallel to the [210]-direction. The succession of Ag(I) ions and ligands generates a zigzag [Ag-ligand-]$_\infty$ chain. The trigonal coordination of Ag(I) is completed by a trifluoromethanesulfonate anion. The sum of the bond angles around silver is 359.9°.

This 1D-chain can be considered as having a Y-shaped topology (Figure 4.1.4). From a crystallographic point of view, the silver atom is bound to two half ligands, the other half being generated by a crystallographic center of symmetry. Hence, there are two S···S separations with respective values of 6.944(1) and 6.915(1) Å.

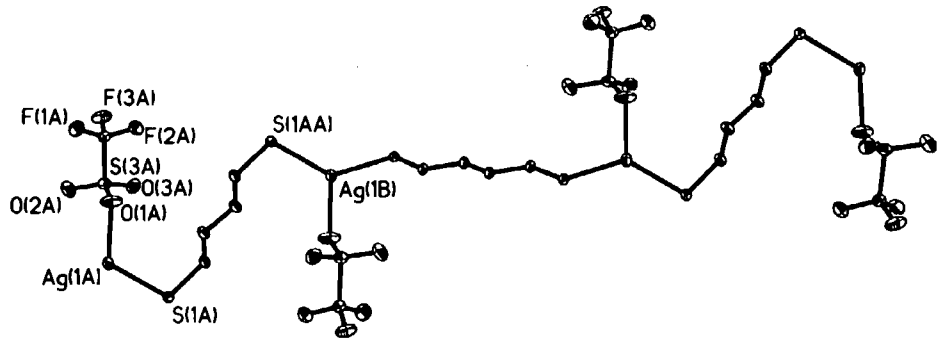

Figure 4.1.4. 1D-coordination polymer of **4** extending alongside the [210]-direction. The anion is coordinated to the silver atoms. The phenyl groups and the hydrogen atoms are omitted for clarity.

Perfluorocarboxylates of $L^{4\text{-}Ph}$. The three perfluororocarboxylates, **$[Ag_2(L^{4\text{-}Ph})_{0.5}(CF_3CO_2)_2]_\infty$ (5)**, **$[Ag_2L^{4\text{-}Ph}(CF_3CF_2CO_2)_2]_\infty$ (6)**, and **$[Ag_2L^{4\text{-}Ph}(CF_3CF_2CF_2CO_2)_2]_\infty$ (7)**, are grouped under this heading since it was observed that for the complexes with the 1,3-bis(phenylthio)propane ligand, increasing the length of the anion influenced the type of network adopted.[7b] Interestingly, the complexes all form centrosymmetric tetrameric units, although **5** has an Ag:L stoichiometry of 4:1 while both **6** and **7** have a 2:1 stoichiometry. The tetrameric units are compared in Figure 4.1.5.

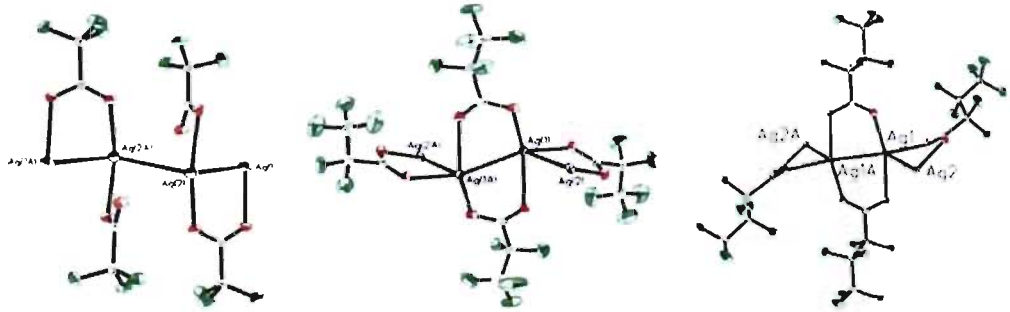

(a) (b) (c)

Figure 4.1.5. Comparison of the tetrameric units in the $L^{4\text{-Ph}}$ complexes formed with (a) the trifluoroacetate anion, **5**; (b) the pentafluoropropionate anion, **6**; and (c) the heptafluorobutyrate anion, **7**.

There are two kinds of silver atoms in **5**: Ag(1) and Ag(2). Adjacent silver atoms, Ag(1) and Ag(2), are bridged by a trifluoroacetate group so as to form a dimer. Another trifluoroacetate group is bound to Ag(2) in a monoatomic mode. A tetrameric unit, $(AgO_2CCF_3)_4$, results from a weak silver···silver interaction between Ag(2) atoms (Ag(2)···Ag(2): 3.1688(7) Å) (Figure 4.1.5a).

A 2-D network is generated by the coordination of one $L^{4\text{-Ph}}$ ligand to four tetramers, via two μ_2-S bridges (Figure 4.1.6a and Figure S6, Annexe VI). The repeat unit of this complex consists of two 12-membered sub units, $Ag_5(L^{4\text{-Ph}})S$, sharing a ligand molecule. Both the central bond of the tetramer and that of the ligand are on crystallographic centers of symmetry.

Interestingly, this structure reveals the cooperation between the anions and the $L^{4\text{-Ph}}$ ligand in the 2D-network formation (Figure S6, Annexe VI). The projection of one layer of **5** (Figure 4.1.7) brings about the existence of two networks. One of them is made up of Ag(I) ions interconnected by the $L^{4\text{-Ph}}$ ligands, while the other network is constituted of the same Ag(I) ions and the anions (Figure S6a, b, Annexe VI). These two networks have the Ag(I) atoms in common and **5** can be described equally well by emphasizing the role of the $L^{4\text{-Ph}}$ ligand or that of the anions.

The tetrahedral coordination of Ag(1) in **5** consists of two sulfur atoms from two distinct ligands, an oxygen atom from a trifluoroacetate group, and Ag(2) with Ag(2)···Ag(1): 3.3212(6) Å. On the other hand, Ag(2) is coordinated to three oxygen atoms from three different trifluoroacetate groups, to Ag(2) (Ag(2)···Ag(2): 3.1688(7) Å) and to Ag(1). Hence, Ag(2) adopts a very distorted trigonal bipyramid.

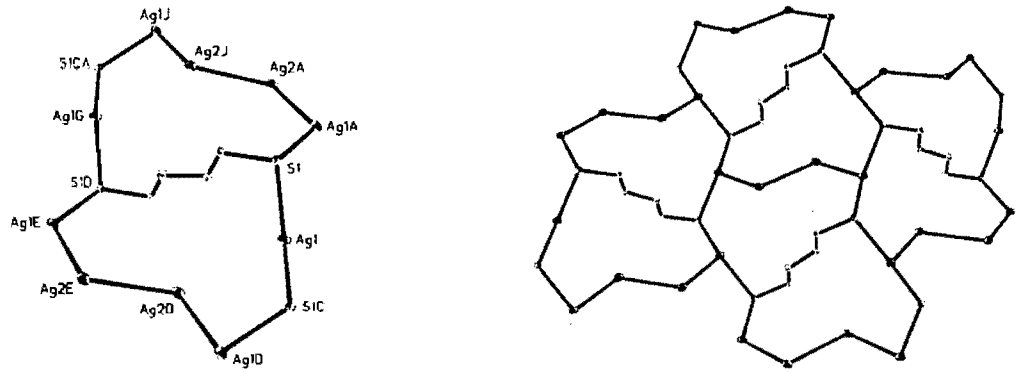

(a)

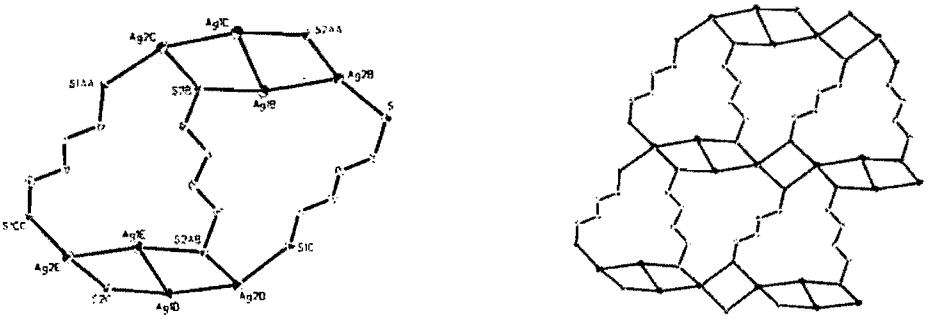

(b)

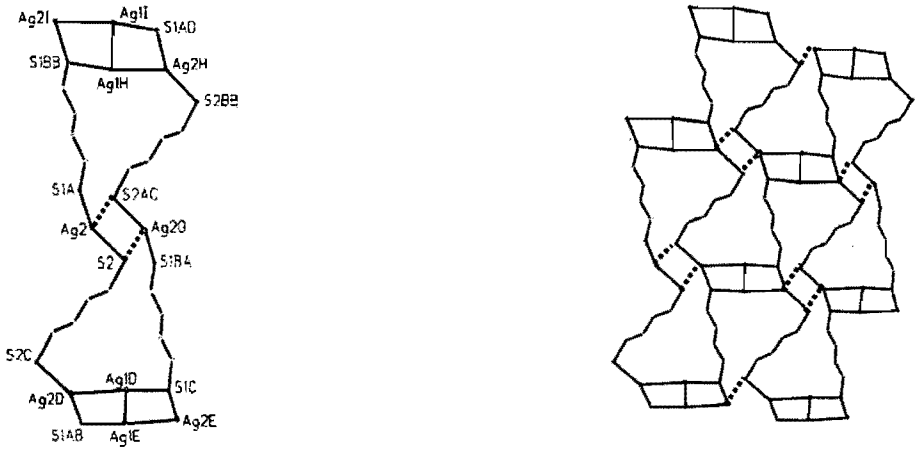

(c)

Figure 4.1.6. Comparison of the repeat units and the 2D-coordination networks in complexes formed with (a) the trifluoroacetate anion, **5**, in which the 2D-network is parallel to the (100)-plane, (b) the pentafluoropropionate anion **6**, (c) the heptafluorobutyrate anion, **7**. The 2D-networks in both **6** and **7** are parallel to (001)-plane. The anions, the phenyl groups, and the H atoms have been omitted for clarity.

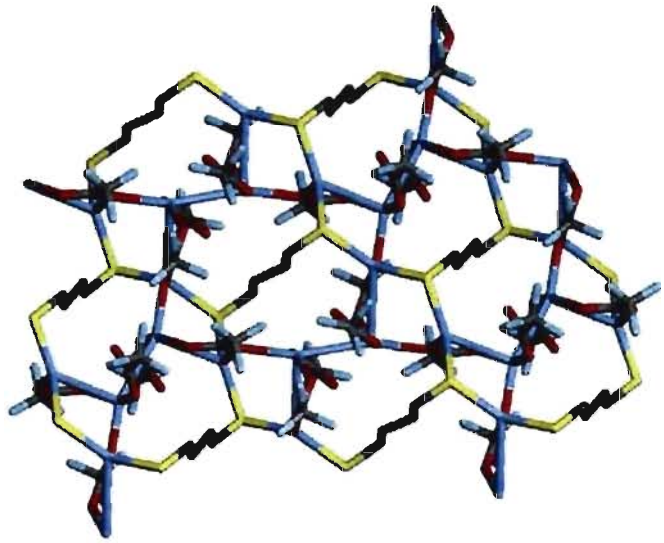

Figure 4.1.7. Projection of one layer of **5** revealing the two interconnected networks. The blue and red "diamond" network is that formed by the anions linked to the silver(I). The yellow and grey "hexagonal" network is formed by the $\mathbf{L}^{4\text{-Ph}}$ ligands and the silver(I) ions. Grey : carbon atoms; yellow: sulfur atoms; blue: silver atoms and red: oxygen atoms.

The nearly identical complexes **6** and **7** contain two sorts of silver atoms. A bridged dimer is formed with two centrosymmetrically related Ag(1) atoms and two perfluorocarboxylate groups in a dibridging mode. In turn, each Ag(1) also forms a weak bond with another silver atom, Ag(2). This is reinforced by another perfluorocarboxylate monobridging Ag(1) and Ag(2). Hence, the $(AgO_2CCF_2CF_3)_4$ and $(AgO_2CCF_2CF_2CF_3)_4$ tetramers are formed in **6** and **7**, respectively (Figure 4.1.5b, c).

The tetramers are connected to each other by the $\mathbf{L}^{4\text{-Ph}}$ ligand, via μ_2-S bridges, producing neutral $[Ag\mathbf{L}^{4\text{-Ph}}(CF_3CF_2CO_2)]_\infty$ and $[Ag\mathbf{L}^{4\text{-Ph}}(CF_3CF_2CF_2CO_2)]_\infty$ layers perpendicular to the *c*-axis (Figure 4.1.6b, c). The repeat unit of these complexes may be described as two 15-membered $Ag_3(\mathbf{L}^{4\text{-Ph}})_2$ macrocycles that share their ligand edges and four 4-membered, Ag_3S diamond shaped ring.

The Ag(1) atom in **6** has an octahedral coordination: Ag(1) is linked to the sulfur atoms of a ligand, to three oxygen atoms of pentafluoropropionate groups, and to two adjacent silver atoms (Ag(1)···Ag(2): 3.1048(6) and Ag(1)···Ag(1): 2.9137(8)Å). On the other hand, the Ag(2) atom is connected to three sulfur atoms, to the oxygen atom of a pentafluoropropionate group, and to another silver atom (Ag(2)···Ag(1): 3.1048(6) Å). Therefore, Ag(2) has a distorted triangular bipyramid environment.

In complex 7, adjacent Ag(1) atoms are dibridged by two heptafluorobutyrate groups and at the same time each Ag(1) is connected to Ag(2) in a monobridging mode by one heptafluorobutyrate group in order to form a tetramer similar to that of **6** (Figure 4.1.5c). However, the Ag_2S_2 diamond, shown by dotted lines in Figure 6c, has an Ag(2)-S* distance, 3.050(2) Å, clearly longer than in **6** (Figure 4.1.6c). Although it is at a rather long distance, this sulfur atom should be considered as being part of the environment of Ag(2), especially in view of the packing similarity between **6** and **7**. Exceptionally long Ag-S interactions, 3.0006(8) Å, has already been reported by Ahmed *et al.*[21] Thus, the Ag(1) silver atoms are octahedrally bound to one ligand, to one adjacent Ag(1) (Ag(1)···Ag(1): 2.8669(9) Å), to a neighbouring Ag(2) (Ag(1)···Ag(2): 3.1594(6) Å), and to three oxygen atoms from three different heptafluorobutyrate groups. The other silver atom, Ag(2), is linked to an oxygen atom from an heptafluorobutyrate group, to two different ligands, to a more distant sulfur atom located at 3.050(2) Å and to Ag(1) (Ag(2)···Ag(1): 3.1594(6) Å). The coordination is that of a distorted trigonal bipyramid.

$\{[Ag_2L^{6\text{-Ph}}(CF_3CO_2)_2.H_2O].H_2O\}_\infty$ (8). In complex **8,** which crystallizes with two water molecules, adjacent silver atoms are linked to the $L^{6\text{-Ph}}$ building block in a μ_2-S bridging mode so as to form neutral sheets parallel to the (100)-plane (Figure 4.1.8b). The repeat unit of these layers is a 22-membered metallomacrocycle, $Ag_4(L^{6\text{-Ph}})_2S_2$ (Figure 4.1.8a). The trifluoroacetate group adopts a monodentate-coordinating mode and completes the coordination sphere of the silver atom (Scheme 1c). It is worth noting that in this complex, there are two kinds of water molecules. The OW(3) water molecules, which are situated on a two-fold axis of rotation, link two symmetrically related Ag atoms, and in doing so, build up a three-dimensional network (Figure 4.1.8c,d). The other water molecules, OW(4), are located in between consecutive 22-membered metallomacrocycles (Figure S7, Annexe VI). The 3D-network of **8** is constituted of diamondlike channels in which the phenyl groups of the spacer, as well as the trifluoroacetate anions, are located (Figure S7, Annexe VI). In this complex, the silver atoms are tetrahedrally coordinated to two sulfur atoms from two distinct ligands, to an oxygen atom from a trifluoroacetate group, and to another oxygen from the OW(3) water molecule (Ag–OW(3): 2.417(2) Å).

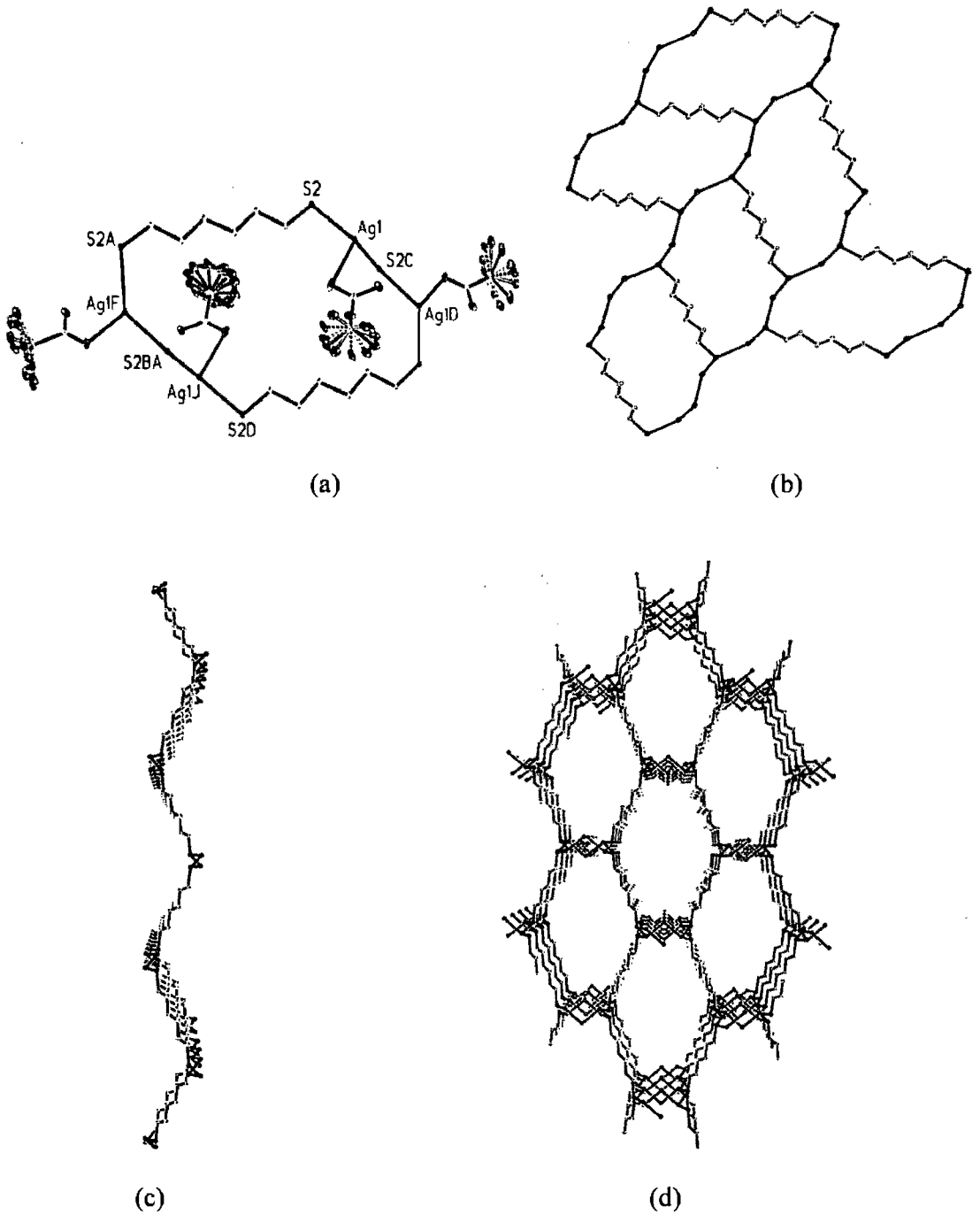

Figure 4.1.8. (a) The repeat unit of the 2D-network of **8**. The OW(4) water molecules, not shown, are located above and below the ring center. (b) One wavy sheet of **8**, parallel to the (100)-plane. The phenyl groups, the anions and the hydrogen atoms have been omitted for clarity. (c) One sheet shown edge-on, i.e., at 90° from b. (d) The 3D-network obtained when sheets of **8** are linked together by the oxygen atoms of water molecules. The phenyl and the trifluoroacetate groups, the water molecules inserted between the layers, as well as the hydrogen atoms have been omitted for clarity.

$[AgL^{6\text{-}Ph}(CF_3CF_2CO_2)]_\infty$ (9). There are two kinds of silver atoms in complex **9**. Two neighbouring Ag(1) atoms are connected in a diatomic bridging mode by two pentafluoropropionate group in order to form the $(Ag(1)O_2CCF_2CF_3)_2$ dimer in which the Ag(1)···Ag(1) distance is 3.0052(4) Å. A different dimer is formed with Ag(2) atoms, with a longer Ag(2)···Ag(2) distance of 3.3898(5) Å. Neighboring dimers, $(Ag(1)O_2CCF_2CF_3)_2$ and $(Ag(2)O_2CCF_2CF_3)_2$, which are almost orthogonal to one another (Φ: 89.6 (1)°), form a $[Ag_2(O_2CCF_2CF_3)_2]_\infty$ chain, via the oxygen atom of the pentafluoropropionate group, that extends parallel to the *a*-axis (Figure 4.1.9a). Adjacent chains are joined by the 1,6-bis(phenylthio)hexane, $\mathbf{L^{6\text{-}Ph}}$, thus building a 2D-box like structure parallel to the (010)-plane (Figure 4.1.9b).

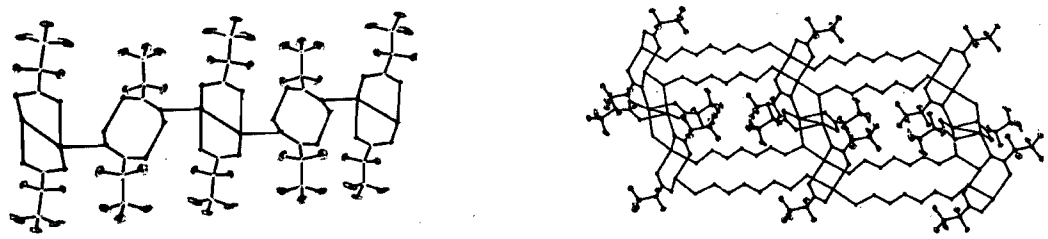

(a) (b)

Figure 4.1.9. (a) A chain of **9** made up of a succession of dimeric units extending along the *a*-axis. Note that consecutive dimers are nearly at 90° to one another. (b) The 2D-coordination network of **9** parallel to the *ac*-plane. This layer is obtained as the ligands link the chains shown above. The hydrogen atoms and the phenyl groups have been omitted for clarity.

Each Ag(1) silver atom is linked to three oxygen atoms from distinct pentafluoropropionates, to a sulfur atom, and to an adjacent Ag(1) silver atom (Ag(1)···Ag(1): 3.0052(4) Å). Thus, Ag(1) has a distorted trigonal bipyramid coordination. By contrast, Ag(2) is coordinated to two oxygen atoms from different pentafluoropropionate groups, and to two sulfur atoms from different $\mathbf{L^{6\text{-}Ph}}$ ligands, resulting in a distorted tetrahedral coordination.

$[Ag(L^{6\text{-}Ph})_{0.5}(CF_3CF_2CF_2CO_2)]_\infty$ (10). Two centrosymmetrically related silver atoms are bound in a diatomic bridging mode by two heptafluorobutyrate anions, forming the $(AgO_2CCF_2CF_2CF_3)_2$ dimer. Dimers are linked to one another by the $\mathbf{L^{6\text{-}Ph}}$ building block, via a μ_2-S bridge, so as to build up a two-dimensional coordination network parallel to the (001)-plane (Figure 4.1.10). The repeat unit is an 18-membered metallomacrocycle,

$Ag_2(L^{6\text{-Ph}})_2$. Taking part in this large ring are two 6-membered hexagonal rings, Ag_4S_2 (Figure 4.1.10a). The phenyl and the heptafluorobutyrate groups occupy both sides of the layers (Figure 4.1.10b). The silver atom adopts a very distorted trigonal bipyramid environment. The silver atoms are connected to two oxygen atoms from distinct anions, to two sulfur atoms from different ligands, and to another silver atom (Ag···Ag: 2.9730(5) Å).

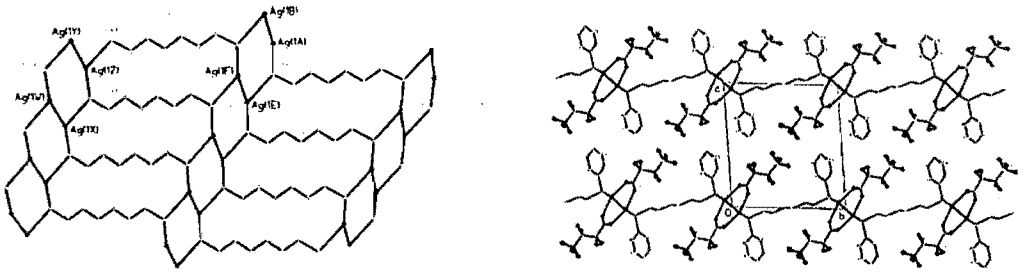

(a) (b)

Figure 4.1.10. (a) The hexagonal Ag_4S_2 rings are linked by the $L^{6\text{-Ph}}$ ligands and yield the layer structure of **10** (the phenyl groups, the anions and the H atoms have been omitted for clarity). (b) Projection on the *bc*-plane showing the packing of the layers. The H atoms are omitted for clarity.

$[AgL^{10\text{-Ph}}(NO_3)]_\infty$ (11). To further study the influence of the length of the building block upon the networks, the 1,10-bis(phenylthio)decane ligand, $L^{10\text{-Ph}}$, was synthesized.[9d] In complex **11**, adjacent silver atoms are brought together by the nitrate anion which acts as a bidentate ligand. The result is a $[Ag\text{-}NO_3]_\infty$ chain, parallel to the *a*-axis (Figure 4.1.11a). Adjacent chains are interconnected by the $L^{10\text{-Ph}}$ ligand, resulting in a corrugated 2D-polymer network parallel to the (020)-plane (Figure 4.1.11b) as the $L^{10\text{-Ph}}$ ligand is present in two distinct conformations. Although the two crystallographically different $L^{10\text{-Ph}}$ ligands each possesses a center of symmetry, one of them is in the completely extended conformation, while the other has the *gggttttg⁻g⁻g⁻* conformation. It is the presence of these three gauche torsion angles that is responsible for the corrugated aspect of the 2D-layer.

In most of the structures reported here, the ligand part of the complex sits on a crystallographic center of symmetry and the ligand is usually in the fully-extended conformation; that is, all the torsion angles along the aliphatic segment are trans.

An aliphatic sequence containing an even number of methylene groups is usually centrosymmetric and adopts preferentially the trans conformation. For example, piperazinium 1-n-alkanecarboxylates[22a] or dibenzamido alkanes[22b] all contain aliphatic

sequences which, when the number of CH_2 groups is even, these are centrosymmetric and adopt a fully-extended conformation.

This is also true for the free ligands[9] $L^{4\text{-Ph}}$, $L^{6\text{-Ph}}$, $L^{8\text{-Ph}}$, and $L^{10\text{-Ph}}$. Thus, in the supramolecular architectures built with the ligands $L^{4\text{-Ph}}$ and $L^{6\text{-Ph}}$, it is not surprising to find that the ligands keep an all-trans conformation. In **11**, $L^{10\text{-Ph}}$ has two conformations, an extended one and a gauche conformation. This prevents the structure from having large voids. The case of $L^{2\text{-Ph}}$ is an interesting one since it is in the cis conformation and hence is chelated to Ag(I) in complex **3**, but adopts the trans conformation in **1**, **2** and also in **3**.

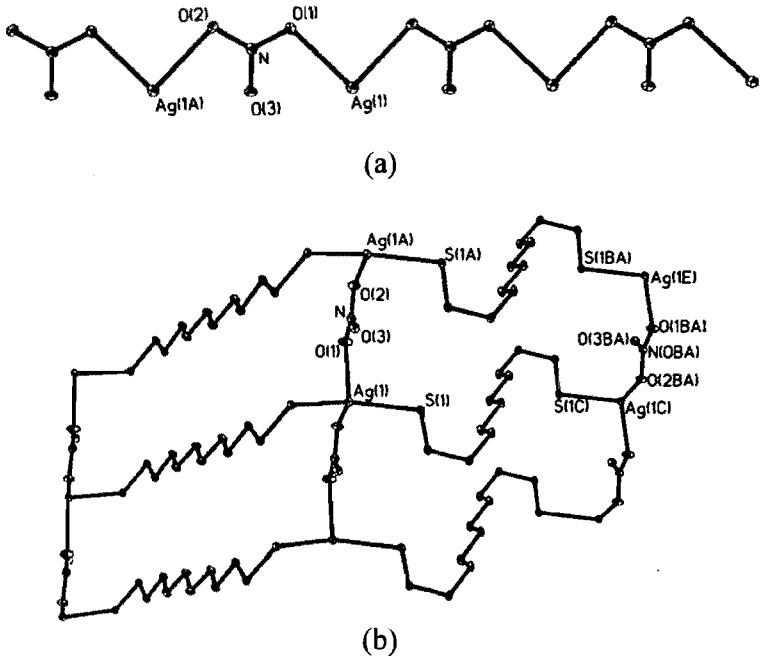

Figure 4.1.11. (a) The 1D-coordination polymer of $[Ag\text{-}NO_3]_\infty$ shown parallel to the *a*-axis. (b) Adjacent chains of $[Ag\text{-}NO_3]_\infty$ are interconnected by the $L^{10\text{-Ph}}$ ligand, thus forming a corrugated 2D-coordination network parallel to the (020)-plane. Note that the $L^{10\text{-Ph}}$ connector adopts two distinct conformations. The hydrogen atoms and the phenyl groups have been omitted for clarity.

The repeat unit of **11** is a 34-membered metallomacrocycle. The silver atom is bound to two oxygen atoms from distinct nitrates, and to two sulfur atoms from different $L^{10\text{-Ph}}$ building blocks, and has a slightly distorted tetrahedral coordination. Indeed, this complex is similar to that formed by the combination of $L^{4\text{-Ph}}$ with the nitrate anion,[4] in which the neighboring silver atoms are linked through the nitrate in a μ-O,O' coordination mode, thereby yielding a 1D-coordination polymer, $[Ag\text{-}NO_3]_\infty$. The chains are linked by

the $L^{4\text{-Ph}}$ ligand thereby yielding a corrugated 2D-coordination network identical to that of complex **11**.

Infrared Spectroscopy. Infrared spectroscopy is usually used for the carboxylate moieties when X-ray structures are not available in order to differentiate the distinct coordination mode of the carboxylate groups, such as the bridging bidentate, chelating bidentate or unidentate modes on the basis of $\Delta\nu$ values ($\Delta\nu = \nu_{asym}(CO_2)-\nu_{sym}(CO_2)$).[23] The bands observed at 1661 and 1384 cm^{-1} in the IR spectrum of complex **2** are assigned to the characteristic antisymmetric and symmetric stretching vibrations of the carboxylate group, respectively. Furthermore, the value of $\Delta\nu = [\nu_{asym}(CO_2)-\nu_{sym}(CO_2)]$, 277$cm^{-1}$, obviously points to the occurrence of the dibridging mode,[24] in agreement with the established crystal structure. This observation applies also to **6**, **7**, **9** and **10**, where the values of $\Delta\nu$ corroborate the X-ray results (Table 4.1.3a). The value of $\Delta\nu$ found for complex **8** (301 cm^{-1}) indicates the occurrence of the monoatomic binding mode,[7a] as shown by the X-ray analysis of **8**. Although the crystal structure of **5** reveals the presence of both the diatomic-bridging mode and the monoatomic-binding mode (Scheme 2a,c), only the latter is identified from its infrared spectrum, where the value of $\Delta\nu$ is 301 cm^{-1}.

The unambiguous assignment of the vibration modes of the $CF_3SO_3^-$ anion in complexes **1** and **4** is quite difficult because of the mixing of CF_3, SO_3, and organic ligand vibrations in the stretching-mode region between 1300 and 1000 cm^{-1}.[23,25] However, for the trifluoromethanesulfonate silver salt, as well as the coordination polymers containing the triflate, the absorption bands at 1270 and 1043 cm^{-1} have been assigned to the $\nu[SO_3(E)]$ and $\nu[SO_3(A_1)]$ vibrations.[25-27] The two absorption bands observed here for complexes **1** and **4**, listed in Table 4.1.3, are consistent with the triflate being coordinated to the silver atom.[7,28] The band at 1384 cm^{-1} for **11** is assigned to the $\nu_3(E')$ of the nitrate.[29] The perchlorate in complex **3** is present with two distinct coordination modes: unidentate (C_{3v}) and bridging bidentate (C_{2v}) (Figure 4.1.3). The observed absorption extending from 1041 to 1179 cm^{-1}, with a maximum at 1091 cm^{-1}, corresponds to assignments for both the C_{2v} and the C_{3v} symmetries.[30]

Table 4.1.3. Comparison of the COO^- stretching frequencies (cm^{-1}) and SO_3^- vibration frequencies (cm^{-1}) obtained by FTIR spectroscopy. ($\Delta = [\nu_{asym}(CO_2) - \nu_{sym}(CO_2)]$).

Complex		$\nu_{asym}(CO_2)$	$\nu_{sym}(CO_2)$	Δ
2	$[Ag_2L^{2\text{-}Ph}(CF_3CO_2)_2]$	1661	1384	277
5	$[Ag_2(L^{4\text{-}Ph})_{0.5}(CF_3CO_2)_2]$	1685	1384	301
6	$[Ag_2L^{4\text{-}Ph}(CF_3CF_2CO_2)_2]$	1679	1413	266
7	$[Ag_2L^{4\text{-}Ph}(CF_3CF_2CF_2CO_2)_2]$	1667	1407	260
8	$[Ag_2L^{6\text{-}Ph}(CF_3CO_2)_2.2H_2O]$	1684	1383	301
9	$Ag_2L^{6\text{-}Ph}(CF_3CF_2CO_2)_2]$	1682	1411	271
10	$[Ag(L^{6\text{-}Ph})_{0.5}(CF_3CF_2CF_2CO_2)]$	1683	1407	276
	$[Ag_2L^{3\text{-}Ph}(CF_3COO)_2]^a$	1685	1410	275
	$[Ag_2L^{3\text{-}Ph}(CF_3CF_2CO_2)_2(CH_3COCH_3)]^a$	1679	1411	268
	$[AgL^{3\text{-}Ph}(CF_3CF_2CF_2CO_2)]^a$	1681	1411	270
	$[AgL^{1\text{-}Ph}(CF_3CO_2)]^b$	1690	1390	300
	$[AgL^{1\text{-}Ph}(CF_3CF_2CF_2CO_2)]^b$	1682	1403	279
	$[AgL^{1\text{-}Ph}(OOCCF_2CF_2COO)]^b$	1683	1407	276
	$Ag_2(CF_3COO)_2(dppm)]^c$	1670	1407	263
	$[Ag_2(CF_3CF_2COO)_2(dppm)]^c$	1672	1406	266
	$[Ag_2(CF_3CF_2CF_2COO)_2(dppm)]^c$	1670	1396	274

Complex	$\nu_{asym}(SO_3)$	$\nu_{sym}(SO_3)$
1	1254	1033
4	1257	1033
$[AgL^{1\text{-}Ph}(CF_3SO_3)]^a$	1258	1032
$[Ag_2(L^{1\text{-}Ph})2(CF_3SO_3)_2]^a$	1254	1027
$[Ag_2L^{3\text{-}Ph}(CF_3SO_3)_2(CH_3COCH_3)]^b$	1258	1033
$[Ag_2L^{3\text{-}Ph}(CF_3SO_3)_2]^b$	1260	1034
$[Ag_2L^{3\text{-}Ph}(CF_3SO_3)_2]^b$	1257	1030
$[Ag_2L(CF_3SO_3)_2]^d$	1257	1035

[a]Reference 7a; [b] Reference 7b; [c] Reference 24; [d]Reference 28 (**L**: dibenzo[d, def]chrysene).

4.1.5 Discussion

I. Description and Topology of the Networks. The main reason for our interest in the role of the anions upon the topology is to synthesize materials with useful properties, such as molecular separation/recognition, especially anion-exchange and luminescence. In earlier work, we reported that the structure of networks based on flexible diarylthioether building blocks and silver salts were influenced by the nature of the counteranion, the metal-to-ligand ratio and the solvent used for recrystallization.[4,7] The difficulty in controlling all these factors is usually considered as the main reason for the lack of structure predictability.

However, to gain more insight, we have investigated one at a time the effect of each parameter upon the topology of the networks formed. In this context, we have studied the role of the counteranion, which may be considered as a charged ligand, upon the structure of the resulting supramolecular networks when diarylthioether ligands are used as building blocks.[4, 7] We explored the effect of the size and/or the coordination ability of several anions in the series PF_6^-, SbF_6^-, ClO_4^-, BF_4^-, NO_3^-, $pTsO^-$, $CF_3SO_3^-$, $CF_3CO_2^-$, $CF_3CF_2CO_2^-$, $CF_3CF_2CF_2CO_2^-$ and $^-OOCF_2CF_2COO^-$.[7] The type of coordination network may be characterized on the basis of the role of the anion *versus* that of the ligand. We thus define a "ligand dominated" network by a structure, where the silver and the ligand generate the structure and the anion only completes the coordination sphere of the metal center. The "anion-dominated" structures would be constituted of silver atoms and anions, while the ligand would have a secondary role. Finally, there are structures that could be described equally well by one or the other definition, in which neither the ligand nor the anion dominate. In this case, the silver atoms are part of two networks, $(Ag\text{-anion})_\infty$ and $(Ag\text{-ligand})_\infty$, which reinforce one another.

Influence of the counteranions upon the networks. In metal-organic crystal engineering, it has been reported that the type of anion has a strong influence upon the topology of the coordination networks.[31] In the same way, we reported that the supramolecular architecture of silver(I) salts with diarylthiother building blocks, such as $\mathbf{L^{1\text{-}Ph}}$ and $\mathbf{L^{3\text{-}Ph}}$, is significantly influenced by the nature of the counteranions used.[7]

Group 1 counteranions usually act as templates and counter-balance the charge of the networks formed by the self-assembly of the silver(I) atom and the organic ligand.[7] Thus, we may consider that group 1 anions favor the formation of networks in which the organic spacer is indispensable. In other words, the organic ligand assures the expansion of the networks and the elements of group 1 counter-balance the charge of the networks or complete only the coordination sphere of the silver(I). We refer to this network as ''ligand-dominated''. For the complexes of the 1,3-bis(phenylthio)propane spacer, $\mathbf{L^{3\text{-}Ph}}$, the noncoordinating anions allow for the formation of cationic layer structures, with a metal-to-ligand ratio 1:2 and in which the anions are inserted between the sheets.[7a] In addition, the bulk of the anions prevents the layers from getting too close to one another, thus allowing for the presence of guest molecules between the cationic layers.[7b,32,33]

The building block $L^{5\text{-Ph}}$ reacted with Ag salts of XY_4^- and XY_6^- also form cationic-layer networks,[34-36] similar to those obtained with $L^{3\text{-Ph}}$ with a 1:2 metal-to-ligand ratio. There is also a report of a comparable 2D-coordination network when $L^{4\text{-Ph}}$ is reacted with silver(I) perchlorate.[4] Hence, when the ligand is of an intermediate size ($L^{3\text{-Ph}}$, $L^{4\text{-Ph}}$, and $L^{5\text{-Ph}}$), one obtains a 2D-coordination network that is "ligand-dominated". Attempts to obtain comparable 2D-coordination networks with $L^{2\text{-Ph}}$ or $L^{6\text{-Ph}}$ were unsuccessful. So it seems that these structures are stable only when the ligand has an optimum dimension to form a relatively rigid network. For ligands larger than $L^{5\text{-Ph}}$, the aliphatic segment is too flexible, i.e., it has too many torsion angles. For example, in the ClO_4^- complex of $L^{6\text{-Ph}}$, the 1:1 metal-to-ligand ratio is preferred and a dinuclear unit (0D-structure) was reported by Bu *et al.*[37] In this structure, the perchlorate is coordinated to the silver atom. In the silver nitrate complex with $L^{10\text{-Ph}}$ (**11**), where the NO_3^- anion has a bulk size comparable to that of BF_4^- or ClO_4^-, one finds that the ligand's aliphatic segment is present in two different conformations, again showing an insufficient rigidity for the formation of a 2D-cationic layer structures.

The perchlorate group is a particular case among the group 1 anions, in the sense that it sometimes coordinates to the silver atom as an unidentate ligand or acts as a bridging unit, as reported here for complex **3**. The perchlorate plays a non-negligible part in the construction of the network of **3**. Indeed, it is the bridging perchlorate which assures the expansion of the network into a two-dimensional one (Figure 4.1.3). Thus, the question is "at what point can we consider a network as being 'ligand-dominated' or 'anion-dominated' and when do the neutral ligand and the charged ligand (anion) cooperate rather than compete for the construction of the coordination-networks ?"

Sulfonates or Group 2 anions. In this work, the multidentate trifluoromethanesulfonate does not take part into the network formation. In both complexes **1** and **4**, it merely completes the trigonal coordination of Ag(I) through one of its oxygen atoms. It was reported earlier[7a] that $CF_3SO_3^-$ acts with $L^{1\text{-Ph}}$ as a single donor. However, in most other compounds, the sulfonate anions (*p*-TsO^- or $CF_3SO_3^-$) act as bidentate ligands.[7a,b] The sulfonate anions seem to be ambivalent as to whether a 1D- or a 2D-coordination network is generated. It should be mentioned that these anions have the property of generating solvent-induced supramolecular polymorphism.[7b]

Perfluorocarboxylates or Group 3 anions. These anions may adopt different coordination modes (Scheme 2). The perfluorocarboxylate which assumes a monodentate coordination mode, as in complex **8** (Figure 4.1.8a), is not considered necessary for the network formation since it only completes the coordination sphere of the silver atom. Hence, this network may be considered as 'ligand-dominated'. A comparable situation is noted with $\mathbf{L}^{\mathbf{1\text{-}Ph}}$ and the trifluoroacetate anion.[7a]

As expected, the bidentate perfluorocarboxylate anions favor the formation of silver(I) dimers, as in the silver trifluoroacetate or the silver heptafluorobutyrate salts.[16, 39] Less frequently, tetramers are also present (Figure 4.1.5a-c). In both cases, the group 3 anions are as necessary to the propagation of the networks as the neutral ligands, since the latter expand the dimers or the tetramers into networks (Figures 4.1.2, 4.1.6, 4.1.10). That is, both the anion and the neutral ligand are equally involved in the network; there is cooperation instead of competition, between these structural unit.

In addition, the oxygen atoms of the perfluoroacarboxylate contain *syn* and *anti* lone pairs capable of coordinating to metal centers (Scheme 2d). It is worth pointing out that the structure of silver(I) trifluoroacetate is a 1D-polymeric chain consisting of interconnected dimers *via* the *anti*-lone pair of the oxygen atoms (Figure S9, Annexe VI).[37] Group 3 anions may thus form 1D-coordination polymer or 2D-networks with the metal atoms (Figure 4.1.7, 4.1.9a). For example, in complex **9** with $\mathbf{L}^{\mathbf{6\text{-}Ph}}$, one anti-lone pair of one oxygen of the $(AgOOCCF_2CF_3)_2$ dimer is coordinated to the silver atom of an adjacent dimer in order to generate the 1D-coordination polymer $[Ag_2(CF_3CF_2CO_2)_2]_\infty$ (Figure 4.1.9a). These 1D-chains are linked to one another by the $\mathbf{L}^{\mathbf{6\text{-}Ph}}$ spacer in order to create a 2D-network (Figure 4.1.9b). In this case, one observes that the neutral ligand, an organic building block and the charged ligand, the perfluorocarboxylate cooperate in order to form a 2D-network. In other words, when the charged ligand forms a one-dimensional coordination polymer with the silver atom, the ligand contributes to an increase in the dimensionality of the network.

In addition, a 1D-coordination polymer is formed when silver(I) tetrafluorosuccinate is reacted with $\mathbf{L}^{\mathbf{1\text{-}Ph}}$.[7a] This chain has been described as a succession of pairs of silver atoms bridged at one end of the tetrafluorosuccinate anion and another pair of silver atoms is bridged at the other end, and so on, thus forming a $[Ag_2\text{-}OOCCF_2CF_2COO\text{-}]_\infty$ ribbon (Figure S8a, Annexe VI). However, in this case, the neutral ligand does not increase the dimensionality of the network, as expected, but only reinforces

the $[Ag_2\text{-}OOCCF_2CF_2COO\text{-}]_\infty$ chain by linking consecutive silver atoms (Figure S8, Annexe VI).

The perfluorocarboxylates in **5** form a two-dimensional structure with the silver atoms (Figure 4.1.7), which may be seen as consisting of two intertwined networks. Neither the ligand nor the anions seem to dominate (Figure S6, Annexe VI).

The small nitrate group may easily approach the metal center so that it should be considered as fairly coordinating.[8] Since this charged ligand is a coordinating one, we can expect that it contributes to the construction of the network. With both $\mathbf{L}^{\mathbf{4\text{-}Ph}}$ and $\mathbf{L}^{\mathbf{10\text{-}Ph}}$, the nitrate anions link adjacent silver atoms in a μ-O,O' mode resulting in the 1D-coordination polymer, $[Ag\text{-}NO_3]_\infty$. These chains, in turn, are linked to each other by the building block (Figure 4.1.11).[4] However, with $\mathbf{L}^{\mathbf{6\text{-}Ph}}$, the nitrate adopts a μ-O,O monoatomic bridging mode that links adjacent silver atoms and gives rise to an Ag_2O_2 ring. Neighbouring rings are inter-connected by the ligand so as to build a 2-D coordination network, that is different from that formed with the former ligands.[38]

Thus, the coordination ability of the anions, charged ligands, plays a non-negligible role upon the formation of the supramolecular architectures in metal-organic crystal engineering. However, the versatile coordination mode of coordinating anions, such as those of Group 3 or the nitrate, limits the predictability of the structure of the networks formed with the silver atoms. It is worth noting that in all the perfluoroacetate-based networks[7] there are weak silver-silver interactions.

II- Silver-Silver Contacts. As expected, bidentate perfluorocarboxylate anions favor the formation of silver(I) dimers or tetramers (Scheme 2, Figure 4.1.5). Dimers are reported for the silver trifluoroacetate or the silver heptafluorobutyrate salts.[16, 39] We have also observed theses structures in networks based on the $\mathbf{L}^{\mathbf{1\text{-}Ph}}$ and the $\mathbf{L}^{\mathbf{3\text{-}Ph}}$ ligands with trifluoroacetate, pentafluoropropionate, heptafluorobutyrate or tetrafluorosuccinate.[7] In all cases, two adjacent silver atoms are bonded together in a binuclear bridging mode by two perfluorocarboxylate groups in order to form $(AgOOCR)_2$ dimers (R = CF_3, CF_3CF_2, $CF_3CF_2CF_2$ or CF_2CF_2COO). Consequently, weak silver-silver interactions occur between the silver atoms of the dimers. The observed Ag···Ag distances are listed in Table 4.1.4 and compared with those reported in other perfluorocarboxylate dimers. All these distances are shorter than the sum of the van der Waals radii of two silver atoms (3.40 Å[17]), and slightly

longer than 2.89 Å, twice the radius of metallic silver[17], indicating the presence of weak silver-silver interactions.[40,41]

Description of the dimers. Dimers were observed in complexes **2**, **9** and **10**. Complexes **2** and **9** have two crystallographically distinct $(AgOOCR)_2$ dimers which differ by the strength of the silver-silver interaction. There is always a short and a long Ag···Ag interaction, the longer distance being almost equal to the sum of the van der Waals radius of two silver atoms. In these cases, we believe that there are no interactions between the silver atoms. On the other hand, the short distances in **2**, **9**, and **10** are clearly less than the silver-silver separation of 3.16 Å observed for the trifluoroacetate-bridged silver-silver systems according to Bosch *et al.*,[40b] and points to a weak interaction between the silver atoms as described by Wang *et al.*[41a]

Table 4.1.4. Comparison of the short Ag···Ag contact distances (Å) observed herein with corresponding values reported for similar ligands.

Complex	Ligand	Anion	Ag···Ag contact	Structural unit
	[a]$L^{1\text{-Ph}}$	$CF_3CF_2CF_2COO^-$	3.1593(3)	dimer
	[a]$L^{1\text{-Ph}}$	$^-OOCCF_2CF_2COO^-$	2.9836(5), 3.0168(5)	dimer
2	$L^{2\text{-Ph}}$	CF_3COO^-	3.0813(5), 3.3813(6)	dimer
	[b]$L^{3\text{-Ph}}$	CF_3COO^-	3.2459(5)	dimer
	[b]$L^{3\text{-Ph}}$	$CF_3CF_2COO^-$	3.0502(7)	dimer
	[b]$L^{3\text{-Ph}}$	$CF_3CF_2CF_2COO^-$	3.1594(4)	dimer
5	$L^{4\text{-Ph}}$	CF_3COO^-	3.1688(7), 3.3212(6)	tetramer
6	$L^{4\text{-Ph}}$	$CF_3CF_2COO^-$	2.9137(8), 3.1048(6)	tetramer
7	$L^{4\text{-Ph}}$	$CF_3CF_2CF_2COO^-$	2.8669(9), 3.1594(6)	tetramer
9	$L^{6\text{-Ph}}$	$CF_3CF_2COO^-$	3.0052(4), 3.3898(5)	dimer
10	$L^{6\text{-Ph}}$	$CF_3CF_2CF_2COO^-$	2.9730(5)	dimer

[a]Reference 7a. [b]Reference 7b

Description of the tetramers. It is of interest to note that tetramers are only observed with the $L^{4\text{-Ph}}$ ligand. A schematic description of the two kinds of tetramers is illustrated in Figure 4.1.12. Complexes **6** and **7** are nearly identical, but differ significantly from **5**. All of the tetramers are centrosymmetric and the silver atoms form a zigzag rather than a linear

chain since all of the Ag-Ag-Ag bond angles are in the range of 96 to 99°. The Ag···Ag distances are all very short and the central bond is always the shortest.

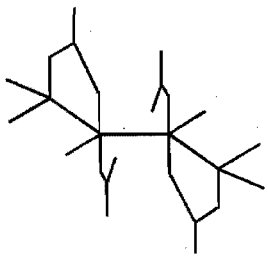

5 3.3212(6), 3.1688(7)

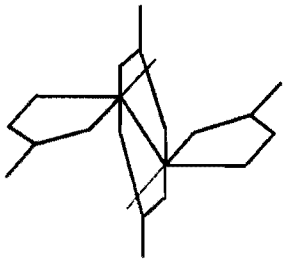

6 3.1048(6), 2.9137(8)
7 3.1594(6), 2.8669(9)

Figure 4.1.12. Schematic representation of the tetrameric units obtained with $\mathbf{L^{4\text{-}Ph}}$ and Ag···Ag distances (Å) in complexes **5**, **6** and **7**. All three complexes are centrosymmetric.

In **5**, the two extreme silver atoms are monobridged by one trifluoroacetate group, while a second ligand is attached to the central silver through one of its oxygens (Figure 4.1.12). There obviously must be a genuine Ag-Ag bond between the central atoms since these are not bridged by a trifluoroacetate. Thus, we think that the short distance between adjacent silver atoms may be attributed to weak silver-silver interactions rather than a geometrical restriction, especially since the central Ag···Ag distance is shorter than those between silver atoms held in a binuclear mode by one trifluoroacetate.

Complexes **6** and **7** are nearly identical. The central silver atoms are dibridged by two perfluorocarboxylate ligands, while the extreme silver atoms are monobridged. The central Ag···Ag distances are among the shortest, these being almost equal to twice the radius of metallic silver or to the separation of silver atoms in silver metal, 2.89 Å.[17] Specifically, in **6**, the Ag1···Ag1 separation, 2.9137(8) Å, is merely 0.03Å longer than the distance in silver metal,[17] indicating a moderate argentophilic interaction,[40] while the central bond in **7** is even shorter, with a value of 2.8669(9) Å.

Nevertheless, it is not clear how the electron-withdrawing power, due to an increase in the number of fluorine atoms in the counteranions, affects the coordination strength of the carboxylate groups, and consequently, the Ag···Ag interactions. On the other hand, such short Ag···Ag distances are not unusual in Ag(I) dinuclear complexes. For example, an Ag···Ag bond, 2.9710(4) Å long has been reported for the trifluoroacetate groups bridging two silver cations in a 2:1 complex of bis(dimethylphenyl)pyrazine and silver(I)

trifluoroacetate crystallized in acetonitrile and 3.1014(3) Å in the 2:2 complex crystallized in dichloromethane.[42] In the tetrafluorosuccinate silver acetylenediide,[43] the Ag···Ag distances are close to that in silver metal: in the crown-like [C2@Ag7] cage, they range from 2.8848(8) to 2.9526(8) Å. A longer distance of 3.116(1) Å is reported for Ag···Ag in the tetrameric silver thiolate phosphine complex.[21] Some Ag···Ag distances shorter than that found in metallic silver have been reported, for exemple, in diaquabis(betaine)disilver(I) dinitrate (2.898(1) Å), and bis(pyridine betaine)disilver(I) diperchlorate,[47] (2.897(2) Å) or bis (3-hydroxyl-4-phenyl-2,2,3,-trimethylcyclohexanecarboxylato)disilver(I) dihydrate (2.778(5) Å).[46]

In most coordination networks incorporating perfluorocarboxylate counteranions and flexible diarylthioether ligands, there are $[Ag_2(\text{carboxylate-}O,O')_2]$ dimers or $[Ag_4(\text{carboxylate-}O,O')_4]$ tetramers in which the Ag···Ag separation presents some argentophilicity,[44] which, according to Schmidbaur, may be regarded as an extension of the well-established concept of the aurophilicity for gold(I).[45]

4.1.6 Conclusions

Of the 11 complexes containing the 1,n-bis(phenylthio)alkane ligands, n = 2, 4, 6, 10, and anions of different coordinating abilities, all but two complexes generate 2D-coordination networks. One (**4**) forms a 1D-coordination polymer while a 3D-network is noted for **8**, where water molecules join adjacent 2D-sheets.

The weakly coordinating anions (PF_6^-, SbF_6^-, ClO_4^-, BF_4^-) form layer structures with $\mathbf{L^{3\text{-}Ph}}$, $\mathbf{L^{4\text{-}Ph}}$, and $\mathbf{L^{5\text{-}Ph}}$ in which the anions are inserted within the layers. In the 1D-coordination polymers formed with Ag and $\mathbf{L^{1\text{-}Ph}}$, the anions are coordinated to the silver atoms. Here, we find that both the perchlorate and the nitrate groups act as bidentate anions. In **3**, ribbons made up of all three structural units are inter-connected by the $\mathbf{L^{2\text{-}Ph}}$ ligand through two bidentate perchlorates, resulting in a very unusual 2D-network.

The binding of silver atoms through the bidentate nitrate in **11** produces polymeric chains. These, in turn, are cross-linked through the $\mathbf{L^{10\text{-}Ph}}$ ligands, thus producing a 2D-coordination network.

Trifluoromethanesulfonate is a weak-to-medium coordinating anion, as with $\mathbf{L^{1\text{-}Ph}}$, or **1** (with $\mathbf{L^{2\text{-}Ph}}$) and **4** (with $\mathbf{L^{4\text{-}Ph}}$). It only completes the trigonal coordination of the metal.

The perfluorocarboxylates are strongly coordinated to the silver atoms, forming dimeric (**2**, **9**, **10**) or tetrameric units (**5**, **6**, **7**). It is of interest to note that the tetramers are obtained only with the $\mathbf{L^{4\text{-}Ph}}$ ligand. These units have a zigzag shape, since the Ag-Ag-Ag angles are close to 98°. The perfluorocarboxylates form dimeric units with $\mathbf{L^{2\text{-}Ph}}$ and $\mathbf{L^{6\text{-}Ph}}$. Both the dimers, and especially the tetramers, have very short metal-metal distances indicating the presence of weak silver···silver interactions.

Acknowledgements. This project was funded by the Natural Sciences and Engineering Research Council of Canada (F.B.). M.O.A. would like to thank the Programme Canadien de Bourse de la Francophonie for a scholarship. We also thank Dr. M. Simard and F. Bélanger-Gariépy for discussion, and H. Dinel for the elemental analyses.

Supplementary Material Available: X-ray crystallographic information files (CIF) for all the compounds (**1-11**). Details on the characterization of the ligands, tables of bond distances and angles, and illustrations S1-S9. This material is available free of charge via the Internet at http://pubs.acs.org

4.1.7 References

(1) (a) Stumpf, H. O.; Ouahab, L.; Pei, Y.; Grandjean, D.; Kahn, O. *Science* **1993**, *261*, 447. (b) Yaghi, O.M.; Li, G.; Li, H. *Nature* **1995**, *378*, 703.

(2) (a) Withersby, M. A.; Blake, A. J.; Champness, N. R.; Cooke, P. A.; Hubberstey, P.; Li, W. S.; Shröder, M. *Inorg. Chem.* **1999**, *38*, 2259. (b) Blake, A. J.; Champness, N. R.; Cooke, P. A.; Nicolson, J. E. B.; Wilson, C. *J. Chem. Soc., Dalton Trans.* **2000**, 3811.

(3) For example: (a) Withersby, M. A.; Blake, A. J.; Champness, N. R.; Hubberstey, P.; Li, W. S.; Schröder, M. *Angew. Chem. Int. Ed.* **1997**, *36*, 2327. (b) Noro, S.; Kitaura, R.; Kondo, M.; Kitagawa, S.; Ishii, T.; Matsuzaka, H.; Yamashita, M. *J. Am. Chem. Soc.* **2002**, *124*, 2568. (c) Chatterton, N. P.; Goodgame, D. M. L.; Grachvogel, D.A.; Hussain, I.; White, A. J. P.; Williams, D. J. *Inorg. Chem.* **2001**, *40*, 312.

(4) Bu, X. H.; Chen, W.; Hou, W. F.; Du, M.; Zhang, R. H.; Brisse, F. *Inorg. Chem.* **2002**, *41*, 3477.

(5) (a) Reed, C. A. *Acc. Chem. Res.* **1998**, *31*, 133. (b) Turner, B.; Shterenberg, A.; Kapon, M.; Suwinska, K.; Eichen, Y. *J. Chem. Soc., Chem. Commun.* **2001**, 13. (c) Beer, P. D.; Gale, P. A.; *Angew. Chem. Int. Ed.* **2001**, *40*, 486. (d) Gale, P. A. *Coord. Chem. Rev.* **2000**, *199*, 181.

(6) (a) Wu, H. P.; Janiak, C.; Rheinwald, G.; Lang, H. *J. Chem. Soc., Dalton Trans.* **1999**, 183.

(b) Janiak, C.; Uehlin, L.; Wu, H. P.; Klüfers, P.; Piotrowski, H.; Scharmann, T. G. *J. Chem. Soc., Dalton Trans.* **1999**, 3121.

(7) (a) Awaleh, M. O.; Badia, A.; Brisse, F. *Cryst. Growth Des.* **2005**, *5*, 1897.
(b) Awaleh, M. O.; Badia, A.; Brisse, F. *Inorg. Chem.* **2005**, *44*, 7833.

(8) (a) Jung, O. S.; Kim, Y. J.; Lee, Y. A.; Park, K. M.; Lee, S. S. *Inorg. Chem.* **2003**, *42*, 844. (b) Jung, O. S.; Kim, Y. J.; Park, J. Y.; Choi, S. N. *J. Mol. Struct.* **2003**, *657*, 207.

(9) (a) Awaleh, M. O.; Badia, A.; Brisse, F. *Acta Crystallogr.* **2005**, *E61*, o2479. (b) Chen, W.; Hou, B. H.; Zhou, L. N.; Wang, J. K.; Li, H. *Acta Crystallogr.* **2005**, *E61*, o1890. (c) Awaleh, M. O.; Badia, A.; Brisse, F. *Acta Crystallogr.* **2005**, *E61*, o2476. (d) Awaleh, M. O.; Badia, A.; Brisse, F. *Acta Crystallogr.* **2005**, *E61*, o2473. (e) Chen, W.; Yin, Q.-X.; Xie, C.; Wang, J.-K.; Li, H. *Acta Crystallogr.* **2004**, *E60*, o2147.

(10) Hartley, F. R.; Murray, S. G.; Levason, W.; Soutter, H. E.; McAuliffe, C. A. *Inorg. Chim. Acta* **1979**, *35*, 265.

(11) SAINT Release 6.06, Integration Software for Single Crystal Data. Bruker AXS Inc.: Madison, WI, 1999.

(12) Sheldrick, G. M. SADABS Bruker Area Detector Absorption Corrections. Bruker AXS Inc.: Madison, WI, 1996.

(13) XPREP Release 5.10; X-ray Data Preparation and Reciprocal Space Exploration Program. Bruker AXS Inc., Madison, WI, 1997.

(14) SHELXTL Release 5.10, The Complete Software Package for Single-Crystal Structure Determination. Brucker AXS Inc.: Madison, WI, 1997.

(15) (a) Sheldrick, G. M. SHELXS97, Program for the Solution of Crystal Structures. University of Göttingen: Göttingen, Germany, 1997. (b) Sheldrick, G. M. SHELXL97, Program for the Refinement of Crystal Structures. University of Göttingen: Göttingen, Germany, 1997.

(16) Griffin, R. G.; Ellett, Jr., J. D.; Mehring, M.; Bullitt, J. G.; Waugh, J. S. *J. Chem. Phys.* **1972**, *57*, 2147.

(17) Porterfield, W. W. *Inorganic Chemistry: A Unified Approach*, Addison-Wesley, 1984, p.168, 180.

(18) Hong, M.; Su, W.; Cao, R.; Zhang, W.; Lu, J. *Inorg. Chem.* **1999**, *38*, 600.

(19) Blake, A. J.; Champness, N. R.; Howdle, S. M.; Webb, P. B. *Inorg. Chem.* **2000**, *39*, 1035.

(20) Liao, S.; Su, C. Y.; Yeung, C. H.; Xu, A. W.; Zhang, H. X.; Liu, H. Q. *Inorg. Chem. Commun.* **2000**, *3*, 405.

(21) Ahmed, L. S.; Dilworth, J. R.; Miller, J. R.; Wheatley, N. *Inorg. Chim. Acta* **1998**, *278*, 229 and references therein.

(22) (a) Vanier, M. M.Sc. Thesis, Department of Chemistry, Université de Montréal. 1982. (b) Pineault, C. M.Sc. Thesis, Department of Chemistry, Université de Montréal. 1982.

(23) Effendy, Nicola, C. D.; Nitiatmodjo, M.; Pettinari, C.; Skelton, B. W.; White, A. H. *Inorg. Chim. Acta* **2005**, *358*, 735.

(24) Szlyk, E.; Szymanska, I.; Surdykowski, A.; Glowiak, T.; Wojtczak, A.; Golinski, A. *J. Chem. Soc., Dalton Trans.* **2003**, 3404 and references therein.

(25) Johnston, D. H.; Shriver, D. F. *Inorg. Chem.* **1993**, *32*, 1045.

(26) Lawrance, G. A. *Chem. Rev.* **1986**, *86*, 17 and references therein.

(27) Batchelor, R. J.; Ruddick, J. N. R.; Sams, J. R.; Aubke, F. *Inorg. Chem.* **1977**, *16*, 1414 and references therein.

(28) Zhong, J. C.; Munakata, M.; Kuroda-Sowa, T.; Maekawa, M.; Suenaga, Y.; Konaka, H. *Inorg. Chem.* **2001**, *40*, 3191.

(29) Nakamoto, K. *Infrared Spectra of Inorganic and Coordination Compounds*. 3rd ed. Wiley-VCH: New York, 1978.

(30) Rosenthal, M. R. *J. Chem. Educ.* **1973**, *50*, 331 and references therein.

(31) (a) Blake, A. J.; Champness, N. R.; Cooke, P. A.; Nicolson, J. E. B.; Wilson. C. *J. Chem. Soc., Dalton Trans.* **2000**, 3811. (b) Withersby, M. A.; Blake, A. J.; Champness, N. R.; Cooke, P. A.; Hubberstey, P.; Li, W. S.; Schröder, M. *Angew. Chem. Int. Ed.* **1997**, *36*, 2327

(32) Black, J. R.; Champness, N. R.; Levason, W.; Reid, G. *J. Chem. Soc. ,Chem. Comm.* **1995**, 1277.

(33) Black, J. R.; Champness, N. R.; Levason, W.; Reid, G. *J. Chem. Soc., Dalton Trans.* **1995**, 3439.

(34) Chen, W.; Du, M.; Zhang, R. H.; Bu, X. H. *Acta Crystallogr.* **2001**, *E57*, m213.

(35) Du, M.; Zhao, X. J. *Acta Crystallogr.* **2004**, *E60*, m193.

(36) Bu, X. H.; Hou, W. F.; Du, M.; Chen, W.; Zhang, R. H. *Cryst Growth Des.* **2002**, *2*, 303.

(37) Karpova, E. V.; Boltalin, A.I.; Korenev, Yu. M.; Troyanov, S.I. *Russ. J. Coord. Chem.* **1999**, *25*, 65.

(38) Chen, W.; Du, M.; Bu, X. H.; Zhang, R. H.; Mak, T. C. W. *CrystEngComm.* **2003**, *5*, *20*, 96.

(39) Blakeslee, A. E.; Hoard, J. L. *J. Am. Chem. Soc.* **1956**, *78*, 3029.

(40) (a) Powell, J.; Horvarth, M. J.; Lough, A.; Phillips, A.; Brunet, J. *J. Chem. Soc., Dalton Trans.* **1998**, 637. (b) Bosch, E.; Barnes, C. L. *Inorg. Chem.* **2001**, 2468. (c) Brammer, L.; Burgard, M. D.; Rodger, C. S.; Swearingen, J. K.; Rath, N. P. *J. Chem. Soc., Chem. Comm.* **2001**, 2468. (d) Brammer, L.; Burgard, M. D.; Eddleston, M. D.; Rodger, C. S.; Rath, N. P.; Adams, H. *CrystEngComm.* **2002**, *4*, 239. (e) Brandys, M.-C.; Puddephatt, R. J. *J. Am. Chem. Soc.* **2002**, *124*, 3946.

(41) (a) Wang, Q. M.; Mak, T. C. W. *J. Am. Chem. Soc.* **2001**, *123*, 7594. (b) Ara, I.; Bahij, F.; Lachkar, M. *Acta Crystallogr.* **2003**, *C59*, m265.

(42) Schultheiss, N.; Powell, D. R.; Bosch, E. *Inorg. Chem.* **2003**, *42*, 5304.

(43) Wang, Q. M.; Guo, G. C.; Mak, T. C. W. *J. Cluster Sci.* **2002**, *13*, 63.

(44) Zhang, X.; Guo, G. C.; Zheng, F. K.; Zhou, G. W.; Mao, J. G.; Dong, Z. C.; Huang, J. S.; Mak, T. C. W. *J. Chem. Soc., Dalton Trans.* **2002**, 1344 and references therein.

(45) Schmidbaur, H. *Chem. Soc. Rev.* **1995**, 391.

(46) Coggon, P.; McPhail, A. T. *J. Chem. Soc., Chem. Comm.* **1972**, 91

(47) Chen, X. M.; Mak, T. C. W. *J. Chem. Soc., Dalton Trans.* **1991**, 1219.

4.2 Supramolecular architectures based on the self-assembly of dithioethers building blocks and silver(I) salts: syntheses, structures and thermal stability.[†]

4.2.1 Abstract

The reaction of 1,3-bis(phenylthio)propane, $\mathbf{L^{3\text{-}Ph}}$, with silver(I) tetrafluorosuccinate and the trifluoromethanesulfonate yields the 2D-coordination network **1**, $[Ag_6(\mathbf{L^{3\text{-}Ph}})_3(CO_2CF_2CF_2CO_2)_3]_\infty$, and **2**, $[Ag_5(\mathbf{L^{3\text{-}Ph}})_2(CF_3SO_3)_5(CH_3COCH_3)_2]_\infty$, respectively. The self-assembly of the smaller organic connector, bis(methylthio)methane, $\mathbf{L^{1\text{-}Me}}$, with 1-naphthalenesulfonate silver(I) leads to the formation of the 1D-coordination polymer **3**, $[Ag\mathbf{L^{1\text{-}Me}}(C_{10}H_7SO_3)]_\infty$. The reaction of 1,2-bis(phenylthio)ethane, $\mathbf{L^{2\text{-}Ph}}$, and silver(I) nitrate gives rise to the 1D-tubular coordination polymer, **4**, $[Ag_{10}(\mathbf{L^{2\text{-}Ph}})_4(NO_3)_{10}]_\infty$. The 2D-coordination networks of both **1** and **2** consist of two meshed networks, $(Ag\text{-anion})_\infty$ and $(Ag\text{-ligand})_\infty$, which share their silver atoms. In complex **1**, the silver tetraflurosuccinate form a 2D-coordination network, $[Ag\text{-}OOCCF_2CF_2COO]_\infty$, in which the silver-silver distances, ranging from 2.9474(4) to 3.2807(5) Å, may indicate some weak argentophilicity. The second network contains the silver atoms and the $\mathbf{L^{3\text{-}Ph}}$ ligand, $[Ag\text{-}\mathbf{L^{3\text{-}Ph}}]_\infty$. There are two sub-networks in **2**, $[Ag\text{-}CF_3SO_3]_\infty$ and $[Ag\text{-}\mathbf{L^{3\text{-}Ph}}]_\infty$, which again share their silver atoms. The acetone molecules are coordinated to the silver atoms. In **2**, the silver atoms adopt different coordination modes: tetrahedral, trigonal bipyramidal, and the less common square-planar. In addition, this complex is a solvent-induced supramolecular isomer.

In **3**, $[Ag\mathbf{L^{1\text{-}Me}}]_2$ dimers are generated when two adjacent silver atoms are dibridged by two bis(methylthio)methane ligands, $\mathbf{L^{1\text{-}Me}}$. These dimers are connected by two 1-naphthalenesulfonate anions, thus yielding a 1D-coordination polymer. The short silver-silver separation, 3.248(2) Å, may be related to a very weak metal-metal interaction. In **4**, the nitrate ions possess several coordination modes. In the monodentate case, a nitrate oxygen is tetrahedrally coordinated to silver, while in the bridging mode the anion participates in the formation of the coordination polymer. The stoichiometry of **4** depends on the initial metal-to-ligand ratio of the starting materials, while the stoichiometries of **1-3** do not. The thermogravimetric analyses of **1** and **2** reveal that they decompose in a single

[†] Awaleh, M. O.; Badia, A.; Brisse, F. *CrystEngComm.* Soumis pour publication. **2007**.

step to metallic silver. Complex **3** shows a two-step weight loss in the range of 80-215 °C. The first step leads to the formation of an intermediate compound, $[Ag_3(\mathbf{L}^{1\text{-}Me})_2(C_{10}H_7SO_3)_3]$, between 80-150 °C. This, in turn, undergoes a further decomposition to produce metallic silver. Compound **4** displays a more complex weight loss. The $\mathbf{L}^{2\text{-}Ph}$ ligands are lost first, followed by the nitrate anions, leaving Ag at 400 °C.

4.2.2 Introduction

The organic-inorganic supramolecular hybrid architectures produced by the spontaneous self-assembly of inorganic metal centres and organic building blocks is a field of considerable current interest because of its relationship to materials science.[1,2]

The interest underlying the design and synthesis of metal-organic frameworks (MOFs) is to control the size and shape of the supramolecular products so as to build extended solid-state functional materials with tunable physical properties. However, there is still a long way to go before the synthesis of a coordination polymer with a predictable topology, and therefore desirable functionality, is achieved. Nevertheless, the synthesis and characterization of new MOFs, as well as the study of the factors determining their structural complexity will contribute to the growing body of knowledge concerning the parameters that affect the topology of metal-organic polymers. There are several factors that influence the topology of the expected metallosupramolecular architectures.[3] In order to study the factors that affect the topology of the coordination polymers, it is necessary to undertake a systematic investigation of the self-assembly of a given set of organic building blocks and a selected metal center which has some affinity to the organic spacers. In this context, we have undertaken to study the parameters that influence the formation of coordination polymers, made up of flexible dithiolate ligands, $RS(CH_2)_nSR$, $\mathbf{L}^{n\text{-}R}$, where n is the number of CH_2 groups and R is an alkyl or an aryl group, and silver(I) centers.
The parameters under investigation are: the type of anions, the length of the organic building blocks, the metal-to-ligand ratio, as well as the recrystallization solvent.[4-7]

An understanding of the factors that control the supramolecular isomerism in MOFs is a major issue in modern crystal engineering.[2d] We have noted the existence of solvent-induced supramolecular isomerism with sulfonate-bearing anions, bis(phenylthio)methane, and 1,3-bis(phenylthio)propane.[4,5] The polar solvents seem to favour the formation of coordination polymers in which the sulfonates adopt a mono-atomic or mono-bridged coordination mode toward the silver(I) centres, while with non-polar solvents, the

sulfonates exhibit a double-bridged coordination mode.[4,5] Therefore, in order to further probe the influence of the solvent polarity upon the supramolecular isomerism, we have used a mixture of polar and non-polar solvents with different ratios as the recrystallization solvent.

Anion control of the solid-state network formation has been achieved in some cases.[8-16] Anions are charged ligands, and the resulting supramolecular architectures may be directed by exploiting their coordinating ability. The group of Schröder, for example, studied a series of coordination polymers based on bis(4-pyridyl)tetrazine. The authors found that the non-coordinating anions, BF_4^- and PF_6^-, did not influence the structure of the polymer. They, however, reported that as the nitrate group bridged silver centers, it was considered as a structure influencing anion.[8]

We report here on the structure determining role of the anions. Complexes of silver(I) trifluoromethanesulfonate or tetrafluorosuccinate and 1,3-bis(phenylthio)propane, are characterized by the presence of the combination of two sub-networks, $(Ag\text{-ligand})_\infty$ and $(Ag\text{-anion})_\infty$ which share their silver atoms. Are these structures more stable? A thermogravimetric investigation was thus undertaken in order to determine whether the coexistence of the two sub-networks $(Ag\text{-anion})_\infty$ and $(Ag\text{-ligand})_\infty$ increases the structure's thermal stability compared to that of complexes formed exclusively of a $(Ag\text{-ligand})_\infty$ network, where the anions are coordinated to the metal.

We report herein the syntheses and characterization of four new silver-dithiolate supramolecular architectures based on the self-assembly of bis(methylthio)methane, 1,2-bis(phenylthio)ethane, and 1,3-bis(phenylthio)propane with different silver(I) salts. The following complexes were obtained: $[Ag_6(\mathbf{L}^{\mathbf{3\text{-}Ph}})_3(CO_2CF_2CF_2CO_2)_3]_\infty$, **1**; $[Ag_5(\mathbf{L}^{\mathbf{3\text{-}Ph}})_2(CF_3SO_3)_5(CH_3COCH_3)_2]_\infty$, **2**; $[Ag\mathbf{L}^{\mathbf{1\text{-}Me}}(C_{10}H_7SO_3)]_\infty$, **3**; $[Ag_{10}(\mathbf{L}^{\mathbf{2\text{-}Ph}})_4(NO_3)_{10}]_\infty$, **4**.

4.2.3 Experimental Section

Materials and General Methods. Bis(methylthio)methane, 1,2-bis(phenylthio)ethane, and 1,3-bis(phenylthio)propane were synthesized according to a method reported in the literature.[17] The other reagents required for the syntheses were commercially available and employed without further purification. The elemental analyses were performed by the Laboratoire d'Analyse Élémentaire (Université de Montréal), and IR spectra were

measured on a Perkin-Elmer 1750 FTIR spectrometer (4000-450 cm^{-1}), with samples prepared as KBr pellets for the solid complexes, while NaCl plates were used for liquid samples. The ^{1}H (300 MHz) and ^{19}F (376.31 MHz) solution NMR spectra were recorded on a Bruker AV300 spectrometer at 25 °C. ^{1}H chemical shifts are reported in parts per million and are referenced to residual solvent signals of the following deuterated solvents: DMSO (δ_{1H} = 2.50) and acetone (δ_{1H} = 2.05). The chemical shifts were referenced to $C_6H_5CF_3$ (-63.9 ppm) for ^{19}F. The thermogravimetric analyses were performed, under a nitrogen atmosphere, on a TG Instrument 2950 TGA HR V5.3C thermal analyzer at a scan rate of 10 °C min^{-1}. The X-ray powder diffraction patterns were recorded at a scan rate of 0.02 $(2\theta)^{\circ}$ s^{-1}on a D8 Discover diffractometer at 25 °C, using CuKα radiation (40 kV, 40 mA).

Syntheses. **Bis(methylthio)methane, $L^{1\text{-}Me}$**. Oil. Yield: 41%. Anal. Found: C, 33.45; H, 7.32. Calcd for $C_3H_8S_2$: C, 33.29; H, 7.45. ^{1}H NMR (DMSO-d_6, 300 MHz): δ 2.16 (*s*, 6H, CH_3-S-CH_2-S-CH_3), 3.63 (*s*, 2H, CH_3-S-CH_2-S-CH_3). IR (KBr, cm^{-1}): 2973m, 2915s, 2855m, 2828m, 2756w, 2588w, 2380w, 2269w, 2181w, 2128w, 2076w, 2034w, 1671w, 1435m, 1422m, 1384m, 1316m, 1203s, 1154m, 1123w, 985m, 958m, 805m, 745s, 693s, 648w.

1,2-bis(phenylthio)ethane, $L^{2\text{-}Ph}$. White powder. Yield: 43%. Anal. Found: C, 68.25; H, 6.09. Calcd for $C_{14}H_{14}S_2$: C, 68.24; H, 5.73. ^{1}H NMR (acetone-d_6, 300 MHZ): δ 3.16 (*s*, 4H, -S-$(CH_2)_2$-S-), 7.23-7.37 (*m*, 10H, C_6H_5-). IR (KBr, cm^{-1}): 3411w, 3055w, 1580s, 1478s, 1436s, 1207m, 1185w, 1152w, 1121w, 1085w, 1071w, 1023m, 893w, 734vs, 714w, 690s, 476m.

1,3-bis(phenylthio)propane, $L^{3\text{-}Ph}$. Oil. Yield: 82%. Anal. Found: C, 69.36; H, 6.35. Calcd for $C_{15}H_{16}S_2$: C, 69.18; H, 6.19. ^{1}H NMR (DMSO-d_6, 300 MHz): δ 2.02 (qt, 2H, -S-CH_2-CH_2-CH_2-S-), 3.08 (t, 4H, -S-CH_2-CH_2- CH_2-S-), 7.15-7.36 (*m*, 10H, C_6H_5-).

IR (KBr, cm^{-1}): 3052m, 2917m, 2849w, 2668w, 2604w, 1943w, 1871w, 1792w, 1583m, 1479m, 1438m, 1342w, 1297m, 1255m, 1201w, 1183w, 1155w, 1089m, 1069w, 1024m, 1000w, 957w, 895w, 836w, 736m, 689m.

$[Ag_6(L^{3\text{-}Ph})_3(OOCCF_2CF_2COO)_3]_\infty$ (1). An amount of 283 mg (1.50 mmol) of tetrafluorosuccinic acid was added to 708 mg (2.53 mmol) of silver carbonate in 10 mL of acetone. The mixture was vigorously stirred and then filtered in order to remove the unreacted Ag_2CO_3. To this filtrate was added a solution of $L^{3\text{-}Ph}$ (0.4 mL, 1.6 mmol) and the reaction mixture was refluxed at 70°C for 6 hours. The resulting solution was filtered

and recrystallized by diffusion of diethyl ether into the solution at room temperature. Single crystals suitable for X-ray analysis were grown over a few days. Yield: 42 % based on $HOOCCF_2CF_2COOH$. Anal. Found: C, 34.33: H, 2.29. Calculated for $C_{57}H_{48}Ag_6F_{12}O_{12}S_6$: C, 34.36; H, 2.43. ^1H NMR (acetone-d_6, 300 MHz): δ 2.04 (qt, 2H, -S- (CH_2)-(CH_2)-), 3.11 (t, 4H, -S- (CH_2)-), 7.16-7.37 (*m*, 10H, C_6H_5-).

$^{19}F\{^1H\}$ NMR (acetone-d_6, 376.31 MHz): δ -118.3 (CF_2). IR (KBr, cm^{-1}): 3439m, 3057w, 2918w, 1684vs, 1584w, 1480m, 1439m, 1418m, 1407, 1260m, 1196w, 1148w, 1105s, 1089m, 1025w, 985m, 821m, 770m, 739s, 690m, 633w, 607w, 520w, 492w.

$[Ag_5(L^{3\text{-}Ph})_2(CF_3SO_3)_5(CH_3COCH_3)_2]_\infty$ (2). To a solution of $AgCF_3SO_3$ (614 mg, 2.39 mmol) in acetone (5 mL) was added a solution of $L^{3\text{-}Ph}$ (0.30 mL, 1.31 mmol) in diethyl ether (5 mL). The mixture was refluxed at 60 °C for 160 min, then layered on a mixture of 1:1 petroleum ether and diethyl ether in covered container, and left to stand at room temperature. Crystals suitable for an X-ray study appeared after about five weeks. Yield: 81 % based on $AgCF_3SO_3$. Anal. Found: C, 25.90; H, 1.89. Calculated for $C_{41}H_{44}Ag_5F_{15}O_{17}S_9$: C, 25.63; H, 2.31. ^1H NMR (DMSO-d_6, 300MHz): 2.04 (qt, 2H, -S-(CH_2)-(CH_2)-), 2.09 (*s*, 6H, CH_3-CO-CH_3), 3.12 (t, 4H, -S-(CH_2)-), 7.16 - 7.37 (*m*, 10H, C_6H_5-).

$^{19}F\{^1H\}$ NMR (DMSO-d_6, 376.31 MHz): -78.8 (s, **F**-C). IR (KBr, cm^{-1}): 3421w, 3055w, 2925w, 1713w, 1582s, 1479s, 1437s, 1390m, 1254vs, 1180s, 1086m, 1071w, 1027s, 884w, 815m, 469w, 733s, 687s, 643s, 580w, 518m, 473m.

$[AgL^{1\text{-}Me}(C_{10}H_7SO_3)]_\infty$ (3). This complex was synthesized by the self-assembly of $L^{1\text{-}Me}$ and the reaction product of 1-naphthalenesulfonic acid and Ag_2CO_3.

The 1-naphthalenesulfonic acid (345 mg, 1.66 mmol) and silver carbonate (760 mg, 2.76 mmol) were combined in 5 mL of acetone and stirred at room temperature for 3 h. The filtrate was then mixed with a solution of $L^{1\text{-}Me}$ (0.30 mL, 2.935 mmol) in diethyl ether (5 mL) and the mixture was refluxed at 70 °C for 2 h. The resulting solution was filtered and recrystallized by diffusion of petroleum ether into the solution. Single crystals suitable for X-ray analysis were found within a few days. Yield: 59% based on $C_{10}H_7SO_3H$. Anal. Found: C, 36.99; H, 3.69. Calcd for $C_{13}H_{15}AgS_3O_3$: C, 36.88; H, 3.57. No NMR spectra is reported for **3** since this complex could not be solubilized.

IR (KBr, cm^{-1}): 3522m, 3089w, 3053w, 3010w, 2975w, 2915w, 2854w, 1714vw, 1645w, 1621w, 1505m, 1431w, 1384w, 1346w, 1262w, 1204vs, 1190s, 1163m, 1150m, 1068m, 1058s, 1023w, 986w, 972w, 864w, 826w, 801s, 769s, 693s, 622s, 569w, 523m.

$[Ag_{10}(L^{2\text{-Ph}})_4(NO_3)_{10}]_\infty$ (**4**). To a solution of $AgNO_3$ (187 mg, 1.10 mmol) in methanol (5 mL) was added a solution of $L^{2\text{-Ph}}$ (109 mg, 0.44 mmol) in diethyl ether (5 mL). The mixture was refluxed at 60 °C for 90 min and then filtered. The filtrate was kept at room temperature in covered container. After a few days, crystals suitable for X-ray analysis were found. Yield: 76 % based on $AgNO_3$. Anal. Found: C, 24.97: H, 1.96; N, 5.09. Calculated for $C_{56}H_{56}Ag_{10}N_{10}O_{30}S_8$: C, 25.06; H, 2.10; N, 5.22. ^{1}H NMR (acetone-d_6, 300 MHz): 3.28 (*s*, 4H, -S-(CH_2)$_2$-S-), 7.37-7.62 (*m*, 10H, C_6H_5-). IR (KBr, cm^{-1}): 3437m, 3055w, 2925w, 2853w, 1631m, 1580m, 1479m, 1437m, 1384vs, 1262w, 1207w, 1153w, 1085w, 1023w, 905w, 860w, 824w, 809w, 734m, 689m, 476w.

Crystal Structure Determinations. X-ray crystallographic data of the complexes **1** and **2** were acquired on a Brucker AXS Platform diffractometer equipped with a SMART 2K CCD area detector using monochromatic Cu Kα (λ = 1.54178 Å), while for complexes **3** and **4**, the X-ray intensity data were obtained on a SMART 6K CCD equipped with a rotating anode (Cu Kα) and a Mirror Montel 200 Optics as monochromator. The program SAINT[18] was used for the data reduction processing. An empirical absorption correction, based on the multiple measurements of equivalent reflections, was applied using the program SADABS.[19] The space group was confirmed by the XPREP[20] routine in the program SHELXTL.[21] The structures were solved by direct methods and difference Fourier techniques with SHELXS-97.[22] The refinements were done on F^2 by full matrix least squares. In complex **2**, the thermal parameters of the carbon atom of one triflate anion were found to be high because of disorder. Thus, the thermal displacement parameters of this carbon, as well as the C-S distance of this anion, were constrained such that they kept the same values as those in the corresponding entities from a non-disordered triflate anion (EADP[22] and SADI[22]). Crystal data and data collection parameters are listed in Table 1.

All non-hydrogen atoms were refined anisotropically, while the hydrogen atoms were introduced at calculated positions and were included in the refinement in the riding-model approximation, with U_{iso}(H) = 1.5U_{eq}(C) for methyl groups and U_{iso}(H) = 1.2U_{eq}(C) for others. A final verification of possible voids was performed with the VOID routine of the Platon program,[23] which indicated a void of 37 Å^3 in complex **1**. The SQUEEZE[23] procedure of the Platon program showed the presence of two cavities of 37 Å^3, each occupied by two electrons which indicated the non-occurence of any solvent molecules in the cavities.

Table 4.2.1. Crystal data and X-ray data collection parameters.

	1	2	3	4
formula	$C_{57}H_{48}Ag_6F_{12}O_{12}S_6$	$C_{41}H_{44}Ag_5F_{15}O_{17}S_9$	$C_{13}H_{15}AgO_3S_3$	$C_{56}H_{56}Ag_{10}N_{10}O_{30}S_8$
mol wt	1992.53	1921.65	423.30	2684.29
cryst size (mm)	0.39x0.14x0.07	0.34x0.10x0.04	0.18x0.02x0.02	0.14x0.10x0.07
cryst syst	*monoclinic*	*monoclinic*	*monoclinic*	*monoclinic*
space group	$P2_1/c$	$P2_1/c$	$P2_1/c$	$P2_1/n$
a (Å)	10.4359(2)	17.4256(2)	8.3129(2)	9.6877(2)
b (Å)	23.9932(4)	24.3524(3)	21.5540(5)	25.1542(6)
c (Å)	25.6039(4)	14.9472(2)	8.9118(2)	32.2345(7)
α (deg)	90	90	90	90
β (deg)	93.868(1)	104.595(1)	110.390(1)	96.929(1)
γ (deg)	90	90	90	90
V (Å^3)	6396.37(19)	6138.24(13)	1496.73(6)	7797.7(3)
Z	4	4	4	4
D(calc) (g cm^{-3})	2.069	2.079	1.879	2.286
F(000)	3888	3760	848	5200
T (K)	100	100	150	150
μ, (mm^{-1})	17.122	16.427	14.752	22.452
θ_{max} (deg)	72.64	72.98	68.69	68.64
$R1$[a] [$I > 2\sigma(I)$]	0.0343	0.0421	0.0646	0.0412
Rw[b] [$I > 2\sigma(I)$]	0.0871	0.0984	0.1924	0.0963
R [*all data*]	0.0414	0.0614	0.0809	0.0690
Rw [*all data*]	0.0896	0.1199	0.1988	0.1051
S[c]	1.013	0.820	1.130	0.922

[a] $R = \Sigma \, || F_o | - | F_c || / \Sigma \, | F_o |$. [b] $Rw = [\Sigma \, w(F_o^2 - F_c^2)^2 / \Sigma \, w(F_o^2)^2]^{1/2}$.
[c] $S = [\Sigma \, w(F_o^2 - F_c^2)^2 / (m-n)]^{1/2}$ (m is the number of reflections and n the number of parameters).

4.2.4 Results and Discussion

In earlier works we have reported the supramolecular networks based on the 1,3-bis(phenylthio)propane, $\mathbf{L}^{\mathbf{3\text{-}Ph}}$, and the bis(phenylthio)methane, $\mathbf{L}^{\mathbf{1\text{-}Ph}}$, ligands and a variety of silver(I) salts (PF_6^-, SbF_6^-, ClO_4^-, BF_4^-, NO_3^-, $pTsO^-$, $CH_3SO_3^-$, $CF_3SO_3^-$, $CF_3CO_2^-$, $CF_3CF_2CO_2^-$, $CF_3CF_2CF_2CO_2^-$, $^-OOCCF_2CF_2COO^-$).[4, 5] The structures of the networks constructed by the self-assembly of the diarylthioether and the silver(I) salts were found to

be influenced by the length of the organic spacer, $RS(CH_2)_nSR$, the bulk of the R substituent, the solvent of recrystallization, as well as the coordinating strength of the anions.[4-7]

When the Ag(I) perfluorocarboxylates (trifluoroacetate, pentafluoropropionate and heptafluorobutyrate) were reacted with $\mathbf{L^{3\text{-}Ph}}$, $[Ag_2(O_2C(CF_2)_nCF_3)_2]$ (n = 0 – 2) dimers were obtained. These, in turn, were bound to one another by the ligands to form 1D or 2D networks.[4] The same type of dimers were noted when silver(I) heptafluorobutyrate was reacted with $\mathbf{L^{1\text{-}Ph}}$.[5]

We hoped to increase the dimensionality of the networks when the syntheses were made with dicarboxylates instead of monocarboxylates. This strategy was unsuccessful when the bis(methylthio)methane or the bis(phenylthio)methane ligands were used.[5, 7] Success was met, however, with 1,3-bis(methylthio)propane.[7b] Thus, we attempted to synthesize complexes of $\mathbf{L^{3\text{-}Ph}}$ with silver(I) tetrafluorosuccinate, hexafluoroglutarate or tetrafluoroterephthalate. Only complex **1**, containing the silver(I) tetrafluorosuccinate was obtained.

$\mathbf{[Ag_6(L^{3\text{-}Ph})_3(OOCCF_2CF_2COO)_3]_\infty}$ **(1)**. Interestingly, the structure of **1** reveals the participation of all the structural subunits, the anions, the Ag(I) cations and the $\mathbf{L^{3\text{-}Ph}}$ ligands, in the construction of the 2D-network (Figure 4.2.1). The projection of one layer of **1** reveals the existence of two sub-networks. One of them is made up of Ag(I) cations interconnected by the $\mathbf{L^{3\text{-}Ph}}$ organic ligands, $(Ag\text{-ligand})_\infty$ (Figure 4.2.1d) while the other sub-network is constituted of the same Ag(I) cations and the anions, $(Ag\text{-anion})_\infty$ (Figure 4.2.1c). These two networks have the Ag(I) atoms in common and **1** can be described equally well by emphasizing the role of the $\mathbf{L^{3\text{-}Ph}}$ ligands or that of the anions. Seemingly the two sub-units reinforce one another and a more stable complex could be expected.

The repeat unit of the $(Ag\text{-anion})_\infty$ network is a macrocycle (unit **A**) containing four $OOCCF_2CF_2COO$ groups and ten silver(I), $Ag_{10}(OOCCF_2CF_2COO)_4$ (Figure 4.2.1a). In turn, these macrocycles are linked to each other, *via* the lone pair of the oxygen atoms into a double chain which is parallel to the *a*-axis (Figure 4.2.1b). Adjacent double chains are connected by tetrafluorocarboxylates thus generating a 2D-network parallel to the *ab*-plane (Figure 1c). In so doing, another macrocycle, unit **B**, $Ag_{16}(OOCCF_2CF_2COO)_6$, is created.

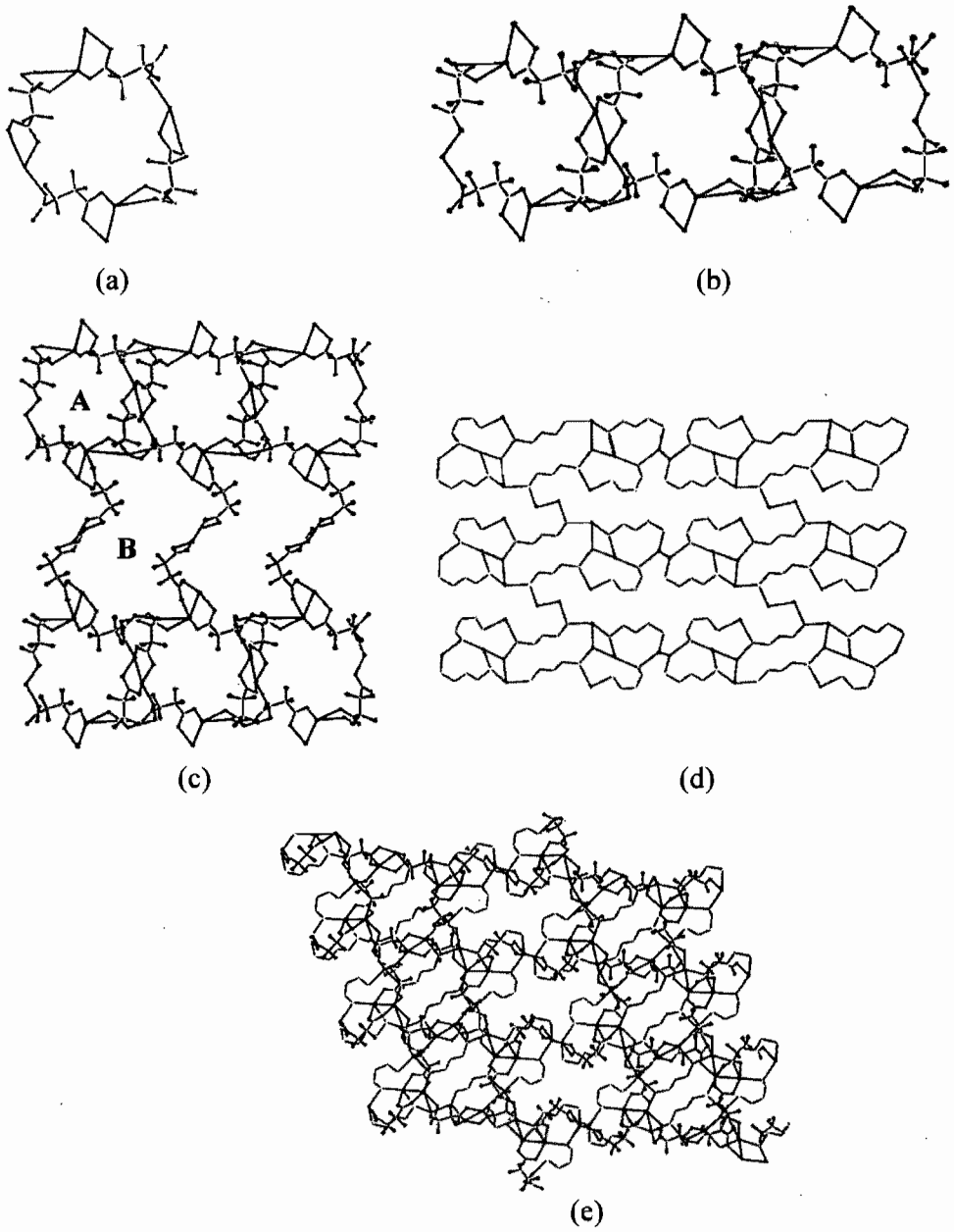

Figure 4.2.1. (a) The repeat of **1** made up of silver(I) centers and tetrafluorosuccinate anions, **A** = $Ag_{10}(OOCCF_2CF_2COO)_4$. (b) The double chain of $(Ag\text{-anion})_\infty$. (c) The 2D-sub-network of $(Ag\text{-anion})_\infty$ and the **B** macrocycle (d) The 2D-sub-network of the $(Ag\text{-ligand})_\infty$. (e) The actual structure where the combined 2D-networks of $(Ag\text{-anion})_\infty$ and $(Ag\text{-ligand})_\infty$ share their silver atoms. (Phenyl groups and H atoms have been removed for clarity).

Previously, we have reported that the 1,4-bis(phenylthio)butane organic ligand, $\mathbf{L}^{4\text{-Ph}}$, formed with the silver(I) trifluoroacetate, a two-dimensional structure that consisted of two intertwined two-dimensional coordination networks. These networks $(Ag\text{-}CF_3CO_2)_\infty$ and $(Ag\text{-}\mathbf{L}^{4\text{-Ph}})_\infty$ could strengthen one another.[6]

Recently, the group of Munakata reported extended solid state networks in which the silver tetrafluorosuccinate formed a one-dimensional columnar coordination polymer $(Ag\text{-anion})_\infty$, $(Ag\text{-}OOCCF_2CF_2COO)_\infty$. In turn, adjacent chains were linked by the [2.2]paracyclophane ligand (pcp) so as to form a two-dimensional coordination polymer. On the other hand, the silver hexafluoroglutarate formed a two-dimensional network made up by the combination of the metal centers and the $^-OOCCF_2CF_2CF_2COO^-$ anions. Furthermore, these sheets were connected to each other by the organic ligand, [2.2]paracyclophane in order to form a microporous 3D-network in which THF molecules were located.[24]

In the structure of **1**, there are six crystallographically different silver(I) atoms. The five silver atoms, Ag(1), Ag(3), Ag(4), Ag(5) and Ag(6), all have a coordination of five with a distorted trigonal bipyramidal environment (Table S1, Annexe VII). Atom Ag(2) is coordinated by three oxygens from two distinct tetrafluorosuccinate groups (Ag(2)-O: 2.271, 2.325(3) and 2.420(4) Å) to a sulfur atom from the ligand (Ag(2)-S: 2.635 Å), and weakly coordinated to two adjacent silver atoms (Ag(2)···Ag: 3.2807(5) and 2.9474(4) Å). Thus, Ag(2) has a coordination of six and adopts a distorted octahedral environment (O-Ag(2)-O: 154.76(11); Ag(1)-Ag(2)-Ag(3): 87.33(1); S-Ag(2)-Ag(1): 116.6(1); O-Ag(2)-S: 104.5(1); O-Ag(2)-Ag(3): 56.9(1)°).

Complex **1** has five relatively short silver-silver distances, ranging from 2.9474(4) to 3.2807(5) Å that are shorter than the sum of the van der Waals radii of two silver atoms (3.40 Å),[25] but slightly longer than 2.89 Å, twice the radius of metallic silver.[25] Such short Ag···Ag separations (3.0502(7) to 3.2459(5) Å long[4]) which have been observed in complexes with the same building block, $\mathbf{L^{3\text{-}Ph}}$, and perfluorocarboxylate anions may indicate weak argentophilic interactions.[16]

$[Ag_5(L^{3\text{-}Ph})_2(CF_3SO_3)_5(CH_3COCH_3)_2]_\infty$ (2). This complex adopts a 2D-coordination network whose sheets are parallel to the (010)-plane (Figure 4.2.2). Its structure reveals, as in **1**, the existence of two sub-networks. One of them is made up of Ag(I) ions interconnected by the $\mathbf{L^{3\text{-}Ph}}$ building blocks, $(Ag\text{-ligand})_\infty$, (Figure 4.2.2a), while the other network is constituted of the same Ag(I) ions and the triflate anions, $(Ag\text{-anion})_\infty$. The repeat unit of the $(Ag\text{-ligand})_\infty$ sub-network is a 30-membered metallomacrocycle,

$Ag_8(L^{3\text{-Ph}})_4S_2$ (Figure S1a, Annexe VII). On the other hand, the neutral $(Ag\text{-anion})_\infty$ sheets have a repeat unit consisting of a 36-membered metallomacrocycle, $Ag_9(CF_3SO_3)_9$ (Figure S1c, Annexe VII). As in complex **1**, these two networks have the Ag(I) atoms in common.

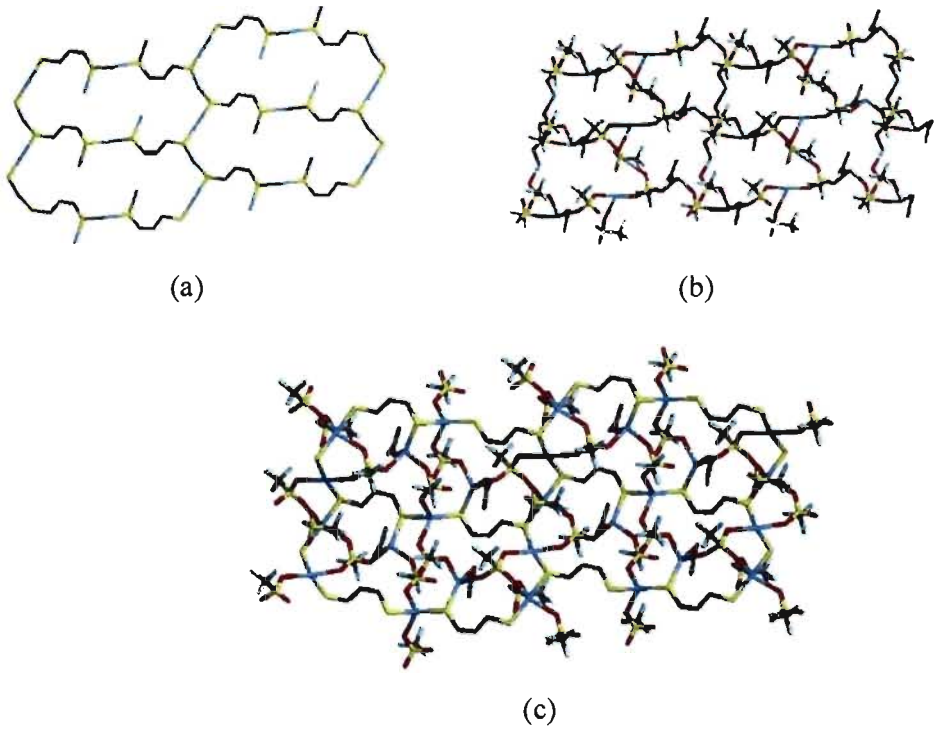

Figure 4.2.2. The two-dimensional network in **2** made up by the combination of: (a) the sub-network consisting of the metal centres and the ligands, $(Ag\text{-ligand})_\infty$ and (b) the two-dimensional sub-network of the metal centres and the trifluoromethanesulfonate anions (Ag-anions). The acetone molecules complete the tetrahedral coordination of some silver(I) atoms. (c) The actual structure where the two (Ag-ligand) and (Ag-anion) networks sharing their silver atoms are combined. (Phenyl groups and H atoms have been removed for clarity).

These complexes may be described equally well by highlighting the role of either the $L^{3\text{-Ph}}$ ligands or that of the anions. The acetone molecules complete the tetrahedral coordination of some silver atoms (Figure 4.2.2b, c).

The group of Shimizu reported the structure of the $Ag(CF_3SO_3)(EtOH)_{0.5}$ complex.[26, 27] We had hoped that it contained the $(Ag\text{-}CF_3SO_3)_\infty$ network as found in **2**. However, in that structure all the sulfonate groups coordinate three silver atoms (Scheme 2c) and thus differ significantly from **2** (Figure S2, Annexe VII).

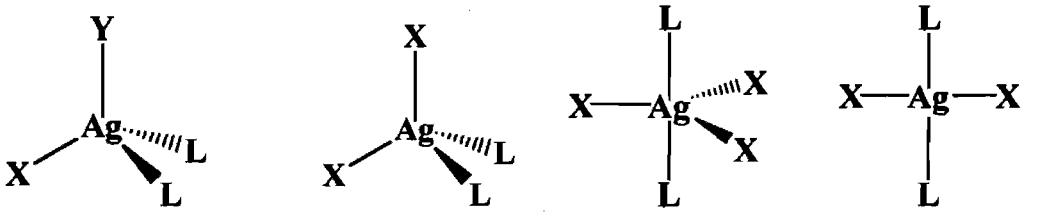

1a (Ag1, Ag3) **1b** (Ag2) **1c** (Ag4) **1d** (Ag5)

Scheme 1. The coordination environment of silver in complex **2**.
L : 1,3-bis(phenylthio)propane; **X** : trifluoromethanesulfonate anion; **Y** : acetone molecule

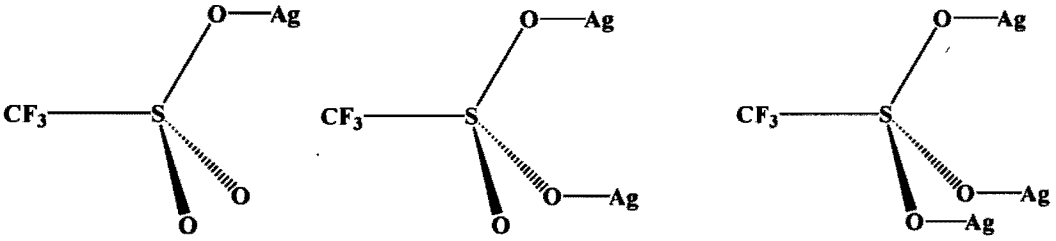

2a **2b** **2c**

Scheme 2. The coordination modes adopted by the trifluoromethanesulfonate anions in complex **2** with 1, 2 or 3 silver atoms respectively.

In complex **2,** the sulfonate anion is linked to either one, two or three silver atoms (Figure 4.2.2c, Scheme 2), and there are five crystallographically distinct silver atoms. Ag(1) is coordinated to one sulfur atom of the 1,3-bis(phenylthio)propane (Ag(1)-S: 2.529(1) Å), to two oxygen atoms from distinct triflate anions (Ag(1)-O: 2.359(4) and 2.501(4) Å), and to one oxygen atom from an acetone molecule (Ag(1)-O: 2.357(4) Å). This silver atom has a distorted tetrahedral environment (O-Ag(1)-O: 93.3(2)°, 128.2(2)° and 83.9(2)°; O-Ag(1)-S: 129.6(1)°) (Scheme 1a, Figure S3). The Ag(2) atom is coordinated to two oxygen atoms from distinct anions (Ag(2)-O: 2.401(4) and 2.479(4) Å) and to two sulfur atoms from different building blocks (Ag(2)-S: 2.455(1) and 2.551(1) Å). Ag(2) has a distorted tetrahedral coordination (O-Ag(2)-S: 124.8(1), 93.8(1), 123.0(1) and 93.5(2)°) (Scheme 1b, Figure S3). The environment of the Ag(3) atom has a strikingly similar environment to that of Ag(1) (Scheme 1a, Figure S3). On the other hand, Ag(4) has a deformed trigonal bipyramidal environment (Scheme 1b, Figure S3, Annexe VII) since the S-Ag(4)-S bond angle, with a value of 176.2(1)°, is approximately linear, and the sum of the three O-Ag(4)-O angles is 352.2°. The Ag(4)-O distances, in the range of 2.597(4) to

2.622(4) Å, fall in the normal interval for the silver(I) diarylthioether complexes (2.268(3)-2.859(8)).[4-7]

In this complex, the Ag(5) atoms present the uncommon square-planar environment as the sum of the angles around Ag(5) is 360.1° (Figure 4.2.3, Scheme 1d). Although this environment is unusual[28], a small number of examples of silver(I) in a square planar coordination has been reported.[29]

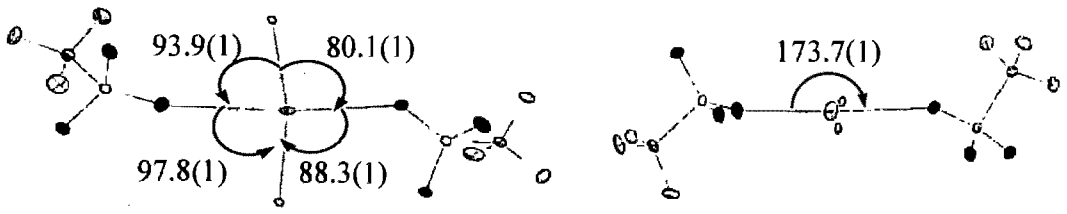

Figure 4.2.3. Two views of the nearly square-planar coordination of Ag(5) in complex **2**.

Supramolecular isomerism. This property was reported for complexes of paratoluenesulfonate, or trifluoromethanesulfonate, anions combined with the $\mathbf{L}^{3\text{-Ph}}$ or the $\mathbf{L}^{1\text{-Ph}}$ ligands.[4,5] The non polar solvents (petroleum ether, hexane, pentane or heptane) brought about structures in which the sulfonate groups participate in a double-bridged coordination mode toward the silver(I) atoms while the polar solvents (diethyl ether) favored the formation of coordination polymers where the sulfonate groups assume a monobridged coordination mode.[4]

However, it is not clear how the polarity of the solvent influences the coordination modes of the silver centres during the crystallization process. In order to gain some insigth on the effect of the solvent polarity upon the crystallization process we decided to use mixtures of polar and non-polar solvent as a recrystallisation medium. Despite the variation of the proportions of the polar and the non-polar solvents, the same complex **2** was always formed. Complex **2** described herein was crystallized from a mixture of diethyl ether and petroleum ether. The sulfonate groups adopt not one but three types of coordination: monoatomic, dibridging as well as the tribridging modes (Scheme 2).

Since the anions bearing the sulfonate groups (paratoluenesulfonate or trifluoromethanesulfonate) display solvent-induced supramolecular isomerism when their silver(I) salts were reacted with 1,3-bis(phenylthio)propane, $\mathbf{L}^{3\text{-Ph}}$, we decided to react this

ligand with 1-naphthalenesulfonate silver(I). Unfortunately, no complex could be obtained with $L^{3\text{-Ph}}$. However, with the $L^{1\text{-Me}}$ organic spacer, a new complex, **3**, was obtained.

$[AgL^{1\text{-Me}}(C_{10}H_7SO_3)]_\infty$ (3). The reaction of the $\mathbf{L^{1\text{-Me}}}$ spacer with 1-naphthalenesulfonate silver(I) lead to the formation of a 1D-coordination polymer. In this complex, two adjacent silver atoms are united by two bis(methylthio)methane ligands, $\mathbf{L^{1\text{-Me}}}$, so as to form the $[Ag(\mathbf{L^{1\text{-Me}}})]_2$ dimer (Figure 4.2.4a). The silver-silver distance in this dimer, 3.248(2) Å, is slightly shorter than the sum of the van der Waals radii of two silver atoms (3.40 Å),[25] hence, this may indicate a weak metal-metal interaction.[16] On the other hand, neighboring $[Ag(\mathbf{L^{1\text{-Me}}})]_2$ dimers were connected to each other by two 1-naphthalenesulfonate silver(I) so as to build up a 1D-coordination polymer extended parallel to the *a*-axis (Figure 4.2.4).

In another description of this complex, the sulfonate groups of the counteranions link two adjacent silver atoms in a dibridging mode, thus forming the $[Ag(C_{10}H_7SO_3)]_2$ dimer. The silver-silver separation is 5.263 Å, indicating that there are no silver-silver interactions in the dimer. Adjacent $[Ag(C_{10}H_7SO_3)]_2$ dimers are linked by one $[Ag(\mathbf{L^{1\text{-Me}}})]_2$ dimer so that a 1D coordination polymer formed by the alternation of these two dimers is generated. The $[Ag(\mathbf{L^{1\text{-Me}}})]_2$ and $[Ag(C_{10}H_7SO_3)]_2$ dimers form an angle of 81.7(2) °; these may be considered to be nearly perpendicular to one another (Figure 4.2.4c). In other words, each of the dimers is almost perpendicular to the ribbon that constitutes the polymeric chain.

The silver atom is coordinated by two oxygen atoms from distinct 1-naphthalensulfonate anions (Ag-O: 2.425(8) and 2.553(7) Å), by two sulfur atoms from different bis(methylthio)methane ligands (Ag-S: 2.471(3) and 2.505(3) Å), and weakly by an adjacent silver atom (Ag-Ag: 3.248(2) Å). Hence, the silver atom adopts a distorted trigonal bipyramidal environment (Table S1, Annexe VII).

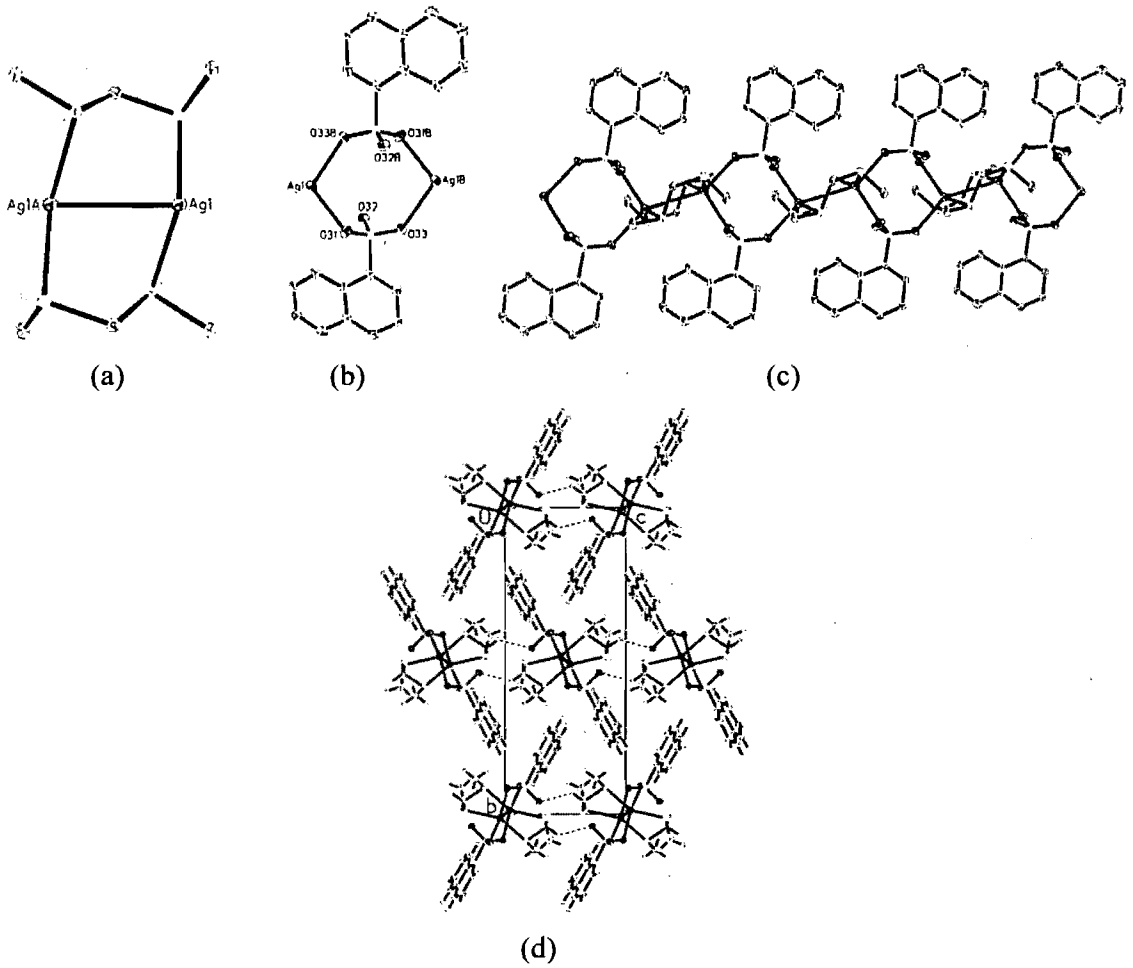

Figure 4.2.4. (a) The $[Ag\text{-}L^{1\text{-}Me}]_2$ dimer of **3**. (b) The $[Ag\text{-}(C_{10}H_7SO_3)]_2$ dimer in **3**. (c) The 1D-coordination polymer of **3** consists of the alternation of the two dimers. (d) The 1D-chains form a 2D-network through hydrogen bonds (shown as dashed lines) between the oxygen atoms of the 1-naphthalensulfonate and the H atoms of the methylene group of the bis(methylthio)methane ligand (C···O(32)^{i}: 3.183 Å and C–H···O(32)^{i}: 127°; symmetry code (i): x, y, 1 + z). The 1D-chains are shown perpendicular to the *bc*-plane. Each chain is surrounded by six others.

On the other hand, there are weak hydrogen bonds between a methylene hydrogen of the building block of one chain (C···O(32)^{i}: 3.183 Å and C–H···O(32)^{i}: 127°; symmetry code (i): x, y, 1 + z) and the sulfonate oxygen atom that is not engaged with the silver(I) centre of an adjacent unit. Thus, each $[AgL^{1\text{-}Me}(C_{10}H_7SO_3)]_\infty$ is surrounded by two others so as to build a neutral 2D network parallel to the *ac*-plane (Figure 4.2.4d). We have previously reported the coordination network $[AgL^{1\text{-}Me}(CH_3SO_3)]_\infty$, which contains $[Ag(L^{1\text{-}Me})]_2$ dimers similar to those found in complex **3**, $[AgL^{1\text{-}Me}(C_{10}H_7SO_3)]_\infty$ (Figure S4, Annexe VII). In addition, $[AgL^{1\text{-}Me}(CH_3SO_3)]_\infty$ and complex **3**, $[AgL^{1\text{-}Me}(C_{10}H_7SO_3)]_\infty$, are

topologically comparable 1D- coordination polymers (Figure S5, Annexe VII). However, complex $[AgL^{1\text{-}Me}(CH_3SO_3)]_\infty$ forms a 3D-coordination network through weak hydrogen bonds, while complex **3**, $[AgL^{1\text{-}Me}(C_{10}H_7SO_3)]_\infty$, forms a 2D-network (Figure S6, Annexe VII). This difference is likely due to the hindrance of the naphthalene groups of the anions in **3**, which prevents the formation of a 3D-network (Figure S6, Annexe VII). Nevertheless, these two complexes have the same hexagonal packing (Figure S6, Annexe VII).

In complex **3**, there are some weak C-H···π interactions between the methyl group of the $L^{1\text{-}Me}$ ligand of one $[AgL^{1\text{-}Me}(C_{10}H_7SO_3)]_\infty$ chain and the naphthalene group of an adjacent chain (H···Cg: 2.686 Å; C-H···Cg: 165.0°). Individual C-H···π and π···π interactions are very weak. However, according to Park *et al.*[30], their cooperative effect makes the structure more stable.Therefore, the weak interactions between neighboring $[AgL^{1\text{-}Me}(C_{10}H_7SO_3)]_\infty$ chains are likely one of the driving forces that make each chain be surrounded by six others (Figure 4.2.4d).[30]

$[Ag_{10}(L^{2\text{-}Ph})_4(NO_3)_{10}]_\infty$ (4). The combination of 1,2-bis(phenylthio)ethane, $L^{2\text{-}Ph}$, and silver nitrate leads to the formation of a tubular coordination polymer parallel to the *a*-axis. The repeat unit of this complex is a 26-membered metallomacrocycle, $Ag_{10}(L^{2\text{-}Ph})_4(NO_3)_{10}$ (Figure 4.2.5a).

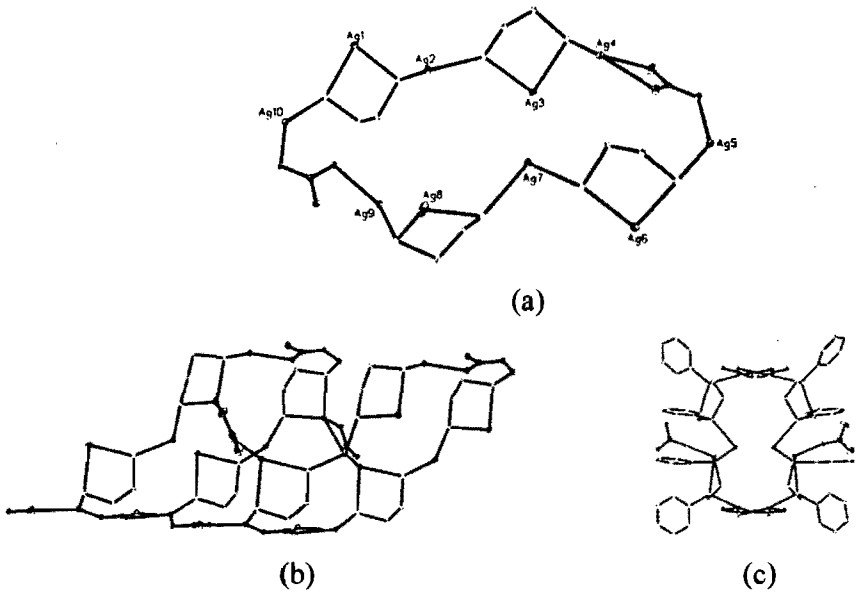

Figure 4.2.5. (a) The 26-membered metallomacrocycle, $Ag_{10}(L^{2\text{-}Ph})_4(NO_3)_{10}$ of complex **4** (the phenyl groups and the hydrogen atoms have been omitted for clarity). (b) The tubular coordination polymer extending parallel to the *a*-axis (the phenyl groups and the hydrogen atoms have been omitted for clarity). (c) Projection of the polymeric tube down the *a*-axis. The nitrates within the tube have been omitted.

Here, the nitrate anions adopt five different coordination modes toward the silver(I) ions (Scheme 3 and Figure S7, Annexe VII). When the nitrate assumes the monodentate or the chelate coordination modes, it completes the tetrahedral coordination of Ag(I), whereas other nitrates with bridging coordination mode allow the connection of neighboring silver atoms, and hence the extension of the network (Figure S8, Annexe VII).

The ligand in **4**, 1,2-bis(phenylthio)ethane, is in the *cis* conformation, although that of the free ligand is *trans* (Figure 4.2.5a).[31] In addition, the phenyl groups of the ligands are located outside the inner part of the polymeric tube, which also contains more nitrates (Figure 4.2.5b).

There are some weak $\pi\cdots\pi$ interactions between the phenyl groups from adjacent ligands (inter center distances, d_c-d_c = 3.666-3.668 Å and inter-planar distances, d-d = 2.496-3.340 Å). The silver atoms adopt the coordination 3 and 4, with a deformed trigonal and tetrahedral coordination. It is of interest to signal that the Ag(I) tubular coordination networks are very scarce.[32]

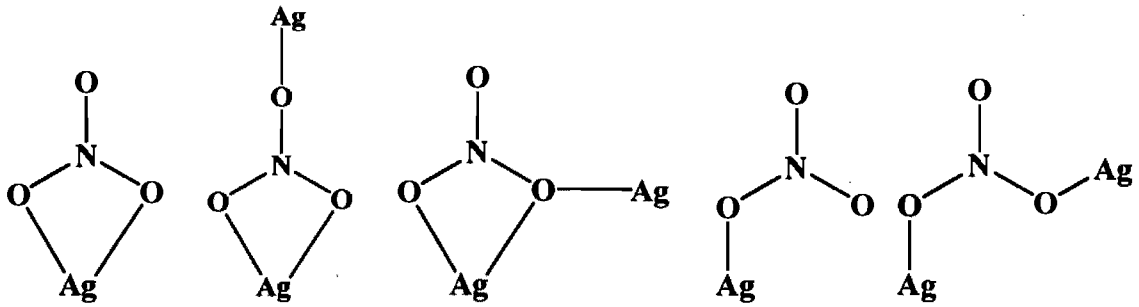

Scheme 3. The five coordinations observed for the nitrate groups in **4**.

Metal-to-ligand ratio. The metal-to-ligand ratio plays a non negligible role upon the formation of metal-based polymers.[33-35] In complexes **1-3**, these ratios were found to be different from those of the starting materials. No matter what the starting metal-to-ligand ratio was, crystals with identical compositions were always obtained, as confirmed by the unit-cell measurements. In the case of complex **4**, the crystals of composition $[Ag_{10}(L^{2\text{-}Ph})_4(NO_3)_{10}]_\infty$, were obtained only for a ratio of 5:2 (metal:ligand) for the starting materials, which is that of the resulting complex.

Infrared Spectroscopy. It is generally accepted that the infrared spectroscopy may be used in order to distinguish the coordination modes of the carboxylate groups.[36, 37] The peaks observed at 1684 and 1418 cm^{-1} in the IR spectrum of **1** are assigned respectively to the characteristic antisymmetric and symmetric stretching bands of the carboxylate group. Furthermore, the value of 266 cm^{-1}, [$\nu_{asym}(CO_2)$ - $\nu_{sym}(CO_2)$], points to the occurrence of the dibridging mode,[38] in agreement with the observation in the crystal structure of complex **1**. On the other hand, in complex **2**, the unambiguous assignment of the vibration modes of the $CF_3SO_3^-$ anion is quite difficult because of the mixing of CF_3 and SO_3 vibrations in the stretching-mode region between 1000 and 1300 cm^{-1}.[39-42] However, in accordance to the literature, the peaks at 1254 and 1027 cm^{-1} for the silver(I) coordination polymers containing the triflate, have been assigned respectively to the $\nu[SO_3(E)]$ and $\nu[SO_3(A_1)]$ vibrations.[39-42] Complex **3**, which includes the 1-naphthalenesulfonate group, has bands at 1190 and 1150 cm^{-1}. These bands are assigned to $\nu[SO_3(E)]$ and $\nu[SO_3(A_1)]$, respectively, following the work of Sharma *et al.* [43] on copper(II) naphthalenesulfonate complexes. These authors observed absorption bands at 1195 and 1137 cm^{-1}. The band at 1384 cm^{-1} in complex **4** is assigned to the $\nu_3(E')$ of the nitrate.[44]

Thermogravimetric Investigation. Thermogravimetric experiments were performed in order to study the thermal stability of the coordination **1-4** complexes. Since complex **1** (and **2**) is made up of two 2D-coordination networks sharing silver atoms, respectively $(Ag\text{-}anion)_\infty$ and $(Ag\text{-}ligand)_\infty$, which could reinforce one another, it was expected that complexes **1** and **2** would be more thermally stable than the previously reported complexes, which only contain one network, the $(Ag\text{-}ligand)_\infty$.

The thermogram of $[Ag_6(\mathbf{L^{3\text{-}Ph}})_3(OOCCF_2CF_2COO)_3]_\infty$ (**1**) is shown in Figure 4.2.6. It reveals a one-step decomposition which starts at about 180°C and is completed at 330°C. The weight loss corresponds to the departure of the $\mathbf{L^{3\text{-}Ph}}$ ligands and the succinate groups (expt/theor = 65.5/67.5%). The TGA curve of **2**, $[Ag_5(\mathbf{L^{3\text{-}Ph}})_2(CF_3SO_3)_5(CH_3COCH_3)_2]_\infty$, is comparable to that of **1**. Complex **2** is stable up to 180°C. The weight loss occurring in the 180-320°C interval corresponds to the removal of the acetones, the $\mathbf{L^{3\text{-}Ph}}$ ligands, and the trifluoromethanesulfonate anions. The remaining residue is metallic silver (expt/theor = 69.6/71.9%) (Figure S9, Annexe VII).

Complex **1** has a thermal behavior nearly identical to that of the perfluorocarboxyalte (trifluoroacetate, pentafluoropropionate and heptafluorobutyrate) complexes of $\mathbf{L}^{\mathbf{3\text{-}Ph}}$, although their structures consist of a single $(Ag\text{-ligand})_\infty$ network.

The same observation can be made for **2**, consisting of $(Ag\text{-ligand})_\infty$ and $(Ag\text{-anion})_\infty$, and its supramolecular isomer, $(Ag\text{-ligand})_\infty$.[4] Thus, the coexistence of the two sub-networks, $(Ag\text{-anions})_\infty$ and $(Ag\text{-ligand})_\infty$, in **1** (or **2**), does not seem to increase its thermal stability. We can speculate that the thermal stability is mainly associated to that of the $(Ag\text{-}\mathbf{L}^{\mathbf{3\text{-}Ph}})_\infty$ network.

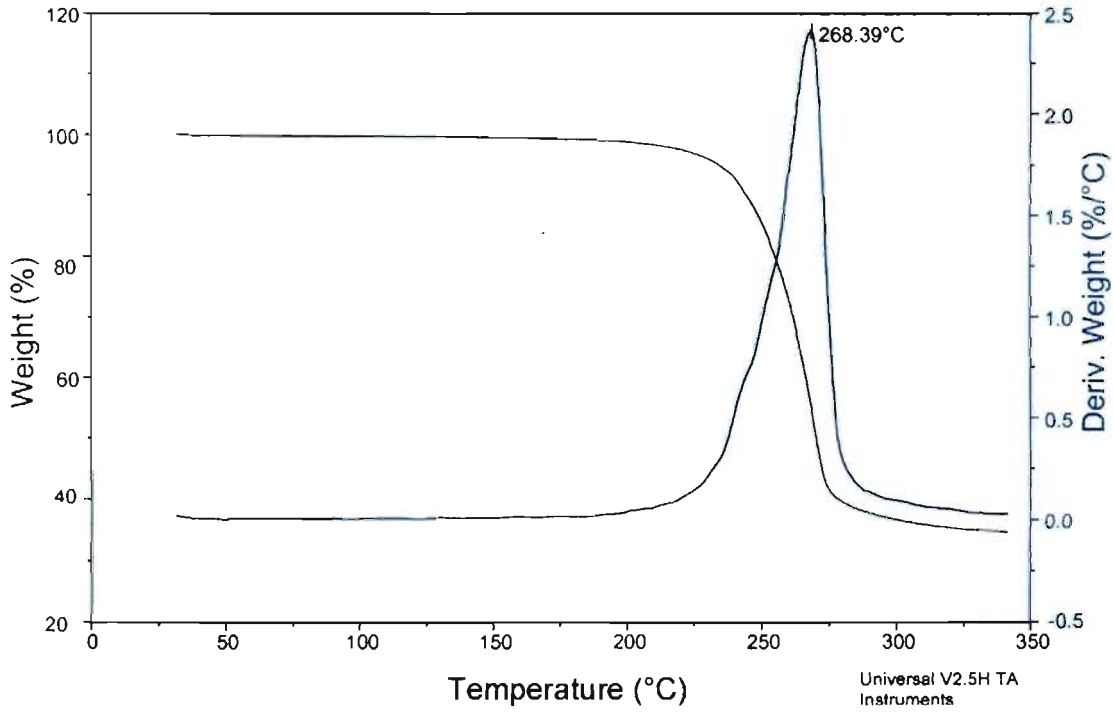

Figure 4.2.6. The TGA and DTGA curves for complex **1** recorded at a heating rate of 10 °C min^{-1}. The ligand $\mathbf{L}^{\mathbf{3\text{-}Ph}}$ and the succinate group of **1** are lost in a single step between 180 and 330 °C. The final product is metallic silver.

The thermogravimetric analysis (TGA) of complex **3**, $[Ag\mathbf{L}^{\mathbf{1\text{-}Me}}(C_{10}H_7SO_3)]_\infty$, shows a two-step weight loss in the temperature range of 80-215°C (Figure 4.2.7). We decided to characterize the product of the first thermal decomposition step.

A sample of complex **3** was kept for about two hours in an oven maintained at 100°C. Afterward, the residue, characterized by elemental analysis, was shown to have the

$[Ag_3(L^{1\text{-}Me})_2(C_{10}H_7SO_3)_3]$[45] composition. Furthermore, the FTIR spectrum of this residue confirms the presence of the ligand and the anion.[46] With the assumption that $[Ag_3(L^{1\text{-}Me})_2(C_{10}H_7SO_3)_3]$ was formed in the first thermal decomposition, we propose the following thermal decomposition for complex **3**:

$$3\,[AgL^{1\text{-}Me}(C_{10}H_7SO_3)] \rightarrow L^{1\text{-}Me} + [Ag_3(L^{1\text{-}Me})_2(C_{10}H_7SO_3)_3] \quad (1)$$

$$[Ag_3(L^{1\text{-}Me})_2(C_{10}H_7SO_3)_3] \rightarrow 2\,L^{1\text{-}Me} + 3\,(C_{10}H_7SO_3) + 3\,Ag \quad (2)$$

The first step of the decomposition seems to correspond to the departure of one ligand from three molecules of **3** (exp/theor = 8.3/8.5%). The second weight loss of **3**, that takes place at 150-230°C, may correspond to the thermal decomposition of the intermediate product that is consistent with the removal of two ligands $L^{1\text{-}Me}$ and three 1-naphthalenesulfonate anions (expt/theor = 69.4/72.2%).

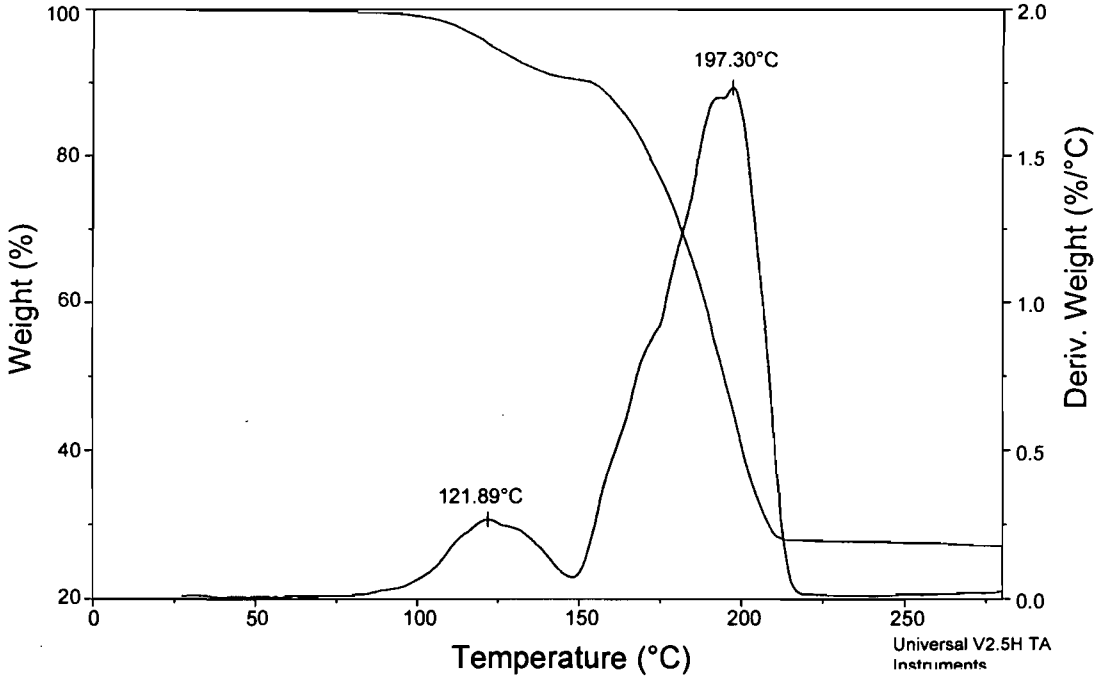

Figure 4.2.7. TGA and DTGA curves of **3** recorded at a heating rate of 10 °C min^{-1}. This complex decomposes between 80 and 215 °C. The weight loss is consistent with the removal of the ligand, $L^{1\text{-}Me}$, and the 1-naphthalenesulfonate anions.

We also performed an additional thermogravimetric experiment at a rate of 1 °C min^{-1}. The process was stopped after the first step, at 115 °C. The elemental analysis of this residue demonstrated that this product has the metal-to-ligand ratio of 3:2 which is in good agreement with the proposed intermediate product, $[Ag_3(L^{1\text{-}Me})_2(C_{10}H_7SO_3)_3]$.[47]

The formulation proposed for this intermediate product, on the basis of the elemental analysis matches reasonably well with the weight loss of the thermogravimetric analysis of **3**. Finally, the X-ray powder diffraction of the intermediate compound, as depicted in Figure 4.2.8, differs significantly from that of complex **3**, thus indicating a different material.

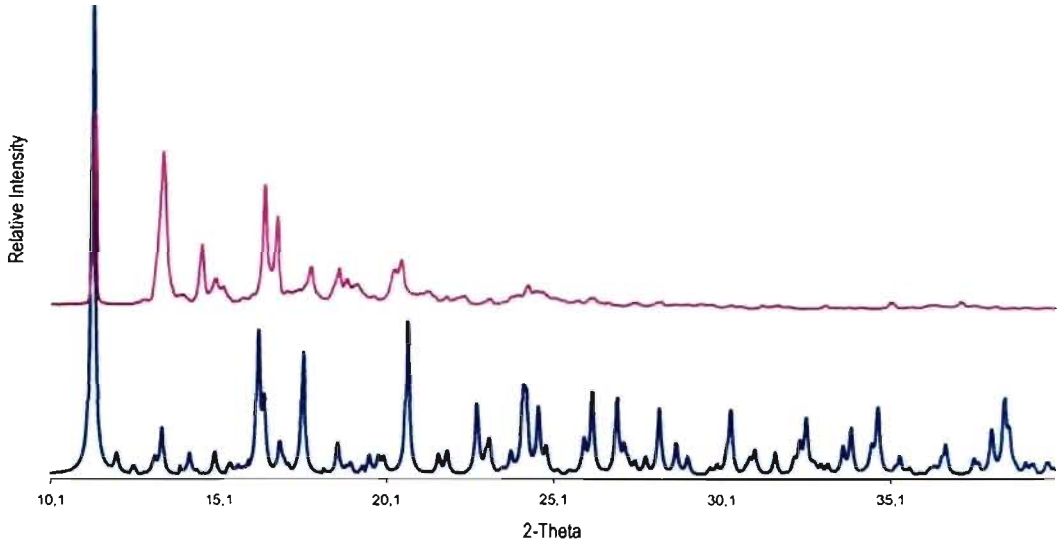

Figure 4.2.8. The X-ray powder diffraction pattern of complex **3** (blue line) and of the intermediate product (pink line).

The TGA curve of **4**, $[Ag_{10}(\mathbf{L}^{2\text{-Ph}})_4(NO_3)_{10}]_\infty$, exhibits a more complex thermal degradation. The first step, which occurs in the interval of 140-230 °C, corresponds to the departure of the ligands $\mathbf{L}^{2\text{-Ph}}$ (expt/theor = 37.5/36.7%). The second step, that occurs between 230 and 400 °C, is consistent with the loss of the nitrate anions (expt/theor = 24.6/23.1%) (Figure S10, Annexe VII) that leaves behind metallic silver.

Audebrand *et al.*, have reported the departure of the nitrate anions from the $Ag_2Ce_2(H_2O)(NO_3)_5$ compound, in the range of 230-310 °C, leaving behind silver and CeO_2.[48] Complexes **1** and **2** consisting of 1,3-bis(phenylthio)propane, $\mathbf{L}^{3\text{-Ph}}$, are stable up to 180°C while **4**, obtained with 1,2-bis(phenylthio)ethane, $\mathbf{L}^{2\text{-Ph}}$, is stable up to 140 °C, and **3**, with bis(methylthio)methane, $\mathbf{L}^{1\text{-Me}}$, is only stable up to 80 °C. For all the complexes,

removal of the ligands and the anions is concomitant with the collapse of the framework, and silver is always deposited, as confirmed by XRPD.

4.2.5 Conclusions

Four novel metal organic frameworks based on the self-assembly of ditopic organic connectors of different sizes, and silver(I) salts of various anions have been prepared and characterized. The metal-organic coordination polymers **1** and **2** are described as the combination of two sub-networks $(Ag\text{-anion})_\infty$ and $(Ag\text{-ligand})_\infty$. Complex **2**, in which some silver atoms adopt the unusual square-planar environment, is a solvent-dependant supramolecular isomer of previously reported networks.

The one-dimensional coordination polymer **3** is made by the alternation of $[Ag\text{-}\mathbf{L}^{\mathbf{1\text{-}Me}}]_2$ and $[Ag\text{-}(C_{10}H_7SO_3)]_2$ dimers sharing their silver atoms. In **4**, the nitrate anions adopt several coordination modes towards the silver centers. In the dibridging mode, the nitrate links adjacent silver atoms to form chains of $[AgNO_3]_\infty$, In turn, the chains are connected to one another by the ligand, producing a tubular coordination polymer.

The thermogravimetric analysis reveals that **1**, in which there are intertwined networks of $(Ag\text{-anion})_\infty$ and $(Ag\text{-ligand})_\infty$, has a similar thermal behavior to that of the perfluorocarboxylates (trifluoroacetate, pentafluoropropiuonate and heptafluorobutyrate) complexes of $\mathbf{L}^{\mathbf{3\text{-}Ph}}$ although their structures consist of the $(Ag\text{-ligand})_\infty$ network. A comparable observation can be made when comparing the thermal decomposition of complex **2** and that of its supramolecular isomer. Thus, the thermal stability may be related to the $(Ag\text{-ligand})_\infty$ network. A two-step thermal decomposition is observed for **3**. The loss of some of the ligand molecules in the first step yields a new phase, $[Ag_3(\mathbf{L}^{\mathbf{1\text{-}Me}})_2(C_{10}H_7SO_3)_3]$, that is stable between 80-150 °C. The second step is completed at 300 °C, and a residue of metallic silver is left behind.

Weak argentophilic interactions are noted for **1** and **3**. The stoichiometries of complexes **1-3** do not depend on the ratio of the starting materials, while that of **4** does.

Acknowledgements. This work was supported by the Natural Sciences and Engineering Research Council of Canada (F.B). M.O.A. wishes to thank the Organisation Internationale de la Francophonie (OIF) and the Programme des bourses d'excellence de la Francophonie du Canada (PCBF) for a graduate scholarship. The authors also thank Dr T. Maris for helpful discussions.

Supporting Information Available: Table of the bond distances and angles involving the silver atoms and Figures S1-S10; X-ray crystallographic information files (CIF) for compounds **1-4**. This material is available free of charge via the Internet at http://pubs.acs.org.

4.2.6 References

(1) For example: (a) Stumpt, H. O.; Ouahab, L.; Pei, Y.; Grandjean, D.; Kahn, O. *Science* **1993**, *261*, 447. (b) Gardner, G. B.; Venkataraman, D.; Moore, J. S.; Lee, S. *Nature* **1995**, *374*, 792. (c) Yaghi, O. M.; Li, G.; Li, H. *Nature* **1995**, *378*, 703. (d) Munakata, M.; Wu, L. P.; Yamamoto, M.; Kuroda-Sowa, T.; Maekawa, M. *J. Am. Chem. Soc.* **1996**, *118*, 3117. (e) Zaworotko, M. J.; *Angew. Chem. Int. Ed.* **2000**, *39*, 3052 and references therein. (f) Chen, C. T.; Suslick, K. S. *Coord. Chem. Rev.* **1993**, *128*, 293.

(2) (a) Leininger, S.; Olenyuk, B.; Stang, P. J. *Chem. Rev.* **2000**, *100*, 853. (b) Holliday, B. J.; Mirkin, C. A. *Angew. Chem. Int. Ed.* **2001**, *40*, 2022. (c) McCleverty, J. A.; Ward, M. D. *Acc. Chem. Res.* **1998**, *31*, 842. (d) Moulton, B.; Zaworotko, M. J. *Chem. Rev.* **2001**, *101*, 1629.

(3) (a) Withersby, M. A.; Blake, A. J.; Champness, N. R.; Cooke, P. A.; Hubberstey, P.; Li, W. S.; Schröder, M. *Inorg. Chem.* **1999**, *38*, 2259. (b) Blake, A. J.; Champness, N. R.; Cooke, P. A.; Nicolson, J. E. B.; Wilson, C. *J. Chem. Soc., Dalton Trans.* **2000**, 3811. (c) Noro, S.; Kitaura, R.; Kondo, M.; Kitagawa, S.; Ishii, T.; Matsuzaka, H.;Yamashita, M. *J. Am. Chem. Soc.* **2002**, *124*, 2568. (d) Chatterton, N. P.; Goodgame, D. M. L.; Grachvogel, D. A.; Hussain, I.; White, A. J. P.; Williams, D. J. *Inorg. Chem.* **2001**, *40*, 312.

(4) Awaleh, M. O.; Badia, A.; Brisse, F. *Inorg. Chem.* **2005**, *44*, 7833.

(5) Awaleh, M. O.; Badia, A.; Brisse, F. *Cryst. Growth Des.* **2005**, *5*, 1897.

(6) Awaleh, M. O.; Badia, A.; Brisse, F.; Bu, X. *Inorg. Chem.* **2006**, *45*, 1560.

(7) (a) Awaleh, M. O.; Badia, A.; Brisse, F. *Cryst. Growth Des.* **2006**, *6*, 2674.

(b) Awaleh, M. O.; Badia, A.; Brisse, F. *To be published.*

(8) Withersby, M. A.; Blake, A. J.; Champness, N. R.; Hubberstey, P.; Li, W. S.; Schröder, M. *Angew. Chem. Int. Ed.* **1997**, *36*, 2327.

(9) Sailaja, S.; Rajasekharan, M. V. *Inorg. Chem.* **2003**, *42*, 5675.

(10) Hong, M.; Su, W.; Cao, R.; Fujita, M.; Lu, J. *Chem. Eur. J.* **2000**, *6*, 42.

(11) Hirsch, K.A.; Wilson , A. S. R.; Moore, J. S., *Chem. Eur. J.* **1997**, *3*, 765.

(12) Jung, O. S.; Kim, Y. J.; Lee, Y. A.; Chae, H. K.; Jang, H. G.; Hong, J. *Inorg. Chem.* **2001**, *40*, 2105.

(13) Schultheiss, N.; Powell, D. R.; Bosch, E. *Inorg. Chem.* **2003**, *42*, 8886.

(14) Zhang, G.; Yang, G.; Ma, J. S. *Cryst. Growth Des.* **2006**, *6*, 1897.

(15) (a) Zhang, L. P.; Du, M.; Lu, W. J.; Mak, T. C. W. *Inorg. Chem. Commun.* **2005**, *8*, 623. (b) Ning, G. L.; Munakata, M.; Wu, L. P.; Maekawa, M.; Suenaga, Y.; Kuroda-Sowa, T.; Sugimoto, K. *Inorg. Chem.* **1999**, *38*, 5668.

(16) Zhang, X.; Guo, G. C.; Zheng, F. K.; Zhou, G. W.; Mao, J. G.; Dong, Z. C.; Huang, J. S.; Mak, T. C. W. *J. Chem. Soc., Dalton Trans.* **2002**, 1344 and references therein.

(17) Hartley, F. R.; Murray, S. G.; Levason, W.; Soutter, H.E; McAuliffe, C. A. *Inorg. Chim. Acta* **1979**, *35*, 265.

(18) *SAINT Integration Software for Single-Crystal Data*, release 6.06, Bruker AXS Inc.: Madison, WI, **1999**.

(19) Sheldrick, G. M. *SADABS Bruker Area Detector Absorption Corrections*; Bruker AXS Inc.: Madison, WI, **1996**.

(20) *XPREP X-ray Data Preparation and Reciprocal Space Exploration Program*, release 5.10 Bruker AXS Inc., Madison, WI, **1997**.

(21) *SHELXTL The Complete Software Package for Single-Crystal Structure Determination*, release 5.10, Brucker AXS Inc.: Madison, WI, **1997**.

(22) (a) Sheldrick, G. M. *SHELXS97, Program for the Solution of Crystal Structures*; University of Göttingen: Göttingen, Germany, **1997**. (b) Sheldrick, G.M. *SHELXL97, Program for the Refinement of Crystal Structures*; University of Göttingen: Göttingen, Germany, **1997**.

(23) Spek, A. L. *PLATON Molecular Geometry Program*, 2000 version University of Utrecht, Utrecht, Holland, **2004**.

(24) Liu, S. Q.; Konaka, H.; Kuroda-Sowa, T.; Maekawa, M.; Suenaga, Y.; Ning, G. L.; Munakata, M. *Inorg. Chim. Acta* **2005**, *358*, 919.

(25) Porterfield, W. W. *Inorganic Chemistry: A Unified Approach*, Addison-Wesley, 1984, p.168, 180.

(26) Côté, A. P.; Shimizu, G. K. H. *Coord. Chem. Rev.* **2003**, *245*, 49 and references therein.

(27) Côté, A. P.; Ferguson, M. J.; Khan, K. A.; Enright, G. D.; Kulynych, A. D.; Dalrymple, S. A.; Shimizu, G. K. H. *Inorg. Chem.* **2002**, *41*, 287.

(28) F. A. Cotton and G. Wilkinson, *Advanced Inorganic Chemistry.* 5rd ed. John Wiley and Sons, **1988**.

(29) (a) Reger, D. L.; Gardinier, J. R.; and Smith, M. D. *Polyhedron* **2004**, *23*, 291. (b) Carmona, D.; Viguri, F.; Lahoz, F. J.; and Oro, L. A. *Inorg. Chem.* **2002**, *41*, 2385 and references therein. (c) Mascal, M.; Hansen, J.; Blake, A. J.; Li, W. S. *J. Chem. Soc., Chem. Comm.* **1998**, 355.

(30) Park, B. I.; Chun, I. S.; Lee, Y. A.; Park, K. M.; Jung, O. S. *Inorg. Chem.* **2006**, *45*, 4310.

(31) Awaleh, M. O.; Badia, A.; Brisse, F. *Acta Crystallogr.* **2005**, *E61*, o2479.

(32) Chen, C. L.; Kang, B. S.; Su, C. Y. *Aust. J. Chem.* **2006**, *59*, 3 and references therein.

(33) Feazell, R. P.; Carson, C. E.; Klausmeyer, K. K. *Inorg. Chem.* **2006**, *45*, 2635.

(34) Feazell, R. P.; Carson, C. E.; Klausmeyer, K. K. *Inorg. Chem.* **2006**, *45*, 2627.

(35) Feazell, R. P.; Carson, C. E.; Klausmeyer, K. K. *Inorg. Chem.* **2006**, *45*, 935.

(36) Effendy; Nicola, C. D.; Nitiatmodjo, M.; Pettinari, C.; Skelton, B. W.; White, A. H. *Inorg. Chim. Acta* **2005**, *358*, 735.

(37) Cingolani, A.; Effendy; Pettinari, C.; Skelton, B. W.; White, A. H. *Inorg. Chim. Acta* **2006**, *359*, 2170.

(38) Szlyk, E.; Szymanska, I.; Surdykowski, A.; Glowiak, T.; Wojtczak, A.; Golinski, A. *J. Chem. Soc. Dalton Trans.* **2003**, 3404 and references therein.

(39) Johnston, D. H.; Shriver, D. F. *Inorg. Chem.* **1993**, *32*, 1045.

(40) Lawrance, G. A. *Chem. Rev.* **1986**, *86,* 17 and references therein.

(41) Batchelor, R. J.; Ruddick, J. N. R.; Sams, J. R.; Aubke, F. *Inorg. Chem.* **1977**, *16*, 1414 and references therein.

(42) Zhong, J. C.; Munakata, M.; Kuroda-Sowa, T.; Maekawa, M.; Suenaga, Y.; Konaka, H. *Inorg. Chem.* **2001**, *40*, 3191.

(43) Sharma, R. P.; Sharma, R.; Bala, R.; Rychlewska, U.; and Warzajtis, B. *J. Mol. Struct.* **2005**, *738*, 291.

(44) Nakamoto, K. *Infrared Spectra of Inorganic and Coordination Compounds*. 3rd ed. Wiley-VCH: New York, 1978.

(45) Elemental analysis of the residue: Anal. Found: C, 36.97: H, 3.68. Calculated for $C_{36}H_{37}Ag_3O_9S_7$: C, 37.22; H, 3.21.

(46) IR of the residue: IR of the residue: 3443m, 2917m, 2849m, 1627m, 1543w, 1504w, 1464w, 1422vw, 1384m, 1189m, 1150w, 1053m, 826w, 800w, 768w, 720vw, 690m, 648w, 616m, 522w.

(47) Elemental analysis of the residue: Anal. Found: Anal. Found: C, 36.86: H, 2.83. Calculated for $C_{36}H_{37}Ag_3O_9S_7$: C, 37.22; H, 3.21.

(48) Audebrand, N.; Auffredic, J. P.; Louër, D. *Journal of Solide State Chemistry* 1997, *132*, 361.

Chapitre 5. Gold(I)-dithioethers coordination polymers: synthesis, characterization and luminescence.[†]

5.1 Abstract

A series of discrete compounds and coordination polymers were synthesized by the self-assembly of the dithiolate building block and $HAuCl_4.3H_2O$. A slight excess of the ligand reduced Au(III) to Au(I). Complex **1** containing bis(methylthio)methane, $\mathbf{L^{1\text{-}Me}}$, is a polymer in which adjacent [Au $\mathbf{L^{1\text{-}Me}}$ Cl] units are connected to one another via aurophilic interactions. Complex **1** features the presence of nearly linear $[Au\text{-}Au\text{-}]_\infty$ chains. The bis(phenylthio)propane, $\mathbf{L^{1\text{-}Ph}}$, complex consists of $[Au_2\mathbf{L^{1\text{-}Ph}}Cl_2]$ units, linked through aurophilic interactions into a one-dimensional coordination polymer, **2**. Three polymorphs, **3-5**, are obtained with the 1,3-bis(phenylthio)propane, $\mathbf{L^{3\text{-}Ph}}$, ligand. The structures of **2**, **3** and **5** consist of very similar 1D-coordination polymers with the same stoichiometry (2Au:1L) whereas **4** forms the $[Au_2\mathbf{L^{3\text{-}Ph}}Cl_2]$ molecular complex. The use of 1,3-bis(methylthio)propane, $\mathbf{L^{3\text{-}Me}}$, leads to complex **6**, [Au$\mathbf{L^{1\text{-}Me}}$ Cl] .

With 1,2-bis(phenylthio)ethane, $\mathbf{L^{2\text{-}Ph}}$, the 2D-coordination network **7** that contains $[Au\text{-}Au\text{-}]_\infty$ chains is obtained. Complex **8**, obtained with 1,4-bis(phenylthio)butane, $\mathbf{L^{4\text{-}Ph}}$, is the molecular compound $[Au_2\mathbf{L^{4\text{-}Ph}}Cl_2]$. The UV-visible spectrum shows that the absorption bands of these complexes are allowed ligand-centered transitions between 230 and 260 nm. Complexes **1** and **7** show solid-state luminescence at 5 K with vibronic progressions and band maxima at approximately 570 nm.

5.2 Introduction

The synthesis and characterization of gold(I) self-assembled supramolecules is an active research area owing to their interesting photoluminescence properties.[1,2] In addition, the use of thiolate molecules bearing hydrophobic aliphatic tails *via* metal (e.g. Au, Ag, Cu)-thiolate interactions is common in surface chemistry to form self-assembled monolayers (SAMs).[3] Moreover, dithiolate molecules with an aliphatic segment between the sulfur atoms may be used for the formation of functionalized surface matrices, in which one S atom may assure the connection of the organic molecule with the metal substrate in

[†] Awaleh, M. O.; Baril-Robert, F.; Reber, C.; Badia, A.; Brisse, F. *Crystal Growth and Design.* **2007**. Soumis pour publication.

order to form self-assembled monolayers while the second thiol may further be used to increase the dimensionality of the organic thin film.[4]

One powerful technique used to probe structured organic thin films formed by self-assembly or the Langmuir-Blodgett technique, is Atomic Force Microscopy.[5] However, even if the scanning probe microscopy techniques allow the characterization with nanometer resolution of the structured thin film on metal substrates, model systems are needed to study the supramolecular gold-dithiolate aggregates. Thus, we were interested to study the structured inorganic-organic frameworks built up by self-assembling dithiolate organic building blocks with Ag(I) and Au(I).

We have chosen dithioether building blocks with aliphatic chains between the sulfur atoms, $RS(CH_2)_nSR$, where n is the number of CH_2 groups and R is an alkyl group, $\mathbf{L^{n\text{-}R}}$, to combined them with Ag(I) in order to form hybrid inorganic-organic supramolecular architectures.[6] The selection of those ligands was motivated by four reasons: (i) according to the Pearson hard-soft acid-base (HSAB) concept of acids and bases,[7] the silver(I) and gold(I) ions are soft Lewis acids and hence have a good ability to coordinate to thioether ligands that are soft Lewis bases, (ii) those symmetrical dithioether building blocks afford two coordination sites to d^{10} metals centers to expand the coordination sphere of the metal centers into extended solid-state networks, (iii) the variation of the aliphatic segment between the S atoms may increase the conformation degree of those ligands[8] so as to get some insight into the effect of the flexibility of the organic building blocks upon the resulting coordination polymers, (iv) the hindrance of the coordination sphere of the d^{10} metal centers may be affected by the bulk of the R substituant of the dithioether ligands, thus the variation of the bulk of R can allow us to study the effect of the shape of the organic building blocks upon the topology of the resulting coordination polymers.

However, the Ag(I) and Au(I), d^{10} metals, adopt different coordination environments.[9] The silver(I) atoms have flexible coordination sphere, from 2 to 6, while Au(I) ions adopt mostly linear two-coordination environment.[10]

In the supramolecular metal-organic frameworks obtained by the combination of those dithioether organic spacers and silver(I) salts, the coordination sphere of Ag(I) was expanded by the neutral dithioether ligands while their charge was balanced naturally by the counteranion.[6]

On the other hand, usually the aurophilic interaction between adjacent gold(I) atoms allows the expansion of complexes into hybrid inorganic-organic extended solid-state

networks.[2, 10-14] This interaction has an energy order of 5-10 kcal mol^{-1} for a Au(I)–Au(I) distance of 3.05 Å, which is comparable to that of hydrogen bonds.[2,15] Individual Au(I)-Au(I) interactions may be considered weak. However, those weak interactions could cooperate in the solid state in order to form more strength interaction so that many of gold(I)-thioether complexes were found to be insoluble in common organic solvents.[15]

Because of their insolubility they could not be crystallized, hence it is difficult to define accurately the structures of those gold(I) coordination polymers.[15] Thus, the need to synthesize soluble gold(I)-thioether compounds, which can be crystallized, so as to determinate their structures.[15]

To the best of our knowledge, there is only one fully structurally characterized gold(I)-$RS(CH_2)_nSR$ complex.[16] The structure of $[Au_2L^{2\text{-}Ph}Cl_2]$ was established at room temperature.

One of our goals was to transpose our previous study of the Ag(I)-$RS(CH_2)_nSR$[6] metal organic frameworks (MOFs) to gold(I) by the synthesis and characterization of supramolecular gold(I)-$L^{n\text{-}R}$ complexes. In addition, we were interested to the photoluminescence properties of those kinds of gold(I)-dithioether complexes.

The self-assembly of dithioether molecules, $L^{n\text{-}R}$, and gold halide salts may lead to the formation of neutral molecular entity, in which the halide counter-balance the charge of the gold(I) while the sulfur atoms of $L^{n\text{-}R}$ were coordinated to one or two gold(I) atoms, in turn those discrete compounds may increase their dimensionality *via* aurophilic interactions as depicted in scheme I.

Here we report on the synthesis and structural characterization of several gold(I) complexes obtained by the self-assembly process of several dithioether building blocks and $HAuCl_4.3H_2O$. The organic building blocks used in this study were: bis(methylthio)methane, $L^{1\text{-}Me}$, bis(phenylthio)methane, $L^{1\text{-}Ph}$, 1,2-bis(phenylthio)ethane, $L^{2\text{-}Ph}$, 1,3-bis(phenylthio)propane, $L^{3\text{-}Ph}$, 1,3-bis(methylthio)propane, $L^{3\text{-}Me}$, and 1,4-bis(phenylthio)butane, $L^{4\text{-}Ph}$. Moreover, we report here the solid-state luminescence of some of those complexes.

Scheme 1

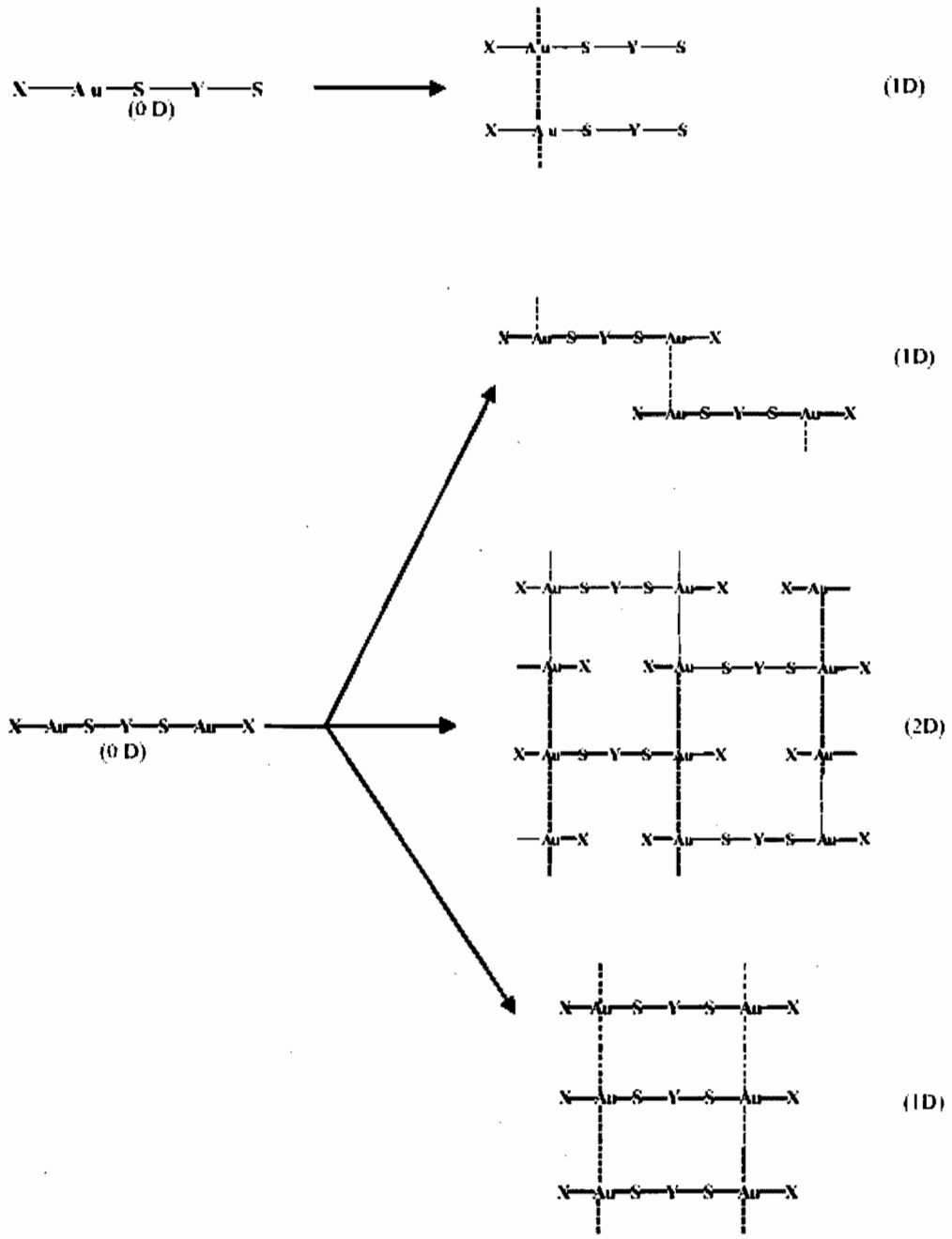

X = Halide; Y = $(CH_2)_n$

OD discrete molecules can be aggregate into 1D or 2D networks via aurophilic interaction.

5.3 Experimental Section

Materials and General Methods. Except for the ligands, all the regents required were commercially available and employed without further purification. The elemental analyses were performed by the Laboratoire d'analyse élémentaire (Université de Montréal). The ^{1}H (300 MHz) NMR spectra in solution were recorded at 25 °C on a Bruker AV300.

^{1}H chemical shifts are reported in parts per million and are referenced to residual solvent signals of the following deuterated solvents: DMSO (δ_{1H} = 2.50); acetone (δ_{1H} = 2.05) and chloroform (δ_{1H} = 7.26). Luminescence spectra were measured using a single-channel spectrometer, and the UV lines (333.6-363.8 nm) of an argon ion laser (Spectra-Physics Stabilite 2017) were used to excite crystalline samples inside a closed-cycled He cryostat (Sumitomo Heavy Industries SRDK-205). Luminescence was collected and dispersed by a 0.5-m monochromator (SPEX 500 M, 600 lines/mm) with a long-pass filter to remove the excitation (Schott KV-418). Emitted light was detected by a photomultiplier tube (Hamamatsu R928) connected to a photon-counter (Stanford Instruments SR 400). All spectra were corrected for instrument response with a tungsten lamp (Oriel 63350) using a literature procedure.[17] The Raman spectra were recorded with a Raman microscope (Renishaw system 3000). UV-visible spectroscopy was carried out with a Cary 500i spectrometer.

Syntheses. The ligands were synthesized according to a published report.[18]

Bis(methylthio)methane, $\mathbf{L^{1\text{-}Me}}$. Colorless oil. Yield: 41%. Anal. Found: C, 33.45; H, 7.32. Calcd for $C_3H_8S_2$: C, 33.29; H, 7.45. ^{1}H NMR (DMSO-d_6, 300 MHz): δ 2.16 (s, 6H, CH_3-S-CH_2-S-CH_3), 3.63 (s, 2H, CH_3-S-CH_2-S-CH_3).

Bis(phenylthio)methane ligand, $\mathbf{L^{1\text{-}Ph}}$. White powder. Yield 85%. Anal. Found: C, 67.03; H, 5.07. Calcd for $C_{13}H_{12}S_2$: C, 67.20; H, 5.21. ^{1}H NMR (DMSO-d_6, 300 MHz): δ 4.54 (s, 2H, -S-(CH_2)-S-), 7.22-7.46 (m, 10H, C_6H_5-).

1,2-bis(phenylthio)ethane, $\mathbf{L^{2\text{-}Ph}}$. White powder. Yield: 43%. Anal. Found: C, 68.25; H, 6.09. Calcd for $C_{14}H_{14}S_2$: C, 68.24; H, 5.73. ^{1}H NMR (acetone-d_6, 300 MHZ): δ 3.16 (s, 4H, -S-(CH_2)$_2$-S-), 7.23-7.37 (m, 10H, C_6H_5-).

1,3-bis(phenylthio)propane, $\mathbf{L^{3\text{-}Ph}}$. Colorless oil. Yield: 82%. Anal. Found: C, 69.36; H, 6.35. Calcd for $C_{15}H_{16}S_2$: C, 69.18; H, 6.19. ^{1}H NMR (DMSO-d_6, 300 MHz): δ 2.02 (qt, 2H, -S-CH_2- CH_2-CH_2-S-), 3.08 (t, 4H, -S-CH_2-CH_2- CH_2-S-),
7.15 - 7.36 (m, 10H, C_6H_5-).

1,3-bis(methylthio)propane, $\mathbf{L^{3\text{-}Me}}$. Colorless oil. Yield: 46%. Anal. Found: C, 44.15; H, 9.25. Calcd for $C_5H_{12}S_2$: C, 44.07 H, 8.88. ^{1}H NMR ($CDCl_3$, 300 MHz): δ 1.91 (qt, 2H, $CH_3SCH_2\mathbf{CH_2}CH_2SCH_3$), 2.13 (s, 6H, $\mathbf{CH_3}SCH_2CH_2CH_2S\mathbf{CH_3}$), 2.62 (t, 4H, $CH_3S\mathbf{CH_2}CH_2\mathbf{CH_2}SCH_3$).

1,4-bis(phenylthio)butane, $\mathbf{L^{4\text{-}Ph}}$. White powder. Yield: 82%. Anal. Found: C, 69.79; H, 6.65. Calcd for $C_{16}H_{18}S_2$: C, 70.02; H, 6.61. ^{1}H NMR (acetone-d_6, 300 MHz): δ 1.80 (qt, 4H, -S-CH_2-($\mathbf{CH_2}$)$_2$- CH_2-S-), 3.01 (t, 4H, -S-$\mathbf{CH_2}$-(CH_2)$_2$-$\mathbf{CH_2}$-S-), 7.17 - 7.45 (m, 10H, $\mathbf{C_6H_5}$-).

[AuL$^{1\text{-}Me}$Cl]$_\infty$ (1). 65 mg of $HAuCl_4.3H_2O$ (0.2 mmol) was dissolved in 10 mL of anhydrous ethanol at room temperature. This resulted in a yellow solution. Upon the addition of 0.30 mL of $\mathbf{L^{1\text{-}Me}}$ (2.93 mmol) the solution turned orange then became colorless within 20 minutes. Colorless hair-like crystals suitable for an X-ray analysis grew from this solution within minutes. Yield: 90% based on $HAuCl_4.3H_2O$. Anal. Found: C, 10.09; H, 2.05. Calculated for $C_3H_8S_2AuCl$: C, 10.58; H, 2.37. ^{1}H NMR (DMSO-d_6, 300 MHz):
δ 2.09 (s, 6H, $\mathbf{CH_3}$-S-CH_2-S-$\mathbf{CH_3}$), 3.70 (s, 2H, CH_3-S-$\mathbf{CH_2}$-S-CH_3).
Raman. ν(Au-S): 264.4 cm^{-1}; ν(Au-Cl): 387.6 cm^{-1}.

[Au$_2$(L$^{1\text{-}Ph}$Cl$_2$]$_\infty$ (2). To 10 mL of anhydrous ethanol was dissolved at room temperature 128 mg of $HAuCl_4.3H_2O$ (0.32 mmol) yielding a yellow solution. This mixture turned orange upon the addition of 498 mg of $\mathbf{L^{1\text{-}Ph}}$ (2.14 mmol). The dropwise addition of diethyl ether (10 mL) over an hour turned the solution from orange to colorless. Then the solution was left to stand at room temperature. After about few weeks colorless crystals were obtained. Yield: 54% based on $HAuCl_4.3H_2O$. Anal. Found: C, 22.71; H, 1.77. Calculated for $C_{13}H_{12}S_2Au_2Cl_2$: C, 22.40; H, 1.73. ^{1}H NMR (DMSO-d_6, 300 MHz): δ 4.66 (s, 2H, -S-($\mathbf{CH_2}$)-S-), 7.22-7.43 (m, 10H, $\mathbf{C_6H_5}$-).
Raman. ν(Au-S): 257.7 cm^{-1}; ν(Au-Cl): 366.6 cm^{-1}.

[Au$_2$L$^{3\text{-}Ph}$Cl$_2$]$_\infty$ (3). This complex was synthesized in the same manner as **2** using $HAuCl_4.3H_2O$ (133 mg, 0.338 mmol) and $\mathbf{L^{3\text{-}Ph}}$ (0.30 mL, 1.31 mmol). After about three weeks crystals suitable for an X-ray analysis were deposited. Yield: 76 % based on $HAuCl_4.3H_2O$. Anal. Found: C, 24.74; H, 2.36. Calculated for $C_{15}H_{16}S_2Au_2Cl_2$: C, 24.84; H, 2.22. ^{1}H NMR (DMSO-d_6, 300 MHz): δ 1.84 (qt, 2H, -S-CH_2- $\mathbf{CH_2}$-CH_2-S-), 3.06 (t, 4H, -S-$\mathbf{CH_2}$-CH_2- $\mathbf{CH_2}$-S-), 7.14-7.33 (m, 10H, $\mathbf{C_6H_5}$-).
Raman. ν(Au-S): 264.2cm^{-1}; ν(Au-Cl): 341.7 cm^{-1}.

$[Au_2L^{3\text{-}Ph}Cl_2]$ (4). This complex was synthesized as follows: 135 mg of $HAuCl_4.3H_2O$ (0.343 mmol) was dissolved in 10 mL of anhydrous ethanol at room temperature. This yellow solution turned orange upon the addition of $L^{3\text{-}Ph}$ (0.30 mL, 1.31 mmol). The solution was left to stand at room temperature for a few weeks, until light-orange prismatic crystals suitable for X-ray analysis appared. Yield: 68 % based on $HAuCl_4.3H_2O$. Anal. Found: C, 24.67; H, 2.24. Calculated for $C_{15}H_{16}S_2Au_2Cl_2$: C, 24.84; H, 2.22.

^{1}H NMR (DMSO-d_6, 300 MHz): δ 2.02 (qt, 2H, -S-CH_2- CH_2-CH_2-S-), 3.09 (t, 4H, -S-CH_2-CH_2- CH_2-S-), 7.14-7.45 (m, 10H, C_6H_5-).

Raman. ν(Au-S): 266.3 cm^{-1}; ν(Au-Cl): 342.4 cm^{-1}.

$[Au_2L^{3\text{-}Ph}Cl_2]_\infty$ (5). To 10 mL of anhydrous ethanol was added 121 mg of $HAuCl_4.3H_2O$ (0.31 mmol) producing a yellow solution. Upon the addition of 0.30 mL of $L^{3\text{-}Ph}$ (1.31 mmol), the solution became orange. The dropwise addition of diethyl ether (10 mL) turned the solution colorless. This solution yielded crystals by diffusion of petroleum ether into the solution. After few weeks colorless crystals suitable for an X-ray analysis were deposited. Yield: 62 % based on $HAuCl_4.3H_2O$. Anal. Found: C, 24.33; H, 2.44. Calculated for $C_{15}H_{16}S_2Au_2Cl_2$: C, 24.84; H, 2.22. ^{1}H NMR (DMSO-d_6, 300 MHz): δ 1.85 (qt, 2H, -S-CH_2- CH_2-CH_2-S-), 3.05 (t, 4H, -S-CH_2-CH_2- CH_2-S-), 7.13 -7.32 (m, 10H, C_6H_5-). Raman. ν(Au-S): 265.4 cm^{-1}; ν(Au-Cl): 344.1 cm^{-1}.

$[AuL^{3\text{-}Me}Cl]$ (6). To 10 mL of anhydrous ethanol was added 127 mg (0.32 mmol) of $HAuCl_4.3H_2O$ at room temperature yielding yellow mixture. Upon the addition of 0.30 mL of $L^{3\text{-}Me}$ (1.31 mmol), an orange precipitate was formed and after about few minutes a colorless microcrystalline powder was deposited. Yield: 82 % based on $HAuCl_4.3H_2O$.

No NMR spectra is reported for **3** since this complex could not be solubilized.

Anal. Found: C, 16.34; H, 3.07. Calculated for $C_5H_{12}S_2AuCl$: C, 16.29; H, 3.28.

Raman. ν(Au-S): 260.1 cm^{-1}; ν(Au-Cl): 370.1 cm^{-1}.

$[Au_2L^{2\text{-}Ph}Cl_2]_\infty$ (7). This complex was synthesized in the same manner as **2** using $HAuCl_4.3H_2O$ (132 mg, 0.34 mmol) and $L^{2\text{-}Ph}$ (150 mg, 0.61 mmol). After few weeks colorless crystals suitable for an X-ray analysis were deposited. Yield: 79 % based on $HAuCl_4.3H_2O$. Anal. Found: C, 23.34; H, 2.11. Calculated for $C_{14}H_{14}S_2Au_2Cl_2$: C, 23.64; H, 1.98. ^{1}H NMR (DMSO-d_6, 300 MHZ): δ 3.15 (s, 4H, -S-$(CH_2)_2$-S-), 7.22-7.43 (m, 10H, C_6H_5-). Raman. ν(Au-S): 273.3 cm^{-1}; ν(Au-Cl): 375.3 cm^{-1}.

$[Au_2L^{4\text{-}Ph}Cl_2]$ (8). This complex was synthesized in the same manner as **2** using $HAuCl_4.3H_2O$ (123 mg, 0.31 mmol) and $L^{4\text{-}Ph}$ (209 mg, 0.76 mmol). After few weeks colorless crystals suitable for an X-ray analysis were deposited. Yield: 85 % based on $HAuCl_4.3H_2O$. Anal. Found: C, 25.60; H, 2.11. Calculated for $C_8H_9S_1Au_1Cl_1$: C, 25.99; H, 2.45. ^{1}H NMR (acetone-d_6, 300 MHz): δ 1.82 (qt, 4H, -S-CH_2-(CH_2)$_2$- CH_2-S-), 3.02 (t, 4H, -S-CH_2-(CH_2)$_2$-CH_2-S-), 7.18 - 7.46 (m, 10H, C_6H_5-).

Raman. ν(Au-S): 262.2 cm^{-1}; ν(Au-Cl): 337.4 cm^{-1}.

Structure Determination. The X-ray intensity data for complex **1** was obtained on an SMART 6K CCD equipped with a rotating anode (Cu Kα, λ = 1.54178 Å) using Mirror Montel 200 Optics as monochromator. X-ray data for **2**, **3**, **5**, **7** and **8** were obtained on a Brucker AXS Platform diffractometer equipped with a SMART 2K CCD area detector and a Cu Kα graphite-monochromatized radiation. The program SAINT[19] was used for the cell refinement and data reduction processing of **1-3**, **5**, **7**, **8**. An empirical absorption correction, which was based on multiple measurements of equivalent reflections, was applied using the program SADABS.[20] The diffraction data for **4** were collected on a Enraf-Nonius CAD-4 diffractometer by the ω-scan technique using Mo Kα graphite-monochromatized radiation, λ = 0.71073 Å. The unit-cell parameters were refined using the CAD-4 software,[21] while NRC-2 and NRC-2A were used for the data reduction.[22] For complex **4**, an absorption correction based on the crystal geometry was applied.[22]

The space groups were confirmed by the XPREP[23] routine in the program SHELXTL.[24] The structures of **1-5** were solved by Patterson method and difference Fourier techniques with SHELXS-97.[25] The refinements were done on F^2 by full matrix least squares analysis.[24] On the other hand, the structure of **8** were solved by the direct method and refined by the full-matrix least-squares on F^2 using the SHELXTL program.[24] For complex **5**, XPREP gave the three possible space groups *C*2, *Cm* and *C*2/*m*. Since our starting materials were not chiral, we tried first to solve its structure in the space groups *Cm* and *C*2/*m*, but both of them did not give reasonable structures. On this basis, we finally solve **5** in the space group *C*2. The Flack parameter,[26] which took the value of 0.01(5) for **5**, confirmed that the reported structure is of the correct hand. All non-hydrogen atoms were refined anisotropically, while the hydrogen atoms were introduced at calculated positions and were included in the refinement in the riding-model approximation,

with U_{iso}(H) = 1.5U_{eq}(C) for methyl groups and U_{iso}(H) = 1.2U_{eq}(C) for others. Crystal data, data collection and refinement parameters are listed in Table 5.1. The distances and angles are listed in Table 5.2.

Table 5.1. Crystal data and X-ray data collection parameters.

	1	2	3	4	5	7	8
formula	$C_3H_8S_2AuCl$	$C_{6.5}H_6SAuCl$	$C_{15}H_{16}S_2Au_2Cl_2$	$C_{7.5}H_8SAuCl$	$C_{7.5}H_8SAuCl$	$C_{14}H_{14}S_2Au_2Cl_2$	C_8H_9SAuCl
mol wt	340.63	348.60	725.23	362.615	362.615	711.21	369.63
cryst size (mm)	0.06 0.04×0.02	0.07×0.05×0.03	0.12×0.07×0.05	0.25×0.17×0.12	0.10×0.07×0.04	0.03×0.05×0.08	0.10x 0.07×0.04
λ (Å)	1.54178	1.54178	1.54178	0.71073	1.54178	1.54178	1.54178
space group	$P2_1/c$	$C2/c$	$P2_1/c$	$C2/c$	$C2$	P-1	$P2_1/c$
a (Å)	5.9972(2)	19.7419(4)	11.6093(3)	21.353(9)	21.4504(6)	6.2629(2)	11.9960(6)
b (Å)	20.3108(5)	10.5996(2)	8.5159(2)	10.049(7)	5.6699(2)	8.9090(2))	9.7548(5)
c (Å)	6.3029(1)	7.4895(2)	19.0202(5)	8.346(3)	7.7774(2)	14.7547(4)	8.5660(5)
α (deg)	90	90	90	90	90	93.667(1)	90
β (deg)	97.706(1)	98.275(2)	102.788(2)	91.04(3)	106.423(1)	92.614(1))	107.620(3)
γ (deg)	90	90	90	90	90	100.891(1)	90
V (Å^3)	760.81(3)	1550.91(6)	1833.74(8)	1790.6(16)	907.31(5)	805.37(4)	955.35(9)
Z	4	8	4	8	4	2	4
D(calc) (g cm^{-3})	2.974	2.986	2.627	2.690	2.665	2.993	2.570
F(000)	616	1256	1320	1320	660	644	676
T (K)	150	200	220	100	220	100	220
μ, (mm^{-1})	43.824	40.595	34.373	16.889	34.736	39.109	33.008
θ_{max} (deg)	68.28	72.75	72.90	26.49	72.01	68.91	72.02
$R1^a$ [$I > 2\sigma(I)$]	0.0337	0.0492	0.0419	0.0363	0.1014	0.0618	0.0538
Rw^b [$I > 2\sigma(I)$]	0.0885	0.1234	0.0960	0.0809	0.2372	0.1463	0.1338
R [*all data*]	0.0359	0.0497	0.0460	0.0747	0.1019	0.0707	0.0561
Rw [*all data*]	0.0896	0.1245	0.0982	0.0843	0.2379	0.1567	0.1371
S^c	1.110	1.105	1.015	0.974	1.195	1.037	1.021

$^aR = \Sigma \, ||F_o| - |F_c|| / \Sigma \, |F_o|$. $^bR_w = [\Sigma \, w(F_o^2 - F_c^2)^2 / \Sigma \, w(F_o^2)^2]^{1/2}$.
$^cS = [\Sigma \, w(F_o^2 - F_c^2)^2 / (m\text{-}n)]^{1/2}$ (m is the number of reflections and n the number of parameters).

Table 5.2. Selected bond distances (Å) and angles (°) for compounds **1-5**, **7** and **8**.

[AuL$^{1\text{-Me}}$Cl] (1)			
Au(1)-S(1)	2.240(2)	S(1)-Au(1)-Cl(1)	173.3(1)
Au(1)-Cl(1)	2.247(2)	S(1)-Au(1)-Au(1)#1	76.9(1)
Au(1)-Au(1)#1	3.1658(4)	Cl(1)-Au(1)-Au(1)#1	96.8(1)
Au(1)-Au(1)#2	3.1658(4)	S(1)-Au(1)-Au(1)#2	94.8(1)
Cl(1)-Au(1)-Au(1)#2	91.8(1)		
Au(1)#1-Au(1)-Au(1)#2	169.1(1)		
#1 x,-y+3/2,z+1/2 #2 x,-y+3/2,z-1/2			
[Au$_2$L$^{1\text{-Ph}}$Cl$_2$] (2)			
Au(1)-S(1)	2.266(2)	S(1)-Au(1)-Cl(1)	173.1(1)
Au(1)-Cl(1)	2.273(2)	S(1)-Au(1)-Au(1)#1	94.6(1)
Au(1)-Au(1)#1	3.0347(4)	Cl(1)-Au(1)-Au(1)#1	87.5(1)
#1 -x+2,y,-z-1/2			
[Au$_2$L$^{3\text{-Ph}}$Cl$_2$] (3)			
Au(1)-S(1)	2.259(2)	S(1)-Au(1)-Cl(1)	177.4(1)
Au(1)-Cl(1)	2.276(2)	S(1)-Au(1)-Au(2)	91.2(1)
Au(1)-Au(2)	3.2997(4)	Cl(1)-Au(1)-Au(2)	89.5(1)
Au(2)-Cl(2)	2.260(2)	Cl(2)-Au(2)-S(2)#1	175.7(1)
Au(2)-S(2)#1	2.2705(19)	Cl(2)-Au(2)-Au(1)	103.9(1)
S(2)#1-Au(2)-Au(1)	79.0(1)		
#1 x,-y+3/2,z+1/2			
[Au$_2$L$^{3\text{-Ph}}$Cl$_2$] (4)			
Au(1)-S(1)	2.250(3)	S(1)-Au(1)-Cl(1)	173.9(1)
Au(1)-Cl(1)	2.259(3)		
[Au$_2$L$^{3\text{-Ph}}$Cl$_2$] (5)			
Au(1)-S(1)	2.263(4)	S(1)-Au(1)-Cl(1)	172.17(17)
Au(1)-Cl(1)	2.267(5)	S(1)-Au(1)-Au(1)#1	101.76(9)
Au(1)-Au(1)#1	3.1918(9)	Cl(1)-Au(1)-Au(1)#1	85.32(13)
#1 -x+1,y,-z+1			
[Au$_2$L$^{2\text{-Ph}}$Cl$_2$] (7)			
Au(1)-S(1)	2.274(3)	S(1)-Au(1)-Cl(1)	178.17(9)
Au(1)-Cl(1)	2.291(2)	S(1)-Au(1)-Au(2)	88.34(7)
Au(1)-Au(2)	3.1204(5)	Cl(1)-Au(1)-Au(2)	90.16(6)
Au(1)-Au(2)#1	3.1499(5)	S(1)-Au(1)-Au(2)#1	97.17(7)

Au(2)-S(2)	2.272(3)	Cl(1)-Au(1)-Au(2)#1	84.31(6)
Au(2)-Cl(2)	2.277(2)	Au(2)-Au(1)-Au(2)#1	174.44(2)
S(2)-Au(2)-Au(1)	100.29(6)	S(2)-Au(2)-Cl(2)	173.94(9)
S(2)-Au(2)-Au(1)#2	82.66(6)		
Cl(2)-Au(2)-Au(1)	84.39(7)		
Cl(2)-Au(2)-Au(1)#2	93.00(7)		

#1 x-1,y,z #2 x+1,y,z

$[Au_2L^{4\text{-}Ph}Cl_2]$ (8)

Au(1)-S(1)	2.253(2)	S(1)-Au(1)-Cl(1)	174.67(8)
Au(1)-Cl(1)	2.261(2)		

5.4 Results

Synthesis of the complexes. The syntheses all started from Au(III) salts. These were reduced to the Au(I) state by the ligand used in excess. The yellow solution of $HAuCl_4.3H_2O$ in anhydrous ethanol turned to orange then changed quickly to colorless as the ligand was added to the solution. The stoichiometry of the resulting complexes confirmed that gold was in the (I) oxidation state.

Al-Sa'ady *et al.* reported that usually for the synthesis of gold(I)-thioether complexes, it was better to start from a gold(III) halide salt where the thioether ligand reduced gold(III) in gold(I).[27] On the other hand, it was reported in the literature that the spontaneous reduction of square-planar Au(III) to linear Au(I) by various thiols is a favourable reaction.[28] Crystals suitable for X-ray analysis were obtained for $L^{1\text{-}Me}$ and $L^{n\text{-}Ph}$, with n = 1, 3 and 4. We noticed that the crystals of the complexes **1**, with $L^{1\text{-}Me}$, and **6**, with $L^{3\text{-}Me}$, were formed within twenty minutes while crystals of the others complexes were obtained after a few weeks. When methanol or propanol were used to dissolve the gold salts instead of anhydrous ethanol, only complex **1** was formed, whereas the others complexes were not produced. Attempts to obtain complexes with different stoichiometries always failed, since when the metal-to-ligand ratios of the starting materials were varied the resulting complexes always had the same unit-cell parameters.

It is worth signaling the polymorphism observed for complexes **3-5**, resulting from the self-assembly of $L^{3\text{-}Ph}$ and $HAuCl_4.3H_2O$. Complexes **3** and **5** were obtained as colorless crystals while the crystals of **4** were light-orange. All these complexes are soluble

in common solvents except for complex **6** with 1,3-bis(methylthio)propane, $\mathbf{L^{3\text{-}Me}}$, which was found to be insoluble in all organic solvents.

Description of the Crystal structures. Complexes **1**, **2**, **3**, **5** form 1D-coordination polymers, of which **2**, **3** and **5** are topologically identical. The complex **7** form a 2D coordination network. On the other hand, the complexes **4** and **8** form discrete molecules. The coordination of the gold atom is square planar in **1** and **7**, triangular in **2**, **3** and **5**, and linear in **4** and **8**.

$[AuL^{1\text{-}Me}Cl]_\infty$ (1). The self-assembly of the $\mathbf{L^{1\text{-}Me}}$, bis(methylthio)methane, building block with the gold salt lead to the formation of a 1D-coordination polymer $[AuL^{1\text{-}Me}Cl]_\infty$ with a ligand-to-metal ratio of 1:1 (Figure 5.1). The backbone of the polymer is an infinite chain of gold atoms. A ligand molecule and a chloride anion are coordinated to each gold atom. Each gold atom is surrounded by four neighbours in a slightly distorted square planar coordination (Cl, S and two Au atoms) (Figure 5.1c and Figure S1, Annexe VIII). In this complex, only one sulfur atom of the building block is coordinated to the gold centre, whereas the second sulfur atom of the ligand and its methyl group lie between polymeric chains, in a plane parallel to the *ac*-plane at *b*/2 intervals (Figure 5.1b). The Au(I)···Au(I) distance between adjacent units is 3.1658(4) Å long. This distance is in the normal range, indicating some aurophilic interaction between adjacent $[AuL^{1\text{-}Me}Cl]$ repeats.[29-39] There are no interactions between the S atoms since the S···S distance is 3.715 Å, a value larger than the sum of the van der Waals radii (3.60 Å)[40] of the sulfur atoms.

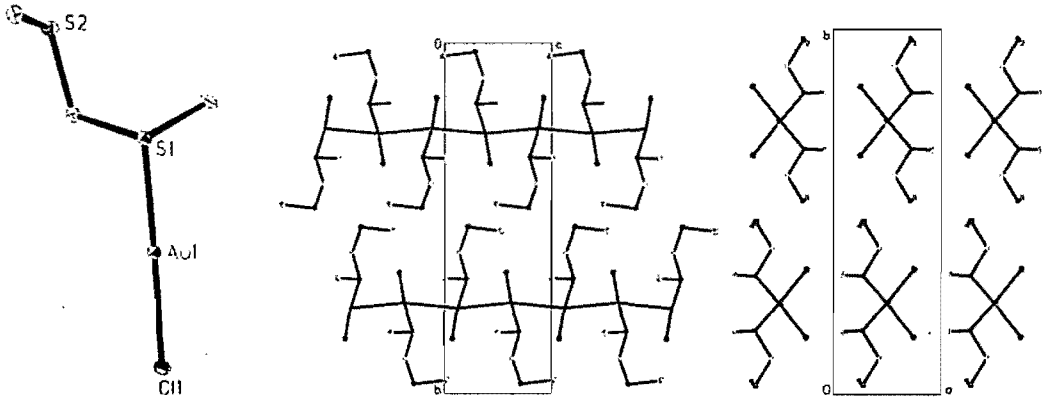

Figure 5.1. Complex **1**. (a) The repeat unit. (b) Side-view of the chains in the unit cell. (c) Projection down the chain axis. Color code: C: grey; Cl: green; S: yellow; Au: orange.

$[Au_2L^{2\text{-}Ph}Cl_2]_\infty$ (7). Complex 7 was obtained by the reaction of the 1,2-bis(phenylthio)ethane building block, $L^{2\text{-}Ph}$, and gold salt. One organic ligand is linked to two Au(I) metal centres so as to form $[Au_2L^{2\text{-}Ph}Cl_2]$ entity with the 1:2 ligand-to-metal ratio (Figure 5.2). On the other hand, the gold(I) atoms of neighbouring entities are linked to one another via aurophilic interactions, so as to form an infinite chain of gold atoms [Au-Au-]$_\infty$ parallel to the a-axis (Figure 5.2c). Furthermore, adjacent [Au-Au-]$_\infty$ chains are connected by the spacer, thus yielding a two-dimensional coordination network, $[L^{2\text{-}Ph} - (AuCl)_2]_\infty$. In fact, the Au(I)···Au(I) separations are 3.1204(5) and 3.1499(5) Å, a value in the normal range for an aurophilic interaction (2.7690(7)- 3.341(2) Å).[29-39] The repeat unit of 7 consists of a 14-membered metallomacrocycle, $Au_6(L^{2\text{-}Ph})_2$ (Figure 5.2a). In this complex, there are two crystallographically independent Au(I) metal centres, which have similar coordination environment (Table 5.2). As in **1**, each gold(I) atom is surrounded by four neighbours in a sligthly distorted square planar coordination (Figure S1, Annexe VIII).

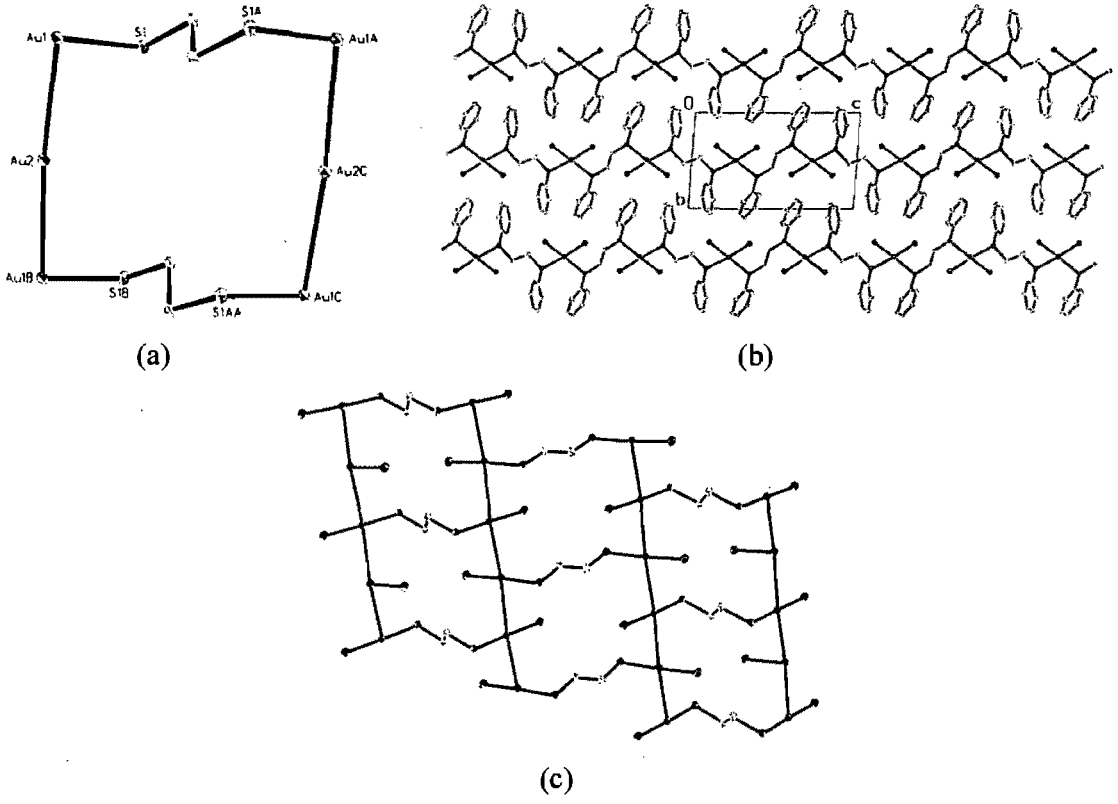

Figure 5.2. Complex 7. (a) The repeat unit. The phenyl ring have been removed for clarity. (b) The 1D-coordination polymer chains parallel to the *c*-axis. (c) Projection showing the (Au-Au-)$_\infty$ chains of 7. Color code: C: grey; Cl: green; S: turquoise; Au: red.

Structures of 2, 3, and 5. The complexes **2**, **3** and **5** have the same stoichiometry (2Au:1L) and adopt very comparable structures. They all form 1D-coordination polymers, where the repeat unit is [Au(Cl)-Au(Cl)-$\mathbf{L^{n\text{-}R}}$-]. Each gold atom, in **2** has four neighbours (Au, S and two Cl), while in **3** and **5**, the gold atom has three neighbours (Au, Cl, S).

$[Au_2L^{1\text{-}Ph}Cl_2]_\infty$ (2). The self-assembly of $\mathbf{L^{1\text{-}Ph}}$, bis(phenylthio)methane, and the gold salt give rise of a one-dimensional coordination polymer (Figure 5.3a). In this complex, one bis(phenylthio)methane is coordinated to two gold(I) atoms yielding $[C_{13}H_{12}S_2Au_2CL_2]$ entities. Adjacent entities are bound to one another by an aurophilic interaction, with an Au(I)···Au(I) separation of 3.0347(4) Å, so as to form a 1D-coordination polymer extending parallel to the c-axis (Figure 5.3b). There are weak Au···Cl interactions between neighbouring polymer chains, since the Au···Cl distance (3.284(1) Å) is shorter than the sum of the van der Waals radii of Au···Cl, 3.41 Å.[40] Thus, this complex may be best described as a columnar coordination polymer (Figure 5.3d). Such secondary interaction was observed for the self-assembly of gold salt and dimethylglyoxime with an Au···Cl separation of 3.323 (4) Å.[41] According to Allen *et al.*[42] and Simonov *et al.*,[41] there are 17 gold complexes in the Cambridge Data Base containing a weak Au···Cl interaction with a separation ranging from 3.281 to 3.526 Å.

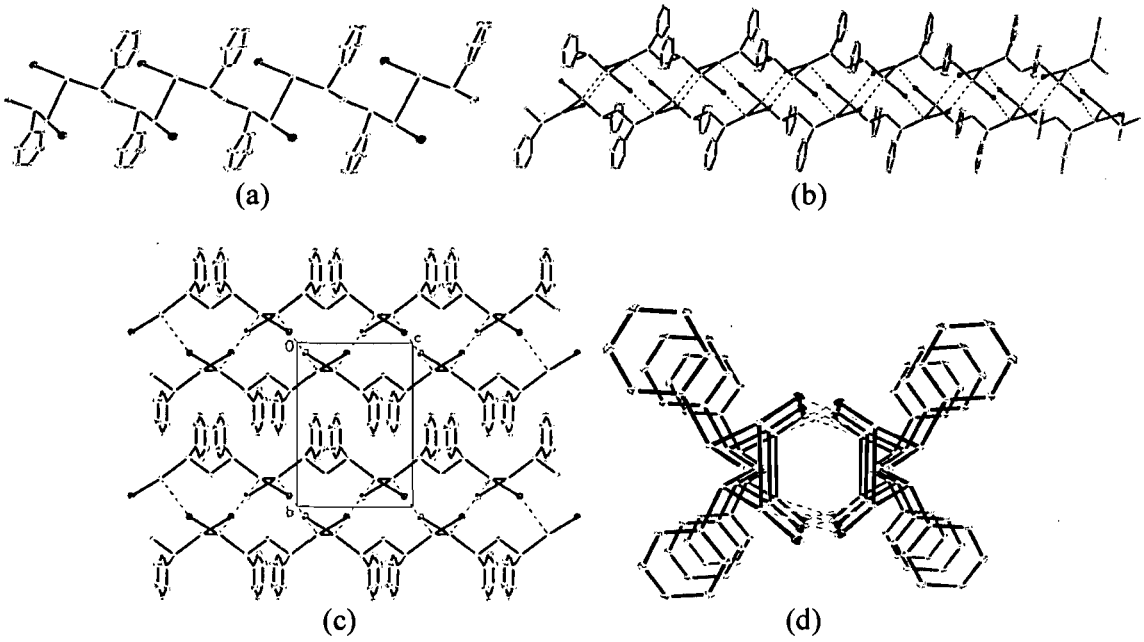

Figure 5.3. Complex **2**. (a) A single chain. (b) Formation of a double chain through weak Au···Cl interactions. (c) The *bc*-plane projection of **2**. (d) Projection along the chain axis. Color code: C: grey; Cl: green; S: yellow; Au: orange.

Complexes 3 and 5 $[Au_2L^{3\text{-}Ph}Cl_2]_\infty$. The complexes **3** and **5** form very similar 1D-coordination polymers. However, the ligand torsion angles differ for **3** and **5** (Figure 5.4a, 5.5a and Table 5.3). The chains extend parallel to the *c*-axis and neighbouring $[Au_2L^{3\text{-}Ph}Cl_2]$ units are associated through short intermolecular Au(I)···Au(I) contacts (auriphilicity)[29-39] (Figures 5.4b, 5.5b). Indeed, the Au···Au distances for **3** and **5** which are respectively 3.2997(4) and 3.1918(9) Å fall in the normal range, 2.7690(7) - 3.341(2) Å, indicating Au···Au aurophilic interaction. [29-39] The packing of the chains is shown by projections on the *ab*-plane (Figure 5.4c, 5.5c).

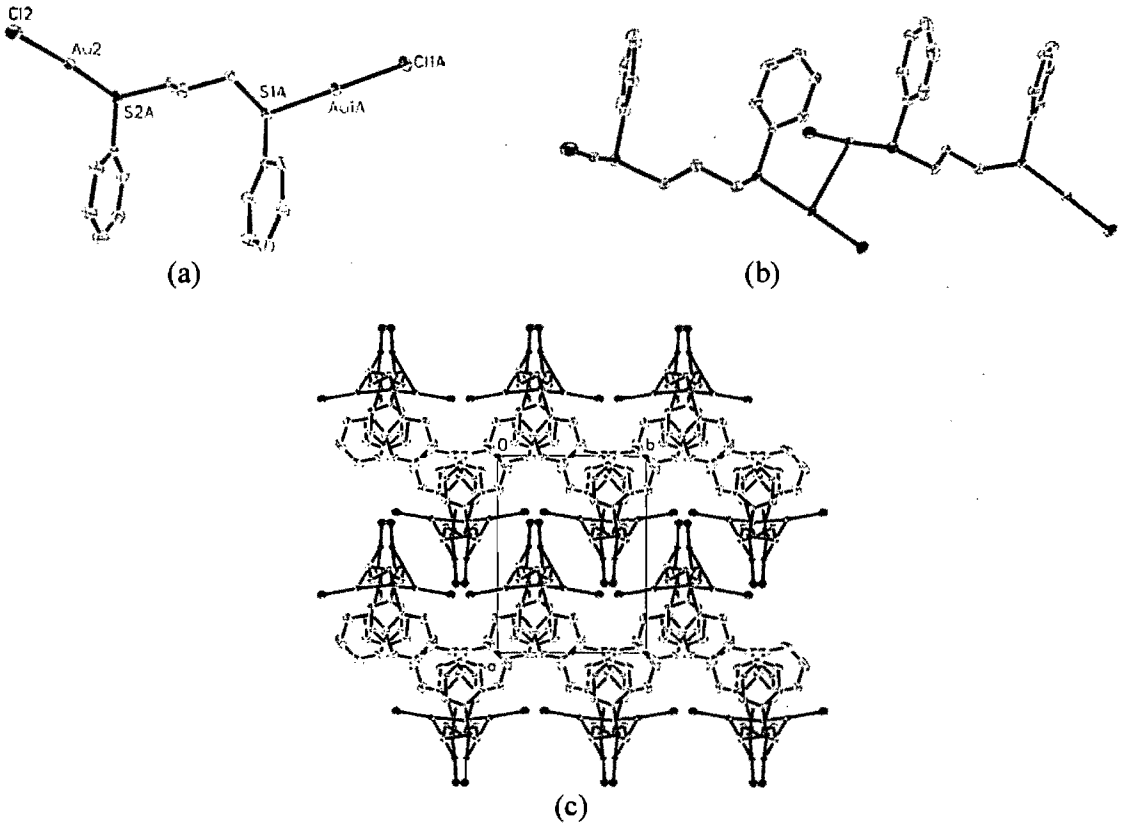

Figure 5.4. Complex **3**. (a) The repeat unit. (b) The 1D-coordination polymer.
(c) Projection of **3** on the *ab*-plane. Color code: C: grey; Cl: green; S: turquoise; Au: red.

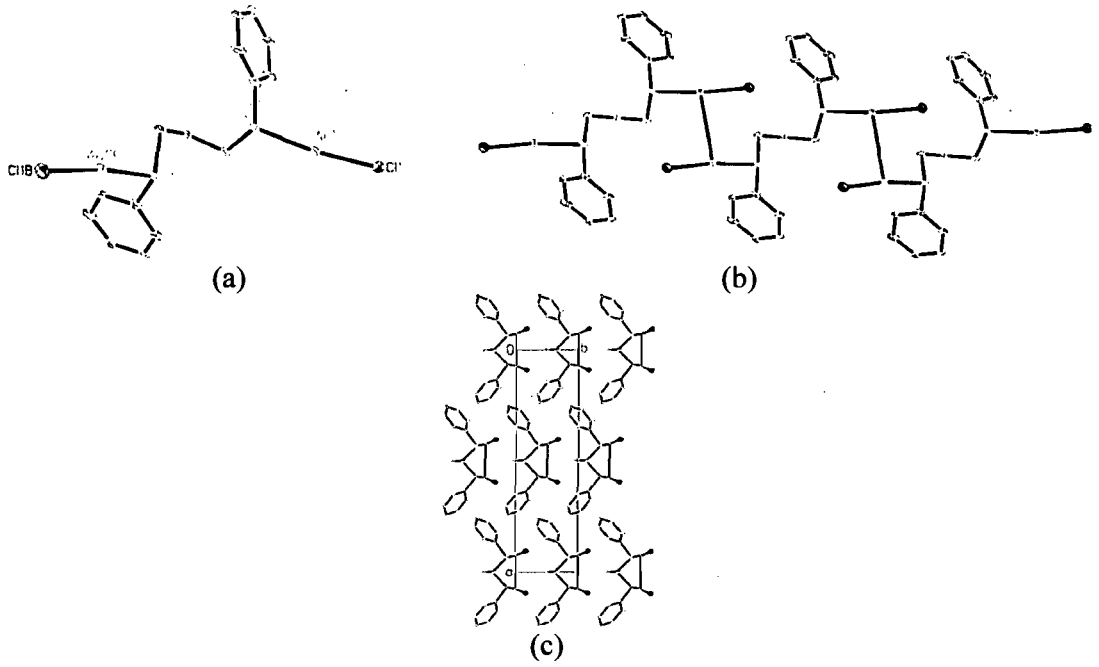

Figure 5.5. Complex **5**. (a) The repeat unit. (b) Formation of the 1D-coordination polymer extending along the *c*-axis. (c) Projection of the chains of **5** onto the *ab*-plane. Color code: C: grey; Cl: green; S: yellow; Au: orange.

Molecular complexes $[Au_2L^{3\text{-}Ph}Cl_2]$ (4) and $[Au_2L^{4\text{-}Ph}Cl_2]$ (8).

Complexes **4** and **8** were obtained by the combination of gold(I) with $L^{3\text{-}Ph}$ and $L^{4\text{-}Ph}$ respectively. In complex **4**, the Au···Au distance (3.615 Å) in adjacent $[Au_2L^{3\text{-}Ph}Cl_2]$ components and the Au···Au separation (4.555 Å) from neighbouring $[Au_2L^{4\text{-}Ph}Cl_2]$ molecules in **8** are clearly longer than twice the van der Waals radius of Au, 3.32 Å,[40] indicating the absence of aurophilic interactions. In both **4** and **8** the gold atoms have a linear coordination (Figure 5.6, 5.7).

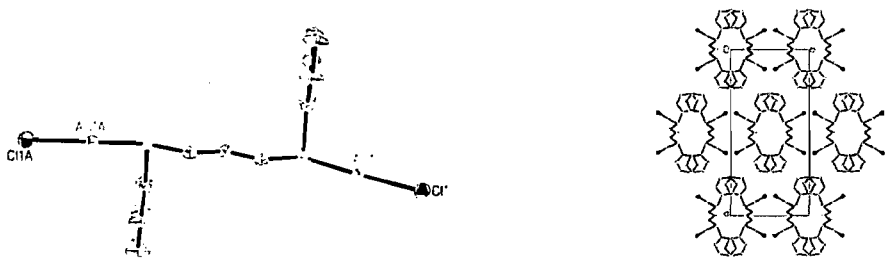

Figure 5.6. Complex **4**. (a) The repeat unit. (b) Projection along the *b*-axis showing the packing of **4**. Color code: C: grey; Cl: green; S: yellow; Au: orange.

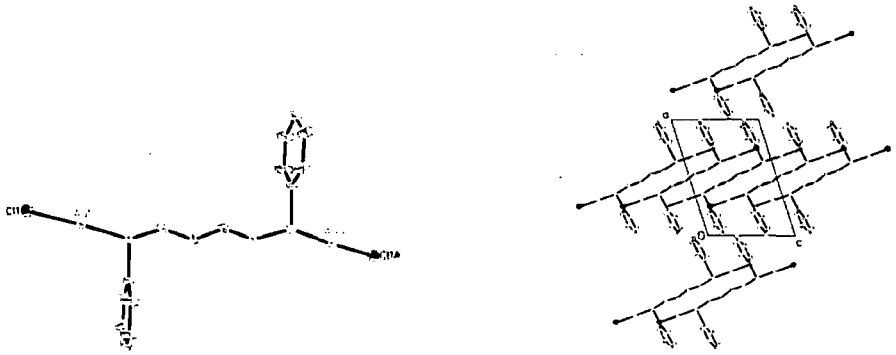

(a) (b)

Figure 5.7. Complex **8.** (a) The repeat unit. (b) Packing of the molecules projected onto the *ac*-plane. Color code: C: grey; Cl: green; S: yellow; Au: orange.

Table 5.3. Torsion angles of interest (°) for complexes **1-5**, **7** and **8**.

	3	**4**	**5**
Au-S-C-C	-173.7(1)	-176.2(1)	-170.5(1)
S-C-C-C	67.5(1)	-178.9(1)	-51.2(1)
C-C-C-S	178.4(1)	-178.9(1)	-51.2(1)
C-C-S-Au	-49.5(1)	-176.2(1)	-170.5(1)
	1		
Au-Au-Au-Au	180		
	2		
Au-S-C-S	178.9(1)		
S-C-S –Au	178.9(1)		
	7		
Au-S-C-C	-179.0(1)		
S-C-C-S	180		
C-C-S-Au	179.0(1)		
Au-Au-Au-Au	180		
	8		
Au-S-C-C	176.5(1)		
S-C-C-C	175.6(1)		
C-C-C-C	180		
C-C-C-S	-175.6(1)		
C-C-S-Au	-176.5(1)		

5. 5 Discussion

One may see the effect of the bulk of the R substituent upon the networks, when the structures of complexes **1** and **2** were compared (Figures 5.1 and 5.3). Indeed, for R = Ph, $\mathbf{L}^{\mathbf{1\text{-}Ph}}$, the two sulfur atoms of the ligand were coordinated to the gold centre in order to form $[Au_2\mathbf{L}^{\mathbf{1\text{-}Ph}}Cl_2]$ repeat units, while for R = Me, $\mathbf{L}^{\mathbf{1\text{-}Me}}$ only one sulfur atom of the ligand was bonded to metal centre, $[Au\mathbf{L}^{\mathbf{1\text{-}Me}}Cl]$. For both complexes, the repeat units were expanded *via* aurophilic interactions, except that for **1** the aurophilic interaction seems to be cooperative, leading to the formation of a chain of Au(I) (Figure 5.1b).

Furthermore, for the complexes **3** and **5** made up with $\mathbf{L}^{\mathbf{3\text{-}Ph}}$, the repeat units $[Au_2\mathbf{L}^{\mathbf{3\text{-}Ph}}Cl_2]$ were connected to each others *via* aurophilic interactions, so as to form topologically similar a one-dimensional coordination polymer (Figures 5.4, 5.5). The absence of Au···Au contacts between adjacent $[Au_2\mathbf{L}^{\mathbf{3\text{-}Ph}}Cl_2]$ units in **4**, and $[Au_2\mathbf{L}^{\mathbf{4\text{-}Ph}}Cl_2]$ in **8** results in molecular structures.

Thus, the phenyl group seems to favour the formation of $[Au_2\mathbf{L}^{\mathbf{n\text{-}Ph}}Cl_2]$ repeat units, where n = 1, 3 and 4, with the ligand-to-metal ratio 1:2 in which one dithioether ligand is coordinated to two metal centers. Whereas, the less bulky methyl group seems to privilege the presence of $[Au\mathbf{L}^{\mathbf{1\text{-}Me}}Cl]$ repeat units, with the ligand-to-metal ratio 1:1 with only one sulfur coordination site of the organic ligand engaged with a metal centre.

The self-assembly of $\mathbf{L}^{\mathbf{3\text{-}Me}}$ and gold lead to the formation of a complex **6** with a 1:1 ligand-to-metal ratio. However, we were unable to elucidate its structure since the crystals of this complex were found to be too small in size and not unique. However, a very small piece was mounted on a Smart 6000K diffractometer equipped with a rotating anode (CuKα). Unfortunately the data was not of good suffisantly quality and the structure could not be solved.

The structure of the complex **7**, with $\mathbf{L}^{\mathbf{2\text{-}Ph}}$, which had been reported by Drew and Riedl[16] from room temperature X-ray data, is a 2D-coordination polymer (Figure 5.2). The low temperature measurement (100 K) was undertaken at a temperature closer to that of the luminescence measurements. The 100 K Au···Au distances (3.1204(5) and 3.1499(5) Å) are shorter than the corresponding quantities obtained at room temperature (3.187(2) and 3.309(2) Å) reflecting the volume decrease from 833.2 to 805.4 $Å^3$.[16] The repeat unit of **7**, $[Au_2\mathbf{L}^{\mathbf{2\text{-}Ph}}Cl_2]$, is similar to that of the gold(I) complexes obtained with $\mathbf{L}^{\mathbf{1\text{-}Ph}}$, $\mathbf{L}^{\mathbf{3\text{-}Ph}}$ and

$L^{4\text{-}Ph}$. This leads us to believe that the phenyl groups seem to favor the 2:1 metal:ligand stoichiometry. Nevertheless, contrary to what is noted for **2**, **3** and **5**, there are $[Au\text{-}Au\text{-}]_\infty$ chains in **7** (Figure 5.2).

In **7**, adjacent $[Au\text{-}Au\text{-}]_\infty$ chains are linked by $L^{2\text{-}Ph}$ ligands. In order to demonstrate if this situation is related to the size of the ligand $L^{2\text{-}Ph}$, we attempted to synthesize the related gold(I) complex of $L^{2\text{-}Me}$. Unfortunately this complex could not be obtained.

Polymorphism was observed for the 1,3-bis(phenylthio)propane, $L^{3\text{-}Ph}$. The three polymorphs **3-5** have identical unit, $[Au_2L^{3\text{-}Ph}Cl_2]$. Nevertheless, they have distinct Au···Au separations. Complexes **3** and **5**, where the Au(I)···Au(I) distances are 3.2997(4) and 3.1918(9) Å respectively, form 1D-coordination polymers while **4**, with a Au(I)···Au(I) separation of 3.615 Å, is composed of discrete molecules (Figures 5.4, 5.5 and 5.6). As shown in Table 5.3, the polymorphs adopt different conformations (Table 5.3). In **3** and **5** the phenyl groups of the same $L^{3\text{-}Ph}$ ligand are located on the same side of the aliphatic chain while in **4**, the phenyl groups are located on opposite sides of the aliphatic chain (Figure 5.4a, 5.5a and 5.6a). Complex **3** has a *trans-gauche-trans-gauche* conformation, while the conformation of **4** is all-*trans* and that of **5** is *trans-gauche-gauche-trans*. Consequently, the disposition in the solid state differ from one another in these three complexes (Figures 5.4c, 5.6b and 5.5c). Complexes **4**, with $L^{3\text{-}Ph}$ and **2**, with $L^{1\text{-}Ph}$ adopt an identical packing mode (Figure S2, Annexe VIII).

The $L^{4\text{-}Ph}$ ligand in complex **8** and $L^{2\text{-}Ph}$ in **7**, which have an even number of CH_2 groups, are in the fully extended conformation (Table 5.3). This situation is not uncommon for symmetrical related molecules that have an even number of methylene groups in their aliphatic chain, such as the free ligands $L^{2\text{-}Ph}$, $L^{4\text{-}Ph}$, $L^{6\text{-}Ph}$, $L^{8\text{-}Ph}$ and $L^{10\text{-}Ph}$ which all contain a centre of symmetry in the middle of their central CH_2–CH_2 bond and all adopt the all trans conformation.[8]

UV-visible spectroscopy. The electronic absorption data of the title complexes, measured in acetonitrile, are listed in Table 5.4. Since complex **6** is insoluble in common organic solvants, the absorption spectrum of this complex cannot be reported. All complexes display moderately intense absorption bands in the 234-256 nm range. The spectra of the complexes are similar to those of the corresponding free ligands as shown in Figures S3-S7, annexe VIII, and the main absorption bands of the complexes can therefore be assigned as ligand-centered transitions.

Table 5.4. Spectroscopic and Photophysical Data of **1-5**, **7** and **8**.

	1	**2**	**3**	**4**	**5**	**7**	**8**
λ_{max} (nm)	234	256	254	256	255	255	254
ε ($dm^3 mol^{-1} cm^{-1}$)	10216	15276	14308	15783	14588	12072	13018

Table 5.5. Luminescence of complexes **1** and **7**.

	1	**7**
E_{max} (cm^{-1})	17250	17900
$W_{1/2Height}$ (cm^{-1})	2400	2300

Luminescence. The solid-state emission spectra at 5 K of complexes **1** and **7** were obtained and are shown in Figure 5.8. The main characteristics of these spectra are listed in Table 5.5. Luminescence intensities decrease as the temperature increase and the compounds did not emit at room temperature.

The emitting compounds contain 1D polymeric chains ($\mathbf{L^{1\text{-}Me}}$, $\mathbf{L^{2\text{-}Ph}}$). Many different interpretations of the luminescence of gold(I) compounds have been proposed: ligand-centred (LC),[43] metal-ligand charge transfer (MLCT),[44] ligand-metal charge transfer (LMCT),[45] metal-centered (MC)[46] or a combination of these categories.[47]

Ab initio calculations (MP2 and CIS) on gold(I) cationic dimers containing thioether ligands[48] assigned the luminescence to a predominantly metal centred transition. These transitions shift to lower energy as Au(I)···Au(I) distances decrease.[49] In contrast, the luminescence band maximum E_{max} of complex **7**, with $\mathbf{L^{2\text{-}Ph}}$, is slightly higher in energy, 17900 cm^{-1}, than the luminescence of **1**, with $\mathbf{L^{1\text{-}Me}}$, 17250 cm^{-1}, even though the Au···Au distance in **7** is shorter. This could be due to the phenyl group on the thiol ligand affecting the ligand strength and the energy of the Au d_{z2} molecular orbital, the difference in the S-Au-Au-S torsion angle affecting the overlap of the gold orbitals or other structural features affecting the HOMO and/or the LUMO energies. Unfortunately, the experimental spectra do not allow to unambiguously identify the differences in electronic structure leading to the different luminescence band maxima. The apparent importance of the Au···Au interactions on the energy of the first excited state rules out purely ligand-centred transitions.

The luminescence spectra of the two compounds show vibronic progressions (shoulders), as shown in Figure 5.8. The average progression interval is on the order of 600 cm^{-1}, indicating that emitting-state distortions occur along normal coordinates other than the low-frequency metal-metal modes, leading to the large luminescence bands. Metal-centred luminescence has been reported for gold(I) compounds with sulfur ligands (dithiocarbonates) and leads to band widths of 1000 cm^{-1}.[34] The assignment as a purely metal-centered transition is therefore too simplistic, as the vibrational progressions reveal a contribution from the ligands (Figure S8, S9, Annexe VIII).

Luminescence spectra can be calculated[50] and show a satisfactory agreement with the experimental spectra as illustrated in Figure 5.8.

The calculated spectra were obtained with electronic origins set to 18950 and 19300 cm^{-1}, vibrational frequencies of 610 cm^{-1} and dimensionless excited-state distortions of 2.22 and 2.52, for complexes **1** and **7**, respectively. The different values obtained for the excited-state distortion reveal small but significant differences in the emitting-state characteristics of the two complexes, quantitatively showing the influence of differences in ligand structure on solid-state luminescent properties. We suspect that the luminescence of **2-6** and **8** could not be excited with the 350 nm laser used.

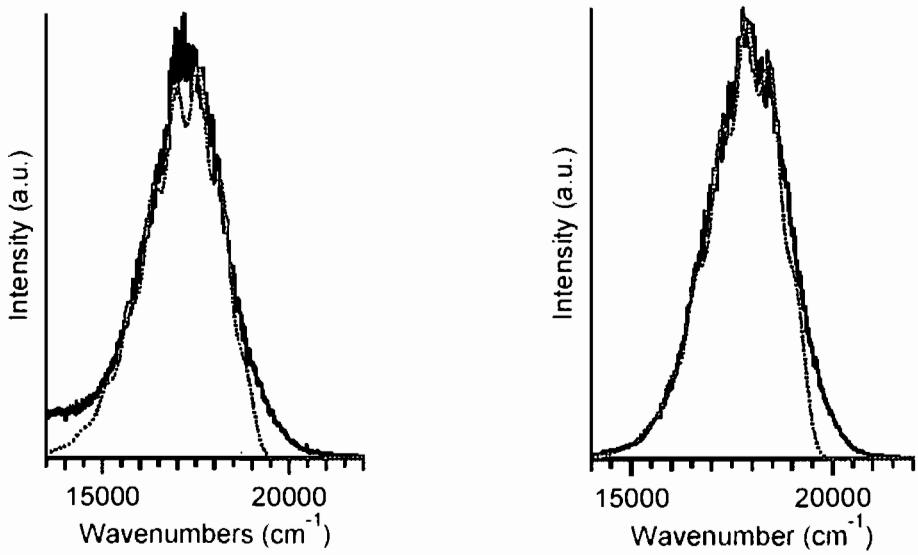

Figure 5.8. (a) Solid-state luminescence spectra of complex **1** and (b) Solid-state luminescence spectra of complex **7**. (Experimental spectrum: black line; luminescence fit: red line).

5. 6 Concluding remarks

In summary, we have prepared and characterized a series of gold(I)-dithiolate bearing aliphatic chain complexes. The phenyl group of the $RS(CH_2)_nSR$ ligands allows the formation of gold(I) complexes, where the repeat unit is $[Au_2L^{n\text{-}Ph}Cl_2]$ while the methyl group leads to $[AuL^{n\text{-}Me}Cl]$ repeat unit. These repeat units are linked to each others (**1-3**, **5** and **7**) *via* aurophilic interactions to form to supramolecular compounds.

The polymeric compounds **1** and **7** have ligand-unsupported Au(I) chains, $[Au\text{-}Au\text{-}]_\infty$. Polymorphism was observed for the 1,3-bis(phenylthio)propane, $L^{3\text{-}Ph}$.

Except for **6**, all the complexes are soluble in common organic solvents. Complexes **1** and **7** show solid-state luminescence at 5 K. Their spectra show vibronic progressions.

Supplementary Material Available.

X-ray crystallographic information files (CIF) for compounds (**1-5**, **7** and **8**). Figures (S1 – S9). This material is available free of charge via the Internet at http://pubs.acs.org.

Acknowledgements.

The authors would like to thank the Natural Sciences and Engineering Research Council of Canada. M.O.A would like to thank the Organisation International de la Francophonie and the Programme Canadien de Bourse de la Francophonie (PCBF) for a graduate scholarship.

5.7 References

(1) Yip, S. K.; Cheng, E. C. C.; Yuan, L. H.; Zhu, N.; Yam, V. W. W. *Angew. Chem. Int. Ed.* **2004**, *43*, 4954.

(2) Schmidbaur, H. *Chem. Soc. Rev.* **1995**, 24, 391-400.

(3) (a) Laibinis, P. E.; Bain, C. D.; Nuzzo, R. G.; Whiteside, G. M. *J. Phys. Chem.* **1995**, *99*, 7663. (b) Aizemberg, J.; Black, A. J.; Whiteside, G. M. *J. Am. Chem. Soc.* **1999**, *121*, 4500.

(4) Burst, M.; Blass, P. M.; Bard, A. J. *Langmuir* **1997**, *13*, 5602.

(5) (a) Moraille, P.; Badia, A. *Langmuir* **2003**, 19, 8041. (b) Sanchez, J.; Badia, A. *Thin Solid Films* **2003**, 440, 223. (c) Moraille, P.; Badia, A. *Angew. Chem. Int. Ed.* **2002**, 41, 4303. (d) Moraille, P.; Badia, A. *Langmuir* **2002**, 18, 4414. (e) Badia, A.; Lennox, R.B.; Reven, L. *Acc. Chem. Res.* **2000**, 33, 475.

(6) (a) Bu, X. H.; Chen, W.; Hou, W. F.; Du, M.; Zhang, R. H.; Brisse, F. *Inorg. Chem.*

2002, *41*, 3477. (b) Awaleh, M. O.; Badia, A.; Brisse, F. *Inorg. Chem.* **2005**, *44*, 7833. (c) Awaleh, M. O.; Badia, A.; Brisse, F.; Bu, X. H. *Inorg. Chem.* **2006**, *45*, 1560. (d) Awaleh, M. O.; Badia, A.; Brisse, F. *Cryst. Growth Des.* **2005**, *5*, 1897. (e) Awaleh, M. O.; Badia, A.; Brisse, F. *Cryst. Growth Des.* **2006**, *6*, 2674. (f) Awaleh, M. O.; Badia, A.; Brisse, F. *Inorg.Chem.* **2006**, *Submitted for publication.*

(7) (a) Pearson, R. G. *J. Am. Chem. Soc.* **1963**, *85*, 3533. (b) Pearson, R. G. *J. Chem. Educ.* **1968**, *45*, 581. (c) Pearson, R. G. *J. Chem. Educ.* **1968**, *45*, 643.

(8) (a) Awaleh, M. O.; Badia, A.; Brisse, F. *Acta Crystallogr.* **2005**, *E61*, o2479. (b) Chen, W.; Hou, B. H.; Zhou, L. N.; Wang, J. K.; Li, H. *Acta Crystallogr.* **2005**, *E61*, o1890. (c) Awaleh, M. O.; Badia, A.; Brisse, F. *Acta Crystallogr.* **2005**, *E61*, o2476. (d) Chen, W.; Yin, Q.-X.; Xie, C.; Wang, J.-K.; Li, H. *Acta Crystallogr.* **2004**, *E60*, o2147. (e) Awaleh, M. O.; Badia, A.; Brisse, F. *Acta Crystallogr.* **2005**, *E61*, o2473.

(9) Cotton, F. A.; Wilkinson, G. *Adavanced Inorganic Chemistry.* 5rd ed. John Wiley and Sons, 1988.

(10) Puddephatt, R. J. In *The Chemistry of Gold*; Clark, R. J. H., Ed.; Elsevier: Amsterdam, 1978.

(11) Leznoff, D. B.; Lefebvre, J. *Gold Bull.* **2005**, *38*, 47.

(12) Tzeng, B. C.; Schier, A.; Schmidbaur, H. *Inorg. Chem.* **1999**, *38*, 3978.

(13) Hollatz, C.; Schier, A.; Schimidbaur, H. *J. Am. Chem. Soc.* **1997**, *119*, 8115.

(14) (a) Puddephatt, R. J. *Coord. Chem. Rev.* **2001**, *216-217*, 313 and references therein. (b) Schimdbaur, H. Gold: Progress in Chemistry, Biochemistry and Technology, Wiley, New York, 1999.

(15) Corbierre, M. K.; Lennox, R. B. *Chem. Mater.* **2005**, *17*, 5691 and references therein.

(16) Drew, M. G. B.; Riedl, M. J. *J. Chem. Soc., Dalton Trans.* **1973**, 52.

(17) Davis, M. J.; Reber, C. *Inorg. Chem.* **1995**, *34*, 4585.

(18) Hartley, F. R.; Murray, S. G.; Levason, W.; Soutter, H. E.; McAuliffe, C. A. *Inorg. Chim. Acta* **1979**, *35*, 265.

(19) SAINT Release 6.06, Integration Software for Single Crystal Data; Bruker AXS Inc.: Madison, WI, **1999**.

(20) Sheldrick, G.M. SADABS Bruker Area Detector Absorption Corrections; Bruker AXS Inc.: Madison, WI, **1996**.

(21) Enraf-Nonius. CAD-4 Software, Version 5.0. Enraf-Nonius; Delft, Holland, **1989**.

(22) Gabe, E. J.; Le Page, Y.; Charlant, J. P.; Lee, F. L.; White, P. S. *J. Appl Crystallogr.* **1989**, *22*, 384.

(23) XPREP Release 5.10; X-ray Data Preparation and Reciprocal Space Exploration Program. Bruker AXS Inc., Madison, WI, **1997**.

(24) SHELXTL Release 5.10. The Complete Software Package for Single-Crystal Structure Determination; Brucker AXS Inc.: Madison, WI, **1997**.

(25) Sheldrick, G.M. SHELXS97, Program for the Solution of Crystal Structures; University of Göttingen: Göttingen, Germany, **1997**.

(26) Flack, H. D.; Schwarzenbach, D. *Acta Crystallogr., Sect. A* **1988**, *44*, 499.

(27) Al-Sa'ady, A. K.; McAuliffe, C. A.; Parish, R. V.; Sandbank, J. A. *Inorg. Synth.* **1985**, *23*, 191.

(28) (a) Canumalla, A. J.; Al-Zamil, N.; Phillips, M.; Isab, A. A.; Shaw III, C. F. *J. Inorg. Bio.* **2001**, *85*, 67. (b) Konno, T.; Hattori, M.; Yoshimura, T.; Hirotsu, M. *Chemistry Letters* **2002**, 230.

(29) Pyykkö, P.; Zhao, Y.-F. *Angew. Chem. Int. Ed.* **1991**, *30*, 604; *Angew. Chem.* **1991**, *103*, 622.

(30) Sladek, A.; Smidbaur, H. *Inorg. Chem.* **1996**, *35*, 3268 and references therein.

(31) Li, J.; Pyykkö, P. *Chem. Phys. Lett.* **1992**, *197*, 586.

(32) Schmidbaur, H. *Pure Appl. Chem.* **1993**, *65*, 691.

(33) Li, J.; Pyykkö, P. *Inorg. Chem.* **1993**, *32*, 2630.

(34) King, C.; Wang, J. C.; Khan, N. I.; Flacker, Jr., J. P. *Inorg. Chem.* **1989**, *28*, 2145.

(35) Leznoff, D. B.; Xue, B. Y; Batchelor, R. J.; Einstein, F. W. B.; Patrick, B. O. *Inorg. Chem.* **2001**, *40*, 6026.

(36) Tzeng, B. C.; Liao, J. H.; Lee, G. H.; Peng, S. M. *Inorg. Chem. Acta* **2004**, *357*, 1405.

(37) Mansour, M. A.; Connick, W. B.; Lachiotte, R. J.; Glysling, H. J.; Eisemberg, R. *J. Am. Chem. Soc.* **1998**, *120*, 1329.

(38) Tzeng, B. C.; Yeh, H. T.; Huang, Y. C.; Chao, H. Y.; Lee, G. H.; Peng, S. M. *Inorg. Chem.* **2003**, *42*, 6008.

(39) Forward, J. M.; Bohmann, D.; John P. Flacker, Jr.; Staples, R. J. *Inorg. Chem.* **1995**, *34*, 6330.

(40) Porterfield, W. W. *Inorganic Chemistry: A Unified Approach*, Addison-Wesley, 1994, p.168.

(41) Simonov, Y.; Bologa, O.; Bourosh, P.; Gerbeleu, N.; Lipkowski, J.; Gdaniec, M. *Inorg. Chem. Acta* **2006**, *359*, 721.

(42) Allen, F. H.; Kennard, O. *Chem. Des. Autom. News* **1993**, *8*, 31.

(43) Watase, S.; Nakamoto, M.; Kitamura, T.; Kanehisa, N.; Kai, Y. Yanagida, S. *J. Chem. Soc., Dalton Trans.* **2000**, 3585.

(44) Flamigni, L.; Talarico, A. M.; Chambron, J. C.; Heitz, V.; Linke, M.; Fijita, N.; Sauvage, J. P. *Chem. Eur. J.* **2004**, *10*, 2689.

(45) Hanna, S. D.; Zink, J. I. *Inorg. Chem.* **1996**, *35*, 297.

(46) Tang, S. S.; Chang, C.; Lin, I. J. B.; Liou, L.; Wang, J. *Inorg. Chem.* **1997**, *36*, 2294.

(47) Lee, Y. A.; McGarrah, J. E.; Lachicotte, R. J.; Eisenberg, R. *J. Am. Chem. Soc.* **2002**, *124*, 10662.

(48) Pan, Q. J.; Zhang, H. X. *Inorg. Chem.* **2004**, *43*, 593.

(49) (a) Fischer, P.; Mesot, J.; Lucas, B.; Ludi, A.; Patterson, H. H.; Hewat, A. *Inorg. Chem.* **1997**, *36*, 2751. (b) Yersin, H.; Riedl, U. *Inorg. Chem.* **1995**, *34*, 1642.

(50) (a) Brunold, T. C.; Güdel, H. U. In *Inorg. Elect. Struct and Spect*, E. I. Salomon, A. B. P. Lever (Editors) Vol I, p 259. (b) Zink, J. I. *Coord. Chem. Rev.* **2001**, *211*, 69.

Chapitre 6. Discussion générale.

En 2000, Brisse et Bu ont débuté une étude des paramètres expérimentaux qui influencent les structures obtenues par l'autoassemblage du 1,4-bis(phénylthio)butane, $\mathbf{L^{4\text{-}Ph}}$, et des ions argent(I).[1] Cette étude a montré que le rapport métal:ligand, le solvant de recristallisation et la nature des anions influençaient la formation des réseaux métallosupramoléculaire pour ce ligand.[1]

Au cours de ce travail, il était signalé que la stœchiométrie des complexes dépendait du rapport métal:ligand des produits de départ. Avec l'anion perchlorate, le rapport métal:ligand 2:3 permettait de générer un réseau bidimensionnel neutre de type hexagonal où l'anion était coordonné au métal, tandis que le rapport métal:ligand 1:2 conduisait à un réseau lamellaire cationique de type carré où les anions perchlorates, localisés entre les feuillets, équilibraient les charges. D'un autre côté, le nitrate, anion coordonnant, participait à la formation d'un réseau bidimensionnel neutre où le ligand reliait deux atomes d'argent pour générer des chaînes $[Ag\text{-ligand}]_{\infty}$. Ces dernières, reliées les unes aux autres par des nitrates, formaient un réseau 2D.[1]

Mon projet de recherche s'inscrit dans la lignée de ces travaux. Ainsi, le but du travail était d'étudier les facteurs pouvant influencer la formation des réseaux, quand des ligands dithiolatés symétriques (Schéma 6.1) sont autoassemblés avec de l'argent(I) ou de l'or(I). De ce fait, nous nous sommes intéressés aux paramètres tels que la taille du substituant **R** du ligand, la longueur de la chaîne aliphatique, la nature du contre-ion, le rapport métal:ligand des produits de départ, ainsi que les solvants de recristallisation.

Schéma 6.1. Les ligands connecteurs choisis où **n** est le nombre de groupements méthylène et **R** = Ph, *t*Bu, Benz, Et et Me. (b) Les angles de torsion décrivant la conformation du ligand.

L'autoassemblage des ligands $\mathbf{L^{n\text{-}R}}$, $\mathbf{RS(CH_2)_nSR}$, où **n** = 1-10 et **R** = Ph, *t*Bu, Benz, Et, Me, et des sels d'argent ont permis de générer principalement des composés métallosupramoléculaires.[2,3] En fait, ces ligands possèdent deux sites de coordination. Par

conséquent, quand un atome de soufre du ligand est engagé dans une liaison de coordination avec un atome d'argent, le second atome de soufre du ligand a la possibilité de se coordonner à un autre métal permettant ainsi la propagation du centre métallique dans un réseau. Nous avons classé dans les tableaux 9.1 - 9.8, en annexe IX, les complexes dont nous avons établi la structure, ainsi que ceux publiés par d'autres chercheurs.[2,3]

6.1 Description des structures des différents types de réseaux observés.

Les structures des complexes sont décrites en termes de topologie. En général, ces composés métallosupramoléculaires forment des réseaux étendus à l'état solide (1D, 2D et 3D) et très rarement des composés moléculaires.

6.1.1 Polymères de coordination à une dimension

L'examen détaillé des structures révèle l'existence de plusieurs types de chaînes linéaires. Ces chaînes peuvent être simples, tubulaires ou doubles (Schéma 6.2).

Chaînes simples

Une chaîne simple est générée quand le ligand ditopique connecte deux atomes d'argent adjacents. Pour ces chaînes, l'anion ne fait que compléter la sphère de coordination du métal. De ce fait, la coordination de l'argent est 3 et, grâce à l'environnement trigonal du métal, la topologie de ces polymères de coordination est une chaîne en zig-zag (Schéma 6.2a).

Le bis(phénylthio)méthane, $\mathbf{L^{1\text{-}Ph}}$, et le bis(*tert*-butylthio)méthane, $\mathbf{L^{1\text{-}tBu}}$, mènent principalement à la formation de polymères de coordination 1D où les anions de petite taille se coordonnent seulement au métal.[2a,3a]

Chaînes ''tubulaires''

Les chaînes tubulaires sont rares pour les polymères de coordination d'argent(I).[4] Néanmoins, une chaîne tubulaire a été obtenue seulement quand le 1,2-bis(phénylthio)éthane, $\mathbf{L^{2\text{-}Ph}}$, a été combiné avec le nitrate d'argent (Schéma 6.2b).[2e]

Chaînes doubles

Une chaîne double peut être générée quand deux chaînes simples adjacentes sont reliées. Les anions portant des groupes carboxyliques peuvent assurer un tel pontage. Dans une moindre mesure, les anions sulfonatés peuvent aussi raccorder des chaînes simples voisines (Schémas 6.2c-g).

Par exemple, le bis(phénylthio)méthane, $\mathbf{L^{1\text{-}Ph}}$ permet de générer des doubles chaînes quand il est autoassemblé avec $CF_3CF_2CF_2COOAg$ ou $AgOOCCF_2CF_2COOAg$ (Schémas 6.2c et 6.2d).[2a] De même, $\mathbf{L^{3\text{-}Ph}}$ donne avec $CF_3CF_2CF_2COOAg$ ou *p*-TsOAg des chaînes doubles similaires (Schéma 6.2c).[2b] Il est à noter que dans ces chaînes doubles, des distances Ag-Ag courtes sont seulement observées avec les carboxylates.[2a,2b]

Un autre type de chaîne double qui est observé pour certains de ces ligands est illustrée au schéma 6.2e. En fait, dans ces doubles chaînes, deux ligands pontent deux atomes d'argent contigus pour former un dimère, $[Ag\text{-ligand}]_2$. Les dimères adjacents ont en commun les atomes d'argent. Ces doubles chaînes, plus précisément des chaînes croisées, sont cationiques et les anions équilibrent seulement la charge du réseau.
De telles chaînes sont obtenues, par exemple, quand le 1,3-bis(méthylthio)propane, $\mathbf{L^{3\text{-}Me}}$, ou le 1,3-bis(éthylthio)propane, $\mathbf{L^{3\text{-}Et}}$, sont autoassemblés avec des anions faiblement ou non coordonnants.[3b,3c]

Dans un autre type de chaîne double, deux ligands connectent deux atomes d'argent voisins pour former le dimère $[Ag\text{-ligand}]_2$. De plus, les dimères sont reliés par un troisième ligand afin de générer la double chaîne (Schéma 6.2f). L'autoassemblage des ligands $\mathbf{L^{4\text{-}tBu}}$, $\mathbf{L^{6\text{-}tBu}}$ et $\mathbf{L^{4\text{-}Benz}}$ avec le perchlorate d'argent, permet l'élaboration de telles doubles chaînes. Le perchlorate est seulement coordonné au métal.[3a,3b]

Dans un dernier type de chaîne double, des dimères $[Ag\text{-ligand}]_2$ voisins sont connectés par le biais de deux anions pour la génération d'une chaîne double (Schéma 6.2g). En d'autres termes, ces réseaux sont caractérisés par l'alternance des dimères $[Ag\text{-ligand}]_2$ et $[Ag\text{-anion}]_2$. De tels réseaux sont obtenus avec les combinaisons ($\mathbf{L^{1\text{-}Me}}$, CH_3SO_3Ag),[2d] ($\mathbf{L^{1\text{-}Me}}$, $C_{10}H_7SO_3Ag$)[2e] et ($\mathbf{L^{1\text{-}Benz}}$, $AgClO_4$)[3b].

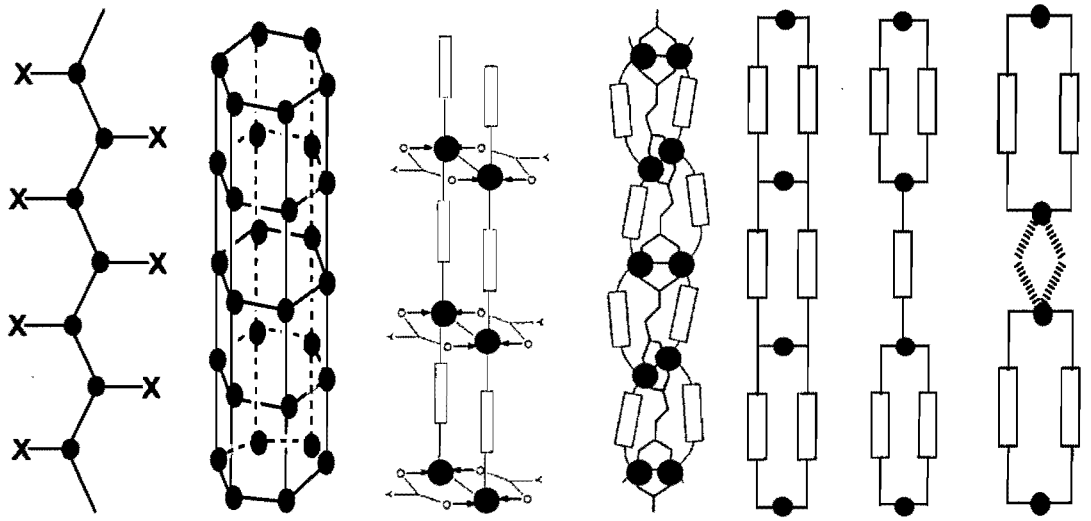

(a) (b) (c) (d) (e) (f) (g)

Schéma 6.2. (a) Chaîne en zigzag. (b) Réseau tubulaire. (Pour les schémas a et b, le point noir représente un atome métallique et le bâtonnet reliant deux points voisins est le ligand ditopique. X est un anion. Dans (b), les anions ne sont pas représentés).
(c) Chaîne double où les anions associent deux chaînes simples voisins (Y est le reste de l'anion). (d) Chaîne double où se superposent les réseaux $(Ag\text{-ligand})_\infty$ et $(Ag\text{-anion})_\infty$. (e) Chaîne double cationique où deux dimères $[Ag\text{-ligand}]_2$ adjacents ont en commun les atomes d'argent (les anions qui équilibrent les charges du réseau ne sont pas représentés). (f) Chaîne double dont des dimères $[Ag\text{-ligand}]_2$ adjacents sont reliés par un ligand (les anions coordonnés au métal ne sont pas représentés pour plus de clartés). (g) Chaînes doubles faites de l'alternance des dimères $[Ag\text{-ligand}]_2$ et $[Ag\text{-anion}]_2$ (les traits en pointillés représentent les anions pontants). (Pour les schémas c-g, le point noir représente un atome métallique et le rectangle reliant deux cercles voisins est le ligand ditopique).

6.1.2 Réseaux de coordination bidimensionnels

Il existe une grande variétés de structures bidimensionnelles. Nous pouvons les classer en quatre catégories:

(i) Structures constituées de feuillets cationiques $[Ag\text{-ligand}]_\infty^+$ entre lesquels sont intercalés les anions.

(ii) Structures à base de feuillets neutres $[Ag(X)\text{-ligand}]_\infty$ où les anions X complètent la coordination tétraédrique du métal.

(iii) Structures constituées de feuillets où sont incorporés les atomes d'argent, les ligands et les anions.

(iv) Structures où des chaînes sont reliées par des interactions faibles pour former des feuillets.

i) Feuillets cationiques [Ag-ligand]$_\infty^+$ entre lesquels les anions sont intercalés

Ces réseaux sont principalement observés quand des contre-ions non coordonnants ou faiblement coordonnants sont autoassemblés avec des ligands de taille intermédiaire, $\mathbf{L^{n\text{-}Ph}}$, avec **n** = 3, 4 et 5.[1,2b,3c-g] Dans ces structures, les anions, intercalés entre les feuillets, contre-balancent les charges du réseau (Schéma 6.3a). Un réseau cationique similaire a été obtenu quand le ligand $\mathbf{L^{4\text{-}Et}}$ a été combiné avec $AgClO_4$[3b] ou encore pour la combinaison ($\mathbf{L^{1\text{-}Me}}$, $AgBF_4$) (Chapitre 3.2).

ii) Feuillets neutres [Ag(X)-ligand]$_\infty$ où les anions complètent la coordination tétraédrique du métal

Dans ce type de réseaux bidimensionnels, les ligands propagent les centres métalliques où sont coordonnés les anions (Schéma 6.3b). Ces structures ont été observées quand le ligand $\mathbf{L^{1\text{-}Me}}$ a été autoassemblé avec les anions comme NO_3^-, ClO_4^-, *p*-TsO^-, $CF_3CO_2^-$, $CF_3SO_3^-$ et $CF_3CF_2CF_2CO_2^-$.[2d] Un tel réseau a aussi été observé quand le bis(éthylthio)méthane, $\mathbf{L^{1\text{-}Et}}$ ou le 1,2-bis(*tert*-butylthio)éthane, $\mathbf{L^{2\text{-}tBu}}$, ont été combinés au perchlorate d'argent.[3a-b]

Dans les deux types de réseaux bidimensionnels neutres et cationiques, [Ag(X)-ligand]$_\infty$ et [Ag-ligand]$_\infty^+$ décrits ci-dessus, les anions ne jouent pas un rôle dominant pour l'élaboration du réseau. En d'autres termes, les contre-ions ne participent pas à la propagation du réseau.

iii) Feuillets où sont incorporés les atomes d'argent, les ligands et les anions

Dans ces réseaux, les anions participent au développement du réseau au même titre que les ligands. En général, les anions très coordonnants (les nitrates ou les anions possédant un groupe carboxylate) favorisent la formation de tels réseaux. Néanmoins, nous avons observé dans une moindre mesure de tels réseaux avec des anions sulfonatés, moins coordonnants et même avec le perchlorate qui est un anion peu coordonnant.[2b-c] Ces réseaux étant assez complexes, une représentation très simplifiée en illustre les structures (Schéma 6.3c).

iv) Chaînes reliées par des interactions faibles pour former des feuillets

Des chaînes linéaires, simples ou doubles, sont obtenues par la combinaison du petit ligand $\mathbf{L^{1\text{-}Ph}}$ et des anions comme le perchlorate, le tétrafluoroborate, le triflate ou les perfluorocarboxylates (Schéma 6.2a).[2a] Ces chaînes sont retenues entre elles par des interactions faibles C–H···X (X=O ou F).[2a] De tels réseaux sont aussi observés pour les

combinaisons ($L^{1\text{-}Me}$, $C_{10}H_7SO_3Ag$)[2e] et ($L^{2\text{-}Et}$, $AgClO_4$).[3b] D'autre part, les doubles chaînes générées par l'autoassemblage de $L^{1\text{-}Me}$ et $C_6H_5COO^-$ sont retenues entre elles par le biais d'interaction $\pi\cdots\pi$ entre les groupes phényles des anions, conduisant ainsi à la formation d'un réseau bidimensionnel.[2d]

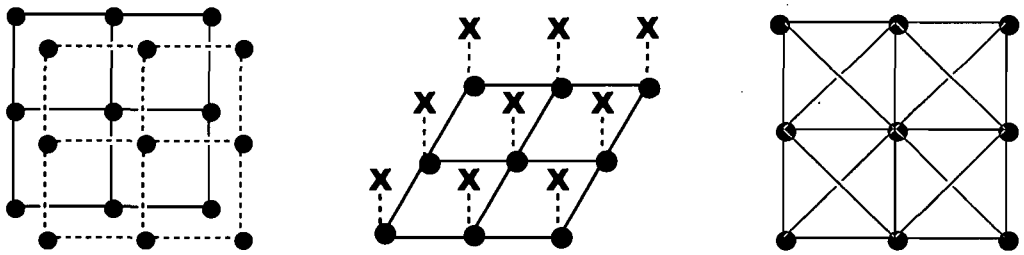

(a) (b) (c)

Schéma 6.3. (a) Feuillets cationiques $[Ag\text{-ligand}]_\infty^+$ où les anions, non montrés ici, sont intercalés entre les feuillets. (b) Feuillets neutres $[Ag(X)\text{-ligand}]_\infty$ où les anions complètent la sphère de coordination de l'argent. (Le point noir représente un atome métallique et le bâtonnet noire reliant deux atomes voisins est le ligand ditopique, et X est un anion). (c) Feuillets neutres où sont incorporés les atomes d'argent, les ligands et les anions (Dans cette représentation très simplifiée, l'anion qui participe à l'élaboration du réseau est représenté par des lignes rouges).

6.1.3 Réseaux de coordination tridimensionnels

Les réseaux tridimensionnels obtenus avec ces ligands sont très limités. Nous les avons regroupés en deux catégories:

(i) Réseaux 3D obtenus par des liaisons de coordination

(ii) Réseaux 3D engendrés par le biais de liaisons hydrogène

i) Réseaux 3D obtenus par des liaisons de coordination

Trois composés sont connus avec de tels réseaux qui sont constitués d'un assemblage de canaux occupés par les anions. Une structure tridimensionnelle cationique a été obtenue par l'autoorganisation de $L^{1\text{-}Me}$ et du triflate d'argent (Chapitre 3.2). Les anions trifluorométhanesulfonates sont localisés dans les canaux. De même, la combinaison de $L^{1\text{-}Ph}$ avec $AgClO_4$ a donné un réseau tridimensionnel cationique où les perchlorates sont situés dans les canaux.[5] Enfin, une structure 3D neutre a été engendrée dans la combinaison ($L^{6\text{-}Ph}$, CF_3COOAg).[2c] Dans ce dernier cas, les canaux sont occupés par les anions trifluoroacétates, coordonnés aux métaux, accompagnés de molécules d'eau.[2c]

ii) Réseaux 3D engendrés par le biais de liaison hydrogène

De la réaction du bis(méthylthio)méthane, $\mathbf{L}^{\mathbf{1\text{-}Me}}$, avec $CH_3SO_3^-$ est obtenue une chaîne faite de l'alternance des dimères $[Ag\text{-}(L^{1\text{-}Me})]_2$ et $[Ag\text{-}(CH_3SO_3)]_2$ (Schéma 6.2g).[2d] L'association de ces chaînes, retenues par des liaisons hydrogène, conduit à un réseau 3D.[2d]

Nous venons de voir un bref aperçu des différents types de réseaux obtenus par l'autoorganisation des ligands $\mathbf{L}^{\mathbf{n\text{-}R}}$ et des sels d'argent. Nous avons étudié l'effet des paramètres suivants qui influencent la formation de ces réseaux: (i) l'encombrement stérique du substituant R, (ii) la longueur du ligand, (iii) la nature de l'anion, (iv) le rapport métal:ligand des produits de départ et (v) le rôle du solvant.

6.2 Études des facteurs influençant la formation des réseaux

6.2.1 Effet de l'encombrement stérique du substituant R sur la topologie des réseaux

Afin d'établir comment la taille du groupe R des ligands influence la topologie des réseaux, nous comparons les structures des complexes à base du perchlorate d'argent et les ligands de petites tailles, **RS**(CH_2)**SR** (**R** = Ph, *t*Bu, Me, Et, Benz) à la figure 6.1.

On constate qu'avec le ligand court, bis(**R**-thio)méthane, les groupes encombrants, *tert*-butyle[3a], phényle,[2a] et benzyle[3b] mènent à un réseau 1D où chaque atome d'argent est lié à deux atomes de soufre provenant de deux ligands différents. Les deux premiers substituants conduisent à des chaînes simples (Figure 6.1a, b). Le groupe benzyle, encombrant mais avec un certain degré de flexibilité, permet la formation d'un réseau unidimensionnel où des dimères $[\mathbf{AgL}^{\mathbf{1\text{-}Benz}}]_2$ adjacents sont maintenus par deux perchlorates (Figure 6.1c).

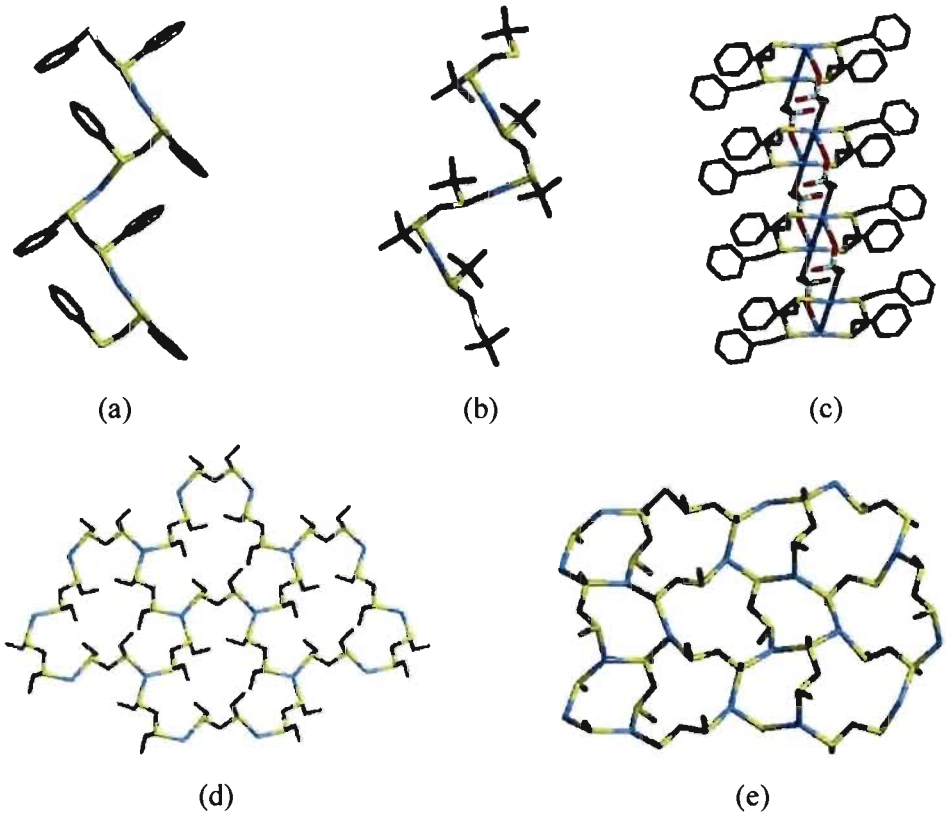

Figure 6.1. Comparaison des structures des complexes formés par la combinaison du ligand **R**S(CH_2)S**R** avec le perchlorate d'argent. (a) Chaîne obtenue avec **R** = Ph. (b) Chaîne formée avec **R** = *t*Bu. (c) Double chaîne obtenue avec **R** = Benz. (d) Réseau bidimensionnel type hexagonal engendré avec **R** = Et. (e) Réseau bidimensionnel élaboré quand **R** = Me. (Les atomes d'hydrogène ainsi que les perchlorates ne sont pas montrés pour plus de clarté).

Les groupes moins encombrants, méthyle[2d] et éthyle,[3b] conduisent à un réseau 2D dans lequel chaque atome d'argent est lié à 3 atomes de soufre de trois ligands distincts (Figure 6.1d, e). Les anions complètent la coordination tétraédrique de l'argent.

Nous spéculons que le petit substituant méthyle, de par son faible encombrement, et contrairement aux groupes phényle, *tert*-butyle et benzyle, pourrait permettre à plus de ligands, $\mathbf{L}^{\mathbf{1\text{-}Me}}$, de s'approcher des centres métalliques.[2d] Ainsi, le groupe méthyle accommoderait la formation de réseaux de plus haute dimensionalité que les groupes phényle et *tert*-butyle en général. D'autre part, le groupe éthyle conduirait aussi à la formation de réseau bidimensionnel.[3b] Cette situation est probablement inhérente à la taille du groupe éthyle plus proche de celle du méthyle que du phényle ou du *tert*-butyle.

Ainsi, de l'analyse des topologies des réseaux obtenus en utilisant le même anion, ClO_4^-, et des ligands de même taille, **R**S(CH_2)S**R**, nous proposons de classifier les substituants **R** en deux groupes :

(i) le groupe 1 favorise la formation de réseaux 2D. Il contient les petits substituants, méthyle et éthyle.

(ii) le groupe 2 forme des polymères de coordination 1D. Ceci est observé avec des substituants plus gros: phényle, *tert*-butyle, et benzyle.

Pour s'assurer que cette classification tient aussi pour des ligands plus longs, nous avons comparé les réseaux obtenus avec différent substituant R pour des ligands de même longueur et avec le même type d'anion.

Malheureusement cette tendance n'est pas observée pour des ligands $\mathbf{L}^{\mathbf{n\text{-}R}}$ plus longs. Par exemple, les perchlorates des complexes de $\mathbf{L}^{\mathbf{3\text{-}R}}$ avec **R** = Me, Et sont constitués de chaînes doubles (Figure 6.2a, b).[3b-c] Cette situation est l'inverse de ce que nous avons rapporté plus haut avec $\mathbf{L}^{\mathbf{1\text{-}R}}$ où **R** = Me, Et. Dans ces cas, il y a formation de réseaux 2D (Figure 6.1d, e).

De la même manière les complexes de $\mathbf{L}^{\mathbf{2\text{-}R}}$ où **R** = Ph, *t*Bu, Benz ont généralement des structures en feuillets, i.e, des réseaux 2D.[2c,3a-b,6] Ceci est l'opposé des structures polymériques des complexes avec $\mathbf{L}^{\mathbf{1\text{-}R}}$ (Figure 6.1 et 6.2).

Par conséquent, il ne semble pas possible de tirer des conclusions cohérentes de l'ensemble des structures rapportées. On pourrait trouver la cause de cette incohérence dans le fait que les complexes synthétisés n'ont pas tous la même stoichiométrie.

La flexibilité des ligands pourrait aussi contribuer à la difficulté de rationalisation des structures ayant le même type d'anion, le même type de substituant et où seule la longueur du ligand varie. Finalement, des molécules de solvants (acétone, méthanol, diéthyléther ou eau) font quelquefois partie des structures. Il y a trop de paramètres, sur lesquels nous n'avons aucun contrôle, qui influencent la structure adoptée.

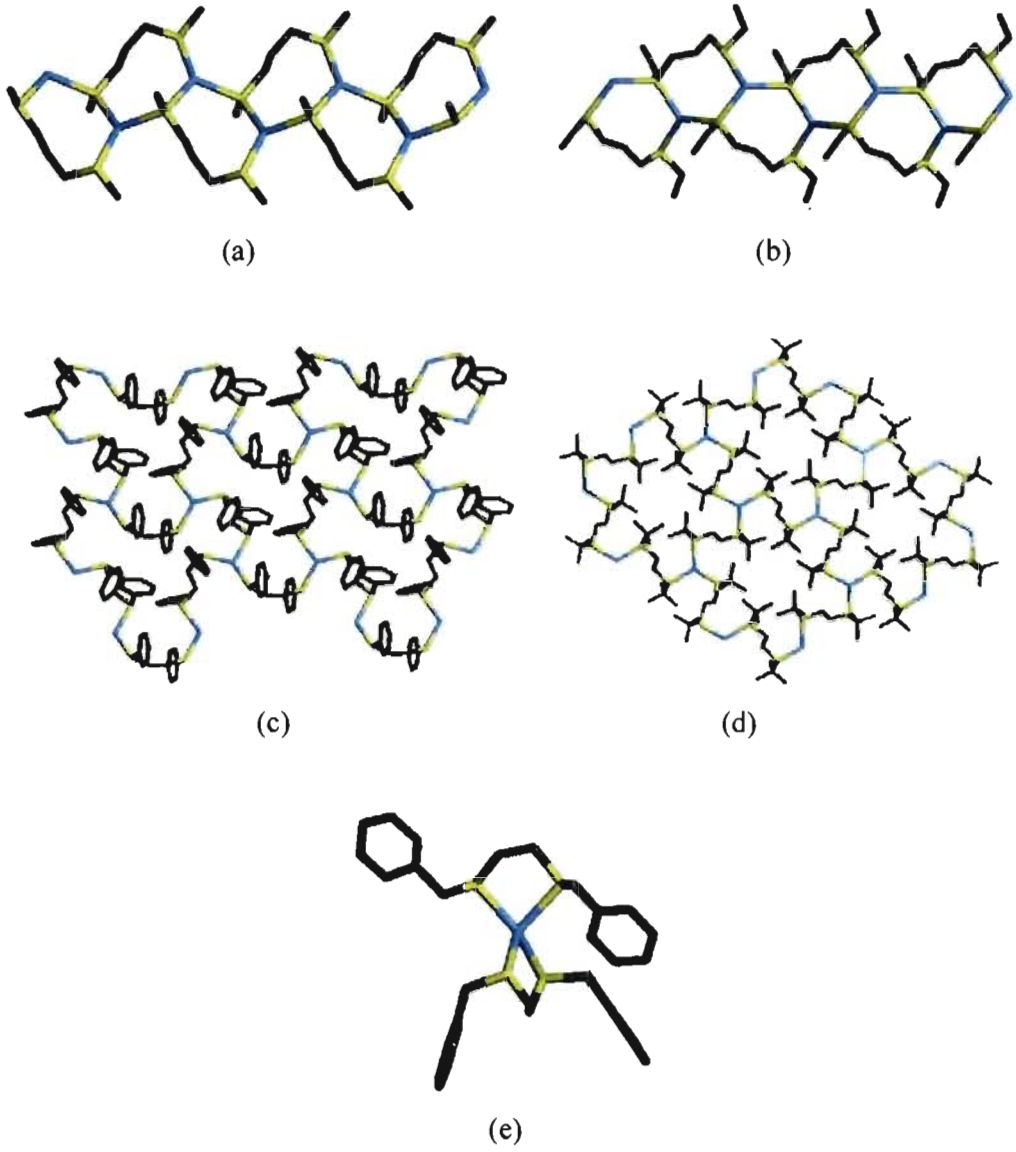

(a) (b)

(c) (d)

(e)

Figure 6.2. (a) Chaîne double élaborée avec $\mathbf{L}^{\mathbf{3\text{-}Me}}$.[3c] (b) Chaîne double formée avec $\mathbf{L}^{\mathbf{3\text{-}Et}}$.[3b] (c) Réseaux 2D formé avec $\mathbf{L}^{\mathbf{2\text{-}Ph}}$.[6] (d) Réseau 2D obtenu avec $\mathbf{L}^{\mathbf{2\text{-}tBu}}$.[3a] (e) Composé moléculaire cationique formée avec $\mathbf{L}^{\mathbf{2\text{-}Benz}}$.[3b] (Les atomes d'hydrogène ainsi que les perchlorates ne sont pas montrés pour plus de clarté).

6.2.2 Effet de la longueur de la séquence aliphatique des ligands

L'augmentation du nombre des angles de torsions est concomitante avec l'accroissement de la longueur de la chaîne méthylénique des ligands $\mathbf{L}^{\mathbf{n\text{-}R}}$.

Nous comparons les angles de torsions des ligands libres, quand ils sont disponibles, et ceux des complexes dans lesquels ils sont engagés (Tableaux 10.1 – 10.10, annexe IX).

Les ligands libres ayant un nombre pair de groupes méthylène possèdent tous un centre de symétrie cristallographique au milieu du lien $CH_2 - CH_2$ central (Schéma 6.4a, Tableaux 10.1-10.10, annexe IX). En conséquence, l'angle de torsion au milieu de la liaison centrale, φ_2 pour $\mathbf{L^{2\text{-}Ph}}$, est *trans* et les autres angles de torsions ont des valeurs opposées, $\varphi_1 = -\varphi_3$ (Schéma 6.4a). De plus, dans la plupart des complexes, les ligands possédant un nombre pair de groupe méthylène possèdent aussi un centre de symétrie au milieu du lien $CH_2 - CH_2$ central.

D'un autre côté, les ligands possédant un nombre impair de groupe méthylène ne possèdent pas de centre de symétrie. Par contre, l'atome de carbone central pourrait être sur un axe de rotation d'ordre 2, alors $\varphi_1 = \varphi_2$ (Schéma 6.4b).

(a) (b)

Schéma 6.4. (a) Ligands pairs (centre d'inversion potentiel). (b) Ligand impairs (axe 2 possible).

Les angles de torsions prennent des valeurs très souvent à l'intérieur des trois conformations suivantes: *trans* = $t = 180 \pm 30°$, *gauche*$^+$ = $g = 60 \pm 30°$ et *gauche*$^-$ = $g^- = -60 \pm 30°$

Conformations des ligands dans les complexes

Nous observons que le ligand $\mathbf{L^{1\text{-}Ph}}$ adopte toujours la conformation *gg* qu'il soit seul ou engagé dans des réseaux métallosupramoléculaires (Tableau 10.1, Annexe IX).[2a] Le ligand $\mathbf{L^{2\text{-}Ph}}$ seul possède la conformation centro symétrique gtg^-.[7] Cependant, l'autoassemblage de ce ligand avec différents sels d'argent conduit celui-ci à adopter des conformations variées (gtg^-, *tgt*, *ttt*, *ggg* et *tgg*). Pour ce ligand, aucune de ces 5 conformations n'est majoritaire (Tableau 10.2, Annexe IX).

D'autre part, nous remarquons que les ligands $\mathbf{L^{3\text{-}Ph}}$ et $\mathbf{L^{4\text{-}Ph}}$ adoptent dans les complexes très majoritairement les conformations *gttg* et $gtttg^-$ respectivement. Dans quelques cas, ces ligands adoptent aussi les conformations (*gtgg*, *tttg*, *tttt*) et (*ttttt*, $tgtg^-t$, $ggtg^-g^-$) respectivement (Tableau 10.3 et 10.4, Annexe IX). Le ligand $\mathbf{L^{5\text{-}Ph}}$ adopte à égalité les deux conformations *gttttg* et *gtttgt* (Tableau 10.5, Annexe IX). Le ligand $\mathbf{L^{6\text{-}Ph}}$ seul

possède la conformation *tttttt*.[8] Par contre, dans les complexes ce ligand adopte différentes conformations comme *gtttttg*$^-$, *gttttg* et *gtggttt*.

La flexibilité des ligands est démontrée par le fait qu'un ligand donné n'a pas toujours la même conformation d'un complexe à un autre. Il arrive aussi qu'un ligand adopte différentes conformations au sein d'un même complexe (Tableaux 10.1-10.10, Annexe IX). Par conséquent, afin de sonder l'influence de la longueur de la séquence aliphatique des ligands $\mathbf{L}^{n\text{-}R}$, nous allons comparer les réseaux obtenus pour le même anion, perchlorate, le même groupe R, phényle, et dont seul le nombre de groupe méthylène, n, varie (Figure 6.3).

Nous avons rapporté dans le chapitre 2, que pour le petit ligand $\mathbf{L}^{1\text{-}Ph}$, qui a dans tous les cas la conformation *gg*, des chaînes sont obtenues quelle que soit la nature des anions.[2a] Autrement dit, dans ces cas-ci, l'anion n'a pas d'influence sur la dimensionalité des structures.

Le ligand $\mathbf{L}^{2\text{-}Ph}$ donne avec le perchlorate deux réseaux 2D (Figure 6.3a, b).[2c,6] Dans le premier, des molécules d'acétone sont coordonnées aux atomes d'argent et les ligands perchlorato, qui optent pour une coordination pontante, participent à l'expansion du réseau (Figure 6.3a).[2c] Dans l'autre structure, qui ne contient pas de molécules de solvant, les ligands perchlorato complètent seulement la sphère de coordination des atomes d'argent (Figure 6.3b).[6] La différence de structure entre ces deux complexes pourrait être attribuée aux modes de coordination du ligand perchlorato. Il se pourrait aussi que la différence de stœchiométrie ainsi que la présence de molécule de solvant pour l'un de ces deux composés contribuent à leur différence de topologie (Figure 6.3a, b).

Les ligands $\mathbf{L}^{3\text{-}Ph}$, $\mathbf{L}^{4\text{-}Ph}$, et $\mathbf{L}^{5\text{-}Ph}$ conduisent à la formation de réseaux cationiques similaires de type carré (Figures 6.3c-e).[1,2b, 3g] On pourrait penser qu'une évolution des angles de torsion maintiendrait la forme ''carrée'' de l'unité de base. Ceci n'en est pas le cas puisque malgré la similitude apparente de ces réseaux cationiques, les ligands y ont des conformations différentes. Dans le complexe $[Ag(\mathbf{L}^{3\text{-}Ph})_2(ClO_4)]_\infty$, $\mathbf{L}^{3\text{-}Ph}$ adopte trois conformations: *tttt*, *gttg* et *ggtg*. Dans $[Ag(\mathbf{L}^{4\text{-}Ph})_2(ClO_4)]_\infty$, le ligand $\mathbf{L}^{4\text{-}Ph}$ adopte trois conformations *ttttt*, *gtttg*$^-$ et *tgtg*$^-$*t* alors que pour le complexe $[Ag(\mathbf{L}^{5\text{-}Ph})_2(ClO_4)]_\infty$, le ligand $\mathbf{L}^{5\text{-}Ph}$ présente les conformations *gttttg* et *gtttgt*. Finalement, le ligand $\mathbf{L}^{6\text{-}Ph}$ ne forme pas de réseau mais un composé discret binucleaire (Figure 6.3f).[9]

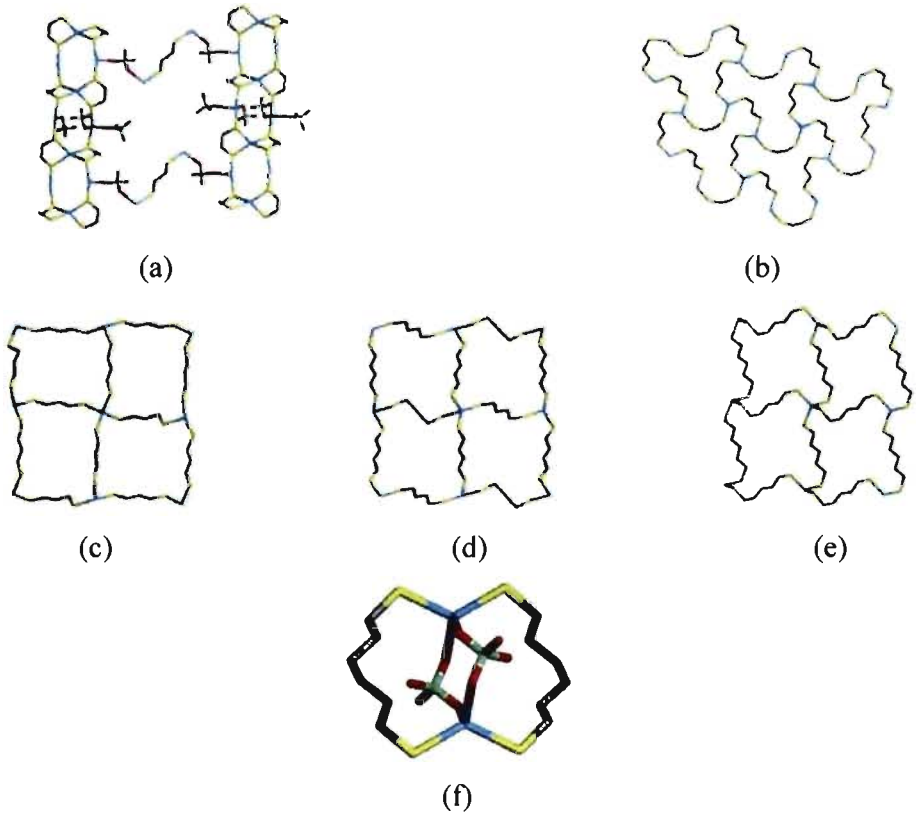

Figure 6.3. (a) Réseau 2D, $[Ag_4(\mathbf{L}^{\mathbf{2\text{-}Ph}})_{2.5}(ClO_4)_4(CH_3COCH_3)_2]_\infty$ (Les molécules de solvant sont omises pour plus de clarté).[2c] (b) Réseau 2D, $[Ag_2(\mathbf{L}^{\mathbf{2\text{-}Ph}})_3(ClO_4)_2]_\infty$ (Les ligands perchlorato qui ne se coordonnent qu'aux métaux sont omis pour plus de clarté).[6] (c)-(e) Feuillets lamellaires cationiques, $[Ag(\mathbf{L}^{\mathbf{n\text{-}Ph}})_2]_\infty^+$, **n** = 3, 4 et 5, dont les charges sont équilibrées par ClO_4^-.[1,2b,3g] (f) Dimère $[Ag(\mathbf{L}^{\mathbf{6\text{-}Ph}})(ClO_4)]_2$.[9] (Les groupes phényles ainsi que les atomes d'hydrogène ne sont pas montrés pour ne pas charger les figures).

De l'analyse des topologies des réseaux obtenus en utilisant le même anion, ClO_4^-, et le même substituant **R** = Ph, mais avec des ligands de différentes longueurs, il ressort principalement deux groupes:

(i) le ligand très court, **n** = 1, permet la formation de chaînes.

(ii) les ligands plus longs engendrent principalement des réseaux 2D.

Nous avons compilé dans la figure 6.4, les topologies des réseaux obtenus avec $\mathbf{L}^{\mathbf{n\text{-}Ph}}$, en fonction de la longueur du ligand et de la nature de l'anion du sel d'argent.

On constate clairement quelque soit la nature de l'anion, mais à une exception près, des chaînes ou polymères de coordination à une dimension sont observés avec le bis(phénylthio)méthane, $\mathbf{L}^{\mathbf{1\text{-}Ph}}$. D'autre part, la majorité des complexes obtenus avec $\mathbf{L}^{\mathbf{n\text{-}Ph}}$,

$\mathbf{n} \geq 2$, forme des réseaux bidimensionnels (Figure 6.4). Ainsi, pour l'ensemble des anions monovalents recensés dans cette étude:

(i) le ligand le plus court donne principalement des chaînes (■).

(ii) les ligands autre que $\mathbf{L}^{\mathbf{1\text{-}Ph}}$ donnent majoritairement des réseaux bidimensionnels (●,⊕).

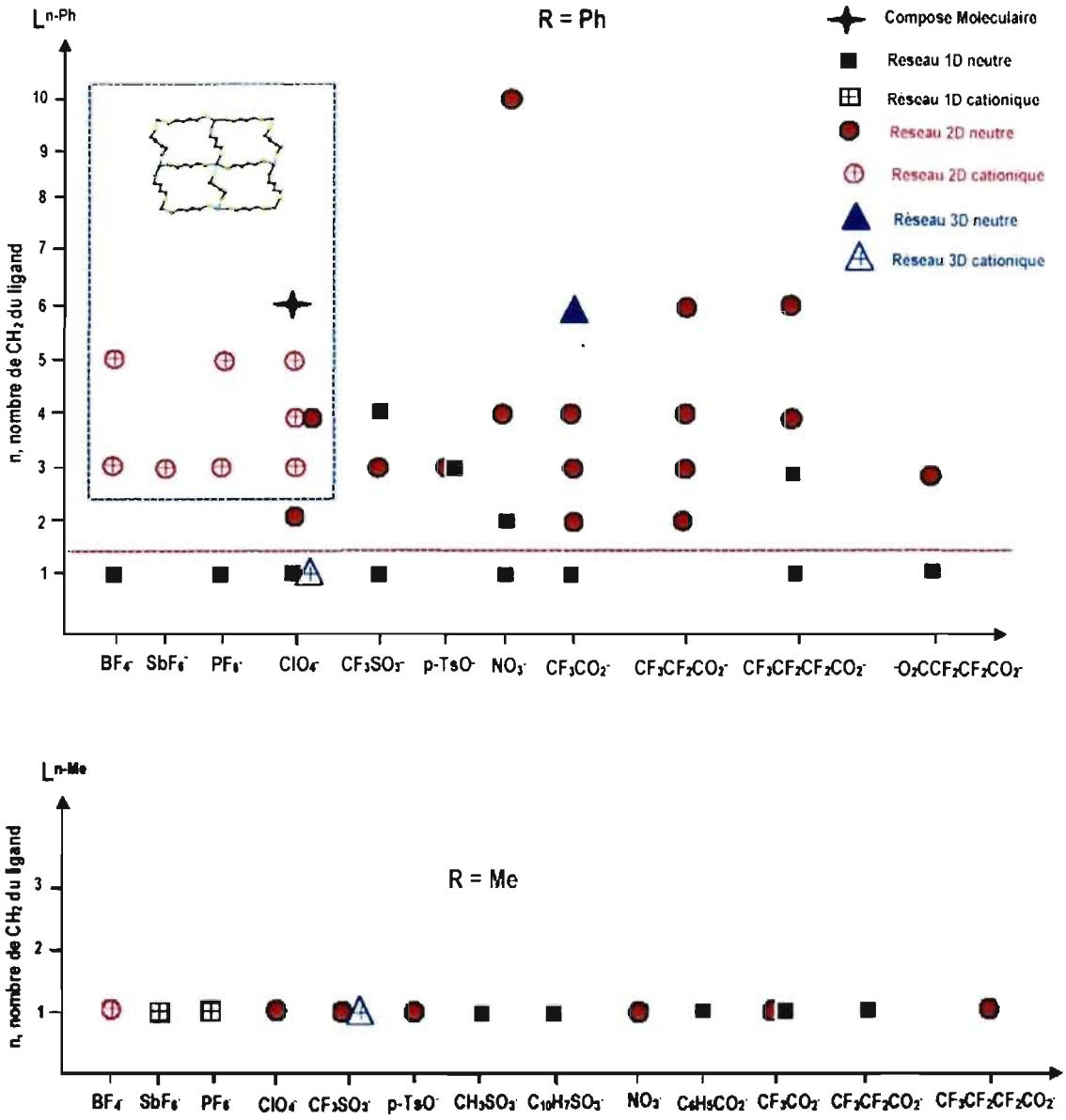

Figure 6.4. Réseaux 1D, 2D et 3D obtenus par la combinaison de $\mathbf{L}^{\mathbf{n\text{-}R}}$ et AgX en fonction du nombre **n** de groupe CH_2 et de l'anion X. En haut, **R** = Ph; au-dessous **R** = Me.

Quand le ligand $\mathbf{L}^{\mathbf{n\text{-}R}}$ possède seulement un groupe méthylène et que le substituant est **R** = Me, on constate la formation de chaînes 1D et de réseaux 2D (dans une proportion

50/50). Il ressort donc clairement, que c'est seulement avec le petit ligand (**n** = 1) que l'on obtient une structure à une dimension majoritairement, que **R** soit Me ou Ph.

6.2.3 Effet des anions sur la topologie des réseaux

Nous nous sommes intéressés à l'influence des anions sur la formation des réseaux dans le but de synthétiser des matériaux hybrides possédant des propriétés d'échange anioniques. Dans ce but nous cherchons à établir l'influence des contre-ions sur la topologie des réseaux obtenus avec les ligands $\mathbf{L^{n\text{-}Ph}}$. Nous avons fait varier la nature des anions pour un ligand de longueur donnée. Ces travaux ont été rapportés dans les chapitres 2 et 4.[2a-c,2e]

Les sels d'argent(I) nous permettent d'avoir accès à un grand éventail d'anions. D'autres sels d'argent(I), non disponible commercialement, ont été obtenus en partant des acides correspondants. Par exemple, la réaction de l'acide tétrafluorosuccinique avec du carbonate d'argent nous a permis de former le tétrafluorosuccinate d'argent, $AgOOCCF_2CF_2COOAg$.[2a,2e] La même procédure avec l'acide 1-naphthalènesulfonique nous a permis d'avoir accès au 1-naphthalènesulfonate d'argent, $C_{10}H_7SO_3Ag$.

La majorité des sels d'argent sont solubles dans les solvants utilisés lors des synthèses. Par contre, nous n'avons pas pu former des complexes avec $Ag_2(SO_4)$.
Ce sel est insoluble dans les solvants organiques communs bien que $Ag_2(SO_4)$ ne soit que partiellement soluble dans l'eau. Malheureusement, nos ligands qui portent des chaînes aliphatiques hydrophobes sont totalement insolubles dans l'eau. Par conséquent, nous n'avons pas pu sonder l'influence de l'ion divalent SO_4^{2-} ou de sa charge. Comme le sel Ag_3PO_4 est aussi insoluble dans les solvants communs, nous n'avons pas pu l'incorporer dans des complexes. Ainsi, nous avons limité notre travail aux anions monovalents suivants: BF_4^-; PF_6^-; SbF_6^-; ClO_4^-; NO_3^-; p-TsO^-; $CF_3SO_3^-$; $CH_3SO_3^-$; $C_{10}H_7SO_3^-$, $C_6H_5COO^-$; CF_3COO^-; $CF_3CF_2COO^-$; $CF_3CF_2CF_2COO^-$ et $^-OOCCF_2CF_2COO^-$.

Pour interpréter les résultats structuraux, nous avons regroupé les anions en fonction de leur coordinabilité:

(i) les anions non coordonnants (BF_4^-, PF_6^-, SbF_6^-).

(ii) l'anion faiblement coordonnant ClO_4^- qui peut présenter différents modes de coordination.

(iii) les anions moyennement coordonnants: sulfonates.

(iv) les anions fortement coordonnants: carboxylates et perfluorocarboxylates.

(v) l'anion NO_3^- est fortement coordonnant et peut adopter différents modes de coordination.

Il ressort de la figure 6.4 que seulement deux réseaux à trois dimensions (sur un total de 39 structures) ont été rapportés pour les ligands $\mathbf{L^{n\text{-}Ph}}$.

Dans le cas du ligand court $\mathbf{L^{1\text{-}Ph}}$, des chaînes simples sont observées avec les anions BF_4^-, ClO_4^-, NO_3^-, CF_3COO^- alors que les anions $CF_3CF_2CF_2COO^-$ et $^-OOCCF_2CF_2COO^-$ sont incorporés dans des chaînes doubles (Chapitre 2.1).[2a] Pour ce même ligand, le triflate a donné deux polymorphes, constitués respectivement d'une chaîne simple et d'une chaîne double (Chapitre 2.1).[2a] Donc l'anion ne semble pas influencer la dimensionalité des réseaux lorsque le ligand est court (**n** =1).

Pour les ligands autres que le bis(phénylthio)méthane, la majorité des complexes forme des réseaux à deux dimensions. Comme cela a été signalé plutôt, il existe plusieurs sortes de réseaux à 2D (Schéma 6.3). L'un d'entre eux est constitué de feuillets cationiques, entre lesquels sont localisés les anions. Comme les anions ne font qu'équilibrer les charges des feuillets, ces matériaux sont susceptibles de présenter des propriétés d'échanges anioniques. Les complexes ayant cette structure ont été obtenus avec les ligands $\mathbf{L^{n\text{-}Ph}}$ où **n** = 3, 4, 5 (Figure 6.3c-e). Toutefois, il faudrait autoassembler $\mathbf{L^{n\text{-}Ph}}$, **n** $\geq$ 6, avec les anions non coordonnants BF_4^-, PF_6^-, SbF_6^- afin de vérifier si cette tendance reste valable pour les ligands plus longs ou si des composés moléculaires sont obtenus.

Les réseaux générés par la réaction du bis(méthylthio)méthane, $\mathbf{L^{1\text{-}Me}}$, avec différents anions, rapportés dans le chapitre 3, sont identifiés dans le diagramme au bas de la figure 6.4. Avec $\mathbf{L^{1\text{-}Me}}$, nous avons obtenu des complexes ayant des réseaux 1D, 2D et seulement un complexe 3D. Dans le cas de ce ligand peu encombrant, les chaînes sont toutes des chaînes doubles. Pour ce qui est des réseaux à deux dimensions, on note que les anions complètent la sphère de coordination de l'argent (Schéma 6.3b) (Chapitre 3).[2d]

Pour les ligands $\mathbf{RS(CH_2)_nSR}$, **R** = Ph et Me: (i) les anions non coordonnants favorisent majoritairement la formation de réseaux cationiques (Figure 6.4), (ii) les anions carboxylates fortement coordonnants permettent l'élaboration de réseaux neutres avec des distances Ag-Ag courtes. Nous avons observé que les anions coordonnants, carboxylates ou nitrates participent majoritairement à l'édification des réseaux, au même titre que les ligands $\mathbf{L^{n\text{-}R}}$ (Chapitres 2 et 4).[2a-c,2e]

Toutefois, ces conclusions sont assez générales et il n'est pas surprenant d'y trouver des exceptions pour des raisons signalées plutôt: stœchiométries différentes, flexibilité des ligands et présence de solvant.

6.2.4 Effet du rapport métal:ligand

Les stœchiométries des complexes ne correspondent pas toujours à celles des produits de départ. Nous avons rassemblé dans les tableaux 9.1-9.8 (Annexe IX) les complexes synthétisés et les stœchiométries correspondantes.

Du point de vue de stœchiométrie, nous pouvons distinguer trois catégories de complexes: (i) un complexe est obtenu seulement pour un rapport métal:ligand bien spécifique des produits de départ. Dans ce cas-ci, ce rapport est identique à la stœchiométrie du complexe. (ii) plusieurs complexes sont formés chacun pour un rapport métal:ligand particulier des produits de départ. (iii) un seul complexe est formé indépendamment du rapport métal:ligand des produits de départ.

Il est intéressant de noter que seulement les combinaisons du $\mathbf{L^{4\text{-}Ph}}$ et des anions ClO_4^- et NO_3^-,[1] ainsi que celle du $\mathbf{L^{2\text{-}Ph}}$ avec NO_3^-,[2e] ont des stœchiométries qui dépendent directement du rapport métal:ligand des produits de départ (ligand et sels d'argent).[1,2e]
Pour toutes les autres combinaisons (ligand, anion), le produit résultant de l'autoassemblage est indépendant du rapport métal:ligand des produits de départ.

Pour la combinaison ($\mathbf{L^{1\text{-}Ph}}$, $AgClO_4$), le rapport métal:ligand des produits de départ 1:2 mène au complexe 3D, $\{[Ag_2(\mathbf{L^{1\text{-}Ph}})_3](ClO_4)_2\}_\infty$,[5] alors que pour tous les autres rapports des produits de départs, seul le complexe 1D, $[Ag(\mathbf{L^{1\text{-}Ph}})(ClO_4)]_\infty$, est obtenu.[2a]

Quand le ligand $\mathbf{L^{2\text{-}Ph}}$ a été combiné avec $AgClO_4$ avec un rapport métal:ligand des produits de départ de 2:1 ou 3:1, un complexe bidimensionnel a été synthétisé, $[Ag_4(\mathbf{L^{2\text{-}Ph}})_{2.5}(ClO_4)_4(CH_3COCH_3)_2]_\infty$.[2c] Par contre, le complexe $[Ag_2(\mathbf{L^{2\text{-}Ph}})_3(ClO_4)_2]_\infty$, est obtenu en présence d'acétone, seulement pour les rapports métal:ligand 1:1, 2:3 et 3:2.[6] Pour les autres rapports métal:ligand, aucun complexe n'a pu être isolé.

Pour toutes les autres combinaisons (ligand, anion), quand nous avons fait varier les rapports métal:ligand des produits de départ en partant d'un excès de ligand jusqu'à un excès de sel d'argent (1:10 à 10:1), un même complexe a toujours été obtenu. Par conséquent, la stœchiométrie de ces métallosupramolécules est indépendante des rapports des produits de départ.

Au vu de ces observations, on constate qu'il est pratiquement impossible de prévoir quelle serait la stœchiométrie du complexe synthétisé et que nous n'avons aucun contrôle sur ce paramètre.

6.2.5 Effet du solvant

Nous avons synthétisé plusieurs complexes où des molécules de solvant (acétone, diéthyléther, méthanol, eau) y sont incorporées. Par exemple, pour la combinaison ($\mathbf{L}^{\mathbf{4\text{-}Ph}}$, $AgClO_4$), quand le diéthyléther a été utilisé comme solvant de recristallisation, le complexe $[Ag_2(\mathbf{L}^{\mathbf{4\text{-}Ph}})_3(ClO_4)_2]_\infty$ a été obtenu alors qu'avec le méthanol comme solvant de recristallisation, le complexe $[Ag_2(\mathbf{L}^{\mathbf{4\text{-}Ph}})_3(ClO_4)_2.CH_3OH]_\infty$ a été formé.[1]

Dans le cas du ligand $\mathbf{L}^{\mathbf{2\text{-}Ph}}$, la synthèse des complexes $[Ag_2(\mathbf{L}^{\mathbf{2\text{-}Ph}})_3(ClO_4)_2]_\infty$[7] et $[Ag_4(\mathbf{L}^{\mathbf{2\text{-}Ph}})_{2.5}(ClO_4)_4(CH_3COCH_3)_2]_\infty$,[2c] diffère seulement par le rapport métal:ligand des produits de départ (1:1, 2:3 et 3:2 pour le premier complexe et 2:1 et 3:1 pour le second complexe). Toutefois, il n'est pas clair comment le rapport des produits de départ influence l'incorporation ou non de molécules de solvant.

L'isomérie supramoléculaire a été rapportée avec les anions sulfonatés. Cette isomérie, observée pour les complexes des ligands $\mathbf{L}^{\mathbf{1\text{-}Ph}}$ et $\mathbf{L}^{\mathbf{3\text{-}Ph}}$, semble être influencée par la polarité du solvant de recristallisation.[2a-b] Nous avons montré que les solvants polaires favorisaient la formation de supramolécules dans lesquelles les groupes sulfonates des anions adoptaient une coordination unidentate. Avec les solvants apolaires, des isomères supramoléculaires sont générés où, cette fois-ci, les groupes sulfonates optent majoritairement pour une coordination bidentate. Enfin, quand nous avons utilisé un mélange de solvant polaire et apolaire comme solvants de recristallisation (1:7 à 7:1), un seul composé a été obtenu avec $\mathbf{L}^{\mathbf{3\text{-}Ph}}$. Celui-ci présente, quelque soit le pourcentage des solvants polaire:apolaire, les modes de coordination unidentate, bidentate et tridentate pour les sulfonates.[2e]

Comme dans ces isomères supramoléculaires il n'y a aucune molécule de solvant polaire ou apolaire incorporée dans les structures, il n'est pas clair comment la polarité du solvant de recristallisation affecte le mode de coordination des groupes sulfonates envers le centre métallique.

6.2.6 Conclusions sur les facteurs influençant la formation des réseaux

Nous avons tenté de déterminer l'influence de certains paramètres sur la topologie des réseaux obtenus par l'autoassemblage de ligands flexibles dithiolatés et de sels d'argent. Ces paramètres sont la nature des anions, la longueur et l'encombrement des ligands, le rapport métal-ligand des produits de départ et les solvants de recristallisation. Pour ce faire, nous avons varié un seul paramètre à la fois.

Tout d'abord on observe que quelque soit la nature de l'anion monovalent, le ligand court $\mathbf{L^{1\text{-}Ph}}$ permet la formation de réseau 1D, tandis que les ligands plus longs, $\mathbf{L^{n\text{-}Ph}}$ ($\mathbf{n \geq 2}$), conduisent majoritairement à des réseaux 2D.

Nous mettons en évidence que les anions non coordonnants permettent la formation de réseaux cationiques. Dans ces réseaux, le ligand propage le centre métallique alors que les anions ne font qu'équilibrer la charge du réseau. De ce fait, ces réseaux cationiques sont susceptibles de présenter des propriétés d'échange anionique.

Les anions coordonnants permettent la formation de réseaux neutres. Ces anions participent souvent au même titre que les ligands au développement du réseau.
D'autre part, les carboxylates conduisent à des réseaux où il y a souvent des courtes distances argent-argent.

Il est difficile de faire ressortir l'influence de l'encombrement des substituants des ligands sur la topologie des réseaux. Néanmoins, nous avons observé que les substituants moins encombrants comme le méthyle et l'éthyle, conduisent à des réseaux de même dimensionalité (1D ou 2D) (Figure 6.1 et Figure 6.2). De même, les substituants plus encombrants comme le phényle, le *tert*-butyle et le benzyle, donnent grosso modo des réseaux de même dimensionalité (1D ou 2D) (Figure 6.1 et Figure 6.2).

Enfin, il y a des paramètres sur lesquels nous n'avons aucun contrôle tels que la stœchiométrie des complexes, la conformation des ligands ou l'incorporation éventuelle de molécules de solvant. Tout ceci contribue à la difficulté de prédire la topologie des réseaux.

6.3 Coordination de l'argent

L'argent(I) a une souplesse de coordination qui lui permet d'adopter différentes modes de coordination, allant de 2 à 6.[10] Pour nos complexes, la coordination de l'argent varie de 3 à 6. Les différentes géométries de coordination observées pour nos composés sont illustrées dans les Schémas 6.5.

Dans les polymères de coordination de topologie ''chaînes simples'', schéma 6.2a, chaque atome d'argent est coordonné à deux ligands distincts et un contre-ion. Ainsi, la géométrie de coordination de l'argent est trigonale (Schéma 6.5a).

La coordination plan-carré, pas très courante pour l'argent(I)[11] a été observée une seule fois (Schéma 6.5b).

Nous avons illustré dans les schémas 6.5c-g, les différentes situations observées pour la coordination tétraédrique. Dans les réseaux cationiques (1D, 2D ou 3D), l'argent qui est coordonné à quatre ligands différents présente une géométrie de coordination tétraédrique (Schéma 6.5c). La coordination tétraédrique est aussi observée pour les réseaux neutres 1D type ''double chaîne'' ou 2D dans lesquels l'anion est coordonné à l'argent. De plus, dans certains de nos complexes, des molécules de solvant complètent la sphère de coordination de l'argent (Schéma 6.5e).

D'un autre côté, nous avons remarqué que les carboxylates permettent la formation de réseaux où l'argent adopte la coordination 5 (Schéma 6.5h, i, k). Cette coordination vient de la présence de liaison métal-métal plus courte que la somme des rayons de van der Waals de deux atomes d'argent. Il est à noter que dans ces cas, la géométrie bipyramide trigonale est très majoritaire (4 liaisons de coordination et une liaison métal-métal) (Schéma 6.5h, i, k).

Toutefois, la coordination 5 a été aussi observée pour un complexe où il n'y a pas d'interaction métal-métal, $[Ag_5(L^{3\text{-}Ph})_2(CF_3SO_3)_5(CH_3COCH_3)_2]_\infty$, (Schéma 6.5j).

La coordination 6 n'a été rapportée qu'avec les anions carboxylates (Schéma 6.5 l, m). Par exemple, nous avons décrit les complexes $[Ag_2L^{4\text{-}Ph}(CF_3CF_2CO_2)_2]_\infty$ et $[Ag_2L^{4\text{-}Ph}(CF_3CF_2CF_2CO_2)_2]_\infty$ où les atomes d'argent adoptent la coordination 6 octaédrique comme illustrée au schéma 6.5 l. D'un autre côté, dans le complexe $[AgL^{1\text{-}Me}(HOOCCF_2CF_2COO)]_\infty$, l'atome d'argent présente aussi la coordination octaédrique comme illustrée par le schéma 6.5m.

Il est intéressant de noter qu'au sein d'un même complexe, les atomes d'argent présentent différents modes de coordination. Par exemple, dans le complexe $[Ag_5(L^{3\text{-}Ph})_2(CF_3SO_3)_5(CH_3COCH_3)_2]_\infty$ les atomes d'argent adoptent les coordinations tétraédrique (schéma 6.5d et e), plan-carré (schéma 6.5b) et bipyramide trigonale (schéma 6.5j). Ceci démontre bien la difficulté de contrôler la géométrie de la sphère de coordination de l'argent pour nos complexes. Cette situation est probablement inhérente au

fait qu'au sein d'un même complexe, le contre-ion peut adopter différente mode de coordination et que des molécules de solvant se coordonnent à certains atomes d'argent alors qu'elles ne se coordonnent pas à d'autres.

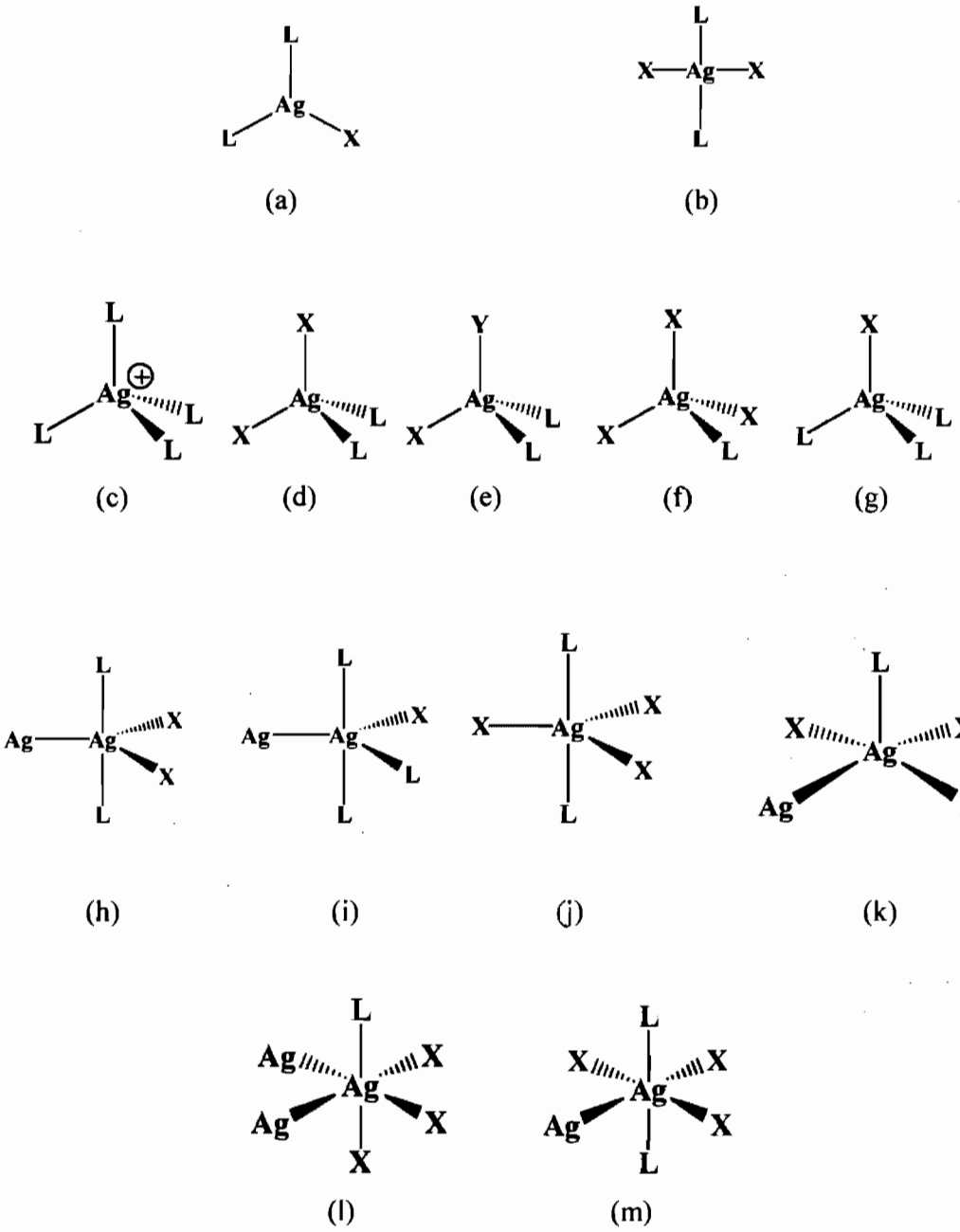

Schéma 6.5. (a) Coordination trigonale; (b) Plan carré; (c)-(g) Tétraédrique; (h)-(j) Bipyramide trigonale; (k) Pyramide à base carrée; (l) et (m) Octaédrique. (**L** : Ligand 1, n-bis(R-thiol)alcane; **X** : anion; **Y** : molécule de solvant).

6.4 Interaction métal-métal

L'interaction Au(I) – Au(I), communément acceptée, a été établie par des études spectroscopiques qui ont confirmé les prédictions des calculs théoriques.[12] Par contre, l'interaction Ag(I) – Ag(I) n'a pas été mise en évidence de manière aussi claire que dans le cas des complexes de l'or, mais il semble que l'interaction argentophilique existe bien.[13]

En effet, une étude par spectroscopie vibrationnelle, utilisant la spectroscopie Raman de résonance, a bien établi la présence d'interactions argentophiliques pour des complexes bimétalliques d'argent(I).[13]

Che *et al.* ont rapporté des complexes d'argent(I) binucléaires qui luminescent à la température de la pièce. Un de ces complexes est $[Ag_2(\mu\text{-dcpm})_2(CF_3SO_3)_2]$ (Figure 6.5).[13] Dans ce dimère, deux molécules de bis(dicyclohexylphosphine)méthane, dcpm, pontent par les phosphores deux atomes d'argent. Les anions triflates ne font que compléter la sphère de coordination des atomes d'argent (Figure 6.5). Les distances métal-métal rapportées pour ce complexe sont 2.936(1) et 2.960(1) Å.[13]

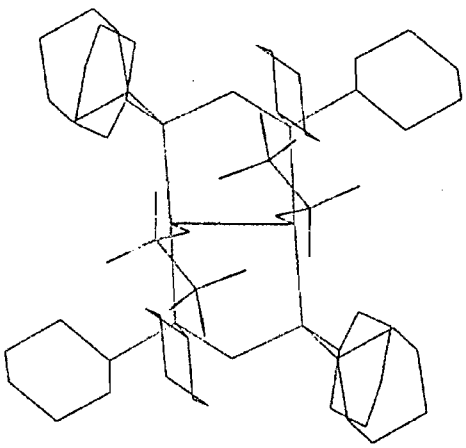

Figure 6.5. $[Ag_2(\mu\text{-dcpm})_2](CF_3SO_3)_2$, complexe binucléaire. (Ag: bleu; C: gris; P: violet, O: rouge; S: jaune; F: vert). (dcpm = bis(dicyclohexylphosphine)méthane). (Les atomes d'hydrogène ne sont pas montrés pour ne pas charger la figure).

Les auteurs ont enregistré le spectre UV-visible du $[Ag_2(\mu\text{-dcpm})_2(CF_3SO_3)_2]$ dans l'acétonitrile et observé une bande à 261nm. À cause de la transparence du ligand dans cette zone, cette transition électronique à été assignée à la transition $4d\sigma^* \longrightarrow 5p\sigma$ provenant de l'interaction Ag(I) – Ag(I).[13] La spectroscopie Raman de résonance, obtenue avec une excitation de 273.9 nm, a confirmé cette attribution. En effet, les signaux Raman

correspondent à la région des bandes associées à la vibration d'élongation de la liaison Ag(I) – Ag(I).[13] La fréquence de vibration d'élongation observée pour la liaison Ag(I) – Ag(I) de ce complexe est 80 cm^{-1}.

Il est intéressant de noter que le groupe de Patterson[14] a rapporté pour le composé Tl[$Ag(CN)_2$] une distance Ag(I) – Ag(I) de 3.110(3) Å. Pour ce composé, la fréquence de vibration obtenue par spectroscopie Raman, qui est de 88 cm^{-1}, a été assignée à la vibration d'élongation de la liaison Ag(I) – Ag(I).[14] Sur la base de ces résultats expérimentaux et de calculs théoriques, les auteurs en tirent la conclusion qu'il y a une interaction Ag – Ag dans ce complexe.[14]

La somme des rayons de van der Waals de deux atomes d'argent est environ 3.44 Å et la somme des rayons métalliques de l'argent est 2.89 Å.[15] Plusieurs groupes de chercheurs considèrent que les composés présentant des distances argent-argent qui sont dans l'intervalle 2.9 – 3.3 Å, pourrait posséder une faible interaction métal-métal.[16]

Souvent, les ions argent (I) adjacents forment des dimères grâce aux ligands. De ce fait, certains se demandent si les courtes distances intermétalliques observées sont dues à une contrainte géométrique plutôt qu'à une authentique interaction intermétallique. Par exemple, la présence de l'interaction argentophilique a été établie pour le complexe [$Ag_2(\mu$-dcpm)$_2$](CF_3SO_3)$_2$ où les atomes d'argent semblent liés entre eux par deux bis(dicyclohexylphosphine)méthane (Figure 6.5).[13] Ainsi, la présence de l'interaction Ag(I) – Ag(I) pourrait être indépendante des contraintes géométriques que semblent lui imposer les ligands pontant deux atomes d'argent voisins.

D'un autre côté, il existe des complexes où les atomes d'argent(I) se trouvent à des distances inférieures de 3.44 Å sans que ces atomes soient liés par l'intermédiaire d'un ligand. Ainsi, Singh *et al.* pensent que la présence d'une distance Ag(I) – Ag(I) courte (3.227(2) Å) dans le complexe [Ag_3(2-(3(5)-pz)py)$_3$].2py ne semble pas être dictée par le ligand mais résulte d'une interaction métal-métal.[17] Néanmoins, seule une étude spectroscopique pourrait établir de façon claire la présence d'une telle interaction au sein de ce composé.

Nos complexes, surtout des carboxylates et quelques sulfonates, conduisent à la formation de composés supramoléculaires où les distances Ag(I) – Ag(I) sont inférieures à la somme des rayons de van der Waals de l'argent. Les distances observées s'étalent entre 2.8669(9) et 3.389(5) Å (Tableau 6.1).[2a-e] Les atomes d'argent appartiennent en majorité à

des unités dimériques, $[RCOOAg]_2$, reliées entre elles par les ligands organiques édifiant ainsi des structures supramoléculaires (Figure 6.6).[2a-e]

Dans le cas des complexes du 1,4-bis(phénylthio)butane, $\mathbf{L^{4\text{-}Ph}}$, des unités tétramériques avec des distances Ag-Ag courtes ont été obtenues, $[RCOOAg]_4$.[2c] Un de ces tétramères est montré à la Figure 6.6b. Dans ce complexe, $[Ag_2(\mathbf{L^{4\text{-}Ph}})_{0.5}(CF_3COO)_2]_\infty$, la liaison métal-métal centrale non retenue par les groupes acétates, 3.1688(7) Å, est plus courte que celles où les groupes carboxylates pontent les atomes d'argent, 3.3212(6) Å.[2c] D'autre part, on constate dans un autre tétramère, $[CF_3CF_2CF_2COOAg]_4$ dans le complexe $[Ag_2(\mathbf{L^{4\text{-}Ph}})(CF_3CF_2CF_2COO)_2]_\infty$, que la distance Ag-Ag est plus courte que la somme des rayons métallique de l'argent: 2.8669(9) Å.[2c]

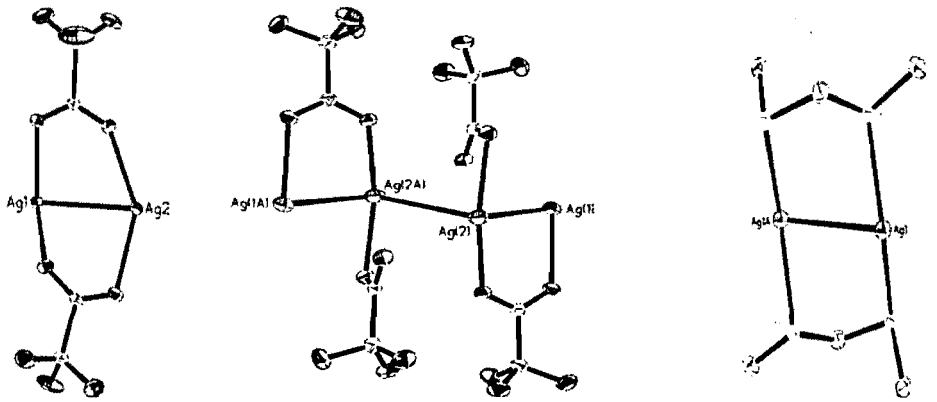

(a) (b) (c)

Figure 6.6. (a) Le dimère $[(CF_3COO)Ag]_2$ dans le complexe $[Ag_2(\mathbf{L^{3\text{-}Ph}})(CF_3COO)_2]_\infty$ (Ag(I) – Ag(I) = 3.2459(5) Å).[2b] (b) Le tétramère $[(CF_3COO)Ag]_4$, dans le complexe $[Ag_2(\mathbf{L^{4\text{-}Ph}})_{0.5}(CF_3COO)_2]_\infty$ (Ag(I) – Ag(I) = 3.1688(7) Å).[2c] (c) Le dimère $[Ag(\mathbf{L^{1\text{-}Me}})]_2$, $[Ag(\mathbf{L^{1\text{-}Me}})(CH_3SO_3)]_\infty$ (Ag(I) – Ag(I) = 3.2430(5) Å)[2d] (Les atomes d'hydrogène ne sont pas montrés pour ne pas charger la figure).

Quand les sulfonates pontent des atomes d'argent dans les complexes du 1,3-bis(phenylthio)propane, $\mathbf{L^{3\text{-}Ph}}$, la distance métal-métal qui est largement supérieure à 3.44 Å indique l'absence d'interaction argentophilique. Par contre, l'utilisation du petit ligand, $\mathbf{L^{1\text{-}Me}}$, bis(méthylthio)méthane, conduit à la formation des unités dimériques $[Ag\mathbf{L^{1\text{-}Me}}]_2$, dans le complexe $[Ag(\mathbf{L^{1\text{-}Me}})(CH_3SO_3)]_\infty$, où la distance Ag(I) – Ag(I) est 3.2430(5) Å.
Le pontage est ici assuré par le ligand (Figure 6.6c).[2d]

Il serait intéressant d'enregistrer les spectres Raman de nos composés, qui présentent des distances Ag(I) – Ag(I) courtes, dans une fenêtre de déplacement Raman

inférieure à 200 cm^{-1} afin de sonder la fréquence de vibration de la liaison Ag – Ag, que des chercheurs ont estimée à environ 75-125 cm^{-1}.[13,14]

Tableau 6.1. Comparaison des distances Ag(I) – Ag(I) courtes observées dans les complexes de ce travail et de quelques autres où les auteurs établissent l'existence d'une interaction argentophilique.

Complexes	Ag-Ag (Å)		Références Aux Schémas 6.5
$[Ag_2L^{2\text{-Ph}}(CF_3CO_2)_2]_\infty$[2c]	3.0813(5); 3.3813(6)	Dimère	b
$[Ag_2(L^{4\text{-Ph}})_{0.5}(CF_3CO_2)_2]_\infty$[2c]	3.1688(7); 3.3212(6)	Tétramère	a + c
$[Ag_2L^{4\text{-Ph}}(CF_3CF_2CO_2)_2]_\infty$[2c]	2.9137(8); 3.1048(6)	Tétramère	a + b
$[Ag_2L^{4\text{-ph}}(CF_3CF_2CF_2CO_2)_2]_\infty$[2c]	2.8669(9); 3.1594(6)	Tétramère	a + b
$[Ag_2L^{6\text{-Ph}}(CF_3CF_2CO_2)_2]_\infty$[2c]	3.0052(4); 3.3898(5)	Dimère	e
$[Ag(L^{6\text{-Ph}})_{0.5}(CF_3CF_2CF_2CO_2)]_\infty$[2c]	2.9730(5)	Dimère	b
$[Ag_2L^{3\text{-ph}}(CF_3COO)_2]_\infty$[2b]	3.2459(5)	Dimère	b
$[Ag_2L^{3\text{-Ph}}(CF_3CF_2CO_2)_2(CH_3COCH_3)]_\infty$[2b]	3.0502(7)	Dimère	b + g
$[AgL^{3\text{-Ph}}(CF_3CF_2CF_2CO_2)]_\infty$[2b]	3.1594(4)	Dimère	b
$[AgL^{1\text{-Ph}}(CF_3CF_2CF_2CO_2)]_\infty$[2a]	3.1593(3)	Dimère	b
$[AgL^{1\text{-Ph}}(OOCCF_2CF_2COO)]_\infty$[2a]	2.9836(5), 3.0168(5)	Dimère	b
$[AgL^{1\text{-Me}}(C_6H_5COO)]_\infty$[2d]	2.9114(4)	Dimère	b
$[AgL^{1\text{-Me}}(OOCCF_2CF_2COOH)]_\infty$[2d]	2.9836(5)	Dimère	b et c
$[AgL^{1\text{-Me}}(CH_3SO_3)]_\infty$[2d]	3.2430(5)	Dimère	
$[AgL^{1\text{-Me}}(C_{10}H_7SO_3)]_\infty$[2e]	3.248(2)	Dimère	
$[Ag_6(L^{3\text{-Ph}})_6(OOCCF_2CF_2COO)_3]_\infty$[2e]	2.9474(4), 3.2807(5) 2.9590(6), 3.1392(6)	Dimère	a + b + c
$[Ag_2(\mu\text{-dcpm})(\mu\text{-}O_2CCF_3)_2]$[13]	2.8892(9)	Dimère	b
$[Ag(PCy_3)(O_2CCF_3)]_2$[13]	3.095(1)	Dimère	c

6.5 Spectroscopie infrarouge des groupes acétates

Nous avons utilisé la spectroscopie infrarouge surtout pour caractériser les composés synthétisés. Cependant, cette technique peut être mise à profit pour identifier le mode de coordination du groupe acétate alors qu'une structure cristallographique n'est pas disponible. En 1980, Deacon et Phillips ont rapporté une remarquable étude où ils relient le type de coordination du groupe carboxylate à la différence entre les fréquences des vibrations d'élongation asymétrique et symétrique du groupe carboxylate, $\Delta = [\nu_{asym}\ (CO_2) - \nu_{sym}\ (CO_2)]$.[18] À partir des données cristallographiques et de spectroscopie infrarouge de 70 complexes acétates et 14 complexes trifluoroacétates, ils ont proposé la tendance empirique suivante:

$$\Delta_{unidentate} > \Delta_{bidentate\ pontant} \approx \Delta_{ionique} > \Delta_{chélatant}$$

Pour avoir des informations sur le mode de coordination des carboxylates dans les complexes, il est courant de comparer la valeur Δ du groupe carboxylate dans le complexe, $\Delta_{complexe} = [\nu_{asym}\ (CO_2) - \nu_{sym}\ (CO_2)]$, avec celle de l'espèce ionique, $\Delta_{ionique}$.[18,19]

Deacon et Phillips ont suggéré que quand la valeur de $\Delta_{complexe}$ est proche de celle de $\Delta_{ionique}$, le groupe carboxylate dans le complexe pourrait avoir une coordination bidentate pontant. Tandis que pour $\Delta_{complexe} > \Delta_{ionique}$, le groupe carboxylate dans le complexe pourrait avoir le mode de coordination unidentate. Alors que pour $\Delta_{complexe} < \Delta_{ionique}$, les auteurs suggèrent une coordination chélatante pour le groupe carboxylate du complexe.[18]

Łakomska et Szłyk ont rapporté pour les perfluorocarboxylates de sodium les valeurs de $\Delta_{ionique}$ = 223 – 272 cm^{-1}.[20] Ils se basent sur ces valeurs et sur la tendance empirique de Deacon et Phillips pour spéculer sur le mode de coordination de leurs complexes perfluorocarboxylatés, bien que souvent les structures n'aient pas été établies.[20] En d'autres termes, pour des valeurs de $\Delta_{complexe}$ proche de Δ_{ionic} des perfluorocarboxylates de sodium, 223-272 cm^{-1}, la coordination bidentate pontant est acceptée. Par exemple, Szłyk *et al.* proposèrent la coordination bidentate pontant pour des complexes de perfluorocarboxylates d'argent qui ont des valeurs de Δ = 263-276 cm^{-1}.[20c]

De leur côté, Che *et al.* ont rapporté des complexes perfluorocarboxylatés dont les structures ont été établies par rayons X et des données de spectroscopie infrarouge.[13] Par exemple, le complexe $[Ag_2(\mu\text{-dcpm})(\mu\text{-}O_2CCF_3)_2]$, présentant une coordination bidentate pontante, possède un Δ = 281 cm^{-1} alors que pour le complexe $[Ag(PCy_3)(O_2CCF_3)]_2$, montrant une coordination unidentate, Δ = 294 cm^{-1}.[13]

Pour nos composés, la corrélation entre la valeur de Δ, calculée à partir des données de spectroscopie infrarouge, et le mode de coordination du groupe COO, déterminés avec les données cristallographiques, est établie sur 17 complexes perfluoroacétates et un complexe acétate (Tableau 6.2).

Il ressort clairement de ces données, que la coordination bidentate pontante est observée pour les valeurs de Δ entre 264 et 279 cm^{-1}. Tandis que pour Δ = 299 – 301 cm^{-1}, la coordination unidentate est observée.

D'un autre côté, il est intéressant de noter qu'il peut y avoir différentes modes de coordination pour les groupes carboxylates dans les complexes. Dans le schéma 6.5 où nous montrons les types de coordination observés pour les groupes COO dans nos complexes, nous pouvons voir qu'il y a différents modes de pontage. En d'autres termes, les modes de coordination illustrés dans les schémas 6.6a,b,d-f font tous intervenir une coordination bidentate pontante. De ce fait, bien que la spectroscopie infrarouge puisse nous aider à identifier au sein d'un complexe la présence du mode de coordination pontante du groupe acétate, elle ne peut pas trancher entre les 5 modes de coordination pontant (Schéma 6.6a,b,d-f).

Le tableau 6.2 montre deux composés qui possèdent à la fois la coordination bidentate pontante et la coordination unidentate au sein d'un même complexe. Ainsi, dans le complexe $[AgL^{1\text{-}Me}(OOCCF_2CF_2COOH)]$,[2d] les deux modes de coordination ont pu être identifiés par spectroscopie infrarouge (Tableau 6.2). Par contre pour le complexe $[Ag_2(L^{4\text{-}Ph})_{0.5}(CF_3CO_2)_2]$,[2c] seule la coordination unidentate a été détectée par infrarouge, bien que la détermination structurale indique aussi l'existence d'une coordination bidentate.

Les composés de coordination avec les perfluorocarboxylates d'argent sont perçus depuis très récemment comme des précurseurs intéressants pour la technique de dépôt chimique en phase vapeur (CVD).[20,21] D'une part, ces précurseurs sont des complexes d'argent dont les anions sont des perfluorocarboxylates portant des ''longues'' chaînes aliphatiques fluorés.[20,21] D'autre part, le mode de coordination des groupes carboxylates des composés utilisés pour le CVD est discuté sur la base de la différence Δ des fréquences des vibrations asymétrique et symétrique des groupes COO, puisque souvent les structures ne sont pas disponibles pour ces composés.[20,21]

Les données du tableau 6.2, basées sur la corrélation entre les modes de coordination des groupes COO bien établis par rayons X et les valeurs de Δ, pourraient être

très utiles pour attribuer le type de coordination des groupes carboxylates des complexes perfluorocarboxylates d'argent utilisés pour la technique CVD, dont des structures ne sont pas souvent disponibles.

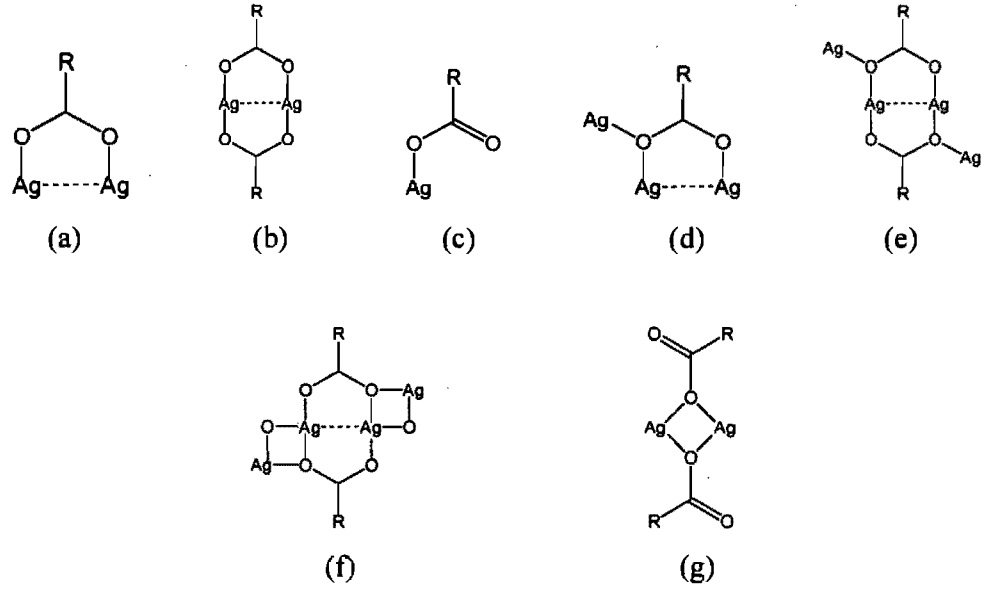

Schéma 6.6. Différents modes de coordination des acétates ou perfluoroacétates.

Tableau 6.2. Comparaison des fréquences du groupe acétate COO (cm^{-1}) obtenues par spectroscopie infrarouge ($\Delta = [\nu_{asym}(CO_2) - \nu_{sym}(CO_2)]$; $\nu_{as}(CO_2) = \nu_{asym}(CO_2)$ et $\nu_s(CO_2) = \nu_{sym}(CO_2)$).

Complexes	$\nu_{as}(CO_2)$	$\nu_s(CO_2)$	Δ	Références aux Schémas 6.5
Groupe COO bidentate pontant				
$[Ag_2L^{2Ph}(CF_3CO_2)_2]^{2c}$	1661	1384	277	b
$[Ag_2L^{4Ph}(CF_3CF_2CO_2)_2]^{2c}$	1679	1413	266	a + b
$[Ag_2L^{4ph}(CF_3CF_2CF_2CO_2)_2]^{2c}$	1667	1407	260	a + b
$[Ag_2L^{6Ph}(CF_3CF_2CO_2)_2]^{2c}$	1682	1411	271	e
$[Ag(L^{6Ph})_{0.5}(CF_3CF_2CF_2CO_2)]^{2c}$	1683	1407	276	b
$[Ag_2L^{3ph}(CF_3COO)_2]^{2b}$	1685	1410	275	b
$[Ag_2L^{3Ph}(CF_3CF_2CO_2)_2(CH_3COCH_3)]^{2b}$	1679	1411	268	b + g
$[AgL^{3Ph}(CF_3CF_2CF_2CO_2)]^{2b}$	1681	1411	270	b
$[AgL^{1Ph}(CF_3CF_2CF_2CO_2)]^{2a}$	1682	1403	279	b
$[AgL^{1Ph}(OOCCF_2CF_2COO)]^{2a}$	1683	1407	276	b
$[Ag_6(L^{3Ph})_6(OOCCF_2CF_2COO)_3]^{2e}$	1684	1418	266	a + b + d
$[AgL^{1Me}(C_6H_5COO)]^{2d}$	1645	1381	264	b
Groupe COO unidentate				
$[AgL^{1-Me}(CF_3CF_2CF_2COO)]^{2d}$	1683	1382	301	c
$[AgL^{1-Me}(CF_3CF_2CF_2COO)]^{2d}$	1683	1382	301	c
$[Ag_2L^{6-Ph}(CF_3CO_2)_2.2H_2O]^{2c}$	1684	1383	301	c
$[AgL^{1-Ph}(CF_3CO_2)]^{2a}$	1690	1390	300	c
$[AgL^{1-Me}(CF_3COO)]^{2d}$	1683	1384	299	c
Groupe COO bidentate pontant + Groupe COO unidentate				
$[Ag_2(L^{4-Ph})_{0.5}(CF_3CO_2)_2]^{2c}$	1685	1384	301	a + c
$[AgL^{1-Me}(OOCCF_2CF_2COOH)]^{2d}$	1680	1372	308	c
	1641	1372	269	b

6.6 Propriétés des polymères de coordination

6.6.1 Échange anionique

Les polymères de coordination susceptibles de présenter des propriétés d'échange anioniques sont souvent constituées de réseaux cationiques (1D, 2D ou 3D) dont la charge est compensée par l'anion qui est non coordonnant ou faiblement coordonnant.

Nous avons suivi les échanges anioniques des polymères de coordination du bis(méthylthio)méthane par spectroscopie infrarouge, analyse élémentaire, et diffraction des rayons X sur poudre (Chapitre 3.2).

Les spectres infrarouges enregistrés à différent temps nous ont permis de suivre les processus d'échange anioniques de façon qualitative en suivant les fréquences de vibration caractéristiques des anions. La diminution de l'intensité du pic de fréquence de vibration propre à l'anion sortant et l'augmentation de celui correspondant à l'anion entrant ont permi de suivre le processus. Nous considérons que la fin de l'échange correspond à la disparition de la fréquence de vibration caractéristique de l'anion sortant.

L'analyse élémentaire permet de s'assurer quantitativement que l'échange a été complété. Enfin, la diffraction des rayons X sur poudre permet de montrer que le réseau a été préservé à la fin de l'échange. On compare le diffractogramme de poudre du matériau avant l'échange à celui résultant de l'échange. La similarité de ces deux diffractogrammes est interprétée comme un signe que durant l'échange la structure a été maintenue.[22]

Échanges dans les canaux hexagonaux

L'autoassemblage du triflate d'argent avec le petit ligand $\mathbf{L}^{\mathbf{1\text{-}Me}}$ donne un réseau cationique tridimensionnel (Figure 6.7a, b) (Chapitre 3.2). Les anions triflates sont localisés dans les canaux de ce complexe $[Ag_3(\mathbf{L}^{\mathbf{1\text{-}Me}})_6(CF_3SO_3)_3]_\infty$ (Figure 6.7a, b). Nous avons discuté dans le chapitre 3.2, des échanges anioniques de ce complexe. Nous avons mis en évidence que les triflates peuvent s'échanger avec les anions comme le perchlorate (54.4 Å^3),[23] le nitrate (40.2 Å^3)[24] ou le tétrafluoroborate (53.4 Å^3)[23]. Néanmoins, il ne nous a pas été possible de pouvoir échanger les triflates (86.9 Å^3)[23] avec les anions comme l'hexafluorophosphate (73.0 Å^3)[23] ou l'hexafluoroantimonate (88.7 Å^3)[23]. Ainsi il existe quatre matériaux isostructuraux de composition $[Ag_3(\mathbf{L}^{\mathbf{1\text{-}Me}})_6(X)_3]_\infty$ où X = $CF_3SO_3^-$; BF_4^-; ClO_4^-; NO_3^-.

Nous avons observé que ces échanges étaient réversibles. En effet, quand les triflates du complexe $[Ag_3(\mathbf{L}^{\mathbf{1\text{-}Me}})_6(CF_3SO_3)_3]_\infty$ ont été remplacés par les anions

perchlorates, il se forme le composé isostructural $[Ag_3(\mathbf{L}^{\mathbf{1\text{-}Me}})_6(ClO_4)_3]_\infty$ (Chapitre 3.2). Quand ce dernier composé est trempé dans une solution aqueuse de $NaCF_3SO_3$ pendant environ deux heures, le composé initial $[Ag_3(\mathbf{L}^{\mathbf{1\text{-}Me}})_6(CF_3SO_3)_3]_\infty$ est obtenu comme confirmé par l'analyse élémentaire et la spectroscopie infrarouge.

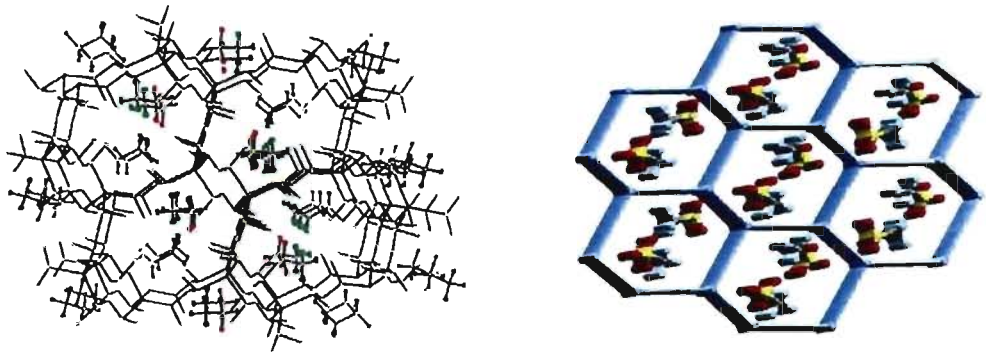

(a) (b)

Figure 6.7. (a) et (b) Réseau 3D $[Ag_3(\mathbf{L}^{\mathbf{1\text{-}Me}})_6(CF_3SO_3)_3]_\infty$. Dans (b), les coins des hexagones représentent les atomes d'argent tandis que les côtés schématisent les ligands).

Échanges dans les structures à une dimension

La réaction de $\mathbf{L}^{\mathbf{1\text{-}Me}}$ avec $AgPF_6$ et $AgSbF_6$ génère des doubles chaînes cationiques (Figure 6.8a, b). Dans ces composés, les anions hexafluorophosphate et hexafluoroantimonate sont présents pour équilibrer les charges des polymères de coordination. Ces complexes métallosupramoléculaires sont capables d'échanges anioniques (Chapitre 3.2). Nous avons observé que les anions PF_6^- (73.0 Å^3)[23] et SbF_6^- (88.7 Å^3)[23] peuvent être échangés reversiblement avec des anions de plus petites tailles comme le nitrate (40.2 Å^3),[24] le perchlorate (54.4 Å^3),[23] ou le tétrafluoroborate (53.4 Å^3).[23] Par contre les anions PF_6^- et SbF_6^- ne peuvent pas s'échanger entre eux ni avec le triflate (86.9 Å^3).[23] Nous pensons que ceci pourrait être dû à la taille des anions mis en jeu lors de l'échange. Autrement dit, pour un anion de départ donné, les anions de plus petite taille que lui pourrait s'échanger avec lui contrairement aux anions de taille semblable ou plus gros. Il est à noter que les produits résultants de l'échange avec le complexe $[Ag(\mathbf{L}^{\mathbf{1\text{-}Me}})_2(SbF_6)(Et_2O)_{0.5}]_\infty$ ne contiennent pas de molécules de diéthyléther comme l'indique l'analyse élémentaire.

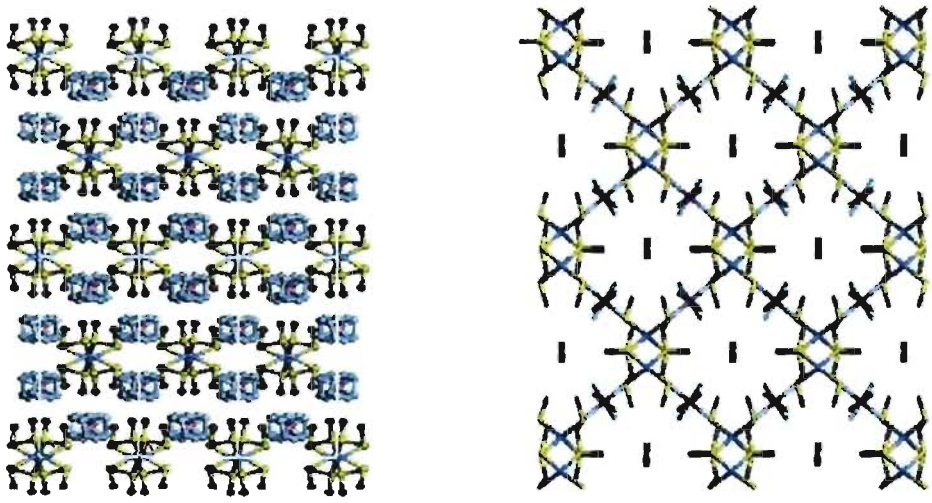

(a) (b)

Figure 6.8. (a) Projection le long de l'axe de chaîne du complexe 1D $[Ag(\mathbf{L}^{\mathbf{1\text{-}Me}})_2(PF_6)]_\infty$. Les chaînes sont en jaune alors que les PF_6^- désordonnés sont en bleu. (b) Projection du complexe $[Ag(\mathbf{L}^{\mathbf{1\text{-}Me}})_2(SbF_6)(Et_2O)_{0.5}]_\infty$. Les chaînes doubles sont en jaune. Les anions SbF_6^- sont placés entre chaînes voisines. Les molécules Et_2O très désordonnées occupent les centres des canaux hexagonaux.

Échange dans les structures à 2Dimension

Des réseaux cationiques 2D lamellaires ont été obtenus lors de la réaction des ligands $\mathbf{L}^{\mathbf{n\text{-}Ph}}$ (**n** = 3, 4, 5) avec des anions non coordonnants ou faiblement coordonnants (BF_4^-, PF_6^-, SbF_6^-, ClO_4^-) (Figure 6.3c-e). Ces réseaux sont constitués de feuillets cationiques, entre lesquels sont localisés les anions (Figure 6.9). Comme ces anions ne font qu'équilibrer les charges des feuillets, ils pourraient être échangés avec d'autres anions non coordonnants ou faiblement coordonnants. De ce fait, ces matériaux peuvent potentiellement présenter des propriétés d'échanges anioniques.

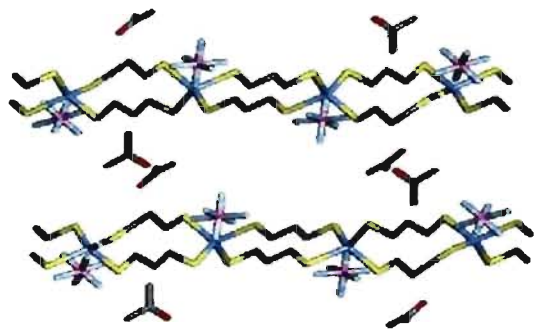

Figure 6.9. Feuillets cationiques du complexe $\{[Ag_2(\mathbf{L}^{\mathbf{3\text{-}Ph}})_4](PF_6)_2(CH_3COCH_3)_2\}_\infty$.
Les anions PF_6^- ainsi que les molécules d'acetone sont placés entre des feuillets adjacentes.

6.6.2 Luminescence

La luminescence des complexes d'or (I) a été étudiée.[25] Nous avons synthétisé deux composés moléculaires: $[\mathbf{L}^{3\text{-Ph}}(AuCl)_2]$ et $[\mathbf{L}^{4\text{-Ph}}(AuCl)_2]$ (Figure 6.10a, b). D'autre part, nous avons isolé trois polymorphes pour le ligand $\mathbf{L}^{3\text{-Ph}}$. Une de ces trois formes est le complexe moléculaire $[\mathbf{L}^{3\text{-Ph}}(AuCl)_2]$. Les deux autres composés forment des chaînes où des unités $[\mathbf{L}^{3\text{-Ph}}(AuCl)_2]$ adjacentes sont retenues par le biais d'interactions aurophiliques, $[\mathbf{L}^{3\text{-Ph}}(AuCl)_2]_\infty$ (Figure 6.9c, d). Le ligand $\mathbf{L}^{1\text{-Ph}}$ conduit aussi à une chaîne, $[\mathbf{L}^{1\text{-Ph}}(AuCl)_2]_\infty$, similaire à celles obtenues avec $\mathbf{L}^{3\text{-Ph}}$ (Figure 6.10e).

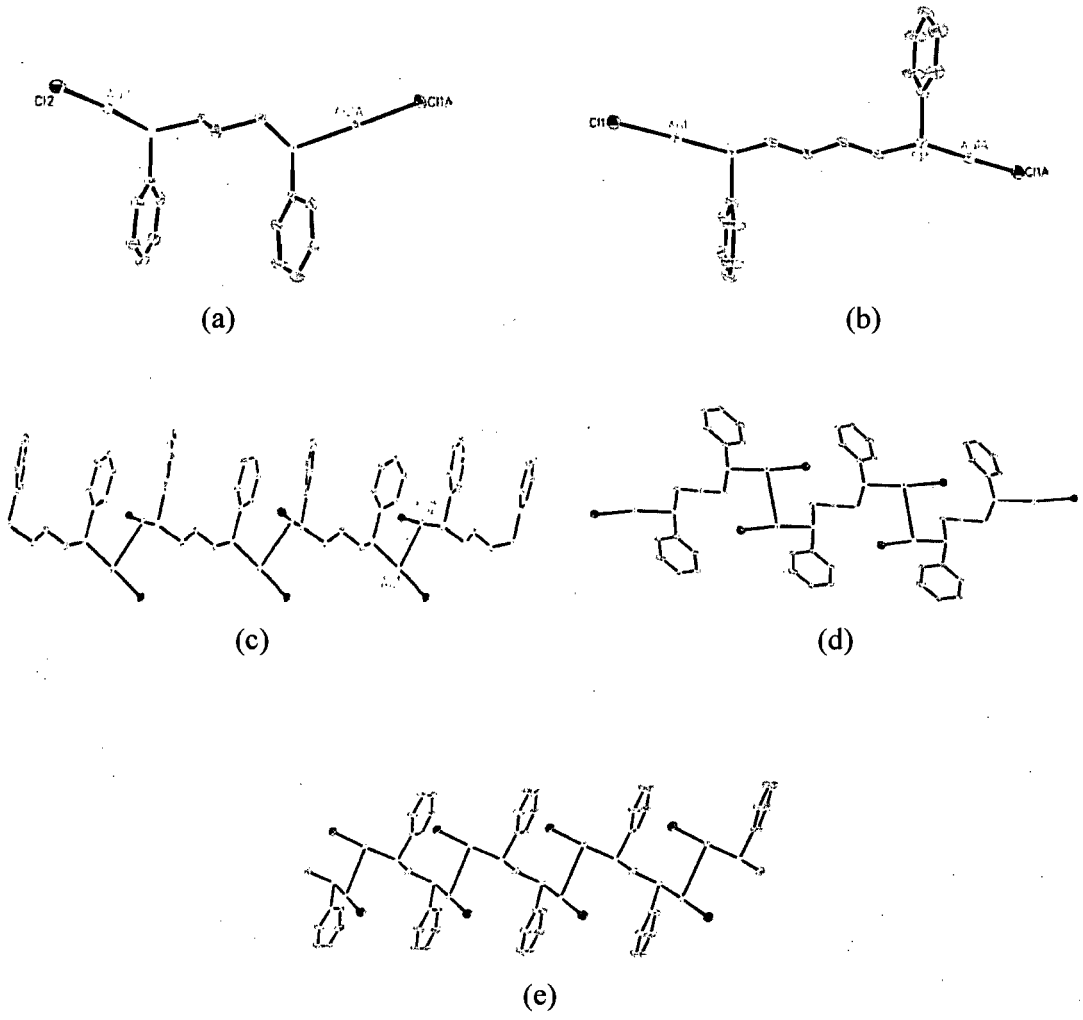

Figure 6.10. (a) Composé moléculaire $[\mathbf{L}^{3\text{-Ph}}(AuCl)_2]$. (b) Composé moléculaire $[\mathbf{L}^{4\text{-Ph}}(AuCl)_2]$. (c) et (d) Chaînes $[\mathbf{L}^{3\text{-Ph}}(AuCl)_2]_\infty$ où des unités $[\mathbf{L}^{3\text{-Ph}}(AuCl)_2]$ adjacentes sont retenues par le biais d'interactions aurophiliques. (e) Chaîne $[\mathbf{L}^{1\text{-Ph}}(AuCl)_2]_\infty$.

Les complexes $[L^{1\text{-}Me}(AuCl)]_\infty$ et $[L^{2\text{-}Ph}(AuCl)_2]_\infty$, formés respectivement avec $L^{1\text{-}Me}$ et $L^{2\text{-}Ph}$, possèdent des chaînes d'or $[\text{-Au-Au-}]_\infty$ (Figure 6.11).[25] Le premier forme une chaîne et le second un réseau bidimensionnel (Figure 6.11).

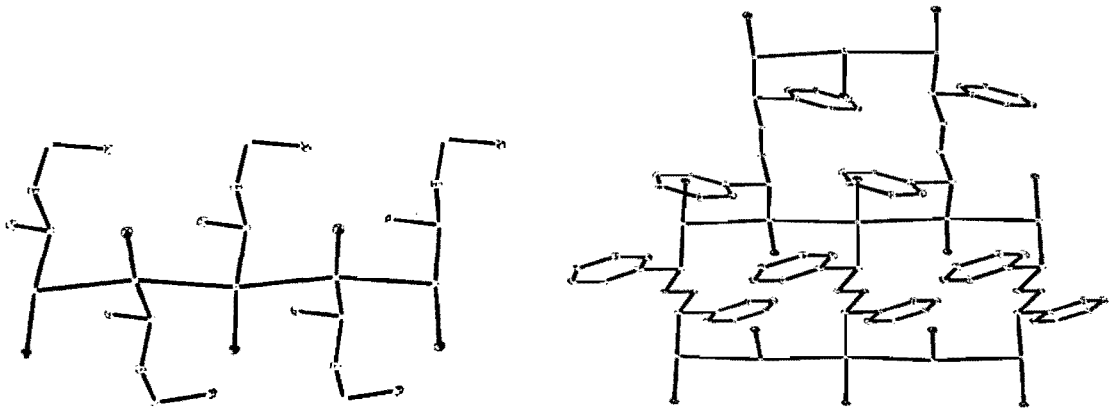

(a) (b)

Figure 6.11. (a) Chaîne 1D $[L^{1\text{-}Me}(AuCl)]_\infty$. (b) Réseau 2D $[L^{2\text{-}Ph}(AuCl)_2]_\infty$.

Les complexes $[L^{1\text{-}Me}(AuCl)]_\infty$ et $[L^{2\text{-}Ph}(AuCl)_2]_\infty$ qui contiennent des chaînes infinies d'or $[\text{-Au-Au-}]_\infty$ montrent un phénomène de luminescence à l'état solide à 5K. Nous suggérons que la luminescence des autres composés dimériques n'a pu être excitée avec le laser 350 nm utilisé parce que, l'énergie du laser est probablement inférieure à l'énergie du premier état excité.

Les spectres des composés $[L^{1\text{-}Me}(AuCl)]_\infty$ et $[L^{2\text{-}Ph}(AuCl)_2]_\infty$ montrent des progressions vibroniques de l'ordre de 600 cm^{-1} (Figure 6.12).[25] Ces progressions vibroniques sont dû à une variation de la densité électronique affectant un mode vibrationnel centré sur le ligand.

Les spectres de luminescence calculés ont été obtenu en prenant des origines à 18950 et 19300 cm^{-1}, respectivement pour les composés $[L^{1\text{-}Me}(AuCl)]_\infty$ et $[L^{2\text{-}Ph}(AuCl)_2]_\infty$, et une fréquence de vibration de 610 cm^{-1}.[26] L'accord entre les spectres de luminescence calculés et expérimentaux de ces composés est satisfaisant (Figure 6.12).

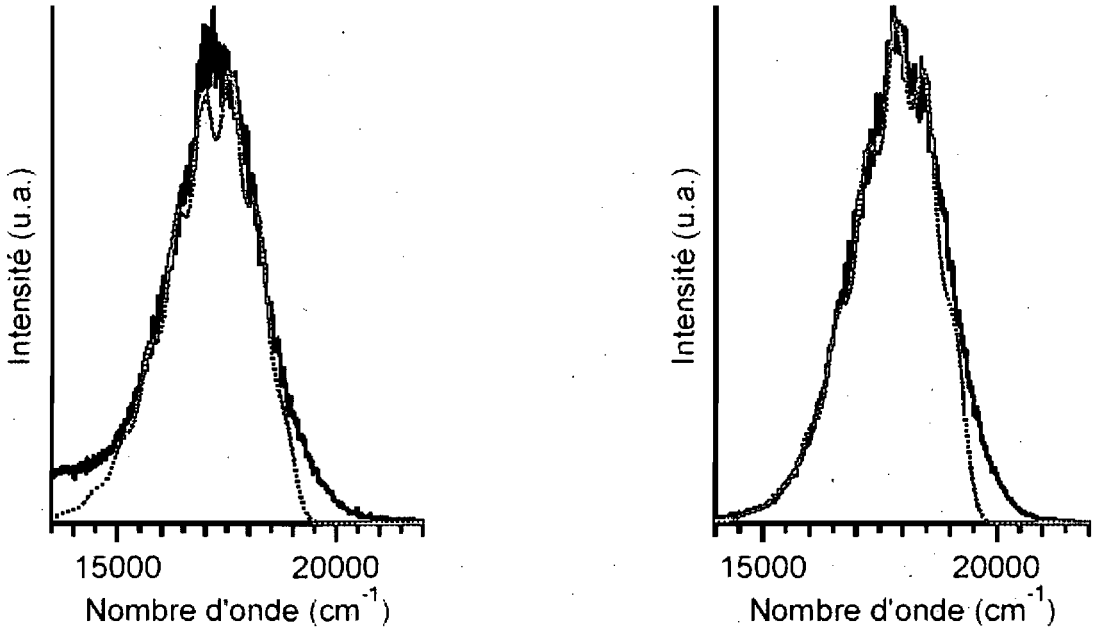

Figure 6.12. Ligne noire: Spectre de luminescence expérimental. Ligne rouge: Spectre de luminescence calculé. (a) $[\mathbf{L}^{\mathbf{1\text{-}Me}}(AuCl)]_\infty$ et (b) $[\mathbf{L}^{\mathbf{2\text{-}Ph}}(AuCl)_2]_\infty$.

6.7 Références.

(1) Bu, X. H.; Chen, W.; Hou, W. F.; Du, M.; Zhang, R. H.; Brisse, F. *Inorg. Chem.* **2002**, *41*, 3477.

(2) (a) Awaleh, M. O.; Badia, A.; Brisse, F. *Cryst. Growth Des.* **2005**. *5*, 1897. (b) Awaleh, M. O.; Badia, A.; Brisse, F. *Inorg. Chem.* **2005**. *44*, 7833. (c) Awaleh, M. O.; Badia, A.; Brisse, F.; Bu, X. H. *Inorg. Chem.* **2006**. *45*, 1560. (d) Awaleh, M. O.; Badia, A.; Brisse, F. *Cryst. Growth Des.* **2006**. *6,* 2674. (e) Awaleh, M. O. ; Badia, A.; Brisse, F. *Inorg. Chem.* **2006**. *Soumis pour publication.*

(3) (a) Li, J. R. ; Zhang, R. H. ; Bu, X. H. *Cryst. Growth. Des.* **2003**, *3*, 829. (b) Li, J. R.; Bu, X. H.; Jiao, J.; Du, W. P. ; Xu, X. H. ; Zhang, R. H. *J. Chem. Soc., Trans Dalton.* **2005**, 464. (c) Black, J. R.; Champness, N. R.; Levason, W.; Reid, G. *J. Chem. Soc., Chem. Comm.* **1995**, 1277. (d) Black, J. R.; Champness, N. R.; Levason, W.; Reid, G. *J. Chem. Soc., Dalton Trans.* **1995**, 3439. (e) Chen, W.; Du, M.; Zhang, R. H.; Bu, X. H. *Acta Crystallogr.* **2001**, *E57*, m213. (f) Du, M.; Zhao, X. J. *Acta Crystallogr.* **2004**, *E60*, m193. (g) Bu, X. H.; Hou, W. F.; Du, M.; Chen, W.; Zhang, R. H. *Cryst. Growth*

Des. **2002**, *2*, 303.

(4) Chen, C. L.; Kang, B. S.; Su, C. Y. *Aust. J. Chem.* **2006**, *59*, 3. Et références citées.

(5) Bu, X. H.; Chen, W.; Du, M.; Biradha, K. ; Wang, W. Z. ; Zhang, R. H. *Inorg. Chem.* **2002**, *41*, 437.

(6) Chen, W.; Li, J. R.; Wang, W. Z.; Bu, X. H.; Zhang, R. H.; Chen, R. T. *Gaodeng Xuexiao Huaxue Xuebao* **2001**, *22*, 22.

(7) Awaleh, M. O.; Badia, A.; Brisse, A. *Acta Crystallogr.* **2005**, *E60*, o2476.

(8) Awaleh, M. O.; Badia, A.; Brisse, A. *Acta Crystallogr.* **2005**, *E60*, o2476.

(9) Chen, W.; Du, M.; Bu, X. H.; Zhang, R. H.; Mak, T. C. W. *CrystEngComm.* **2003**, *5*, 96.

(10) Cotton, F. A.; Wilkinson, G. *Adavanced Inorganic Chemistry.* 5rd ed. John Wiley and Sons, 1988.

(11) Hanton, L. R.; Young, A. G. *Cryst. Growth Des.* **2006**, *6*, 833.

(12) (a) Pyykkö, P. *Chem. Rev.* **1997**, *97*, 597. (b) Häberlen, O. D.; Schmidbaur, H.; Rosch, N. *J. Am. Chem. Soc.* **1994**, *116*, 8241. (c) Che, C. M.; Kwong, H. L.; Yam, V. W. A.; Cho, K. C. *J. Chem. Soc., Chem. Comm.* **1989**, 885. (d) King, C.; Wang, J. C.; Khan, N. I.; Fackler Jr.; J. P. *Inorg. Chem.* **1989**, *28*, 2145. (e) Phillips, L. D.; Che, C. M.; Leung, K. H.; Mao, Z.; Tse, M. C. *Coord. Chem. Rev.* **2005**, *249*, 1476. (f) Che, C. M.; Lai, S. W. *Coord. Chem. Rev.* **2005**, *249*, 1296.

(13) Che, C. M.; Tse, M. C. ; Chan, M. C. W.; Cheung, K. K. ; Phillips, D. L.; Leung, K. K. *J. Am. Chem. Soc.* **2000**, *122*, 2464.

(14) Omary, M. A.; Webb, T. R.; Assefa, Z.; Shankle, G. E.; Patterson, H. H. *Inorg. Chem.* **1998**, *37*, 1380.

(15) Porterfield, W. W. *Inorganic Chemistry: A Unified Approach*, Addison-Wesley, 1994.

(16) (a) Ahmed, L. S.; Dilworth, J. R.; Miller, J. R.; Wheatley, N. *Inorg. Chim. Acta* **1998**, *278*, 229. (b) Jung, O. S.; Kim, Y. J.; Lee, Y. A.; Kang, S. W.; Choi, S. N. *Cryst Growth Des.* **2004**, *4*, 23. (c) Reger, D. L.; Semeniuc, F.; Captain, B.; Smith, M. D. *Inorg. Chem.* **2005**, *44*, 2995. (d) Bosch, E.; Barnes, C. L. *Inorg. Chem.* **2002**, *41*, 2543. (e) Wang, Q. M.; Mak, T. C. W. *J. Am. Chem. Soc.* **2001**, *123*, 7594.

(17) Singh, K.; Long, J. R.; Stavropoulos, P. *J. Am. Chem. Soc.* **1997**, *119*, 2942.

(18) Deacon, G. B.; Phillips, R. J. *Coord. Chem. Rev.* **1980**. *33*, 227.

(19) Robert, V; Lemercier, G. *J. Am. Chem. Soc.* **2006**, *128*, 1183.

(20) (a) Łakomska, I.; Grodzicki, A. *Thermochimica. Acta* **1997**, *303*, 41. (b) Łakomska, I.;

Szłyk, E.; Grodzicki, A. *Thermochimica. Acta* **1998**, *315*, 121. (c) Szłyk, E.; Szymańska, I.; Surdykowski, A.; Głowiak, T.; Wojtczak, A.; Goliński, A. *J. Chem. Soc., Dalton. Trans.* **2003**, 3404.

(21) Grodzicki, A.; Łakomska, I.; Piszczek, P.; Szymańska, I.; Szłyk, E. *Coord. Chem. Rev.* **2005**, *249*, 2232.

(22) Jung, O. S.; Kim, Y. J.; Lee, Y. A.; Park, J. K.; Chae, H. K. *J. Am. Chem. Soc.* **2000**, *122*, 9921.

(23) Yamada, M.; Hagiwara, H.; Torigoe, H.; Matsumoto, N.; Kojima, M.; Dahan, F.; Tuchagues, J. P.; Re, N.; Iijima, S. *Chem. Eur. J.* **2006**, *12*, 4536.

(24) Le volume moléculaire du nitrate a été calculé en utilisant le programe Spartan dans les mêmes conditions que les auteurs de la référence 23 ont calculé avec le même programe les volumes moléculaires des anions BF_4^-; ClO_4^-; PF_6^-; SbF_6^- et $CF_3SO_3^-$ (voir référence 23).

(25) Awaleh, M. O.; Baril-Robert, F.; Reber, C.; Badia, A.; Brisse, F. *Cryst. Growth Des.* **2007**. *Soumis pour publication.*

(26) (a) Brunold, T. C.; Güdel, H. U. *In Inorg. Elect. Struct and Spect*, Salomon, Vol I, p 259. (b) Zink, J. I. *Coord. Chem. Rev.* **2001**, *211*, 69.

Chapitre 7: Conclusions et perspectives

L'objectif de cette recherche consistait à étudier les paramètres influençant la formation des composés à structure étendue à l'état solide qui sont générés par autoassemblage de ligands dithioéthers flexibles avec des sels d'argent(I) et d'or(I). Cette étude systématique visait à sélectionner les réseaux de coordination susceptibles de présenter des propriétés d'échange ou de luminescence sur la base de leurs topologies, afin d'étudier les propriétés de ces matériaux hybrides.

Parmi les paramètres étudiés, les anions jouent un rôle très important. Nous avons classé les anions sur la base de leur habilité à se coordonner à l'argent dans nos composés métallosupramoléculaires:

(i) les anions non coordonnants (BF_4^-, PF_6^- et SbF_6^-) équilibrent seulement les charges des réseaux cationiques formés par le métal et le ligand $(Ag\text{-ligand})_\infty^+$;

(ii) l'anion perchlorate est faiblement coordonnant puisqu'il complète souvent la sphère de coordination du métal dans les réseaux $(Ag\text{-ligand})_\infty$ et dans certains cas il ne fait que compenser la charge des réseaux cationiques $(Ag\text{-ligand})_\infty^+$;

(iii) les anions sulfonates sont considérés comme moyennement coordonnants du fait qu'ils sont souvent coordonnés à l'argent. Dans d'autres cas ils forment des dimères $(Ag\text{-anion})_2$ qui se constituent en réseau par l'intermédiaire des ligands.

(iv) le nitrate et les anions qui comportent des groupes carboxylates sont fortement coordonnants car ils participent souvent à l'expansion du réseau au même titre que les ligands. On a aussi observé que des réseaux $(Ag\text{-ligand})_\infty$ et $(Ag\text{-anions})_\infty$, partageant leurs atomes d'argent, coexistent au sein d'un même complexe.

L'étude systématique entreprise dans le cadre de cette thèse montre qu'il y a des très fortes chances d'élaborer des réseaux cationiques en combinant les ligands $\mathbf{L^{n\text{-}Me}}$ avec des anions non coordonnants ou des anions faiblement coordonnants, indépendamment du rapport métal-ligand des produits de départ.

L'autoassemblage du ligand $\mathbf{L^{1\text{-}Me}}$, $MeS(CH_2)SMe$, avec des sels d'argent incorporant des anions faiblement ou non coordonnants permit de générer des réseaux cationiques (1D, 2D) où les anions équilibrent seulement la charge du réseau. Des réseaux identiques sont obtenus quelque soit le rapport métal-ligand des produits de départ. Ces matériaux présentent des propriétés d'échanges anioniques réversibles.

De la même manière, la combinaison des ligands $\mathbf{L^{n\text{-}Ph}}$, $PhS(CH_2)_nSPh$, de taille intermédiaire (n = 3, 4 et 5), avec des sels d'argent dont les contre-ions sont faiblement ou non coordonnants, générèrent systématiquement des réseaux cationiques lamellaires. Ces matériaux peuvent potentiellement présenter des propriétés d'échanges anioniques.

La majorité des composés métallosupramoléculaires obtenus par la combinaison des ligands $\mathbf{L^{n\text{-}Ph}}$ avec des carboxylates d'argent présentent des distances Ag-Ag courtes. Pour certains de ces composés, spécifiquement les tétramères d'argent, ces distances sont mêmes plus courtes que la somme des rayons métalliques de l'argent. Il est possible que des interactions argentophiliques existent dans ces matériaux.

Une analyse thermogravimétrique a révélé que les métallosupramolécules au sein desquelles coexistent les deux réseaux $(Ag\text{-ligand})_\infty$ et $(Ag\text{-anion})_\infty$ ont la même stabilité thermique que les complexes semblables contenant seulement le réseau $(Ag\text{-ligand})_\infty$ où les anions complètent la sphère de coordination de l'argent.

Deux complexes d'un nouveau type ont été obtenus par autoassemblage du bis(méthylthio)méthane, $\mathbf{L^{1\text{-}Me}}$, et du trifluoroacétate ou du pentafluoropropionate d'argent. La particularité de ces matériaux est qu'ils contiennent des agrégats $Ag_{12}S_6$ possédant la géométrie d'un cuboctaèdre déformé. Ces agrégats sont formés d'anions $^-SCH_3$, résultant du clivage du ligand, et de cations Ag(I). Chaque anion $^-SCH_3$ relie quatre atomes d'argent par un pontage μ_4-SCH_3. Les ligands bis(méthylthio)méthane coordonnent ces agrégats formant ainsi des polymères de coordination. Il est à noter que les agrégats sont seulement obtenus avec le petit ligand $\mathbf{L^{1\text{-}Me}}$. Il faut au moins quatre mois pour en obtenir des cristaux.

Des complexes moléculaires et des composés métallosupramoléculaires d'or(I) ont été synthétisés quand les ligands dithioéthers ont été autoassemblés avec l'acide tétrachloroaurique trihydraté. Les composés arborant des chaînes d'or, $[Au\text{-}Au\text{-}]_\infty$, exhibent des propriétés de luminescence à basse température. Les spectres de luminescence de ces composés montrent des progressions vibroniques de l'ordre de 600 cm^{-1} impliquant une contribution des ligands.

Perspectives et travaux futurs

Dans la discussion générale, nous avions récapitulé l'influence de certains paramètres sur la formation des réseaux obtenus par auto-assemblage des ligands $\mathbf{L^{n\text{-}R}}$ et des sels d'argent(I). Dans ce chapitre nous soulignions la difficulté de contrôler la topologie

des réseaux métallosuprmaoléculaires d'argent(I). Ainsi, il y a encore beaucoup de travail à faire pour arriver à contrôler le rôle de plusieurs paramètres (solvent, stoechiométrie, etc). Néanmoins, dans le domaine du génie cristallin des composés dithiolatés d'argent(I), il reste quelques axes de recherche intéressants à explorer.

1- Domaine d'existence des réseaux cationiques 2D

a- Nous avons mis en évidence la formation de réseaux cationiques lamellaires avec les sels d'argent(I) incorporant des anions non coordonnants ou faiblement coordonnants et les ligands $\mathbf{L^{n\text{-}Ph}}$ (**n** = 3-5) et $\mathbf{L^{n\text{-}tBu}}$ (**n** = 1). Il serait intéressant d'auto-assembler les ligands $\mathbf{L^{n\text{-}R}}$ (**R** = *t*Bu, Benz ; **n** = 3-5) avec les sels d'argent(I) afin de vérifier si des réseaux lamellaires cationiques vont se former. Ceci nous permettrait d'étudier l'influence du substituant **R** sur la formation de ces réseaux.

b- D'autre part, il faudrait combiner les ligands $\mathbf{L^{n\text{-}Ph}}$ (**n** = 6-10) avec les sels AgX (X = BF_4^-, PF_6^-, AsF_6^-, SbF_6^-) afin de tester si des réseaux lamellaires cationiques vont se former. Cette étude permettrait d'établir l'influence de la longueur des ligands $\mathbf{L^{n\text{-}Ph}}$ sur la formation des réseaux cationiques 2D.

c- Nous avons établit que la combinaison du ligand $\mathbf{L^{1\text{-}Me}}$ avec des sels d'argent(I) conduisait à des réseaux cationiques (1D, 2D et 3D). De plus, nous avons observé que les ligands $\mathbf{L^{1\text{-}Me}}$ et $\mathbf{L^{1\text{-}Et}}$ menaient à des réseaux de même dimensionalité. De ce fait, une suite logique de ce travail serait de combiner les ligands $\mathbf{L^{n\text{-}R}}$ (**R** = Me, Et ; **n** = 2 - 6) et des sels d'argent possédant des contre-ions non coordonnants ou faiblement coordonnants afin de générer des réseaux cationiques. Cette étude systématique permettrait d'examiner comment la longueur du ligand influence la topologie des réseaux cationiques

2- Échange d'anions

Un axe de recherche concernerait l'étude systématique de l'échange d'anions de tous les réseaux cationiques formées. Cette étude permettrait de sélectionner les réseaux cationiques qui se prétent facilement aux échanges d'anions.

3- Agrégats

Nous avons obtenus des agrégats en combinant $\mathbf{L^{1\text{-}Me}}$ avec CF_3CO_2Ag ou $CF_3CF_2CO_2Ag$. Ces agrégats mettent plusieurs mois pour se former avec des faibles rendements. Dans ceux-ci, il y a des entités $^-SCH_3$, provenant du clivage du ligand. Une petite étude préliminaire a montré que l'utilisation du $NaSCH_3$ en combinaison avec $\mathbf{L^{1\text{-}Me}}$ et CF_3CO_2Ag permettait de générer ces agrégats dans un délai de moins d'un mois avec un très bon rendement. Il serait très intéressant de transposer cette voie de synthèse

prometteuse aux ligands $\mathbf{L}^{\mathbf{n\text{-}R}}$ (**n** = 2 - 6, **R** = Me, Ph, etc). Ceci nous permettrait de sonder l'influence de la longueur et de l'encombrement des ligands sur la formation d'agrégats.

4- Interactions entre atomes d'argent

Les agrégats possèdent des liaisons argent-argent plus courtes que la somme des rayons de van der Waals de deux atomes d'argent laissant prévoir l'existence d'interaction Ag–Ag coopératives. Par ailleurs, de nombreux complexes sont constitués de dimères Ag–Ag ou de tétramères Ag–Ag–Ag–Ag où les distances internucléaires sont courtes.
Il serait intéressant de voir si ces matériaux possèdent des propriétés de luminescence. Une étude par spectroscopie Raman permettrait de sonder la fréquence de vibration de la liaison Ag – Ag et d'établir l'existence d'interactions argentophiliques.

5- Stabilité thermique

Les composés de coordination avec des perfluorocarboxylates d'argent sont considérés depuis très récemment comme des précurseurs intéressants pour le dépôt chimique en phase vapeur (CVD). Il a été rapporté que des tels précurseurs obtenus avec $CF_3CF_2CF_2Ag$ se décomposaient entre 250 et 380 °C. Comme certains de nos complexes, obtenus par réaction entre $\mathbf{L}^{\mathbf{3\text{-}Ph}}$ et $CF_3CF_2CO_2Ag$ ou $AgOOCCF_2CF_2COOAg$, se décomposent au-dessous de 300 °C ils pourraient être utilisés pour le dépôt chimique de film d'argent en phase vapeur. L'étude de la volatilité des complexes permettrait de tester si nos composés se prêteraient à la technique CVD.

Références.

(1) Grodzicki, A.; Łakomska, I.; Piszczek, P.; Szymańska, I.; Szłyk, E. *Coord. Chem. Rev.* **2005**, *249*, 2232.

(2) Edwards, D. N.; Harker, R. M.; Mahon, M. F.; Molloy, K. C. *Inorg. Chim. Acta* **2002**, *328*,134.

(3) (a) Awaleh, M. O.; Badia, A.; Brisse, F. *Inorg. Chem.* **2005**. *44*, 7833.

(b) Awaleh, M. O. ; Badia, A.; Brisse, F. *CrystEngComm.* **2007**. *Soumis pour publication* (Chapitre 4.2).

Annexe I

Table S1. Comparison of the bond distances (Å) and angles (°) involving the silver atom in the seven complexes synthesized.

Bond		*Angle*			*Symmetry position*
1	ClO_4^-				
Ag(1)-S(1)	2.5368(7)	S(1)-Ag(1)-S(2)#1	121.4(1)	#1	-x+3/2; y+1/2; -z+1/2
Ag(1)-S(2)#1	2.5212(7)	O(1)-Ag(1)-S(1)	111.0(1)		
Ag(1)-O(1)	2.412(2)	O(1)-Ag(1)-S(2)#1	126.5(1)		
2	BF_4^-				
Ag(1)-S(1)#1	2.5174(8)	S(2)-Ag(1)-S(1)#1	123.5(1)	#1	-x+1/2; y-1/2; -z+3/2
Ag(1)-S(2)	2.5269(8)	F(1)-Ag(1)-S(1)#1	125.6(1)		
Ag(1)-F(1)	2.535(3)	F(1)-Ag(1)-S(2)	109.2(1)		
3	CF_3COO^-				
Ag(1)-S(1)	2.651(4)	O(1)-Ag(1)-S(2)#1	151.5(4)	#1	x+1; y; z
Ag(1)-S(2)#1	2.468(5)	O(1)-Ag(1)-S(1)	112.8(3)		
Ag(1)-O(1)	2.186(12)	S(1)-Ag(1)-S(2)#1	95.5(1)		
4	$CF_3SO_3^-$				
Ag(1)-S(1)	2.434(2)	S(1)-Ag(1)-S(2)#1	145.9(1)	#1	+1/2; -y+1/2; z+1/2
Ag(1)-S(2)#1	2.477(2)	O(1)-Ag(1)-S(1)	125.6(2)		
Ag(1)-O(1)	2.378(5)	O(1)-Ag(1)-S(2)#1	86.7(2)		
5	$CF_3SO_3^-$				
Ag(1)-S(4)	2.5160(13)	S(4)-Ag(1)-S(6)#2	126.4(1)	#1	-x; -y+1; -z
Ag(1)-S(6)#2	2.4826(12)	S(4)-Ag(1)-O(5)#1	93.4(2)	#2	-x+1; -y+2; -z+1
Ag(1)-O(4)	2.377(4)	S(4)-Ag(1)-O(4)	99.3(2)		
Ag(1)-O(5)#1	2.466(6)	O(4)-Ag(1)-O(5)#1	99.4(2)		
		O(4)-Ag(1)-S(6)#2	121.2(2)		
		O(5)#1-Ag(1)-S(6)#2	110.6(2)		
Ag(2)-S(3)	2.4758(14)	S(5)-Ag(2)-O(2)	104.7(1)		
Ag(2)-S(5)	2.4646(15)	S(5)-Ag(2)-O(3)#2	105.3(1)		
Ag(2)-O(2)	2.429(4)	S(3)-Ag(2)-O(2)	105.4(1)		
Ag(2)-O(3)#2	2.450(4)	O(2)-Ag(2)-O(3)#2	100.4(2)		
		S(3)-Ag(2)-S(5)	139.6(1)		
		S(3)-Ag(2)-O(3)#2	95.1(1)		
6	$CF_3CF_2CF_2COO^-$				
Ag(1)-S(2)#2	2.5826(6)	S(1)-Ag(1)-Ag(1)#1	152.6(1)	#1	-x+1; -y+1; -z+1
Ag(1)-S(1)	2.6154(6)	O(11)-Ag(1)-O(12)#1	136.6(1)	#2	x+1; y; z
Ag(1)-O(11)	2.321(2)	O(11)-Ag(1)-S(2)#2	100.0(1)		
Ag(1)-O(12)#1	2.311(2)	O(12)#1-Ag(1)-S(2)#2	115.4(1)		

Ag(1)-Ag(1)#1	3.1593(3)	S(1)-Ag(1)-S(2)#2	104.2(1)		
		S(1)-Ag(1)-O(11)	103.3(1)		
		S(1)-Ag(1)-O(12)#1	92.0(1)		
		S(2)#2-Ag(1)-Ag(1)#1	102.4(1)		
		O(12)-Ag(1)-Ag(1)#1	70.5(1)		
		O(11)-Ag(1)-Ag(1)#1	78.4(1)		

7 $^{-}OOCCF_2CF_2COO^{-}$

Ag(1)-S(1)#1	2.5826(9)	S(1)-Ag(1)-S(3)	101.2(1)	#1	-x+1; -y; -z+1
Ag(1)-S(3)	2.6243(8)	S(1)-Ag(1)-O(1)	109.1(1)	#2	x; y; z+1
Ag(1)-O(1)	2.311(2)	S(1)-Ag(1)-O(2)	106.9(1)	#3	-x+1; -y; -z+2
Ag(1)-O(2)	2.314(2)	S(3)-Ag(1)-O(1)	92.2(1)		
Ag(1)-Ag(1)#1	2.9836(5)	S(3)-Ag(1)-O(2)	99.3(1)		
		O(1)-Ag(1)-O(2)	139.1(1)		
		S(1)-Ag(1)-Ag(1)#1	104.2(1)		
		S(3)-Ag(1)-Ag(1)#1	154.5(1)		
		O(1)-Ag(1)-Ag(1)#1	77.4(1)		
		O(2)-Ag(1)-Ag(1)#1	75.6(1)		
Ag(2)-S(2)	2.6540(8)	S(2)-Ag(2)-S(4)	107.1(1)		
Ag(2)-S(4)#2	2.6409(9)	S(2)-Ag(2)-O(3)#1	88.6(1)		
Ag(2)-O(3)#1	2.281(2)	S(2)-Ag(2)-O(4)#2	100.9(1)		
Ag(2)-O(4)#2	2.280(2)	S(4)#2-Ag(2)-O(3)#1	103.0(1)		
Ag(2)-Ag(2)#3	3.0168(5)	S(4)#2-Ag(2)-O(4)#2	93.1(1)		
		O(3)#1-Ag(2)-O(4)#2	158.1(1)		
		S(2)-Ag(2)-Ag(2)#3	138.7(1)		
		S(4)#2-Ag(2)-Ag(2)#3	114.2(1)		
		O(3)#1-Ag(2)-Ag(2)#3	81.8(1)		
		O(4)#2-Ag(2)-Ag(2)#3	78.1(1)		

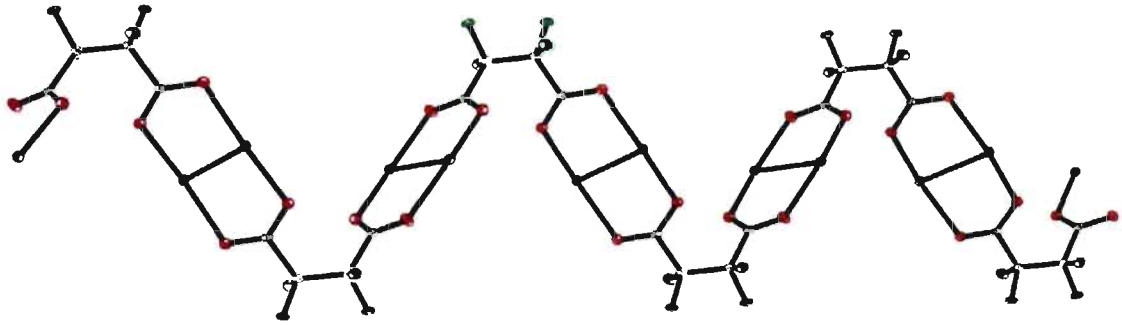

(a)

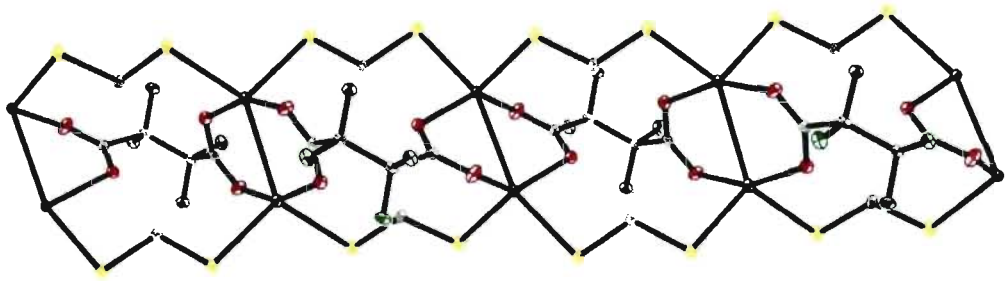

(b)

Figure S1. (a) The 1D-coordination polymer in complex **7** showing the anions bridging consecutive dimers thus yielding the polymeric chain. (b) The same chain now including the ligands which reinforce the structure through Ag-S bonds.

Annexe II

Table S1. Comparison of the bond distances (Å) and angles (°) involving the silver atoms in the complexes synthesized.

(1) PF_6^-				
Ag(1)-S(3)	2.538(1)	S(3)-Ag(1)-S(5)	116.0(1)	#1 1-x, y-½, ½-z
Ag(1)-S(5)	2.565(1)	S(3)-Ag(1)-S(2)#1	116.5(1)	#2 x, y-1, z
Ag(1)-S(2)#1	2.584(1)	S(5)-Ag(1)-S(2)#1	107.6(1)	#3 –x, ½+y, ½-z
Ag(1)-S(1)	2.596(1)	S(3)-Ag(1)-S(1)	105.9(1)	
Ag(2)-S(4)	2.589(1)	S(5)-Ag(1)-S(1)	105.2(1)	
Ag(2)-S(7)	2.597(1)	S(1)-Ag(1)-S(2)#1	104.4(1)	
Ag(2)-S(6)#2	2.541(1)	S(4)-Ag(2)-S(7)	108.5(1)	
Ag(2)-S(8)#2	2.577(1)	S(4)-Ag(2)-S(6)#2	108.6(1)	
		S(4)-Ag(2)-S(8)#2	99.0(1)	
		S(6)#2-Ag(2)-S(8)#3	128.6(1)	
		S(6)#2-Ag(2)-S(7)	107.1(1)	
		S(8)#3-Ag(2)-S(7)	103.7(1)	
(2) CF_3COO^-				
Ag(1)-O(3)	2.268(3)	O(3)-Ag(1)-O(1)	110.2(2)	#1 x, ½-y, z-½
Ag(1)-O(1)	2.348(1)	O(3)-Ag(1)-S(1)	133.0(1)	
Ag(1)-S(1)	2.478(1)	O(1)-Ag(1)-S(1)	112.1(1)	
Ag(1)-S(1)#1	2.697(1)	O(3)-Ag(1)-S(1)#1	83.7(1)	
Ag(1)-Ag(2)	3.2459(5)	O(1)-Ag(1)-S(1)#1	97.3(1)	
		S(1)-Ag(1)-S(1)#1	110.0(1)	
		O(3)-Ag(1)-Ag(2)	84.7(1)	
		O(1)-Ag(1)-Ag(2)	66.9(1)	
		S(1)-Ag(1)-Ag(2)	93.6(1)	
		S(1)#1-Ag(1)-Ag(2)	155.6(1)	
(3) $CF_3CF_2COO^-$				
Ag(1)-O(11)	2.345(4)	O(11)-Ag(1)-O(12)#1	123.8(2)	#1 1-x, y, ½-z
Ag(1)-O(12)#1	2.359(4)	O(11)-Ag(1)-S(1)	123.7(2)	#2 1-x, 1-y, -z
Ag(1)-S(1)	2.500(1)	O(12)#1-Ag(1)-S(1)	103.6(1)	
Ag(1)-S(2)	2.625(1)	O(11)-Ag(1)-S(2)	82.7(2)	
Ag(1)-Ag(1)#1	3.0502(7)	O(12)#1-Ag(1)-S(1)	97.7(1)	
Ag(2)-O(82)	2.333(4)	S(1)-Ag(1)-S(2)	122.0(1)	
Ag(2)-O(42)	2.354(4)	O(11)-Ag(1)-Ag(1)#1	82.3(1)	
Ag(2)-O(42)#2	2.408(4)	O(12)#1-Ag(1)-Ag(1)#1	70.6(1)	
Ag(2)-S(2)	2.488(1)	S(1)-Ag(1)-Ag(1)#1	87.4(1)	
		S(2)-Ag(1)-Ag(1)#1	150.6(1)	
		O(82)-Ag(2)-O(42)	110.4(2)	
		O(82)-Ag(2)-O(42)#2	105.1(1)	
		O(42)-Ag(2)-O(42)#2	78.6(1)	
		O(82)-Ag(2)-S(2)	125.8(1)	
		O(42)-Ag(2)-S(2)	115.8(1)	

		O(42)#2-Ag(2)-S(2)	110.5(1)	

(4) $CF_3CF_2CF_2COO^-$

Ag(1)-O(1)	2.417(2)	O(1)-Ag(1)-O(2)#1	119.4(1)	#1 –x, y, ½-z
Ag(1)-O(2)#1	2.330(2)	S(1)-Ag(1)-O(2)#1	110.2(1)	#2 x, 1+y, z
Ag(1)-S(1)	2.503(1)	S(1)-Ag(1)-O(1)	117.1(1)	
Ag(1)-S(2)#2	2.591(1)	S(2)#2-Ag(1)-O(2)#1	99.8(1)	
Ag(1)-Ag(1)#1	3.1594(4)	S(2)#2-Ag(1)-O(1)	83.7(1)	
		S(1)-Ag(1)-S(2)#2	123.9(2)	
		O(2)#1-Ag(1)-Ag(1)#1	70.0(1)	
		O(1)-Ag(1)-Ag(1)#1	77.5(1)	
		S(1)-Ag(1)-Ag(1)#1	86.2(1)	
		S(2)#2-Ag(1)-Ag(1)#1	149.5(1)	

(5) *p*-Tso^-

Ag(1)-O(1)	2.472(4)	O(1)-Ag(1)-O(2)#1	109.2(2)	#1 –x, 2-y, -z
Ag(1)-O(2)#1	2.348(4)	S(1)-Ag(1)-O(2)#1	131.5(1)	#2 x, 1+y, z
Ag(1)-S(1)	2.496(1)	O(1)-Ag(1)-S(1)	103.6(1)	
Ag(1)-S(2)#2	2.578(1)	O(2)#1-Ag(1)-S(2)#2	88.2(2)	
		O(1)-Ag(1)-S(2)#2	86.7(1)	
		S(1)-Ag(1)-S(2)#2	129.1(1)	

(6) *p*-Tso^-

Ag(1)-S(1)	2.461(1)	S(1)-Ag(1)-O(3)#1	113.8(1)	#1 1-x, -y, 2-z
Ag(1)-S(2)#2	2.468(1)	S(2)#2-Ag(1)-O(3)#1	92.9(1)	#2 x, ½-y, ½+z
Ag(1)-O(3)	2.491(3)	S(1)-Ag(1)-S(2)#2	150.3(1)	
Ag(1)-O(3)#1	2.400(3)	O(3)-Ag(1)-O(3)#1	74.9(1)	
		S(1)-Ag(1)-O(3)	100.6(1)	
		S(2)#2-Ag(1)-O(3)	98.9(1)	

(7) $CF_3SO_3^-$

Ag(1)-O(32)	2.356(4)	O(32)-Ag(1)-O(41)	84.9(2)	#1 ½+x, ½-y, z-½
Ag(1)-O(41)	2.463(5)	O(32)-Ag(1)-S(2)#1	118.7(1)	#2 x-½, ½-y, ½+z
Ag(1)-S(1)	2.590(1)	O(41)-Ag(1)-S(2)#1	131.4(1)	#3 1+x, y, z
Ag(1)-S(2)#1	2.516(1)	O(32)-Ag(1)-S(1)	103.9(1)	
Ag(2)-O(7)	2.486(4)	O(41)-Ag(1)-S(1)	83.1(1)	
Ag(2)-O(31)	2.518(5)	S(2)#1-Ag(1)-S(1)	124.6(1)	
Ag(2)-O(43)#2	2.393(4)	O(7)-Ag(2)-O(43)#2	88.1(2)	
Ag(2)-S(1)	2.602(1)	O(31)-Ag(2)-O(43)#2	83.6(2)	
Ag(2)-S(2)#3	2.631(1)	O(7)-Ag(2)-O(31)	170.6(2)	
		O(43)#2-Ag(2)-S(1)	128.1(1)	
		O(7)-Ag(2)-S(1)	93.6(1)	
		O(31)-Ag(2)-S(1)	88.1(2)	
		O(43)#2-Ag(2)-S(2)#3	106.3(1)	
		O(7)-Ag(2)-S(2)#3	97.3(1)	
		O(31)-Ag(2)-S(2)#3	89.4(2)	
		S(1)-Ag(2)-S(2)#3	124.8(1)	

(**8**) $CF_3SO_3^-$

Ag(1)-O(1)	2.459(4)	O(1)#1-Ag(1)-S(1)	136.6(1)	#1 –x, 2-y, -z
Ag(1)-O(1)#1	2.415(4)	O(1)#1-Ag(1)-O(1)	79.6(1)	#2 x, 1+y, z
Ag(1)-O(3)#2	2.481(4)	O(1)-Ag(1)-O(3)#2	77.4(1)	
Ag(1)-S(1)	2.445(2)	O(1)#1-Ag(1)-O(3)#2	82.7(1)	
		S(1)-Ag(1)-O(1)	141.0(1)	
		S(1)-Ag(1)-O(3)#2	115.1(1)	

(**9**) $CF_3SO_3^-$

Ag(1)-S(1)	2.549(1)	S(1)-Ag(1)-O(1)	126.2(1)	#1 ½+x, ½-y, z-½
Ag(1)-S(2)#2	2.549(1)	S(1)-Ag(1)-O(5)#1	94.9(1)	#2 ½+x, ½-y, ½+z
Ag(1)-O(1)	2.515(4)	S(1)-Ag(1)-S(2)#2	121.7(4)	#3 x-½, ½-y, ½+z
Ag(1)-O(5)	2.340(3)	S(2)#2-Ag(1)-O(1)	86.2(9)	
Ag(2)-S(1)	2.553(1)	S(2)#2-Ag(1)-O(5)#1	131.0(1)	
Ag(2)-S(2)#3	2.531(1)	O(1)-Ag(1)-O(5)#1	97.8(1)	
Ag(2)-O(4)	2.361(4)	S(1)-Ag(2)-O(4)	107.5(1)	
Ag(2)-O(3)#3	2.422(3)	S(1)-Ag(2)-O(3)#3	101.5(1)	
		S(1)-Ag(2)-S(2)#3	123.8(4)	
		S(2)#3-Ag(2)-O(4)	120.2(1)	
		S(2)#3-Ag(2)-O(3)#3	106.7(1)	
		O(3)#3-Ag(2)-O(4)	89.3(1)	

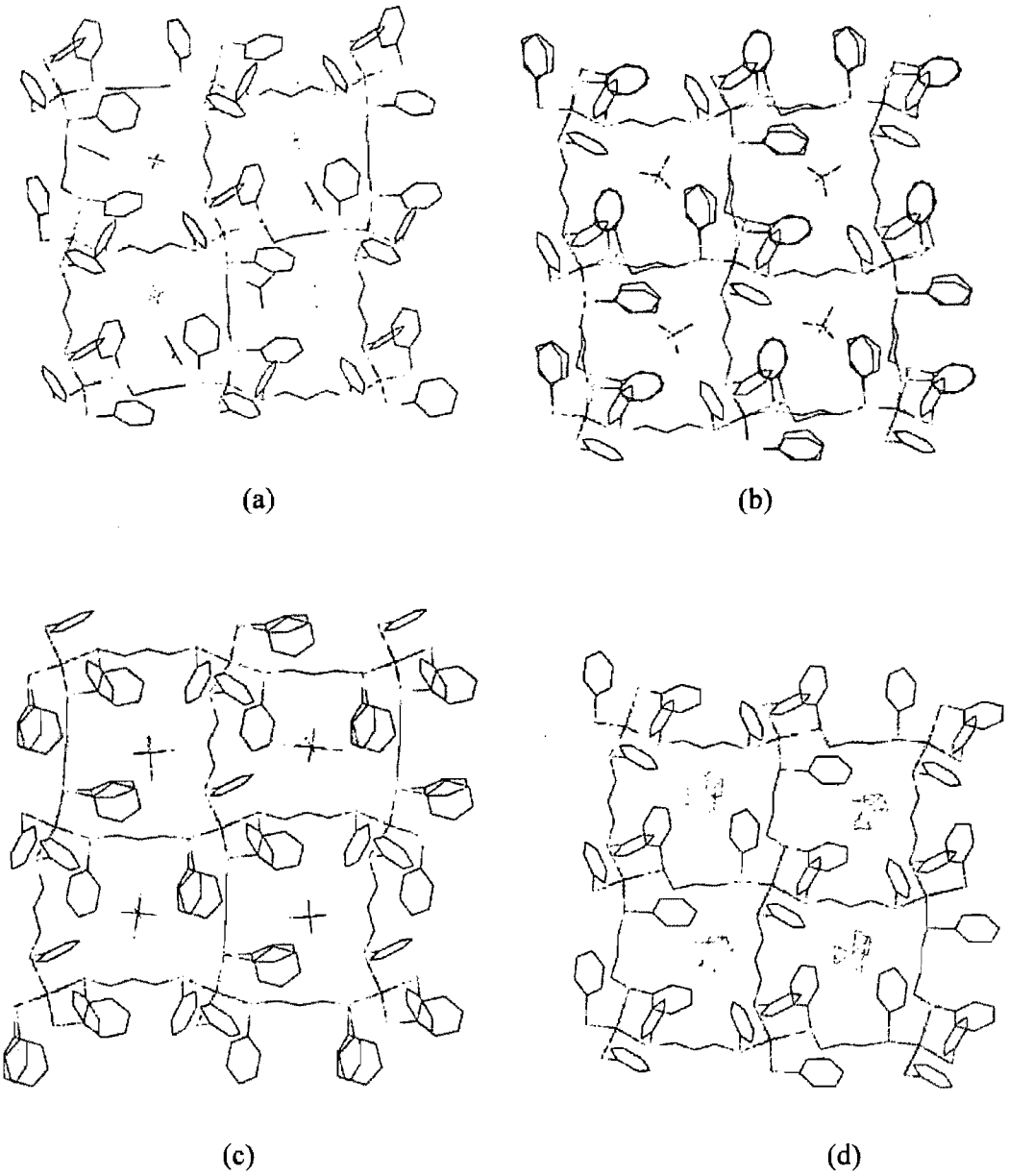

Figure S1. Comparison of the host guest structures with the cationic layers of $[Ag_2(\mathbf{L}^{3\text{-Ph}})_4]_\infty$, where the anions and the solvent molecules are inserted between layers. (a) PF_6^-, (b) ClO_4^-, (c) SbF_6^- and (d) BF_4^-. The cationic layers are parallel to the (001)-plane. In (b) and (c), the acetone molecules are too disordered to be shown. The structure with BF_4^- is taken from ref 18. The water molecules were not shown in the original publication.

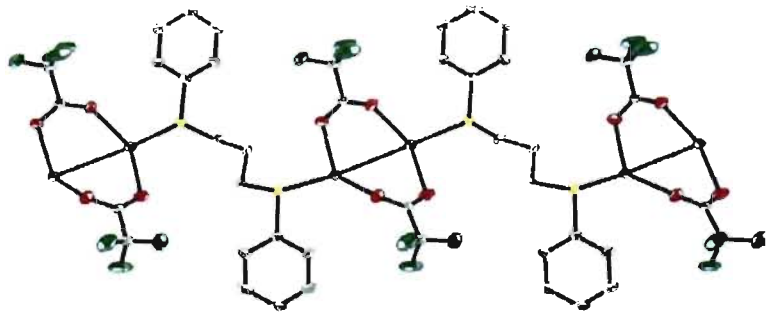

Figure S2. The dimers of **2** are linked through the ligand molecules and form a 1D-chain parallel to the *b*-axis. Each sulfur atoms is also bound to the silver ion of another chain thus generating a 2D-coordination network.

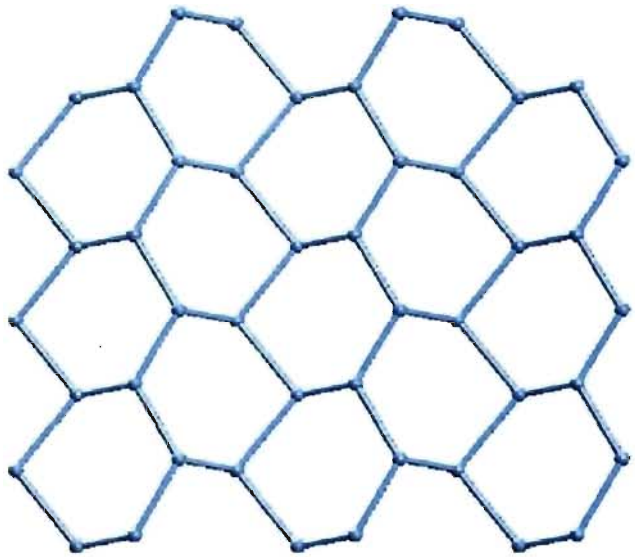

Figure S3. Topology of complex **2**. Ag-to-Ag connectivity showing the wavy honeycomb structure. The layers are parallel to (100)-plane.

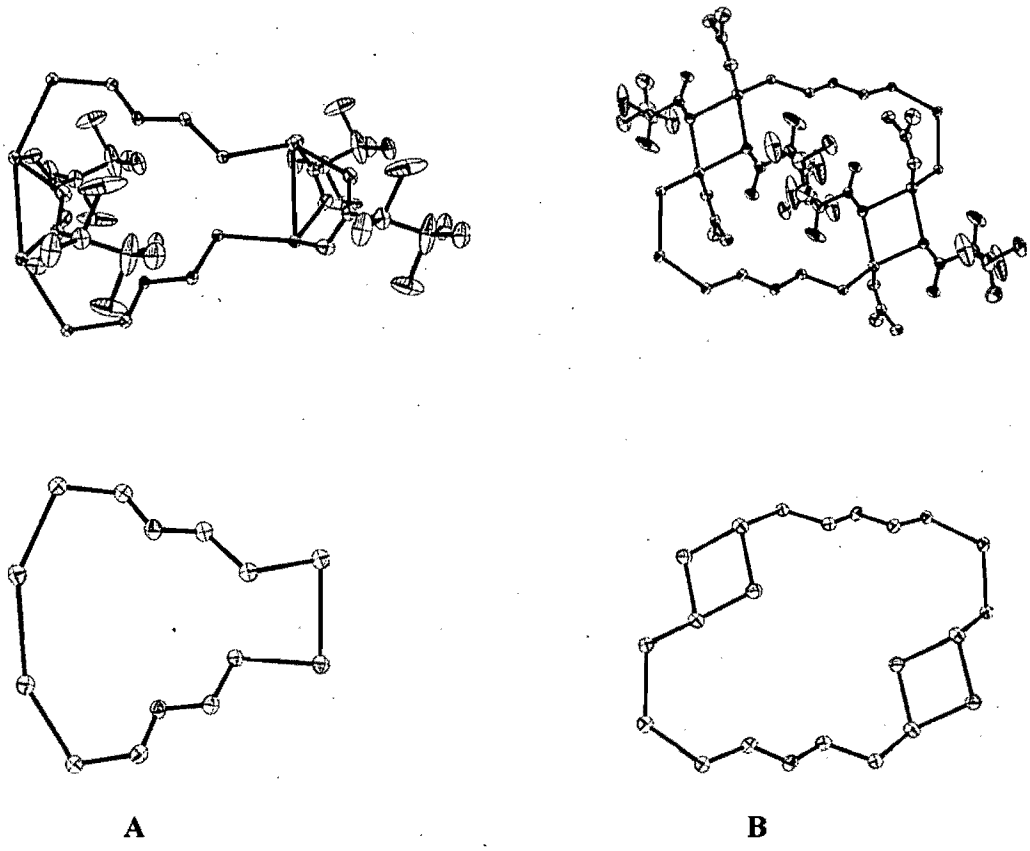

A B

Figure S4. The two units (**A** and **B**) in complex **3**. Above, the anions and acetone are included. Below, they were omitted for clarity.

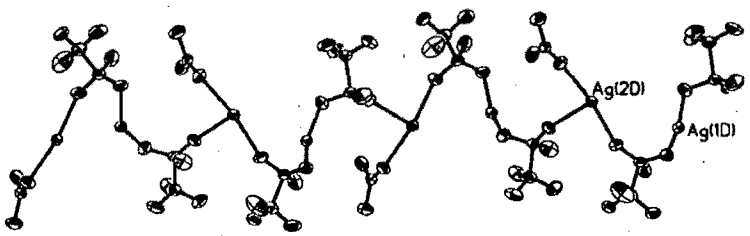

Figure S5. The trifluoromethanesulfonate 1D-chain along the [202]-direction of complex **7**. An acetone molecule is coordinated to every second silver ion, i.e., on Ag(2).

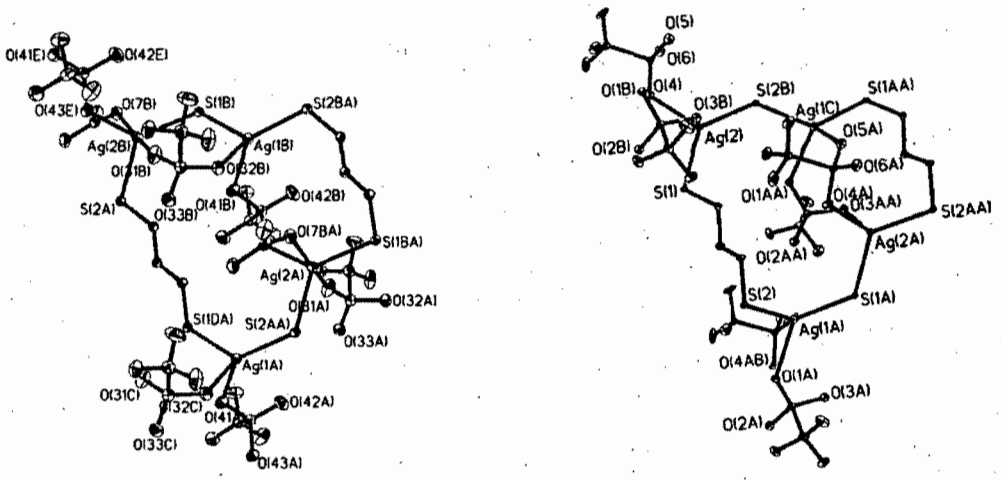

(a) (b)

Figure S6. Comparison of the structural units in **7** (a) and **9** (b). The main $Ag_4(\mathbf{L}^{3\text{-Ph}})_2S_2$ rings are identical, while the anions bridge the silver ions in different ways.

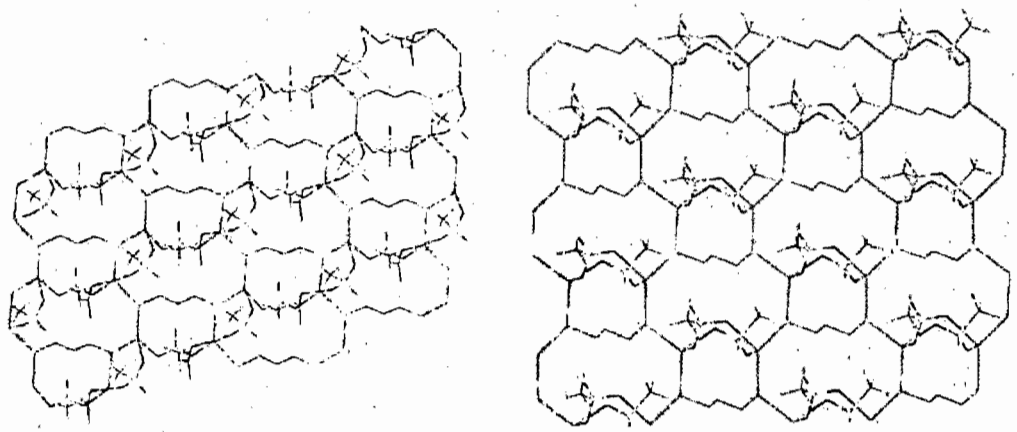

(a) (b)

Figure S7. Comparison of the 2D-networks in (a) complex **7** and (b) complex **9**. The sheets are parallel to the *ac*-plane in both complexes.

Complex **7**

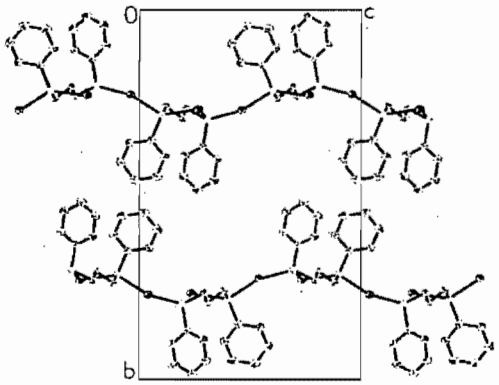

Complex **9**

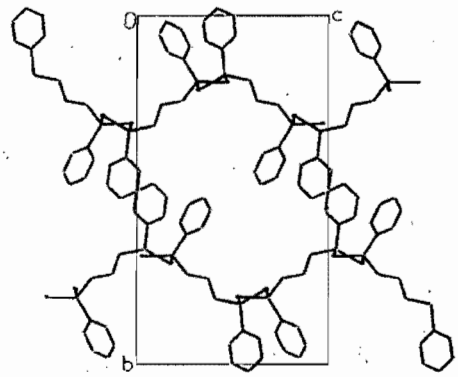

Complex **2**

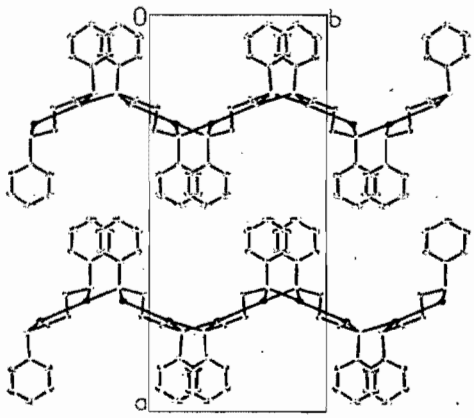

Figure S8. Packing of **2**, **7** and **9**.showing that the layers are not flat but undulated. The phenyl groups clearly stick away from the layers. (a) Packing diagram of **7** illustrating the "in-phase" relative disposition of the sheets. (b) Packing diagram of **9** showing the "out-of-phase" disposition of consecutive sheets. (c) Another form of "in-phase" organization is found in **2**.

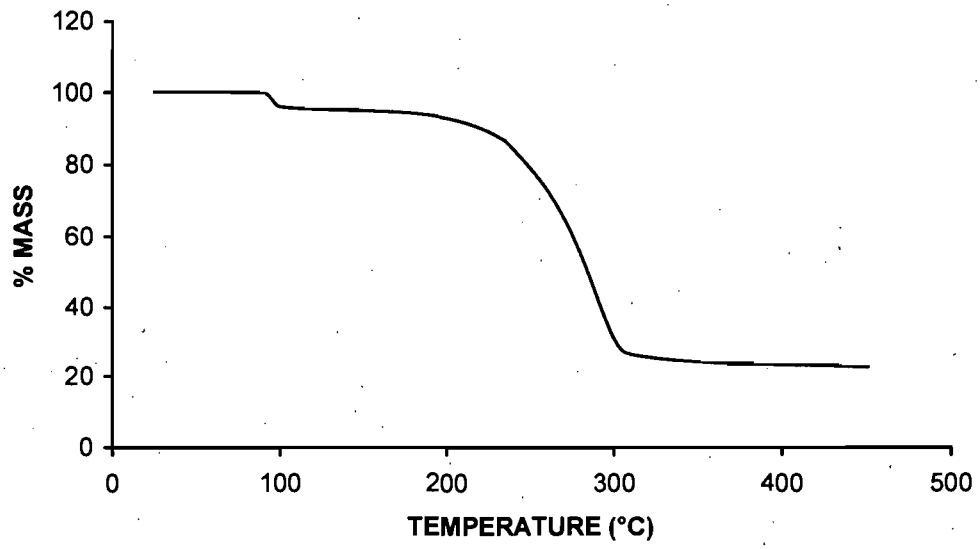

Figure S9. TGA of complex **10.** Recorded at a heating rate of 10 °C min^{-1}. A two-step decomposition. First step: loss of acetone between 95 and 110 °C. Second step: loss of the ligand between 180 and 310 °C.

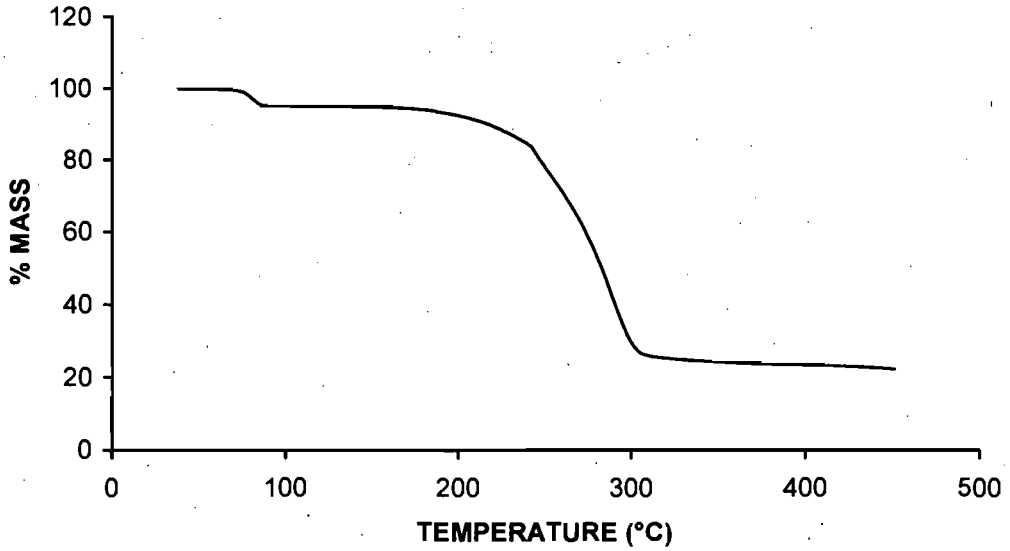

Figure S10. TGA of complex **11.** Recorded at a heating rate of 10 °C min^{-1}. First step: loss of acetone between 75 and 90 °C. Second step: loss of the ligand, between 160 and 310 °C.

Annexe III

Table S1. Comparison of the bond distances (Å) and angles (°) for the silver atoms in the complexes synthesized.

(1) $L^{1\text{-}Me}$ / NO_3

Ag(1)-S(4)	2.5245(17)	S(4)-Ag(1)-S(3)	118.1(1)
Ag(1)-S(3)	2.5418(18)	S(4)-Ag(1)-S(2)	127.7(1)
Ag(1)-S(2)	2.5518(17)	S(3)-Ag(1)-S(2)	114.1(1)
Ag(1)-O(4)	2.571(5)	S(4)-Ag(1)-O(4)	95.0 (1)
Ag(2)-O(1)	2.377(5)	S(3)-Ag(1)-O(4)	91.5(1)
Ag(2)-S(2)	2.5315(17)	S(2)-Ag(1)-O(4)	87.3(1)
Ag(2)-S(1)	2.5496(17)	O(1)-Ag(2)-S(2)	125.8(1)
Ag(2)-S(4)#1	2.6205(18)	O(1)-Ag(2)-S(1)	98.8(1)
		S(2)-Ag(2)-S(1)	114.1(1)
		O(1)-Ag(2)-S(4)#1	93.9(1)
		S(2)-Ag(2)-S(4)#1	104.9(1)
		S(1)-Ag(2)-S(4)#1	119.1(1)

#1 x-1/2,-y+3/2,-z+2

(2) $L^{1\text{-}Me}$ / ClO_4

Ag(2)-S(4)	2.5025(16)	S(4)-Ag(2)-S(3)	126.3(1)
Ag(2)-S(3)	2.5283(17)	S(4)-Ag(2)-S(2)	124.8(1)
Ag(2)-S(2)	2.5574(14)	S(3)-Ag(2)-S(2)	107.9(1)
Ag(2)-O(8)	2.619(5)	S(4)-Ag(2)-O(8)	95.9(1)
Ag(1)-O(4)	2.461(5)	S(3)-Ag(2)-O(8)	97.4(1)
Ag(1)-S(2)	2.5453(15)	S(2)-Ag(2)-O(8)	86.3(1)
Ag(1)-S(1)	2.5458(17)	O(4)-Ag(1)-S(2)	110.2(1)
Ag(1)-S(4)#1	2.5805(17)	O(4)-Ag(1)-S(1)	99.7(1)
		O(4)-Ag(1)-S(4)#1	92.9(2)
		S(2)-Ag(1)-S(4)#1	113.3(1)
		S(1)-Ag(1)-S(4)#1	127.1(1)
		S(1)-Ag(1)-S(2)	109.9(1)

#1 -x+1,-y+1,z+1/2

(3) $L^{1\text{-}Me}$ / ClO_4

Ag(2)-S(2)	2.527(1)	S(2)-Ag(2)-S(3)#1	121.7(1)
Ag(2)-S(3)#1	2.538(1)	S(2)-Ag(2)-S(3)	113.6(1)
Ag(2)-S(3)	2.570(1)	S(3)#1-Ag(2)-S(3)	121.2(1)
Ag(1)-S(1)	2.498(1)	S(1)-Ag(1)-S(4)#2	126.5(1)
Ag(1)-S(4)#2	2.557(1)	S(1)-Ag(1)-O(1)	119.0(1)
Ag(1)-O(1)	2.574(4)	S(4)#2-Ag(1)-O(1)	93.2(1)
Ag(1)-S(2)	2.667(1)	S(1)-Ag(1)-S(2)	121.3(1)
Ag(2)-O(5)	2.633(4)	S(4)#2-Ag(1)-S(2)	104.9(1)

O(1)-Ag(1)-S(2)	79.7(1)
S(3)-Ag(2)-O(5)	91.4(1)
S(2)#2-Ag(2)-O(5)	111.0(1)
S(3)#1-Ag(2)-O(5)	86.3(1)

#1 x,-y+1/2,z+1/2; #2 x,-y+1/2,z-1/2

(4) $L^{1\text{-}Me}$ / *p*-TsO

Ag(1)-O(1)	2.343(2)	O(1)-Ag(1)-S(2)#1	109.8(1)
Ag(1)-S(2)#1	2.5332(7)	O(1)-Ag(1)-S(2)	108.7(1)
Ag(1)-S(2)	2.5431(7)	S(2)#1-Ag(1)-S(2)	123.6(1)
Ag(1)-S(1)	2.5830(7)	O(1)-Ag(1)-S(1)	102.7(1)
		S(2)#1-Ag(1)-S(1)	108.5(1)
		S(2)-Ag(1)-S(1)	101.3(1)

#1 -x+1/2,y+1/2,z

(5) $L^{1\text{-}Me}$ / CF_3CO_2

Ag(1)-O(1)	2.305(6)	O(1)-Ag(1)-S(2)	109.3(2)
Ag(1)-S(2)	2.539(3)	O(1)-Ag(1)-S(1)	100.6(2)
Ag(1)-S(1)	2.577(2)	S(2)-Ag(1)-S(1)	105.7(1)
Ag(1)-S(2)#1	2.584(3)	O(1)-Ag(1)-S(2)#1	107.3(2)
		S(2)-Ag(1)-S(2)#1	124.1(1)
		S(1)-Ag(1)-S(2)#1	107.4(1)

#1 -x+1/2,y,z+1/2

(6) $L^{1\text{-}Me}$ / $CF_3CF_2CF_2CO_2$

Ag(1)-O(1)	2.306(4)	O(1)-Ag(1)-S(2)	108.6(1)
Ag(1)-S(1)	2.5940(12)	S(2)-Ag(1)-S(1)	102.1(1)
Ag(1)-S(2)#2	2.6006(16)	O(1)-Ag(1)-S(2)#2	107.3(1)
Ag(1)-S(2)	2.567(2)	S(2)-Ag(1)-S(2)#2	123.8(1)
		S(1)-Ag(1)-S(2)#2	105.9(1)

#2 -x+1/2,y,z+1/2

(7) $L^{1\text{-}Me}$ / CF_3SO_3

Ag(1)-O(1)	2.487(2)	O(1)-Ag(1)-S(3)	101.04(6)
Ag(1)-S(3)	2.5634(7)	O(1)-Ag(1)-S(2)	101.32(6)
Ag(1)-S(2)	2.5672(7)	S(3)-Ag(1)-S(2)	130.58(2)
Ag(1)-S(4)#1	2.5704(7)	O(1)-Ag(1)-S(4)#1	97.23(6)
Ag(2)-O(4)	2.473(2)	S(3)-Ag(1)-S(4)#1	114.88(2)
Ag(2)-S(2)	2.5686(7)	S(2)-Ag(1)-S(4)#1	105.22(2)
Ag(2)-S(6)	2.5778(7)	O(4)-Ag(2)-S(2)	103.67(5)
Ag(2)-S(3)#2	2.5803(7)	O(4)-Ag(2)-S(6)	96.69(5)
		S(2)-Ag(2)-S(6)	117.01(2)
		O(4)-Ag(2)-S(3)#2	96.13(5)

S(2)-Ag(2)-S(3)#2	128.62(2)
S(6)-Ag(2)-S(3)#2	106.85(2)

#1 x,-y+3/2,z-1/2; #2 x+1,y,z

(8) $L^{1\text{-}Me}$ / $C_6H_5CO_2$

Ag(1)-O(1)	2.267(2)	O(1)-Ag(1)-O(2)#1	128.4(1)
Ag(1)-O(2)#1	2.413(2)	O(1)-Ag(1)-S(2)#2	113.8(1)
Ag(1)-S(2)#2	2.5634(7)	O(2)#1-Ag(10-S(2)#2	91.6(1)
Ag(1)-S(1)	2.6288(7)	O(1)-Ag(1)-S(1)	119.3(1)
Ag(1)-Ag(1)#1	2.9114(4)	O(2)#1-Ag(1)-S(1)	99.9(1)
		S(2)#2-Ag(1)-S(1)	96.5(1)
		O(1)-Ag(1)-Ag(1)#1	75.7(1)
		O(2)#1-Ag(1)-Ag(1)#1	71.9(1)
		S(2)#2-Ag(1)-Ag(1)#1	163.1(1)
		S(1)-Ag(1)-Ag(1)#1	90.1(1)

#1 -x+1,-y+1,-z+1; #2 x-1,y,z

(9) $L^{1\text{-}Me}$ / CH_3SO_3

Ag(1)-O(1)	2.440(3)	O(1)-Ag(1)-O(3)#1	104.8(1)
Ag(1)-O(3)#1	2.461(3)	O(1)-Ag(1)-S(1)	101.9(1)
Ag(1)-S(1)	2.4891(8)	O(3)#1-Ag(1)-S(1)	115.1(1)
Ag(1)-S(2)	2.5193(8)	O(1)-Ag(1)-S(2)	96.8(1)
Ag(1)-Ag(1)#2	3.2430(5)	O(3)#1-Ag(1)-S(2)	95.4(1)
		S(1)-Ag(1)-S(2)	138.4(1)
		O(1)-Ag(1)-Ag(1)#2	169.6(1)
		O(3)#1-Ag(1)-Ag(1)#2	71.1(1)
		S(1)-Ag(1)-Ag(1)#2	88.8(1)
		S(2)-Ag(1)-Ag(1)#2	74.4(1)

#1 -x+1,-y+1,-z; #2 -x+1,-y,-z

(10) $L^{1\text{-}Me}$ / $OOCCF_2CF_2COOH$

Ag-S(1)	2.4788(8)	S(1)-Ag-S(2)#1	169.3(1)
Ag-S(2)#1	2.4790(8)	S(1)-Ag-O(3)	92.6(1)
Ag-O(3)	2.627(2)	S(2)#1-Ag-O(3)	97.7(1)
Ag-Ag#1	3.0672(5)	S(1)-Ag-Ag#1	86.8(1)
Ag-O(2)#2	2.859(8)	S(2)#1-Ag-Ag#1	91.4(1)
Ag-O(4)#1	2.786(8)	O(3)#1-Ag-Ag#1	82.5(1)
		O(2)#2-Ag-O(3)#2	69.8(1)
		O(4)-Ag-O(2)#2	128.0(1)
		O(4)-Ag-Ag#1	79.6(1)

#1 -x, -y, 2-z; #2 1-x, -y, 2-z

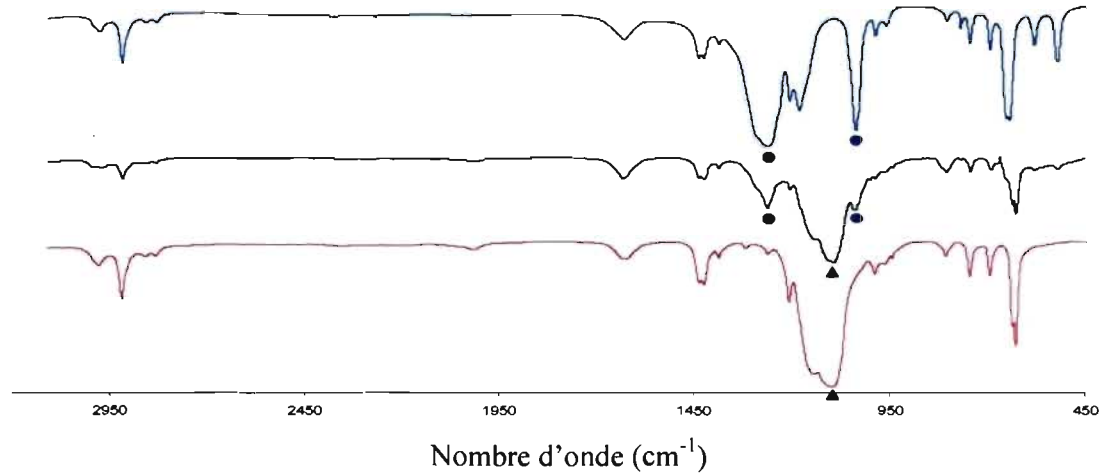

Figure S1. Evolution of the IR spectra (KBr pellet) during the anion-exchange procedure between $[Ag_2(L^{1\text{-}Me})_2(ClO_4)_2]_\infty$ and an aqueous solution of CF_3SO_3Na.
(a) The red spectrum is that of complex **2**, $[Ag_2(L^{1\text{-}Me})_2(ClO_4)_2]_\infty$. The characteristic band of $ClO4^-$ is $\nu_1(A_1)$ at 1092 cm^{-1} (▲).
(b) The black IR spectrum is that of complex **2** treated with an aqueous solution of CF_3SO_3Na for 2 hours. It shows the gradual disappearance of the perchlorate characteristic band and the growth of the trifluoromethanesulfonate characteristic bands $\nu[SO_3(E)]$ at 1270 cm^{-1} (●) and $\nu[SO_3(A_1)]$ at 1030 cm^{-1} (●).
(c) The blue spectrum indicates the complete disappearance of the perchlorate, after 4 hours, and corresponds to the IR of complex **8**, $[Ag_2(L^{1\text{-}Me})_2(CF_3SO_3)_2]_\infty$.

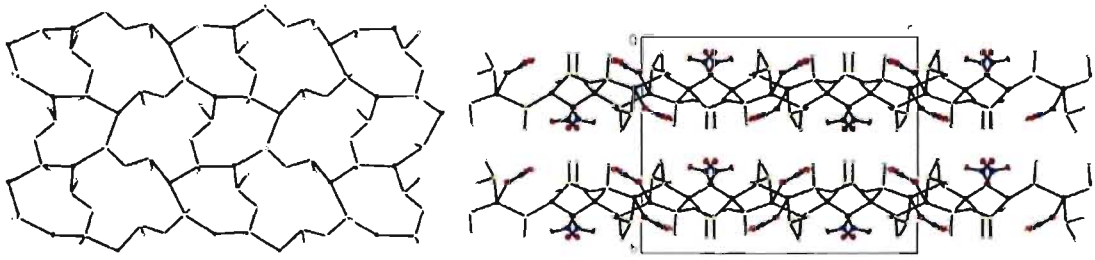

(a) (b)

Figure S2. (a) Neutral layers of **1** parallel to *ac*-plane. The nitrate anions and the hydrogen atoms are omitted for clarity. (b) View-down the *a*-axis of complex **1**. The nitrates are coordinated to the silver atom in monoatomic mode and are located between the sheets.

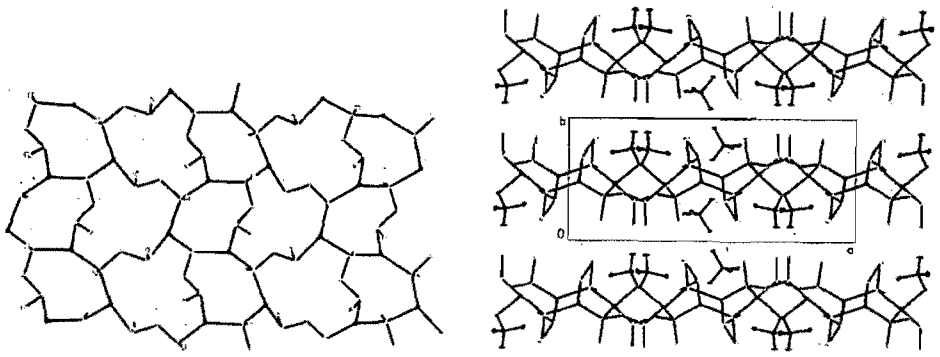

(a) (b)

Figure S3. (a) Neutral sheet of **2** shown projected along the *b*-axis. (The perchlorate anions and the hydrogen atoms are omitted for clarity). (b) The *ab*-plane projection of complex **2**. The perchlorates, coordinated to the silver atom in the monoatomic mode, are located between the sheets.

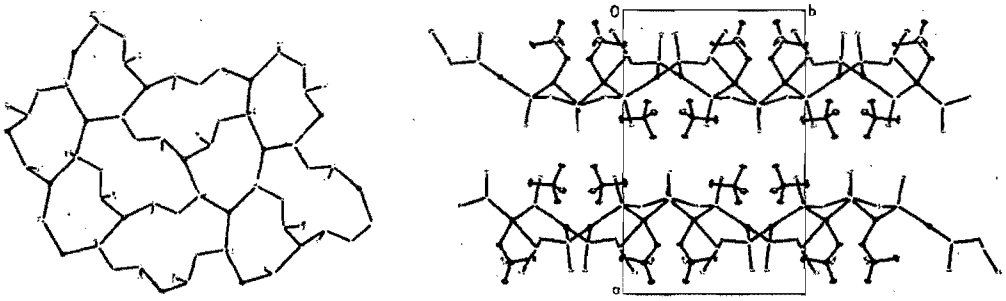

Figure S4. Complex **3**, the second form of the perchlorate complex, has a topology comparable to those of **1** and **2**.

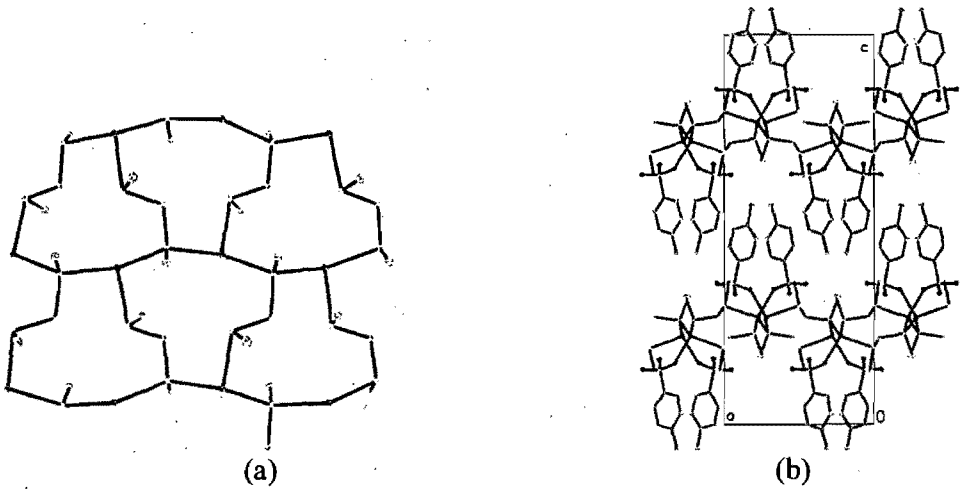

(a) (b)

Figure S5. (a) Neutral layer of **4** parallel to the *ab*-plane. The anions and the hydrogen atoms are omitted for clarity. (b) Packing of **4**. The paratoluenesulfonate anions are located between the neutral sheets and there is no π-π stacking between the phenyl groups of the anions.

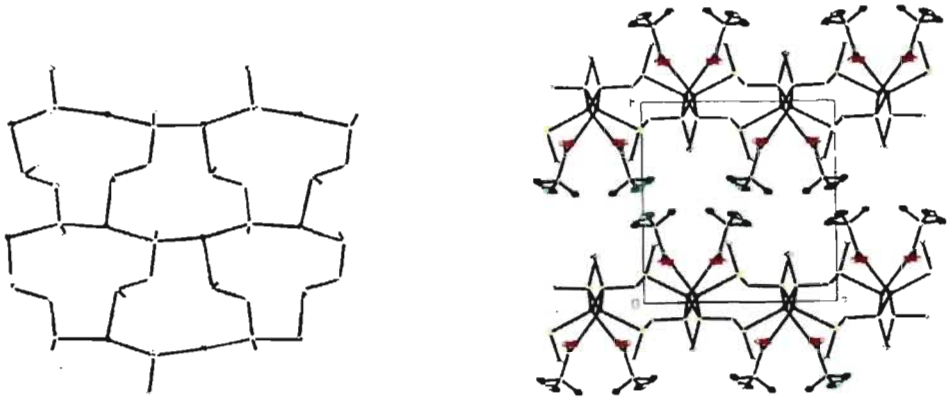

(a) (b)

Figure S6. (a) Neutral layer of **5** parallel to *ac*-plane. The anions and the hydrogen atoms are omitted for clarity. (b) Packing of **5**. The trifluoroacetate anions are located between the neutral sheets.

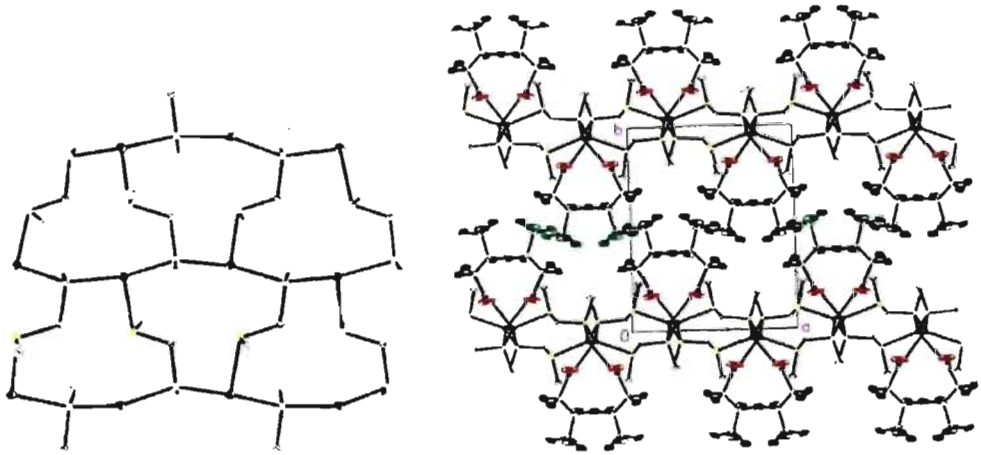

(a) (b)

Figure S7. (a) Neutral layer of **6** parallel to *ac*-plane. The anions and the hydrogen atoms are omitted for clarity. (b) Packing of **6**. The heptafluorobutyrate anions are located between the neutral sheets.

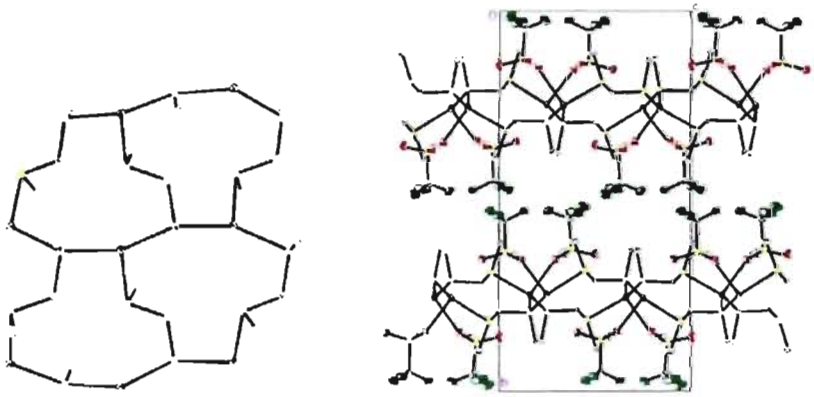

Figure S8. Layer and side view of complex **7**, with CF_3SO_3.

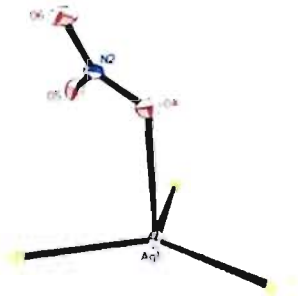

(a)

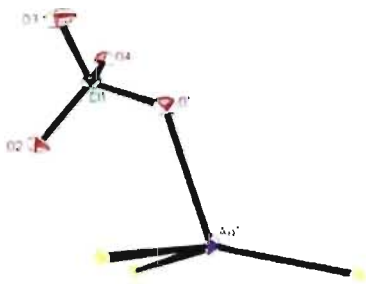

(b)

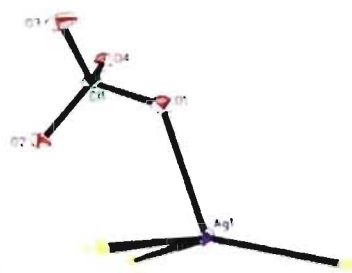

(c)

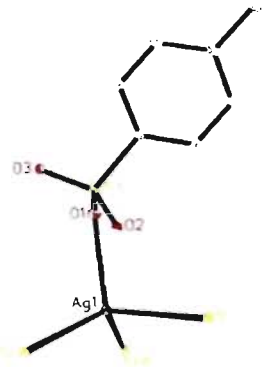
O3
O1
O2
Ag1

(d)

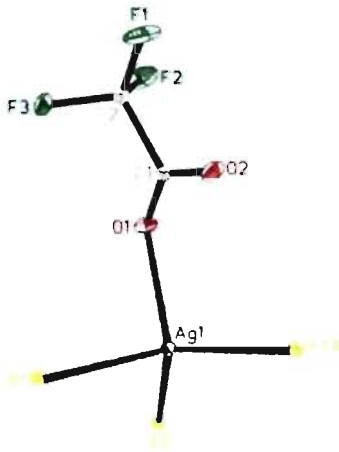
F1
F2
F3
O2
O1
Ag1

(e)

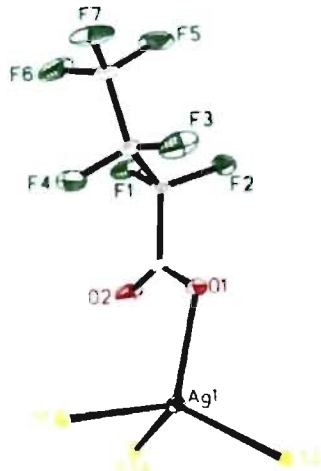
F7
F5
F6
F3
F4
F1
F2
O2
O1
Ag1

(f)

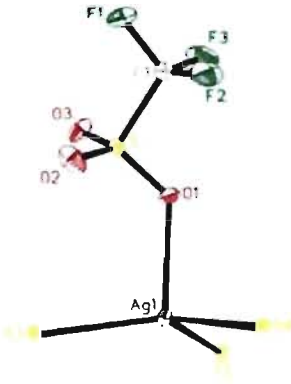
F1
F3
F2
O3
O2
O1
Ag1

(g)

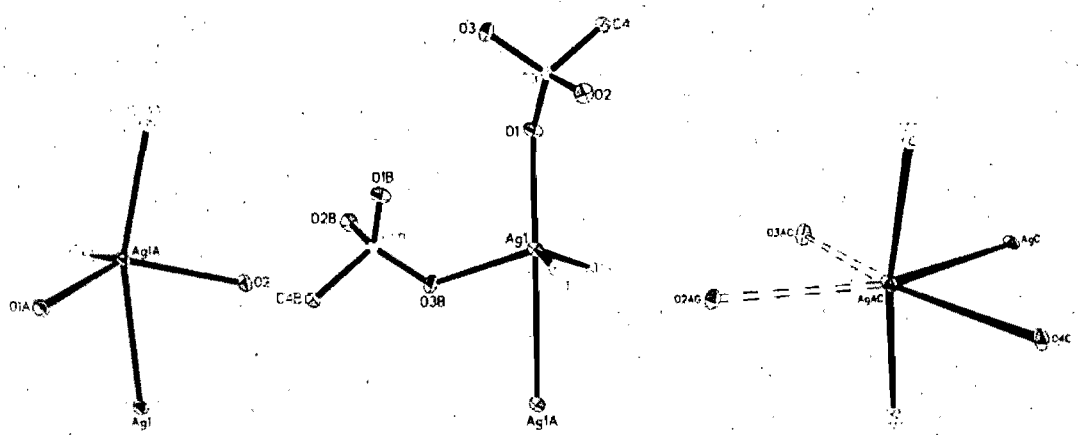

(h) (i) (j)

Figure S9. Coordination of Ag(I) in complexes **1-10**: (a) Complex **1**; (b) Complex **2**; (c) Complex **3**; (d) Complex **4**; (e) Complex **5**; (f) Complex **6**; (f) Complex **7**; (h) Complex **8**; (i) Complex **9**. (j) Complex **10**.

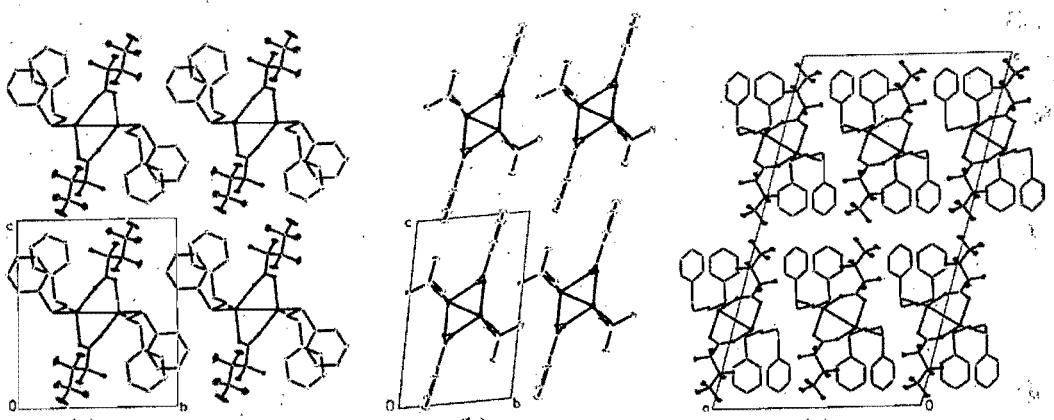

(a) (b) (c)

Figure S10. (a) Projection down the *a*-axis of the packing of the double-stranded 1D-coordination polymer obtained by self-assembly of $L^{1\text{-Ph}}$ and hepatfluorobutyrate.[a] (b) Projection down the *a*-axis showing the packing of the double-stranded 1D-coordination polymer **8**. (c) The double-stranded 1D-coordination polymer obtained by self-assembly of $L^{3\text{-Ph}}$ and hepatfluorobutyrate shown perpendicular to the *ac*-plane.[b]

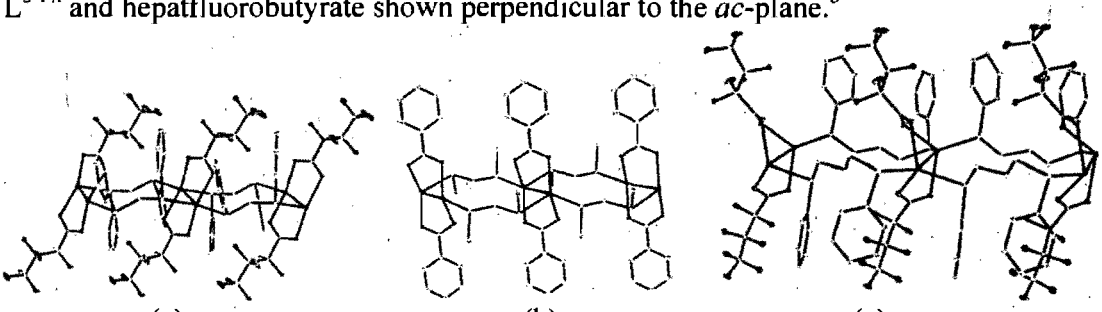

(a) (b) (c)

Figure S11. (a) The double-stranded 1D-coordination polymer obtained by self-assembly of $L^{1\text{-Ph}}$ and hepatfluorobutyrate.[a] (b) The 1D-coordination polymer **8**. (c) The double-stranded 1D-coordination polymer obtained by self-assembly of $L^{3\text{-Ph}}$ and hepatfluorobutyrate.[b]

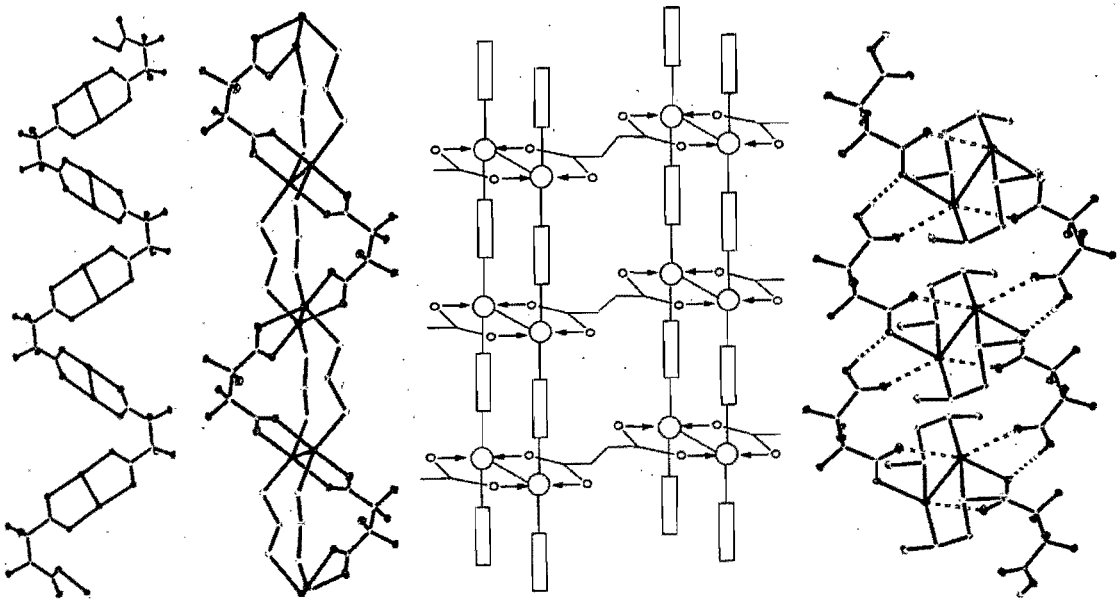

Figure S12. (a) The 1D-coordination polymer $[L^{1\text{-}Ph}\text{-}OOCCF_2CF_2COO]$[a] showing the anions bridging consecutive dimers, thereby yielding the polymeric chain. (b) The same chain now including the ligands which reinforce the structure through Ag-S bonds. (c) Expected extension of $L^{1\text{-}Me}\text{-}OOCCF_2CF_2COO$ into a 2D-network.
(d) $[L^{1\text{-}Me}\text{-}OOCCF_2CF_2COOH]$ which forms a 1D-coordination polymer through hydrogen-bond interactions.

[a]Awaleh, M. O; Badia, A.; Brisse, F. *Cryst. Growth and Design* **2005**, *5,* 1897.
[b]Awaleh, M. O; Badia, A.; Brisse, F. *Inorg. Chem.* **2005**, *44*, 7833.

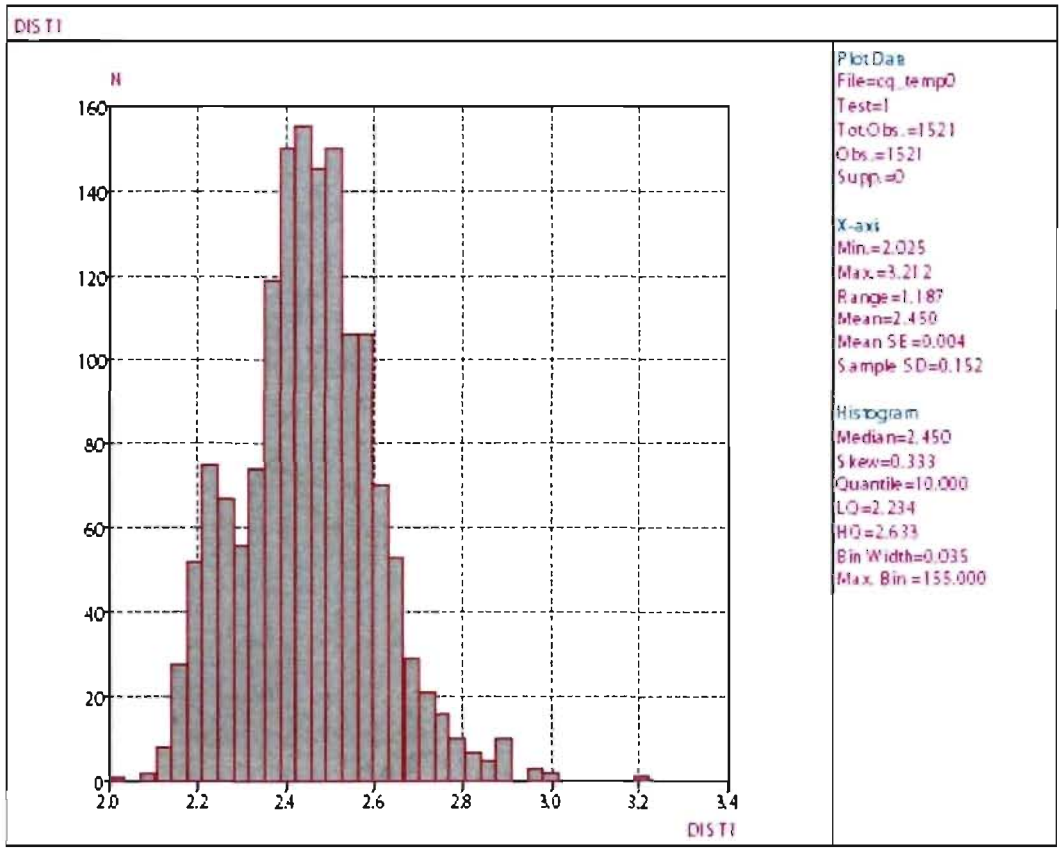

Coordination number: 4
Ag-O, 711 hits, 1521 distances taken into account

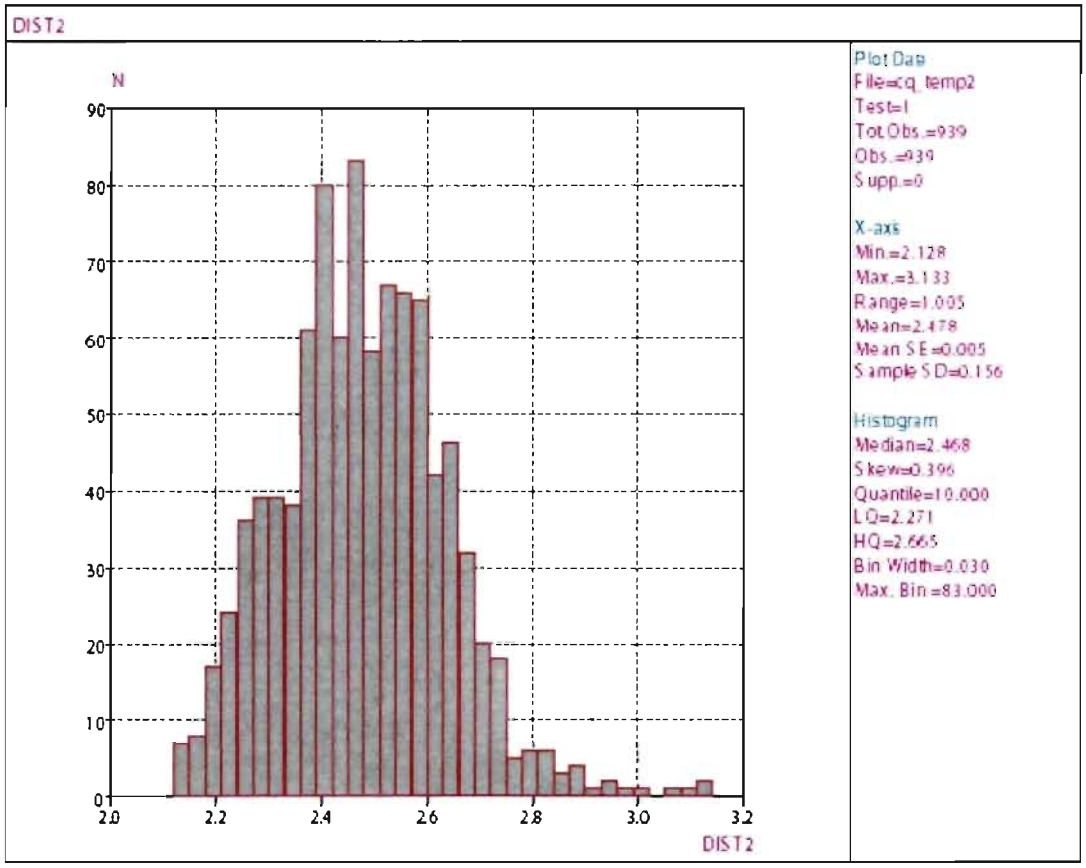

Coordination number: 5
Ag-O, 342 hits, 932 distances taken into account

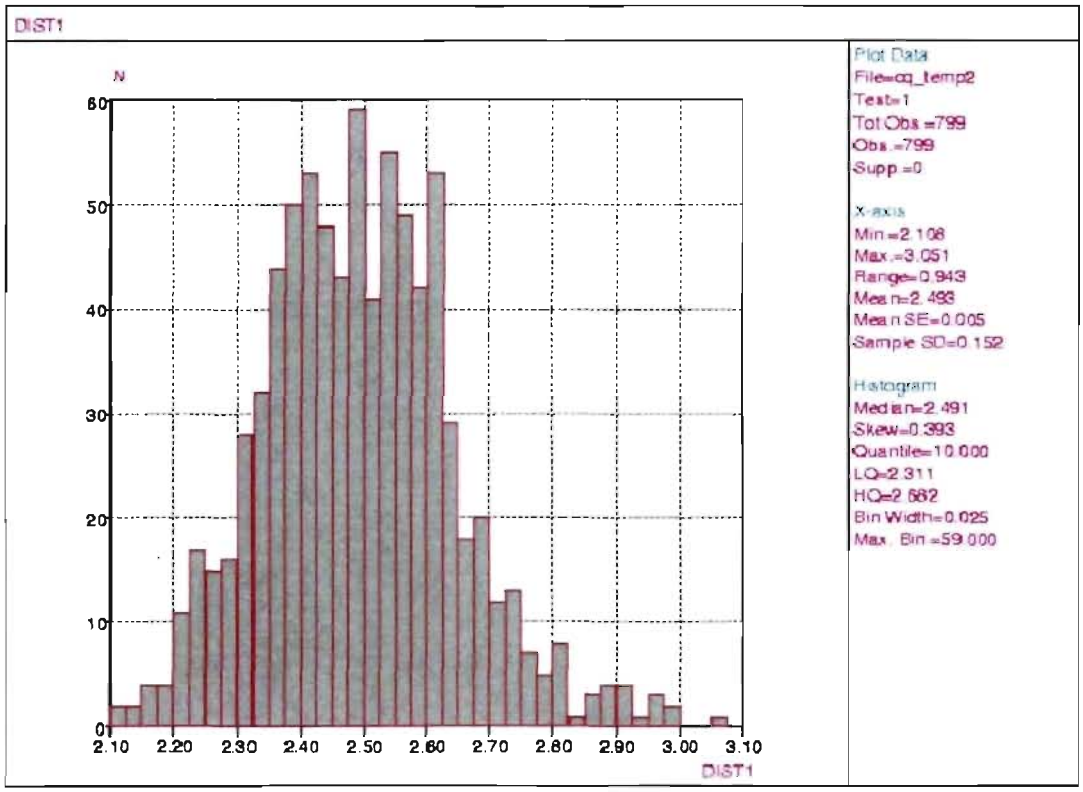

Coordination number : 6.
Ag-O, 226 hits, 785 distances taken into account.

Figure S13. Distribution of the Ag-O distances in the three main coordinations: 4, 5 and 6.

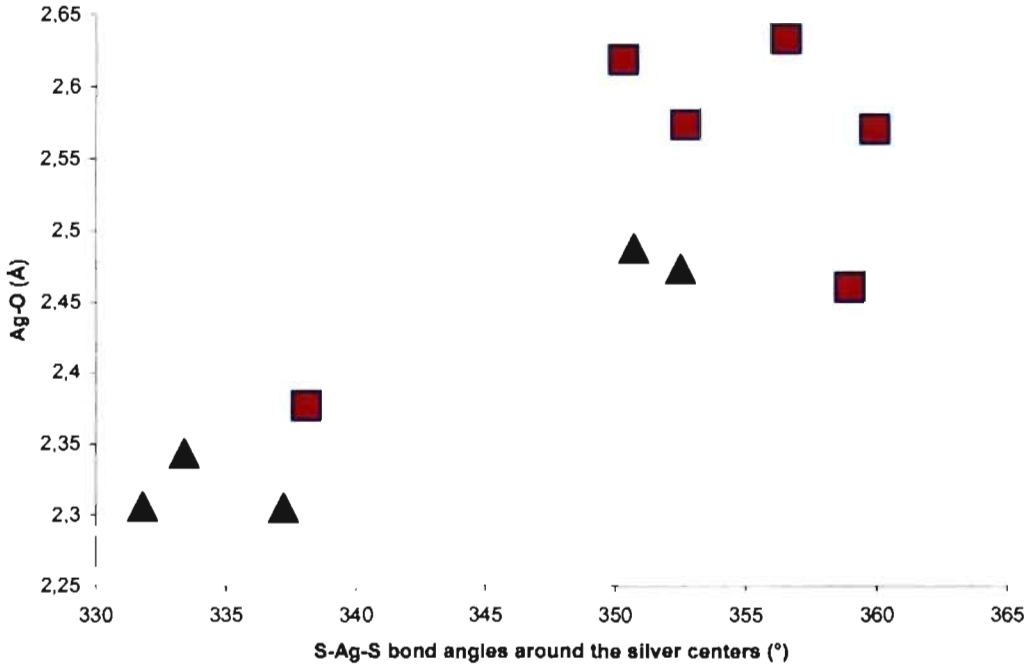

Figure S14. Plot of the sum of the S-Ag-S bond angles around the silver centers as a function of the Ag-O distance. Group 1(■) and group 2 (▲).

Annexe IV

Tableau S1. Les longueurs de liaison (Å) et angles (°) des complexes **1-4**.

(1) $L^{1\text{-}Me}$ / CF_3SO_3

Ag(1)-S(5)	2.532(1)	S(5)-AG1-S(4)	123.41(4)
Ag(1)-S(4)	2.562(1)	S(5)-AG1-S(10)	106.65(4)
Ag(1)-S(10)	2.622(1)	S(4)-AG1-S(10)	112.69(4)
Ag(1)-S(7)	2.660(1)	S(5)-AG1-S(7)	110.45(4)
Ag(2)-S(11)	2.526(1)	S(4)-AG1-S(7)	96.56(4)
Ag(2)-S(13)	2.531(1)	S(10)-AG1-S(7)	105.46(4)
Ag(2)-S(8)	2.594(1)	S(11)-AG2-S(13)	127.02(4)
Ag(2)-S(2)	2.698(1)	S(11)-AG2-S(8)	104.58(4)
Ag(3)-S(12)	2.557(1)	S(13)-AG2-S(8)	116.76(4)
Ag(3)-S(6)	2.562(1)	S(11)-AG2-S(2)	106.76(4)
Ag(3)-S(9)	2.570(1)	S(13)-AG2-S(2)	94.16(4)
Ag(3)-S(3)	2.596(1)	S(8)-AG2-S(2)	104.20(4)
		S(12)-AG3-S(6)	113.75(4)
		S(12)-AG3-S(9)	121.73(4)
		S(6)-AG3-S(9)	104.47(4)
		S(12)-AG3-S(3)	100.87(4)
		S(6)-AG3-S(3)	112.72(4)
		S(9)-AG3-S(3)	102.88(4)

(2) $L^{1\text{-}Me}$ / PF_6

Ag(1)-S(1)	2.595(1)	S(1)-AG1-S(1)#1	115.67(5)
Ag(1)-S(1)#1	2.595(1)	S(1)-AG1-S(2)	102.92(4)
Ag(1)-S(2)	2.612(1)	S(1)#1-AG1-S(2)	108.30(4)
Ag(1)-S(2)#1	2.612(1)	S(1)-AG1-S(2)#1	108.30(4)
		S(1)#1-AG1-S(2)#1	102.92(4)
		S(2)-AG1-S(2)#1	119.35(6)

#1 -x,y,-z+3/2

(3) $L^{1\text{-}Me}$ / SbF_6

Ag(1)-S(1)#1	2.552(1)	S(1)#1-AG1-S(1)	122.38(5)
Ag(1)-S(1)	2.552(1)	S(1)#1-AG1-S(2)#1	108.81(3)
Ag(1)-S(2)#1	2.602(1)	S(1)-AG1-S(2)#1	102.68(3)
Ag(1)-S(2)	2.602(1)	S(1)#1-AG1-S(2)	102.68(3)
		S(1)-AG1-S(2)	108.81(3)
		S(2)#1-AG1-S(2)	111.58(5)

#1 -x,y,-z+1/2

(4) $L^{1\text{-}Me}$ / BF_4

Ag(1)-S(4a)	2.519(5)	S(4A)-AG1-S(4)	119.78(13)
Ag(1)-S(4)	2.528(2)	S(4A)-AG1-S(1)	120.97(14)
Ag(1)-S(1)	2.550(1)	S(4)-AG1-S(1)	118.85(6)
Ag(1)-S(2)	2.624(2)	S(4A)-AG1-S(2)	119.2(14)
Ag(1)-S(3)	2.633(1)	S(4)-AG1-S(2)	104.27(6)
		S(1)-AG1-S(2)	105.32(4)
		S(4A)-AG1-S(3)	99.05(12)
		S(4)-AG1-S(3)	116.84(5)
		S(1)-AG1-S(3)	106.18(5)
		S(2)-AG1-S(3)	103.69(5)

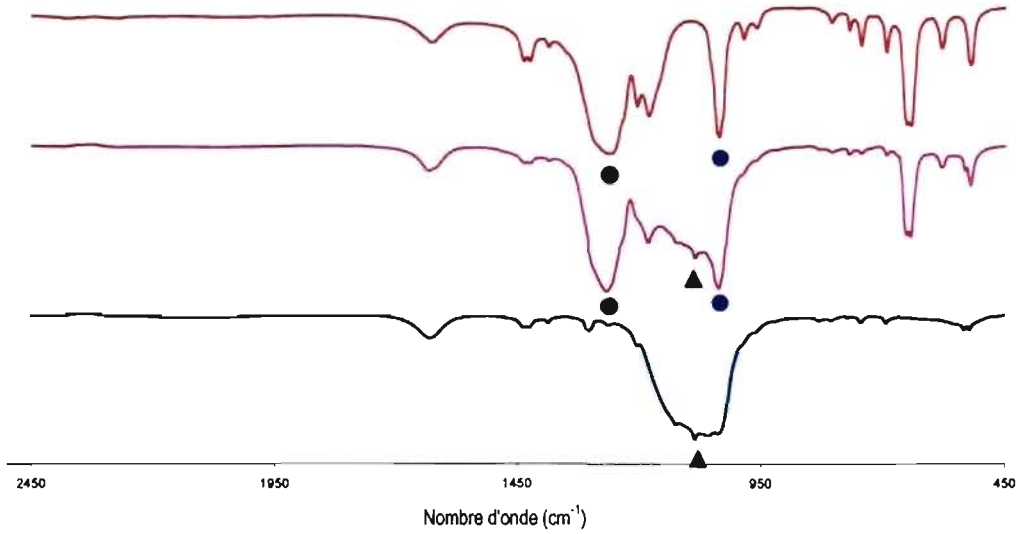

Figure S1. Evolution des spectres infrarouges durant l'échange des anions triflates du complexe **1**, $[Ag_3(L^{1\text{-}Me})_6(CF_3SO_3)_3]_\infty$, avec les anions tétrafluoroborates. Le spectre rouge est celui du complexe **1**, $[Ag_3(L^{1\text{-}Me})_6(CF_3SO_3)_3]_\infty$, comme préparé (Les bandes de vibrations caractéristiques du triflate sont $\nu[SO_3(E)]$: 1270 cm^{-1} (●), et $\nu[SO_3(A_1)]$: 1030 cm^{-1} (●)).[a,b] Le spectre en violet est celui du complexe **1** agité avec une solution aqueuse de $LiBF_4$ durant 40 min, montrant la décroissance de l'intensité des bandes caractéristique du triflate (● : 1270 cm^{-1}, $\nu[SO_3(E)]$, et ● :1030 cm^{-1}, $\nu[SO_3(A_1)]$) et l'augmentation de l'intensité de la bande caractéristique du perchlorate (▲ : 1078 cm^{-1}, $\nu_{as}(F_2)$).[c] Le spectre bleu est celui du produit résultant de l'échange après deux heures et correspond au compose $[Ag_3(L^{1\text{-}Me})_6(BF_4)_3]_\infty$.

[a]Lawrance, G. A. *Chem. Rev.* **1986**, *86*, 17.
[b]Batchelor, R. J.; Ruddick, J. N. R.; Sams, J. R.; Aubke, F. *Inorg. Chem.* **1977**, *16*, 1414 and references therein.
[c]Mikuli, E.; Gorska, N.; Wrobel, S.; Sciesinski, J.; Sciesinska, E. *J. Mol. Struct.* **2004**, *692*, 231.

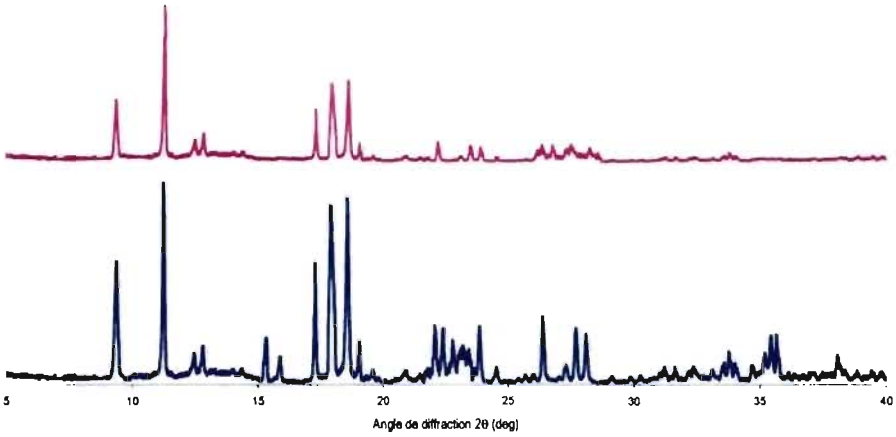

Figure S2. En bleu: Diagramme de poudre du complexe **1** comme synthétisé. En violet: Diagramme de poudre du produit résultant de l'échange **1** + $LiBF_4$.

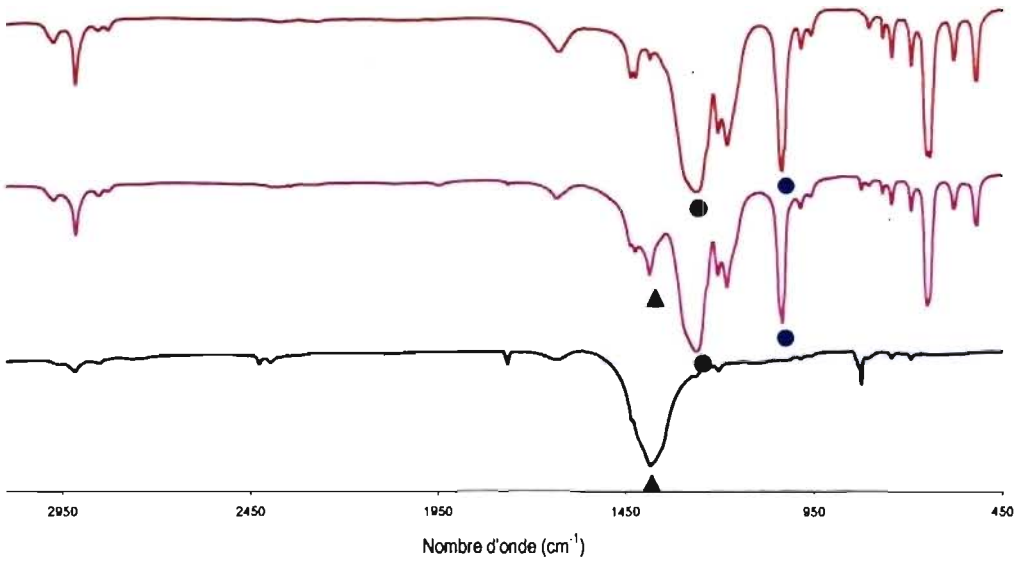

Figure S3. Evolution des spectres infrarouges durant l'échange des anions triflates du complexe **1**, $[Ag_3(L^{1\text{-}Me})_6(CF_3SO_3)_3]_\infty$, avec les anions nitrates. Le spectre rouge est celui du complexe **1**, $[Ag_3(L^{1\text{-}Me})_6(CF_3SO_3)_3]_\infty$, comme préparé (Les bandes de vibrations caractéristiques du triflate sont $\nu[SO_3(E)]$: 1270 cm^{-1} (●), et $\nu[SO_3(A_1)]$: 1030 cm^{-1} ●)).[a,b] Le spectre en violet est celui du complexe **1** agité avec une solution aqueuse de $NaNO_3$ durant 40 min, montrant la décroissance de l'intensité des bandes caractéristique du triflate (● : 1270 cm^{-1}, $\nu[SO_3(E)]$, et ● :1030 cm^{-1}, $\nu[SO_3(A_1)]$) et l'augmentation de l'intensité de la bande caractéristique du perchlorate (▲ : 1384 cm^{-1}, $\nu_3(E')$)).[d] Le spectre bleu est celui du produit résultant de l'échange après deux heures et correspond au compose $[Ag(L^{1\text{-}Me})_6(NO_3)_3]_\infty$.

[a]Lawrance, G. A. *Chem. Rev.* **1986**, *86*, 17.
[b]Batchelor, R. J.; Ruddick, J. N. R.; Sams, J. R.; Aubke, F. *Inorg. Chem.* **1977**, *16*, 1414 and references therein.
[d]Nakamoto, K. *Infrared Spectra of Inorganic and Coordination Compounds,* 3rd ed.; Wiley-VCH: New York, 1978.

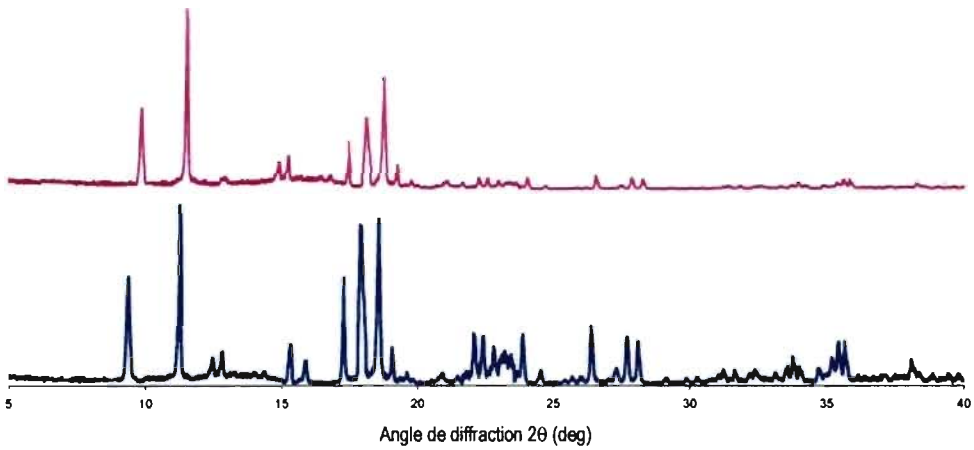

Figure S4. En bleu: Diagramme de poudre du complexe **1** comme synthétisé. En violet: Diagramme de poudre du produit résultant de l'échange **1** + $NaNO_3$.

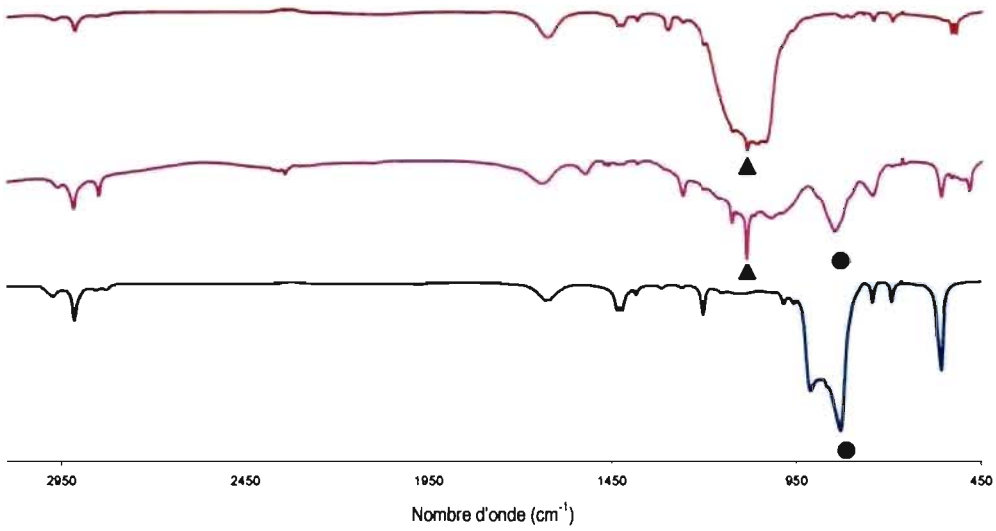

Figure S5. Evolution des spectres infrarouges durant l'échange des anions hexafluorophosphates du complexe **2**, $[Ag(L^{1\text{-}Me})_2(PF_6)]_\infty$, avec les anions tétrafluoroborates. Le spectre bleu est celui du complexe **2**, $[Ag(L^{1\text{-}Me})_2(PF_6)]_\infty$,comme préparé (Vibration caractéristique du l'hexafluorophosphate (● : 835 cm^{-1}, $\nu_3(T_{1u})$). [e-g] Le spectre en violet est celui du complexe **2**, agité dans une solution aqueuse de $LiClO_4$ durant 40 min, montrant la décroissance de l'intensité de la bande caractéristique de l'hexafluorophosphate (● : 835 cm^{-1}, $\nu_3(T_{1u})$) [e-g] et l'augmentation de l'intensité de la bande caractéristique du perchlorate (▲ : 1074 cm^{-1}, $\nu_{as}(F_2)$).[c] Le spectre rouge est celui du produit résultant de l'échange après deux heures et correspond au compose $[Ag(L^{1\text{-}Me})_2(BF_4)]_\infty$.

[c]Mikuli, E.; Gorska, N.; Wrobel, S.; Sciesinski, J.; Sciesinska, E. *J. Mol. Struct.* **2004**, *692*, 231.
[e]Matsumoto, K.; Hagiwara, R.; Ito, Y.; Tamada, O. *Solid State. Sci.* **2002**, *4*, 1465.
[f]Reger, D. L.; Semeniuc, R. F.; Rassolov, V.; Smith, M. D. *Inorg. Chem.* **2004**, *43*, 537.
[g]Jung, O. S.; Kim, Y. J.; Lee, Y. A.; Chae, H. K.; Jang, H. G.; Hong , J. *Inorg. Chem.* **2001**, *40*, 2105.

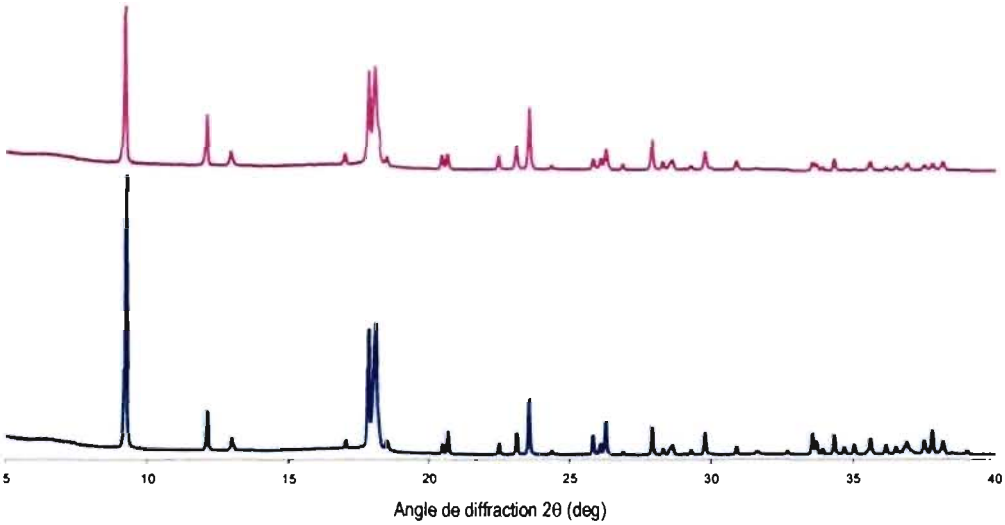

Figure S6. En bleu: Diagramme de poudre du complexe **2** comme synthétisé. En violet: Diagramme de poudre du produit résultant de l'échange **2** + $LiBF_4$.

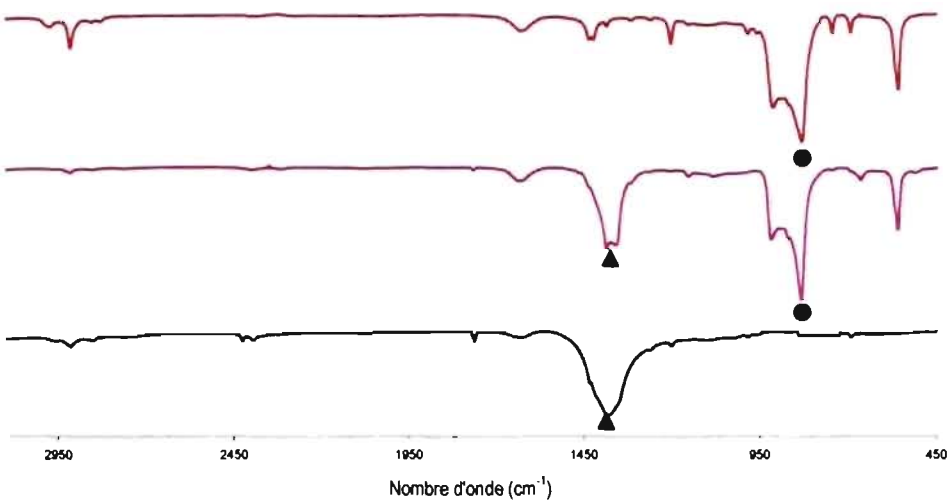

Figure S7. Evolution des spectres infrarouges durant l'échange des anions hexafluorophosphates du complexe **2**, $[Ag(L^{1\text{-}Me})_2(PF_6)]_\infty$, avec les anions nitrates.
Le spectre rouge est celui du complexe **2**, $[Ag(L^{1\text{-}Me})_2(PF_6)]_\infty$,comme préparé (Vibration caractéristique du l'hexafluorophosphate (● : 835 cm^{-1}, $\nu_3(T_{1u})$). [e-g] Le spectre en violet est celui du complexe **2**, agité dans une solution aqueuse de $NaNO_3$ durant 40 min, montrant la décroissance de l'intensité de la bande caractéristique de l'hexafluorophosphate (● : 835 cm^{-1}, $\nu_3(T_{1u})$) [e-g] et l'augmentation de l'intensité de la bande caractéristique du perchlorate (▲ : 1384 cm^{-1}, $\nu_3(E')$).[d] Le spectre bleu est celui du produit résultant de l'échange après deux heures et correspond au compose $[Ag(L^{1\text{-}Me})_2(NO_3)]_\infty$.

[d]Nakamoto, K. *Infrared Spectra of Inorganic and Coordination Compounds,* 3rd ed.; Wiley-VCH: New York, 1978.
[e]Matsumoto, K.; Hagiwara, R.; Ito, Y.; Tamada, O. *Solid State. Sci.* **2002**, *4*, 1465.
[f]Reger, D. L.; Semeniuc, R. F.; Rassolov, V.; Smith, M. D. *Inorg. Chem.* **2004**, *43*, 537.
[g]Jung, O. S.; Kim, Y. J.; Lee, Y. A.; Chae, H. K.; Jang, H. G.; Hong , J. *Inorg. Chem.* **2001**, *40*, 2105.

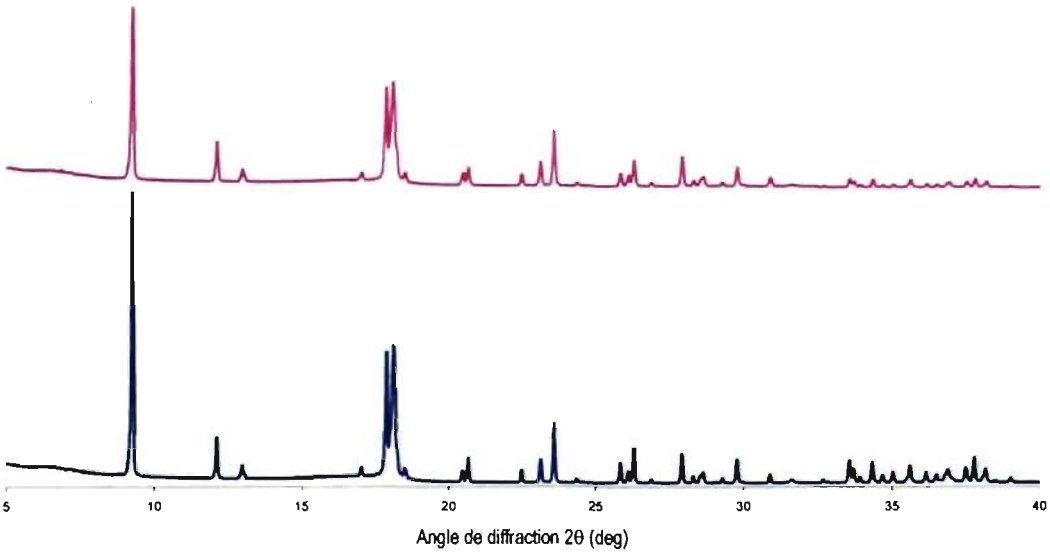

Figure S8. En bleu: Diagramme de poudre du complexe **2** comme synthétisé. En violet: Diagramme de poudre du produit résultant de l'échange **2** + $NaNO_3$.

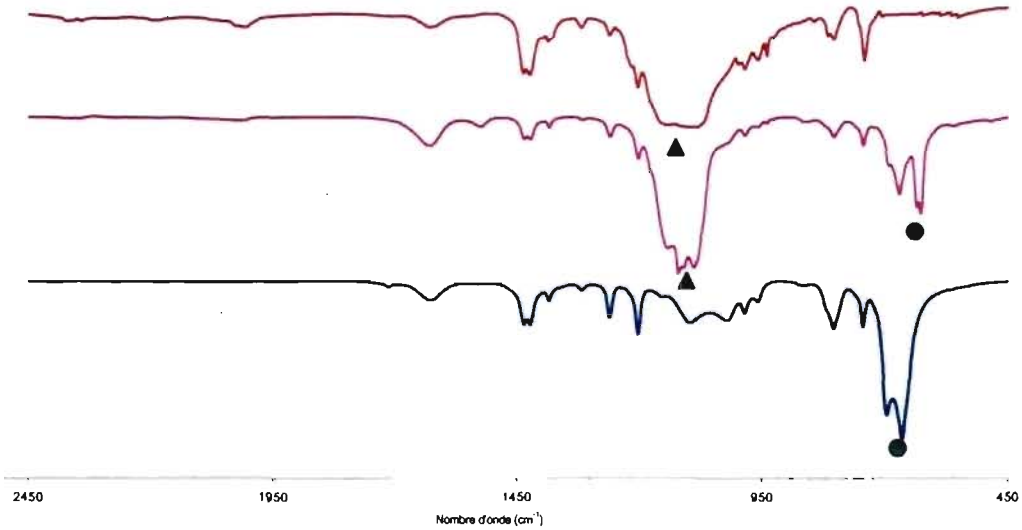

Figure S9. Evolution des spectres infrarouges durant l'échange des anions hexafluoroantimonate du complexe **3**, $[Ag(L^{1\text{-}Me})_2(SbF_6)(Et_2O)_{0.5}]_\infty$, avec les anions tétrafluoroborates. Le spectre bleu est celui du complexe **3**, $[Ag(L^{1\text{-}Me})_2(SbF_6)(Et_2O)_{0.5}]_\infty$,comme préparé (Vibration caractéristique de l'hexafluoroantimonate (● : 664 cm^{-1}, $\nu_3(T_{1u})$).[d, h] Le spectre en violet est celui du complexe **3**, agité dans une solution aqueuse de $LiBF_4$ durant 40 min, montrant la décroissance de l'intensité de la bande caractéristique de l'hexafluoroantimonate (●: 664 cm^{-1}, $\nu_3(T_{1u})$)[d,h] et l'augmentation de l'intensité de la bande caractéristique du perchlorate (▲ : 1078 cm^{-1}, $\nu_{as}(F_2)$).[c] Le spectre rouge est celui du produit résultant de l'échange après deux heures et correspond au compose $[Ag(L^{1\text{-}Me})_2(BF_4)]_\infty$.

[c]Mikuli, E.; Gorska, N.; Wrobel, S.; Sciesinski, J.; Sciesinska, E. *J. Mol. Struct.* **2004**, *692*, 231.
[d]Nakamoto, K. *Infrared Spectra of Inorganic and Coordination Compounds,* 3rd ed.; Wiley-VCH: New York, 1978.
[h]Bernhardt, E.; Bach, C.; Bley, B.; Wartchow, R.; Westphal, U.; Sham, I. H. T.; Ahrsen, B. V.; Wang, C.; Willner, H.; Thompson, R. C.; Aubke, F. *Inorg. Chem.* **2005**, *44*, 4189.

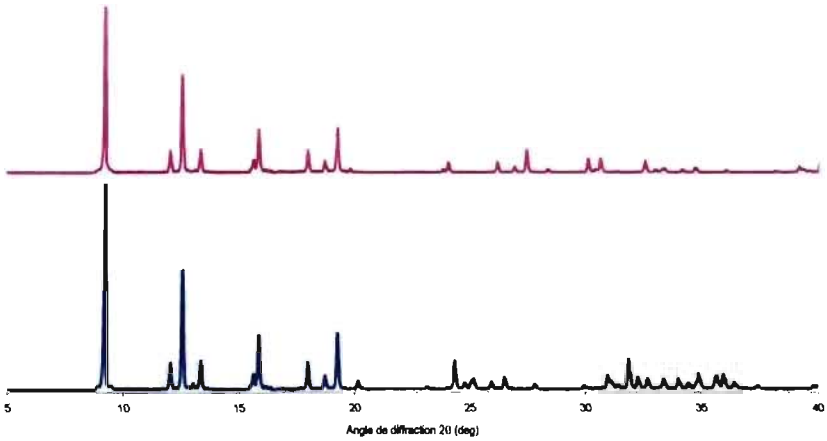

Figure S10. En bleu: Diagramme de poudre du complexe **3** comme synthétisé. En violet: Diagramme de poudre du produit résultant de l'échange **3** + $LiBF_4$.

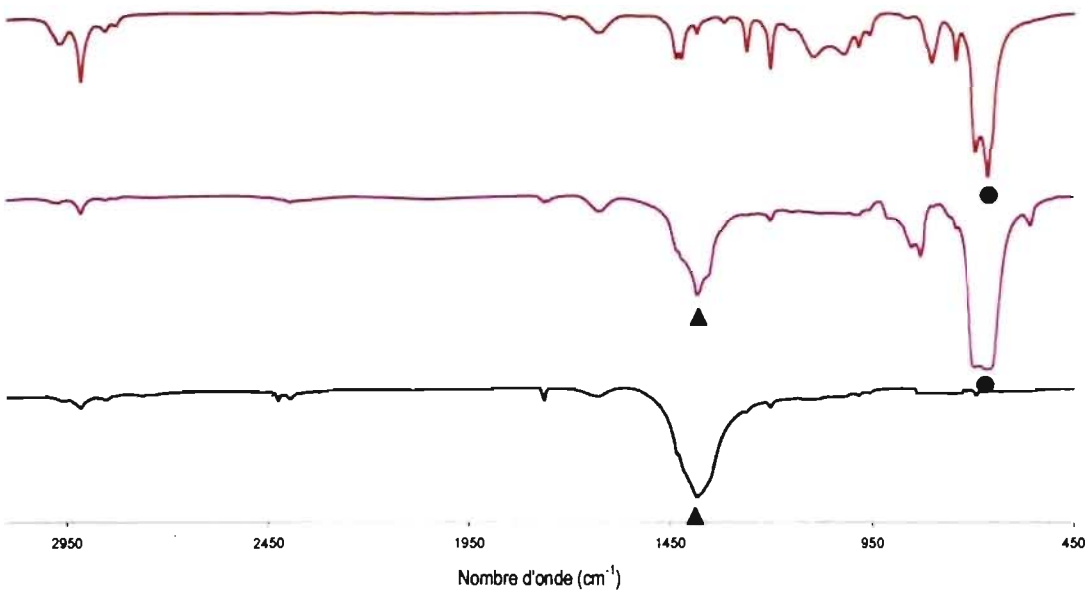

Figure S11. Evolution des spectres infrarouges durant l'échange des anions hexafluoroantimonate du complexe **3**, $[Ag(L^{1\text{-}Me})_2(SbF_6)(Et_2O)_{0.5}]_\infty$, avec les anions nitrates. Le spectre rouge est celui du complexe **3**, $[Ag(L^{1\text{-}Me})_2(SbF_6)(Et_2O)_{0.5}]_\infty$,comme préparé (Vibration caractéristique de l'hexafluoroantimonate (● : 664 cm^{-1}, $\nu_3(T_{1u})$).[d, h] Le spectre en violet est celui du complexe **3**, agité dans une solution aqueuse de $NaNO_3$ durant 40 min, montrant la décroissance de l'intensité de la bande caractéristique de l'hexafluoroantimonate (●: 664 cm^{-1}, $\nu_3(T_{1u})$) [d,h] et l'augmentation de l'intensité de la bande caractéristique du perchlorate (▲ : 1384 cm^{-1}, $\nu_3(E')$).[d] Le spectre bleu est celui du produit résultant de l'échange après deux heures et correspond au compose $[Ag(L^{1\text{-}Me})_2(NO_3)]_\infty$.

[d]Nakamoto, K. *Infrared Spectra of Inorganic and Coordination Compounds,* 3rd ed.; Wiley-VCH: New York, 1978.
[h]Bernhardt, E.; Bach, C.; Bley, B.; Wartchow, R.; Westphal, U.; Sham, I. H. T.; Ahsen, B. V.; Wang, C.; Willner, H.; Thompson, R. C.; Aubke, F. *Inorg. Chem.* **2005**, *44*, 4189.

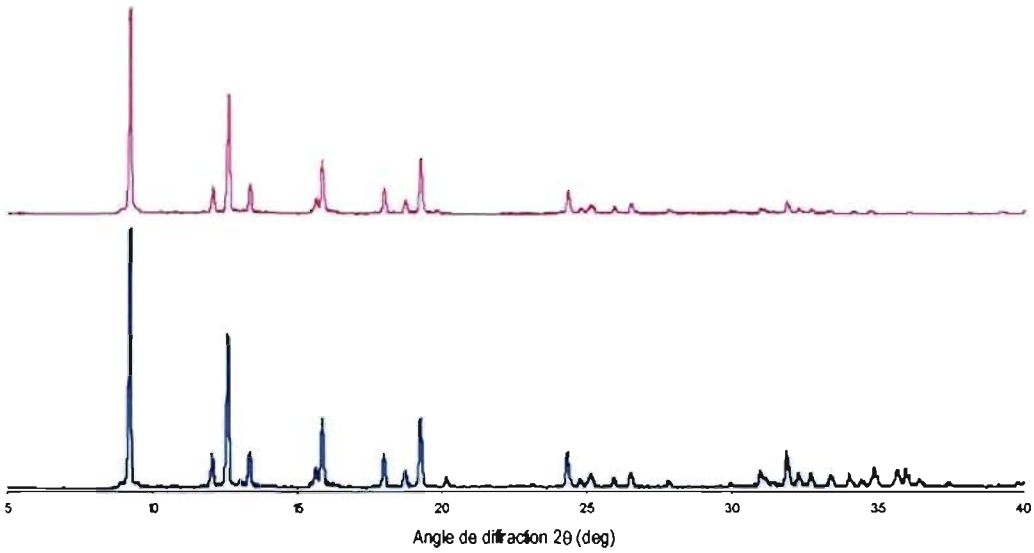

Figure S12. En bleu: Diagramme de poudre du complexe **3** comme synthétisé. En violet: Diagramme de poudre du produit résultant de l'échange **3** + $NaNO_3$.

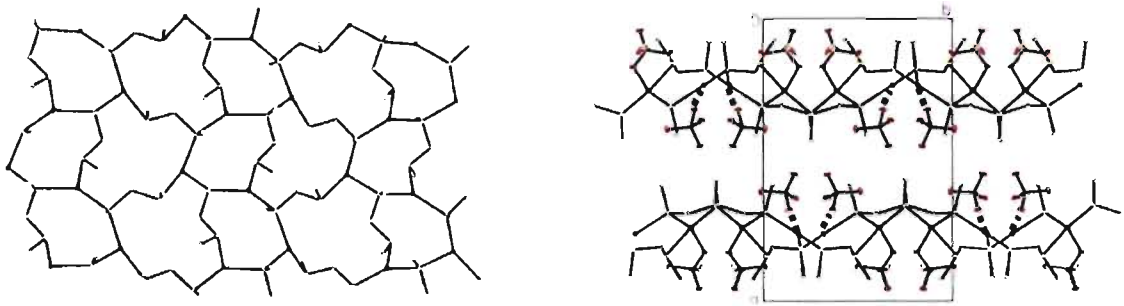

(a) (b)

Figure S13. (a) Réseau 2D du composé $[Ag_2(L^{1\text{-}Me})_2(ClO_4)_2]_\infty$. (Les atomes hydrogènes et les anions perchlorates ont été omis pour plus de clarté). (b) Projection le long de l'axe cristallographique c du complexe $[Ag_2(L^{1\text{-}Me})_2(ClO_4)_2]_\infty$. Les perchlorates coordonnés aux atomes d'argent sont localises entres des feuillets adjacents.[j]

[j]Awaleh, M. O.; Badia, A.; Brisse, F. *Cryst. Growth and Design.* **2006**. *6,* 2674.

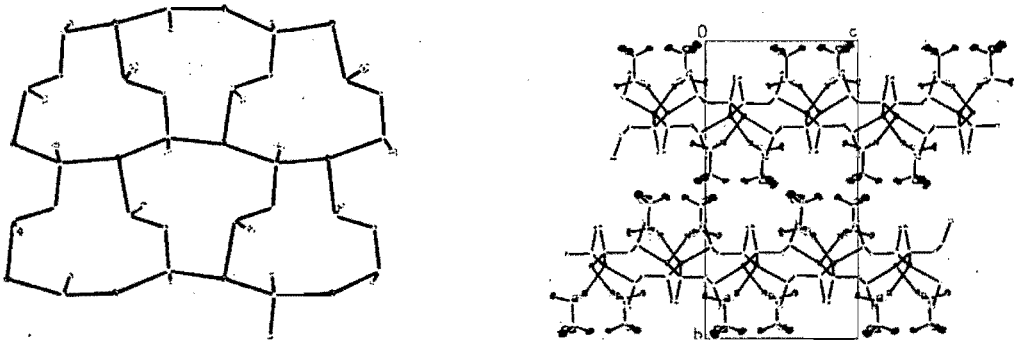

(a) (b)

Figure S14. (a) Le réseau 2D du composé $[Ag_2(L^{1\text{-}Me})_2(CF_3SO_3)_2]_\infty$, obtenu par une procédure de synthèse impliquant le complexe $[Ag_2(L^{1\text{-}Me})_2(ClO_4)_2]_\infty$ (montré à la figure S15).[j] (Les anions triflates et les atomes hydrogènes ont été omis pour plus de clarté). (b) Projection le long de l'axe cristallographique a du complexe $[Ag_2(L^{1\text{-}Me})_2(CF_3SO_3)_2]_\infty$. Les triflates coordonnés aux atomes d'argent sont localises entres des feuillets adjacents.[j]

[j]Awaleh, M. O.; Badia, A.; Brisse, F. *Cryst. Growth and Design.* **2006**. *6,* 2674.

Crystal data and structure refinement for Complex **1**: $C_{21}H_{48}Ag_3F_9O_9S_{15}$.

Identification code	awal55	
Empirical formula	C21 H48 Ag3 F9 O9 S15	
Formula weight	1420.10	
Temperature	100(2)K	
Wavelength	1.54178 Å	
Crystal system	Monoclinic	
Space group	C2	
Unit cell dimensions	a = 17.3226(2) Å	α = 90°
	b = 9.28200(10) Å	β = 93.7260(1)°
	c = 29.8388(3) Å	γ = 90°
Volume	4787.59(9)Å^3	
Z	4	
Density (calculated)	1.970 Mg/m^3	
Absorption coefficient	16.567 mm^{-1}	
F(000)	2832	
Crystal size	0.12 x 0.03 x 0.03 mm	
Theta range for data collection	1.48 to 72.88°	
Index ranges	$-21 \le h \le 21$, $-10 \le k \le 9$, $-36 \le \ell \le 35$	
Reflections collected	19371	
Independent reflections	7496 [R_{int} = 0.035]	
Absorption correction	Semi-empirical from equivalents	
Max. and min. transmission	0.608 and 0.420	
Refinement method	Full-matrix least-squares on F^2	
Data / restraints / parameters	7496 / 1 / 527	
Goodness-of-fit on F^2	1.004	
Final R indices [I>2sigma(I)]	R_1 = 0.0298, wR_2 = 0.0700	
R indices (all data)	R_1 = 0.0313, wR_2 = 0.0707	
Absolute structure parameter	0.008(5)	
Largest diff. peak and hole	0.763 and -0.696 e/Å^3	

Table 2. Atomic coordinates (x 10^4) and equivalent isotropic displacement parameters ($Å^2$ x 10^3) for $C_{21}H_{48}Ag_3F_9O_9S_{15}$. U_{eq} is defined as one third of the trace of the orthogonalized Uij tensor.

	Occ.	x	y	z	U_{eq}
Ag(1)	1	5026(1)	886(1)	1117(1)	13(1)
Ag(2)	1	8193(1)	1059(1)	2206(1)	13(1)
Ag(3)	1	8335(1)	-56(1)	4438(1)	14(1)
S(6)	1	9245(1)	1971(1)	4720(1)	13(1)
S(7)	1	5838(1)	-1344(1)	1452(1)	12(1)
S(8)	1	7430(1)	-1233(1)	1950(1)	13(1)
S(9)	1	8868(1)	-2319(1)	4847(1)	14(1)
S(10)	1	5454(1)	3088(1)	1625(1)	12(1)
S(12)	1	8024(1)	-24(2)	3588(1)	14(1)
S(3)	1	6959(1)	187(1)	4726(1)	15(1)
S(11)	1	9574(1)	526(1)	2037(1)	15(1)
S(4)	1	5621(1)	934(2)	353(1)	14(1)
S(5)	1	3597(1)	511(1)	1208(1)	11(1)
S	1	8348(1)	-318(1)	642(1)	13(1)
S(2)	1	7674(1)	3110(1)	1621(1)	11(1)
S(13)	1	7739(1)	2365(1)	2886(1)	12(1)
S(18)	1	6496(1)	4857(2)	4023(1)	18(1)
S(21)	1	4542(1)	182(2)	2580(1)	16(1)
F(1)	1	8331(2)	2057(4)	160(1)	26(1)
F(3)	1	9093(2)	417(4)	-64(1)	26(1)
F(2)	1	9420(2)	1650(4)	530(1)	26(1)
F(8)	1	5333(2)	-662(4)	3312(1)	36(1)
F(7)	1	5062(2)	1605(4)	3302(1)	26(1)
F(5)	1	6823(3)	5462(4)	3198(1)	42(1)
F(6)	1	7466(2)	6692(5)	3706(2)	49(1)
F(4)	1	6277(2)	7181(5)	3534(1)	42(1)
F(9)	1	4173(2)	43(4)	3415(1)	28(1)
O(1)	1	8148(2)	497(4)	1028(1)	22(1)
O(2)	1	7705(2)	-798(5)	347(1)	22(1)
O(4)	1	7102(3)	3809(5)	4028(1)	35(1)
O(7)	1	5247(2)	553(5)	2382(1)	29(1)
O(9)	1	3934(2)	1238(5)	2515(1)	24(1)
O(8)	1	4303(2)	-1299(5)	2524(1)	25(1)
O(5)	1	6495(2)	5733(5)	4420(1)	31(1)
O(6)	1	5748(3)	4370(6)	3856(2)	37(1)
O(3)	1	8947(2)	-1378(4)	730(1)	19(1)
C(61)	1	10000	887(8)	5000	11(1)
C(81)	1	6607(3)	-252(6)	1706(2)	13(1)
C(51)	1	3076(3)	221(6)	672(2)	19(1)
C(31)	1	6344(3)	541(7)	4225(2)	24(1)
C(62)	1	9763(3)	2544(7)	4244(2)	20(1)
C(71)	1	6325(3)	-2081(6)	983(2)	19(1)
C(41)	1	6480(3)	2042(6)	427(2)	17(1)
C(1)	1	8816(3)	1016(6)	297(2)	16(1)
C(12)	1	8183(3)	1824(6)	3422(2)	13(1)
C(13)	1	9526(3)	-1267(6)	1805(2)	12(1)
C(42)	1	5000	2097(8)	0	16(2)
C(52)	1	3609(3)	-1280(6)	1447(2)	13(1)
C(17)	1	5674(3)	4511(6)	1237(2)	17(1)
C(22)	1	7416(3)	4582(5)	1979(2)	14(1)

C(15)	1	6737(3)	1969(6)	2967(2)	18(1)
C(92)	1	7965(3)	-3036(6)	5030(2)	12(1)
C(2)	1	6776(3)	6115(7)	3593(2)	23(1)
C(4)	1	4785(3)	288(6)	3182(2)	19(1)
C(25)	1	8764(3)	-968(6)	3304(2)	21(1)
C(82)	1	7024(3)	-2000(6)	2441(2)	21(1)
C(91)	1	9088(3)	-3618(7)	4422(2)	26(1)
C(35)	1	10192(3)	262(8)	2540(2)	28(2)

Table 3. Hydrogen coordinates (x 10^4) and isotropic displacement parameters ($Å^2$ x 10^3) for $C_{21}H_{48}Ag_3F_9O_9S_{15}$.

	Occ.	x	y	z	U_{eq}
H(61A)	0.50	10231	259	4776	14
H(61B)	0.50	9769	259	5224	14
H(81A)	1	6394	346	1943	16
H(81B)	1	6788	410	1474	16
H(51A)	1	3407	-299	472	29
H(51B)	1	2928	1152	537	29
H(51C)	1	2610	-349	715	29
H(31A)	1	5841	895	4310	36
H(31B)	1	6271	-349	4051	36
H(31C)	1	6587	1271	4043	36
H(62A)	1	10236	3053	4350	29
H(62B)	1	9435	3190	4054	29
H(62C)	1	9900	1699	4068	29
H(71A)	1	6541	-1293	811	29
H(71B)	1	5954	-2626	787	29
H(71C)	1	6743	-2721	1096	29
H(41A)	1	6710	2158	137	25
H(41B)	1	6854	1577	641	25
H(41C)	1	6341	2989	542	25
H(12A)	1	7989	2465	3655	16
H(12B)	1	8747	1984	3418	16
H(13A)	1	9141	-1280	1545	15
H(13B)	1	9343	-1936	2034	15
H(42A)	0.50	5314	2720	-187	19
H(42B)	0.50	4686	2720	187	19
H(52A)	1	3987	-1302	1710	15
H(52B)	1	3790	-1966	1222	15
H(17A)	1	5324	4441	966	25
H(17B)	1	6210	4412	1155	25
H(17C)	1	5607	5449	1380	25
H(22A)	1	7825	4720	2218	21
H(22B)	1	6928	4359	2112	21
H(22C)	1	7356	5465	1800	21
H(15A)	1	6684	949	3044	26
H(15B)	1	6423	2175	2689	26
H(15C)	1	6560	2567	3210	26
H(92A)	1	7765	-2368	5253	14
H(92B)	1	7582	-3066	4769	14
H(25A)	1	8719	-726	2983	31
H(25B)	1	8698	-2009	3341	31

H(25C)	1	9276	-681	3433	31
H(82A)	1	6881	-1224	2642	32
H(82B)	1	7408	-2627	2598	32
H(82C)	1	6563	-2564	2348	32
H(91A)	1	9149	-4574	4559	40
H(91B)	1	9569	-3343	4289	40
H(91C)	1	8665	-3642	4188	40
H(35A)	1	9992	-533	2714	42
H(35B)	1	10203	1145	2720	42
H(35C)	1	10717	32	2459	42

Table 4. Anisotropic parameters ($Å^2 \times 10^3$) for $C_{21}H_{48}Ag_3F_9O_9S_{15}$. The anisotropic displacement factor exponent takes the form: $-2\pi^2 [h^2 a^{*2} U_{11} + ... + 2 h k a^* b^* U_{12}]$.

	U11	U22	U33	U23	U13	U12
Ag(1)	11(1)	17(1)	12(1)	0(1)	4(1)	-2(1)
Ag(2)	11(1)	16(1)	12(1)	-1(1)	3(1)	0(1)
Ag(3)	12(1)	18(1)	12(1)	2(1)	2(1)	0(1)
S(6)	12(1)	15(1)	13(1)	2(1)	2(1)	1(1)
S(7)	10(1)	14(1)	14(1)	1(1)	2(1)	-1(1)
S(8)	12(1)	13(1)	13(1)	0(1)	2(1)	0(1)
S(9)	12(1)	16(1)	13(1)	3(1)	3(1)	1(1)
S(10)	9(1)	12(1)	14(1)	-1(1)	3(1)	0(1)
S(12)	15(1)	16(1)	11(1)	1(1)	3(1)	2(1)
S(3)	13(1)	13(1)	18(1)	-1(1)	5(1)	0(1)
S(11)	14(1)	14(1)	17(1)	-2(1)	7(1)	0(1)
S(4)	13(1)	19(1)	10(1)	2(1)	3(1)	2(1)
S(5)	10(1)	12(1)	12(1)	1(1)	3(1)	-2(1)
S	12(1)	16(1)	10(1)	-1(1)	3(1)	-1(1)
S(2)	10(1)	12(1)	10(1)	1(1)	2(1)	-1(1)
S(13)	12(1)	16(1)	10(1)	1(1)	2(1)	1(1)
S(18)	20(1)	21(1)	14(1)	-2(1)	5(1)	0(1)
S(21)	15(1)	25(1)	9(1)	-1(1)	1(1)	-5(1)
F(1)	23(2)	17(2)	37(2)	10(1)	4(1)	6(1)
F(3)	30(2)	30(2)	19(2)	2(1)	12(1)	2(1)
F(2)	21(2)	26(2)	32(2)	1(2)	-1(1)	-9(1)
F(8)	40(2)	39(2)	26(2)	1(2)	-12(2)	18(2)
F(7)	23(2)	28(2)	26(2)	-11(1)	-1(1)	-1(1)
F(5)	73(3)	35(3)	19(2)	8(2)	14(2)	12(2)
F(6)	33(2)	52(3)	60(3)	18(2)	3(2)	-19(2)
F(4)	51(3)	28(2)	48(2)	11(2)	6(2)	20(2)
F(9)	33(2)	34(2)	19(2)	3(2)	13(1)	-3(2)
O(1)	21(2)	29(2)	15(2)	-2(2)	7(2)	1(2)
O(2)	17(2)	29(2)	20(2)	-5(2)	1(2)	-6(2)
O(4)	54(3)	30(3)	25(2)	15(2)	20(2)	23(2)
O(7)	23(2)	44(3)	20(2)	-7(2)	10(2)	-10(2)
O(9)	21(2)	30(3)	19(2)	8(2)	-6(2)	1(2)
O(8)	24(2)	30(2)	21(2)	-12(2)	2(2)	-4(2)
O(5)	24(2)	51(3)	18(2)	-14(2)	8(2)	2(2)

O(6)	34(3)	45(3)	30(2)	-3(2)	-5(2)	-17(2)
O(3)	20(2)	20(2)	16(2)	2(2)	3(2)	4(2)
C(61)	18(3)	7(4)	9(3)	0	-4(2)	0
C(81)	12(2)	11(3)	17(2)	0(2)	-1(2)	0(2)
C(51)	18(3)	25(3)	15(2)	3(2)	-3(2)	-2(2)
C(31)	12(2)	36(4)	23(3)	-10(2)	0(2)	0(2)
C(62)	21(3)	24(3)	14(2)	2(2)	2(2)	-7(2)
C(71)	23(3)	21(3)	15(2)	1(2)	6(2)	3(2)
C(41)	13(2)	23(3)	14(2)	-1(2)	3(2)	1(2)
C(1)	13(2)	16(3)	20(2)	1(2)	2(2)	-4(2)
C(12)	15(2)	15(3)	9(2)	-3(2)	1(2)	-2(2)
C(13)	8(2)	13(3)	16(2)	2(2)	3(2)	1(2)
C(42)	19(4)	16(4)	11(3)	0	-3(3)	0
C(52)	13(2)	13(3)	12(2)	4(2)	1(2)	1(2)
C(17)	15(2)	16(3)	20(3)	2(2)	7(2)	-6(2)
C(22)	17(2)	10(3)	16(2)	-1(2)	7(2)	4(2)
C(15)	13(2)	25(3)	14(2)	-3(2)	0(2)	0(2)
C(92)	13(2)	9(3)	14(2)	2(2)	3(2)	4(2)
C(2)	22(3)	18(3)	27(3)	6(2)	2(2)	4(2)
C(4)	19(3)	21(3)	17(3)	-3(2)	-1(2)	3(2)
C(25)	26(3)	15(3)	21(3)	0(2)	5(2)	6(2)
C(82)	26(3)	21(3)	16(3)	2(2)	7(2)	-1(2)
C(91)	28(3)	26(4)	26(3)	-4(2)	12(2)	9(2)
C(35)	17(3)	43(4)	25(3)	-17(3)	2(2)	0(2)

Table 5. Bond lengths [Å] and angles [°] for $C_{21}H_{48}Ag_3F_9O_9S_{15}$.

		S(11)-C(35)	1.803(6)
Ag(1)-S(5)	2.5316(12)	S(4)-C(41)	1.811(5)
Ag(1)-S(4)	2.5624(11)	S(4)-C(42)	1.812(5)
Ag(1)-S(10)	2.6222(13)	S(5)-C(51)	1.806(5)
Ag(1)-S(7)	2.6602(13)	S(5)-C(52)	1.808(5)
Ag(2)-S(11)	2.5256(12)	S-O(1)	1.440(4)
Ag(2)-S(13)	2.5308(12)	S-O(3)	1.443(4)
Ag(2)-S(8)	2.5942(13)	S-O(2)	1.443(4)
Ag(2)-S(2)	2.6976(12)	S-C(1)	1.834(6)
Ag(3)-S(12)	2.5571(12)	S(2)-C(22)	1.807(5)
Ag(3)-S(6)	2.5616(13)	S(2)-C(52)#3	1.823(5)
Ag(3)-S(9)	2.5700(13)	S(13)-C(12)	1.800(5)
Ag(3)-S(3)	2.5961(12)	S(13)-C(15)	1.807(5)
S(6)-C(62)	1.809(5)	S(18)-O(4)	1.430(4)
S(6)-C(61)	1.811(4)	S(18)-O(6)	1.430(4)
S(7)-C(81)	1.801(5)	S(18)-O(5)	1.439(4)
S(7)-C(71)	1.815(5)	S(18)-C(2)	1.822(6)
S(8)-C(81)	1.804(5)	S(21)-O(7)	1.433(4)
S(8)-C(82)	1.811(5)	S(21)-O(8)	1.442(5)
S(9)-C(91)	1.807(6)	S(21)-O(9)	1.443(4)
S(9)-C(92)	1.816(5)	S(21)-C(4)	1.821(6)
S(10)-C(17)	1.813(5)	F(1)-C(1)	1.328(6)
S(10)-C(13)#1	1.829(5)	F(3)-C(1)	1.327(6)
S(12)-C(25)	1.810(5)	F(2)-C(1)	1.354(6)
S(12)-C(12)	1.812(5)	F(8)-C(4)	1.335(6)
S(3)-C(92)#2	1.805(5)	F(7)-C(4)	1.352(7)
S(3)-C(31)	1.809(6)	F(5)-C(2)	1.335(7)
S(11)-C(13)	1.802(5)	F(6)-C(2)	1.332(7)

F(4)-C(2)	1.318(7)	C(51)-S(5)-AG1	111.16(18)
F(9)-C(4)	1.326(6)	C(52)-S(5)-AG1	100.52(16)
C(61)-S(6)#4	1.811(4)	O(1)-S-O(3)	114.7(2)
C(13)-S(10)#5	1.829(5)	O(1)-S-O(2)	115.7(2)
C(42)-S(4)#6	1.812(5)	O(3)-S-O(2)	114.8(2)
C(52)-S(2)#7	1.823(5)	O(1)-S-C(1)	103.5(2)
C(92)-S(3)#8	1.805(5)	O(3)-S-C(1)	102.9(2)
		O(2)-S-C(1)	102.7(2)
S(5)-AG1-S(4)	123.41(4)	C(22)-S(2)-C(52)#3	101.1(2)
S(5)-AG1-S(10)	106.65(4)	C(22)-S(2)-AG2	103.68(17)
S(4)-AG1-S(10)	112.69(4)	C(52)#3-S(2)-AG2	98.01(16)
S(5)-AG1-S(7)	110.45(4)	C(12)-S(13)-C(15)	100.6(2)
S(4)-AG1-S(7)	96.56(4)	C(12)-S(13)-AG2	116.21(17)
S(10)-AG1-S(7)	105.46(4)	C(15)-S(13)-AG2	111.15(17)
S(11)-AG2-S(13)	127.02(4)	O(4)-S(18)-O(6)	116.0(3)
S(11)-AG2-S(8)	104.58(4)	O(4)-S(18)-O(5)	114.5(3)
S(13)-AG2-S(8)	116.76(4)	O(6)-S(18)-O(5)	114.5(3)
S(11)-AG2-S(2)	106.76(4)	O(4)-S(18)-C(2)	102.4(3)
S(13)-AG2-S(2)	94.16(4)	O(6)-S(18)-C(2)	103.6(3)
S(8)-AG2-S(2)	104.20(4)	O(5)-S(18)-C(2)	103.4(3)
S(12)-AG3-S(6)	113.75(4)	O(7)-S(21)-O(8)	115.3(3)
S(12)-AG3-S(9)	121.73(4)	O(7)-S(21)-O(9)	114.5(3)
S(6)-AG3-S(9)	104.47(4)	O(8)-S(21)-O(9)	115.5(2)
S(12)-AG3-S(3)	100.87(4)	O(7)-S(21)-C(4)	104.2(3)
S(6)-AG3-S(3)	112.72(4)	O(8)-S(21)-C(4)	102.3(3)
S(9)-AG3-S(3)	102.88(4)	O(9)-S(21)-C(4)	102.4(2)
C(62)-S(6)-C(61)	98.4(2)	S(6)-C(61)-S(6)#4	112.5(4)
C(62)-S(6)-AG3	106.50(18)	S(7)-C(81)-S(8)	115.4(3)
C(61)-S(6)-AG3	98.9(2)	F(3)-C(1)-F(1)	108.1(4)
C(81)-S(7)-C(71)	99.7(2)	F(3)-C(1)-F(2)	107.0(4)
C(81)-S(7)-AG1	94.53(17)	F(1)-C(1)-F(2)	107.1(5)
C(71)-S(7)-AG1	105.35(18)	F(3)-C(1)-S	111.6(4)
C(81)-S(8)-C(82)	100.8(2)	F(1)-C(1)-S	111.7(3)
C(81)-S(8)-AG2	94.59(17)	F(2)-C(1)-S	111.1(3)
C(82)-S(8)-AG2	107.50(19)	S(13)-C(12)-S(12)	116.3(3)
C(91)-S(9)-C(92)	101.0(3)	S(11)-C(13)-S(10)#5	113.3(3)
C(91)-S(9)-AG3	107.4(2)	S(4)-C(42)-S(4)#6	106.8(4)
C(92)-S(9)-AG3	98.76(16)	S(5)-C(52)-S(2)#7	114.2(3)
C(17)-S(10)-C(13)#1	100.1(2)	S(3)#8-C(92)-S(9)	114.5(3)
C(17)-S(10)-AG1	105.22(18)	F(4)-C(2)-F(6)	107.6(5)
C(13)#1-S(10)-AG1	101.80(17)	F(4)-C(2)-F(5)	107.4(5)
C(25)-S(12)-C(12)	101.8(2)	F(6)-C(2)-F(5)	107.4(5)
C(25)-S(12)-AG3	110.46(18)	F(4)-C(2)-S(18)	112.0(4)
C(12)-S(12)-AG3	104.86(16)	F(6)-C(2)-S(18)	110.9(4)
C(92)#2-S(3)-C(31)	101.0(3)	F(5)-C(2)-S(18)	111.4(4)
C(92)#2-S(3)-AG3	99.70(15)	F(9)-C(4)-F(8)	108.2(5)
C(31)-S(3)-AG3	104.22(18)	F(9)-C(4)-F(7)	107.4(4)
C(13)-S(11)-C(35)	101.8(3)	F(8)-C(4)-F(7)	106.7(4)
C(13)-S(11)-AG2	103.69(16)	F(9)-C(4)-S(21)	111.5(4)
C(35)-S(11)-AG2	112.20(19)	F(8)-C(4)-S(21)	111.4(4)
C(41)-S(4)-C(42)	100.6(2)	F(7)-C(4)-S(21)	111.4(4)
C(41)-S(4)-AG1	106.04(16)		
C(42)-S(4)-AG1	105.64(6)		
C(51)-S(5)-C(52)	101.7(3)		

Symmetry transformations used to generate equivalent atoms:

#1 x-1/2,y+1/2,z #2 -x+3/2,y+1/2,-z+1

#3 x+1/2,y+1/2,z #4 -x+2,y,-z+1 #5 x+1/2,y-1/2,z

#6 -x+1,y,-z #7 x-1/2,y-1/2,z #8 -x+3/2,y-1/2,-z+1

Table 6. Torsion angles [°] for $C_{21}H_{48}Ag_3F_9O_9S_{15}$.

S(12)-AG3-S(6)-C(62) -22.1(2)	S(10)-AG1-S(4)-C(42) -83.7(2)
S(9)-AG3-S(6)-C(62) 112.9(2)	S(7)-AG1-S(4)-C(42) 166.5(2)
S(3)-AG3-S(6)-C(62) -136.2(2)	S(4)-AG1-S(5)-C(51) 2.1(2)
S(12)-AG3-S(6)-C(61) -123.66(5)	S(10)-AG1-S(5)-C(51) 135.0(2)
S(9)-AG3-S(6)-C(61) 11.33(6)	S(7)-AG1-S(5)-C(51) -110.9(2)
S(3)-AG3-S(6)-C(61) 122.29(5)	S(4)-AG1-S(5)-C(52) 109.23(17)
S(5)-AG1-S(7)-C(81) -139.10(16)	S(10)-AG1-S(5)-C(52) -117.9(1)
S(4)-AG1-S(7)-C(81) 91.53(16)	S(7)-AG1-S(5)-C(52) -3.85(17)
S(10)-AG1-S(7)-C(81) -24.23(16)	S(11)-AG2-S(2)-C(22) -120.5(2)
S(5)-AG1-S(7)-C(71) 119.6(2)	S(13)-AG2-S(2)-C(22) 10.23(17)
S(4)-AG1-S(7)-C(71) -9.8(2)	S(8)-AG2-S(2)-C(22) 129.18(17)
S(10)-AG1-S(7)-C(71) -125.6(2)	S(11)-AG2-S(2)-C(52)#3-16.9(1)
S(11)-AG2-S(8)-C(81) -139.3(2)	S(13)-AG2-S(2)-C(52)#3 113.8(2)
S(13)-AG2-S(8)-C(81) 74.84(16)	S(8)-AG2-S(2)-C(52)#3-127.3(2)
S(2)-AG2-S(8)-C(81) -27.36(16)	S(11)-AG2-S(13)-C(12) -46.1(2)
S(11)-AG2-S(8)-C(82) 117.9(2)	S(8)-AG2-S(13)-C(12) 91.09(19)
S(13)-AG2-S(8)-C(82) -28.0(2)	S(2)-AG2-S(13)-C(12) -160.7(2)
S(2)-AG2-S(8)-C(82) -130.2(2)	S(11)-AG2-S(13)-C(15) -160.2(2)
S(12)-AG3-S(9)-C(91) 8.2(2)	S(8)-AG2-S(13)-C(15) -23.1(2)
S(6)-AG3-S(9)-C(91) -122.2(2)	S(2)-AG2-S(13)-C(15) 85.1(2)
S(3)-AG3-S(9)-C(91) 119.9(2)	C(62)-S(6)-C(61)-S(6)#4 74.1(2)
S(12)-AG3-S(9)-C(92) -96.30(17)	AG3-S(6)-C(61)-S(6)#4 -176.7(1)
S(6)-AG3-S(9)-C(92) 133.26(17)	C(71)-S(7)-C(81)-S(8) -67.2(3)
S(3)-AG3-S(9)-C(92) 15.34(17)	AG1-S(7)-C(81)-S(8) -173.6(2)
S(5)-AG1-S(10)-C(17) -111.7(2)	C(82)-S(8)-C(81)-S(7) -71.8(3)
S(4)-AG1-S(10)-C(17) 26.73(18)	AG2-S(8)-C(81)-S(7) 179.4(2)
S(7)-AG1-S(10)-C(17) 130.85(18)	O(1)-S-C(1)-F(3) 175.3(3)
S(5)-AG1-S(10)-C(13)#1 -7.7(2)	O(3)-S-C(1)-F(3) 55.5(4)
S(4)-AG1-S(10)-C(13)#1130.7 (2)	O(2)-S-C(1)-F(3) -63.9(4)
S(7)-AG1-S(10)-C(13)#1-125.2(2)	O(1)-S-C(1)-F(1) -63.5(4)
S(6)-AG3-S(12)-C(25) 85.3(2)	O(3)-S-C(1)-F(1) 176.7(4)
S(9)-AG3-S(12)-C(25) -41.1(2)	O(2)-S-C(1)-F(1) 57.2(4)
S(3)-AG3-S(12)-C(25) -153.8(2)	O(1)-S-C(1)-F(2) 56.0(4)
S(6)-AG3-S(12)-C(12) -23.71(17)	O(3)-S-C(1)-F(2) -63.8(4)
S(9)-AG3-S(12)-C(12)-150.09(17)	O(2)-S-C(1)-F(2) 176.7(4)
S(3)-AG3-S(12)-C(12) 97.23(17)	C(15)-S(13)-C(12)-S(12) 57.4(3)
S(12)-AG3-S(3)-C(92)#2-112.1(2)	AG2-S(13)-C(12)-S(12) -62.7(3)
S(6)-AG3-S(3)-C(92)#2 9.64(17)	C(25)-S(12)-C(12)-S(13) 83.5(3)
S(9)-AG3-S(3)-C(92)#2121.6(2)	AG3-S(12)-C(12)-S(13) -161.3(2)
S(12)-AG3-S(3)-C(31) -7.9(2)	C(35)-S(11)-C(13)-S(10)#5-
S(6)-AG3-S(3)-C(31) 113.7(2)	66.0(3)
S(9)-AG3-S(3)-C(31) -134.3(2)	AG2-S(11)-C(13)-S(10)#5177.4(2)
S(13)-AG2-S(11)-C(13)140.41(17)	C(41)-S(4)-C(42)-S(4)#6149.2(2)
S(8)-AG2-S(11)-C(13) -0.74(17)	AG1-S(4)-C(42)-S(4)#6-100.69(8)
S(2)-AG2-S(11)-C(13)-110.80(17)	C(51)-S(5)-C(52)-S(2)#7-71.8(3)
S(13)-AG2-S(11)-C(35) 31.4(3)	AG1-S(5)-C(52)-S(2)#7 173.7(2)
S(8)-AG2-S(11)-C(35) -109.8(2)	C(91)-S(9)-C(92)-S(3)#8 62.0(3)
S(2)-AG2-S(11)-C(35) 140.2(2)	AG3-S(9)-C(92)-S(3)#8 171.7(2)
S(5)-AG1-S(4)-C(41) 152.95(19)	O(4)-S(18)-C(2)-F(4) 179.6(4)
S(10)-AG1-S(4)-C(41) 22.57(19)	O(6)-S(18)-C(2)-F(4) 58.6(5)
S(7)-AG1-S(4)-C(41) -87.23(19)	O(5)-S(18)-C(2)-F(4) -61.1(5)
S(5)-AG1-S(4)-C(42) 46.7(2)	O(4)-S(18)-C(2)-F(6) -60.3(5)

O(6)-S(18)-C(2)-F(6)	178.7(4)
O(5)-S(18)-C(2)-F(6)	59.0(5)
O(4)-S(18)-C(2)-F(5)	59.3(5)
O(6)-S(18)-C(2)-F(5)	-61.7(5)
O(5)-S(18)-C(2)-F(5)	178.6(4)
O(7)-S(21)-C(4)-F(9)	176.7(4)
O(8)-S(21)-C(4)-F(9)	-62.9(4)
O(9)-S(21)-C(4)-F(9)	57.1(4)
O(7)-S(21)-C(4)-F(8)	-62.2(5)
O(8)-S(21)-C(4)-F(8)	58.1(5)
O(9)-S(21)-C(4)-F(8)	178.1(4)
O(7)-S(21)-C(4)-F(7)	56.8(4)
O(8)-S(21)-C(4)-F(7)	177.1(4)
O(9)-S(21)-C(4)-F(7)	-62.9(4)

Symmetry transformations used to generate equivalent atoms:
#1 x-1/2,y+1/2,z
#2 -x+3/2,y+1/2,-z+1
#3 x+1/2,y+1/2,z
#4 -x+2,y,-z+1
#5 x+1/2,y-1/2,z
#6 -x+1,y,-z
#7 x-1/2,y-1/2,z
#8 -x+3/2,y-1/2,-z+1

Crystal data and structure refinement for Complex **2**: $C_6H_{16}AgF_6PS_4$.

Identification code	ande30	
Empirical formula	C6 H16 Ag F6 P S4	
Formula weight	469.27	
Temperature	200(2)K	
Wavelength	1.54178 Å	
Crystal system	Monoclinic	
Space group	C2/c	
Unit cell dimensions	a = 8.2468(4) Å	α = 90°
	b = 19.1011(10) Å	β = 107.065(2)°
	c = 10.1381(5) Å	γ = 90°
Volume	1526.67(13)Å^3	
Z	4	
Density (calculated)	2.042 Mg/m^3	
Absorption coefficient	17.161 mm^{-1}	
F(000)	928	
Crystal size	0.10 x 0.06 x 0.04 mm	
Theta range for data collection	4.63 to 69.01°	
Index ranges	$-9 \le h \le 9$, $-23 \le k \le 22$, $-11 \le \ell \le 12$	
Reflections collected	10377	
Independent reflections	1403 [R_{int} = 0.054]	
Absorption correction	Semi-empirical from equivalents	
Max. and min. transmission	0.5703 and 0.335	
Refinement method	Full-matrix least-squares on F^2	
Data / restraints / parameters	1403 / 10 / 87	
Goodness-of-fit on F^2	0.982	
Final R indices [I>2sigma(I)]	R_1 = 0.0436, wR_2 = 0.1193	
R indices (all data)	R_1 = 0.0444, wR_2 = 0.1201	
Largest diff. peak and hole	0.935 and -0.650 e/Å^3	

Table 2. Atomic coordinates (x 10^4) and equivalent isotropic displacement parameters ($Å^2$ x 10^3) for $C_6H_{16}AgF_6PS_4$. U_{eq} is defined as one third of the trace of the orthogonalized Uij tensor.

	Occ.	x	y	z	U_{eq}
Ag(1)	1	0	126(1)	7500	42(1)
S(1)	1	471(1)	849(1)	9748(1)	36(1)
S(2)	1	-2783(2)	-565(1)	7347(1)	39(1)
C(12)	1	2576(6)	622(3)	10830(5)	40(1)
C(11)	1	675(9)	1764(3)	9396(7)	56(2)
C(21)	1	-2486(8)	-1468(3)	6939(6)	51(1)
P(1)	1	5000	1493(1)	7500	42(1)
F(1)	0.40	6095(17)	2066(6)	8574(12)	75(1)
F(2)	0.40	5641(18)	909(6)	8679(11)	75(1)
F(3)	0.40	6433(15)	992(6)	8316(13)	75(1)
F(4)	0.35	4726(18)	1059(7)	8761(12)	75(1)
F(5)	0.35	6712(15)	1103(7)	7529(15)	75(1)
F(6)	0.35	5030(20)	2024(7)	8664(13)	75(1)
F(7)	0.25	4310(30)	1804(10)	8706(18)	75(1)
F(8)	0.25	6700(20)	1939(10)	8110(20)	75(1)
F(9)	0.25	3510(20)	1922(9)	7830(20)	75(1)

Table 3. Hydrogen coordinates (x 10^4) and isotropic displacement parameters ($Å^2$ x 10^3) for $C_6H_{16}AgF_6PS_4$.

	Occ.	x	y	z	U_{eq}
H(12A)	1	2900	165	10520	48
H(12B)	1	3388	976	10694	48
H(11A)	1	451	2046	10130	84
H(11B)	1	-143	1886	8510	84
H(11C)	1	1828	1858	9355	84
H(21A)	1	-1386	-1633	7525	77
H(21B)	1	-2519	-1505	5968	77
H(21C)	1	-3393	-1755	7104	77

Table 4. Anisotropic parameters ($Å^2$ x 10^3) for $C_6H_{16}AgF_6PS_4$. The anisotropic displacement factor exponent takes the form: $-2\pi^2 [h^2 a^{*2} U_{11} + ... + 2 h k a^* b^* U_{12}]$

	U11	U22	U33	U23	U13	U12
Ag(1)	46(1)	41(1)	37(1)	0	12(1)	0
S(1)	35(1)	38(1)	33(1)	0(1)	7(1)	1(1)
S(2)	34(1)	46(1)	34(1)	0(1)	5(1)	-1(1)
C(12)	36(2)	49(3)	35(3)	-2(2)	9(2)	3(2)
C(11)	70(4)	38(3)	54(3)	1(2)	8(3)	1(3)
C(21)	62(3)	47(3)	45(3)	-9(2)	15(3)	-10(3)
P(1)	41(1)	37(1)	48(1)	0	14(1)	0

Table 5. Bond lengths [Å] and angles [°] for $C_6H_{16}AgF_6PS_4$

		F(6)-F(7)	0.739(19)
Ag(1)-S(1)	2.5947(12)	F(6)-F(9)	1.30(2)
Ag(1)-S(1)#1	2.5947(12)	F(6)-F(8)	1.64(2)
Ag(1)-S(2)	2.6122(12)	F(7)-F(9)	0.96(2)
Ag(1)-S(2)#1	2.6122(12)		
S(1)-C(11)	1.802(6)	S(1)-AG1-S(1)#1	115.67(5)
S(1)-C(12)	1.813(5)	S(1)-AG1-S(2)	102.92(4)
S(2)-C(21)	1.807(6)	S(1)#1-AG1-S(2)	108.30(4)
S(2)-C(12)#2	1.808(5)	S(1)-AG1-S(2)#1	108.30(4)
C(12)-S(2)#2	1.808(5)	S(1)#1-AG1-S(2)#1	102.92(4)
P(1)-F(6)	1.551(12)	S(2)-AG1-S(2)#1	119.35(6)
P(1)-F(6)#3	1.551(12)	C(11)-S(1)-C(12)	102.9(3)
P(1)-F(3)#3	1.557(10)	C(11)-S(1)-AG1	109.9(2)
P(1)-F(3)	1.557(10)	C(12)-S(1)-AG1	105.91(17)
P(1)-F(5)#3	1.589(12)	C(21)-S(2)-C(12)#2	101.4(3)
P(1)-F(5)	1.589(12)	C(21)-S(2)-AG1	108.6(2)
P(1)-F(9)#3	1.593(14)	C(12)#2-S(2)-AG1	98.73(17)
P(1)-F(9)	1.593(14)	S(2)#2-C(12)-S(1)	114.8(3)
P(1)-F(4)	1.594(11)	F(6)-P(1)-F(6)#3	98.40(11)
P(1)-F(4)#3	1.594(11)	F(6)-P(1)-F(3)#3	130.2(8)
P(1)-F(8)	1.599(14)	F(6)#3-P(1)-F(3)#3	99.1(7)
P(1)-F(8)#3	1.599(14)	F(6)-P(1)-F(3)	99.1(7)
F(1)-F(8)	0.815(19)	F(6)#3-P(1)-F(3)	130.2(8)
F(1)-F(6)	0.915(15)	F(3)#3-P(1)-F(3)	104.1(9)
F(1)-F(7)	1.60(2)	F(6)-P(1)-F(5)#3	97.8(8)
F(2)-F(4)	0.834(14)	F(6)#3-P(1)-F(5)#3	118.5(7)
F(2)-F(3)	0.853(14)	F(3)#3-P(1)-F(5)#3	33.9(6)
F(2)-F(5)	1.696(17)	F(3)-P(1)-F(5)#3	104.7(7)
F(3)-F(5)	0.917(15)	F(6)-P(1)-F(5)	118.5(7)
F(3)-F(4)	1.604(17)	F(6)#3-P(1)-F(5)	97.8(8)
F(4)-F(7)	1.46(2)	F(3)#3-P(1)-F(5)	104.7(7)
F(5)-F(8)	1.70(2)	F(3)-P(1)-F(5)	33.9(6)

F(5)#3-P(1)-F(5)	124.0(1)	F(7)-F(1)-P(1)	59.9(7)
F(6)-P(1)-F(9)#3	89.1(9)	F(4)-F(2)-F(3)	143.90(17)
F(6)#3-P(1)-F(9)#3	49.0(9)	F(4)-F(2)-P(1)	74.0(1)
F(3)#3-P(1)-F(9)#3	135.8(1)	F(3)-F(2)-P(1)	71.2(9)
F(3)-P(1)-F(9)#3	85.2(9)	F(4)-F(2)-F(5)	131.50(12)
F(5)#3-P(1)-F(9)#3	166.8(9)	F(3)-F(2)-F(5)	17.2(9)
F(5)-P(1)-F(9)#3	60.6(8)	P(1)-F(2)-F(5)	57.4(5)
F(6)-P(1)-F(9)	49.0(9)	F(2)-F(3)-F(5)	146.80(17)
F(6)#3-P(1)-F(9)	89.1(9)	F(2)-F(3)-P(1)	77.6(9)
F(3)#3-P(1)-F(9)	85.2(9)	F(5)-F(3)-P(1)	75.0(1)
F(3)-P(1)-F(9)	135.8(1)	F(2)-F(3)-F(4)	17.8(9)
F(5)#3-P(1)-F(9)	60.6(8)	F(5)-F(3)-F(4)	133.70(12)
F(5)-P(1)-F(9)	166.8(9)	P(1)-F(3)-F(4)	60.5(5)
F(9)#3-P(1)-F(9)	118.20(14)	F(2)-F(4)-F(7)	122.90(16)
F(6)-P(1)-F(4)	72.7(7)	F(2)-F(4)-P(1)	75.8(1)
F(6)#3-P(1)-F(4)	167.5(9)	F(7)-F(4)-P(1)	63.3(8)
F(3)#3-P(1)-F(4)	80.9(7)	F(2)-F(4)-F(3)	18.2(9)
F(3)-P(1)-F(4)	61.2(6)	F(7)-F(4)-F(3)	106.60(11)
F(5)#3-P(1)-F(4)	55.7(6)	P(1)-F(4)-F(3)	58.3(5)
F(5)-P(1)-F(4)	94.3(7)	F(3)-F(5)-P(1)	71.1(1)
F(9)#3-P(1)-F(4)	137.4(9)	F(3)-F(5)-F(2)	16.0(9)
F(9)-P(1)-F(4)	78.4(9)	P(1)-F(5)-F(2)	58.4(5)
F(6)-P(1)-F(4)#3	167.5(9)	F(3)-F(5)-F(8)	83.50(14)
F(6)#3-P(1)-F(4)#3	72.7(7)	P(1)-F(5)-F(8)	58.0(7)
F(3)#3-P(1)-F(4)#3	61.2(6)	F(2)-F(5)-F(8)	84.8(1)
F(3)-P(1)-F(4)#3	80.9(7)	F(7)-F(6)-F(1)	150(3)
F(5)#3-P(1)-F(4)#3	94.3(7)	F(7)-F(6)-F(9)	46.80(19)
F(5)-P(1)-F(4)#3	55.7(6)	F(1)-F(6)-F(9)	135.90(17)
F(9)#3-P(1)-F(4)#3	78.4(9)	F(7)-F(6)-P(1)	80.70(16)
F(9)-P(1)-F(4)#3	137.4(9)	F(1)-F(6)-P(1)	77.3(1)
F(4)-P(1)-F(4)#3	117.4(1)	F(9)-F(6)-P(1)	67.2(9)
F(6)-P(1)-F(8)	62.8(8)	F(7)-F(6)-F(8)	137(2)
F(6)#3-P(1)-F(8)	76.2(9)	F(1)-F(6)-F(8)	17.4(9)
F(3)#3-P(1)-F(8)	167.0(1)	F(9)-F(6)-F(8)	120.40(12)
F(3)-P(1)-F(8)	71.4(8)	P(1)-F(6)-F(8)	60.1(7)
F(5)#3-P(1)-F(8)	158.3(1)	F(6)-F(7)-F(9)	99(3)
F(5)-P(1)-F(8)	64.6(9)	F(6)-F(7)-F(4)	112(2)
F(9)#3-P(1)-F(8)	33.4(8)	F(9)-F(7)-F(4)	110.70(18)
F(9)-P(1)-F(8)	106.7(9)	F(6)-F(7)-F(1)	16.40(14)
F(4)-P(1)-F(8)	106.3(9)	F(9)-F(7)-F(1)	104.40(18)
F(4)#3-P(1)-F(8)	105.8(1)	F(4)-F(7)-F(1)	95.40(12)
F(6)-P(1)-F(8)#3	76.2(9)	F(6)-F(7)-P(1)	72.30(15)
F(6)#3-P(1)-F(8)#3	62.8(8)	F(9)-F(7)-P(1)	71.7(1)
F(3)#3-P(1)-F(8)#3	71.4(8)	F(4)-F(7)-P(1)	62.4(7)
F(3)-P(1)-F(8)#3	167.0(1)	F(1)-F(7)-P(1)	60.6(7)
F(5)#3-P(1)-F(8)#3	64.6(9)	F(1)-F(8)-P(1)	76.60(13)
F(5)-P(1)-F(8)#3	158.3(1)	F(1)-F(8)-F(6)	19.6(1)
F(9)#3-P(1)-F(8)#3	106.7(9)	P(1)-F(8)-F(6)	57.2(7)
F(9)-P(1)-F(8)#3	33.4(8)	F(1)-F(8)-F(5)	123.00(18)
F(4)-P(1)-F(8)#3	105.8(1)	P(1)-F(8)-F(5)	57.4(7)
F(4)#3-P(1)-F(8)#3	106.3(9)	F(6)-F(8)-F(5)	107.60(11)
F(8)-P(1)-F(8)#3	115.60(14)	F(7)-F(9)-F(6)	34.00(13)
F(8)-F(1)-F(6)	143.00(19)	F(7)-F(9)-P(1)	73.3(1)
F(8)-F(1)-F(7)	133.50(17)	F(6)-F(9)-P(1)	63.8(8)
F(6)-F(1)-F(7)	13.20(11)		
F(8)-F(1)-P(1)	74.00(13)		
F(6)-F(1)-P(1)	69.2(1)		

Symmetry transformations used to generate equivalent atoms:

#1 -x,y,-z+3/2 #2 -x,-y,-z+2 #3 -x+1,y,-z+3/2

Table 6. Torsion angles [°] for C6 H16 Ag F6 P S4.

S(1)#1-AG1-S(1)-C(11)	-7.7(3)
S(2)-AG1-S(1)-C(11)	-125.6(3)
S(2)#1-AG1-S(1)-C(11)	107.1(3)
S(1)#1-AG1-S(1)-C(12)	-118.3(2)
S(2)-AG1-S(1)-C(12)	123.85(19)
S(2)#1-AG1-S(1)-C(12)	-3.41(19)
S(1)-AG1-S(2)-C(21)	-134.0(2)
S(1)#1-AG1-S(2)-C(21)	103.0(2)
S(2)#1-AG1-S(2)-C(21)	-14.1(2)
S(1)-AG1-S(2)-C(12)#2	-28.81(18)
S(1)#1-AG1-S(2)-C12)#2	-151.8(2)
S(2)#1-AG1-S(2)-C(12)#2	91.1(2)
C(11)-S(1)-C(12)-S(2)#2	101.8(4)
AG1-S(1)-C(12)-S(2)#2	-142.8(2)
F(6)-P(1)-F(1)-F(8)	-176(2)
F(6)#3-P(1)-F(1)-F(8)	-66.4(2)
F(3)#3-P(1)-F(1)-F(8)	-180(2)
F(3)-P(1)-F(1)-F(8)	64.80(18)
F(5)#3-P(1)-F(1)-F(8)	167.70(17)
F(5)-P(1)-F(1)-F(8)	31.50(18)
F(9)#3-P(1)-F(1)-F(8)	-24.0(2)
F(9)-P(1)-F(1)-F(8)	-156.00(17)
F(4)-P(1)-F(1)-F(8)	125.80(18)
F(4)#3-P(1)-F(1)-F(8)	-4(2)
F(8)#3-P(1)-F(1)-F(8)	-128.3(2)
F(6)#3-P(1)-F(1)-F(6)	109.8(2)
F(3)#3-P(1)-F(1)-F(6)	-3(3)
F(3)-P(1)-F(1)-F(6)	-119.00(13)
F(5)#3-P(1)-F(1)-F(6)	-16.0(2)
F(5)-P(1)-F(1)-F(6)	-152.30(13)
F(9)#3-P(1)-F(1)-F(6)	152.20(16)
F(9)-P(1)-F(1)-F(6)	20.20(15)
F(4)-P(1)-F(1)-F(6)	-58.00(13)
F(4)#3-P(1)-F(1)-F(6)	171.80(12)
F(8)-P(1)-F(1)-F(6)	176(2)
F(8)#3-P(1)-F(1)-F(6)	47.90(15)
F(6)-P(1)-F(1)-F(7)	10.40(15)
F(6)#3-P(1)-F(1)-F(7)	120.20(12)
F(3)#3-P(1)-F(1)-F(7)	7(2)
F(3)-P(1)-F(1)-F(7)	-108.6(1)
F(5)#3-P(1)-F(1)-F(7)	-5.60(12)
F(5)-P(1)-F(1)-F(7)	-141.9(1)
F(9)#3-P(1)-F(1)-F(7)	162.60(12)
F(9)-P(1)-F(1)-F(7)	30.60(11)
F(4)-P(1)-F(1)-F(7)	-47.6(1)
F(4)#3-P(1)-F(1)-F(7)	-177.8(1)
F(8)-P(1)-F(1)-F(7)	-173(2)
F(8)#3-P(1)-F(1)-F(7)	58.40(12)
F(6)-P(1)-F(2)-F(4)	58.60(14)
F(6)#3-P(1)-F(2)-F(4)	168(2)
F(3)#3-P(1)-F(2)-F(4)	-71.60(14)
F(3)-P(1)-F(2)-F(4)	170(2)
F(5)#3-P(1)-F(2)-F(4)	-39.90(14)
F(5)-P(1)-F(2)-F(4)	-177.90(15)
F(9)#3-P(1)-F(2)-F(4)	146.60(15)
F(9)-P(1)-F(2)-F(4)	13.30(16)
F(4)#3-P(1)-F(2)-F(4)	-132.5(1)
F(8)-P(1)-F(2)-F(4)	121.30(15)
F(8)#3-P(1)-F(2)-F(4)	-8.80(19)
F(6)-P(1)-F(2)-F(3)	-111.80(13)
F(6)#3-P(1)-F(2)-F(3)	-2(3)
F(3)#3-P(1)-F(2)-F(3)	117.90(13)
F(5)#3-P(1)-F(2)-F(3)	149.70(13)
F(5)-P(1)-F(2)-F(3)	11.60(12)
F(9)#3-P(1)-F(2)-F(3)	-23.80(16)
F(9)-P(1)-F(2)-F(3)	-157.10(13)
F(4)-P(1)-F(2)-F(3)	-170(2)
F(4)#3-P(1)-F(2)-F(3)	57.0(1)
F(8)-P(1)-F(2)-F(3)	-49.1(1)
F(8)#3-P(1)-F(2)-F(3)	-179.2(1)
F(6)-P(1)-F(2)-F(5)	-123.4(8)
F(6)#3-P(1)-F(2)-F(5)	-14(2)
F(3)#3-P(1)-F(2)-F(5)	106.3(7)
F(3)-P(1)-F(2)-F(5)	-11.60(12)
F(5)#3-P(1)-F(2)-F(5)	138.0(8)
F(9)#3-P(1)-F(2)-F(5)	-35.4(1)
F(9)-P(1)-F(2)-F(5)	-168.8(9)
F(4)-P(1)-F(2)-F(5)	177.90(15)
F(4)#3-P(1)-F(2)-F(5)	45.4(7)
F(8)-P(1)-F(2)-F(5)	-60.8(1)
F(8)#3-P(1)-F(2)-F(5)	169.10(12)
F(4)-F(2)-F(3)-F(5)	-51(6)
P(1)-F(2)-F(3)-F(5)	-35(3)
F(4)-F(2)-F(3)-P(1)	-16(3)
F(5)-F(2)-F(3)-P(1)	35(3)
P(1)-F(2)-F(3)-F(4)	16(3)
F(5)-F(2)-F(3)-F(4)	51(6)
F(6)-P(1)-F(3)-F(2)	69.90(13)
F(6)#3-P(1)-F(3)-F(2)	79.20(11)
F(3)#3-P(1)-F(3)-F(2)	-65.60(11)
F(5)#3-P(1)-F(3)-F(2)	-30.70(13)
F(5)-P(1)-F(3)-F(2)	-161(2)
F(9)#3-P(1)-F(3)-F(2)	158.30(14)
F(9)-P(1)-F(3)-F(2)	32.00(18)
F(4)-P(1)-F(3)-F(2)	5.50(12)
F(4)#3-P(1)-F(3)-F(2)	-122.8(1)
F(8)-P(1)-F(3)-F(2)	127.10(15)
F(8)#3-P(1)-F(3)-F(2)	2(4)
F(6)-P(1)-F(3)-F(5)	-129.00(13)
F(6)#3-P(1)-F(3)-F(5)	-19.8(2)
F(3)#3-P(1)-F(3)-F(5)	95.4(1)
F(5)#3-P(1)-F(3)-F(5)	130.4(1)
F(9)#3-P(1)-F(3)-F(5)	-40.70(13)
F(9)-P(1)-F(3)-F(5)	-167.00(14)
F(4)-P(1)-F(3)-F(5)	166.50(14)

F(4)#3-P(1)-F(3)-F(5) 38.20(12)
F(8)-P(1)-F(3)-F(5) -71.90(14)
F(8)#3-P(1)-F(3)-F(5) 163(3)
F(6)-P(1)-F(3)-F(4) 64.5(8)
F(6)#3-P(1)-F(3)-F(4) 173.7(9)
F(3)#3-P(1)-F(3)-F(4) -71.1(7)
F(5)#3-P(1)-F(3)-F(4) -36.1(8)
F(5)-P(1)-F(3)-F(4) -166.50(14)
F(9)#3-P(1)-F(3)-F(4) 152.8(1)
F(9)-P(1)-F(3)-F(4) 26.50(13)
F(4)#3-P(1)-F(3)-F(4) -128.2(1)
F(8)-P(1)-F(3)-F(4) 121.60(11)
F(8)#3-P(1)-F(3)-F(4) -3(4)
F(3)-F(2)-F(4)-F(7) -29(4)
P(1)-F(2)-F(4)-F(7) -44.30(14)
F(5)-F(2)-F(4)-F(7) -47(3)
F(3)-F(2)-F(4)-P(1) 15(3)
F(5)-F(2)-F(4)-P(1) -2.30(17)
P(1)-F(2)-F(4)-F(3) -15(3)
F(5)-F(2)-F(4)-F(3) -18(2)
F(6)-P(1)-F(4)-F(2) -116.70(15)
F(6)#3-P(1)-F(4)-F(2) -163(3)
F(3)#3-P(1)-F(4)-F(2)106.00(14)
F(3)-P(1)-F(4)-F(2) -5.60(13)
F(5)#3-P(1)-F(4)-F(2)130.70(16)
F(5)-P(1)-F(4)-F(2) 1.90(14)
F(9)#3-P(1)-F(4)-F(2) -47.9(2)
F(9)-P(1)-F(4)-F(2) -167.1(2)
F(4)#3-P(1)-F(4)-F(2) 55.20(12)
F(8)-P(1)-F(4)-F(2) -62.90(16)
F(8)#3-P(1)-F(4)-F(2)173.60(14)
F(6)-P(1)-F(4)-F(7) 22.2(1)
F(6)#3-P(1)-F(4)-F(7) -24(4)
F(3)#3-P(1)-F(4)-F(7) -115.0(1)
F(3)-P(1)-F(4)-F(7) 133.3(1)
F(5)#3-P(1)-F(4)-F(7) -90.4(1)
F(5)-P(1)-F(4)-F(7) 140.8(1)
F(9)#3-P(1)-F(4)-F(7) 91.0(1)
F(9)-P(1)-F(4)-F(7) -28.1(1)
F(4)#3-P(1)-F(4)-F(7) -165.8(1)
F(8)-P(1)-F(4)-F(7) 76.0(1)
F(8)#3-P(1)-F(4)-F(7) -47.4(1)
F(6)-P(1)-F(4)-F(3) -111.1(8)
F(6)#3-P(1)-F(4)-F(3) -157(3)
F(3)#3-P(1)-F(4)-F(3) 111.7(9)
F(5)#3-P(1)-F(4)-F(3) 136.4(9)
F(5)-P(1)-F(4)-F(3) 7.5(8)
F(9)#3-P(1)-F(4)-F(3) -42.3(1)
F(9)-P(1)-F(4)-F(3) -161.4(1)
F(4)#3-P(1)-F(4)-F(3) 60.9(6)
F(8)-P(1)-F(4)-F(3) -57.3(1)
F(8)#3-P(1)-F(4)-F(3) 179.3(9)
F(5)-F(3)-F(4)-F(2) 144(4)
P(1)-F(3)-F(4)-F(2) 162(4)
F(2)-F(3)-F(4)-F(7) 155(4)
F(5)-F(3)-F(4)-F(7) -61(2)
P(1)-F(3)-F(4)-F(7) -42.7(1)
F(2)-F(3)-F(4)-P(1) -162(4)
F(5)-F(3)-F(4)-P(1) -18.20(18)
F(2)-F(3)-F(5)-P(1) 35(3)
F(4)-F(3)-F(5)-P(1) 16.30(16)
P(1)-F(3)-F(5)-F(2) -35(3)
F(4)-F(3)-F(5)-F(2) -19(2)
F(2)-F(3)-F(5)-F(8) 94(3)
P(1)-F(3)-F(5)-F(8) 58.3(6)
F(4)-F(3)-F(5)-F(8) 74.70(18)
F(6)-P(1)-F(5)-F(3) 60.80(14)
F(6)#3-P(1)-F(5)-F(3) 64.80(12)
F(3)#3-P(1)-F(5)-F(3)-93.60(14)
F(5)#3-P(1)-F(5)-F(3)-62.80(11)
F(9)#3-P(1)-F(5)-F(3)131.80(16)
F(9)-P(1)-F(5)-F(3) 44(4)
F(4)-P(1)-F(5)-F(3) -11.90(12)
F(4)#3-P(1)-F(5)-F(3)-132.3(2)
F(8)-P(1)-F(5)-F(3) 94.20(14)
F(8)#3-P(1)-F(5)-F(3) -170(2)
F(6)-P(1)-F(5)-F(2) 71.6(9)
F(6)#3-P(1)-F(5)-F(2) 175.7(7)
F(3)#3-P(1)-F(5)-F(2) -82.8(7)
F(3)-P(1)-F(5)-F(2) 10.80(11)
F(5)#3-P(1)-F(5)-F(2) -52.0(5)
F(9)#3-P(1)-F(5)-F(2)142.60(12)
F(9)-P(1)-F(5)-F(2) 54(4)
F(4)-P(1)-F(5)-F(2) -1.0(8)
F(4)#3-P(1)-F(5)-F(2) -121.5(9)
F(8)-P(1)-F(5)-F(2) 105.00(11)
F(8)#3-P(1)-F(5)-F(2) -159(2)
F(6)-P(1)-F(5)-F(8) -33.40(11)
F(6)#3-P(1)-F(5)-F(8) 70.6(1)
F(3)#3-P(1)-F(5)-F(8) 172.2(1)
F(3)-P(1)-F(5)-F(8) -94.20(14)
F(5)#3-P(1)-F(5)-F(8) -157.0(1)
F(9)#3-P(1)-F(5)-F(8) 37.6(9)
F(9)-P(1)-F(5)-F(8) -51(4)
F(4)-P(1)-F(5)-F(8) -106.1(1)
F(4)#3-P(1)-F(5)-F(8)133.50(12)
F(8)#3-P(1)-F(5)-F(8) 96(3)
F(4)-F(2)-F(5)-F(3) 143(4)
P(1)-F(2)-F(5)-F(3) 140(4)
F(4)-F(2)-F(5)-P(1) 2.70(19)
F(3)-F(2)-F(5)-P(1) -140(4)
F(4)-F(2)-F(5)-F(8) 58(2)
F(3)-F(2)-F(5)-F(8) -85(4)
P(1)-F(2)-F(5)-F(8) 55.3(7)
F(8)-F(1)-F(6)-F(7) 49(8)
P(1)-F(1)-F(6)-F(7) 43(5)
F(8)-F(1)-F(6)-F(9) -31(6)
F(7)-F(1)-F(6)-F(9) -80(5)
P(1)-F(1)-F(6)-F(9) -37(2)
F(8)-F(1)-F(6)-P(1) 6(4)
F(7)-F(1)-F(6)-P(1) -43(5)
F(7)-F(1)-F(6)-F(8) -49(8)
P(1)-F(1)-F(6)-F(8) -6(4)
F(6)#3-P(1)-F(6)-F(7) 128(2)
F(3)#3-P(1)-F(6)-F(7) 19(2)
F(3)-P(1)-F(6)-F(7) -98(2)
F(5)#3-P(1)-F(6)-F(7) 8(2)
F(5)-P(1)-F(6)-F(7) -128(2)

F(9)#3-P(1)-F(6)-F(7)	177(2)	F(2)-F(4)-F(7)-P(1)	49.30(17)
F(9)-P(1)-F(6)-F(7)	47(2)	F(3)-F(4)-F(7)-P(1)	40.2(8)
F(4)-P(1)-F(6)-F(7)	-43(2)	F(8)-F(1)-F(7)-F(6)	-141(6)
F(4)#3-P(1)-F(6)-F(7)	172(3)	P(1)-F(1)-F(7)-F(6)	-132(6)
F(8)-P(1)-F(6)-F(7)	-162(2)	F(8)-F(1)-F(7)-F(9)	-68(3)
F(8)#3-P(1)-F(6)-F(7)	69(2)	F(6)-F(1)-F(7)-F(9)	73(6)
F(6)#3-P(1)-F(6)-F(1)	-71.8(1)	P(1)-F(1)-F(7)-F(9)	-58.90(14)
F(3)#3-P(1)-F(6)-F(1)	178.7(1)	F(8)-F(1)-F(7)-F(4)	45(3)
F(3)-P(1)-F(6)-F(1)	61.40(13)	F(6)-F(1)-F(7)-F(4)	-174(6)
F(5)#3-P(1)-F(6)-F(1)	167.70(12)	P(1)-F(1)-F(7)-F(4)	54.0(8)
F(5)-P(1)-F(6)-F(1)	31.90(15)	F(8)-F(1)-F(7)-P(1)	-9(3)
F(9)#3-P(1)-F(6)-F(1)	-23.50(14)	F(6)-F(1)-F(7)-P(1)	132(6)
F(9)-P(1)-F(6)-F(1)	-153.20(19)	F(6)#3-P(1)-F(7)-F(6)	-58(3)
F(4)-P(1)-F(6)-F(1)	117.30(13)	F(3)#3-P(1)-F(7)-F(6)	-165.3(2)
F(4)#3-P(1)-F(6)-F(1)	-28(4)	F(3)-P(1)-F(7)-F(6)	87(2)
F(8)-P(1)-F(6)-F(1)	-2.10(14)	F(5)#3-P(1)-F(7)-F(6)	-172(2)
F(8)#3-P(1)-F(6)-F(1)	-130.9(2)	F(5)-P(1)-F(7)-F(6)	69(2)
F(6)#3-P(1)-F(6)-F(9)	81.40(11)	F(9)#3-P(1)-F(7)-F(6)	-4(2)
F(3)#3-P(1)-F(6)-F(9)	-28.1(2)	F(9)-P(1)-F(7)-F(6)	-106(3)
F(3)-P(1)-F(6)-F(9)	-145.40(12)	F(4)-P(1)-F(7)-F(6)	127(2)
F(5)#3-P(1)-F(6)-F(9)	-39.1(1)	F(4)#3-P(1)-F(7)-F(6)	-174(3)
F(5)-P(1)-F(6)-F(9)	-174.90(12)	F(8)-P(1)-F(7)-F(6)	16(2)
F(9)#3-P(1)-F(6)-F(9)	129.70(14)	F(8)#3-P(1)-F(7)-F(6)	-102(2)
F(4)-P(1)-F(6)-F(9)	-89.40(13)	F(6)-P(1)-F(7)-F(9)	106(3)
F(4)#3-P(1)-F(6)-F(9)	126(3)	F(6)#3-P(1)-F(7)-F(9)	48.10(19)
F(8)-P(1)-F(6)-F(9)	151.10(13)	F(3)#3-P(1)-F(7)-F(9)	-58.9(2)
F(8)#3-P(1)-F(6)-F(9)	22.30(12)	F(3)-P(1)-F(7)-F(9)	-167.10(17)
F(6)#3-P(1)-F(6)-F(8)	-69.7(9)	F(5)#3-P(1)-F(7)-F(9)	-65.50(17)
F(3)#3-P(1)-F(6)-F(8)	-179.2(1)	F(5)-P(1)-F(7)-F(9)	175.40(15)
F(3)-P(1)-F(6)-F(8)	63.5(1)	F(9)#3-P(1)-F(7)-F(9)	103(2)
F(5)#3-P(1)-F(6)-F(8)	169.8(9)	F(4)-P(1)-F(7)-F(9)	-126(2)
F(5)-P(1)-F(6)-F(8)	34.00(11)	F(4)#3-P(1)-F(7)-F(9)	-67(4)
F(9)#3-P(1)-F(6)-F(8)	-21.4(1)	F(8)-P(1)-F(7)-F(9)	122.30(18)
F(9)-P(1)-F(6)-F(8)	-151.10(13)	F(8)#3-P(1)-F(7)-F(9)	3.90(17)
F(4)-P(1)-F(6)-F(8)	119.4(1)	F(6)-P(1)-F(7)-F(4)	-127(2)
F(4)#3-P(1)-F(6)-F(8)	-26(3)	F(6)#3-P(1)-F(7)-F(4)	174.4(9)
F(8)#3-P(1)-F(6)-F(8)	-128.9(1)	F(3)#3-P(1)-F(7)-F(4)	67.4(1)
F(1)-F(6)-F(7)-F(9)	-110(5)	F(3)-P(1)-F(7)-F(4)	-40.7(1)
P(1)-F(6)-F(7)-F(9)	-67.30(14)	F(5)#3-P(1)-F(7)-F(4)	60.9(9)
F(8)-F(6)-F(7)-F(9)	-91(3)	F(5)-P(1)-F(7)-F(4)	-58.20(14)
F(1)-F(6)-F(7)-F(4)	7(6)	F(9)#3-P(1)-F(7)-F(4)	-131.1(1)
F(9)-F(6)-F(7)-F(4)	117(2)	F(9)-P(1)-F(7)-F(4)	126(2)
P(1)-F(6)-F(7)-F(4)	49.40(15)	F(4)#3-P(1)-F(7)-F(4)	59(4)
F(8)-F(6)-F(7)-F(4)	26(4)	F(8)-P(1)-F(7)-F(4)	-111.3(1)
F(9)-F(6)-F(7)-F(1)	110(5)	F(8)#3-P(1)-F(7)-F(4)	130.3(1)
P(1)-F(6)-F(7)-F(1)	43(5)	F(6)-P(1)-F(7)-F(1)	-12.7(2)
F(8)-F(6)-F(7)-F(1)	19(3)	F(6)#3-P(1)-F(7)-F(1)	-71.0(1)
F(1)-F(6)-F(7)-P(1)	-43(5)	F(3)#3-P(1)-F(7)-F(1)	-178.0(7)
F(9)-F(6)-F(7)-P(1)	67.30(14)	F(3)-P(1)-F(7)-F(1)	73.9(9)
F(8)-F(6)-F(7)-P(1)	-23(3)	F(5)#3-P(1)-F(7)-F(1)	175.5(1)
F(2)-F(4)-F(7)-F(6)	-5(3)	F(5)-P(1)-F(7)-F(1)	56.30(13)
P(1)-F(4)-F(7)-F(6)	-55(2)	F(9)#3-P(1)-F(7)-F(1)	-16.5(1)
F(3)-F(4)-F(7)-F(6)	-14(3)	F(9)-P(1)-F(7)-F(1)	-119(2)
F(2)-F(4)-F(7)-F(9)	104(3)	F(4)-P(1)-F(7)-F(1)	114.60(11)
P(1)-F(4)-F(7)-F(9)	54.80(16)	F(4)#3-P(1)-F(7)-F(1)	174(3)
F(3)-F(4)-F(7)-F(9)	95(2)	F(8)-P(1)-F(7)-F(1)	3.3(1)
F(2)-F(4)-F(7)-F(1)	-3(2)	F(8)#3-P(1)-F(7)-F(1)	-115.1(1)
P(1)-F(4)-F(7)-F(1)	-52.8(7)	F(6)-F(1)-F(8)-P(1)	-6(4)
F(3)-F(4)-F(7)-F(1)	-12.50(13)	F(7)-F(1)-F(8)-P(1)	8(2)

F(7)-F(1)-F(8)-F(6)	14(2)
P(1)-F(1)-F(8)-F(6)	6(4)
F(6)-F(1)-F(8)-F(5)	-41(5)
F(7)-F(1)-F(8)-F(5)	-28(4)
P(1)-F(1)-F(8)-F(5)	-35.50(16)
F(6)-P(1)-F(8)-F(1)	2.30(15)
F(6)#3-P(1)-F(8)-F(1)	109.50(17)
F(3)#3-P(1)-F(8)-F(1)	180(100)
F(3)-P(1)-F(8)-F(1)	-108.80(18)
F(5)#3-P(1)-F(8)-F(1)	-26(3)
F(5)-P(1)-F(8)-F(1)	-145(2)
F(9)#3-P(1)-F(8)-F(1)	141(3)
F(9)-P(1)-F(8)-F(1)	24.70(18)
F(4)-P(1)-F(8)-F(1)	-57.70(18)
F(4)#3-P(1)-F(8)-F(1)	176.80(16)
F(8)#3-P(1)-F(8)-F(1)	59.40(15)
F(6)#3-P(1)-F(8)-F(6)	107.20(12)
F(3)#3-P(1)-F(8)-F(6)	177(3)
F(3)-P(1)-F(8)-F(6)	-111.1(9)
F(5)#3-P(1)-F(8)-F(6)	-28(3)
F(5)-P(1)-F(8)-F(6)	-147.10(11)
F(9)#3-P(1)-F(8)-F(6)	138(2)
F(9)-P(1)-F(8)-F(6)	22.3(1)
F(4)-P(1)-F(8)-F(6)	-60.1(9)
F(4)#3-P(1)-F(8)-F(6)	174.4(8)
F(8)#3-P(1)-F(8)-F(6)	57.0(7)
F(6)-P(1)-F(8)-F(5)	147.10(11)
F(6)#3-P(1)-F(8)-F(5)	-105.7(1)
F(3)#3-P(1)-F(8)-F(5)	-36(4)
F(3)-P(1)-F(8)-F(5)	35.9(6)
F(5)#3-P(1)-F(8)-F(5)	119(2)
F(9)#3-P(1)-F(8)-F(5)	-74.5(2)
F(9)-P(1)-F(8)-F(5)	169.40(11)
F(4)-P(1)-F(8)-F(5)	87.0(9)
F(4)#3-P(1)-F(8)-F(5)	-38.5(9)
F(8)#3-P(1)-F(8)-F(5)	-155.9(1)
F(7)-F(6)-F(8)-F(1)	-147(6)
F(9)-F(6)-F(8)-F(1)	156(5)
P(1)-F(6)-F(8)-F(1)	-173(4)
F(7)-F(6)-F(8)-P(1)	27(3)
F(1)-F(6)-F(8)-P(1)	173(4)
F(9)-F(6)-F(8)-P(1)	-31.10(14)
F(7)-F(6)-F(8)-F(5)	-2(4)
F(1)-F(6)-F(8)-F(5)	144(5)
F(9)-F(6)-F(8)-F(5)	-59.80(17)
F(6)-P(1)-F(9)-F(7)	-35.30(14)
F(6)#3-P(1)-F(9)-F(7)	-137.2(2)
F(3)#3-P(1)-F(9)-F(7)	123.6(2)
F(3)-P(1)-F(9)-F(7)	18(2)
F(5)#3-P(1)-F(9)-F(7)	99(2)
F(5)-P(1)-F(9)-F(7)	-15(5)
F(9)#3-P(1)-F(9)-F(7)	-96.0(2)
F(4)-P(1)-F(9)-F(7)	41.9(2)
F(4)#3-P(1)-F(9)-F(7)	159.9(2)
F(8)-P(1)-F(9)-F(7)	-61.9(2)
F(8)#3-P(1)-F(9)-F(7)	-173(3)
F(6)#3-P(1)-F(9)-F(6)	-101.9(1)
F(3)#3-P(1)-F(9)-F(6)	158.9(1)
F(3)-P(1)-F(9)-F(6)	53.6(2)
F(5)#3-P(1)-F(9)-F(6)	134.2(2)
F(5)-P(1)-F(9)-F(6)	20(5)
F(9)#3-P(1)-F(9)-F(6)	-60.8(9)
F(4)-P(1)-F(9)-F(6)	77.2(1)
F(4)#3-P(1)-F(9)-F(6)	-164.9(1)
F(8)-P(1)-F(9)-F(6)	-26.60(12)
F(8)#3-P(1)-F(9)-F(6)	-138(2)
F(8)-F(6)-F(9)-F(7)	128(3)
P(1)-F(6)-F(9)-F(7)	99(2)
F(1)-F(6)-F(9)-F(7)	138(3)
F(1)-F(7)-F(9)-P(1)	51.8(1)
F(4)-F(7)-F(9)-P(1)	-49.70(13)
F(6)-F(7)-F(9)-P(1)	67.80(17)
P(1)-F(7)-F(9)-F(6)	-67.80(17)
F(1)-F(7)-F(9)-F(6)	-15.90(13)
F(4)-F(7)-F(9)-F(6)	-117(2)
F(2)-F(5)-F(8)-F(6)	-27.10(12)
P(1)-F(5)-F(8)-F(6)	28.6(8)
F(3)-F(5)-F(8)-F(6)	-43.10(15)
F(2)-F(5)-F(8)-P(1)	-55.7(6)
F(3)-F(5)-F(8)-P(1)	-71.80(11)
F(2)-F(5)-F(8)-F(1)	-14(2)
P(1)-F(5)-F(8)-F(1)	42(2)
F(3)-F(5)-F(8)-F(1)	-30(3)
P(1)-F(6)-F(8)-F(5)	-28.7(9)
F(7)-F(6)-F(9)-P(1)	-99(2)
F(1)-F(6)-F(9)-P(1)	39(2)
F(8)-F(6)-F(9)-P(1)	29.00(13)

Symmetry transformations used to generate equivalent atoms:

#1 -x,y,-z+3/2

#2 -x,-y,-z+2

#3 -x+1,y,-z+3/2

Crystal data and structure refinement for complex **3** sans le solvent: $C_6H_{16}S_4AgSbF_6$.

Identification code	Ande26	
Empirical formula	$C_6H_{16}S_4AgSbF_6$	
Formula weight	560.05	
Temperature	100(2)K	
Wavelength	1.54178 Å	
Crystal system	Monoclinic	
Space group	C2/c	
Unit cell dimensions	a = 13.2985(4) Å	α = 90°
	b = 16.1208(4) Å	β = 95.883(2)°
	c = 8.9804(3) Å	γ = 90°
Volume	1915.1(1)Å^3	
Z	4	
Density (calculated)	1.942 Mg/m^3	
Absorption coefficient	23.835 mm^{-1}	
F(000)	1072	
Crystal size	0.14 x 0.11 x 0.09 mm	
Theta range for data collection	4.32 to 72.78°	
Index ranges	$-16 \le h \le 16$, $-19 \le k \le 19$, $-8 \le \ell \le 10$	
Reflections collected	11575	
Independent reflections	1851 [R_{int} = 0.045]	
Absorption correction	Semi-empirical from equivalents	
Max. and min. transmission	0.117 and 0.082	
Refinement method	Full-matrix least-squares on F^2	
Data / restraints / parameters	1851 / 0 / 90	
Goodness-of-fit on F^2	0.961	
Final R indices [I>2sigma(I)]	R_1 = 0.0379, wR_2 = 0.1135	
R indices (all data)	R_1 = 0.0394, wR_2 = 0.1148	
Largest diff. peak and hole	1.244 and -1.564 e/Å^3	

Table 2. Atomic coordinates (x 10^4) and equivalent isotropic displacement parameters ($Å^2$ x 10^3) for $C_6H_{16}S_4AgSbF_6$. U_{eq} is defined as one third of the trace of the orthogonalized Uij tensor.

	x	y	z	U_{eq}
Ag(1)	0	844(1)	2500	21(1)
Sb(1)	7500	2500	5000	17(1)
S(1)	-1272(1)	1607(1)	667(1)	19(1)
S(2)	1156(1)	-64(1)	989(1)	20(1)
F(1)	6821(4)	2112(3)	3226(5)	74(2)
F(2)	8116(4)	3312(3)	3947(6)	78(2)
F(3)	8569(3)	1767(2)	4814(6)	56(1)
C(11)	-878(3)	1158(3)	-1039(5)	19(1)
C(12)	-894(4)	2675(3)	480(6)	28(1)
C(21)	2419(4)	-42(3)	1931(7)	31(1)

Table 3. Hydrogen coordinates (x 10^4) and isotropic displacement parameters ($Å^2$ x 10^3) for $C_6H_{16}S_4AgSbF_6$.

	x	y	z	U_{eq}
H(11A)	-1252	1418	-1929	22
H(11B)	-146	1247	-1087	22
H(12A)	-168	2700	379	42
H(12B)	-1040	2987	1370	42
H(12C)	-1270	2918	-410	42
H(21A)	2414	-270	2942	46
H(21B)	2664	531	1994	46
H(21C)	2866	-377	1368	46

Table 4. Anisotropic parameters ($Å^2$ x 10^3) for $C_6H_{16}S_4AgSbF_6$. The anisotropic displacement factor exponent takes the form: $-2\pi^2 [h^2 a^{*2} U_{11} + ... + 2 h k a^* b^* U_{12}]$

	U11	U22	U33	U23	U13	U12
Ag(1)	20(1)	22(1)	19(1)	0	0(1)	0
Sb(1)	15(1)	17(1)	20(1)	0(1)	-1(1)	5(1)
S(1)	16(1)	21(1)	21(1)	-2(1)	2(1)	3(1)
S(2)	16(1)	19(1)	25(1)	-2(1)	0(1)	2(1)
F(1)	93(4)	73(3)	46(3)	-31(2)	-41(2)	24(3)
F(2)	76(3)	56(3)	107(4)	41(3)	39(3)	-6(2)
F(3)	28(2)	44(2)	94(3)	-21(2)	0(2)	16(2)
C(11)	20(2)	18(2)	18(2)	0(2)	3(2)	0(2)
C(12)	30(3)	20(2)	32(3)	-2(2)	-3(2)	2(2)
C(21)	18(2)	32(3)	41(3)	0(2)	-2(2)	0(2)

Table 5. Bond lengths [Å] and angles [°] for $C_6H_{16}S_4AgSbF_6$

Ag(1)-S(1)#1	2.5519(11)
Ag(1)-S(1)	2.5519(11)
Ag(1)-S(2)#1	2.6022(11)
Ag(1)-S(2)	2.6022(11)
Sb(1)-F(2)#2	1.855(4)
Sb(1)-F(2)	1.855(4)
Sb(1)-F(1)	1.858(4)
Sb(1)-F(1)#2	1.858(4)
Sb(1)-F(3)#2	1.870(3)
Sb(1)-F(3)	1.870(3)
S(1)-C(12)	1.807(5)
S(1)-C(11)	1.819(5)
S(2)-C(21)	1.802(5)
S(2)-C(11)#3	1.803(4)
C(11)-S(2)#3	1.803(4)
S(1)#1-AG1-S(1)	122.38(5)
S(1)#1-AG1-S(2)#1	108.81(3)
S(1)-AG1-S(2)#1	102.68(3)
S(1)#1-AG1-S(2)	102.68(3)
S(1)-AG1-S(2)	108.81(3)
S(2)#1-AG1-S(2)	111.58(5)
F(2)#2-SB1-F(2)	180.0(2)
F(2)#2-SB1-F(1)	89.9(3)
F(2)-SB1-F(1)	90.1(3)
F(2)#2-SB1-F(1)#2	90.1(3)
F(2)-SB1-F(1)#2	89.9(3)
F(1)-SB1-F(1)#2	180.00(1)
F(2)#2-SB1-F(3)#2	91.2(2)
F(2)-SB1-F(3)#2	88.8(2)
F(1)-SB1-F(3)#2	89.0(2)
F(1)#2-SB1-F(3)#2	91.0(2)
F(2)#2-SB1-F(3)	88.8(2)
F(2)-SB1-F(3)	91.2(2)
F(1)-SB1-F(3)	91.0(2)
F(1)#2-SB1-F(3)	89.0(2)
F(3)#2-SB1-F(3)	180.0(3)
C(12)-S(1)-C(11)	101.2(2)
C(12)-S(1)-AG1	110.32(18)
C(11)-S(1)-AG1	97.07(15)
C(21)-S(2)-C(11)#3	101.0(2)
C(21)-S(2)-AG1	108.47(19)
C(11)#3-S(2)-AG1	113.79(15)
S(2)#3-C(11)-S(1)	106.9(2)

Symmetry transformations used to generate equivalent atoms:

#1 -x,y,-z+1/2 #2 -x+3/2,-y+1/2,-z+1
#3 -x,-y,-z

Table 6. Torsion angles [°] for $C_6H_{16}S_4AgSbF_6$.

S(1)#1-AG1-S(1)-C(12)	16.9(2)
S(2)#1-AG1-S(1)-C(12)	139.2(2)
S(2)-AG1-S(1)-C(12)	-102.4(2)
S(1)#1-AG1-S(1)-C(11)	121.7(2)
S(2)#1-AG1-S(1)-C(11)	-116.0(1)
S(2)-AG1-S(1)-C(11)	2.34(15)
S(1)#1-AG1-S(2)-C(21)	11.8(2)
S(1)-AG1-S(2)-C(21)	142.84(19)
S(2)#1-AG1-S(2)-C(21)	-104.6(2)
S(1)#1-AG1-S(2)-C(11)#3	123.3(2)
S(1)-AG1-S(2)-C(11)#3	-105.6(2)
S(2)#1-AG1-S(2)-C(11)#3	6.95(16)
C(12)-S(1)-C(11)-S(2)#3	177.5(2)
AG1-S(1)-C(11)-S(2)#3	65.1(2)

Symmetry transformations used to generate equivalent atoms:

#1 -x,y,-z+1/2 #2 -x+3/2,-y+1/2,-z+1
#3 -x,-y,-z

Crystal data and structure refinement for complex **4**: $C_{7.5}H_{20}S_5AgBF_4$.

Identification code	Ande29
Empirical formula	C7.5 H20 Ag B F4 S5
Formula weight	465.21
Temperature	100(2)K
Wavelength	1.54178 Å
Crystal system	Monoclinic
Space group	C2/c
Unit cell dimensions	a = 16.7916(9) Å α = 90°
	b = 9.1090(4) Å β = 99.676(4)°
	c = 22.6704(11) Å γ = 90°
Volume	3418.2(3)Å^3
Z	8
Density (calculated)	1.808 Mg/m^3
Absorption coefficient	15.393 mm^{-1}
F(000)	1864
Crystal size	0.32 x 0.16 x 0.13 mm
Theta range for data collection	3.96 to 72.85°
Index ranges	$-18 \le h \le 20$, $-11 \le k \le 11$, $-27 \le \ell \le 27$
Reflections collected	20609
Independent reflections	3283 [R_{int} = 0.062]
Absorption correction	Semi-empirical from equivalents
Max. and min. transmission	0.135 and 0.043
Refinement method	Full-matrix least-squares on F^2
Data / restraints / parameters	3283 / 47 / 207
Goodness-of-fit on F^2	0.932
Final R indices [I>2sigma(I)]	R_1 = 0.0580, wR_2 = 0.1528
R indices (all data)	R_1 = 0.0601, wR_2 = 0.1549
Largest diff. peak and hole	1.623 and -2.041 e/Å^3

Table 2. Atomic coordinates (x 10^4) and equivalent isotropic displacement parameters ($Å^2$ x 10^3) for $C_{7.5}H_{20}S_5AgBF_4$. U_{eq} is defined as one third of the trace of the orthogonalized Uij tensor.

	Occ.	x	y	z	U_{eq}
Ag(1)	1	1321(1)	1262(1)	1692(1)	36(1)
S(1)	1	2830(1)	699(2)	1886(1)	37(1)
S(2)	1	630(1)	-1039(1)	2086(1)	37(1)
S(3)	1	1099(1)	3353(1)	2449(1)	31(1)
C(21)	1	0	20(8)	2500	38(2)
C(22)	1	-135(5)	-1718(8)	1497(4)	53(2)
C(31)	1	2125(4)	3970(6)	2721(3)	41(2)
C(32)	1	716(4)	4889(6)	1984(3)	33(1)
C(11)	1	3109(5)	155(9)	1188(4)	58(2)
S(4)	0.723(2)	609(1)	1558(2)	624(1)	38(1)
S(5)	0.723(2)	-647(2)	3636(2)	-70(1)	44(1)
C(41)	0.723(2)	-65(5)	3117(9)	634(3)	38(2)
C(42)	0.723(2)	-1356(5)	2117(12)	-208(5)	52(2)
C(43)	0.723(2)	1324(6)	2310(60)	188(6)	52(2)
S(4A)	0.277(2)	664(3)	2470(6)	733(2)	38(1)
S(5A)	0.277(2)	-814(4)	2181(6)	-253(2)	44(1)
C(41A)	0.277(2)	-189(11)	1361(19)	394(7)	38(2)
C(42A)	0.277(2)	-1342(14)	3540(30)	123(11)	52(2)
C(43A)	0.277(2)	1278(12)	2310(160)	150(12)	52(2)
B(1)	0.680(5)	2879(5)	5324(10)	1203(4)	31(2)
F(1)	0.680(5)	2233(4)	6053(8)	1378(3)	47(1)
F(2)	0.680(5)	3571(4)	6181(7)	1290(3)	57(1)
F(3)	0.680(5)	2675(5)	5105(9)	580(3)	74(2)
F(4)	0.680(5)	3014(6)	3978(9)	1458(5)	100(3)
B(1A)	0.320(5)	2741(11)	5418(18)	1357(7)	31(2)
F(1A)	0.320(5)	3245(7)	5504(14)	1896(5)	47(1)
F(2A)	0.320(5)	2414(9)	4041(14)	1320(6)	57(1)
F(3A)	0.320(5)	3154(10)	5560(20)	883(7)	74(2)
F(4A)	0.320(5)	2159(14)	6500(20)	1289(14)	100(3)

Table 3. Hydrogen coordinates (x 10^4) and isotropic displacement parameters ($Å^2$ x 10^3) for $C_{7.5}H_{20}S_5AgBF_4$.

	Occ.	x	y	z	U_{eq}
H(21A)	1	-352	663	2216	46
H(21X)	0.00	352	663	2784	46
H(22A)	1	-527	-2303	1670	79
H(22B)	1	118	-2332	1224	79
H(22C)	1	-411	-889	1274	79
H(31A)	1	2409	3214	2992	49
H(31B)	1	2415	4070	2377	49
H(32A)	1	733	5777	2230	50
H(32B)	1	157	4692	1795	50
H(32C)	1	1050	5034	1673	50
H(11A)	1	3659	-242	1260	87
H(11B)	1	3086	1009	923	87
H(11C)	1	2733	-599	1000	87
H(41A)	0.723(2)	-443	2890	913	45
H(41B)	0.723(2)	262	3973	798	45
H(42A)	0.723(2)	-1057	1192	-205	77
H(42B)	0.723(2)	-1699	2246	-599	77
H(42C)	0.723(2)	-1694	2093	105	77
H(43A)	0.723(2)	1030	2824	-163	78
H(43B)	0.723(2)	1646	1517	57	78
H(43C)	0.723(2)	1682	3007	435	78
H(41C)	0.277(2)	16	408	273	45
H(41D)	0.277(2)	-532	1157	700	45
H(42D)	0.277(2)	-1373	3203	529	77
H(42E)	0.277(2)	-1889	3681	-100	77
H(42F)	0.277(2)	-1048	4476	145	77
H(43D)	0.277(2)	1515	1329	161	78
H(43E)	0.277(2)	1710	3048	215	78
H(43F)	0.277(2)	940	2477	-241	78

Table 4. Anisotropic parameters ($Å^2$ x 10^3) for $C_{7.5}H_{20}S_5AgBF_4$. The anisotropic displacement factor exponent takes the form: $-2\pi^2 [h^2 a^{*2} U_{11} + ... + 2 h k a^* b^* U_{12}]$

	U11	U22	U33	U23	U13	U12
Ag(1)	33(1)	20(1)	48(1)	0(1)	-12(1)	9(1)
S(1)	31(1)	20(1)	56(1)	6(1)	-8(1)	8(1)
S(2)	33(1)	14(1)	57(1)	-5(1)	-16(1)	3(1)
S(3)	27(1)	14(1)	46(1)	-3(1)	-10(1)	-2(1)
C(21)	38(4)	12(3)	58(5)	0	-7(4)	0
C(22)	55(4)	28(3)	64(4)	-13(3)	-21(3)	-2(3)
C(31)	26(3)	19(3)	70(4)	-8(3)	-11(3)	-3(2)
C(32)	39(3)	15(2)	42(3)	-2(2)	-4(2)	5(2)
C(11)	47(4)	57(5)	63(4)	3(4)	-8(3)	16(3)
S(4)	42(1)	26(1)	42(1)	-7(1)	-8(1)	15(1)
S(5)	68(1)	37(1)	21(1)	3(1)	-11(1)	17(1)
C(41)	52(5)	37(4)	20(3)	-3(3)	-3(3)	23(4)
C(42)	28(4)	67(6)	57(5)	10(4)	0(4)	19(4)
C(43)	51(4)	62(5)	41(4)	-20(5)	0(3)	4(5)
S(4A)	42(1)	26(1)	42(1)	-7(1)	-8(1)	15(1)
S(5A)	68(1)	37(1)	21(1)	3(1)	-11(1)	17(1)
C(41A)	52(5)	37(4)	20(3)	-3(3)	-3(3)	23(4)
C(42A)	28(4)	67(6)	57(5)	10(4)	0(4)	19(4)
C(43A)	51(4)	62(5)	41(4)	-20(5)	0(3)	4(5)
B(1)	32(5)	31(4)	32(6)	2(4)	5(4)	4(3)
F(1)	43(3)	56(4)	38(3)	-8(2)	-3(2)	3(3)
F(2)	51(3)	53(3)	62(3)	-1(3)	-4(3)	-8(2)
F(3)	68(4)	87(5)	62(4)	-27(4)	2(3)	1(4)
F(4)	83(6)	60(5)	163(9)	52(5)	38(6)	25(4)
B(1A)	32(5)	31(4)	32(6)	2(4)	5(4)	4(3)
F(1A)	43(3)	56(4)	38(3)	-8(2)	-3(2)	3(3)
F(2A)	51(3)	53(3)	62(3)	-1(3)	-4(3)	-8(2)
F(3A)	68(4)	87(5)	62(4)	-27(4)	2(3)	1(4)
F(4A)	83(6)	60(5)	163(9)	52(5)	38(6)	25(4)

Table 5. Bond lengths [Å] and angles [°] for $C_{7.5}H_{20}S_5AgBF_4$.

Ag(1)-S(4a)	2.519(5)	C(41)-S(5)-C(42)	101.3(5)
Ag(1)-S(4)	2.528(2)	S(5)-C(41)-S(4)	116.3(4)
Ag(1)-S(1)	2.5502(14)	C(43A)-S(4A)-C(41A)	99(3)
Ag(1)-S(2)	2.6238(16)	C(43A)-S(4A)-AG1	112(2)
Ag(1)-S(3)	2.6325(14)	C(41A)-S(4A)-AG1	108.8(6)
S(1)-C(11)	1.792(8)	C(41A)-S(5A)-C(42A)	99.3(1)
S(1)-C(31)#1	1.805(6)	S(5A)-C(41A)-S(4A)	114.9(1)
S(2)-C(22)	1.800(7)	F(4)-B(1)-F(1)	113.2(8)
S(2)-C(21)	1.807(4)	F(4)-B(1)-F(2)	111.8(8)
S(3)-C(32)	1.805(5)	F(1)-B(1)-F(2)	111.5(7)
S(3)-C(31)	1.819(6)	F(4)-B(1)-F(3)	107.1(8)
C(21)-S(2)#2	1.807(4)	F(1)-B(1)-F(3)	106.6(7)
C(31)-S(1)#3	1.804(6)	F(2)-B(1)-F(3)	106.2(7)
S(4)-C(43)	1.813(19)	F(2A)-B(1A)-F(1A)	106.80(13)
S(4)-C(41)	1.819(7)	F(2A)-B(1A)-F(4A)	112.30(16)
S(5)-C(41)	1.788(7)	F(1A)-B(1A)-F(4A)	112.40(18)
S(5)-C(42)	1.819(11)	F(2A)-B(1A)-F(3A)	106.60(15)
S(4a)-C(43a)	1.81(2)	F(1A)-B(1A)-F(3A)	112.00(15)
S(4a)-C(41a)	1.816(17)	F(4A)-B(1A)-F(3A)	106.80(17)
S(5a)-C(41a)	1.815(15)	C(43)-S(4)-AG1	108.2(4)
S(5a)-C(42a)	1.818(17)	C(43)-S(4)-C(41)	100.40(14)
B(1)-F(4)	1.358(10)	S(1)#3-C(31)-S(3)	113.3(3)
B(1)-F(1)	1.384(9)	S(2)-C(21)-S(2)#2	115.5(4)
B(1)-F(2)	1.387(9)	C(41)-S(4)-AG1	105.5(2)
B(1)-F(3)	1.411(9)	C(31)-S(3)-AG1	102.4(2)
B(1a)-F(2a)	1.365(13)	C(32)-S(3)-AG1	104.79(19)
B(1a)-F(1a)	1.367(13)	C(32)-S(3)-C(31)	100.5(3)
B(1a)-F(4a)	1.375(13)	C(21)-S(2)-AG1	94.7(2)
B(1a)-F(3a)	1.380(13)	C(22)-S(2)-AG1	108.8(3)
S(4A)-AG1-S(4)	19.78(13)	C(22)-S(2)-C(21)	99.3(3)
S(4A)-AG1-S(1)	120.97(14)	C(31)#1-S(1)-AG1	102.6(2)
S(4)-AG1-S(1)	118.85(6)	C(11)-S(1)-AG1	107.6(2)
S(4A)-AG1-S(2)	119.23(14)	C(11)-S(1)-C(31)#1	101.5(4)
S(4)-AG1-S(2)	104.27(6)	S(2)-AG1-S(3)	103.69(5)
S(1)-AG1-S(2)	105.32(4)	S(1)-AG1-S(3)	106.18(5)
S(4)-AG1-S(3)	116.84(5)	S(4A)-AG1-S(3)	99.05(12)

Symmetry transformations used to generate equivalent atoms:
#1 -x+1/2,y-1/2,-z+1/2 #2 -x,y,-z+1/2 #3 -x+1/2,y+1/2,-z+1/2

Table 6. Torsion angles [°] for $C_{7.5}H_{20}S_5AgBF_4$.

S(4A)-AG1-S(1)-C(11)	-36.7(3)
S(4)-AG1-S(1)-C(11)	-14.0(3)
S(2)-AG1-S(1)-C(11)	102.3(3)
S(3)-AG1-S(1)-C(11)	-148.1(3)
S(4A)-AG1-S(1)-C(31)#1	-143.3(3)
S(4)-AG1-S(1)-C(31)#1	-120.6(3)
S(2)-AG1-S(1)-C(31)#1	-4.3(3)
S(3)-AG1-S(1)-C(31)#1	105.3(3)
S(4A)-AG1-S(2)-C(22)	13.8(3)
S(4)-AG1-S(2)-C(22)	-0.2(3)
S(1)-AG1-S(2)-C(22)	-126.1(3)
S(3)-AG1-S(2)-C(22)	122.6(3)
S(4A)-AG1-S(2)-C(21)	-87.75(15)
S(4)-AG1-S(2)-C(21)	-101.76(7)
S(1)-AG1-S(2)-C(21)	132.38(6)
S(3)-AG1-S(2)-C(21)	21.02(6)
S(4A)-AG1-S(3)-C(32)	-8.4(3)
S(4)-AG1-S(3)-C(32)	-17.5(2)
S(1)-AG1-S(3)-C(32)	117.7(2)
S(2)-AG1-S(3)-C(32)	-131.6(2)
S(4A)-AG1-S(3)-C(31)	-112.9(3)
S(4)-AG1-S(3)-C(31)	-122.1(2)
S(1)-AG1-S(3)-C(31)	13.1(2)
S(2)-AG1-S(3)-C(31)	123.9(2)
C(22)-S(2)-C(21)-S(2)#2	72.1(3)
AG1-S(2)-C(21)-S(2)#2	-177.9(1)
C(32)-S(3)-C(31)-S(1)#3	58.0(4)
AG1-S(3)-C(31)-S(1)#3	165.9(3)
S(4A)-AG1-S(4)-C(43)	70.40(17)
S(1)-AG1-S(4)-C(43)	-31.40(16)
S(2)-AG1-S(4)-C(43)	-148.20(16)
S(3)-AG1-S(4)-C(43)	98.10(16)
S(4A)-AG1-S(4)-C(41)	-36.4(5)
S(1)-AG1-S(4)-C(41)	-138.2(3)
S(2)-AG1-S(4)-C(41)	105.0(3)
S(3)-AG1-S(4)-C(41)	-8.7(4)
C(42)-S(5)-C(41)-S(4)	70.6(7)
C(43)-S(4)-C(41)-S(5)	66.3(1)
AG1-S(4)-C(41)-S(5)	178.7(5)
S(4)-AG1-S(4A)-C(43A)	-71(4)
S(1)-AG1-S(4A)-C(43A)	19(4)
S(2)-AG1-S(4A)-C(43A)	-115(4)
S(3)-AG1-S(4A)-C(43A)	134(4)
S(4)-AG1-S(4A)-C(41A)	37.1(7)
S(1)-AG1-S(4A)-C(41A)	126.8(7)
S(2)-AG1-S(4A)-C(41A)	-6.7(7)
S(3)-AG1-S(4A)-C(41A)	-118.1(7)
C(42A)-S(5A)-C(41A)-S(4A)	-74.8(2)
C(43A)-S(4A)-C(41A)-S(5A)	-71(4)
AG1-S(4A)-C(41A)-S(5A)	172.5(8)

Symmetry transformations used to generate equivalent atoms:

#1 -x+1/2,y-1/2,-z+1/2 #2 -x,y,-z+1/2
#3 -x+1/2,y+1/2,-z+1/2

Annexe V

Table S1. Silver-Silver distances, Å, in complexes **1** and **2**.

$[Ag_6(CF_3CO_2)_3(L^{1\text{-}Me})_3(SCH_3)_3]$ (1)

Ag(1)-Ag(5)	2.9644(6)
Ag(1)-Ag(2)	3.1074(5)
Ag(1)-Ag(3)	3.1082(5)
Ag(2)-Ag(4)	2.9390(6)
Ag(2)-Ag(3)	3.0728(5)
Ag(4)-Ag(5)#1	3.3615(6)
Ag(5)-Ag(4)#1	3.3615(6)
Ag(3)-Ag(6)	2.9250(5)

#1: -x+2, -y, -z

$[Ag_6(CF_3CF_2CO_2)_3(L^{1\text{-}Me})_2(SCH_3)_3(H_2O)]$ (2)

Ag(1)-Ag(4)	2.9867(10)
Ag(1)-Ag(5)	3.0121(11)
Ag(1)-Ag(3)	3.0303(11)
Ag(1)-Ag(2)	2.9372(10)
Ag(2)-Ag(3)	2.9908(10)
Ag(4)-Ag(5)	3.3798(11)
Ag(2)-Ag(4)#1	2.9606(11)
Ag(4)-Ag(2)#1	2.9606(11)

#1: -x+1, -y+1 ,-z+2

Table S2. Characteristics of the hydrogen bonds in complex **2**.

D-A	d(D..A), Å	D-H···A, (°)
O(7)-O(2)	2.741(1)	167.3
O(7)-O(2)#2	2.818(1)	160.9

#2: -x+1, -y, -z+2

Table S3. Selected Bond Distances (Å) and Angles (deg) for Complexes **1** and **2**.

$[Ag_6(CF_3CO_2)_3(L^{1\text{-}Me})_3(SCH_3)_3]$ (1).

Ag(1)-S(7)	2.4657(11)	Ag(3)-S(3)	2.6556(14)
Ag(1)-S(5)	2.5041(11)	Ag(6)-S(4)	2.6053(15)
Ag(1)-S(8)	2.5511(13)	Ag(6)-S(5)#1	2.5809(11)
Ag(2)-S(5)	2.4934(12)	Ag(6)-S(7)	2.5729(12)
Ag(2)-O(3)	2.537(5)	Ag(6)-O(7)	2.344(4)
Ag(2)-S(9)	2.5660(11)	Ag(5)-S(6)	2.6148(13)
Ag(2)-S(1)	2.6120(13)	Ag(5)-S(5)	2.5779(12)
Ag(3)-O(4)	2.469(4)	Ag(5)-S(9)#1	2.5515(11)
Ag(3)-S(9)	2.4966(12)	Ag(5)-O(5)	2.438(4)
Ag(3)-S(7)	2.5617(12)	Ag(4)-S(2)	2.6209(15)
Ag(4)-S(9)	2.5530(13)	Ag(4)-S(7)#1	2.5091(12)

Ag(4)-O(11)#1	2.424(5)	S(7)-Ag(1)-S(5)	127.94(4)
S(7)-Ag(1)-S(8)	125.79(5)	S(5)-Ag(1)-S(8)	106.27(4)
S(7)-Ag(1)-Ag(5)	102.24(3)	S(5)-Ag(1)-Ag(5)	55.48(3)
S(8)-Ag(1)-Ag(5)	109.26(3)	S(7)-Ag(1)-Ag(2)	105.65(3)
S(5)-Ag(1)-Ag(2)	51.40(3)	S(8)-Ag(1)-Ag(2)	107.97(4)
Ag(5)-Ag(1)-Ag(2)	103.902(1)	S(7)-Ag(1)-Ag(3)	53.22(3)
S(5)-Ag(1)-Ag(3)	106.39(3)	S(8)-Ag(1)-Ag(3)	115.71(3)
AG5-Ag(1)-Ag(3)	134.89(1)	Ag(2)-Ag(1)-Ag(3)	59.26(1)
S(5)-Ag(2)-O(3)	117.41(14)	S(5)-Ag(2)-S(9)	130.72(4)
O(3)-Ag(2)-S(9)	8.90(13)	S(5)-Ag(2)-S(1)	116.24(4)
O(3)-Ag(2)-S(1)	74.43(11)	S(9)-Ag(2)-S(1)	104.37(4)
S(5)-Ag(2)-Ag(4)	101.95(3)	O(3)-Ag(2)-Ag(4)	140.21(13)
S(9)-Ag(2)-Ag(4)	54.75(3)	S(1)-Ag(2)-Ag(4)	83.61(4)
S(5)-Ag(2)-Ag(3)	107.72(3)	O(3)-Ag(2)-Ag(3)	71.91(11)
S(9)-Ag(2)-Ag(3)	51.61(3)	S(1)-Ag(2)-Ag(3)	133.27(3)
AG4-Ag(2)-Ag(3)	102.63(1)	S(5)-Ag(2)-Ag(1)	51.71(3)
O(3)-Ag(2)-Ag(1)	83.06(11)	S(9)-Ag(2)-Ag(1)	106.43(3)
S(1)-Ag(2)-Ag(1)	144.15(4)	Ag(4)-Ag(2)-Ag(1)	129.67(1)
AG3-Ag(2)-Ag(1)	60.38(1)	O(4)-Ag(3)-S(9)	123.42(11)
O(4)-Ag(3)-S(7)	94.42(12)	S(9)-Ag(3)-S(7)	125.70(4)
O(4)-Ag(3)-S(3)	75.45(13)	S(9)-Ag(3)-S(3)	120.49(4)
S(7)-Ag(3)-S(3)	104.68(4)	O(4)-Ag(3)-Ag(6)	141.95(11)
S(9)-Ag(3)-Ag(6)	94.42(3)	S(7)-Ag(3)-Ag(6)	55.45(3)
S(3)-Ag(3)-Ag(6)	89.39(3)	O(4)-Ag(3)-Ag(2)	81.34(11)
S(9)-Ag(3)-Ag(2)	53.67(3)	S(7)-Ag(3)-Ag(2)	104.22(3)
S(3)-Ag(3)-Ag(2)	143.98(3)	Ag(6)-Ag(3)-Ag(2)	124.97(1)
O(4)-Ag(3)-Ag(1)	65.41(13)	S(9)-Ag(3)-Ag(1)	108.24(3)
S(7)-Ag(3)-Ag(1)	50.43(3)	S(3)-Ag(3)-Ag(1)	128.99(3)
AG6-Ag(3)-Ag(1)	101.60(1)	Ag(2)-Ag(3)-Ag(1)	60.36(1)
O(11)#1-Ag(4)-S(7)#1	107.36(19)	O(11)#1-Ag(4)-S(9)	97.5(2)
S(7)#1-Ag(4)-S(9)	122.12(4)	O(11)#1-Ag(4)-S(2)	85.07(13)
S(7)#1-Ag(4)-S(2)	106.32(4)	S(9)-Ag(4)-S(2)	127.61(4)
O(11)#1-Ag(4)-Ag(2)	143.4(2)	S(7)#1-Ag(4)-Ag(2)	108.11(3)
S(9)-Ag(4)-Ag(2)	55.17(3)	S(2)-Ag(4)-Ag(2)	93.57(4)
O(11)#1-Ag(4)-Ag(5)#1	71.32(14)	S(7)#1-Ag(4)-Ag(5)#1	91.26(3)
S(9)-Ag(4)-Ag(5)#1	48.79(3)	S(2)-Ag(4)-Ag(5)#1	154.06(4)
Ag(2)-Ag(4)-Ag(5)#1	98.99(2)	O(5)-Ag(5)-S(9)#1	115.17(11)
O(5)-Ag(5)-S(5)	121.26(12)	S(9)#1-Ag(5)-S(5)	107.56(4)
O(5)-Ag(5)-S(6)	87.23(13)	S(9)#1-Ag(5)-S(6)	115.88(4)
S(5)-Ag(5)-S(6)	108.61(4)	O(5)-Ag(5)-Ag(1)	76.09(13)
S(9)#1-Ag(5)-Ag(1)	107.69(3)	S(5)-Ag(5)-Ag(1)	53.17(3)
S(6)-Ag(5)-Ag(1)	136.38(3)	O(5)-Ag(5)-Ag(4)#1	76.02(11)
S(9)#1-Ag(5)-Ag(4)#1	48.83(3)	S(5)-Ag(5)-Ag(4)#1	107.77(3)
S(6)-Ag(5)-Ag(4)#1	143.54(3)	Ag(1)-Ag(5)-Ag(4)#1	70.82(1)
O(7)-Ag(6)-S(7)	110.74(15)	O(7)-Ag(6)-S(5)#1	94.26(12)
S(7)-Ag(6)-S(5)#1	112.34(4)	O(7)-Ag(6)-S(4)	100.55(15)
S(7)-Ag(6)-S(4)	124.37(4)	S(5)#1-Ag(6)-S(4)	109.70(4)
O(7)-Ag(6)-Ag(3)	155.52(12)	S(7)-Ag(6)-Ag(3)	55.09(3)
S(5)#1-Ag(6)-Ag(3)	109.43(3)	S(4)-Ag(6)-Ag(3)	77.66(3)

#1 -x+2, -y ,-z #2 -x+1 –y, -z

$[Ag_6(CF_3CF_2CO_2)_3(L^{1\text{-}Me})_2(SCH_3)_3(H_2O)]$ (2).

Ag(1)-O(1)	2.339(7)	Ag(1)-S(4)	2.429(2)
Ag(1)-S(1)	2.443(2)	Ag(2)-O(3)	2.368(7)
Ag(2)-S(7)	2.544(2)	Ag(2)-S(1)	2.553(3)
Ag(2)-S(2)	2.691(3)	Ag(5)-S(7)#1	2.501(2)
Ag(3)-S(4)	2.517(3)	Ag(3)-S(3)	2.526(3)
Ag(3)-S(7)	2.539(2)	Ag(3)-O(5)	2.562(7)
Ag(4)-O(4)#	2.354(7)	Ag(4)-O(10)	2.403(7)
Ag(4)-O(7)	2.385(7)	Ag(4)-S(7)#1	2.501(3)
Ag(4)-S(4)	2.524(3)	Ag(5)-S(1)	2.533(3)
Ag(5)-S(6)	2.510(3)	Ag(6)-S(1)#1	2.522(3)
Ag(6)-S(5)	2.495(3)	Ag(6)-S(4)	2.548(2)
Ag(6)-O(5)	2.534(8)	O(5)-Ag(6)-S(4)	85.80(19)
O(1)-Ag(1)-S(4)	102.7(3)	O(1)-Ag(1)-S(1)	104.2(2)
S(4)-Ag(1)-S(1)	152.08(9)	O(1)-Ag(1)-Ag(2)	104.2(2)
S(4)-Ag(1)-Ag(2)	110.23(6)	S(1)-Ag(1)-Ag(2)	55.73(7)
O(1)-Ag(1)-Ag(4)	120.4(2)	S(4)-Ag(1)-Ag(4)	54.38(6)
S(1)-Ag(1)-Ag(4)	115.34(7)	Ag(2)-Ag(1)-Ag(4)	134.55(3)
O(1)-Ag(1)-Ag(5)	107.5(2)	S(4)-Ag(1)- Ag(5)	122.93(7)
S(1)-Ag(1)-Ag(5)	54.13(7)	Ag(2)-Ag(1)-Ag(5)	107.62(3)
Ag(4)-Ag(1)-Ag(5)	68.58(3)	O(1)-Ag(1)-Ag(3)	97.0(2)
S(4)-Ag(1)-Ag(3)	53.53(6)	S(1)-Ag(1)-Ag(3)	115.45(7)
Ag(2)-Ag(1)-Ag(3)	60.13(2)	Ag(4)-Ag(1)-Ag(3)	103.41(3)
Ag(5)-Ag(1)-Ag(3)	154.96(3)	O(3)-Ag(2)-S(7)	110.6(2)
O(3)-Ag(2)-S(1)	95.0(3)	S(7)-Ag(2)-S(1)	137.36(9)
O(3)-Ag(2)-S(2)	77.6(2)	S(7)-Ag(2)-S(2)	13.52(10)
S(1)-Ag(2)-S(2)	104.72(9)	O(3)-Ag(2)-Ag(1)	143.8(2)
S(7)-Ag(2)-Ag(1)	104.86(6)	S(1)-Ag(2)-Ag(1)	52.28(6)
S(2)-Ag(2)-Ag(1)	94.81(7)	O(3)-Ag(2)-Ag(4)#1	80.90(19)
S(7)-Ag(2)-Ag(4)#1	53.40(6)	S(1)-Ag(2)-Ag(4)#1	100.80(6)
S(2)-Ag(2)-Ag(4)#1	147.76(8)	Ag(1)-Ag(2)-Ag(4)#1	116.49(3)
O(3)-Ag(2)-Ag(3)	150.2(2)	S(7)-Ag(2)-Ag(3)	53.88(6)
S(1)-Ag(2)-Ag(3)	113.36(6)	S(2)-Ag(2)-Ag(3)	86.04(7)
Ag(1)-Ag(2)-Ag(3)	61.48(2)	Ag(4)#1-Ag(2)-Ag(3)	101.65(3)
S(4)-Ag(3)-S(3)	124.85(11)	S(4)-Ag(3)-S(7)	124.19(9)
S(3)-Ag(3)-S(7)	109.08(11)	S(4)-Ag(3)-O(5)	85.86(18)
S(3)-Ag(3)-O(5)	102.2(2)	S(7)-Ag(3)-O(5)	96.74(18)
S(4)-Ag(3)-Ag(2)	106.15(6)	S(3)-Ag(3)-Ag(2)	92.99(8)
S(7)-Ag(3)-Ag(2)	54.03(6)	O(5)-Ag(3)-Ag(2)	150.42(17)
S(4)-Ag(3)-Ag(1)	50.92(5)	S(3)-Ag(3)-Ag(1)	107.90(9)
S(7)-Ag(3)-Ag(1)	102.38(6)	O(5)-Ag(3)-Ag(1)	136.27(17)
Ag(2)-Ag(3)-Ag(1)	58.39(2)	O(4)#1-Ag(4)-O(10)	97.4(3)
O(4)#1-Ag(4)-S(7)#1	115.2(2)	O(10)-Ag(4)-S(7)#1	108.4(2)
O(4)#1-Ag(4)-S(4)	97.3(2)	O(10)-Ag(4)-S(4)	97.4(2)
S(7)#1-Ag(4)-S(4)	134.48(8)	O(4)#1-Ag(4)-Ag(2)#1	81.27(18)
O(10)-Ag(4)-Ag(2)#1	158.7(2)	S(7)#1-Ag(4)-Ag(2)#1	54.74(6)
S(4)-Ag(4)-Ag(2)#1	103.86(6)	O(4)#1-Ag(4)-Ag(1)	148.4(2)

O(10)-Ag(4)-Ag(1)	84.0(2)	S(7)#1-Ag(4)-Ag(1)	93.95(6)
S(4)-Ag(4)-Ag(1)	51.48(5)	Ag(2)#1-Ag(4)-Ag(1)	108.35(3)
O(4)#1-Ag(4)-Ag(5)	155.0(2)	O(10)-Ag(4)-Ag(5)	76.5(2)
S(7)#1-Ag(4)-Ag(5)	47.50(6)	S(4)-Ag(4)-Ag(5)	107.51(6)
Ag(2)#1-Ag(4)-Ag(5)	95.71(3)	Ag(1)-Ag(4)-Ag(5)	56.06(2)
S(7)#1-Ag(5)-S(6)	124.54(10)	S(7)#1-Ag(5)-S(1)	113.71(8)
S(6)-Ag(5)-S(1)	120.93(10)	S(7)#1-Ag(5)-Ag(1)	93.33(6)
S(6)-Ag(5)-Ag(1)	112.82(9)	S(1)-Ag(5)-Ag(1)	51.40(6)
S(7)#1-Ag(5)-Ag(4)	47.49(6)	S(6)-Ag(5)-Ag(4)	110.22(7)
S(1)-Ag(5)-Ag(4)	101.09(6)	Ag(1)-Ag(5)-Ag(4)	55.35(2)
S(5)-Ag(6)-S(1)#1	118.78(9)	S(5)-Ag(6)-O(5)	102.29(18)
S(1)#1-Ag(6)-O(5)	117.53(18)	S(5)-Ag(6)-S(4)	122.00(8)
S(1)#1-Ag(6)-S(4)	106.24(8)	O(5)-Ag(6)-S(4)	85.80(19)

#1 -x+1,-y+1,-z+2 #2 x-1,y,z #3 x+1,y,z

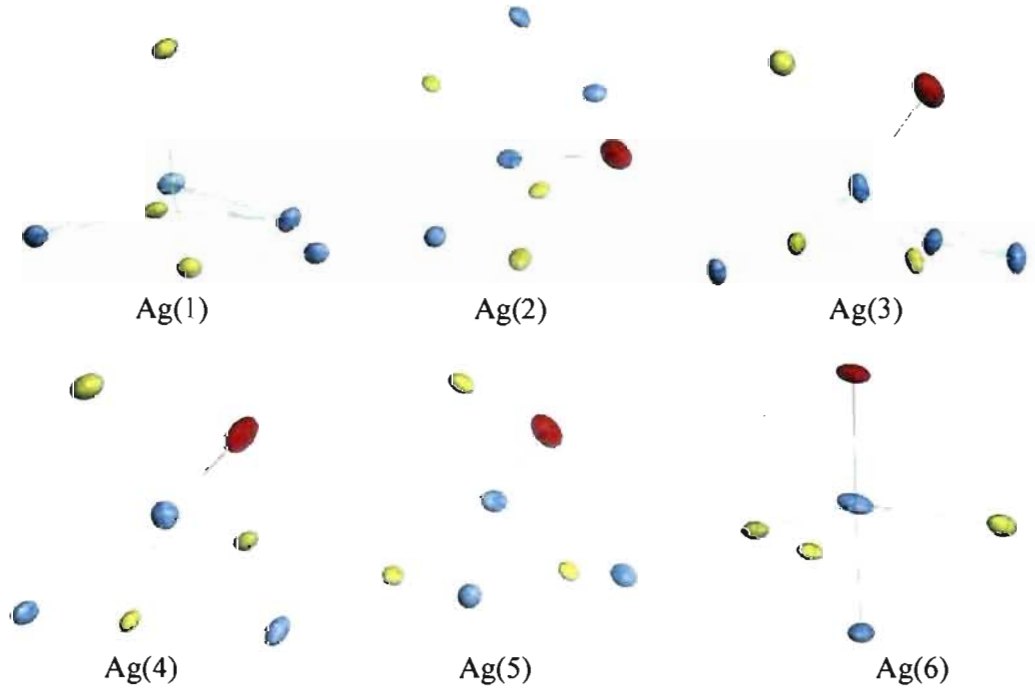

Figure S1. Coordination polyhedra around the silver atoms in cluster **1**. Color code: S: yellow; O: red and Ag: grey.

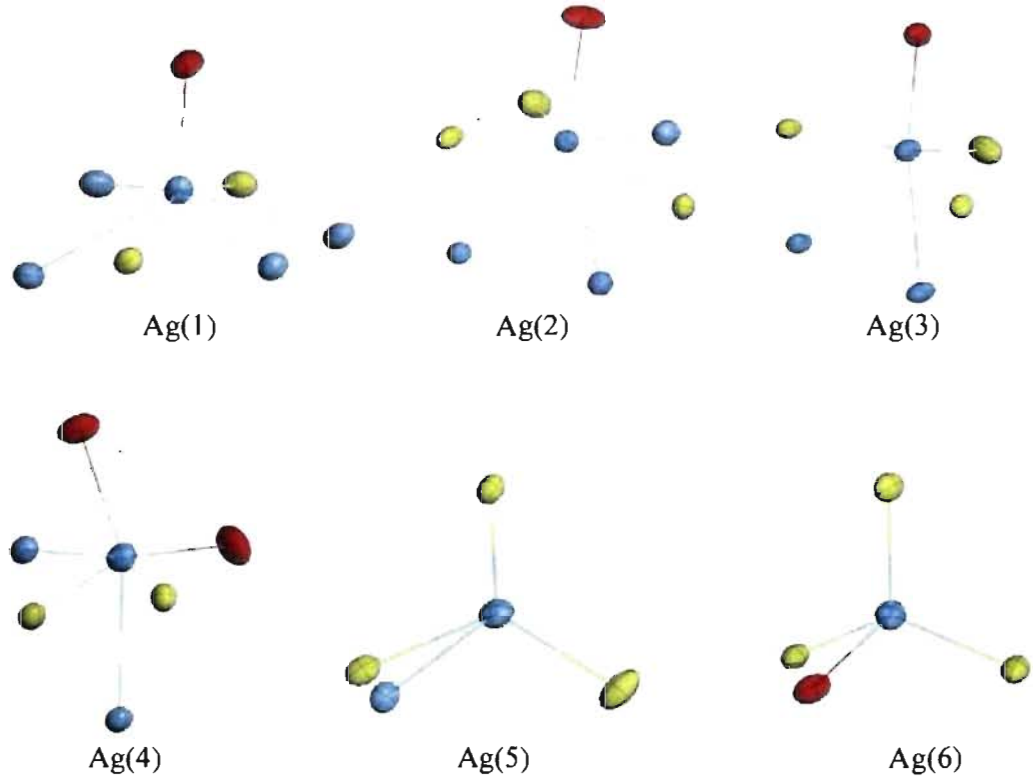

Figure S2. Coordination polyhedra around the silver atoms in cluster **2**. Color code: S: yellow; O: red and Ag: grey.

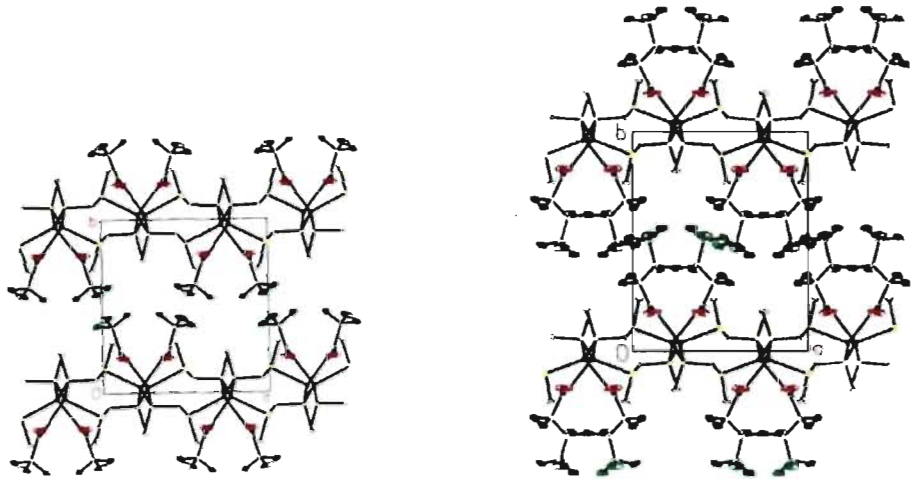

(a) (b)

Figure S3. (a) Polymorph of the trifluoroacetate and (b) structure of the related heptafluorobutyrate. These two complexes are topologically identical.[a]

[a]Awaleh, M.O.; Badia, A.; Brisse, F. *Cryst. Growth Des.* **2006**, *6*, 2674.

Annexe VI

Syntheses of the Ligands. All the ligands were synthesized by the method previously reported in the literature.[a]

1,2-bis(phenylthio)ethane, $\mathbf{L^{2\text{-}Ph}}$, Yield : 43%. Anal. Found: C, 68.25; H, 6.09. Calcd for $C_{14}H_{14}S_2$: C, 68.24; H, 5.73. ^{1}H NMR (acetone-d_6, 300 MHZ): δ 3.14 (s, 4H, -S-$(CH_2)_2$-S-), 7.32-7.60 (m, 10H, C_6H_5-). IR (KBr, cm^{-1}): 3411w, 3055w, 1580s, 1478s, 1436s, 1207m, 1185w, 1152w, 1121w, 1085w, 1071w, 1023m, 893w, 734vs, 714w, 690s, 476m.

1,4-bis(phenylthio)butane, $\mathbf{L^{4\text{-}Ph}}$, Yield : 82%. Anal. Found: C, 69.79; H, 6.65. Calcd for $C_{16}H_{18}S_2$: C, 70.02; H, 6.61. ^{1}H NMR (acetone-d_6, 300 MHz): δ 1.80 (qt, 4H, -S-CH_2-$(CH_2)_2$- CH_2-S-), 3.01 (t, 4H, -S-CH_2-$(CH_2)_2$-CH_2-S-), 7.17-7.45 (m, 10H, C_6H_5-). IR (KBr, cm^{-1}): 3477m, 3054m, 2976m, 2926m, 1937w, 1640w, 1579m, 1479s, 1437s, 1310m, 1196m, 1162m, 1092s, 1070s, 1050s, 1022s, 886m, 685s, 473m, 460m.

1,6-bis(phenylthio)hexane, $\mathbf{L^{6\text{-}Ph}}$, Yield : 87%. Anal. Found: C, 71.43; H, 7.32. Calcd for $C_{18}H_{22}S_2$: C, 71.47; H, 7.33. ^{1}H NMR (acetone-d_6, 400 MHz): δ 1.46 (qt, 4H, -S-$(CH_2)_2$-$(CH_2)_2$-$(CH_2)_2$-S-), 1.63 (qt, 4H, S-CH_2-CH_2-$(CH_2)_2$-CH_2-CH_2-S-), 2.95 (t, 4H, -S-CH_2-$(CH_2)_4$-CH_2-S-), 7.14-7.34 (m, 10H, C_6H_5-). IR (KBr, cm^{-1}): 3436m, 3073w, 3057w, 3018w, 2943w, 2924m, 1937w, 1856w, 1727w, 1635w, 1583m, 1479m, 1458w, 1438m, 1384w, 1356w, 1271m, 1185w, 1163w, 1147w, 1091w, 1071m, 1023m, 947w, 893w, 782w, 765w, 732s, 689m, 614w, 480m, 474m.

1,10-bis(phenylthio)decane, $\mathbf{L^{10\text{-}Ph}}$, Yield : 91%. Anal. Found: C, 73.47; H, 8.59. Calcd for $C_{22}H_{30}S_2$: C, 73.68; H, 8.43. ^{1}H NMR (acetone-d_6, 400 MHz): δ 1.28(t, 4H, -S-$(CH_2)_4$-$(CH_2)_2$-$(CH_2)_4$-S-), 1.30(qt, 4H, -S-$(CH_2)_3$-CH_2-$(CH_2)_2$-CH_2-$(CH_2)_3$-S-), 1.45(qt, 4H, -S-$(CH_2)_2$-CH_2-$(CH_2)_4$-CH_2-$(CH_2)_2$-S-), 1.64(qt, 4H, -S-CH_2-CH_2-$(CH_2)_6$-CH_2-CH_2-S-), 2.97(t, 4H, -S-CH_2-$(CH_2)_8$-CH_2-S-), 7.16-7.35(m, 10H, C_6H_5-). IR (KBr, cm^{-1}): 3466m, 3073m, 2922vs, 2848s, 1938w, 1856w, 1790w, 1730w, 1615s, 1580s, 1470s, 1461s, 1437s, 1377w, 1348w, 1294m, 1232m, 1183w, 1163m, 1146w, 1092s, 1069s, 1022s, 997w, 893s, 839w, 826w, 785w, 731vs, 687vs, 613w, 473s.

[a]Hartley, F. R.; Murray, S. G.; Levason, W.; Soutter, H. E.; McAuliffe, C. A. *Inorg. Chim. Acta*, **1979**, *35*, 265.

Table S1. Comparison of the bond distances (Å) and angles (°) for the silver atoms in the complexes synthesized.

(1) $L^{2\text{-Ph}}$ / CF_3SO_3

Ag(1)-O(41)	2.385(2)	O(41)-Ag(1)-S(2)	113.5(1)
Ag(1)-S(2)	2.482(1)	O(41)-Ag(1)-S(1)	102.1(1)
Ag(1)-S(1)	2.511(1)	S(2)-Ag(1)-S(1)	143.8(1)
Ag(2)-O(31)	2.372(2)	O(31)-Ag(2)-S(1)#1	119.8(1)
Ag(2)-S(1)#1	2.493(1)	O(31)-Ag(2)-S(2)	104.8(1)
Ag(2)-S(2)	2.526(1)	S(1)#1-Ag(2)-S(2)	135.4(1)

#1 x+1, y, z

(2) $L^{2\text{-Ph}}$ / CF_3CO_2

Ag(1)-O(1)	2.279(3)	O(1)-Ag(1)-O(2)#1	122.1(1)
Ag(1)-O(2)#1	2.304(2)	O(1)-Ag(1)-S(1)	125.4(1)
Ag(1)-S(1)	2.495(1)	O(2)#1-Ag(1)-S(1)	112.3(1)
Ag(1)-S(2)	2.834(1)	O(1)-Ag(1)-S(2)	74.3(1)
Ag(1)-Ag(1)#1	3.0813(5)	S(1)-Ag(1)-S(2)	109.0(1)
Ag(2)-O(3)	2.242(3)	O(2)#1-Ag(1)-S(2)	83.6(1)
Ag(2)-O(4)#1	2.304(3)	O(1)-Ag(1)-Ag(1)#1	70.6(1)
Ag(2)-S(2)	2.498(1)	O(2)#1-Ag(1)-Ag(1)#1	85.0(1)
Ag(2)-S(1)#2	2.920(1)	O(3)-Ag(2)-S(2)	125.7(1)
Ag(2)-Ag(2)#1	3.3813(6)	O(4)#1-Ag(2)-S(2)	106.8(1)
		S(2)-Ag(2)-S(1)#2	115.6(1)
		O(3)-Ag(2)-O(4)#1	127.6(1)
		S(2)-Ag(2)-Ag(1)#1	129.0(1)
		S(1)-Ag(2)-O(3)	71.5(1)
		S(1)#2-Ag(2)-O(4)#1	87.1(1)
		Ag(1)#1–Ag(1)–S(2)	129.0(1)

#1 -x, y, -z+1/2; #2 x, y+1, z

(3) $L^{2\text{-Ph}}$ / ClO_4.

Ag(1)-S(1)	2.642(1)	S(2)-Ag(1)-S(3)	136.2(1)
Ag(1)-S(2)	2.625(1)	S(2)-Ag(1)-S(1)	80.5(1)
Ag(1)-S(3)	2.636(1)	S(3)-Ag(1)-S(1)	124.9(1)
Ag(1)-S(4)	2.658(1)	S(2)-Ag(1)-S(4)	118.0(1)
Ag(2)-S(1)	2.493(1)	S(3)-Ag(1)-S(4)	83.8(1)
Ag(2)-S(3)	2.507(1)	S(1)-Ag(1)-S(4)	117.6(1)
Ag(2)-O5)	2.549(4)	S(1)#1-Ag(2)-S(3)	153.7(1)
Ag(3)-S(4)	2.493(1)	S(1)#1-Ag(2)-O(5)	102.1(1)
Ag(3)-S(2)#2	2.509(1)	S(3)-Ag(2)-O(5)	99.6(1)
Ag(3)-O(17)	2.538(4)	S(4)-Ag(3)-S(2)#2	155.5(1)
Ag(3)-O(1)	2.586(4)	S(4)-Ag(3)-O(17)	115.8(1)
Ag(4)-O(6)	2.476(4)	S(2)#2-Ag(3)-O(17)	80.6(1)
Ag(4)-O(9)	2.350(4)	S(4)-Ag(3)-O(1)	105.5(1)

Ag(4)-O(19)	2.302(1)	S(2)#2-Ag(3)-O(1)	94.8(1)
Ag(4)-S(5)	2.452(1)	O(1)-Ag(3)-O(17)	80.6(1)
		O(10)-Ag(4)-O(9)	99.8(1)
		O(10)-Ag(4)-S(5)	132.0(1)
		O(10)-Ag(4)-O(6)	86.9(1)
		O(9)-Ag(4)-S(5)	113.5(1)
		O(9)-Ag(4)-O(6)	110.6(1)
		S(5)-Ag(4)-O(6)	110.6(1)

#1 –x, 1-y, -z #2 –x, 1-y, 1-z

(4) $L^{4\text{-Ph}}$ / CF_3SO_3

Ag(1)-O(1)	2.323(2)	O(1)-Ag(1)-S(1)	117.4(1)
Ag(1)-S(1)	2.475(1)	O(1)-Ag(1)-S(2)	110.5(1)
Ag(1)-S(2)	2.502(1)	S(1)-Ag(1)-S(2)	132.0(1)

(5) $L^{4\text{-Ph}}$ / CF_3CO_2

Ag(1)-O(2)	2.346(3)	O(2)-Ag(1)-S(1)	114.2(1)
Ag(1)-S(1)	2.528(1)	O(2)-Ag(1)-S(1)#1	95.4(1)
Ag(1)-S(1)#1	2.589(1)	S(1)-Ag(1)-S(1)#1	142.77(1)
Ag(1)-Ag(2)	3.3212(6)	O(2)-Ag(1)-Ag(2)	74.6(1)
Ag(2)-O(1)	2.234(3)	S(1)-Ag(1)-Ag(2)	87.5(1)
Ag(2)-O(3)	2.271(3)	S(1)#1-Ag(1)-Ag(2)	123.4(1)
Ag(2)-O(2)#2	2.485(3)	O(1)-Ag(2)-O(3)	151.4(1)
Ag(2)-Ag(2)#3	3.1688(7)	O(1)-Ag(2)-O(2)#2	107.4(1)
		O(3)-Ag(2)-O(2)#2	84.6(1)
		O(1)-Ag(2)-Ag(2)#3	92.0(1)
		O(3)-Ag(2)-Ag(2)#3	82.1(1)
		O(2)#2-Ag(2)-Ag(2)#3	158.9(1)
		O(1)-Ag(2)-Ag(1)	74.9(1)
		O(3)-Ag(2)-Ag(1)	78.3(1)
		O(2)#2-Ag(2)-Ag(1)-	95.4(1)
		Ag(2)#3-Ag(2)-Ag(1)	97.8(1)

#1 x, -y+3/2, z+1/2; #2 x, -y+3/2, z-1/2; #3 -x+1, -y+1,-z

(6) $L^{4\text{-Ph}}$ / $CF_3CF_2CO_2$

Ag(2)-O(1)	2.291(4)	O(1)-Ag(2)-S(2)#1	135.8(1)
Ag(2)-S(2)#1	2.483(1)	O(1)-Ag(2)-S(1)#2	88.2(1)
Ag(2)-S(1)#2	2.577(1)	S(2)#1-Ag(2)-S(1)#2	134.9(1)
Ag(2)-S(1)	2.899(1)	O(1)-Ag(2)-S(1)	87.6(1)
Ag(2)-Ag(1)	3.1048(6)	S(2)#1-Ag(2)-S(1)	103.9(1)
Ag(1)-O(2)	2.247(4)	S(1)#2-Ag(2)-S(1)	83.8(1)
Ag(1)-O(3)	2.334(4)	O(1)-Ag(2)-Ag(2)	77.3(1)
Ag(1)-O(4)#1	2.419(4)	S(2)#1-Ag(2)-Ag(2)	67.8(1)
Ag(1)-S(2)	2.697(1)	S(1)#2-Ag(2)-Ag(1)	128.8(1)

Ag(1)-Ag(1)#1	2.9137(1)	S(1)-Ag(2)-Ag(1)	142.8(1)
		O(2)-Ag(1)-O(3)	113.2(2)
		O(2)-Ag(1)-O(4)#1	92.5(2)
		O(3)-Ag(1)-O(4)#1	137.9(2)
		O(2)-Ag(1)-S(2)	111.9(1)
		O(3)-Ag(1)-S(2)	104.0(1)
		O(4)#1-Ag(1)-S(2)	95.6(1)
		O(2)-Ag(1)-Ag(1)#1	163.5(1)
		O(3)-Ag(1)-Ag(1)#1	81.9(1)
		O(4)#1-Ag(1)-Ag(1)#1	71.2(1)
		S(2)-Ag(1)-Ag(1)#1	68.4(1)
		O(2)-Ag(1)-Ag(2)	78.9(1)
		O(3)-Ag(1)-Ag(2)	77.2(1)
		O(4)#1-Ag(1)-Ag(2)	75.9(1)
		S(2)-Ag(1)-Ag(2)	166.9(1)
		Ag(1)#1-Ag(1)-Ag(2)	-99.0(1)

#1 -x, -y,-z; #2 -x, 1-y, -z

(7) $L^{4\text{-}Ph}$ / $CF_3CF_2CF_2CO_2$

Ag(1)-O(4)	2.268(4)	O(4)-Ag(1)-O(1)	102.4(2)
Ag(1)-O(1)	2.359(4)	O(4)-Ag(1)-O(2)#1	99.9(2)
Ag(1)-O(2)#1	2.372(4)	O(1)-Ag(1)-O(2)#1	138.0(1)
Ag(1)-S(1)	2.654(1)	O(4)-Ag(1)-S(1)	113.4(1)
Ag(1)-Ag(1)#1	2.867(1)	O(1)-Ag(1)-S(1)	106.5(1)
Ag(1)-Ag(2)	3.1594(5)	O(2)#1-Ag(1)-S(1)	96.6(1)
Ag(2)-O(3)	2.312(4)	O(4)-Ag(1)-Ag(1)#1	172.4(1)
Ag(2)-S(1)#1	2.464(1)	O(1)-Ag(1)-Ag(1)#1	81.0(1)
Ag(2)-S(2)	2.525(1)	O(2)#1-Ag(1)-Ag(1)#1	73.5(1)
Ag(2)-S(2)#2	3.050(1)	S(1)-Ag(1)-Ag(1)#1	71.6(1)
		O(4)-Ag(1)-Ag(2)	79.3(1)
		O(1)-Ag(1)-Ag(2)	65.5(1)
		O(2)#1-Ag(1)-Ag(2)	84.4(1)
		S(1)-Ag(1)-Ag(2)	166.8(1)
		Ag(1)#1-Ag(1)-Ag(2)	96.2(1)
		O(3)-Ag(2)-S(1)#1	130.5(1)
		O(3)-Ag(2)-S(2)	85.5(1)
		S(1)#1-Ag(2)-S(2)	143.7(1)
		O(3)-Ag(2)-Ag(1)	74.0(1)
		S(1)#1-Ag(2)-Ag(1)	69.0(1)
		S(2)-Ag(2)-Ag(1)	137.1(1)
		Ag(1)-Ag(2)-S(2)#2	124.4(1)
		S(2)-Ag(2)-S(2)#2	102.5(1)

#1 1-x, 2-y, -z; #2 1-x, 1-y, -z

(8) $L^{6\text{-Ph}}$ / CF_3CO_2

Ag(1)-O(3)	2.417(2)	O(3)-Ag(1)-O(1)	133.0(1)
Ag(1)-O(1)	2.496(4)	O(3)-Ag(1)-S(2)	103.7(1)
Ag(1)-S(2)	2.534(1)	O(1)-Ag(1)-S(2)	94.5(1)
Ag(1)-S(2)#1	2.576(1)	O(3)-Ag(1)-S(2)#1	96.2(1)
		O(1)-Ag(1)-S(2)#1	107.1(1)
		S(2)-Ag(1)-S(2)#1	126.7(1)

#1 x, y, z+1

(9) $L^{6\text{-Ph}}$ / $CF_3CF_2CO_2$

Ag(2)-O(1)	2.419(2)	O(1)-Ag(2)-S(2)#1	99.58(6)
Ag(2)-S(2)#1	2.5098(7)	O(1)-Ag(2)-S(1)	107.23(6)
Ag(2)-S(1)	2.5489(7)	S(2)#1-Ag(2)-S(1)	142.29(2)
Ag(2)-O(4)	2.558(2)	O(1)-Ag(2)-O(4)	135.66(7)
Ag(1)-O(1)#2	2.340(2)	S(2)#1-Ag(2)-O(4)	90.58(6)
Ag(1)-O(3)	2.352(2)	S(1)-Ag(2)-O(4)	88.43(5)
Ag(1)-O(2)	2.418(2)	O(1)#2-Ag(1)-O(3)	82.96(8)
Ag(1)-S(1)	2.536(1)	O(1)#2-Ag(1)-O(2)	89.2(1)
Ag(1)-Ag(1)#2	3.0052(4)	O(3)-Ag(1)-O(2)	132.7(1)
Ag(2)-Ag(2)#2	3.3898(5)	O(1)#2-Ag(1)-S(1)	152.2(1)
		O(3)-Ag(1)-S(1)	112.8(1)
		O(2)-Ag(1)-S(1)	95.2(1)
		O(1)#2-Ag(1)-Ag(1)#2	128.7(1)
		O(3)-Ag(1)-Ag(1)#2	81.8(1)
		O(2)-Ag(1)-Ag(1)#2	67.3(1)
		S(1)-Ag(1)-Ag(1)#2	77.7(2)

#1 x, y, z+1; #2 2-x, 1-y, 1-z

(10) $L^{6\text{-Ph}}$ / $CF_3CF_2CF_2CO_2$

Ag(1)-O(1)	2.256(3)	O(1)-Ag(1)-O(2)	157.6(1)
Ag(1)-O(2)	2.284(3)	O(1)-Ag(1)-S(1)#1	105.4(1)
Ag(1)-S(1)	2.872(1)	O(2)-Ag(1)-S(1)#1	89.8(1)
Ag(1)-S(1)#1	2.644(1)	O(1)-Ag(1)-S(1)	87.0(1)
Ag(1)-Ag(1)#2	2.9730(5)	O(2)-Ag(1)-S(1)	95.6(1)
		S(1)#1-Ag(1)-S(1)	130.8(1)
		O(1)-Ag(1)-Ag(1)#2	80.5(1)
		O(2)-Ag(1)-Ag(1)#2	80.0(1)
		S(1)#1-Ag(1)-Ag(1)#2	160.2(1)
		S(1)-Ag(1)-Ag(1)#2	67.5(1)

#1 1+x, y, z #2 2-x, -y, 2-z

(11) $L^{10\text{-}Ph}$ / NO_3

Ag(1)-O(1)	2.461(3)	O(1)-Ag(1)-O(2)#1	86.3(1)
Ag(1)-O(2)#1	2.491(3)	O(1)-Ag(1)-S(2)	105.2(1)
Ag(1)-S(2)	2.494(1)	O(2)#1-Ag(1)-S(2)	114.5(1)
Ag(1)-S(1)	2.512(1)	O(1)-Ag(1)-S(1)	99.9(1)
		O(2)#1-Ag(1)-S(1)	98.7(1)
		S(2)-Ag(1)-S(1)	139.1(1)

#1 x+1, y, z

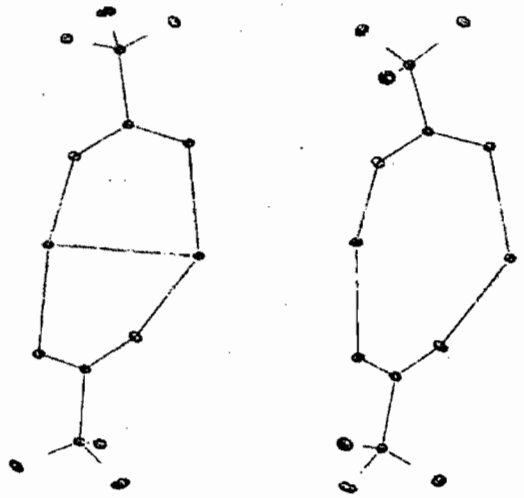

(a) (b)

Figure S1. The two dimers present in **2**. (a) $Ag(1)_2(O_2CCF_3)_2$ in which the Ag···Ag contact is 3.081(5)Å and (b) $Ag(2)_2(O_2CCF_3)_2$ where the Ag…Ag distance is 3.381(6) Å.

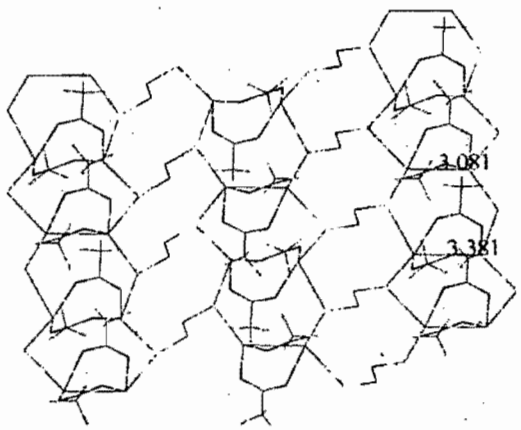

Figure S2. The 2D-network of the complex **2**. The distances in the two dimers are shown in green.

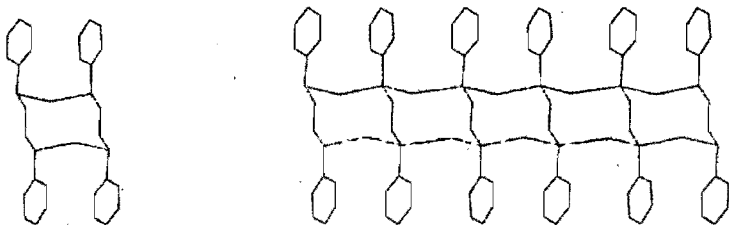

(a) (b)

Figure S3. (a) The Unit **A** formed of 10-membered $Ag_2(L^{2\text{-}Ph})_2$ metallomacrocycle. (b) The units **A** share their ligand edges so that to build up a ribbon parallel to the y-axis. The hydrogen atoms are omitted for clarity.

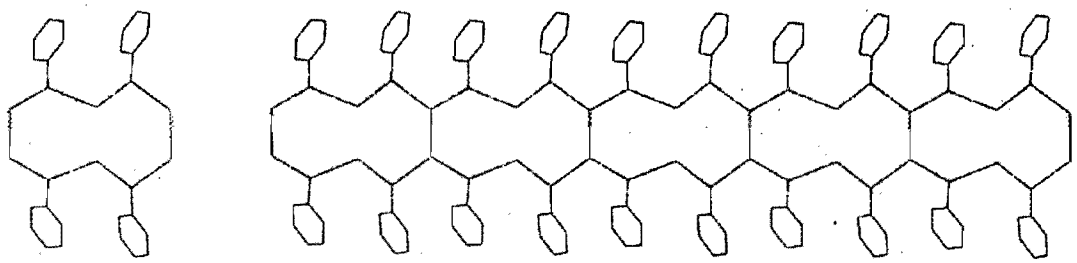

(a) (b)

Figure S4. (a) The Unit **B** is formed by 10-membered Ag_6S_4 metallomacrocycle. (b) The **B** units share Ag...Ag edges in order to give rise to a ribbon alongside the y-axis. The trifluoroacetate groups and the hydrogen atoms are omitted for clarity.

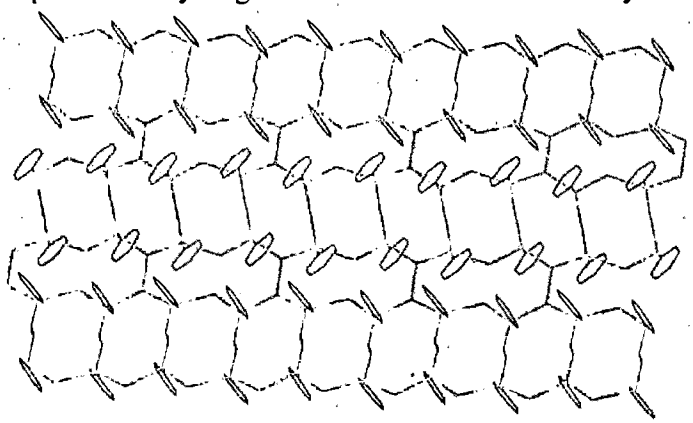

Figure S5. Neighboring **A** and **B** ribbons in complex **2** share their silver and sulfur atoms thus making up a 2D-coordination network perpendicular to the *a*-axis (see also Figure 3c). The trifluoroacetate groups and the hydrogen atoms are omitted for clarity.

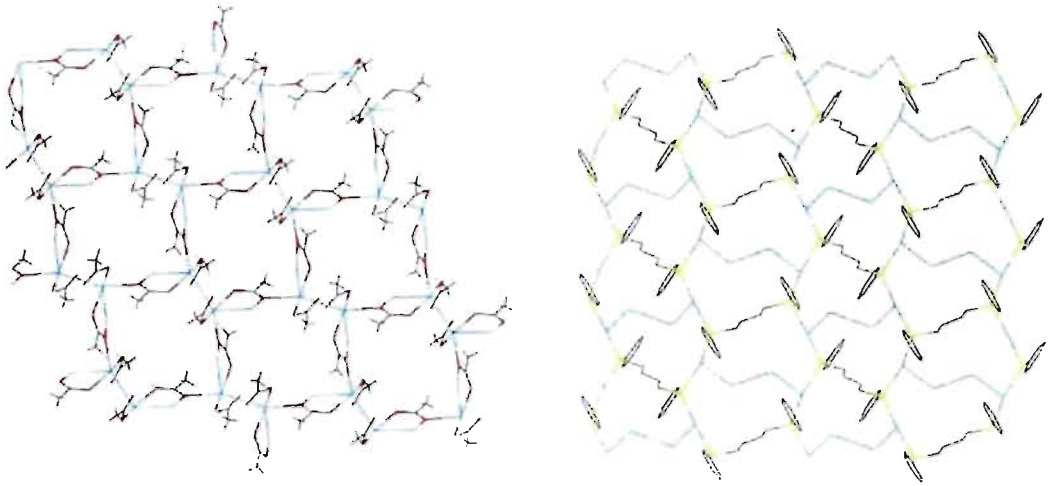

(a) (b)

Figure S6. (a) The 2D-network of **5**. Shown are the anions and the silver(I) ions. (b) The 2D-network of **5**. Shown are the ligands and the silver(I) ions.

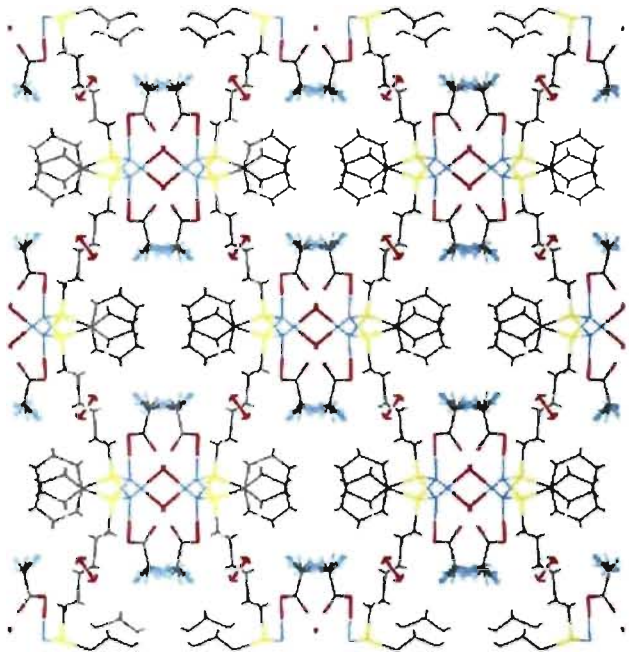

Figure S7. Projection of the 3D-network of complex **8**. The positions of the OW(4) water molecules are shown by red double arrows

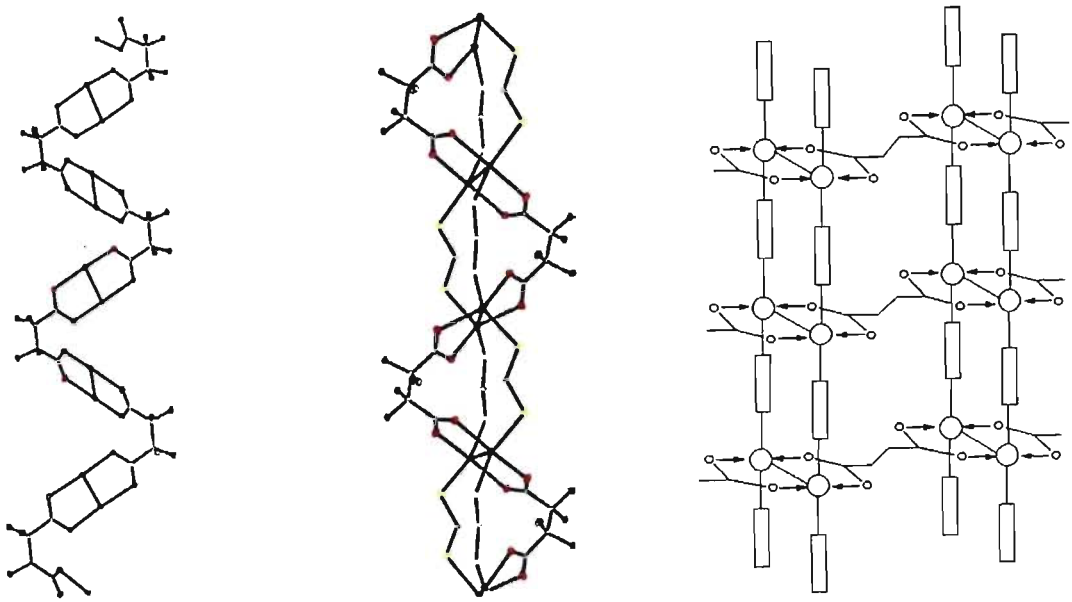

Figure S8. (a) The 1D-coordination polymer of $\mathbf{L}^{\mathbf{1\text{-}Ph}}$-$OOCCF_2CF_2COO$[7a] showing the anions bridging consecutive dimers, thereby yielding the polymeric chain. (b) The same chain now including the ligands which reinforce the structure through Ag-S bonds. (c) Expected extension of $\mathbf{L}^{\mathbf{1\text{-}Ph}}$-$OOCCF_2CF_2COO$ into a 2D-network.

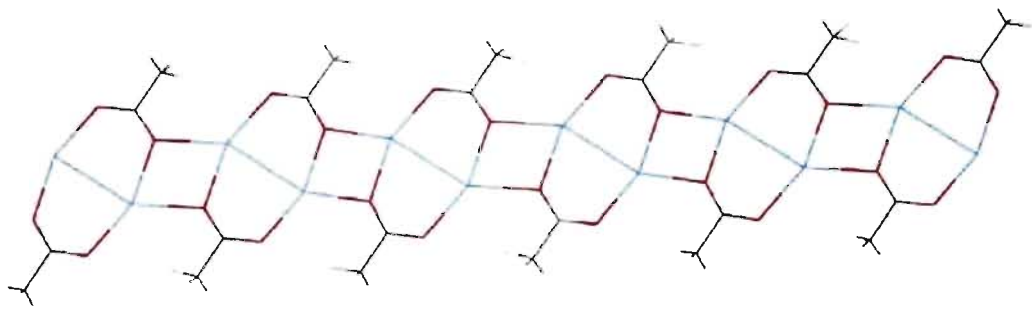

Figure S9. In the trifluoroacetate silver salt, adjacent $(AgCF_3CO_2)_2$ dimers are interconnected via the anti-lone pair of the oxygen atoms so as to build up the $[Ag_2(CF_3CO_2)_2]_\infty$ one-dimensional coordination polymer.[37] Note that both the dimer and the diamond-shaped 4-membered ring are centrosymmetric.

Annexe VII

Table S1. Bond distances, A, and angles (deg) for **1, 2, 3** and **4.**

Complex 1.

Ag(1)-O(9)	2.256(3)	O(9)-Ag(1)-O(5)	157.15(11)
Ag(1)-O(5)	2.271(3)	O(9)-Ag(1)-S(2)	109.86(8)
Ag(1)-S(2)	2.5912(10)	O(5)-Ag(1)-S(2)	89.69(9)
Ag(1)-S(5)	2.7768(11)	O(9)-Ag(1)-S(5)	100.20(8)
Ag(1)-Ag(2)	2.9474(4)	O(5)-Ag(1)-S(5)	81.6(1)
Ag(2)-O(6)	2.271(3)	S(2)-Ag(1)-S(5)	113.76(3)
Ag(2)-O(10)	2.325(3)	O(9)-Ag(1)-Ag(2)	78.23(7)
Ag(2)-O(1)	2.420(3)	O(5)-Ag(1)-Ag(2)	79.53(8)
Ag(2)-S(3)#1	2.6355(11)	S(2)-Ag(1)-Ag(2)	159.95(3)
Ag(2)-Ag(3)	3.2807(5)	S(5)-Ag(1)-Ag(2)	81.57(2)
Ag(3)-O(2)	2.365(3)	O(6)-Ag(2)-O(10)	154.76(11)
Ag(3)-S(5)	2.4622(10)	O(6)-Ag(2)-O(1)	81.64(11)
Ag(3)-O(12)#2	2.474(3)	O(10)-Ag(2)-O(1)	110.29(10)
Ag(3)-S(4)#3	2.5623(10)	O(6)-Ag(2)-S(3)#1	113.95(9)
Ag(4)-O(8)#4	2.309(3)	O(10)-Ag(2)-S(3)#1	85.31(8)
Ag(4)-O(7)	2.377(3)	O(1)-Ag(2)-S(3)#1	104.53(7)
Ag(4)-S(6)	2.6194(12)	O(6)-Ag(2)-Ag(1)	80.46(8)
Ag(4)-S(2)	2.6578(11)	O(10)-Ag(2)-Ag(1)	76.13(7)
Ag(4)-Ag(4)#4	3.1392(6)	O(1)-Ag(2)-Ag(1)	138.89(7)
Ag(5)-O(3)	2.248(3)	S(3)#1-Ag(2)-Ag(1)	116.55(3)
Ag(5)-O(4)#3	2.330(3)	O(6)-Ag(2)-Ag(3)	92.71(9)
Ag(5)-O(11)#5	2.434(3)	O(10)-Ag(2)-Ag(3)	77.01(8)
Ag(5)-S(4)	2.5666(11)	O(1)-Ag(2)-Ag(3)	56.92(7)
Ag(5)-Ag(5)#3	2.9590(6)	S(3)#1-Ag(2)-Ag(3)	145.97(3)
Ag(6)-O(11)	2.362(3)	Ag(1)-Ag(2)-Ag(3)	87.326(12)
Ag(6)-O(2)#1	2.494(3)	O(2)-Ag(3)-S(5)	122.77(8)
Ag(6)-S(1)	2.5859(10)	O(2)-Ag(3)-O(12)#2	95.52(11)
Ag(6)-S(3)#1	2.6829(11)	S(5)-Ag(3)-O(12)#2	95.54(8)
O(2)-Ag(3)-S(4)#3	107.64(8)	O(3)-Ag(5)-O(4)#3	138.92(11)
S(5)-Ag(3)-S(4)#3	127.30(4)	S(2)-Ag(4)-Ag(4)#4	98.00(3)
O(12)#2-Ag(3)-S(4)#3	93.86(8)	S(6)-Ag(4)-Ag(4)#4	126.37(3)
O(2)-Ag(3)-Ag(2)	82.60(7)	O(7)-Ag(4)-Ag(4)#4	69.66(8)
S(5)-Ag(3)-Ag(2)	79.92(3)	O(8)#4-Ag(4)-Ag(4)#4	79.21(8)
O(12)#2-Ag(3)-Ag(2)	172.95(8)	S(6)-Ag(4)-S(2)	131.70(3)
S(4)#3-Ag(3)-Ag(2)	93.18(3)	O(7)-Ag(4)-S(2)	104.23(8)
O(8)#4-Ag(4)-O(7)	136.08(12)	O(8)#4-Ag(4)-S(2)	110.26(9)
O(8)#4-Ag(4)-S(6)	97.24(9)	O(3)-Ag(5)-O(11)#5	103.96(11)
O(7)-Ag(4)-S(6)	78.43(8)	S(4)-Ag(5)-Ag(5)#3	106.47(3)
O(4)#3-Ag(5)-O(11)#5	90.92(10)	O(11)#5-Ag(5)-Ag(5)#3	159.25(7)
O(3)-Ag(5)-S(4)	118.16(9)	O(4)#3-Ag(5)-Ag(5)#3	75.89(7)
O(4)#3-Ag(5)-S(4)	99.19(8)	O(3)-Ag(5)-Ag(5)#3	77.51(8)
O(11)#5-Ag(5)-S(4)	91.22(8)	O(11)-Ag(6)-O(2)#1	98.67(10)
O(11)-Ag(6)-S(1)	113.80(7)	S(1)-Ag(6)-S(3)#1	91.60(3)

O(2)#1-Ag(6)-S(1)	102.36(7)	O(11)-Ag(6)-S(3)#1	89.88(8)
O(2)#1-Ag(6)-S(3)#1	158.89(7)		

#1 x+1,y,z #2 x-1,y,z #3 -x+1,-y+1,-z #4 -x+2,-y+2,-z #5 -x+2,-y+1,-z

Complex 2.

Ag(1)-O(1)	2.357(4)	O(1)-Ag(1)-O(14)	93.26(15)
Ag(1)-O(14)	2.359(4)	O(1)-Ag(1)-O(2)	128.23(15)
Ag(1)-O(2)	2.501(4)	O(14)-Ag(1)-O(2)	83.90(15)
Ag(1)-S(1)	2.5290(14)	O(14)-Ag(1)-S(1)	129.60(11)
Ag(2)-O(3)#1	2.401(4)	O(1)-Ag(1)-S(1)	124.77(11)
Ag(2)-S(2)	2.4547(13)	O(2)-Ag(1)-S(1)	93.76(11)
Ag(2)-O(5)	2.479(4)	O(3)#1-Ag(2)-S(2)	123.03(11)
Ag(2)-S(1)	2.5512(13)	O(3)#1-Ag(2)-O(5)	93.52(15)
Ag(3)-O(8)	2.324(4)	S(2)-Ag(2)-O(5)	124.96(10)
Ag(3)-O(7)#1	2.423(4)	O(3)#1-Ag(2)-S(1)	91.11(11)
Ag(3)-O(17)	2.462(4)	S(2)-Ag(2)-S(1)	130.84(4)
Ag(3)-S(2)	2.513(1)	O(5)-Ag(2)-S(1)	81.06(10)
Ag(4)-S(3)	2.461(1)	O(8)-Ag(3)-O(7)#1	104.19(15)
Ag(4)-S(4)#2	2.509(1)	O(8)-Ag(3)-O(17)	93.62(16)
Ag(4)-O(13)#2	2.597(4)	O(7)#1-Ag(3)-O(17)	85.03(14)
Ag(4)-O(9)#2	2.611(4)	O(7)#1-Ag(3)-S(2)	113.19(10)
Ag(4)-O(16)#2	2.622(4)	O(8)-Ag(3)-S(2)	137.85(11)
Ag(5)-S(4)#3	2.4634(14)	O(17)-Ag(3)-S(2)	107.93(12)
Ag(5)-S(3)	2.4712(13)	O(9)#2-Ag(4)-O(16)#2	89.6(2)
Ag(5)-O(15)#4	2.540(4)	S(3)-Ag(4)-S(4)#2	176.24(5)
Ag(5)-O(12)#4	2.806(4)	O(16)#2-Ag(4)-O(13)#2	130.2(2)
O(9)#2-Ag(4)-O(13)#2	132.4(2)	S(4)#2-Ag(4)-O(13)#2	83.14(11)
S(3)-Ag(5)-O(15)#4	93.99(10)	S(3)-Ag(4)-O(13)#2	96.50(11)
S(4)#3-Ag(5)-O(15)#4	97.83(10)	O(12)#4-Ag(5)-S(3)	80.1(1)
O(12)#4-Ag(5)-S(4)#3	88.3(1)	S(4)#3-Ag(5)-S(3)	167.22(5)
O(15)#4-Ag(5)-O(12)#4	173.74(5)	O(9)#2-Ag(4)-O(13)#2	132.4(2)

#1 x,-y+3/2,z-1/2 #2 x+1,y,z #3 x+1,-y+3/2,z+1/2
#4 x,-y+3/2,z+1/2 #5 x-1,y,z #6 x-1,-y+3/2,z-1/2

Complex 3.

Ag(1)-O(31)	2.425(8)	O(31)-Ag(1)-O(33)#1	106.4(3)
Ag(1)-S(2)	2.471(3)	S(2)-Ag(1)-O(33)#1	87.6(2)
Ag(1)-S(1)	2.505(3)	S(1)-Ag(1)-O(33)#1	88.5(2)
Ag(1)-O(33)#1	2.553(7)	O(31)-Ag(1)-Ag(1)#2	105.2(2)
Ag(1)-Ag(1)#2	3.2481(16)	S(2)-Ag(1)-Ag(1)#2	73.76(6)
O(31)-Ag(1)-S(2)	120.88(19)	S(1)-Ag(1)-Ag(1)#2	91.48(7)
O(31)-Ag(1)-S(1)	95.03(19)	O(33)#1-Ag(1)-Ag(1)#2	148.24(19)
S(2)-Ag(1)-S(1)	143.45(10)		

#1 -x+1,-y+1,-z+1 #2 -x,-y+1,-z+1

Complex 4.

Ag(1)-O(41)#1	2.391(5)	Ag(6)-O(82)	2.552(6)

Ag(1)-O(32)#1	2.469(6)	Ag(6)-S(6)	2.611(2)
Ag(1)-S(2)	2.491(2)	Ag(6)-S(5)	2.686(2)
Ag(1)-O(43)#1	2.495(5)	Ag(7)-O(31)	2.311(6)
Ag(1)-S(1)	2.662(2)	Ag(7)-O(91)	2.407(6)
Ag(2)-O(122)	2.328(6)	Ag(7)-S(6)	2.533(2)
Ag(2)-O(53)#1	2.423(5)	Ag(7)-S(7)	2.713(2)
Ag(2)-S(3)	2.546(2)	Ag(8)-O(82)#1	2.382(5)
Ag(2)-S(2)	2.671(2)	Ag(8)-O(83)#1	2.467(9)
Ag(3)-O(41)	2.505(5)	Ag(8)-S(7)	2.514(2)
Ag(3)-S(3)	2.580(2)	Ag(8)-O(121)	2.559(7)
Ag(3)-S(4)	2.699(2)	Ag(8)-S(8)	2.652(2)
Ag(4)-O(73)#1	2.342(5)	Ag(9)-O(21)	2.385(5)
Ag(4)-S(4)	2.466(2)	Ag(9)-O(12)	2.455(5)
Ag(4)-O(61)	2.504(5)	Ag(9)-S(8)	2.537(2)
Ag(4)-O(62)	2.567(6)	Ag(10)-O(11)	2.395(5)
Ag(5)-O(63)	2.350(5)	Ag(10)-O(23)#1	2.468(5)
Ag(5)-S(5)	2.466(2)	Ag(10)-S(1)	2.525(2)
Ag(5)-O(72)	2.494(5)	Ag(6)-O(93)#2	2.600(5)
Ag(5)-O(71)	2.572(5)	O(41)#1-Ag(1)-O(32)#1	79.6(2)
O(41)#1-Ag(1)-S(2)	125.76(15)	O(41)-Ag(3)-S(3)	122.71(13)
O(32)#1-Ag(1)-S(2)	116.98(14)	O(41)-Ag(3)-S(4)	103.18(14)
O(41)#1-Ag(1)-O(43)#1	51.52(16)	S(3)-Ag(3)-S(4)	81.63(5)
O(32)#1-Ag(1)-O(43)#1	111.55(19)	O(73)#1-Ag(4)-S(4)	138.85(12)
S(2)-Ag(1)-O(43)#1	129.66(14)	O(73)#1-Ag(4)-O(61)	81.07(16)
O(41)#1-Ag(1)-S(1)	149.38(15)	S(4)-Ag(4)-O(61)	138.47(12)
O(32)#1-Ag(1)-S(1)	84.15(18)	O(73)#1-Ag(4)-O(62)	129.80(17)
S(2)-Ag(1)-S(1)	84.77(5)	S(4)-Ag(4)-O(62)	91.30(13)
O(43)#1-Ag(1)-S(1)	113.26(13)	O(61)-Ag(4)-O(62)	49.68(16)
O(122)-Ag(2)-O(53)#1	77.9(2)	O(63)-Ag(5)-S(5)	138.86(12)
O(122)-Ag(2)-S(3)	147.86(18)	O(63)-Ag(5)-O(72)	82.35(16)
O(53)#1-Ag(2)-S(3)	118.70(16)	S(5)-Ag(5)-O(72)	136.54(12)
O(122)-Ag(2)-S(2)	100.5(2)	O(63)-Ag(5)-O(71)	130.57(17)
O(53)#1-Ag(2)-S(2)	117.54(14)	S(5)-Ag(5)-O(71)	90.50(13)
S(3)-Ag(2)-S(2)	95.31(5)	O(72)-Ag(5)-O(71)	49.56(16)
O(82)-Ag(6)-O(93)#2	75.94(18)	O(82)#1-Ag(8)-S(7)	121.37(15)
O(82)-Ag(6)-S(6)	121.17(13)	O(83)#1-Ag(8)-S(7)	134.1(2)
O(93)#2-Ag(6)-S(6)	162.39(13)	O(82)#1-Ag(8)-O(121)	76.6(2)
O(82)-Ag(6)-S(5)	106.05(13)	O(83)#1-Ag(8)-O(121)	114.0(2)
O(93)#2-Ag(6)-S(5)	90.57(14)	S(7)-Ag(8)-O(121)	104.84(17)
S(6)-Ag(6)-S(5)	80.90(5)	O(82)#1-Ag(8)-S(8)	148.40(14)
O(31)-Ag(7)-O(91)	78.6(2)	O(83)#1-Ag(8)-S(8)	123.3(2)
O(31)-Ag(7)-S(6)	149.44(18)	S(7)-Ag(8)-S(8)	85.39(5)
O(91)-Ag(7)-S(6)	118.46(17)	O(121)-Ag(8)-S(8)	80.5(2)
O(31)-Ag(7)-S(7)	97.1(2)	O(21)-Ag(9)-O(12)	89.76(16)
O(91)-Ag(7)-S(7)	118.44(15)	O(21)-Ag(9)-S(8)	140.90(11)
S(6)-Ag(7)-S(7)	95.84(5)	O(12)-Ag(9)-S(8)	128.78(13)
O(82)#1-Ag(8)-O(83)#1	51.1(2)	O(11)-Ag(10)-O(23)#1	88.26(16)
O(11)-Ag(10)-S(1)	141.74(11)	O(23)#1-Ag(10)-S(1)	128.36(13)

#1 x-1,y,z; #2 x+1,y,z

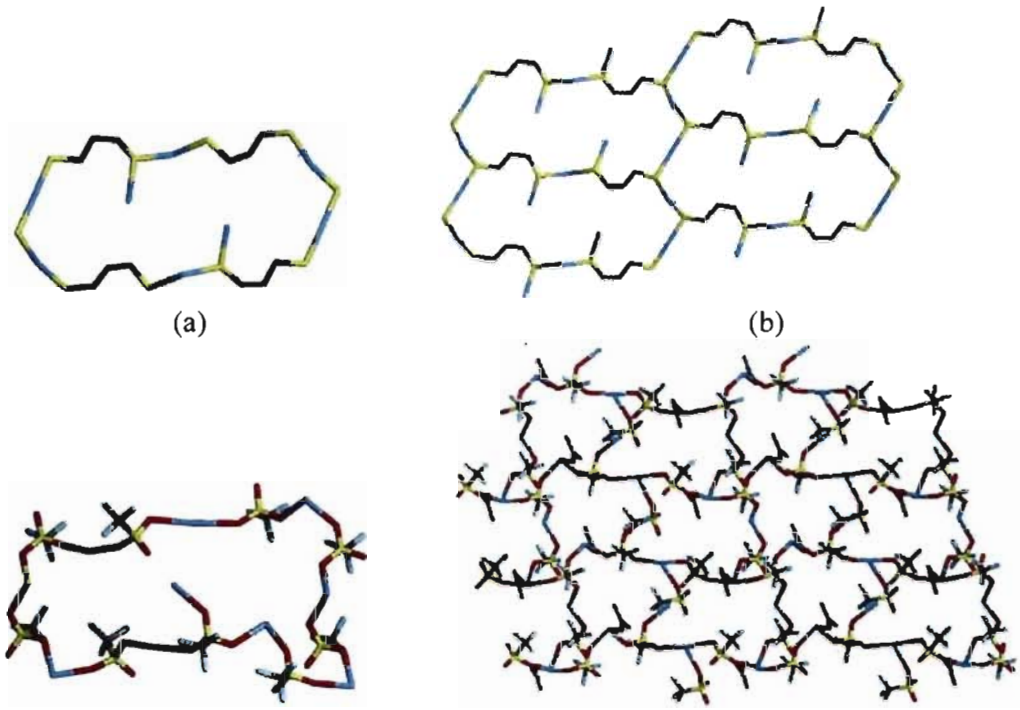

Figure S1. Complex **2**. (a) The repeat of the $(Ag\text{-}L^{3\text{-}Ph})_{\infty}$ network and (b) the corresponding two-dimensional network. (c) The repeat of the $(Ag\text{-}CF_3SO_3)_{\infty}$ network and (d) thecorresponding two-dimensional network. As for **1**, complex **2** is the fusion of both the $(Ag\text{-liand})_{\infty}$ and the $(Ag\text{-anion})_{\infty}$ networks.

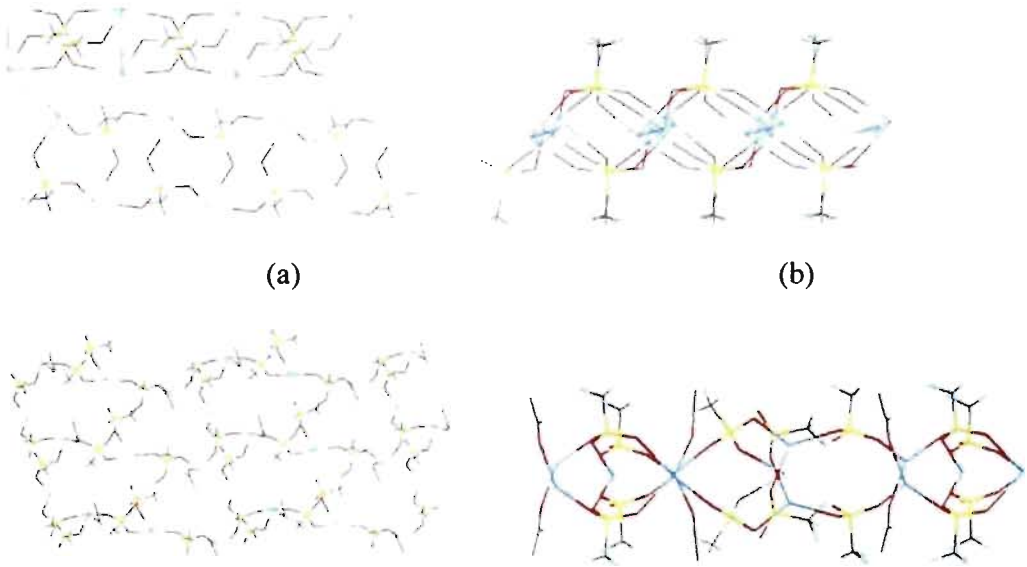

Figure S2. (a) The two-dimensional $(Ag\text{-}CF_3SO_3)_\infty$ network in the $AgOTf.(EtOH)_{0.5}$ complex parallel to the *ab*-plane[a] (b) Side view of the $(Ag\text{-}CF_3SO_3)_\infty$ parallel to the *a*-axis.[a] (c) The 2D $(Ag\text{-}CF_3SO_3)_\infty$ network in complex 2. (d) Side view of the 2D $(Ag\text{-}CF_3SO_3)_\infty$ network in complex **2**.

[a] Côté, A. P.; Ferguson, M. J.; Khan, K. A.; Enright, G. D.; Kulynych, A. D, Dalrymple, S. A.; Shimizu, G. K. H. Inorg. Chem. **2002**, *41*, 287.

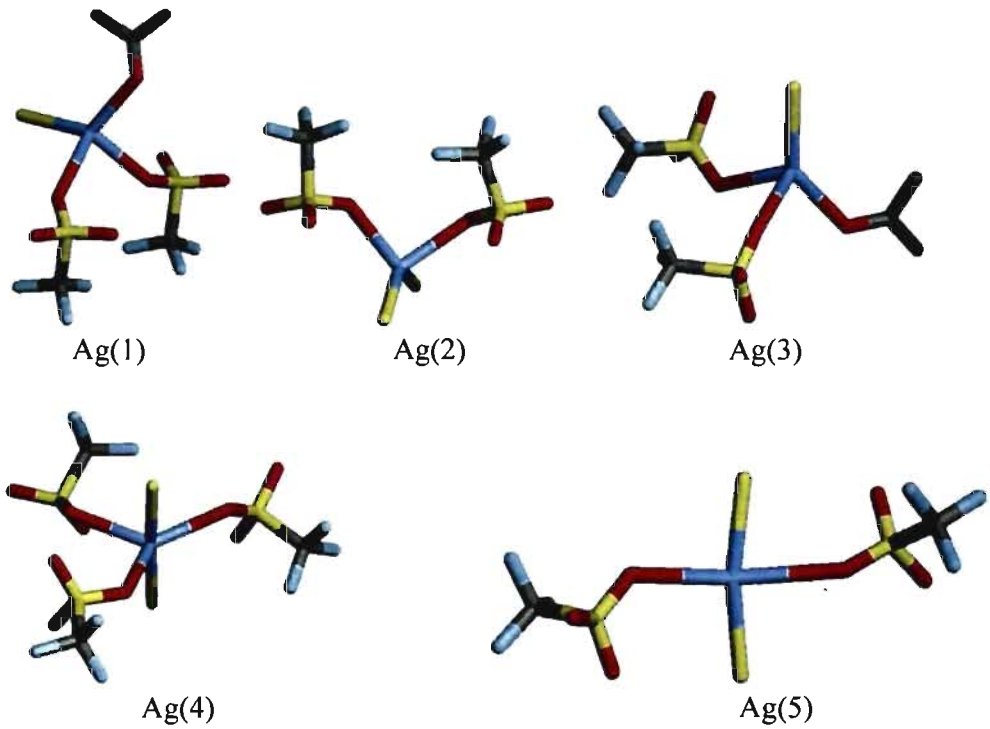

Figure S3. Coordination modes of the five different silver atoms in the complex **2**.

(a) (b)

Figure S4. (a) The [Ag- $\mathbf{L}^{\mathbf{1\text{-}Me}}$]$_2$ dimer in complex **3**. (b) [Ag- $\mathbf{L}^{\mathbf{1\text{-}Me}}$]$_2$ dimer in the complex of $AgCH_3SO_3$ and $\mathbf{L}^{\mathbf{1\text{-}Me}}$.[a]

[a]Awaleh, M. O; Badia, A. ; Brisse, F. *Cryst. Growth and Design,* **2006**, *6,* 2674.

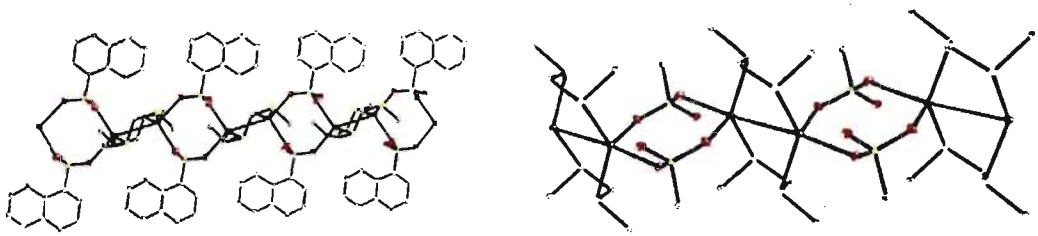

(a) (b)

Figure S5. (a) The 1D-coordination polymer **3**, consisting of a repetition of dimers linked by two $C_{10}H_7SO_3$ anions. (b) The 1D-coordination polymer $AgCH_3SO_3$ and $\mathbf{L}^{\mathbf{1\text{-}Me}}$ consisting of a repetition of dimers linked by two CH_3SO_3 anions.[a]

[a]Awaleh, M. O; Badia, A. ; Brisse, F. *Cryst. Growth and Design,* **2006**, *6,* 2674.

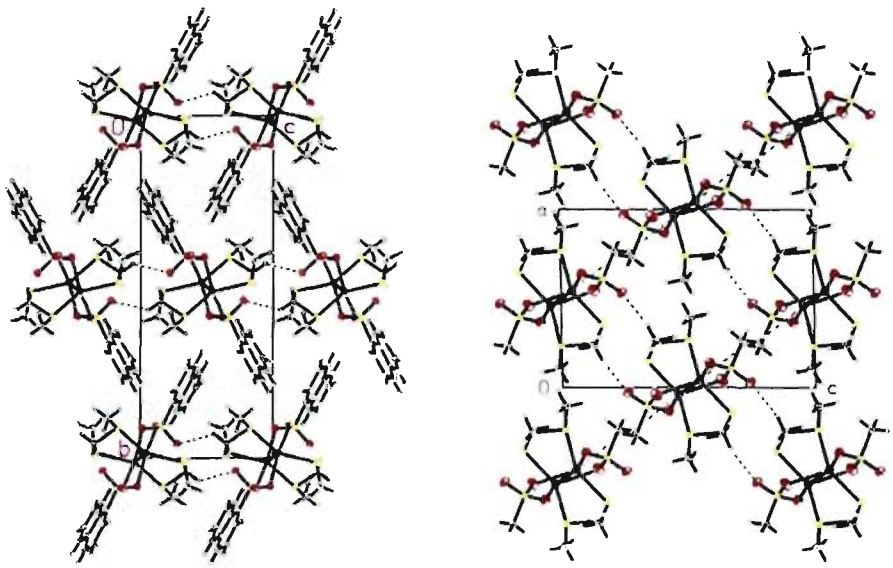

(a) (b)

Figure S6. (a) Packing of complex **3** in its unit cell. (b) Packing of the complex formed with $AgCH_3SO_3$ and $\mathbf{L}^{\mathbf{1\text{-}Me}}$.[a]

[a]Awaleh, M. O; Badia, A. ; Brisse, F. *Cryst. Growth and Design,* **2006**, *6,* 2674.

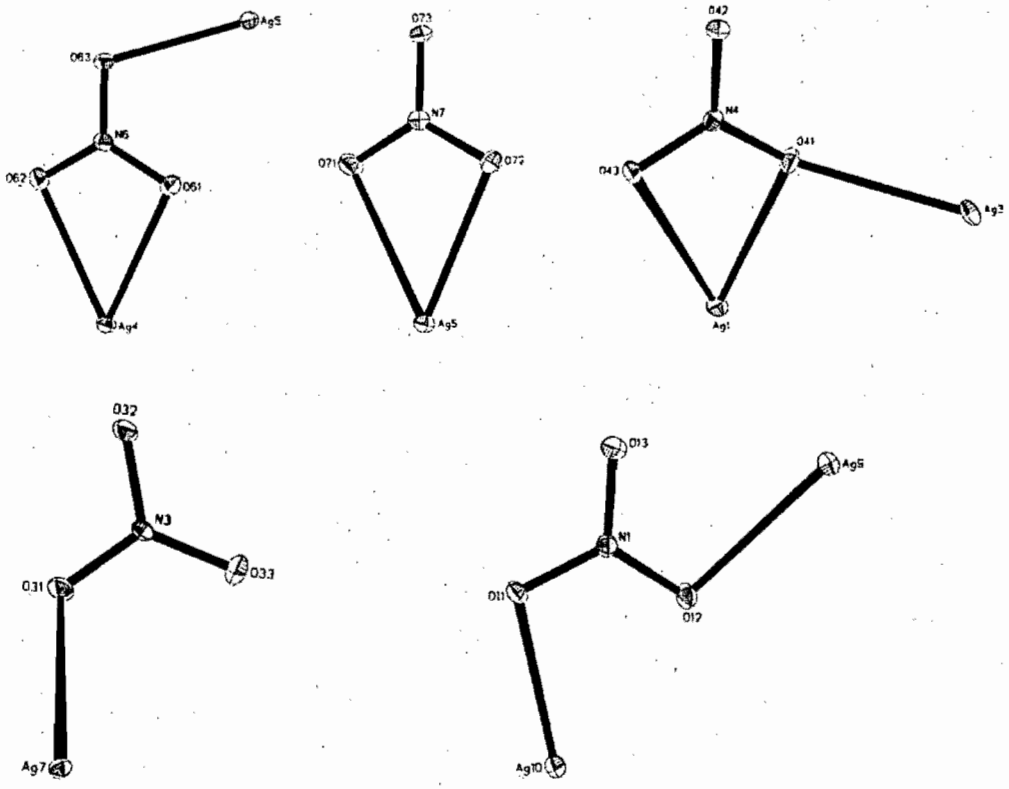

Figure S7. The five coordinations of the nitrate group in complex **4**.

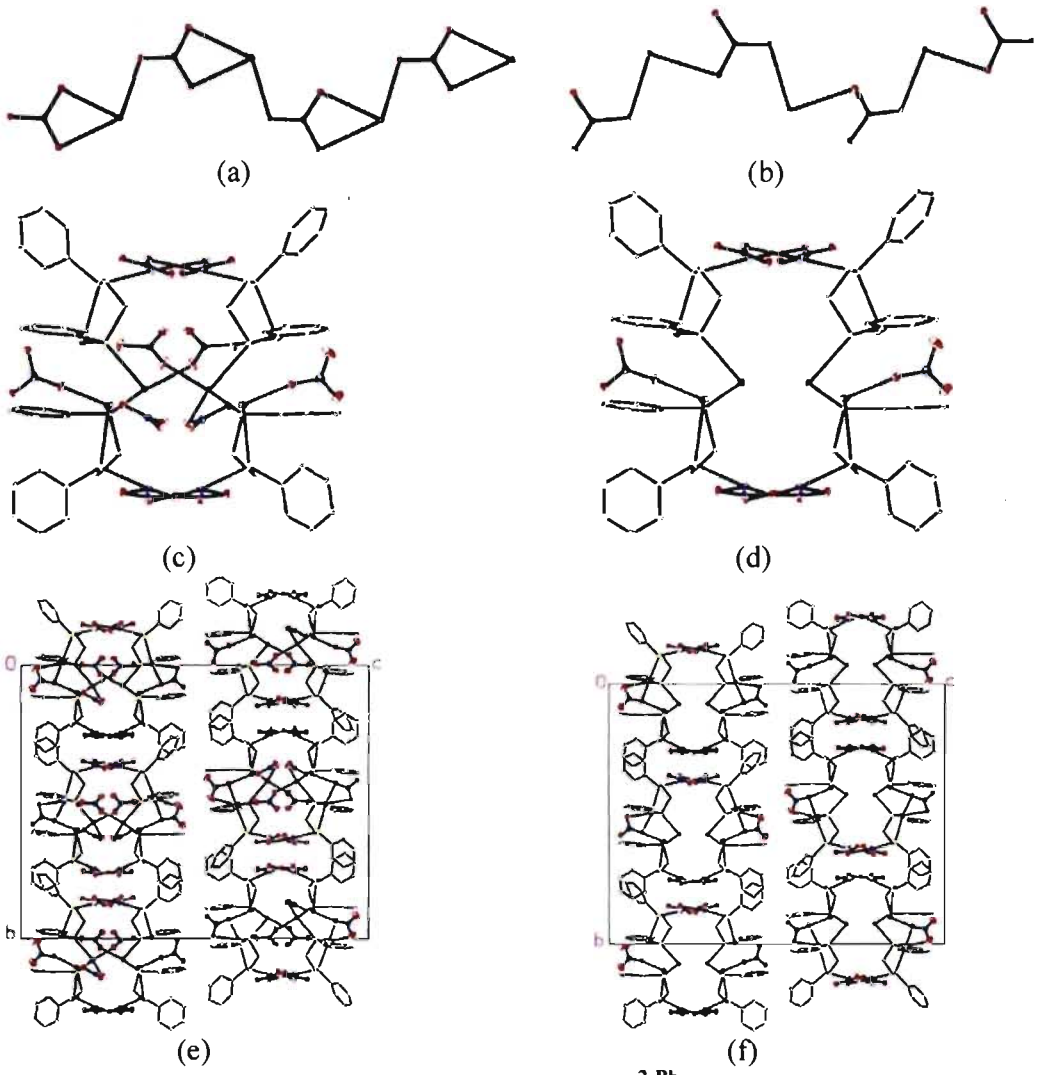

Figure S8. The 1D-coordination polymer, $[Ag_{10}(\mathbf{L}^{\mathbf{2\text{-}Ph}})_4(NO_3)_{10}]_\infty$, **4**. (a) The nitrate anions, $[AgNO_3]_\infty$, link the silver ions in a mix of chelating and bridging coordination modes. (b) In another sequence, the nitrate anions are in the bridging coordination mode. (c) Projection down the *a*-axis of the tube-like coordination polymer **4**, showing all the nitrate anions. (d) The same projection when the nitrates have been removed from the channel. (e) Packing of the tubes with all the nitrates shown. (f) Packing of the tube. Clearly each tube has only four nearest neighbors. The nitrates within the tubes have been removed.

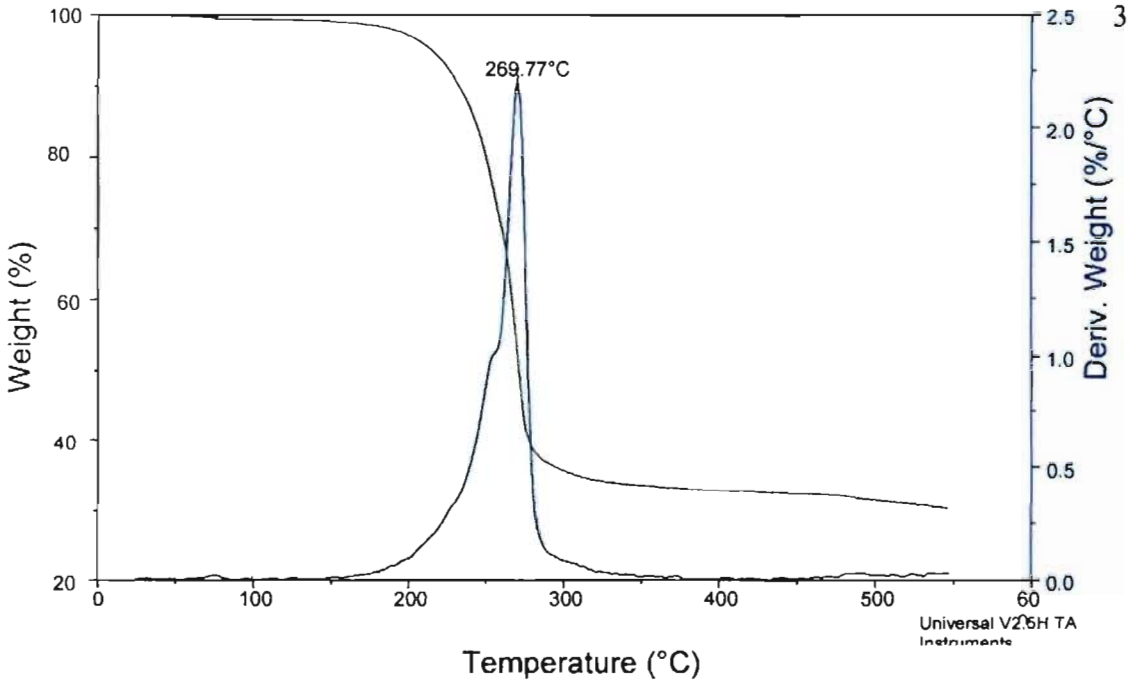

Figure S9. The TGA and DTGA curves of complex **2**, recorded at a heating rate of 10 °C min^{-1}. Complex **2** decomposes in one step, between 180 and 320 °C. The final residue is metallic silver.

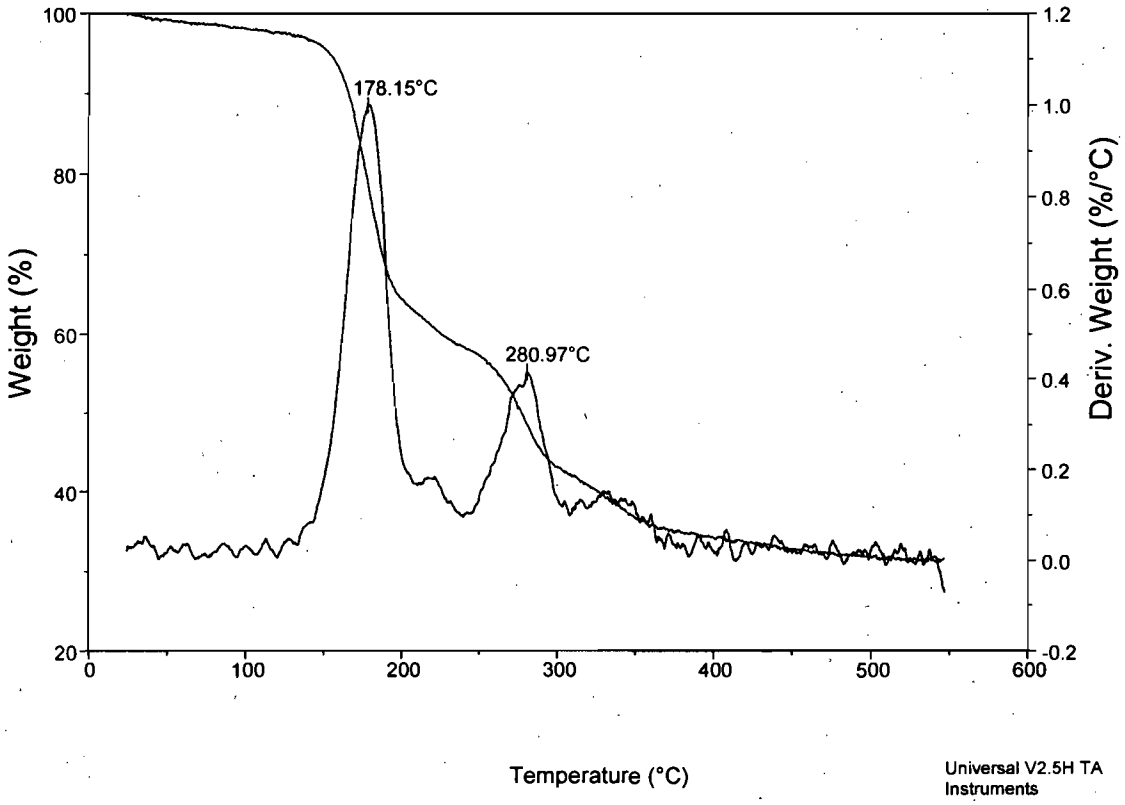

Figure S10. TGA and DTGA curves of **4** recorded at a heating rate of 10 °C min^{-1} show a more complex decomposition. First step: lost of the ligand, $\mathbf{L}^{2\text{-Ph}}$, between 140 and 230 °C. Second step: Lost of the nitrate anion, between 230 and 400 °C.

Annexe VIII

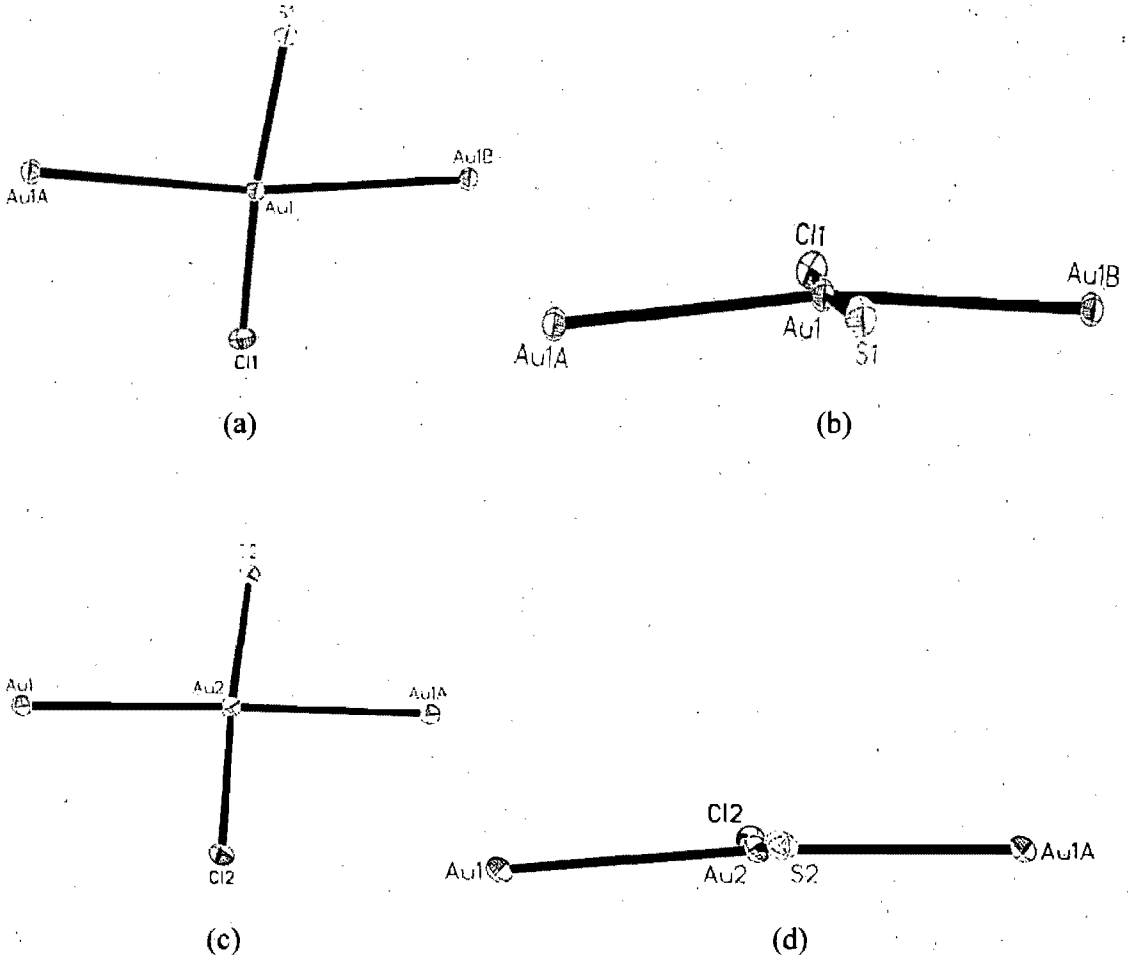

Figure S1. (a), (b): The square-planar environment of the Au(I) in complex 1. (c), (d) the square planar coordination of Au(I) in 7.

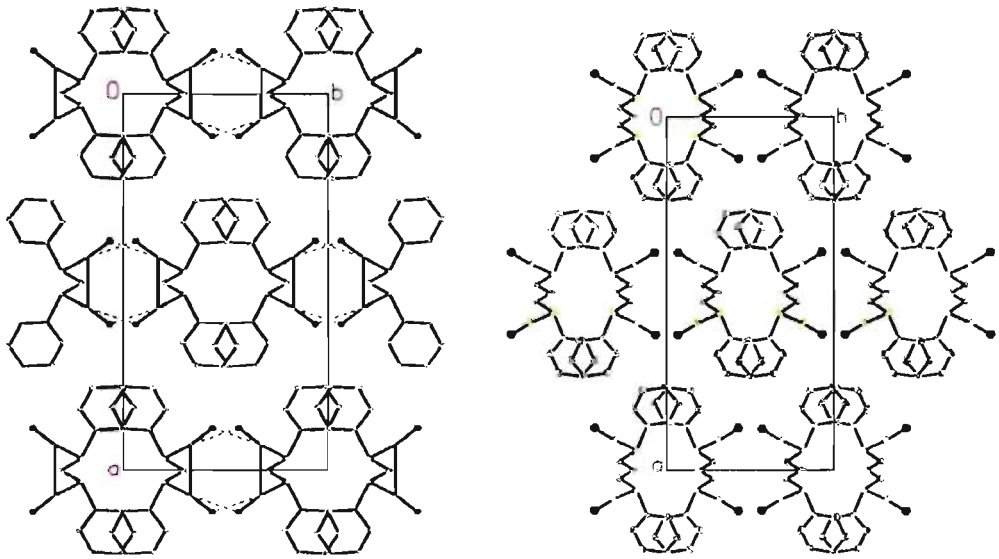

(a) (b)

Figure S2. Comparison of the packing of (a) complex **2** and (b) complex **4** viewed down the *c*-axis.

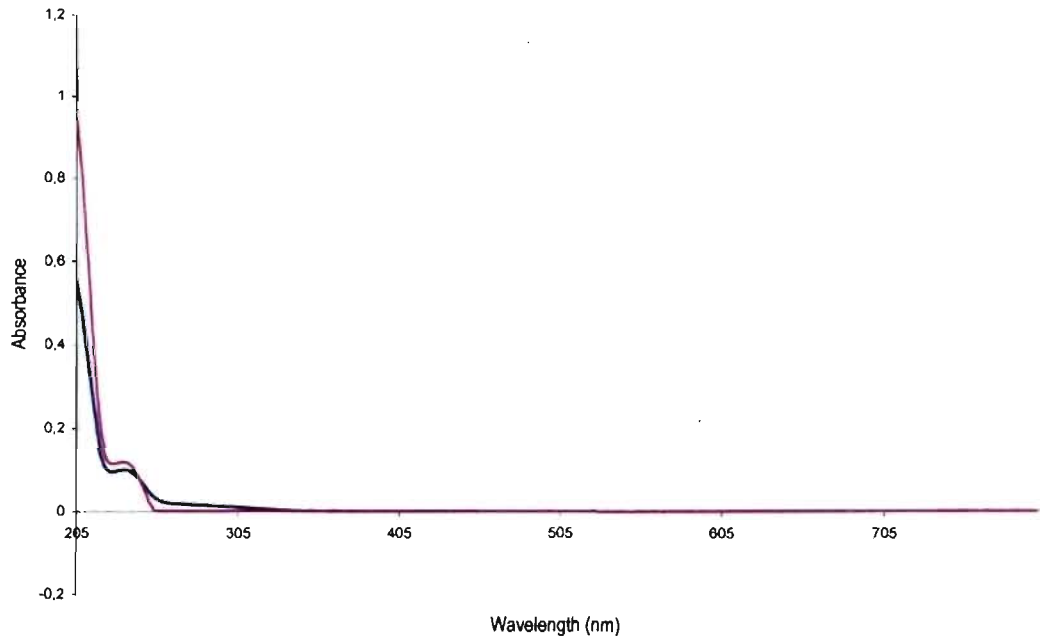

Figure S3. UV-Vis spectrum in $CHCl_3$. Blue line: Ligand $\mathbf{L^{1\text{-}Me}}$ and Pink line: complex **1**, $[AuL^{1\text{-}Me}Cl]_{\infty}$.

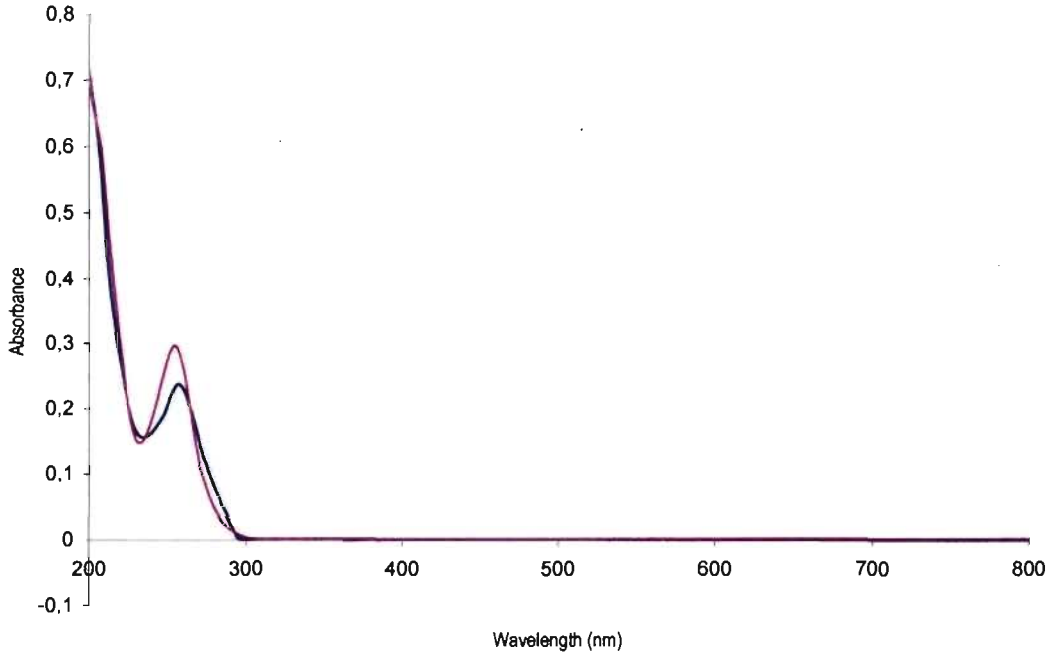

Figure S4. UV-Vis spectrum in $CHCl_3$. Blue line: Ligand $\mathbf{L}^{\mathbf{1\text{-}Ph}}$ and Pink line: complex **2**, $[Au_2\mathbf{L}^{\mathbf{1\text{-}Ph}}Cl_2]_\infty$.

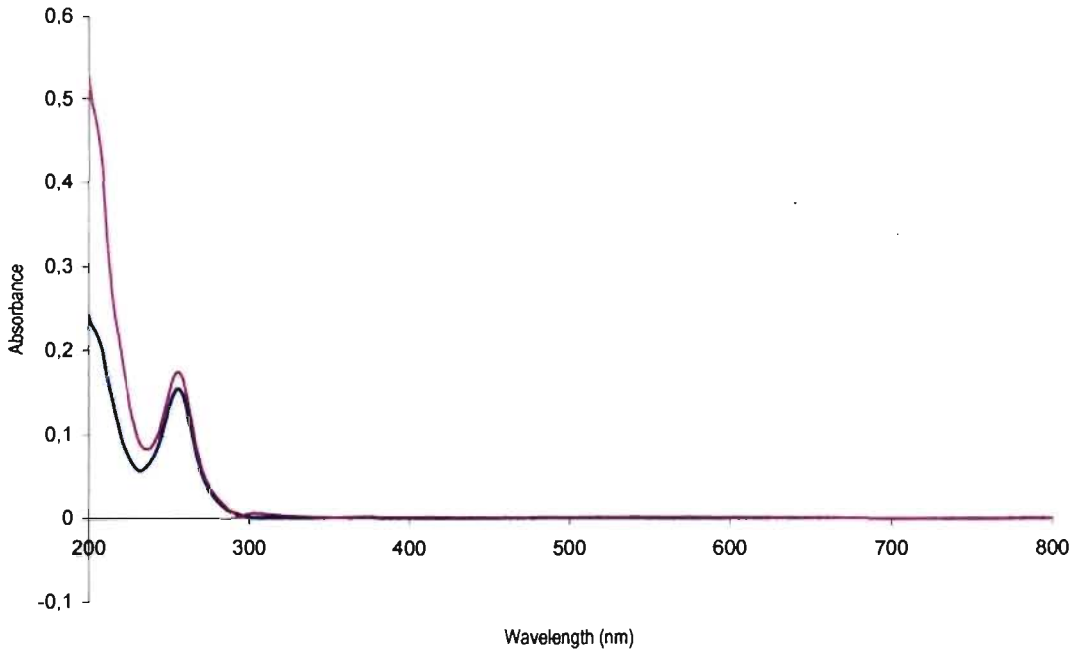

Figure S5. UV-Vis spectrum in $CHCl_3$. Blue line: Ligand $\mathbf{L}^{\mathbf{2\text{-}Ph}}$ and Pink line: complex **7**, $[Au_2\mathbf{L}^{\mathbf{2\text{-}Ph}}Cl_2]_\infty$.

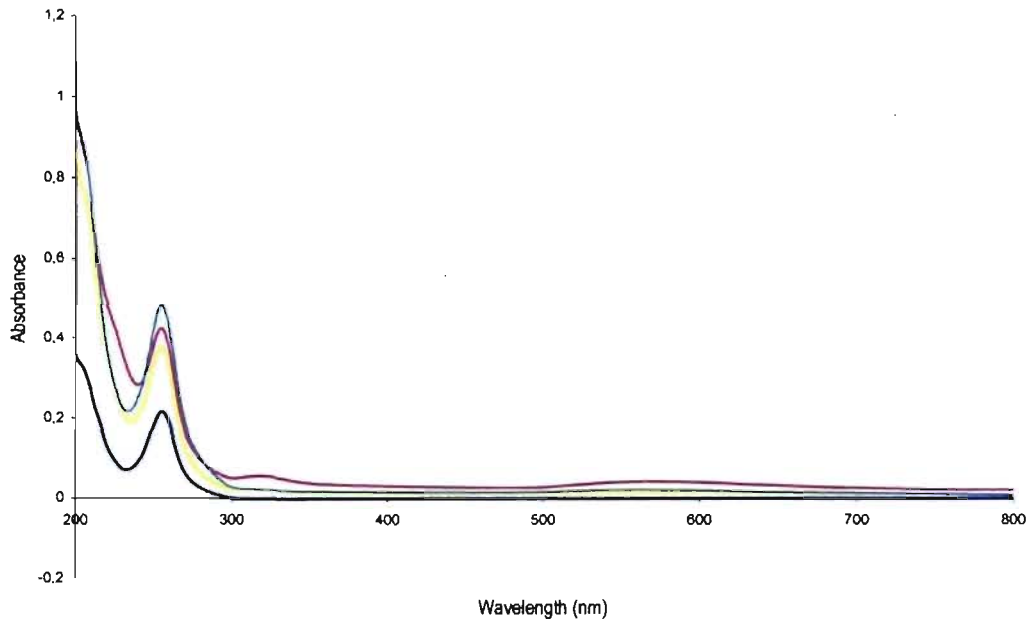

Figure S6. UV-Vis spectrum in $CHCl_3$. Blue line: Ligand $\mathbf{L^{3\text{-}Ph}}$, Yellow line: complex **3**, $[Au_2\mathbf{L^{3\text{-}Ph}}\ Cl_2]_\infty$, Green line: complex **4**, $[Au_2\mathbf{L^{3\text{-}Ph}}\ Cl_2]_\infty$, Pink line: complex **5**, $[Au_2\mathbf{L^{3\text{-}Ph}}Cl_2]_\infty$.

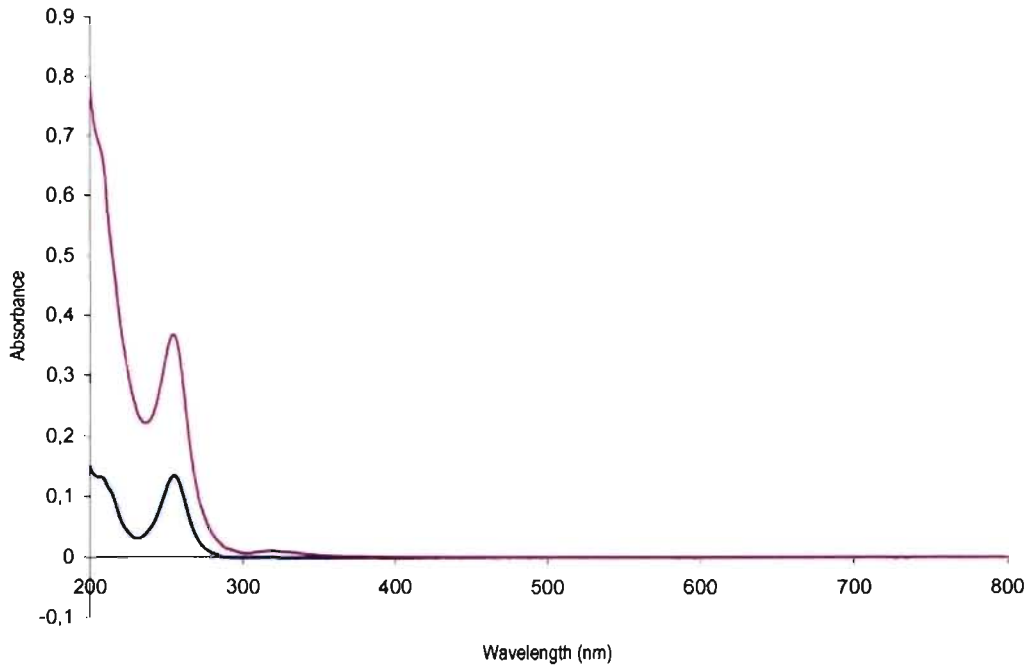

Figure S7. UV-Vis spectrum in $CHCl_3$. Blue line: Ligand $\mathbf{L^{4\text{-}Ph}}$ and Pink line: complex **8**, $[Au_2\mathbf{L^{4\text{-}Ph}}\ Cl_2]$.

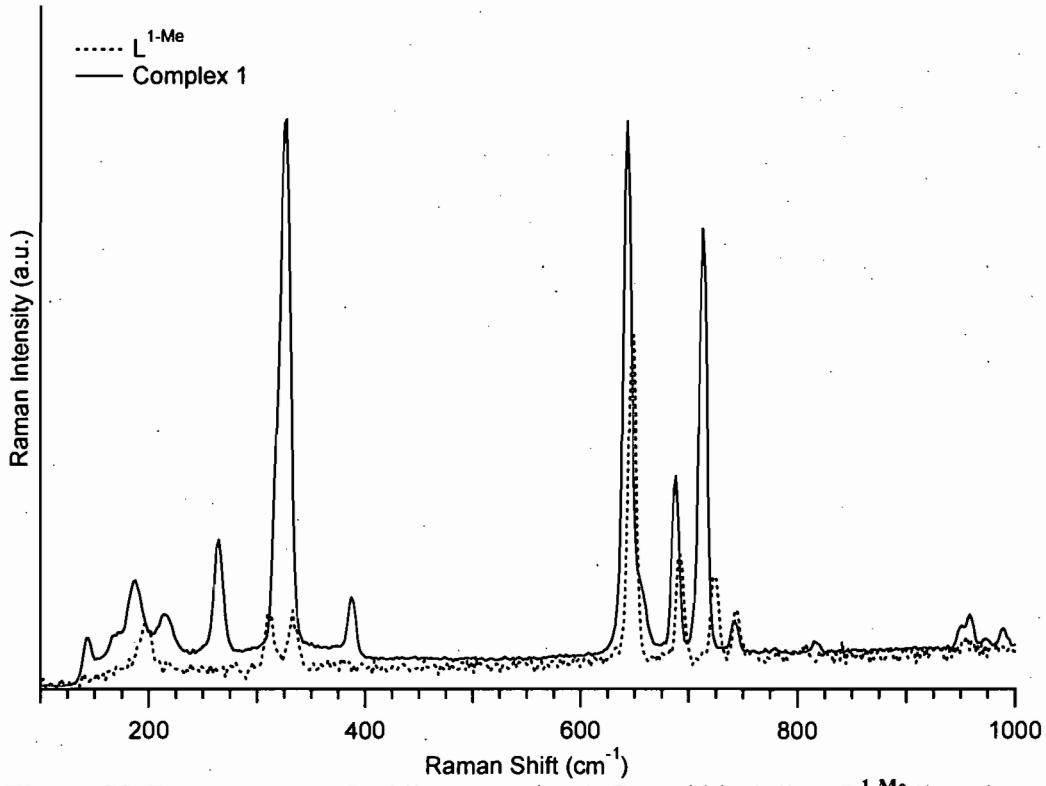

Figure S8. Raman spectra. Red line: complex **1**. Dotted black line: $\mathbf{L^{1\text{-}Me}}$ ligand.

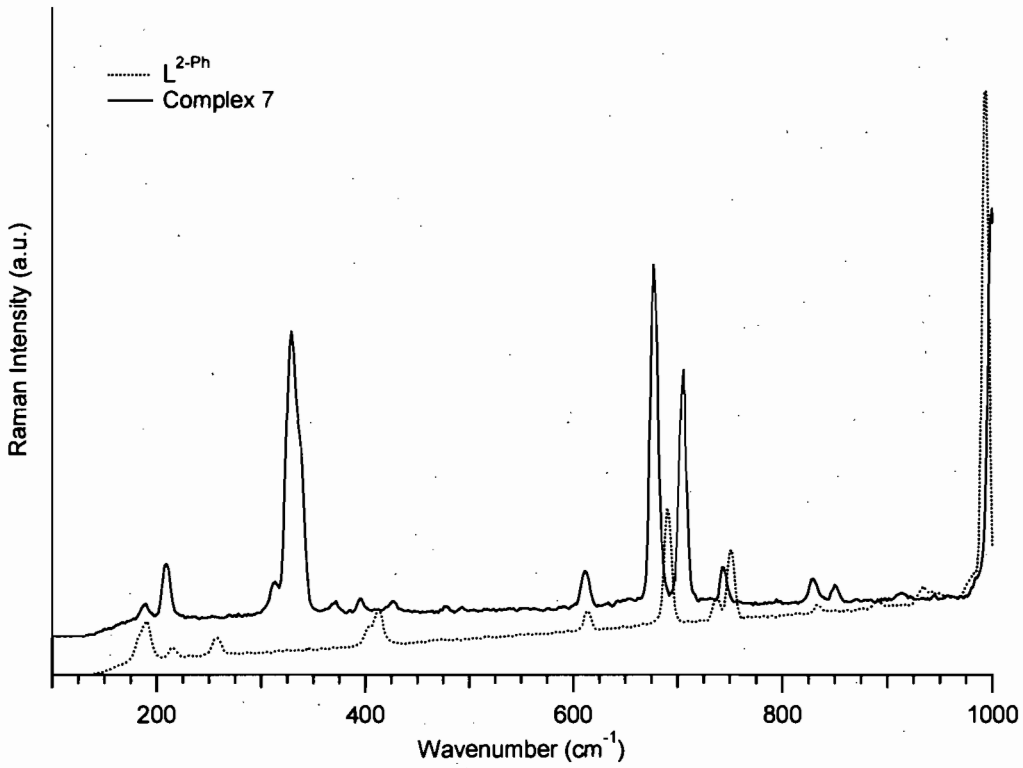

Figure S9. Raman spectra. Red line: complex 7. Dotted black line: $\mathbf{L^{2\text{-}Ph}}$ ligand.

Annexe IX

Tableau 9.1. Composés moléculaires

Formule	Rapport Métal/Ligand	Observation/Commentaire	Ref
$[Ag(L^{6\text{-}Ph})(ClO_4)]_2$	1:1	Dimère	a
$[Ag(L^{3\text{-}tBu})(ClO_4)]_2$	1:1	Dimère	b
$[Ag(L^{5\text{-}tBu})(ClO_4)]_2$	1:1	Dimère	b
$[Ag(L^{2\text{-}Et})(ClO_4)]_4$	1:1	Tétramère	c
$[Ag(L^{1\text{-}Benz})(ClO_4)]_2$	1:1	Dimère	c
$[Ag(L^{2\text{-}Benz})_2](ClO_4)$	1:2	Mononucléaire	b

Tableau 9.2. Chaînes simples.

Formule	Rapport Métal/Ligand	Observation/Commentaire	Ref
$[Ag(L^{1\text{-}Ph})(ClO_4)]_\infty$	1:1		d
$[Ag(L^{1\text{-}Ph})(BF_4)]_\infty$	1:1		d
$[Ag(L^{1\text{-}Ph})(NO_3)]_\infty$	1:1		e
$[Ag(L^{1\text{-}Ph})(CF_3CO_2)]_\infty$	1:1		d
$[Ag(L^{1\text{-}Ph})(CF_3SO_3)]_\infty$	1:1		d
$[Ag(L^{4\text{-}Ph})(CF_3SO_3)]_\infty$	1:1		f
$[Ag(L^{1\text{-}tBu})(ClO_4)]_\infty$	1:1		b

Tableau 9.3. Chaînes doubles

Formule	Rapport Métal/Ligand	Observation/Commentaire	Ref
$[Ag(L^{1\text{-}Ph})(CF_3CF_2CF_2CO_2)]_\infty$	1:1	Courte distance métal-métal	d
$[Ag_2(L^{1\text{-}Ph})_2(OOCCF_2CF_2COO)]_\infty$	1:1	Courte distance métal-métal	d
$[Ag_2(L^{1\text{-}Ph})_2(CF_3SO_3)_2]_\infty$	1:1		d

$[Ag(L^{3\text{-}Ph})(CF_3CF_2CF_2CO_2)]_\infty$	1:1	Courte distance métal-métal	g
$[Ag(L^{3\text{-}Ph})(p\text{-}TsO)]_\infty$	1:1		g
$[Ag(L^{1\text{-}Me})_2(PF_6)]_\infty$	1:2		h
$[Ag(L^{1\text{-}Me})_2(SbF_6)(EtO)_{0.5}]_\infty$	1:2		h
$[Ag(L^{1\text{-}Me})(C_6H_5CO_2)]_\infty$	1:1	Courte distance métal-métal	i
$[Ag(L^{1\text{-}Me})(CH_3SO_3)]_\infty$	1:1		i
$[Ag(L^{1\text{-}Benz})(ClO_4)]_\infty$	1:1		c
$[Ag(L^{3\text{-}Et})(ClO_4)]_\infty$	1:1		c
$[Ag(L^{4\text{-}tBu})_{1.5}(ClO_4)]_\infty$	2:3		b
$[Ag(L^{6\text{-}tBu})_{1.5}(ClO_4)]_\infty$	2:3		b
$[Ag(L^{4\text{-}Benz})_{1.5}(ClO_4)]_\infty$	2:3		c
$[Ag(L^{3\text{-}Me})(ClO_4)]_\infty$	1:1		j
$[Ag(L^{1\text{-}Me})(C_{10}H_7SO_3)]_\infty$	1:1		q

Tableau 9.4. Réseaux bidimensionnels $[Ag\text{-}L^{n\text{-}R}]_\infty$ où l'anion complète la coordination du métal.

Formule	Rapport Métal/Ligand	Observation/Commentaire	Ref
$[Ag_2(L^{1\text{-}Me})_2(NO_3)_2]_\infty$	1:1		k
$[Ag_2(L^{1\text{-}Me})_2(ClO_4)_2]_\infty$	1:1		i
$[Ag_2(L^{1\text{-}Me})_2(p\text{-}TsO)_2]_\infty$	1:1		i
$[Ag(L^{1\text{-}Me})(CF_3CO_2)]_\infty$	1:1		i
$[Ag(L^{1\text{-}Me})(CF_3CF_2CF_2CO_2)]_\infty$	1:1		i
$[Ag_2(L^{1\text{-}Me})_2(CF_3SO_3)_2]_\infty$	1:1		i
$[Ag_2(L^{2\text{-}Ph})_2(CF_3SO_3)_2]_\infty$	1:1		f

$[Ag_2(L^{4\text{-}Ph})_3(ClO_4)_2]_\infty$	2:3	l
$[Ag_2(L^{4\text{-}Ph})_3(ClO_4)_2.CH3OH]_\infty$	2:3	l
$[Ag(L^{2\text{-}tBu})_{1.5}(ClO_4)]_\infty$	2:3	b
$[Ag(L^{1\text{-}Et})_{1.5}(ClO_4)]_\infty$	2:3	c
$[Ag(L^{4\text{-}Et})_2(ClO_4)]_\infty$	1:2	c
$[Ag_2(L^{2\text{-}Ph})_3(ClO_4)_2]_\infty$	2:3	m

Tableau 9.5. Réseaux bidimensionnels où l'anion est intercalé entre les feuillets cationiques $[Ag\text{-}L^{n\text{-}R}]_\infty$.

Formule	Rapport Métal/Ligand	Observation/Commentaire	Ref
$\{[Ag_2(L^{3\text{-}Ph})_4](PF_6)_2(CH_3COCH_3)_2\}_\infty$	1:2		g
$\{[Ag_2(L^{3\text{-}Ph})_4](ClO_4)_2(CH_3COCH_3)_2\}_\infty$	1:2		g
$\{[Ag_2(L^{3\text{-}Ph})_4](SbF_6)_2(CH_3COCH_3)_2\}_\infty$	1:2		g
$\{[Ag_2(L^{3\text{-}Ph})_4](BF_4)_2\}_\infty$	1:2		j
$\{[Ag(L^{4\text{-}Ph})_2](ClO_4)_2\}_\infty$	1:2		l
$\{[Ag(L^{1\text{-}Me})_{2.5}](BF_4)\}_\infty$	2:5		h
$\{[Ag(L^{5\text{-}Ph})_2](ClO_4)_2\}_\infty$	1:2		n
$\{[Ag(L^{5\text{-}Ph})_2](PF_6)_2\}_\infty$	1:2		o
$\{[Ag(L^{5\text{-}Ph})_2](BF_4)_2\}_\infty$	1:2		p
$\{[Ag(L^{4\text{-}Et})_2](ClO_4)_2\}_\infty$	1:2		c

Tableau 9.6. Réseaux bidimensionnels où sont incorporés l'argent, le ligand et l'anion.

Formule	Rapport Métal/Ligand	Observation/Commentaire	Ref
$[Ag_2(L^{3\text{-}Ph})(CF_3CO_2)_2]_\infty$	1:1		g
$[Ag_2(L^{3\text{-}Ph})(CF_3CF_2CO_2)_2(CH_3COCH_3)]_\infty$	2:1		g
$[Ag(L^{3\text{-}Ph})(p\text{-}TsO)]_\infty$	1:1		g
$[Ag_2(L^{3\text{-}Ph})(CF_3SO_3)_2(CH_3COCH_3)]_\infty$	2:1		g
$[Ag_2(L^{3\text{-}Ph})(CF_3SO_3)_2]_\infty$	2:1		g
$[Ag_4(L^{2\text{-}Ph})_{2.5}(ClO_4)_4(CH_3COCH_3)]_\infty$	8:5		f
$[Ag_2(L^{4\text{-}Ph})_{0.5}(CF_3CO_2)_2]_\infty$	4:1		f
$[Ag_2(L^{4\text{-}Ph})(CF_3CF_2CO_2)_2]_\infty$	2:1		f
$[Ag_2(L^{4\text{-}Ph})(CF_3CF_2CF_2CO_2)_2]_\infty$	2:1		f
$[Ag(L^{10\text{-}Ph})(NO_3)]_\infty$	1:1		f
$[Ag(L^{4\text{-}Ph})(NO_3)]_\infty$	1:1		l
$[Ag_2(L^{6\text{-}Ph})(CF_3CF_2CO_2)]_\infty$	2:1		f
$[Ag(L^{6\text{-}Ph})_{0.5}(CF_3CF_2CF_2CO_2)]_\infty$	2:1		f
$[Ag_2(L^{4\text{-}Ph})_{0.5}(CF_3CO_2)_2]_\infty$	4:1	coexistences des réseaux $(Ag\text{-ligand})_\infty$ et $(Ag\text{-anion})_\infty$	f
$[Ag_6(L^{3\text{-}Ph})_3(OOCCF_2CF_2COO)]_\infty$	2:1	coexistences des réseaux $(Ag\text{-ligand})_\infty$ et $(Ag\text{-anion})_\infty$	q
$[Ag_5(L^{3\text{-}Ph})_2(CF_3SO_3)_5(CH_3COCH_3)_2]_\infty$	2:1	coexistences des réseaux $(Ag\text{-ligand})_\infty$ et $(Ag\text{-anion})_\infty$	q
$[Ag_2(L^{2\text{-}Ph})(CF_3CO_2)_2]_\infty$	2:1		f
$[Ag(L^{6\text{-}Ph})(NO_3)]_\infty$	1:1		a

Tableau 9.7. Réseaux bidimensionnels où des chaînes sont retenues à proximité par des interactions faibles.

Formule	Rapport Métal/Ligand	Observation/Commentaire	Ref
$[Ag(L^{1\text{-}Me})(C_6H_5CO_2)]_\infty$	1:1		i
$[Ag(L^{1\text{-}Ph})(ClO_4)]_\infty$	1:1		d
$[Ag(L^{1\text{-}Ph})(BF_4)]_\infty$	1:1		d
$[Ag(L^{1\text{-}Ph})(NO_3)]_\infty$	1:1		e
$[Ag(L^{1\text{-}Ph})(CF_3CO_2)]_\infty$	1:1		d
$[Ag(L^{1\text{-}Ph})(CF_3SO_3)]_\infty$	1:1		d
$[Ag(L^{1\text{-}Ph})(CF_3CF_2CF_2CO_2)]_\infty$	1:1		d
$[Ag_2(L^{1\text{-}Ph})_2(OOCCF_2CF_2COO)]_\infty$	1:1		d
$[Ag_2(L^{1\text{-}Ph})_2(CF_3SO_3)_2]_\infty$	1:1		d
$[Ag(L^{1\text{-}Me})(C_{10}H_7SO_3)]_\infty$	1:1		q
$[Ag_2(L^{2\text{-}Et})_2(ClO_4)_2]_\infty$	1:1		c

Tableau 9.8. Réseaux tridimensionnels

Formule	Rapport Métal/Ligand	Observation/Commentaire	Ref
$\{[Ag_3(L^{1\text{-}Me})_6(CF_3SO_3)_3]\}_\infty$	1:1	Réseau obtenu avec des liaisons de coordination	h
$[Ag(L^{1\text{-}Me})(CH_3SO_3)]_\infty$	1:1	Réseau obtenu avec des liaisons hydrogènes	i
$\{[Ag_2(L^{6\text{-}Ph})\ (CF_3CO_2)_2.H_2O].H_2O\}_\infty$	2:1	Réseau obtenu avec des liaisons de coordination	f
$[Ag_2(L^{1\text{-}Ph})_3(ClO_4)]_\infty$	2:3	Réseau obtenu avec des liaisons de coordination	e

Références

[a]Chen, W.; Du, M.; Bu, X. H.; Zhang, R. H.; Mak, T. C. W. *CrystEngComm.* **2003**, *5*, 96.
[b]Li, J. R.; Zhang, R. H.; Bu, X. H. *Cryst Growth Des.* **2003**, *5*, 829.
[c]Li, J. R.; Bu, X. H.; Jiao, J.; Du, W. P.; Xu, X. H.; Zhang, R. H. *J. Chem. Soc. Dalton.* **2005**, 464.
[d]Awaleh, M. O.; Badia, A.; Brisse, F. *Cryst. Growth Des.* **2005**. *5*, 1897.
[e]Bu, X. H.; Chen, W.; Du, M.; Biradha, K. ; Wang, W. Z. ; Zhang, R. H. *Inorg. Chem.* **2002**, *41*, 437.
[f]Awaleh, M. O.; Badia, A.; Brisse, F.; Bu, X. H. *Inorg. Chem.* **2006**. *45*, 1560.

[g]Awaleh, M. O.; Badia, A.; Brisse, F. *Inorg. Chem.* **2005**. *44*, 7833.
[h]Chapitre 3.2
[i]Awaleh, M. O.; Badia, A.; Brisse, F. *Cryst Growth Des.* **2006**. *Sous presse*
[j]Blake, J. R.; Champness, N. R.; Levason, W.; Reid, G. *J. Chem. Soc. Chem. Comm.* **1995**, 1277
[k]Awaleh, M.O.; Badia, A.; Brisse, F. *Inorg.Chem.* **2006**. Soumis pour publication.
[l]Bu, X. H.; Chen, W.; Hou, W. F.; Du, M.; Zhang, R. H.; Brisse, F. *Inorg. Chem.* **2002**, *41*, 3477.
[m]Chen, W.; Li, J. R.; Wang, W. Z.; Bu, X. H.; Zhang, R. H.; Chen, R. T. *Gaodeng Xuexiao Huaxue Xuebao.* **2001**, *22*, 22.
[n]Bu, X. H.; Hou, W. F.; Du, M.; Chen, W.; Zhang, R. H. *Cryst. Growth Des.* **2002**, *2*, 303.
[o]Chen, W.; Du, M.; Zhang, R. H.; Bu, X. H. *Acta Crystallogr.* **2001**, *E57*, m213.
[p]Du, M.; Zhao, X. J. *Acta Crystallogr.* **2004**, *E60*, m193.
[q]Awaleh, M. O.; Badia, A.; Brisse, F. *Inorg. Chem.* **2006**. *Soumis pour publication*

Tableaux 10. Angles de torsion des ligands libres, quand ils sont disponibles, et dans les complexes (°).

Tableau 10.1.1

$L^{1\text{-}Ph}$ seul[a]	$L^{1\text{-}Ph}/ClO_4$[a]	$L^{1\text{-}Ph}/BF_4$[a]	$L^{1\text{-}Ph}/NO_3$[a]	$L^{1\text{-}Ph}/CF_3CO_2$[a]
φ1: 71.8	φ1: 73.6	φ1: 73.7	φ1: 66.2	φ1: 70.9
φ2: 71.8	φ2: 65.6	φ2: 64.0	φ2: 66.0	φ2: 68.8

Tableau 10.1.2

$L^{1\text{-}Ph}$ seul[a]	$L^{1\text{-}Ph}/CF_3CO_2$[a]	$L^{1\text{-}Ph}/CF_3SO_3$[a]	$L^{1\text{-}Ph}/CF_3SO_3$[a]
φ1: 71.8	φ1: 70.9	φ1: 66.9	φ1: 59.6
φ2: 71.8	φ2: 68.8	φ2: 73.7	φ2: 68.9
			φ1': 114.8
			φ2': -70.3

Tableau 10.1.3

$L^{1\text{-}Ph}$ seul[a]	$L^{1\text{-}Ph}/CF_3CF_2CF_2CO_2$[a]	$L^{1\text{-}Ph}/OOCCF_2CF_2COO$[a]
φ1: 71.8	φ1: 96.8	φ1: -73.6
φ2: 71.8	φ2: -66.7	φ2: -72.1
		φ1': 68.6
		φ2': 66.9

[a]Awaleh, M. O.; Badia, A.; Brisse, F. *Cryst. Growth. Des.* **2005**. *5*, 1897.

Tableau 10.2

$L^{2\text{-}Ph}$ seul[b]	$L^{2\text{-}Ph}/AgClO_4$ [c]	$L^{2\text{-}Ph}/AgCF_3CO_2$ [c]	$L^{2\text{-}Ph}/CF_3SO_3$ [c]	$L^{2\text{-}Ph}/AgNO_3$ [c]
φ1: 83.9	φ1: -65.7	φ1: -179.4	φ1: -166.5	φ1: 62.8
φ2: 180.0	φ2: 180.0	φ2: -179.1	φ2: 178.6	φ2: 66.2
φ3: -83.9	φ3: 65.7	φ3: 175.1	φ3: 174.9	φ3: -65.5
	φ1': -171.3			φ1': -169.9
	φ2': 68.8			φ2': 74.7
	φ3': -171.5			φ3': 65.3
				φ1'': 165.8
				φ2'': -65.9
				φ3'': -60.7
				φ1''': 66.726
				φ2''': -73.577
				φ3''': -64.9

[b]Awaleh, M. O.; Badia, A.; Brisse, F. *Acta Crystallogr.* **2005**, *E61*, o2479.

[c]Awaleh, M. O.; Badia, A.; Brisse, F.; Bu, X. H. Inorg. Chem. **2006**. *45*, 1560.

Tableau 10.3.1

$L^{3\text{-}Ph}$ seul Non disponible	$L^{3\text{-}Ph}/PF_6$ [d]	$L^{3\text{-}Ph}/SbF_6$ [d]	$L^{3\text{-}Ph}/ClO_4$ [d]	$L^{4\text{-}Ph}/BF_4$ [e]
φ1:	φ1: 62.2	φ1: -65.1	φ1: 64.9	φ1: 73.8
φ2:	φ2: 179.6	φ2: -178.4	φ2: -175.3	φ2: 175.4
φ3:	φ3: 179.8	φ3: -177.8	φ3: 177.5	φ3: 67.2
φ4:	φ4: -64.5	φ4: 64.9	φ4: -69.7	φ4: 66.9
	φ1': 67.2	φ1': 65.6	φ1': -69.7	φ1': -61.9
	φ2': 179.6	φ2': 175.3	φ2': 177.5	φ2': 175.0
	φ3': 179.8	φ3': -178.8	φ3': -175.3	φ3': -178.6
	φ4': 64.5	φ4': -73.3	φ4': 64.9	φ4': 68.1
	φ1'': 66.6	φ1'': 64.9	φ1'': -66.2	
	φ2'': 69.9	φ2'': -177.8	φ2'': -68.4	
	φ3'': 172.9	φ3'': -178.4	φ3'': -176.4	
	φ4'': 77.8	φ4'': -65.1	φ4'': -71.9	
	φ1''': 67.1	φ1''': -168.9	φ1''': -177.7	
	φ2''': 179.9	φ2''': 177.4	φ2''': -179.9	
	φ3''': 176.9	φ3''': -176.2	φ3''': -176.6	
	φ4''': -70.8	φ4''': 167.3	φ4''': -174.0	
	φ1'''': -179.7			
	φ2'''': 178.7			
	φ3'''': -175.0			
	φ4'''': 175.1			

[d]Awaleh, M. O.; Badia, A.; Brisse, F. *Inorg. Chem.* **2005**. *44*, 7833.
[e]Black, J. R.; Champness, N. R.; Levason, W.; Reid, G. *J. Chem. Soc., Dalton Trans.* **1995**, 3439.

Tableau 10.3.2

$L^{3\text{-}Ph}$ seul Non disponible	$L^{3\text{-}Ph}/CF_3CO_2$ [d]	$L^{3\text{-}Ph}/CF_3CF_2CO_2$ [d]	$L^{3\text{-}Ph}/CF_3CF_2CF_2CO_2$ [d]
φ1:	φ1: -100.6	φ1: 70.3	φ1: -69.7
φ2:	φ2: -78.2	φ2: 178.0	φ2: 173.3
φ3:	φ3: 170.3	φ3: 177.3	φ3: -164.2
φ4:	φ4: 164.1	φ4: -66.3	φ4: 61.7

Tableau 10.3.3

$L^{3\text{-}Ph}$ seul Non disponible	$L^{3\text{-}Ph}/CF_3SO_3$ [d]	$L^{3\text{-}Ph}/CF_3SO_3$ [d]	$L^{3\text{-}Ph}/CF_3SO_3$ [d]	$L^{3\text{-}Ph}$/p-TsO [d]	$L^{3\text{-}Ph}$/p-TsO [d]
φ1:	φ1: 166.1	φ1: 52.0	φ1: 169.6	φ1: -63.6	φ1: 56.3
φ2:	φ2: 179.5	φ2: 172.8	φ2: 163.4	φ2: 178.6	φ2: -168.5
φ3:	φ3: 159.4	φ3: -176.2	φ3: 163.4	φ3: -68.5	φ3: 172.7
φ4:	φ4: 66.1	φ4: -65.1	φ4: 169.5	φ4: -61.6	φ4: -66.1

Tableau 10.4.1

$L^{4\text{-Ph}}$ seul[f]	$L^{4\text{-Ph}}/CF_3SO_3$[c]	$L^{4\text{-Ph}}/CF_3CO_2$[c]	$L^{4\text{-Ph}}/CF_3CF_2CO_2$[c]	$L^{4\text{-Ph}}/CF_3CF_2CF_2CO_2$[c]
φ1: -172.8	φ1: -77.1	φ1: -83.4	φ1: -80.9	φ1: -175.8
φ2: 179.6	φ2: 178.9	φ2: 178.2	φ2: -173.4	φ2: 168.9
φ3: 180.0	φ3: 180.0	φ3: 180.0	φ3: 180.0	φ3: 180.0
φ4: -179.6	φ4: -178.9	φ4: -178.2	φ4: 173.4	φ4: -168.9
φ5: 172.8	φ5: 77.1	φ5: 83.4	φ5: 80.9	φ5: 175.8
	φ1': 58.7		φ1': -73.9	
	φ2': -177.7		φ2': -172.6	
	φ3': 180.0		φ3': 180.0	
	φ4': 177.7		φ4': 172.6	
	φ5': -58.7		φ5': 73.9	

[c]Awaleh, M. O.; Badia, A.; Brisse, F.; Bu, X. H. Inorg. Chem. **2006**. *45*, 1560.

[f]Chen, W.; Hou, B. H.; Zhou, L. N.; Wang, J. K.; Li, H. *Acta Crystallogr.* **2005**, *E61*, o1890.

Tableau 10.4.2

$L^{4\text{-Ph}}$ seul[f]	$L^{4\text{-Ph}}/NO_3$[g]	$L^{4\text{-Ph}}/ClO_4$[g] M/L: 2/3	$L^{4\text{-Ph}}/ClO_4$[g] M/L: x/y (CH3OH)	$L^{4\text{-Ph}}/ClO_4$[g] M/L: 2/1
φ1: -172.8	φ1: -63.6	φ1: 60.9	φ1: -60.7	φ1: -170.5
φ2: 179.6	φ2: -63.8	φ2: 172.7	φ2: -177.6	φ2: -67.2
φ3: 180.0	φ3: 180.0	φ3: 180.0	φ3: 180.0	φ3: 180.0
φ4: -179.6	φ4: 63.8	φ4: -172.7	φ4: 177.6	φ4: 67.2
φ5: 172.8	φ5: 63.6	φ5: -60.9	φ5: 60.7	φ5: 170.5
		φ1': -81.6	φ1': 62.8	φ1': 74.1
		φ2': -165.9	φ2': -177.4	φ2': 175.5
		φ3': 180.0	φ3': 180.0	φ3': 180.0
		φ4': 165.9	φ4': 177.4	φ4': -175.5
		φ5': 81.6	φ5': -62.8	φ5': -74.1
				φ1'': -170.5
				φ2'': -67.2
				φ3'': 180.0
				φ4'': 67.2
				φ5'': 170.5
				φ1''': 72.9
				φ2''': -179.8
				φ3''': 180.0
				φ4''': 179.8
				φ5''': -72.9
				φ1'''': -162.1
				φ2'''': 175.5
				φ3'''': 180.0

				φ4'''': -175.5 φ5'''': 162.1

[g]Bu, X. H.; Chen, W.; Hou, W. F.; Du, M.; Zhang, R. H.; Brisse, F. *Inorg. Chem.* **2002**, *41*, 3477.

Tableau 10.5

$L^{5\text{-Ph}}$ seul Non disponible	$L^{5\text{-Ph}}/PF_6$[h]	$L^{5\text{-Ph}}/ClO_4$[i]	$L^{5\text{-Ph}}/BF_4$[j]
φ1:	φ1: -83.8	φ1: -70.1	φ1: -68.4
φ2:	φ2: 174.7	φ2: 175.1	φ2: -171.4
φ3:	φ3: 169.3	φ3: -178.3	φ3: 177.9
φ4:	φ4: -174.1	φ4: -175.1	φ4: -170.9
φ5:	φ5: 171.9	φ5: -57.5	φ5: -174.3
φ6:	φ6: 67.2	φ6: -169.9	φ6: 88.0
	φ1': -70.7	φ1': -86.6	φ1': 171.6
	φ2': 174.7	φ2': 174.0	φ2': 56.3
	φ3': -176.9	φ3': 170.1	φ3': 175.5
	φ4': -176.7	φ4': -176.4	φ4': 178.3
	φ5': -59.4	φ5': 170.7	φ5': -175.6
	φ6': -171.6	φ6': 67.8	φ6': 70.5

[h]Chen, W.; Du, M.; Zhang, R. H.; Bu, X. H. *Acta Crystallogr.* **2001**, *E57*, m213.
[j]Du, M.; Zhao, X. J. *Acta Crystallogr.* **2004**, *E60*, m193.
[i]Bu, X. H.; Hou, W. F.; Du, M.; Chen, W.; Zhang, R. H. *Cryst Growth and Design*, **2002**, *2*, 303.

Tableau 10.6

$L^{6\text{-Ph}}$ seul[k]	$L^{6\text{-Ph}}/CF_3CO_2$[c]	$L^{6\text{-Ph}}/CF_3CF_2CO_2$[c]	$L^{6\text{-Ph}}/CF_3CF_2CF_2CO_2$[c]	$L^{6\text{-Ph}}/ClO_4$[l]
φ1: 175.1	φ1: 63.8	φ1: -71.4	φ1: -66.5	φ1: -68.4
φ2: 179.7	φ2: -177.3	φ2: 176.5	φ2: 174.5	φ2: -179.5
φ3: -179.7	φ3: 177.9	φ3: 174.2	φ3: 173.6	φ3: 63.2
φ4: 180.0	φ4: 180.0	φ4: 171.7	φ4: 180.0	φ4: 66.5
φ5: 179.7	φ5: -177.9	φ5: 170.9	φ5: -173.6	φ5: -171.3
φ6: -179.7	φ6: 177.3	φ6: 173.8	φ6: -174.5	φ6: -177.4
φ7: -175.1	φ7: -63.8	φ7: -81.7	φ7: 66.5	φ7: -164.5

[k]Awaleh, M. O.; Badia, A.; Brisse, A. *Acta Crystallogr.* **2005**, *E60*, o2476.

[c]Awaleh, M. O.; Badia, A.; Brisse, F.; Bu, X. H. Inorg. Chem. **2006**. *45*, 1560.

[l]Chen, W.; Du, M.; Bu, X. H.; Zhang, R. H.; Mak, T. C. W. *CrystEngComm.* **2003**, *5*, 96.

Tableau 10.7

$L^{10\text{-}Ph}$ seul[m]	$L^{10\text{-}Ph}/NO_3$[c]
φ1: 173.1	φ1: 71.6
φ2: -179.3	φ2: 67.2
φ3: -179.8	φ3: 69.2
φ4: 179.8	φ4: -179.5
φ5: -179.7	φ5: 178.4
φ6: 180.0	φ6: 180.0
φ7: 179.7	φ7: 178.4
φ8: -179.8	φ8: 179.5
φ9: 179.8	φ9: -69.2
φ10: 179.3	φ10: -67.2
φ10: -173.1	φ11: -71.6
	φ1': 177.7
	φ2': -173.0
	φ3': 172.4
	φ4': 176.8
	φ5': -177.4
	φ6': 180.0
	φ7': 177.4
	φ8': -176.8
	φ9': -172.4
	φ10': 173.0
	φ11': -177.7

[m]Awaleh, M. O.; Badia, A.; Brisse, A. *Acta Crystallogr.* **2005**, *E60*, o2473.

[c]Awaleh, M. O.; Badia, A.; Brisse, F.; Bu, X. H. Inorg. Chem. **2006**. *45*, 1560.

Tableau 10.8

$L^{1\text{-}tBu}/ClO_4^{n}$	$L^{2\text{-}tBu}/ClO_4^{n}$	$L^{3\text{-}tBu}/ClO_4^{n}$	$L^{4\text{-}tBu}/ClO_4^{n}$	$L^{5\text{-}tBu}/ClO_4^{n}$	$L^{6\text{-}tBu}/ClO_4^{n}$
φ1: -85.9	φ1: -176.8	φ1: -171.5	φ1: 95.2	φ1: -171.9	φ1: 178.7
φ2: -156.7	φ2: -180.0	φ2: 178.0	φ2: 171.4	φ2: -178.2	φ2: 74.1
	φ3: 176.8	φ3: -161.8	φ3: -180.0	φ3: 67.8	φ3: 174.6
		φ4: -76.6	φ4: -171.4	φ4: 65.4	φ4: 180.0
			φ5: -95.2	φ5: -176.5	φ5: -174.6
				φ6: -101.5	φ6: -74.1
			φ1': 171.8		φ7: -178.7
			φ2': 177.3		
			φ3': 69.8		
			φ4': 166.4		
			φ5': -175.6		

[n]Li, J. R. ; Zhang, R. H. ; Bu, X. H. *Cryst. Growth. Des.* **2003**, *3*, 829.

Tableau 10.9

$L^{1\text{-}Benz}/ClO_4^{o}$	$L^{2\text{-}Benz}/ClO_4^{o}$	$L^{3\text{-}Benz}/ClO_4^{o}$	$L^{4\text{-}Benz}/ClO_4^{o}$
φ1: 60.7	φ1: 168.1	φ1: -67.1	φ1: 78.1
φ2: 176.0	φ2: -76.9	φ2: 178.5	φ2: -177.9
	φ3: -177.8	φ3: 178.5	φ3: 180.0
		φ4: -67.1	φ4: 177.9
			φ5: -78.1
	φ1': 64.9		
	φ2': 59.7		φ1': 65.9
	φ3': 61.5		φ2': 59.9
			φ3': -175.3
			φ4': -176.4
			φ5': 69.6

[o]Li, J. R.; Bu, X. H.; Jiao, J.; Du, W. P. ; Xu, X. H. ; Zhang, R. H. *J. Chem. Soc. Dalton.* **2005**, 464.

Tableau 10.10

$L^{1\text{-}Et}/ClO_4$ [o]	$L^{2\text{-}Et}/ClO_4$ [o]	$L^{3\text{-}Et}/ClO_4$ [o]	$L^{4\text{-}Et}/ClO_4$ [o]
φ1: -72.0	φ1: 79.8	φ1: -54.9	φ1: -174.3
φ2: -72.0	φ2: 65.8	φ2: -170.4	φ2: -157.7
	φ3: -166.9	φ3: 77.5	φ3: -180.0
		φ4: 164.1	φ4: 157.7
			φ5: 174.3
	φ1': -165.8		
	φ2': 64.6		φ1': -51.2
	φ3': 75.6		φ2': -162.7
			φ3': -82.0
			φ4': -170.1
			φ5': -59.1
			φ1': -67.7
			φ2': -168.4
			φ3': -175.4
			φ4': -164.8
			φ5': -63.6

[o]Li, J. R.; Bu, X. H.; Jiao, J.; Du, W. P. ; Xu, X. H. ; Zhang, R. H. *J. Chem. Soc. Dalton.* **2005**, 464.